DISCOVERIES IN THE TASMANIDES
A Mines & Wines Event

2026
DISCOVERIES IN THE TASMANIDES CONFERENCE

EXTENDED ABSTRACTS VOLUME
9–11 September 2026 | New South Wales, Australia

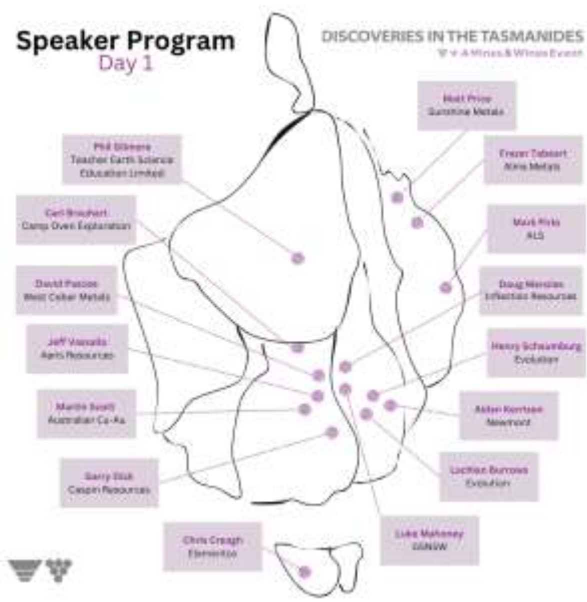

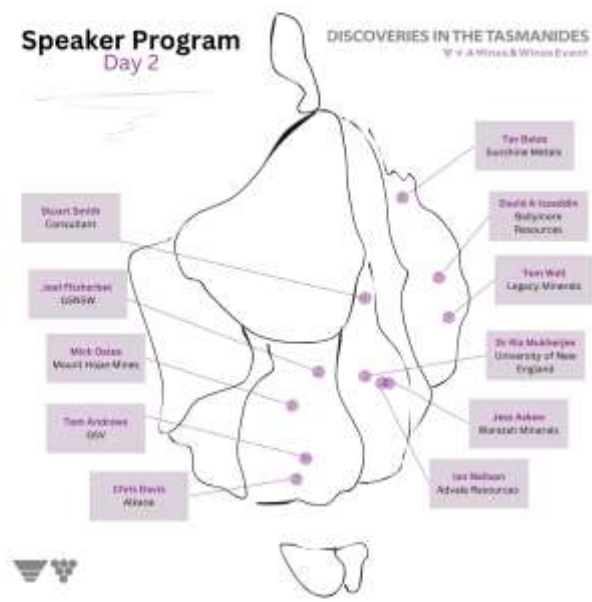

AIG BULLETIN 77
Publisher: Australian Institute of Geoscientists

NEW SOUTH WALES
9–11 September 2026

Australian Institute of Geoscientists
Level 26, 44 Market Street, Sydney NSW 2000.

Telephone: 08 9427 0820
Email aig@aig.org.au

ISBN: 978-1-876118-58-7
ISSN 0812 6089

Bibliographic reference:

Greenfield, J.E. (compiler), 2026. Bulletin 77: Discoveries in the Tasmanides 2026. Australian Institute of Geoscientists, Sydney NSW 2000.

PREFACE

The 2026 Discoveries in the Tasmanides conference marks a significant milestone, two decades since the inaugural event was held in 2006.

In 2006, gold traded at around US$604 per ounce. Artificial intelligence was still the stuff of Spielberg's sci-fi blockbusters, the iPhone had yet to be released, and the Global Financial Crisis was looming just over the horizon. Twenty years later the world looks remarkably different. Gold now trades at more than US$4,000 per ounce, artificial intelligence has moved from science fiction into everyday life, smartphones have transformed the way we communicate, and technological innovation continues to reshape our approach to mineral exploration.

Yet despite two decades of extraordinary change the challenge and excitement of making the next discovery remain unchanged. Against the backdrop of the many challenges our industry faces, the committee continues to be encouraged by the level of engagement and support this conference receives. This year we are again fortunate to present a fantastic spread of presentations from across the Tasmanides, alongside record student engagement and strong support from the geoscience community.

Returning to Orange, NSW this year, the 2026 conference represents the culmination of two years of organisation by a dedicated volunteer committee from industry and government. Committee members generously donate their time to ensure that our community can meet on a biennial basis to network, exchange ideas and discuss exploration and project advances across the Tasmanides. With considerable support from the Australian Institute of Geoscientists and our conference sponsors, this volunteer model not only keeps delivery costs down but it also makes it accessible to a wide variety of people including our pipeline of future geoscientists. We are extremely proud of the dedication and enthusiasm that this group has shown to make the 2026 conference a success.

Discoveries in the Tasmanides conference was inaugurated in 2006 as a collaboration among SMEDG, AIG and the Geological Survey of NSW with the vision of providing exploration geoscientists the opportunity to present on their projects in the Palaeozoic Tasmanides of Eastern Australia. To both complement and contextualise these projects Big Picture presentations are invited from recognised specialists in metallogenesis, tectonism and mineral exploration.

The foundation principles of the Discoveries in the Tasmanides conference are:

1. Conference speakers must recognise that all presentations are to be technical in nature and non-promotional. References to market capitalisation, share price, and the like, are strongly discouraged.
2. All committee members perform their roles on a volunteer, non-paid basis.
3. We encourage students to attend, contribute to the poster sessions and, where appropriate, apply for any financial assistance on offer.
4. Presentations are sought from across the Tasmanides with a diversity of commodities, deposit types, and locations represented.
5. We seek both mineral exploration practitioners to share their projects and specialists to inform us on relevant developments in minerals geoscience.
6. Conferences are preferably held in areas that have significant mineral deposits accessible via field trips.
7. Conferences are held in areas that have access to a recognised wine industry.
8. Socialising over a good wine makes for effective networking in our profession which thrives on shared learnings.

This volume of extended abstracts will be made available through websites of the Discoveries in the Tasmanides, Sydney Mineral Exploration Discussion Group (SMEDG), and the Australian Institute of Geoscientists (AIG).

We would like to once again, extend our appreciation to the volunteer committee members, speakers and sponsors whose support and collaboration have been instrumental in the organisation of this conference. We hope this volume serves as a useful reference and inspires further research and innovation in the important field of mineral exploration and discovery.

Kristyn Adamczyk & Doug Menzies (Co-Chairs)

CONTENTS

Thank you to our 2026 conference sponsors, partners, and booth holders

PLATINUM SPONSORS

ALS Global
www.alsglobal.com

GOLD SPONSORS

Newmont Australia
www.newmont.com

Mitchell Services
www.mitchellservices.com.au

Waratah Minerals
www.waratahminerals.com/

SILVER SPONSOR

Evolution Mining
evolutionmining.com

Anglogold Ashanti
www.anglogoldashanti.com

BRONZE SPONSORS

DDH 1 Drilling
ddh1drilling.com.au

AXT
www.axt.com.au

Bell Potter
bellpotter.com.au

Inflection Resources
inflectionresources.com

CONFERENCE DINNER

Durock Drilling
www.durockdrilling.com.au

FIELD TRIP

Mitchell Services
www.mitchellservices.com.au

ICEBREAKER

Ophir Drilling

WINE DEGUSTATION

Titeline Drilling
www.titelinedrilling.com.au

NAME TAGS

maxgeo
maxgeo.com

COFFEE CART

Anglogold Ashanti
www.anglogoldashanti.com

CORE SHACK

MetaGeo
metageo.io

GOLD-ANTIMONY SYSTEMS IN VICTORIA

Tom Andrews[1], Cameron Cairns[1], Steven Boger[1], Sam Waugh[1], Simon Travers[1], Ross Cayley[1], Zsanett Pintér[2], Nick Farmer[2]

[1] Geological Survey of Victoria, Level 8, 8 Nicholson St, East Melbourne, 3002.

[2] CSIRO Mineral Resources, Research Way, Clayton, 3168.

Key Words: Antimony, gold, Victoria, Devonian, Melbourne Zone, Selwyn Block, orogenic gold, reduced intrusion related gold, MAIA mapper.

INTRODUCTION

Victorian mining is synonymous with high grade gold. Historical production was centred on the famous Golden Triangle – Bendigo, Ballarat, and one of several Stawell Zone goldfields, depending on who's telling the story. Coarse free gold was mined from fault hosted quartz veins emplaced at the end of the Benambran Orogeny, a textbook example of metamorphic gold formed during amagmatic compressional tectonics.

Artisanal mining was perfectly suited to exploit rich alluvial deposits, with thousands of ounces taken from nine square foot claims. Primary, vein hosted mineralisation was nuggety but occupied predictable structural settings easily traceable by pick and shovel, with a lifechanging face only ever a cut away.

But these characteristics don't favour modern mining and resource estimation. Their nuggety nature means that while grade continuity likely exists, it is incredibly difficult to prove. And while 'drill for structure drive for grade' works in practice, it is hard to sell and scale.

But this isn't the only type of gold deposit in Victoria. Mines in the Costerfield Domain, centred in the Melbourne and eastern Bendigo zones, are distinguished by their lower temperature stibnite dominated ore mineral assemblages and refractory gold mineralisation.

Historically these played second fiddle to the coarse free gold deposits in the Bendigo Zone. Refractory mineralisation was arduous to process, and the Melbourne Zone contains no significant alluvial gold deposits.

Costerfield re-entered modern production in the early 2000s, producing up to 64,000 ounces of gold per year at world class grades. It is currently Australia's only antimony mine, contributing up to 3.5% of world demand.

Modern production at Fosterville began in 2005, exploiting unique mineralisation for the Bendigo Zone. Fine-grained, gold-rich arsenopyrite disseminated within the wall rocks surrounding quartz–carbonate veins, accompanied by minor stibnite, contrasts with the coarse free-gold hosted in the same rocks and structures at nearby Bendigo.

Fosterville produced approximately 100,000 ounces of gold a year from refractory mineralisation through the early 2010s. Excess antimony poisoned the bacteria in the BIOX mill, compromising gold recovery, and was avoided.

The discovery of the Swan Zone at Fosterville in 2016 revealed the potential of Victorian gold-antimony systems. Complex structures intercepted down plunge of the resource contained up to wt% gold as fine, native grains in stylolitic quartz carbonate veins, often coincident with massive stibnite.

This single-handedly kicked off a modern gold rush in Victoria, driven by the allure of another Swan.

Southern Cross' diligent exploration at Sunday Creek has shown the greenfields potential of the Melbourne Zone. Systematic drilling of spectacular gold-antimony veins has contributed to an exploration target of 8.1 – 9.6 Mt @ 8.3 – 10.6 AuEq for 2.2 – 3.2 Moz AuEq (as of March 2025).

Costerfield has continued from strength to strength as one of the highest-grade gold mines in the world, becoming more gold-rich with depth.

Gold-antimony systems can match the grade of the famous deposits in the Bendigo Zone. Less nuggety gold means grade continuity is more consistent and amenable to modern resource estimation. The emergence of antimony as a valuable critical mineral strengthens project economic and ESG credentials.

A BIT ABOUT ANTIMONY

Subduction processes cause antimony to become enriched in igneous rocks above average crustal values. Mid-ocean ridge basalt becomes enriched in antimony through seafloor metasomatism (Jochum & Verma, 1996). Subduction of metasomatized crust introduces antimony into the mantle wedge, where it enters arc magmas and becomes enriched in the crust (Hattori & Guillot, 2003).

Antimony is very fluid mobile. The solubility of antimony is strongly temperature controlled, with precipitation from realistic crustal fluids inhibited above ~250°C. This can be observed in modern settings as antimony rich precipitates in geothermal pools, and antimony rich sulphide films in the boiling zones in geothermal power wells. Precipitation is therefore restricted to the shallow or distal parts of ore forming systems.

MINERAL SYSTEMS

Orogenic and reduced intrusion-related gold deposits are the two most likely mineral systems candidates for gold-antimony mineralisation in Victoria, forming at different progressive stages of prograde metamorphism.

During prograde metamorphism, fertile source rocks, including serpentinised ophiolite and arc igneous rocks, pass through the greenschist-amphibolite transition. Chlorite, muscovite and pyrite breakdown and release water, sulphur and fluid mobile trace elements, including gold, antimony, arsenic, molybdenum, bismuth, tungsten and mercury into low salinity, near neutral, CO_2 rich metamorphic fluids (Latheef Thathrampally et al., 2025; Tomkins, 2010). Fluids are focussed through fault zones with enhanced permeability and ascend the crust. Orogenic gold deposits are formed when conduits self-organise to focus fluids through narrow volumes with appropriate physiochemical conditions to transiently seal and fail, precipitating their contained metals (Cox, 1995; Hronsky, 2020).

Vertical zoning in response to geothermal gradients is common in orogenic gold systems (Groves et al., 1998). Deep (hypozonal) levels preserve higher temperature gold-arsenic metals assemblages. Medial (mesozonal) levels preserve gold-arsenic-tungsten-tellurium. Shallow (epizonal) levels preserve gold-antimony, when the enclosing temperature drops below approximately 250°C.

If prograde metamorphism progresses past the wet solidus, remaining metamorphic fluids flux silicate melting. Trace elements remaining in the source rocks can enter these silicate melts, potentially forming intrusion related gold deposits.

Intrusions with ore forming potential are typically small, <5km^2. Large and flat-topped batholiths have poor fluid focussing and ore forming potential. Fluids become concentrated beneath the cooling intrusion carapace. Intrusion related gold deposits form when fluid pressure exceeds the strength of the carapace, which explosively fails. Fluids are released into the wallrock, traversing steep hornfels geotherms. Metals are precipitated in narrow concentric zones in response to steep P/T/pH gradients (Hart, 2005). Antimony mineralisation is deposited in the cool, distal shoulders of the magmatic hydrothermal systems.

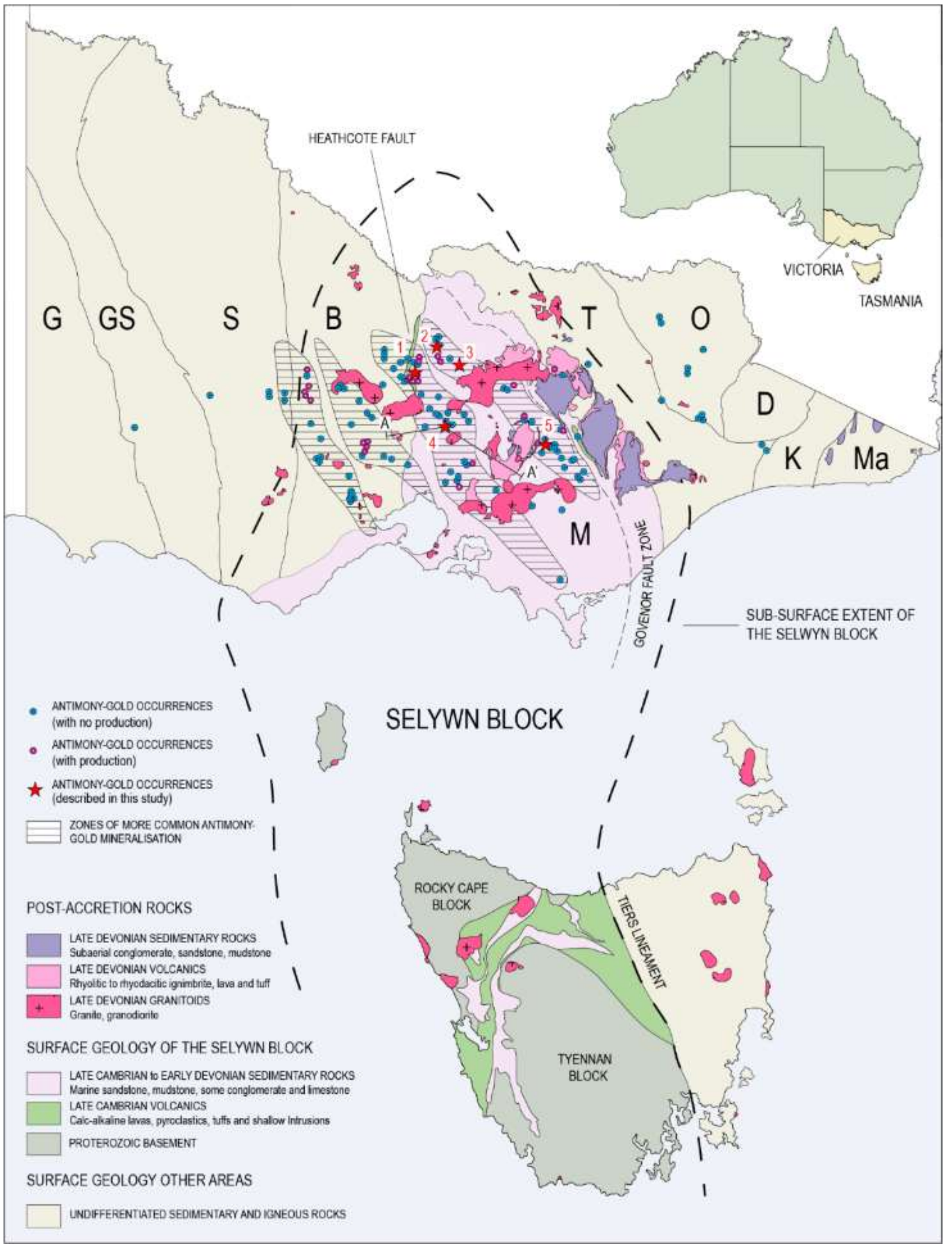

Figure 1: Antimony mineral occurrences, middle-late Devonian magmatism and the Selwyn Block in central Victoria. Red stars show the location of deposits discussed in the text - 1: Fosterville 2: Costerfield 3: Sunday Creek 4: Nagambie 5: Rushworth 6: Whroo 7: Mount Piper 8: Steeles Creek 9: Big River.

DISTRIBUTION

Stibnite occurs as a primary or accessory phase in 344 historical mines in Victoria. One hundred and ninety-eight new occurrences discovered in historical records were recently added to this database (Cairns et al., 2026).

Gold antimony deposits are clustered in central Victoria, dominantly in the Melbourne Zone, but extending into the adjacent zones (Figure 1). Their distribution overlaps more closely with the subsurface projection of the Selwyn Block, the northern extension of the Vandieland microcontinent which forms the basement to the Melbourne Zone. Middle-late Devonian felsic magmatism and gold-antimony mineralisation are spatially coincident in Victoria.

Gold-antimony mineralisation occurs in NW trends which traverse the Heathcote Fault in the Melbourne and Bendigo zones. Gold only mineralisation occurs both within and in between the trends, in the same structural settings as gold-antimony deposits.

HOST GEOLOGY AND MINERALISATION

Victorian gold-antimony systems are hosted in quartz-carbonate veins as disseminated to semi-massive stibnite containing free and refractory gold. Veins range from a few centimetres to 2m wide and persist for tens of metres down dip and hundreds of metres along strike in favourable structures.

Folded and faulted Murrindindi Supergroup and Castlemaine Group sediments host most deposits. Less numerous but equally prospective deposits overprint mafic-felsic dykes. These predate mineralisation and provide a rheological contrast which enhances fracturing and precipitation.

Stibnite is the primary antimony ore mineral, with lesser sulphosalts. Gold occurs as fine disseminated native specs, and in fine acicular arsenopyrite in the wallrocks. Base metal sulphides are a common, low volume accessory phase.

Visible alteration is dominated by narrow sericite-carbonate-pyrite alteration haloes, often less than 5 metres wide. Cryptic enrichment of arsenic and antimony and subtle changes in white mica chemistry can persist greater than 50m from mineralised veins.

Vertical zoning is common, with antimony decreasing and gold increasing with depth. The vertical extent of these deposits is unclear but exceeds 1km.

Vein textures including open vugs containing delicate acicular crystal growths, combined with fluid inclusions indicate formation at shallow crustal levels (<3km) (Gao et al., 1995; Gao & Kwak, 1995).

STRUCTURE

Gold-antimony veins postdate the major deformation events which have affected the Melbourne Zone - the Bindian and Tabberabberan orogenies. They commonly strike NNW-SSE and dip sub vertically.

At Costerfield, NNW striking, west dipping and subvertical veins strike sub-parallel to the stratigraphy and form long veins with strike persistence over hundreds of meters. They range from 10cm to 1.5m in width (Figure 2).

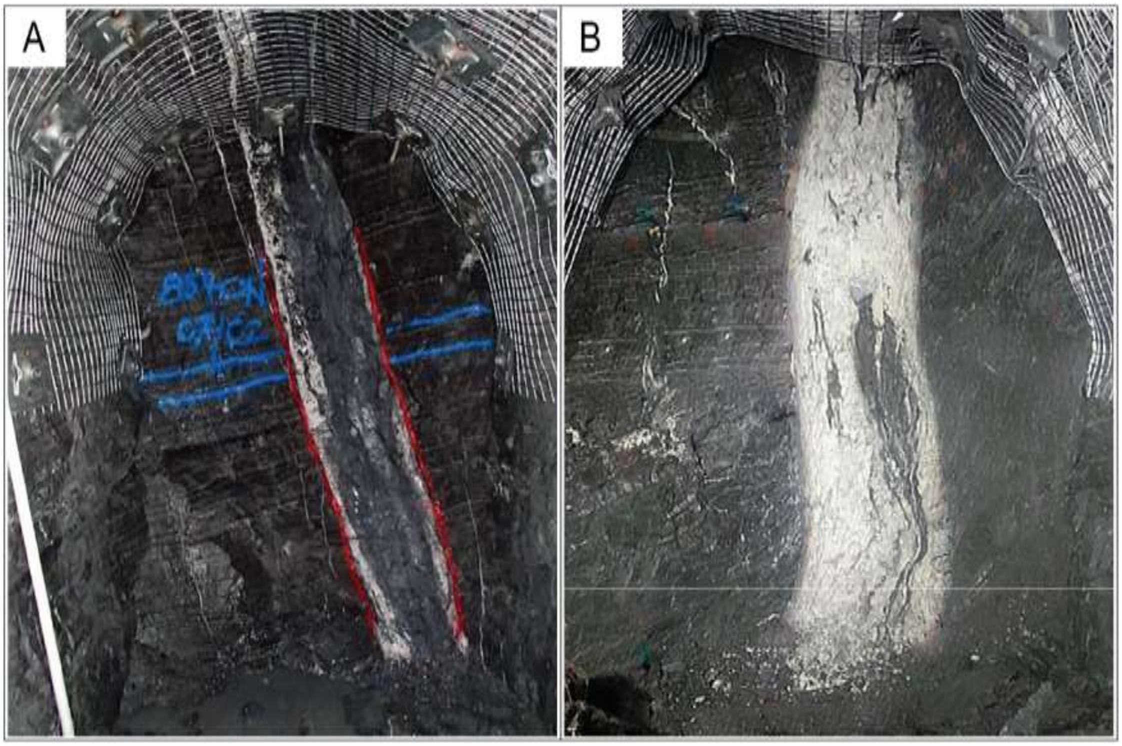

Figure 2: Mineralisation styles at Costerfield. A. Steep dipping vein with massive stibnite (dark grey). Vein cuts bedding at a high angle. Cuffley Lode, Costerfield (Fenwick, 2019). B. Quartz-rich gold-only vein. Youle Lode, 617 Level (Bush & Hudson, 2024).

At Sunday Creek, NNW striking veins crosscut an approximately E-W striking subvertical diorite dyke. Composite transtensional shear and subsidiary extensional tension veins cut the dyke at a high angle.

At Nagambie, Rushworth and Whroo, the enclosing stratigraphy strikes approximately E-W. Free to disseminated gold is hosted in north dipping thrust faults and subsidiary tension veins developed in response to earlier N-S shortening. Antimony veins are subvertical, strike near N-S and are concentrated in the E-W striking anticlines.

Antimony mineralisation locally overprints granitic stocks and hydrothermal breccias. At Mount Piper, wispy quartz stibnite veinlets overprint a low-grade hydrothermal breccia containing polymictic turbidite – dacite clasts. At Steeles Creek, quartz stibnite veinlets overprint a quenched, alerted quartz porphyry. At Big River, quartz stibnite veins overprint an altered granitic intrusive and deformed metasediments.

MINERALOGY AND PARAGENESIS

The paragenesis and ore textures are consistent between gold-antimony deposits in central Victoria.

Paragenetically early laminated quartz-carbonate veins contain free gold surrounded by a halo of fine acicular gold rich arsenopyrite. Free gold in early veins is typically fine, concentrated in stylolites or distributed homogeneously in the quartz.

Antimony mineralisation exploits the same structures but overprints this early gold rich event. Massive stibnite breccias overprint earlier quartz-carbonate veins and refractory mineralisation. Stibnite cemented breccias contain milled vein quartz and fragments of wall rock containing early refractory gold in arsenopyrite mineralisation (Figure 3). Gold can be present or absent in the late stibnite breccias. Where present, gold spots commonly align within the breccia (Figure 4). Arsenopyrite alteration halos can surround massive stibnite veins.

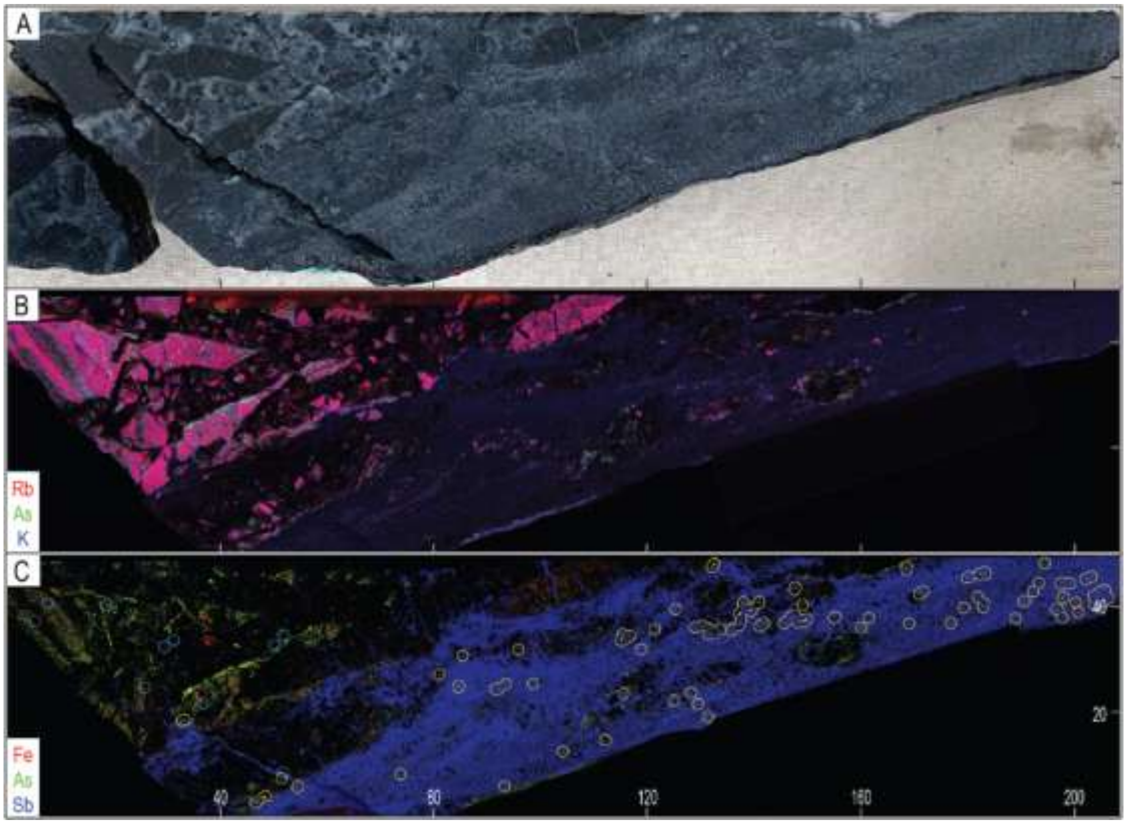

Figure 3: Maia elemental maps and drill core images of GSV sample 322114, Apollo prospect, Sunday Creek. (Cairns et al., 2026). A: Angular wallrock fragments in quartz cemented breccia overprinted by massive stibnite. B: Micaceous sedimentary rock fragments (magenta colours) in quartz breccia showing arsenopyrite (electric blue colours) in discordant veinlets and concentrated in sandy (mica poor) beds. C: Arsenopyrite (yellow colours) does not ring breccia cemented wallrock fragments, implying emplacement prior to brecciation. Yellow and blue circles show gold spots.

AGE

Gold-antimony veins structurally overprint the main periods of deformation in the Melbourne Zone and have historically ascribed a post Tabberabberan age. Mineralisation has been indirectly dated 383 ± Ma and 376 ± 3 Ma, using Ar/Ar geochronology on sericitic alteration at Fosterville (Fu et al., 2009). Recent Re-Os pyrite and arsenopyrite geochronology on Sunday Creek returned a mean weighted age of 379 ± 1 Ma (Waugh et al., 2024). Quartz-stibnite veins overprint felsic igneous units with SHRIMP U-Pb zircon ages overlapping at ~373 Ma (GSV unpublished data) at Steeles Creek and Big River.

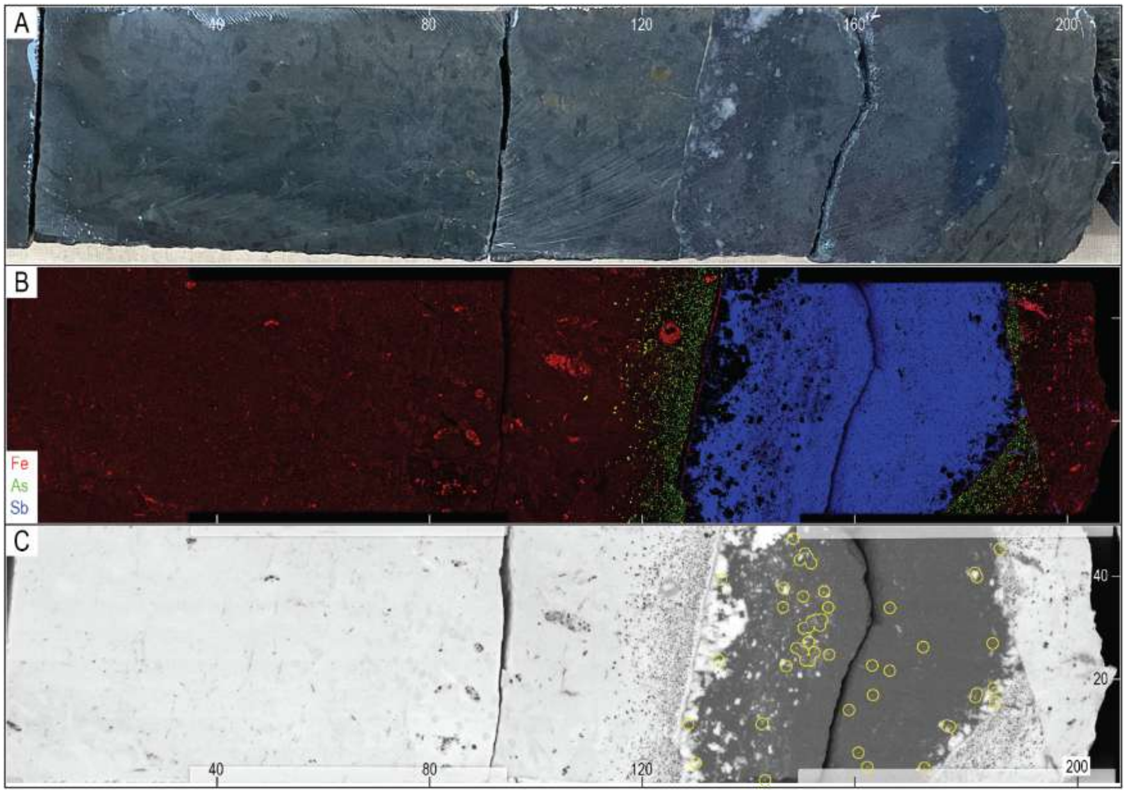

Figure 4: Maia elemental maps and drill core images of GSV sample 310415, Youle lode, Costerfield (Cairns et al., 2026). A: Massive stibnite breccia containing milled vein quartz fragments. B: Massive stibnite (blue) in vein surrounded by halo of fine acicular arsenopyrite (green specks in wallrock). C: Gold spots (yellow circles) in massive stibnite breccia.

The consistent paragenesis demonstrates refractory Au mineralisation predates stibnite mineralisation at Costerfield and Sunday Creek. The Re-Os pyrite-arsenopyrite ages may date the earlier gold-arsenic event, not necessarily the gold-antimony event. The absolute time difference of these events is unknown. They exploit the same structures, implying emplacement in the same stress field. Further work is required to confirm the absolute age of stibnite mineralisation at Costerfield and Sunday Creek and whether it is more closely associated with the early gold-arsenic event or the late gold-antimony event overprinting 373 Ma igneous units.

The duration of the gold-antimony mineralisation immediately precedes and overlaps with the beginning of the large middle-late Devonian magmatic event in central Victoria and Tasmania.

WHY THE MELBOURNE ZONE/SELWYN BLOCK?

Gold-antimony mineralisation in Victoria is strongly spatially correlated with the subsurface projection of the Selwyn Block. This has led many to posit the existence of uniquely antimony rich source rocks in the lower crust of the Melbourne Zone.

The gold only deposits in the Bendigo and Tabberabbera zones are hosted in deformed siliceous turbidites of the Castlemaine/Adaminaby groups. Both zones share a common basement lithology - early Cambrian tholeiitic basalt with lesser island arc lithologies e.g. Lazy Bar Andesite, Sheoak Gully Boninite. Basalt rather than the turbidites is the most likely source of the gold in the Bendigo Zone (Willman et al., 2010).

In comparison to the Bendigo Zone, the lower crust of the Melbourne Zone, the Selwyn Block, is dominated by Proterozoic rocks (Cayley et al., 2011, 2002). The bulk composition of this crust is unknown due to lack of exposure. It consists of deformed, metamorphosed mafic igneous protolith where exposed e.g. Ceres Gabbro, Corduroy Creek Gabbro .

Late Cambrian calc-alkaline volcanics with temporal and geochemical affinities to the Mount Read Volcanics occur in fault bounded windows in the Governor Fault Zone. Surface constrained interpretations from deep reflection seismic show the Cambrian volcanic rocks may persist as a widespread veneer on the lower Proterozoic crust (Cayley et al., 2011).

Large, long wavelength magnetic anomalies in the Melbourne Zone have been modelled as tabular serpentinised ophiolites beneath the turbiditic cover sequence, part of the Selwyn Block (Mclean et al., 2010). This has been confirmed by diamond drilling into a magnetic anomaly near Foster in the southern Melbourne Zone.

This diverse basement is unconformably overlain by a condensed package of Ordovician black shale – Mt Easton Shale, transitioning conformably into the turbiditic, Siluro-Devonian Murrindindi Supergroup.

Whole rock geochemistry was collected on samples from the basement and host lithologies from the Bendigo, Melbourne and Tabberabbera zones (Figure 5).

Median antimony in all lithologies from the Bendigo and Tabberabbera zones, and the Murrindindi Supergroup in the Melbourne Zone is at or below the upper crust average of 0.4 ppm (Rudnick & Gao, 2014). Median antimony in the serpentinised ophiolite intersected in the southern Melbourne Zone is 6.25 times higher than average upper crust.

No unaltered samples for the Jamieson Volcanics are available. Median antimony in similar unaltered late Cambrian calk-alkaline volcanics from the Mount Read Volcanics in Tasmania is 1.8 times higher than the upper crust average (data from Zivkovic et al., 2024). Median antimony is highest in basalts. Andesitic to dacitic volcanics contain the highest outlier antimony concentrations, with samples up to 27 ppm (> 50 times continental average).

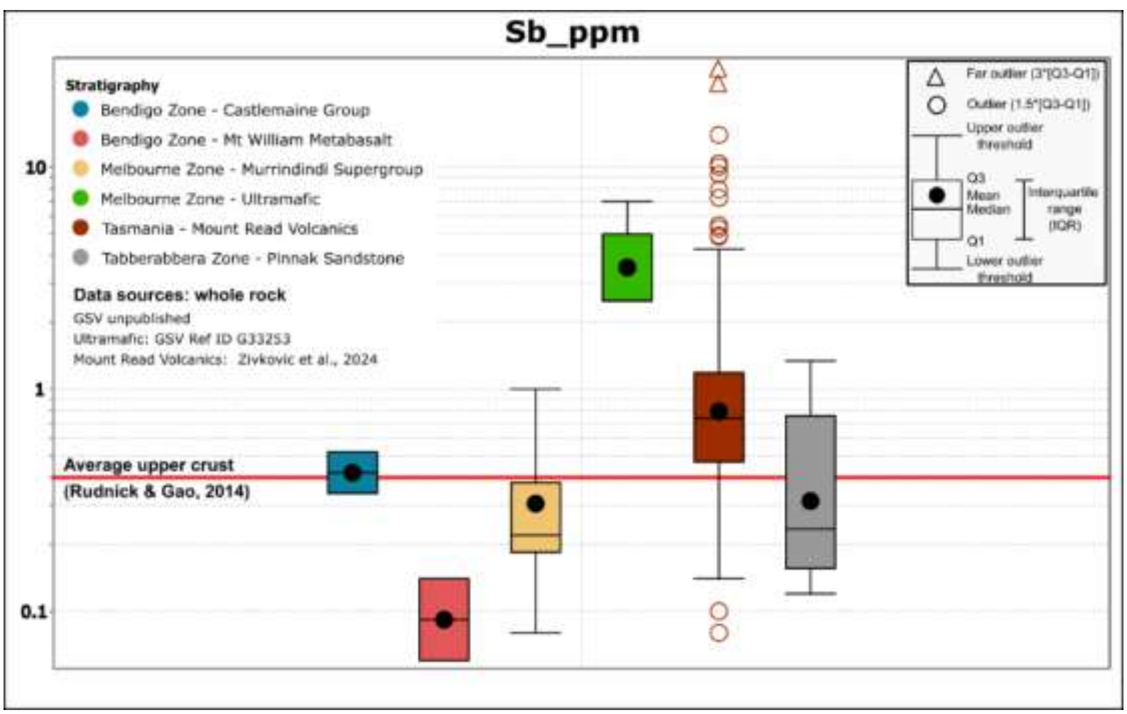

Figure 5: Antimony concentration in the source and host rocks of central Victoria.

THE DRIVER IN VICTORIA

The lower crust in the Melbourne Zone contains rocks which are inherently more antimony rich than those in the adjacent Bendigo and Tabberabbera zones. Gold and antimony must be liberated from this reservoir to be focussed into mineral deposits. The posited driver in Victoria is magmatic underplating, advective heat input and prograde metamorphism.

Boger et al. (2025) note that decompression anatexis cannot account for the volume of middle to late Devonian silicic magma in central Victoria. They posit magmatic underplating advectively contributes the additional required heat.

Platinum Group Elements (PGEs) are strongly chalcophile and can only be extracted from the mantle once melting progresses to the point that sulphur has become completely depleted (Keays, 1995). Boger et al. (2025) assert that the presence of semi-massive sulphide hosted PGEs in mafic dykes at Coopers Creek demands mantle melting extensive enough to cause sulphur depletion and PGE extraction. This melt is posited to have stalled in the lower lithosphere, adding heat adjectivally into the crust.

Advective heat caused prograde metamorphism through the greenschist-amphibolite transition. Fertile source rocks released most of their water, sulphur, gold, antimony and trace elements into metamorphic fluids. These fluids were structurally focussed to form orogenic gold systems with antimony rich epizonal levels.

Prograde metamorphism progressed past the wet solidus and metamorphic fluids fluxed silicate melting. Some of these melts fractionated to form intrusion related gold deposits. Most coalesced to form massive the siliceous batholiths and calderas that characterise the central Victorian middle-late Devonian magmatic event.

This geothermal gradient resulted in a systematic progression of metallogensis related to water, sulphur and trace element release during prograde metamorphism and finally silicate melting.

PRESERVATION

Gold-antimony deposits in Victoria are the shallow expression of vertically extensive hydrothermal systems formed between 370 and 380 million years ago in the middle to late Devonian. Geothermal, textural and fluid inclusion constraints indicate formation between 0.9 and 3 km depth at less than 250°C (Gao et al., 1995; Gao & Kwak, 1995).

Middle-late Devonian subaerial felsic volcanics including the Violet Town Volcanics, Ferny Creek Rhyodacite and the Cerberean Cauldron spatially and temporally overlap with Au-Sb mineralisation in the Melbourne and Bendigo zones. These volcanics, together with coeval rift flank conglomerates (Taggerty Subgroup) mark the paleo surface during the waning stage of the gold-antimony mineralisation in the central Victoria (VandenBerg et al., 2000).

Preservation of volcanic stratigraphy demonstrates the lack of erosion since the formation of gold-antimony mineralisation. Subaerial volcanics emplaced onto the Devonian paleosurface at Lake Mountain (1,433m) and Mount Donna Buang (1,250m) define the high plateaus in the Melbourne Zone, with over 1000m of relief above Costerfield (180m), Sunday Creek (280m) and Fosterville (170m).

Shallow mineralisation and lack of post-mineral erosion combine to affect the alluvial gold potential of the Melbourne Zone. Gold-antimony mineralisation forms in the epizonal levels of orogenic systems (Groves et al., 1998). Above this level, mineralisation typically becomes become gold poor and increasingly antimony and mercury dominated. The preservation of gold-antimony veins implies little mineralised crust has been eroded since their formation.

Historically, alluvial gold production has been used as a proxy for the primary gold endowment of a goldfield. However, the Melbourne Zone produced approximately 20,000 oz of alluvial gold, compared with approximately 12.3 million oz from the Bendigo Zone.

Carrying the logic, this disparity could be interpreted as evidence that the Melbourne Zone has limited primary, vein-hosted gold potential. The exceptional preservation of the hydrothermal system, together with the lack of significant post-mineral erosion, suggests this assumption is locally misleading. Preservation of coeval subaerial volcanic rocks confirms post-mineral erosion has been minimal, while the presence of Au–Sb veins at surface demonstrates that the upper parts of the hydrothermal systems remain intact.

Consequently, the low alluvial gold endowment of the Melbourne Zone is best explained by limited erosion rather than limited primary gold endowment. Very little mineralised material has been eroded, and the small amount that has been removed originated from the uppermost, relatively gold-poor parts of the hydrothermal system.

This implies the entire vertical extent of the middle-late Devonian orogenic systems in central Victoria remain in-situ.

REFERENCES

BOGER S.D., SCHLEGEL T.U., & KEAYS R.R., 2025. Dyke-hosted copper-nickel-platinum group element mineralisation in Victoria (Geological Survey Report No. 7), Victoria's Critical Minerals & Strategic Materials. Geological Survey of Victoria, Melbourne.

BUSH K., & HUDSON M., 2024. Sunday Creek: high-grade gold-antimony discovery in Clonbinane, Victoria, in: AIG Bulletin. Presented at the Discoveries in the Tasmanides, pp. 37–41.

CAIRNS C.P., BOGER S.D., WAUGH S.A.F., Pintér, Z., TRAVERS S.J., FARMER N., & CAYLEY R.A., 2026. Mineralisation & textures of select gold-antimony occurrences from the Melbourne Zone, central Victoria (Geological Survey Report No. 9), Victoria's Critical Minerals & Strategic Materials. Geological Survey of Victoria, Melbourne.

CAYLEY R., KORSCH R., MOORE D., COSTELLOE R., NAKAMURA A., WILLMAN C., RAWLING T., MORAND V., SKLADZIEN P., & O'SHEA P., 2011. Crustal architecture of Central Victoria: Results from the 2006 deep crustal reflection seismic survey. Aust. J. Earth Sci. - AUST J EARTH SCI 58, 113–156. https://doi.org/10.1080/08120099.2011.543151

CAYLEY R.A., TAYLOR D.H., VANDENBERG A.H.M., & MOORE D.H., 2002. Proterozoic – Early Palaeozoic rocks & the Tyennan Orogeny in central Victoria: The Selwyn Block & its tectonic implications. Aust. J. Earth Sci. 49, 225–254. https://doi.org/10.1046/j.1440-0952.2002.00921.x

COX S.F., 1995. Faulting processes at high fluid pressures: An example of fault valve behavior from the Wattle Gully Fault, Victoria, Australia. J. Geophys. Res. Solid Earth 100, 12841–12859. https://doi.org/10.1029/95JB00915

FENWICK M., 2019. Costerfield antimony goldfield. Discoveries in the Tasmanides presentation (smedg.org.au).

FU B., FAIRMAID A., & PHILLIPS D., 2009. New 40Ar/39Ar geochronology of gold deposits in central Victoria: final report. (Geological Survey Report No. 19), Gold Undercover. Geological Survey of Victoria, Melbourne.

GAO Z.L., & KWAK T.A.P., 1995. Turbidite-Hosted Gold Deposits in the Bendigo-Ballarat & Melbourne Zones, Australia. I. Geology, Mineralization, Stable Isotopes, & Implications for Exploration. Int. Geol. Rev. 37, 910–944. https://doi.org/10.1080/00206819509465433

GAO Z.L., KWAK T.A.P., CHANGKAKOTI A., HUSSEIN E., & GRAY J., 1995. Supergene ore & hypogene nonore mineralization at the Nagambie sediment-hosted gold deposit, Victoria, Australia. Econ. Geol. 90, 1747–1763. https://doi.org/10.2113/gsecongeo.90.6.1747

GROVES D.I., GOLDFARB R.J., GEBRE-MARIAM M., HAGEMANN S.G., & ROBERT F., 1998. Orogenic gold deposits: A proposed classification in the context of their crustal distribution & relationship to other gold deposit types. Ore Geol. Rev. 13, 7–27. https://doi.org/10.1016/S0169-1368(97)00012-7

HART C., 2005. Classifying, Distinguishing & Exploring for Intrusion-Related Gold Systems. The Gangue 87.

HATTORI K.H., & GUILLOT S., 2003. Volcanic fronts form as a consequence of serpentinite dehydration in the forearc mantle wedge. Geology 31, 525–528. https://doi.org/10.1130/0091-7613(2003)031%3C0525:VFFAAC%3E2.0.CO;2

HRONSKY J., 2020. Deposit-scale structural controls on orogenic gold deposits: an integrated, physical process–based hypothesis & practical targeting implications. Miner. Deposita 55. https://doi.org/10.1007/s00126-019-00918-z

JOCHUM K., & VERMA S., 1996. JOCHUM K. P. & VERMA S. P. Extreme enrichment of Sb, Tl & other trace elements in altered MORB. Chem. Geol. 130, 289-299. Chem. Geol. - CHEM GEOL 130, 289–299. https://doi.org/10.1016/0009-2541(96)00014-9

KEAYS R.R., 1995. The role of komatiitic & picritic magmatism & S-saturation in the formation of ore deposits. Picrites Komatiites Their Ore Depos. 34, 1–18. https://doi.org/10.1016/0024-4937(95)90003-9

Latheef THATHRAMPALLY A., CHAKRAVARTI R., LAFLAMME C., & OLIN P., 2025. Gold & Trace Element Release From Pyrite During Prograde Metamorphism of Carbonaceous Metapelites: Implications for Orogenic Gold Formation. Econ. Geol. https://doi.org/10.5382/econgeo.5168

MCLEAN M., MORAND V., & CAYLEY R., 2010. Gravity & magnetic modelling of crustal structure in central Victoria: What lies under the Melbourne Zone? Aust. J. Earth Sci. 57, 153–173. https://doi.org/10.1080/08120090903416245

RUDNICK R., & GAO S., 2014. Composition of the Continental Crust. Treatise Geochem. 4. https://doi.org/10.1016/B978-0-08-095975-7.00301-6

TOMKINS A.G., 2010. Windows of metamorphic sulfur liberation in the crust: Implications for gold deposit genesis. Geochim. Cosmochim. Acta 74, 3246–3259. https://doi.org/10.1016/j.gca.2010.03.003

VANDENBERG A.H.M., WILLMAN C.E., MAHER S., SIMONS B.A., CAYLEY R.A., TAYLOR D.H., MORAND V.J., MOORE D.H., & RADOJKOVIC A.M. (Eds.), 2000. The Tasman fold belt system in Victoria : geology & mineralisation of proterozoic to carboniferous rocks. Geological Survey of Victoria, Dept. of Natural Resources & Environment, East Melbourne, Vic.

WAUGH S.A.F., CREASER R.A., CAIRNS C.P., DUNCAN R.A., & CAYLEY R.A., 2024. Re-Os geochronology of Victorian mineral occurrences (Geological Survey Report No. 5), Victoria's Critical Minerals & Strategic Materials. Geological Survey of Victoria, Melbourne.

WILLMAN C.E., KORSCH R.J., MOORE D.H., CAYLEY R.A., LISITSIN V.A., RAWLING T.J., MORAND V.J., & O'SHEA P.J., 2010. Crustal-Scale Fluid Pathways & Source Rocks in the Victorian Gold Province, Australia: Insights from Deep Seismic Reflection Profiles. Econ. Geol. 105, 895–915. https://doi.org/10.2113/econgeo.105.5.895

ZIVKOVIC Z., HALLEY S., VICARY M., BAKER M., CRACKNELL M.J., & BARKER S., 2024. Whole rock lithogeochemical analysis of the Mount Read Volcanics: a new tool for geochemical exploration. Geochem. Explor. Environ. Anal. 24, geochem2024-008. https://doi.org/10.1144/geochem2024-008

SPUR GOLD PROJECT, CARGO DISTRICT, NEW SOUTH WALES: HYDROTHERMAL ALTERATION AND GOLD MINERALISATION IN A TELESCOPED PORPHYRY–EPITHERMAL SYSTEM, MACQUARIE ARC

Jessica Askew[1,2], Malai Ila'ava[1,2,3], S. Meffre[2], T. Wells[2], Y. Cajal Contreras[2], D.R. Cooke[2], and P. Duerden[1]

[1] Waratah Minerals

[2] CODES – University of Tasmania

[3] Ila'ava Lava

Key Words: Spur, Cargo, epithermal gold, hydrothermal alteration, gold mineralisation, pyrite trace elements, telescoped porphyry–epithermal system, Macquarie Arc, Molong Volcanic Belt

INTRODUCTION

The Cargo Cu–Au system, in the Molong Volcanic Belt of the Late Ordovician Macquarie Arc, comprises porphyry-style Cu–Mo mineralisation at depth and superimposed epithermal gold in the overlying volcanic wallrock, a telescoped porphyry–epithermal system in which gold is concentrated at the epithermal level. It forms the Spur Gold Project (EL5238) of Waratah Minerals Limited (ASX:WTM), 5 km west of the Cadia Valley operations in central New South Wales, over the historic Consols and Ironclad goldfields; the project is at exploration stage, with no Mineral Resource estimated. Building on the volcanic and intrusive characterisation of Askew et al. (in prep.), this contribution describes the hydrothermal alteration, gold mineralisation, and pyrite trace-element chemistry of the epithermal system and their relationship to the porphyry environment.

The highest-grade gold in the Macquarie Arc is hosted in the wallrock of porphyry and epithermal systems, as at Ridgeway, Cadia East, Cowal, and Boda, rather than within the intrusive centres that earlier exploration at Cargo targeted; Spur tests that wallrock position.

GEOLOGICAL SETTING

The Macquarie Arc is a dismembered Ordovician to earliest Silurian intra-oceanic arc, preserved as four fault-segmented volcanic belts in the eastern Lachlan Orogen and accreted to Gondwana during the Benambran Orogeny (Crawford et al., 2007; Glen et al., 2012). It contains more than 83 Moz Au and 17.2 Mt Cu (recalculated from Kreuzer et al., 2015) and evolved from basaltic–andesitic sequences to calc-alkaline and locally shoshonitic suites (Cooke et al., 2007).

At Cargo, gold is hosted by the Cargo Volcanics, a submarine succession of Fe-rich, mafic–intermediate lavas and volcaniclastic rocks (Simpson et al., 2007), intruded by the multiphase Cargo Intrusive Complex (monzodiorite to quartz monzonite, with dacite porphyries) emplaced between 471 and 466 Ma (U–Pb zircon; Askew et al., in prep.); its magmatic affinity, calc-alkaline or alkalic, is unresolved. Molybdenite Re–Os ages of 469.8–471.6 Ma and a magmatic–hydrothermal pulse at 466–467 Ma constrain the main mineralising interval. Intrusion, mineralisation, and alteration follow a northwest-trending corridor along a reactivated segment of the Molong Lineament, and the system was later offset by the Essex, Tywi, and Cothi faults.

DEPOSIT GEOLOGY

Gold at Spur occupies a near-surface epithermal corridor, the Spur Gold Corridor and the Consols Zone, in altered basalt and albitised andesite along the margins of the intrusive complex, telescoped onto porphyry-style mineralisation; geophysical and drilling data indicate several intrusive centres rather than a single porphyry. The Consols envelope exceeds 400 m (E–W), 500 m (N–S), and 600 m (vertical) and contains three intercepts of more than 200 g·m Au. Lodes are steep to subvertical (75–80% of true width); grades increase toward syn-mineral monzonite and monzodiorite contacts, whereas post-mineral dykes dilute and truncate ore.

Representative intercepts include 81 m at 2.42 g/t Au from 536 m (Consols, SPD048), 208.7 m at 1.17 g/t Au from 514 m (incl. 38 m at 3.61 g/t Au; Spur, SPRCD062), and 11 m at 10.82 g/t Au from an oxidised skarn at Spur East (SPRC002).[1]

MINERALISATION AND ALTERATION

Gold occurs in several styles: dominant epithermal stringer and lode gold in the Spur and Consols corridors, hosted in altered basalt and albitised andesite; subordinate oxidised skarn (hematite–epidote–pyrite ± magnetite) at Spur East; siliceous stockwork at Spur South; and, at depth, porphyry-style Cu–Au (chalcopyrite ± bornite in A/B veins and potassic magmatic-hydrothermal breccia) at Breccia West. The ore assemblage is pyrite-dominant, with chalcopyrite, minor bornite, and magnetite; gold occurs as free gold, inclusions in chalcopyrite, electrum, and with bismuth tellurides, silver is minor, and molybdenum increases at depth toward the porphyry (Fig. 1).

Gold occupies a multi-stage, reactivated vein sequence logged in oriented core. Early porphyry-stage quartz–magnetite (A-type) and quartz (B-type) veins are overprinted by gold-stage pyrite–chalcopyrite–gold veins with potassic selvages, with quartz–carbonate–pyrite–chalcopyrite (± Au ± bismuthinite), pyrite–quartz–carbonate–chlorite–magnetite–gold, and late-carbonate assemblages. Chlorite–pyrite crackle breccias and the potassic magmatic-hydrothermal breccia of the Breccia West Cu–Mo zone accompany the veins; the highest grades occur where vein sets intersect and early veins are reactivated.

Alteration is zoned and overprinted, intensifying from weakly propylitic distal rocks to near-complete replacement in the most proximal, mineralised units. At depth, potassic (K-feldspar–quartz) and sodic-calcic to calcic (actinolite–albite–magnetite) assemblages with a Cu–Mo signature mark the porphyry (Breccia West, Dalcoath), overprinted by phyllic (quartz–sericite–pyrite) and locally argillic alteration. Outward and upward, the wallrock carries albite and magnetite (skarn) alteration passing into propylitic (chlorite–epidote–carbonate) assemblages, with silica–hematite–pyrite stringers at the shallowest levels. The downward potassic–calcic (Cu–Mo) and upward phyllic–silica–hematite–pyrite transitions vector toward the porphyry and epithermal environments respectively.

PYRITE TRACE-ELEMENT CHEMISTRY

LA-ICP-MS mapping of pyrite (20 mounts, 32 maps) across Spur, Breccia West, and Dalcoath resolves two populations that mirror the telescoped architecture (Fig. 2; cf. Sykora et al., 2018). Porphyry-environment pyrite (Breccia West and deeper holes) is Co–Ni–Se-rich (Co ~200–1000 ppm, locally >10,000 ppm; Se 20–80 ppm) with low As (<~100 ppm), whereas epithermal-corridor pyrite (Spur; e.g. SPRCD062) is As-rich (300–1300 ppm, locally ~7600 ppm) with elevated Sb, Tl, Ag, and Au. Maps of composite grains (SPRCD062; up to ~42 ppm Au, ~7600 ppm As) show gold concentrated in As–Te–Bi-rich domains, consistent with the bismuth-telluride association seen petrographically (Fig. 3-5). This porphyry-to-epithermal trend in pyrite provides an independent geochemical vector that reinforces the alteration and vein evidence for telescoping.

GOLD DEPORTMENT – CURRENT KNOWLEDGE

Initial gold deportment work at the Spur Zone involving uXRF scanning, petrology and gravity separation with sequential leaching on the gravity tails suggests that 90 to 97% of the gold can be recovered using a gravity circuit followed by conventional leaching process. Gravity separation recovered between 15 and 45% of gold with coarse gold grains in the gravity concentrate sizing up to 688um. Similar work is underway for the Consols Zone.[1]

DISCUSSION

The alteration zonation, vein paragenesis, and pyrite chemistry record a telescoped porphyry–epithermal system developed around a multiphase intrusive complex with multiple porphyry centres (Sillitoe, 2010). Telescoping is shown by gold-stage veins overprinting porphyry-stage A/B veins, phyllic–argillic alteration overprinting the potassic core, and the porphyry-to-epithermal trend in pyrite. Porphyry-style mineralisation at depth (potassic–calcic alteration, Cu–Mo, magnetite–quartz–chalcopyrite veins; Breccia West) marks where the intrusive centres exsolved oxidised, metal-bearing magmatic fluids; gold was deposited where these fluids ascended into the epithermal environment and reacted with Fe-rich wallrock, cooling, oxidising, and sulphidising the mafic host. The alteration assemblages, vein sets, and pyrite compositions therefore vector toward both the shallow gold and the deeper porphyry centres.

Sulphur-isotope data are consistent with this model, with sulphide $\delta^{34}S$ of −9.7 to +1.9‰ (n = 163) recording a magmatic sulphur source and the most negative values consistent with epithermal-stage boiling (Askew, in prep.). Cargo is an evolving target: continued drilling and analysis refine its alteration and mineralisation framework, and the magmatic affinity of the complex and the position of the fault-offset porphyry centres remain open questions.

ACKNOWLEDGEMENTS

We thank Waratah Minerals Limited for permission to publish and for access to its drilling, assay, and geophysical datasets, and we are grateful to the Waratah Minerals geology team, whose field, logging, and technical support made this work possible. We thank the CODES team at the University of Tasmania for the analytical facilities, training, and discussion that underpin this study, and Jessica Askew warmly thanks her supervisors for their guidance and mentorship throughout her doctoral research. Exploration results are reported under the JORC Code (2012), with Mr Peter Duerden (RPGeo, AIG) as Competent Person.

[1] Intercepts reported by Waratah Minerals Limited (ASX:WTM) under the JORC Code (2012); Competent Person P. Duerden (RPGeo, AIG). Grades are length-weighted, uncut, at a 0.1 g/t Au lower cut with up to 5 m internal dilution; intervals are downhole lengths (estimated >75–80% of true width for subvertical zones). ASX:WTM releases, 2024–2026.

REFERENCES

COOKE D.R., WILSON A.J., HOUSE M.J., WOLFE R.C., WALSHE J.L., LICKFOLD V., & CRAWFORD A.J., 2007, Alkalic porphyry Au–Cu & associated mineral deposits of the Ordovician to Early Silurian Macquarie Arc, New South Wales: Australian Journal of Earth Sciences, v. 54, p. 445–463.

CRAWFORD A.J., MEFFRE S., SQUIRE R.J., BARRON L.M., & FALLOON T.J., 2007, Middle & Late Ordovician magmatic evolution of the Macquarie Arc, Lachlan Orogen, New South Wales: Australian Journal of Earth Sciences, v. 54, p. 181–214.

GLEN R.A., QUINN C.D., & COOKE D.R., 2012, The Macquarie Arc, Lachlan Orogen, New South Wales: its evolution, tectonic setting & mineral deposits: Episodes, v. 35, p. 177–186.

KREUZER O.P., MILLER A.V.M., PETERS K.J., PAYNE C., WILDMAN C., PARTINGTON G.A., PUCCIONI E., MCMAHON M.E., & ETHERIDGE M.A., 2015, Comparing prospectivity modelling results & past exploration data: A case study of porphyry Cu–Au mineral systems in the Macquarie Arc, Lachlan Fold Belt, New South Wales: Ore Geology Reviews, v. 71, p. 516–544.

REICH M., KESLER S.E., UTSUNOMIYA S., PALENIK C.S., CHRYSSOULIS S.L., & EWING R.C., 2005, Solubility of gold in arsenian pyrite: Geochimica et Cosmochimica Acta, v. 69, p. 2781–2796.

SILLITOE R.H., 2010, Porphyry copper systems: Economic Geology, v. 105, p. 3–41.

SIMPSON C.J., SCOTT R.J., CRAWFORD A.J., & MEFFRE S., 2007, Volcanology, geochemistry & structure of the Ordovician Cargo Volcanics in the Cargo–Walli region, central New South Wales: Australian Journal of Earth Sciences, v. 54, p. 273–300.

SYKORA S., COOKE D.R., MEFFRE S., STEPHANOV A.S., GARDNER K., SCOTT R., SELLEY D., & HARRIS A.C., 2018, Evolution of pyrite trace element compositions from porphyry-style & epithermal conditions at the Lihir gold deposit: Implications for ore genesis & mineral processing: Economic Geology, v. 113, p. 193–208.

FIGURES

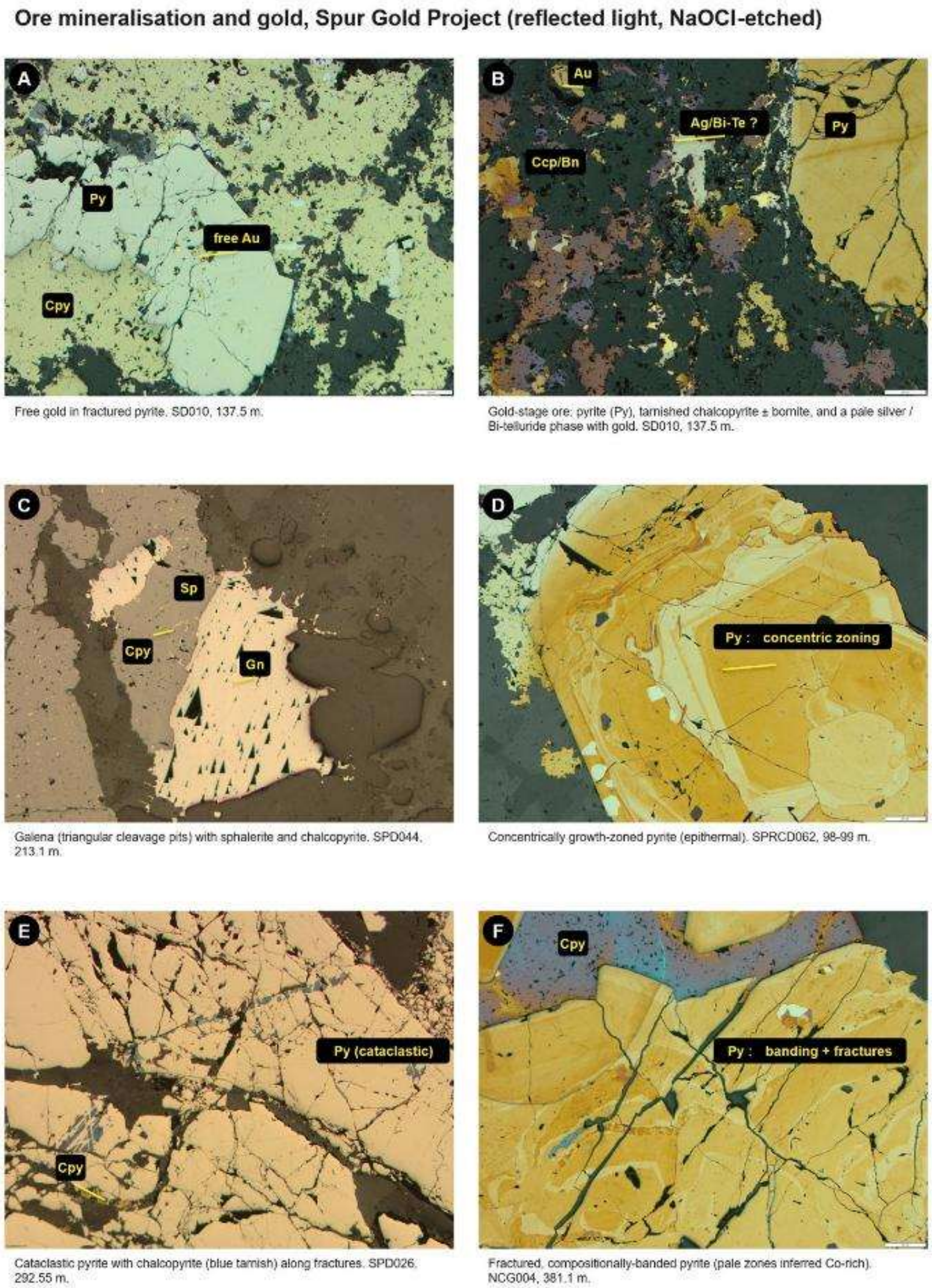

Figure 1. Ore and gold, Spur Gold Project (reflected light, NaOCl-etched): (A) free gold in fractured pyrite (SD010, 137.5 m); (B) gold-stage pyrite, chalcopyrite ± bornite, and a silver/Bi-telluride phase with gold (SD010, 137.5 m); (C) galena with sphalerite (SPD044, 213.1 m); (D) concentrically zoned epithermal pyrite (SPRCD062, 98–99 m); (E) cataclastic pyrite with fracture-controlled chalcopyrite (SPD026, 292.55 m); (F) fractured, compositionally banded pyrite (NCG004, 381.1 m). Scale bars 200 µm; identifications optical, chalcopyrite–bornite and silver/Bi-telluride phases to be confirmed by SEM-EDS.

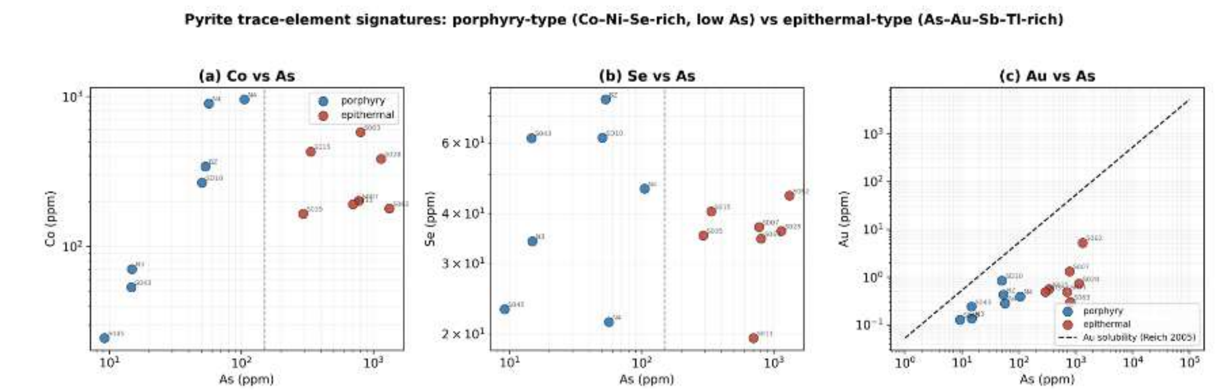

Figure 2. Pyrite trace-element discrimination (LA-ICP-MS, LADR-quantified; geometric-mean concentrations, one point per mount): (a) Co vs As, (b) Se vs As, (c) Au vs As. Porphyry-type pyrite (Co–Ni–Se-rich, low As; blue) is separated from epithermal-type pyrite (As–Au–Sb–Tl-rich; red). Dashed line in (c) is the gold solubility limit of Reich et al. (2005); nearly all pyrite plots below it, indicating lattice-bound gold.

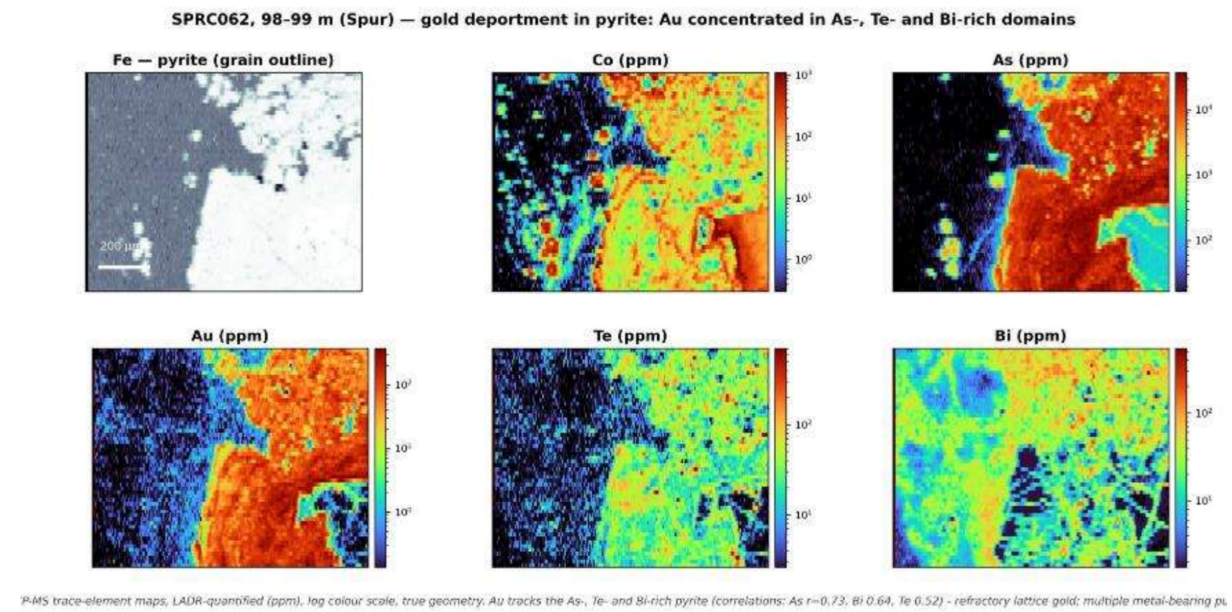

Figure 3. LA-ICP-MS maps of gold-bearing composite pyrite (SPRCD062, 98–99 m, Spur), in ppm (log colour scale). Fe outlines the pyrite; Co, As, Au, Te, and Bi show gold concentrated in As–Te–Bi-rich domains. Scale bar 200 µm.

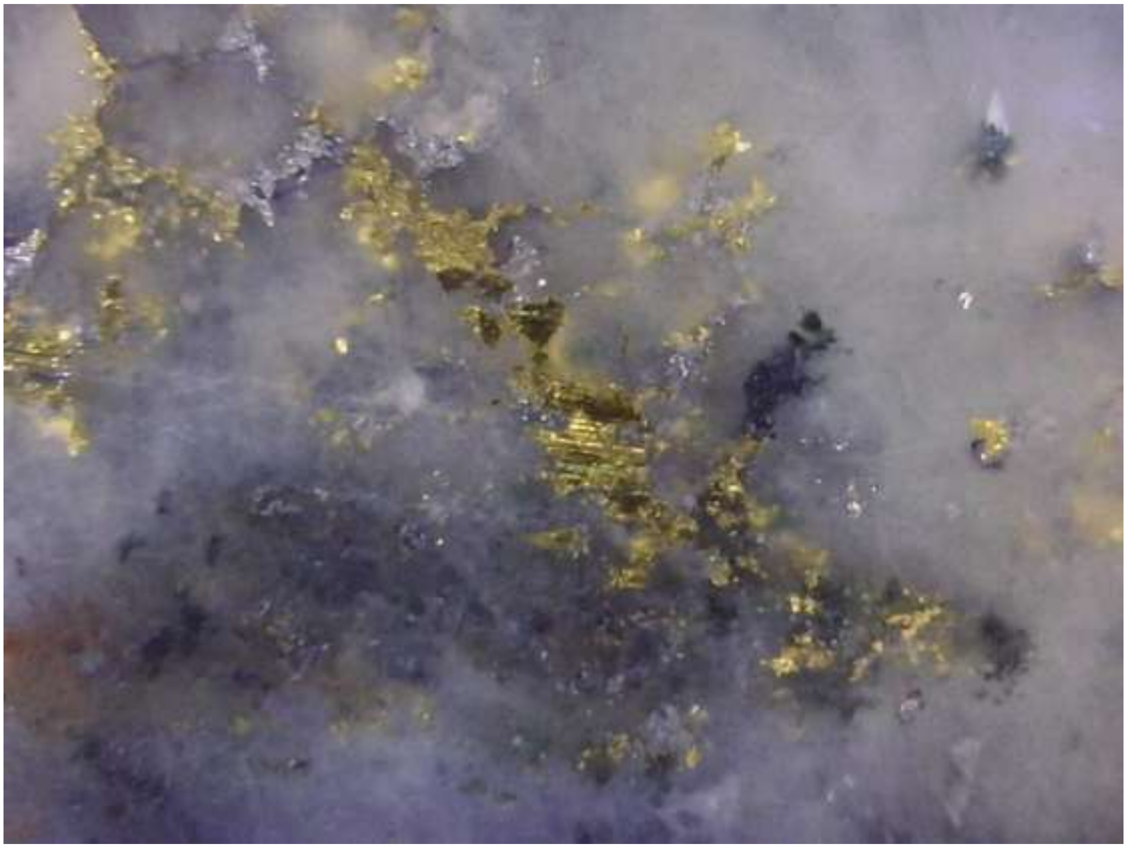

Figure 4. Visible gold, SPD021@330m FOW 10mm.

Figure 5. Visible gold with Bi-tellurides. SPD058 @ 43.3m. FOW 10mm.

LOW SULPHIDATION EPITHERMAL GOLD MINERALISATION HOSTED WITHIN THE SYBIL GRABEN, NORTH QUEENSLAND

Tav Bates, Matt Price

Sunshine Metals Ltd, Townsville, QLD, 4810.

Key Words: Sybil Graben, low sulphidation, epithermal, gold mineralisation, North Queensland

INTRODUCTION

The majority of North Queensland's well known low sulphidation epithermal gold deposits are hosted within the Drummond Basin. These include Pajingo (Osborne & Chambers, 2017), Wirralie (Fellows & Hammond, 1990), Glen Eva (Cunneen & Sillitoe, 1989) and Twin Hills (Sennit, 1991). However, a less widely known low sulphidation epithermal system is situated approximately 170kms further north within the Sybil Graben.

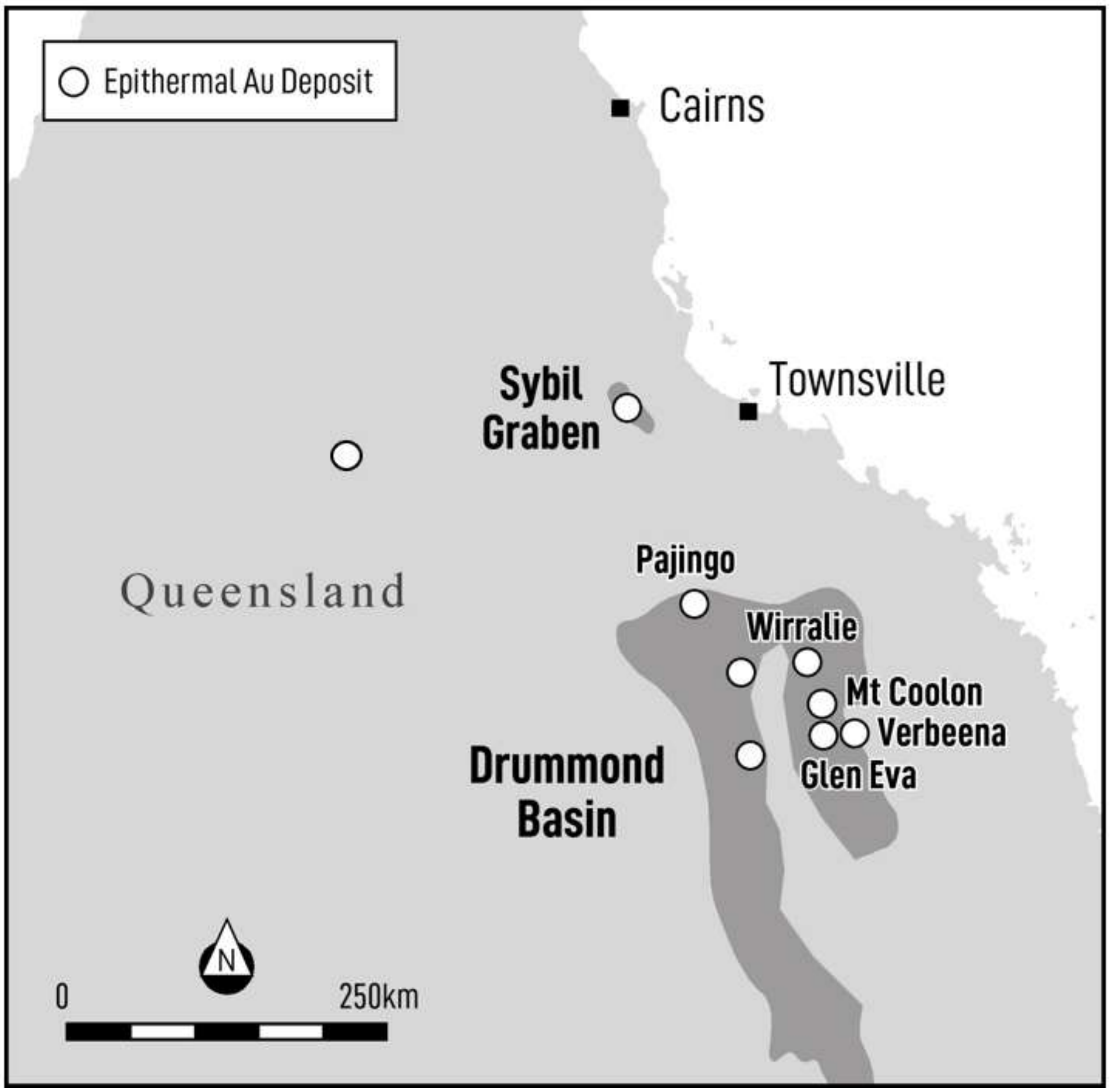

Figure 1. Location of Sybil Graben and other major North Queensland Low Sulphidation Epithermal Deposits

SYBIL GRABEN

The Sybil Graben is situated approximately 135km West of Townsville (Figure 1). The Sybil graben is a 30km long north-westerly trending extensional basin with a width of 20km in the NW and narrowing to10km at the SE.

Silurian-Devonian phyllites and slates of the Kangaroo Hills Formation, together with early Carboniferous marine sandstones, siltstones and shales of the Ruxton Formation, form the basement and floor of the graben. These units are unconformably overlain by the late Carboniferous Hells Gate Formation, a felsic volcanic succession comprising rhyolitic lavas, ignimbrites, autobreccias, crystal tuffs and volcaniclastic rocks, which forms the principal host to epithermal gold mineralisation. The early Permian Marsh Creek Formation conformably overlies the Hells Gate Formation and consists of conglomerates, sandstones and volcaniclastic sediments. Local Tertiary basalt flows have subsequently intruded the graben (Harijoko, 2001) (Figure 2).

The NW trending bounding faults of the Sybil Graben were active during deposition of the contained units. Internal to the graben, smaller scale NNW, NS and EW structures also intersect the area (Draper & Withnall, 1997). These smaller scale faults are possibly acting as linkage structures and potentially controlling the geometry of the epithermal veining.

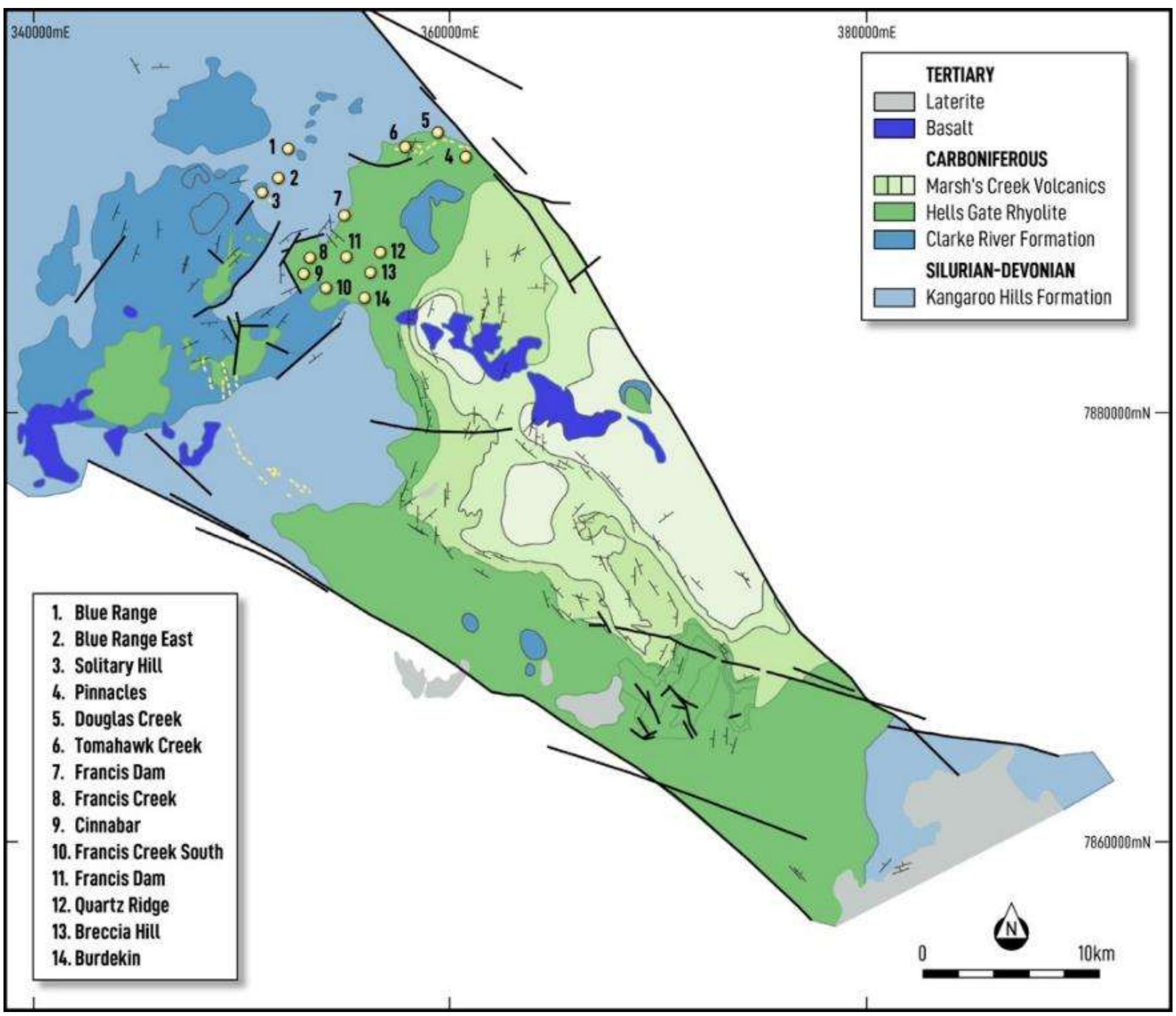

Figure 2. Simplified geology of the Sybil Graben and location of epithermal prospects

DISCOVERY & EXPLORATION HISTORY

Epithermal veining was first recognized in the northwest portion of the Sybil Graben by uranium exploration companies in the late 1970s. The majority of the project area has been explored since 1986 by A.S Marton & Associates (Aranay Holdings, Arshay Holdings, Epithermal Gold Pty Ltd & Queensland Epithermal Minerals Pty Ltd) and under multiple joint-venture arrangements with partners including Homestake, Battle Mountain, Poseidon and Cyprus Gold.

Even though the Francis Creek prospect has historically reported high-grade gold drill intersections, the epithermal mineralisation in the Sybil Graben has received only limited exploration since the 1990s. Many prospects remain poorly explored and have not been adequately drill tested. Exploration efforts have recently been renewed following Sunshine Metals' acquisition of the project in 2025.

MINERALISATION STYLES

Two main styles of epithermal mineralisation are recognised within the Sybil Graben: banded quartz-adularia veins and broad quartz stockworks hosted within intensely fractured, silica-flooded alteration zones.

Banded quartz-adularia veins are best developed at the Francis Creek prospect and are also present at Francis Creek East, Francis Creek South, Francis Dam, Blue Range, Solitary Hill, Pinnacles, Douglas Creek, Tomahawk Creek and Burdekin prospects. These veins occupy fault and/or fissure structures, range from 0.5m to 5m wide, and extend along strike for up to 1,500m.

At Quartz Ridge, intense silicification forms a broad zone of approximately 600m by 400m within a rhyolite dome-flow breccia complex in the upper Hells Gate Rhyolite sequence. This interpreted "silica cap" is cut by a stockwork of 10–50 mm quartz-pyrite-marcasite veinlets (Figure 3.).

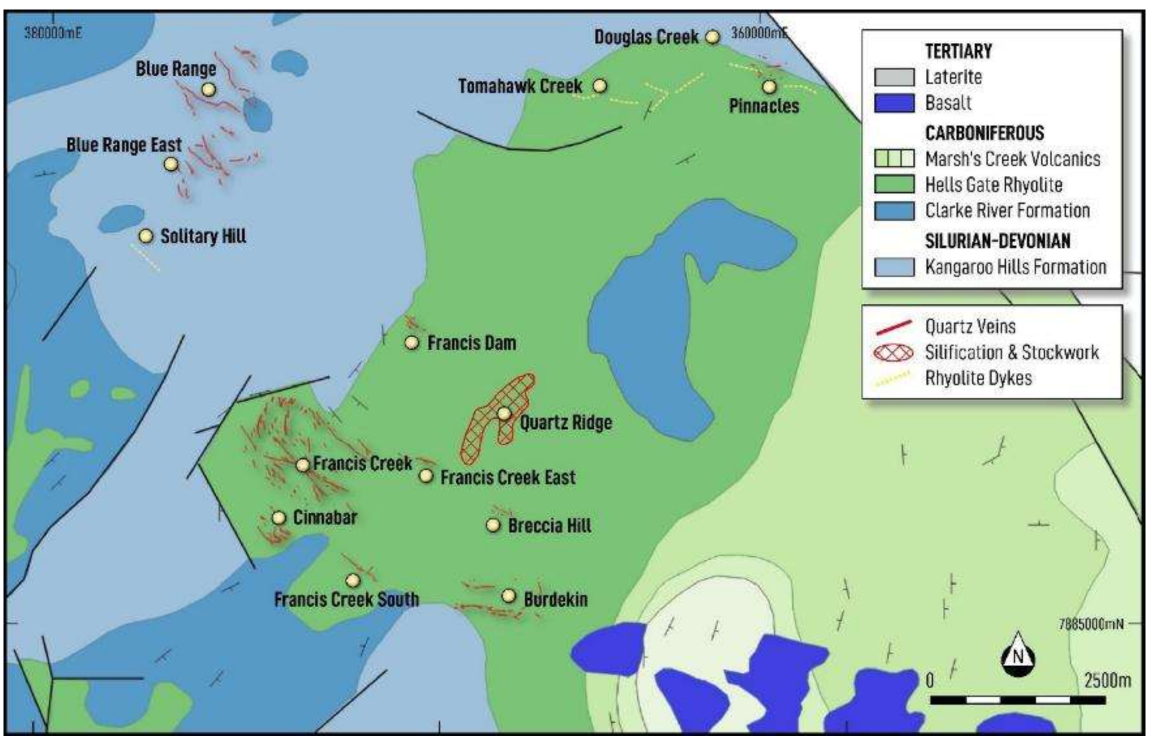

Figure 3. Simplified geology of the northwest Sybil Graben and mineralisation styles of epithermal prospects

VEIN TEXTURES

Common vein textures occurring within the quartz-adularia vein style mineralisation include banded crustiform-colloform quartz-adularia, crustiform-colloform smoky quartz & marcasite ginguro, vein breccia, silica after bladed carbonate pseudomorphs, marcasite clots, cockade and moss textures (Figure 4.).

The quartz-sulphide stockwork present at the Quartz Ridge prospect consists of dark grey comb quartz with disseminated pyrite-marcasite (Figure 4).

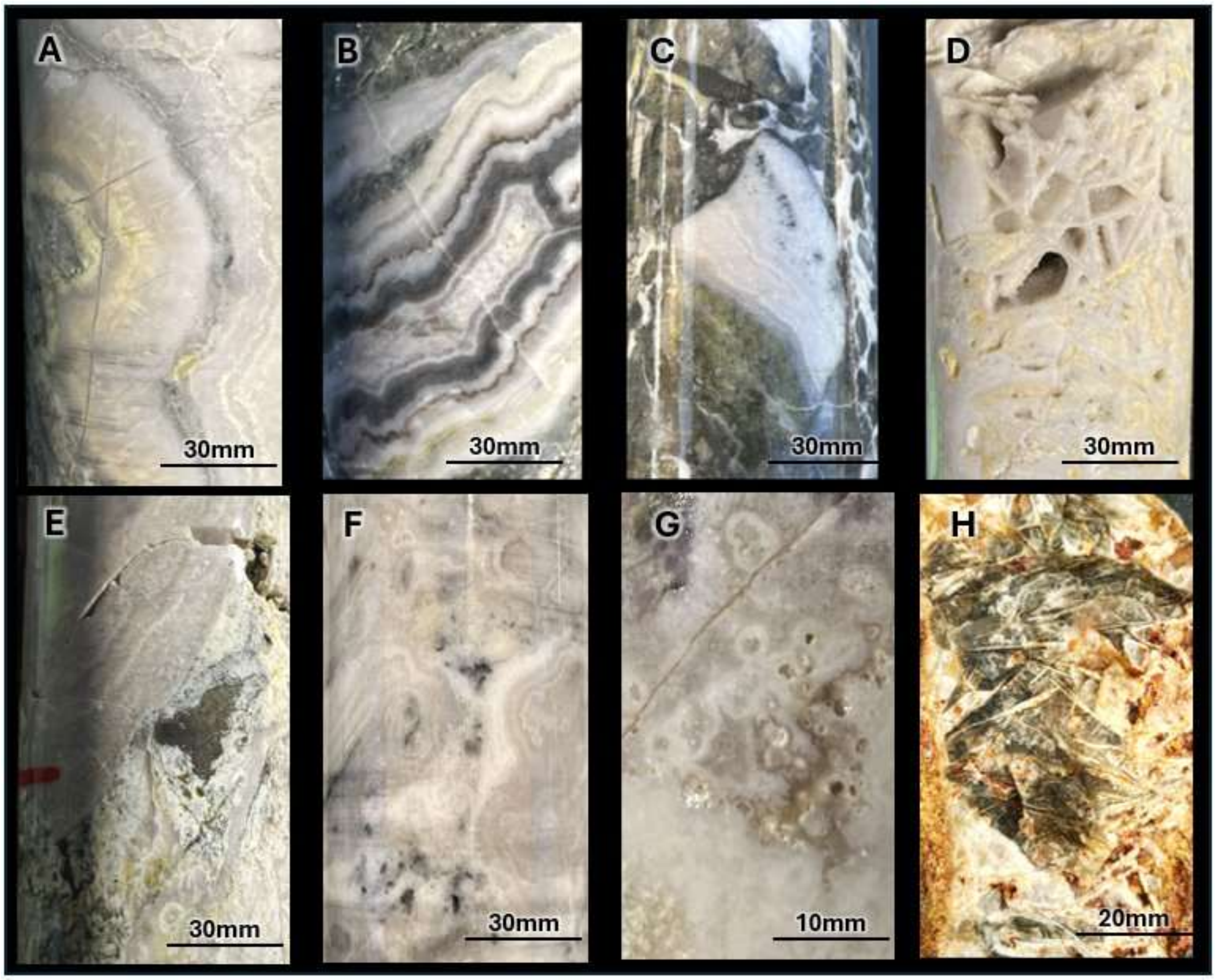

Figure 4. (A) crustiform-colloform quartz-adularia, (B) crustiform-colloform smoky quartz & marcasite ginguro, (C) vein breccia, (D) silica after bladed carbonate pseudomorphs, (E) marcasite clots, (F) cockade, (G) moss, (H) dark grey comb from Quartz Ridge stockwork.

GOLD GRADE

High grade gold is reported in drill results from the Francis Creek and Blue Range prospects and predominantly associated with crustiform-colloform quartz-adularia vein textures. While broad low grade intersections are reported from the Quartz Ridge mineralisation associated with the quartz-sulphide stockwork. Table 1 below summarises the best drill intersections from these three prospects to date.

Table 1. Best gold drill intersections from the Sybil Graben Epithermal mineralisation. SHN – Sunshine Metals Ltd, QEP – Queensland Epithermal Minerals Pty Ltd, CRL – City Resources Ltd

Year	Company	Drillhole	Intercept	Depth from	Prospect
2025	SHN	25FCDD003	4.4m @ 57.51g/t Au	23.6m	Francis Creek
2025	SHN	25FCDD012	4.5m @ 17.23g/t Au	82.5m	Francis Creek
2005	QEP	FCP05	9.0m @ 8.39g/t Au	6m	Francis Creek
2005	QEP	FCP04	3.0m @ 23.2g/t Au	6m	Francis Creek
2005	QEP	FCP17	8.0m @ 8.21g/t Au	5m	Francis Creek
2005	QEP	FCP46	6.0m @ 10.51g/t Au	7m	Francis Creek
2005	QEP	FCP07	4.0m @ 11.19g/t Au	17m	Francis Creek
2025	SHN	25FCDD007	5.2m @ 9.01g/t Au	52m	Francis Creek
2025	SHN	25FCDD010	2.8m @ 15.15g/t Au	37m	Francis Creek
1989	SHN	FSR070	68m @ 0.38g/t Au	36m	Quartz Ridge
1984	CRL	BUP105	2.0m @ 3.27g/t Au	14m	Blue Range

REFERENCES

CUNNEEN R. & SILLITOE R.H. 1989. Palaeozoic hot spring sinter in the Drummond Basin, Queensland, Australia. Economic Geology Vol 84 pp 135-142

DRAPER & WITHNALL, 1997, In: BAIN J.H.C., DRAPER J.J., North-Queensland Geology, AGSO Bulletin 240, Queensland Geology, AGSO, Department of mines & energy.

FELLOWS M.L. & HAMMOND J.M. 1990. Wirralie gold deposit in Hughs (ed) Deposits of Australia & Papua New Guinea – Monograph 14

HARIJOKO A. 2001. Epithermal Mineralisation in the Francis Creek Area, Northeast Queensland, Australia. Unpublished Master Thesis, Kyushu University.

OSBORNE D.J. & CHAMBERS C.D. 2017, Pajingo Gold deposit. In Philips (ed), Australian Ore Deposits. AusIMM. Monograph 23

SENNITT C. M., 1991. Aspects of Epithermal Gold Mineralisation, Twin Hills, Queensland, MSc Thesis, James Cook University

SHN ASX Release, 17th November 2025 'Final Diamond Drill Results".

AUSTRALIAN INTRACRATONIC COPPER-GOLD AND ALLIED DEPOSITS: A CLAN OF MINERAL SYSTEMS

Carl W. Brauhart[1], David Ian Groves[2,3]

[1] Centre for Exploration Targeting, The University of Western Australia, Robert Street Building, Crawley WA 6009, Australia

[2] Department of Geology, The University of Western Australia, Perth, Australia

[3] State Key Laboratory of Geological Processes and Mineral Resources, China University of Geosciences, 29# Xue-Yuan Road, Haidian District, Beijing 10 0 083, China

Key Words: IOCG deposits; Intracratonic Cu-Au (ICG) clan; magmatophile element groups; fertilised mantle lithosphere; cratonic sutures.

INTRODUCTION

A clan of intracratonic Cu-Au (ICG) and allied deposits is proposed to define a diverse genetic group of hydrothermal mineral systems. Although there is far too much variation in both metal budgets and deposit style to be embraced within a single ore deposit class, a sensible clan, or spectrum, of deposit types is united by several common key features.

Deposits lie in the hanging wall of cratonic sutures that mark subduction-driven collision between two cratonic blocks at least some hundreds of millions of years before mineralisation. They have a high-temperature combined geochemical signature that is distinctly magmatophile, with some combination of Cu, Au, Bi, W, Se, F, Mo, Sn, In, Pt, Pd, Ni, Co, U, and REEs. The deposits are broadly coeval with high-temperature, shallow-crustal, late- to post-orogenic felsic and minor basic magmatism with the size of that igneous footprint controlling the total endowment of the province. Broadly coeval felsic intrusions are generally not mineralised, nor do they have zoned alteration around the hot intrusions as they would have if there was a direct hydrothermal connection to mineralisation. Rather they are interpreted to be a separate manifestation of the high heat flow environment that drives the intracratonic mineral systems. Rare, coeval, potassic mantle melts, for example, lamprophyres at Olympic Dam, are interpreted as directly derived from mantle lithosphere that was fertilised by fluids related to ancient subduction. Poorly constrained hydrothermal fluids are also interpreted to be derived from fertilised mantle lithosphere, with F and Se likely critical components. Fluorine is interpreted as an important silicate solvent and ligand and Se as a marker of a distinctly oxidised fluid source.

The ICG Clan was recognised by studying five data-rich Proterozoic districts in Australia, but Andean IOCG deposits are interpreted as a less common "intracratonic-like" variation within a broader convergent tectonic cycle. A similar style of asthenospheric upwelling leading to rifting and high heat flow over fertilised mantle might explain Cu-Au mineralisation in the Cobar District.

WHY AN ICG CLAN?

The proposed ICG clan ranges in Australia from well accepted IOCG deposits (e.g., Olympic Dam), through ironstone hosted Cu-Au and Au-Cu deposits that some workers classify as IOCG (e.g., Tennant Creek field and Starra), through quartz vein hosted Cu-Au (e.g., Winu) and Au-Cu (e.g., Telfer) deposits to small Pb-dominated (e.g., Abra) and Zn-dominated (e.g., Prairie Downs) deposits with minor Cu and Au.

IOCG deposits comprise the only widely recognised ore deposit class amongst this proposed clan, notwithstanding ongoing debate about which deposits qualify as members and the source of their metal endowment (Groves et al., 2010; Skirrow, 2022).

Quartz vein hosted deposits like Telfer (Goellnicht et al., 1989; Rowins et al., 1997) and Abra (Pirajno et al., 2016), do not fit traditional subduction-related ore deposit models despite many superficial similarities. Mineral systems models for VMS, porphyry Cu, epithermal, skarn, granite-related Sn-W, orogenic Au, and foreland basin Pb-Zn deposits all fit into an elegant subduction-related paradigm that explains their progressive development through time and space (Groves and Santosh, 2023). A similar, holistic understanding of Cu-Au and related deposits in intracratonic settings has yet to be properly articulated. From a descriptive point of view, placing quartz-vein hosted ICG deposits into traditional ore deposit pigeonholes is, at least partially, valid. Many ICG deposits have more descriptive features in common with traditional ore deposit classes than they do with other members of the ICG clan. However, their tectonic setting and relationship with coeval felsic intrusions are not the same For example, a quartz vein hosted Au-Cu deposit like Telfer has been described as orogenic (Rowins et al., 1997) and intrusion related Au (Goellnicht et al., 1989; Schindler et al., 2016) but it doesn't fit either of these subduction-related models because the coeval, but barren, Crofton Suite granites are preceded by more than a billion years of intracratonic igneous and sedimentary strata. Such conundrums lead to proposals like 'Telfer-style'. At the Pb-Zn end of the ICG spectrum, deposits like Abra have long proved problematic to classify. It has variously been described as SHMS or stratiform Cu (Vogt and Stumpfl, 1987), SHMS, but with VMS and IOCG characteristics (Pirajno et al., 2016), VMS (Boddington, 1990), intrusion-related breccia pipe (Pirajno et al., 2009), and epithermal (Cooper et al., 1998; McInerney et al., 2019). The variety of interpretations for Abra is not the product of poor-quality observations. Abra shares many common descriptive criteria with each of these classes, but the observations have not been integrated into a rigorous mineral systems model.

It is suggested that confusion surrounding Cu-Au deposits in intracratonic settings can be resolved by starting with a genetic model that unites a whole clan of apparently disparate deposits into a single paradigm that embraces tectonic setting, lithosphere-scale structural control, metals derived from pre-fertilised mantle lithosphere (with likely additions from crustal leaching), and a heat source from asthenosphere upwelling to drive both the hydrothermal system and coeval intracratonic felsic magmatism. It is similar in scope to magmatic-hydrothermal deposits in subduction related settings or the clan of sedimentary basin hosted base-metal deposits. Within this framework, IOCG is the only existing mineral system or class that should be maintained. Suitable descriptive ore deposit models for mineralisation in the Paterson and Capricorn Provinces of Western Australia do not yet exist, contributing to various failed attempts to place them in conventional, subduction-related classes. At this stage, it is considered unwise to define new deposit classes until a critical mass of similar deposits have been recognised and properly documented.

KEY FEATURES OF THE CLAN

Australia has two IOCG provinces that are widely recognised in the literature (Gawler and Cloncurry), a disputed IOCG province at Tennant Creek, as well as quartz-vein hosted members of the proposed ICG clan in the Paterson and Capricorn Provinces (Fig. 1). The regional geology of each province is well understood after many decades of systematic geological mapping by state and federal government agencies, with that mapping supported by extensive U-Pb in zircon dating, direct isotopic dating of mineralisation, Sm-Nd and Lu-Hf

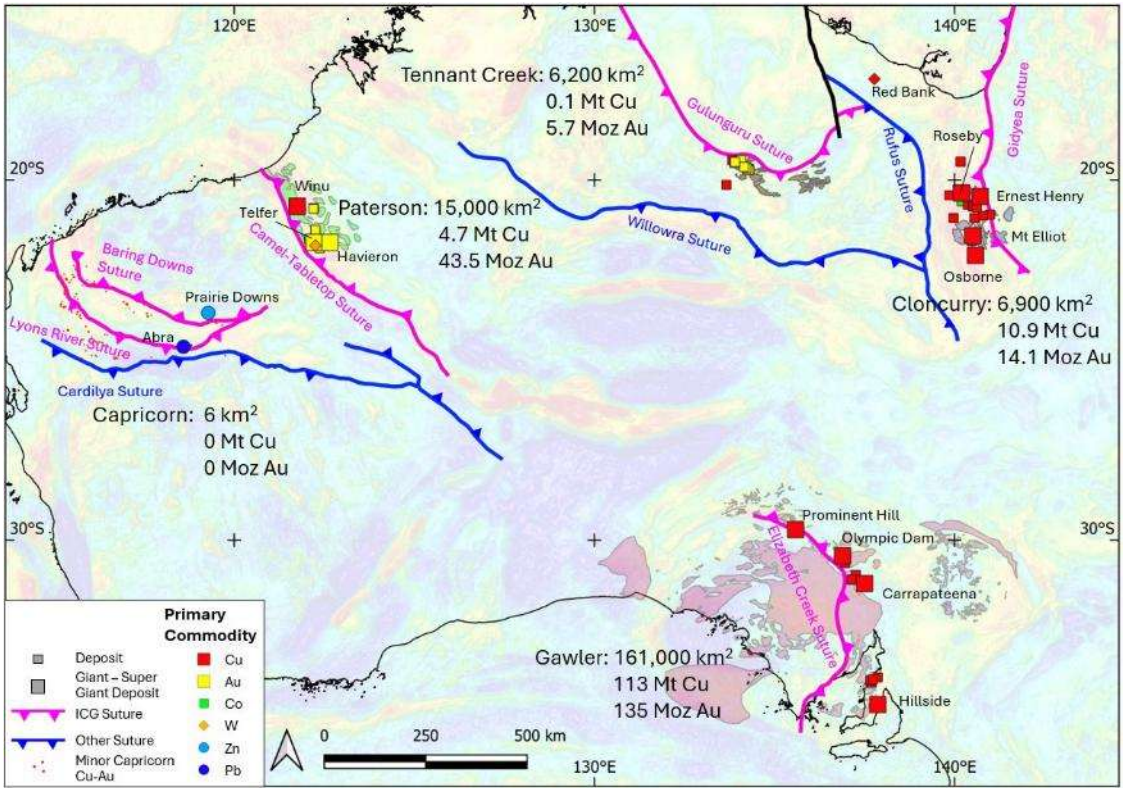

Fig. 1. Significant mineral deposits in five Australian ICG provinces in relation to coeval , largely felsic intracratonic magmatism and ancient crustal sutures. Red Bank explained in the text. Location and dip of cratonic sutures from Johnson et al. (2013); Skirrow et al. (2018); Curtis and Thiel (2019); Jiang et al. (2022); Martin et al. (2022); Doublier and Korsch (2024); Korsch et al. (2024).

isotope data, nationwide aeromagnetic, radiometric and gravity surveys, and province-scale seismic reflection and magneto telluric surveys.

Ore Textures

Variations in ore textures along the ICG spectrum range from milled breccia in IOCG *sensu stricto* deposits of Groves et al., (2010), to less energetic breccias and shear zones in smaller IOCG deposits, to disseminated and lesser semi-massive sulfides with abundant quartz-sulfide veins in deposits like Telfer, to crustiform quartz sulphide veins and massive base-metal sulphides at Abra and Prairie Downs.

Ore and pathfinder element geochemistry

There is a broad range of metal signatures for samples in the OSNACA database from the five Australian ICG provinces and publicly available data for Havieron and Winu, but five key elements; Cu-Au-Bi-W-Se are common to most signatures. Mo, In, and Sn also feature prominently across the range of ICG signatures, and are interpreted as an extension of the main Cu-Au-Bi-W-Se signature . A subset of large IOCG deposits have granophile La and U enrichments, whereas a partly overlapping subset have enrichments in an ‘ultramafic’ suite of elements that includes Co-Ni-Pd-Pt.

Endowment

Grade-tonnage plots for Cu and Au (Fig. 2; Minex Consulting unpublished data) show that Olympic Dam is easily the largest accumulation of both Cu and Au in the clan. Even without Olympic Dam, remaining Gawler deposits have the highest Cu and second largest Au endowment of the five provinces. The largest Cu and Au endowments are with the largest igneous province, the Gawler Province, versus trivial endowments of Cu and Au in the Capricorn Province with its 6 km^2 of Tangadee Rhyolite outcrop.

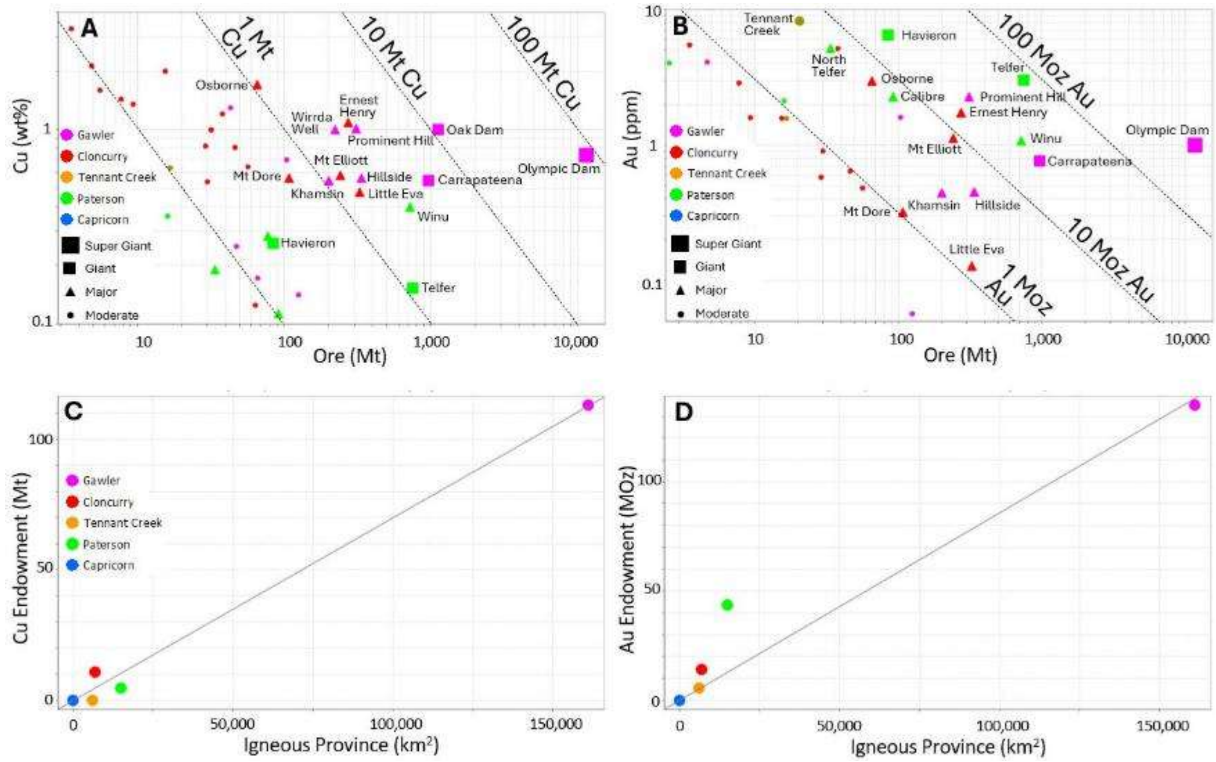

Fig. 2. (A) Tonnes versus grade for Cu endowment of ICG deposits. (B) Tonnes versus grade for Au endowment of ICG deposits. (C) Total Cu endowment versus coeval Igneous Province area. (D) Total Au endowment versus coeval Igneous Province area.

Tectono-stratigraphy

Regional tectono-stratigraphic columns for the five main ICG Provinces recognised in Australia (Fig. 3) include evidence for ancient underlying lithosphere (inherited zircons), the timing of collisions that are marked by cratonic sutures, and key elements of strata exposed at surface or intersected by drilling. Of note are ages for cratonic sutures shown on Figure 1, all of which precede their respective ICG mineral systems by hundreds of millions of years. The most important part of each tectono-stratigraphic column is intracratonic magmatism which is highlighted bright yellow in Figure 3. Each of these igneous events is broadly coeval with local ICG deposits as constrained by direct isotopic dating of that mineralisation (Fig. 3). Figure 1 shows the areal extent and location of coeval intracratonic magmatism with respect to important ore systems and ancient cratonic sutures. Critically, all major ICG deposits are in the hanging wall of those sutures, mostly within 50 km. There does not appear to be a strong relationship between deposit size and distance from suture within that fertile band.

Igneous lithogeochemistry

Lithogeochemical data for broadly coeval felsic units from the five major ICG provinces all have flat Heavy Rare Earth Element (HREE) profiles which indicate shallow crustal melting in the absence of garnet or amphibole (Takahashi, 1986). The most likely mechanism to trigger widespread shallow melting in an intracratonic setting is an asthenosphere upwelling that thins and extends the crust in a similar way to that invoked for the Gawler Craton by Skirrow et al.

(2018). Most granites in Australia have more depleted HREE profiles related to melt sources deeper in the crust in subduction-related tectonic settings.

ICG MODEL

Key attributes of a genetic model (Fig. 4) that can explain the common features of the ICG clan are:

- Establishment of a crustal suture at least some hundreds of millions of years earlier than an ICG mineralisation event, via subduction-related collision of two cratonic blocks. The suture is a permanent trans-lithospheric structural corridor that focuses later hydrothermal fluids and potassic magmas generated from fertilised mantle lithosphere.
- Coeval intracratonic felsic magmatism, commonly with a subordinate basic component, is interpreted to represent another manifestation of the very high heat flow environment necessary to drive the ICG mineral system. Shallow crustal igneous rocks necessarily form during the same intracratonic tectonic event, but they play no direct role in generating ore fluids.
- Thermal plumes related to asthenosphere uprise are the most likely mechanism to explain the very high heat flow required to move metals and ligands from fertilised mantle lithosphere to the upper crust. There is a large gap in research that is required to properly constrain the physio-chemical properties of such a fluid. Samples are rare and the mantle can never be mapped directly. Nevertheless, it is argued that there are sufficient data on the composition of fertilised mantle, and composition of IOCG endmember mineralisation and fluids, to make educated assumptions about what some of the critical features of the endmember fluid must be. These critical features include that the fluid be:
    - silica-undersaturated;
    - F- and Se-rich, and
    - generated by mantle devolatilisation with a possible input from small volume melting of fertilised ultramafic rock
- Deposit morphology and metal budgets vary widely according to how direct hydrothermal fluid flow is from deep mantle source to mid- to upper-crustal trap site. Large IOCG deposits are interpreted to have the most direct link to metal source in that they most faithfully reflect the interpreted metal signature of a fertilised mantle source, are dominated by milled hydrothermal breccias in vertical pipes, are F-rich and are accompanied by the largest intracontinental igneous provinces. Abra and Prairie Downs type Pb and/or Zn deposits have distinctly ICG metal signatures, but they have subeconomic Cu-Au tenor and are accompanied by the smallest intracontinental igneous footprints.
- Potassic mafic-ultramafic rocks derived from the fertilised mantle source, like lamprophyres, are rarely exposed at the same level as ICG deposits. However, lamprophyre dykes at Olympic Dam are regarded as further evidence of the direct link between fertilised mantle lithosphere and ICG deposits.

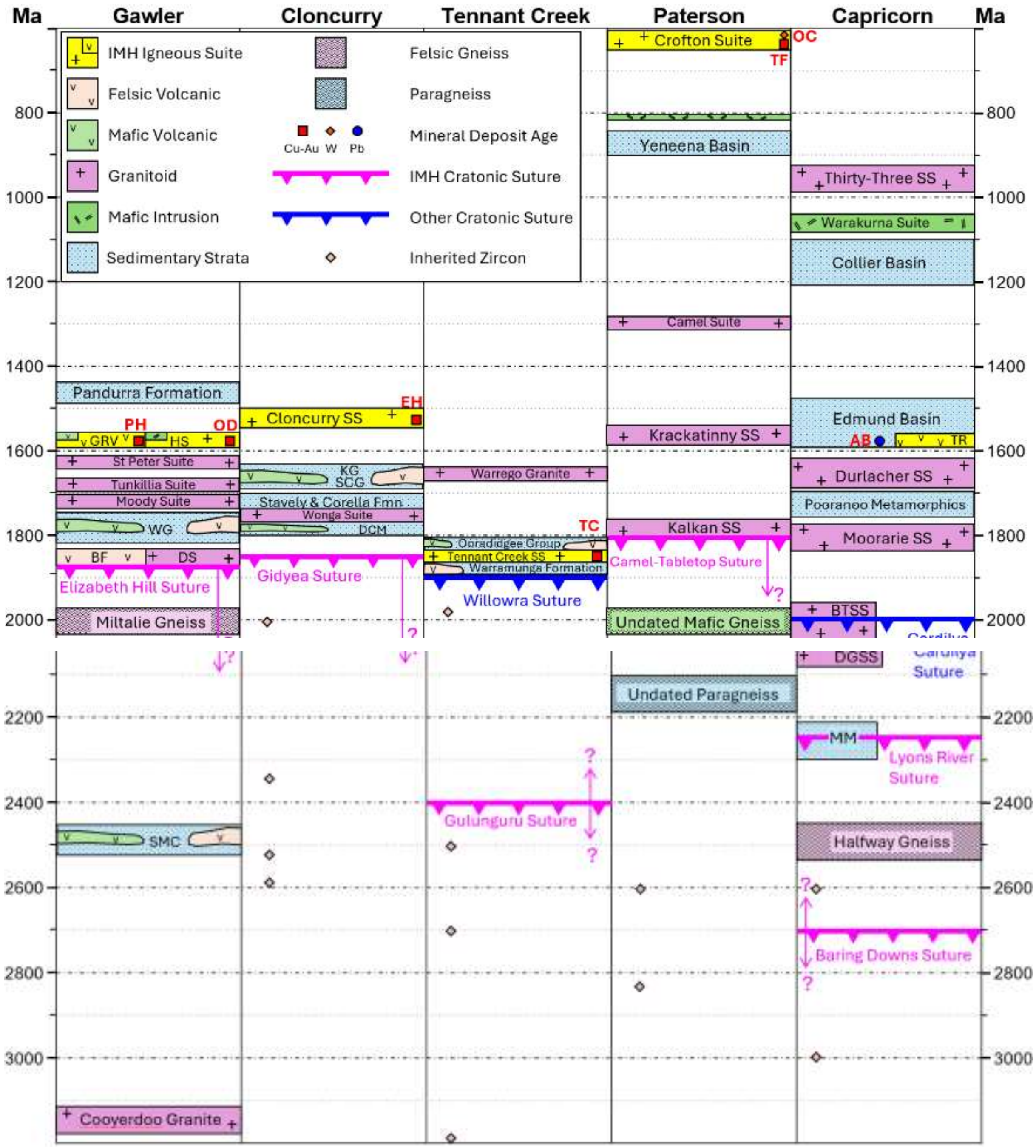

Fig. 3. Tectono- stratigraphic framework for the five major ICG provinces in Australia. Cratonic sutures interpreted to be critical to the development of younger ICG provinces are highlighted in bold magenta. Igneous strata associated with each ICG mineral system are highlighted yellow, and key mineral deposit ages are highlighted in red. References for cratonic sutures are as for Figure 1. Geochronology – see references in Brauhart and Groves (2026) Stratigraphic Abbreviations: BTSS = Betubba Super Suite, DGSS = Dalgaranga Super Suite, GRV = Gawler Range Volcanics, HS = Hiltaba Suite, KG = Kurilla Group, MM = Moogie Metamorphics, SCG = Soldiers Cap Group, SMC = Sleaford and Mulgathing Complexes. Ore Deposit Abbreviations: AB = Abra, EH = Ernest Henry, OC = O'Callaghans, OD = Olympic Dam, PH = Prominent Hill, TC = Tennant Creek Field, TF = Telfer.

ICG DEPOSITS IN THE TASMANIDES?

The Andean arc-hosted subset of IOCG deposits (Sillitoe, 2003; Skirrow, 2022) are also recognised as IOCG *sensu stricto* by Groves et al. (2010), and whole rock geochemical data (Sillitoe 2003), reveal the same style of element enrichments as for Australian ICG Provinces. However, because they are demonstrably within a subduction-related convergent margin, and therefore not intracratonic, it is problematic to include them in the ICG clan. It is proposed that the key to resolving this apparent conundrum is a short-lived tectonic setting akin to asthenospheric upwelling in an intracratonic setting, within a longer-lived convergent setting. Richards et al (2017) propose a model for Andean IOCG mineral systems where subduction stalled owing to slab steepening, leading to back-arc extension and asthenosphere upwelling creating the necessary anomalously high heat flow, shallow crustal melting and extraction of metal from recently fertilised mantle lithosphere.

The enigmatic Cobar Cu-Au deposits have long defied classification (Stegman, 2001),but may be analogous to Andean IOCG deposits where ICG mineralisation formed during an "intracratonic anomaly" within an overall subduction cycle. The Cobar Basin is an intracratonic basin that formed late in the convergent margin history of the Lachlan Fold Belt in the hangingwall to the west-dipping Gilmore Suture (Venkataramani et al., 2016; Fig. 5). Basement Silurian Granites have fractionated HREE profiles, but felsic volcanic rocks in the Cobar Basin and nearby Devonian granites north and south of the Cobar Basin have weakly fractionated to flat HREE profiles. The OSNACA database only has five samples from the Cobar District but three samples from Chesney have high Cu-Au-Bi-Se-W with supporting elevated In and Mo which perfectly matches the ICG metal signature. Two samples from Endeavour contain unusually high Cu-Au-Se-Bi for conventional sedimentary basin hosted Pb-Zn mineralisation.

Many questions remain to be resolved, including evidence for F-rich fluids or other indications of mantle-derived fluids, whether asthenospheric upwelling explains contemporaneous felsic magmatism, and gathering further consistent multielement data for ore samples from Cobar District deposits. However, it is hoped that the ICG paradigm provides a new perspective that helps advance research on the genesis of Cobar deposits.

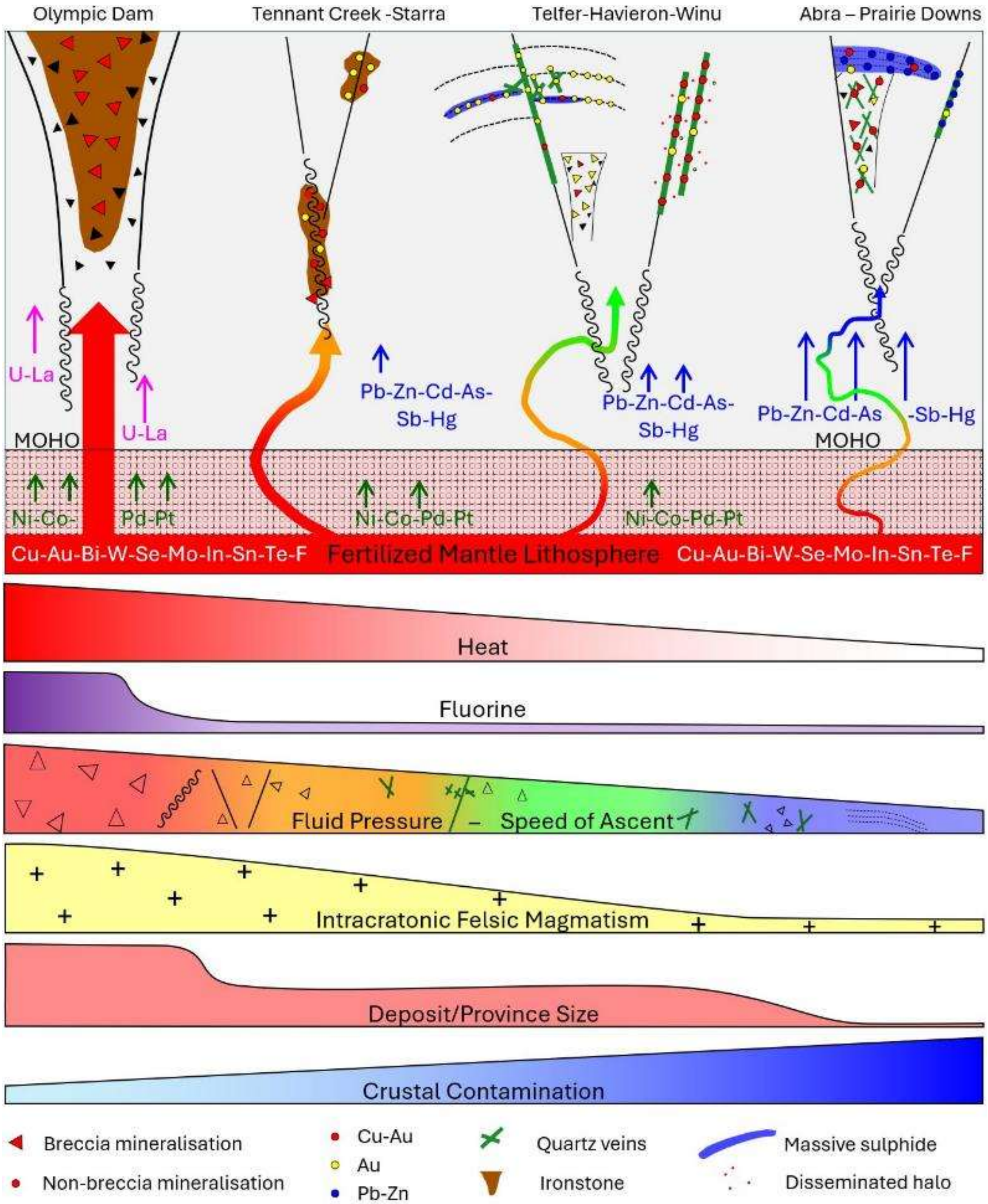

Fig. 4. Schematic illustration of each element of the ICG spectrum. Heat is the master variable which controls the amount of F^- in the ore fluid, fluid pressure and the resultant ore textures, the size of the intracratonic felsic igneous province, the endowment of the ICG province and the degree to which the original fertilised mantle lithosphere signature is contaminated by crustal metal reservoirs.

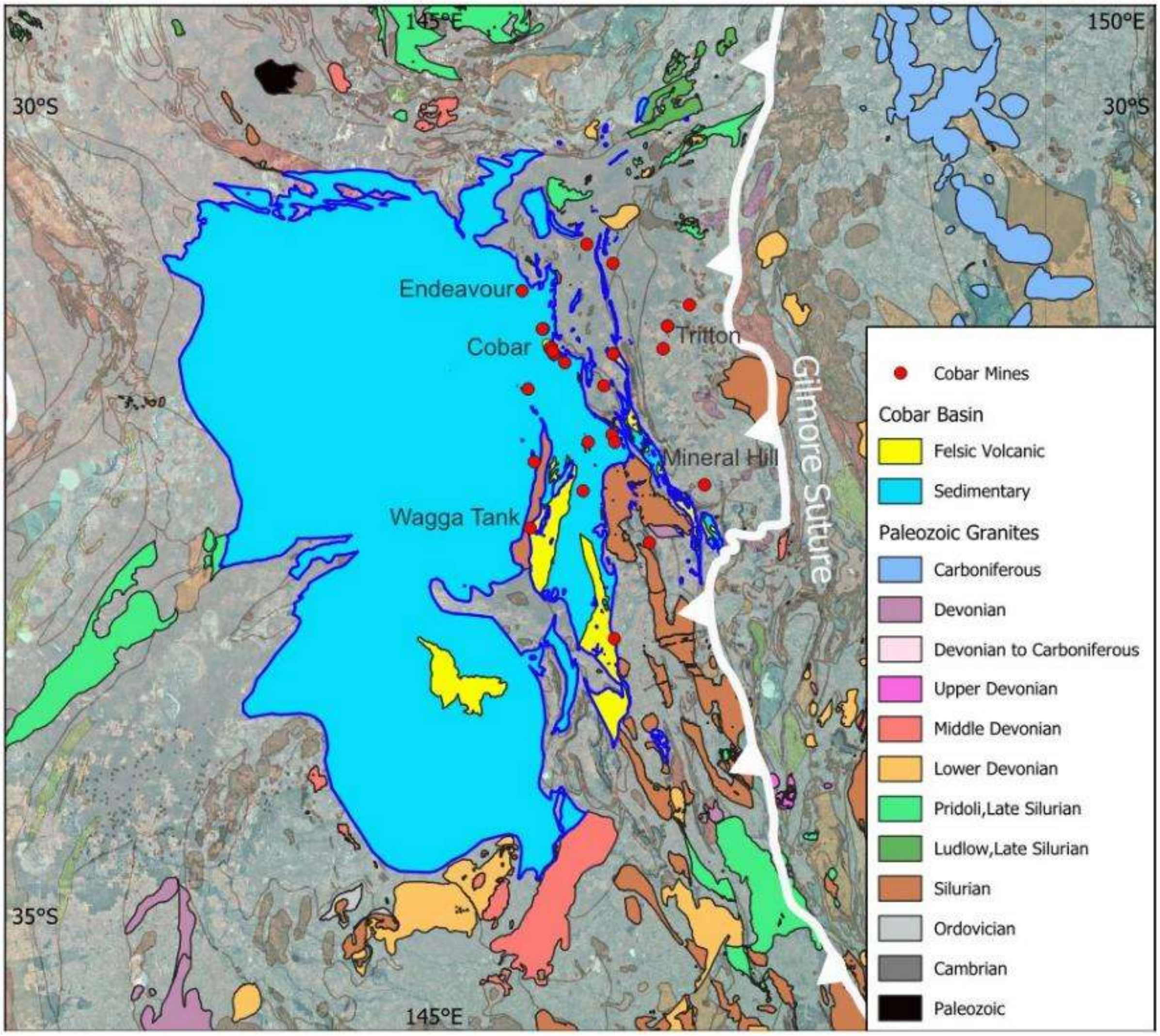

Fig. 5. Cobar Basin and Cobar Mineral Field with respect to the Gilmore Suture and ages of granite intrusions.

REFERENCES

BODDINGTON T. D. M. 1990. Abra lead–silver–copper–gold deposit. In: HUGHES F. E., ed., Mineral deposits of Australia & Papua New Guinea, Volume Monograph 14, Australasian Institute of Mining & Metallurgy, 659–664.

BRAUHART C. W. & GROVES D. I. 2026. Australian intracratonic copper-gold & allied deposits: A clan of mineral systems. Gondwana Research 149, 158-182.

COOPER R. W., LANGFORD R. L. & PIRAJNO F. 1998. Mineral occurrences & exploration potential of the Bangemall Basin. Western Australia Geological Survey, 42 pp.

GOELLNICHT N. M., GROVES D. I., MCNAUGHTON N. J., & DIMO G. 1989. An Epigenetic Origin for the Telfer Gold Deposit, Western Australia. In: KEAYS R. R., RAMSAY W. R. H., & GROVES D. I., eds., The Geology of Gold Deposits: The Perspective in 1988. Monograph 6, Society of Economic Geologists, 151-167.

GROVES D. I., BIERLEIN F. P., MEINERT L. D. & HITZMAN M. W. 2010. Iron Oxide Copper-Gold (IOCG) Deposits through Earth History: Implications for Origin, Lithospheric Setting & Distinction from Other Epigenetic Iron Oxide Deposits. Economic Geology 105, 641-654.

GROVES D. I. & SANTOSH M. 2023. Mineral Systems, Earth Evolution & Global Metallogeny. Elsevier, 251 pp.

MCINERNEY M., MUTTON A. J. & PETERS W. S. 2019. COPPER-LEAD-ZINC: Abra lead-silver-copper-gold deposit, Western Australia: a geophysical case history. ASEG Extended Abstracts 1994, no. 1, 119-132.

PIRAJNO F., HELL A., THORNE A. M. & CUTTEN H. N. 2009. The Abra deposit: a breccia-pipe polymetallic mineral system in the Edmund Basin, Capricorn Orogen: implications for mineral exploration. Geological Survey of Western Australia Record 2009/2, 31-33.

PIRAJNO F., MERNAGH T. P., HUSTON D., CREASER R. A. & SELTMANN R. 2016. The Mesoproterozoic Abra polymetallic sedimentary rock-hosted mineral deposit, Edmund Basin, Western Australia. Ore Geology Reviews 76, 442-462.

RICHARDS J. P., LÓPEZ G. P., ZHU J.-J., CREASER R. A., LOCOCK A. J. & MUMIN A. H. 2017. Contrasting Tectonic Settings & Sulfur Contents of Magmas Associated with Cretaceous Porphyry Cu ± Mo ± Au & Intrusion-Related Iron Oxide Cu-Au Deposits in Northern Chile. Economic Geology 112, 295-318.

ROWINS S. M., GROVES D. I., MCNAUGHTON N. J., PALMER M. R. & ELDRIDGE C. S. 1997. A reinterpretation of the role of granitoids in the genesis of Neoproterozoic gold mineralization in the Telfer Dome, Western Australia. Economic Geology 92, 133-160.

SCHINDLER C., HAGEMANN S. G., BANKS D., MERNAGH T. & HARRIS A. C. 2016. Magmatic Hydrothermal Fluids at the Sedimentary Rock-Hosted, Intrusion-Related Telfer Gold-Copper Deposit, Paterson Orogen, Western Australia: Pressure-Temperature-Composition Constraints on the Ore-Forming Fluids. Economic Geology 111, 1099-1126.

SILLITOE R. H. 2003. Iron oxide-copper-gold deposits: an Andean view. Mineralium Deposita 38, 787-812.

SKIRROW R. G. 2022. Iron oxide copper-gold (IOCG) deposits – A review (part 1): Settings, mineralogy, ore geochemistry & classification. Ore Geology Reviews 140.

SKIRROW R. G., VAN DER WIELEN S. E., CHAMPION D. C., CZARNOTA K. & THIEL S. 2018. Lithospheric Architecture & Mantle Metasomatism Linked to Iron Oxide Cu-Au Ore Formation: Multidisciplinary Evidence from the Olympic Dam Region, South Australia. Geochemistry, Geophysics, Geosystems 19, 2673-2705.

STEGMAN C. L. 2001. Cobar Deposits: Still Defying Classification!. SEG Discovery 44, 1-26.

TAKAHASHI E. 1986. Melting of dry peridotite KLB-1 up to 14 GPa: implications on the origin of peridotitic upper mantle. Journal of Geophysical Research 91, 9367-9382.

VENKATARAMANI D., MUSGRAVE R. & BOUTELIER D. 2016. Understanding the 3D structure of the Gilmore Fault Zone through geophysical modelling: implications for Lachlan tectonic reconstructions. ASEG Extended Abstracts 2016 no. 1, 1-6.

VOGT J. H. & STUMPFL E. F. 1987. Abra; a strata-bound Pb-Cu-Ba mineralization in the Bangemall Basin, Western Australia. Economic Geology 82, 805-825.

CONTINUING TO EXPLORE THE COWAL GOLD CORRIDOR, HOW TO UNCOVER MINERALISATION AFTER 20 YEARS OF OPERATIONS

Lachlan Burrows, Matthew Green, Dianna Villanueva, Daniela Gaibor, Hamish Watson, Timothy Stever, Britney Russell

Evolution Mining (Cowal) Pty Ltd

Key Words: epithermal, Cowal, E41, E42, E46, GR, GRE46

INTRODUCTION

The Cowal Gold Operation is located approximately 350 km west of Sydney and 40 km north-east of West Wyalong in central New South Wales, Australia. Cowal is 100% Evolution Mining owned comprising both open pit and underground mining. Open pit mining commenced in 2005, processing in 2006, with underground production commencing in 2023. Between 2006 and 2026, over 5 Moz of gold has been produced at Cowal. The operation will continue to exploit different open pit and underground ore bodies, with continued resource growth supporting operations to 2042.

The operation is situated within the Junee–Narromine Belt, the westernmost belt of the Macquarie Arc, an Ordovician to early Silurian intra-oceanic volcanic arc preserved within the Eastern Lachlan Orogen. The Macquarie Arc hosts several of Australia's largest gold and copper-gold deposits, including Cowal, Cadia and Northparkes (Figure 1A).

Gold mineralisation at Cowal is classified as epithermal and is hosted within the Cowal Igneous Complex (CIC), and forms within a 15 km long and 3 km wide NS corridor termed the Gold Corridor. Gold mineralisation formed between approximately 455 and 435 Ma during Ordovician to early Silurian magmatic activity. The CIC comprises sedimentary rocks (mudstones, sandstones and conglomerates) and volcanic rocks intruded by a series of gabbroic to dioritic bodies. Gold is predominantly hosted within networks of narrow quartz-carbonate-sulphide veins, pyritic veinlets and disseminated pyrite, with gold typically occurring as micron-sized grains.

Mining at Cowal is currently centred on the E42 and E46 open pits and the Cowal Underground (GRE46). Additional Mineral Resources have been defined at the E41, Galway and Regal (GR). Total Ore Reserves now total 180 Mt at 0.89 g/t Au for 5.1 Moz gold, with Mineral Resources comprising 340 Mt at 0.92 g/t Au for 10 Moz of contained gold[1] demonstrating the scale of the Cowal mineralised system. Together, past production and current resources give an endowment of ~15 Moz of gold. Despite more than two decades of mining, Cowal continues to generate significant exploration opportunities both near existing mine infrastructure and across the broader mineral system.

In this paper, we will discuss recent exploration activities that have focused on improving understanding of mineralisation controls by integrating geological, geophysical, geochemical, drilling, and three-dimensional modelling datasets. This integrated approach has refined exploration targeting, supported continued resource growth and identified new mineralised zones across the Cowal Gold Corridor.

[1] Refer to 'Annual Mineral Resources and Ore Reserves Statement' dated 1 May 2026 and available to view at www.evolutionmining.com. The Company confirms that it is not aware of any new information or data that materially affects the information included in the release and that all material assumptions and parameters underpinning the estimates in the release continue to apply and have not materially changed. The Company confirms that the form and context in which the Competent Persons' findings are presented have not been materially modified from the Reports.

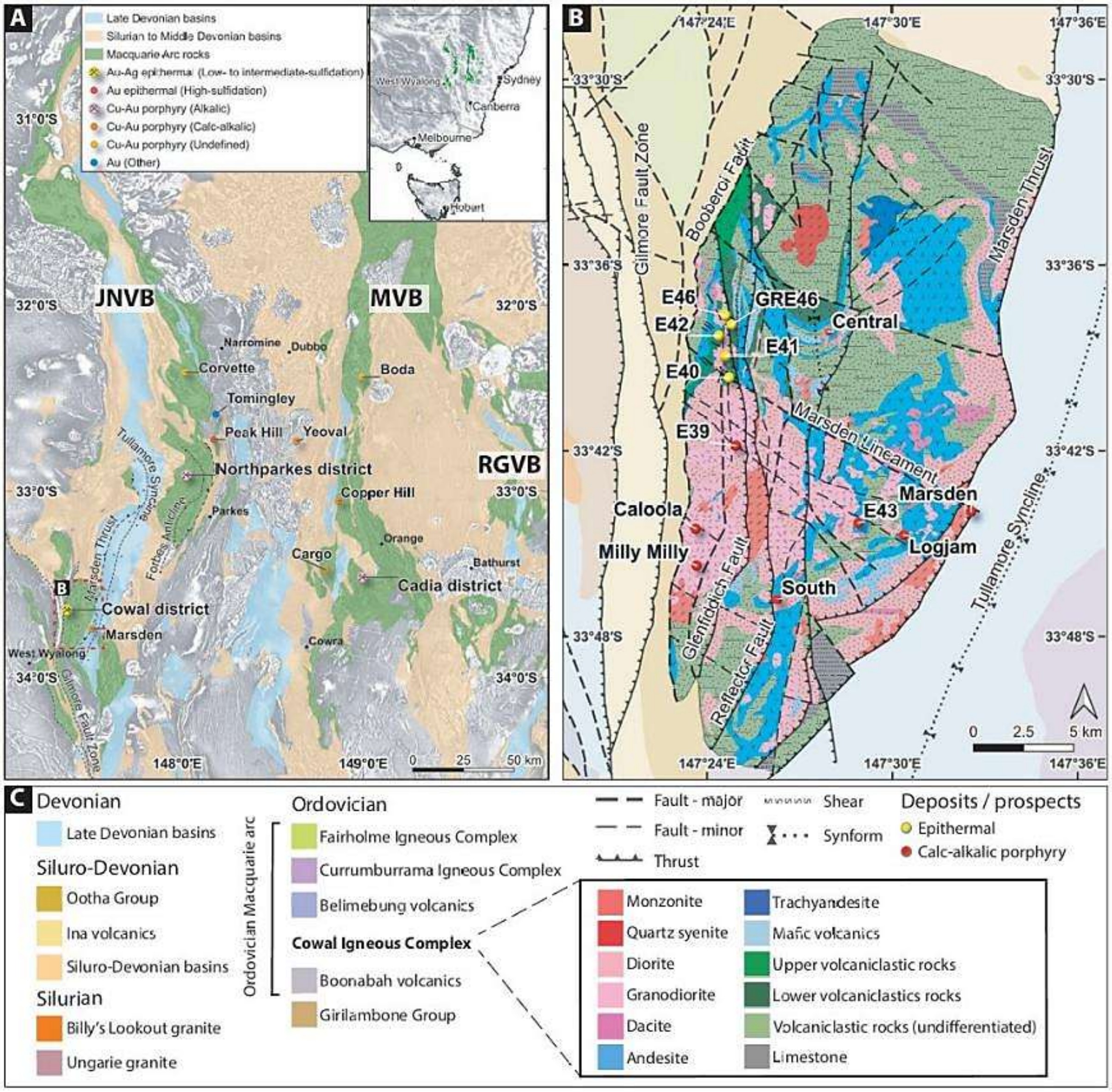

Figure 1:(A) Location and simplified regional geologic map of the Macquarie arc, highlighting the major porphyry and epithermal deposits overlain with the reduced to pole total magnetic intensity (first vertical derivative). Coordinates in EPSG:4326 WGS 84. Abbreviations: JNVB = Junee-Narromine volcanic belt, MVB = Molong volcanic belt, RGVB = Rockley-Gulgong volcanic belt. (B) District scale geology of the Cowal Igneous Complex and surrounding area. The geology and structural interpretation include both local interpretation from Cowal mine geology (D. Radford, pers. commun., 2020) combined with the seamless geology data package (v. 2.3) from the Geological Survey of NSW (Colquhoun et al., 2023). (C) Geologic legend for the Cowal Igneous Complex (B). (Staubmann et al., 2025).

COWAL'S DISCOVERY HISTORY

Prior to the 1980s, exploration in the Lake Cowal area was limited to sporadic, shallow historical prospecting. In 1980, Geopeko, following initial success of the "Endeavour" exploration program exploring for masked Cu-Au porphyry deposits to the north in the Goonumbla Volcanics, discovered an outcropping gossan on the shore of Lake Cowal to be named the E35 prospect. E35 was one of few outcropping areas of the Cowal Igneous Complex, with the remainder of the complex covered by Quaternary post mineral cover.

By 1987, Lake Cowal had dried out sufficiently to allow RAB and AC drilling to commence along the lake shore. Several targets were delineated in a 7.5km x 2km trend with anomalous gold (>0.1ppm), along coincident a magnetic high, now referred to as the "Cowal Gold Corridor" These targets included E40, E41, E42 and E46.

In 1988, Peko Wallsend Ltd was acquired by North Limited, who subsequently executed an extensive RC and Diamond drilling campaign, focusing on the E42 and E41 targets. They defined a massive structurally controlled, low to intermediate sulphidation epithermal deposit at E42. E41 East and West Pods were also defined. In 1993, a Mineral Resource of 30.4 Mt at 1.6 g/t Au for 1.6 Moz gold was declared by Peko Wallsend Operations Ltd (Peko-Wallsend Operations Ltd, 1993).

In 2000, Rio Tinto acquired North Limited. In 2001, following a restructure of mining portfolios, the Cowal Project was sold to Homestake Mining, which in late 2001, merged with Barrick Gold Corporation. By the end of 2002, the Ore Reserves sat at 68.9 Mt at 1.3 g/t Au for 2.8 Moz gold, with Mineral Resources at 58.7 Mt at 1.2 g/t Au for 2.2 Moz gold (Tucker, 2003). Resource drilling and pre-development of the E42 open pit by Barrick in 2005 lead to the discovery of the adjacent Galway and Regal mining zones.

Cowal Gold Operations were acquired by Evolution Mining in 2015, with an Ore Reserve at the time of 72.58 Mt at 0.93g/t Au for 2.18 Moz gold and Mineral Resources of 162.87 Mt at 0.97 g/t Au for 5.09 Moz gold (Evolution Mining Ltd, 2015). Following an extensive review of historic drilling data around underground Mineral Resources, a deep directional drill program was executed. Results from this program indicated that the Galway and Regal zones were not just discrete pods, but a semi-contiguous structurally controlled North-South corridor of veining and gold mineralisation. In 2018, development of the GRE46 underground exploration decline commenced. Following an aggressive drilling campaign, the Dalwhinnie Lode was discovered, a zone of mineralisation associated with a thin andesitic lava unit within the volcaniclastic sediment package adjacent to the Muddy Lake Diorite. The Dalwhinnie Lava is observed to be preferentially brittle fractured, containing a network of high-grade gold quartz-carbonate-pyrite-bearing veins.

Total Ore Reserves now totals 180 Mt at 0.89 g/t Au for 5.1 Moz gold, with Mineral Resources comprising 340 Mt at 0.9 g/t Au for 10 Moz of contained gold (Evolution Mining Ltd, 2026). Operations now sit until 2042, and during that time, ore will be produced from several sources, including E42, E41E, E41W, E46, GR, Regal and Dalwhinnie (Figure 2).

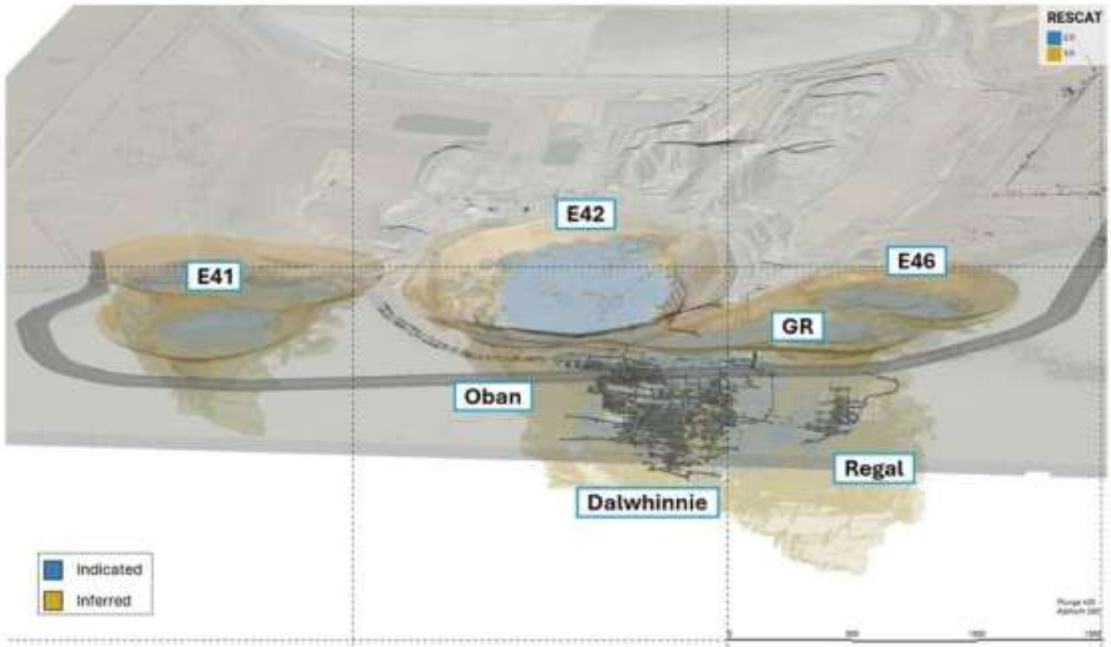

Figure 2. Cowal oblique long section (looking 260° W) with proposed open pits, underground infrastructure and Mineral Resource.

COWAL'S EXPLORATION METHODOLOGY

The exploration methodology at Cowal has evolved many times over the years. With over 70,000 holes and 2,000,000 metres drilled to date within the Gold Corridor, it would be easy to assume that everything has been found. However, through a structured approach of ore body knowledge, drill studies, and robust three-dimensional geological modelling, there is significant upside for further discoveries. One of the truisms of the Gold Corridor is the more we drill, the more we find – a sign of a world class gold system.

Ore Body Knowledge

The geology of the Cowal Igneous Complex (CIC) consists of a ~20x40km fault bounded sequence of semi-conformable, mafic to intermediate volcanic, volcaniclastic and sedimentary rocks depositing in an intra-oceanic arc setting, intruded by a fractionated monzodiorite body (Muddy Lake Diorite) as well as a series of pre and post-mineral dykes (Figure 1, Figure 3). The geology is cross-cut by a set of N-S trending, subvertical faults, both pre- and post-mineralisation. The CIC can be broadly divided into two halves. An older block to the north consisting of volcanics, volcaniclastics and diorite, host to the E42 and GRE46 deposits. And a younger (by ~20Myr) block to the south dominated by dioritic to granodioritic intrusions and host to the E41 deposit (Ila'ava et al., 2024). The sequence is poorly exposed, with almost no outcrop, extensive Cenozoic sediment cover and a deep insitu weathering profile.

[1] Refer to ASX Announcement titled 'Exploration Update' dated 15 April 2026 and available to view at www.evolutionmining.com. The Company confirms that it is not aware of any new information or data that materially affects the information included in the release and that all material assumptions and parameters underpinning the estimates in the release continue to apply and have not materially changed. The Company confirms that the form and context in which the Competent Persons' findings are presented have not been materially modified from the release.

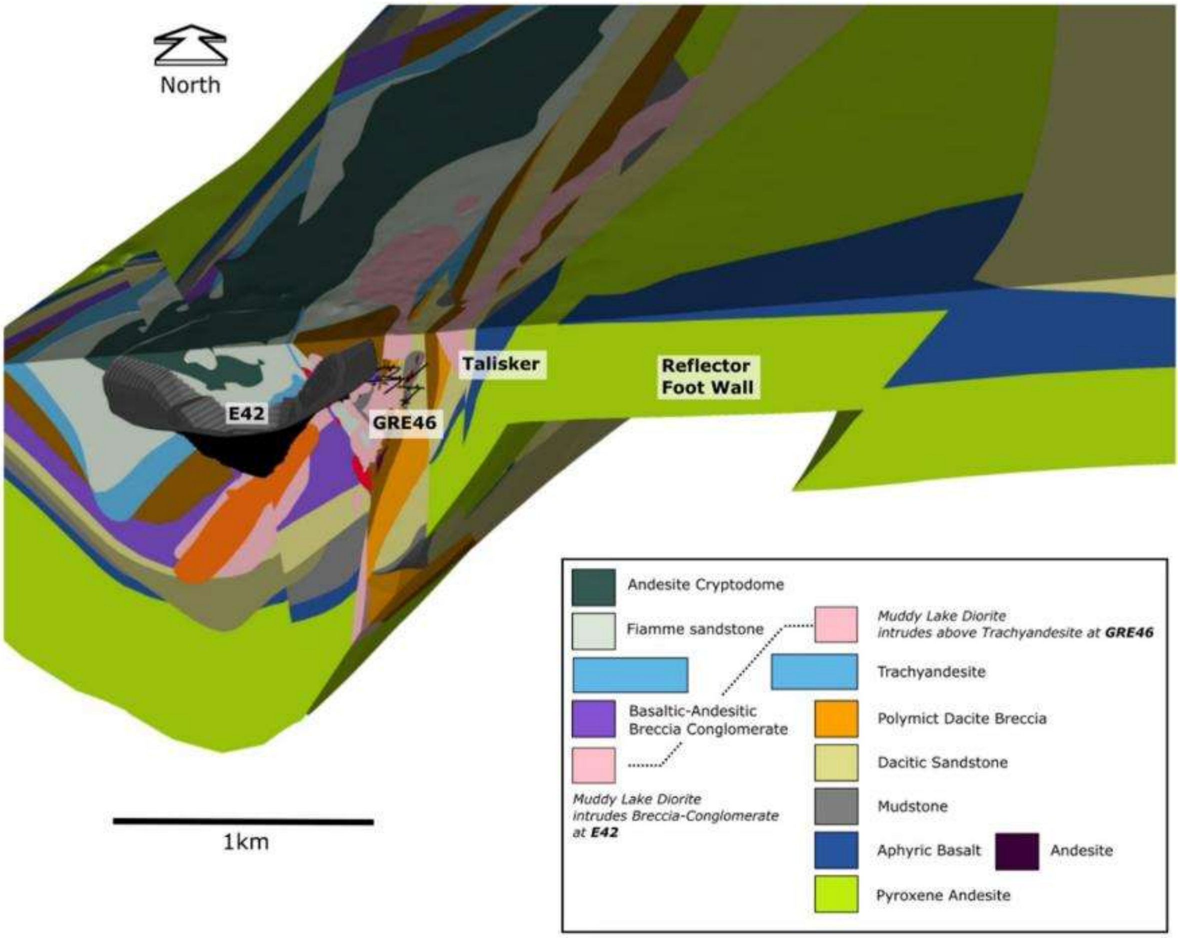

Figure 3: 3D model of ancient and buried volcanic successions in the Cowal Igneous Complex built through a volcanic facies analysis and graphic logging (Ila'ava et al., 2024).

The CIC hosts a variety of styles of mineralisation; however, low sulphidation epithermal (E42, GRE46, E41) and calc-alkalic porphyry (Marsden, E39, E43) styles are the most prevalent. Epithermal mineralisation within the CIC is not confined to a single host unit. There are no bad hosts, though some rock types are observed to be better than others. Mineralisation is instead governed by several factors that may preferentially localise mineralising fluids. These include rheological contrasts between brittle units such as coherent lavas or diorite and more ductile volcaniclastics and sediments. Undulations and overhangs within the diorite contact acting as fluid traps, and proximity to interpreted fluid conduits may also play a role. The deposits within the Gold Corridor are also commonly associated with second and third order NS structures relating to the Gilmore Suture and Booberoi Fault (McInnes and Freer, 2007).

To assist in developing ore body knowledge, Evolution Mining has supported several research studies on Cowal. These include Burns-Nichols (2020); Ila'ava (2024); Leslie (2021); Staubmann (2025); and Zukowski (2014).

Drill Studies

A full appreciation for the vein direction and structural controls of the GRE46 deposit was not realised until partway through the construction of the exploration decline. Due to the majority of the orebody being situated under Lake Cowal, most of the previous drilling was constrained to the lake shore, with holes drilled from west to east (Figure 4B). This caused challenges when discrete grade domain modelling was attempted. To assist in modelling, several vein orientation studies were undertaken by collecting high quality structural data and using the modelling software to quickly select populations to visualise on stereonets and within 3D workspaces (Figure 5). These highlighted the structural complexity of the GRE46 orebody and that vein orientations change significantly throughout the deposit with proximity to fluid conduit structures such as Galway and Manna (Figure 4A), and with the orientation of the intrusive diorite and its overhangs. This work has been extended to other parts of the Gold Corridor, including E41 and makes up a key part of the Cowal exploration methodology.

Modelling

The implementation of three-dimensional modelling has significantly enhanced the geological understanding of the Gold Corridor at Cowal Gold Operations (CGO). Comprehensive 3D lithological, structural, oxidation classification, and domain models are routinely maintained and updated, supporting both resource estimation and drill targeting activities.

As geological understanding of the CGO gold corridor has evolved, the complexity and sophistication of the geological models have increased accordingly. An example of this is the development of implicit modelling of grade at the GRE46 deposit where new domains are added and geometries increasingly complicated as infill drilling is added and mineralisation controls unique to each mining zone become better understood (Figure 6A and 6B).

Recent camp-scale structural reinterpretations, combined with updated lithogeochemical classifications, have improved the understanding of fault block architecture and structural offsets throughout the gold corridor leading to the development of Mining Lease scale lithological and structural models (Figure 6C). Recent work by Ila'ava et al. (2024), involved reconstructing the CIC, through facies analysis, into a 3D model (Figure 3) has been instrumental in expanding the search space away from known ore bodies.

RECENT SUCCESSES AND FUTURE POTENTIAL

Recent exploration work at Cowal has been targeted at challenging traditional beliefs formed in long-lived mines. Over the past 2 years, significant work has been undertaken to test the GRE46 underground deposit west of the Glenfiddich Fault (Figure 7). This fault served as a hard stop when drilling commenced in GRE46. Drilling at the Oban prospect has challenged this boundary and has identified that mineralisation continues west of the Glenfiddich, in a similar stratigraphic position to GRE46, juxtaposed across the Glenfiddich Fault and sitting below E42. While the Oban story is in its infancy, recent results have been encouraging and include:

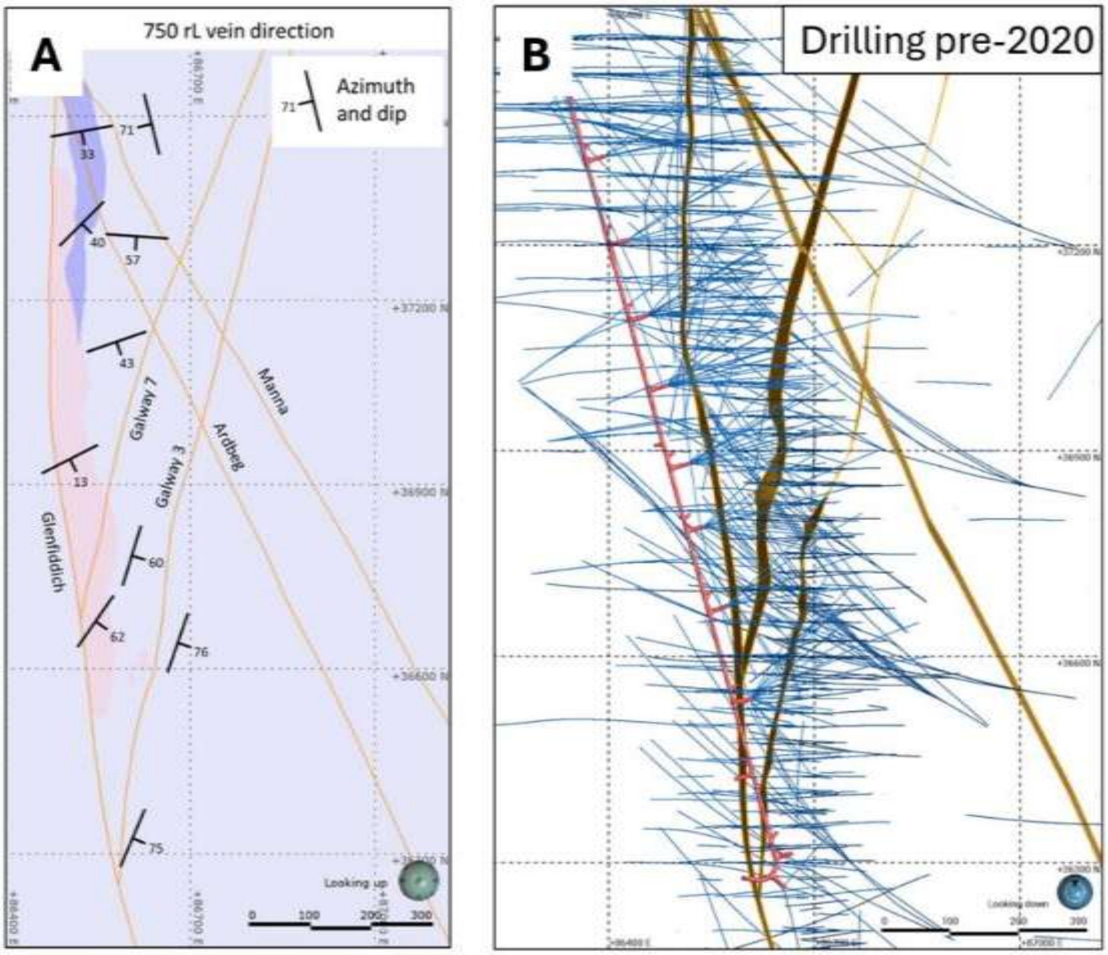

Figure 4:(A) Average vein direction of GRE46 at 750mRL showing the variety of directions the veins take. (B) Drilling pre-2020 showing the majority of holes drilled west to east, sub-optimal to some of the veins at GRE46.

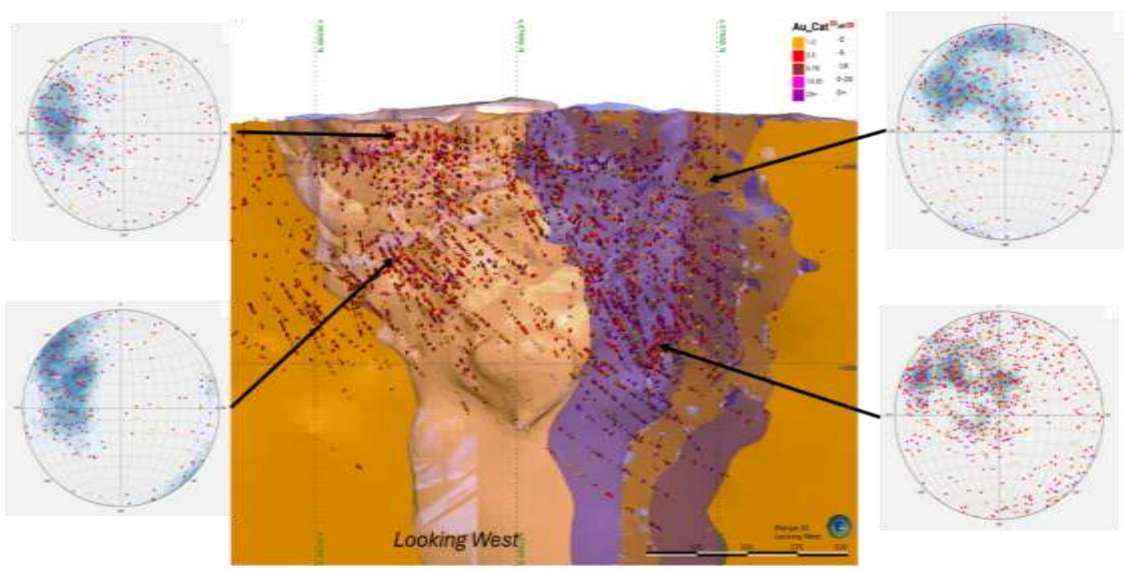

Figure 5: Variation in the preferred gold-bearing vein orientations at GRE46 illustrated by stereonet plots of mineralised veins to highlight the progressive vein rotation and steepening from south to north.

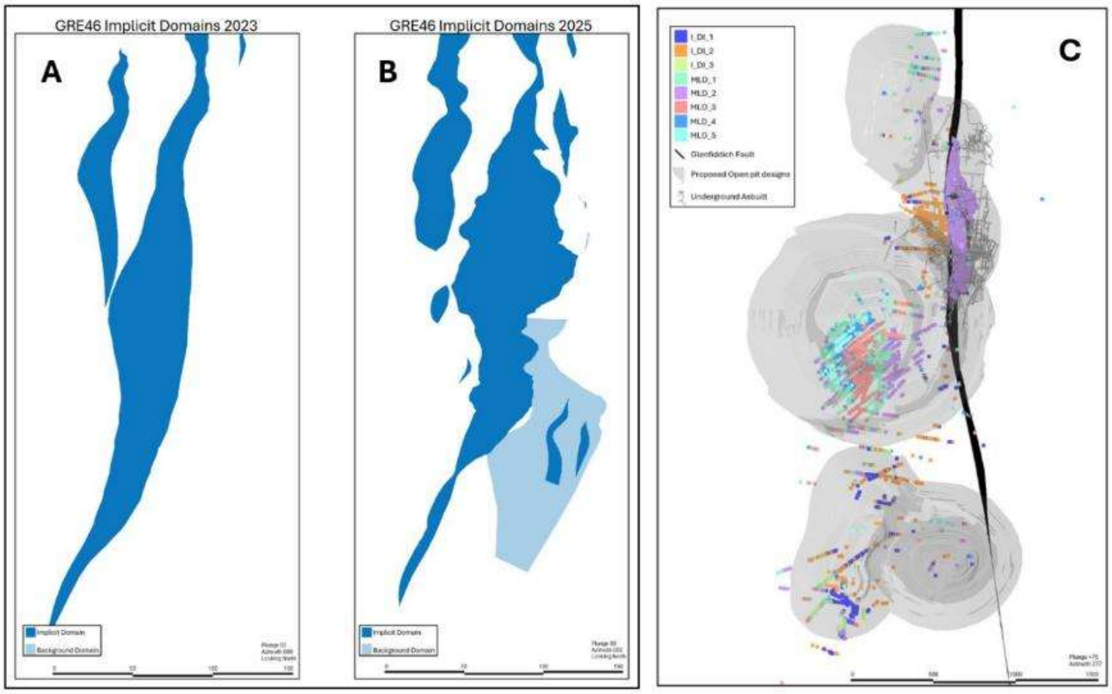

Figure 6: Recent modelling developments. (A) Cross-section looking north through the GRE46 deposit showing the GRE46 implicit domains in 2023 compared to (B), which shows the domains as of 2025. (C) Oblique plan-view looking down Glenfiddich fault displaying the different fractionations in the CGO gold corridor as mapped by lithogeochemistry classification.

- RDU0225 – 20m (14m estimate true width) @ 8.22g/t Au from 456m[1]
- RDU0295 – 3.22m (2.25m estimate true width) @ 17.09g/t Au from 219m[1]
- RDU0296A – 27m (19.6m estimate true width) @ 1.95g/t Au from 289m[1]

Additional work has been undertaken at E41 to test the potential for growth (Figure 8). This work was undertaken after significant vein orientation studies, which determined that previous drilling was done at suboptimal angles. Recent results from E41 include:

- E41D2955 – 13m (9.1m estimate true width) @ 4.05g/t Au from 516m[1]
- E41D2960 – 9m (5.4m estimate true width) @ 5.83/t Au from 379m[1]

Further exploration work at Cowal will involve applying lessons learnt from successes since Evolution acquired the operation, with the goal of discovering new ore bodies within the Gold Corridor that support future production. The focus is on finding additional higher grade resources that could support additional mining fronts as well as potentially displacing current lower grade open cut resources. by continuing to test under-drilled or poorly orientated drill areas within the mining lease, including between E41 and E42, to determine whether these ore bodies could be connected, around E41 to further grow this future ore source and testing the open space west of the Glenfiddich Fault, following recent success at Oban. Cowal Gold Operations holds a significant 1,483km^2 tenement package, with work to test for untouched and unknown wedges of the Cowal Intrusive Complex underway (Figure 8).

[1] Refer to ASX Announcement titled 'Exploration Update' dated 15 April 2026 and available to view at www.evolutionmining.com.

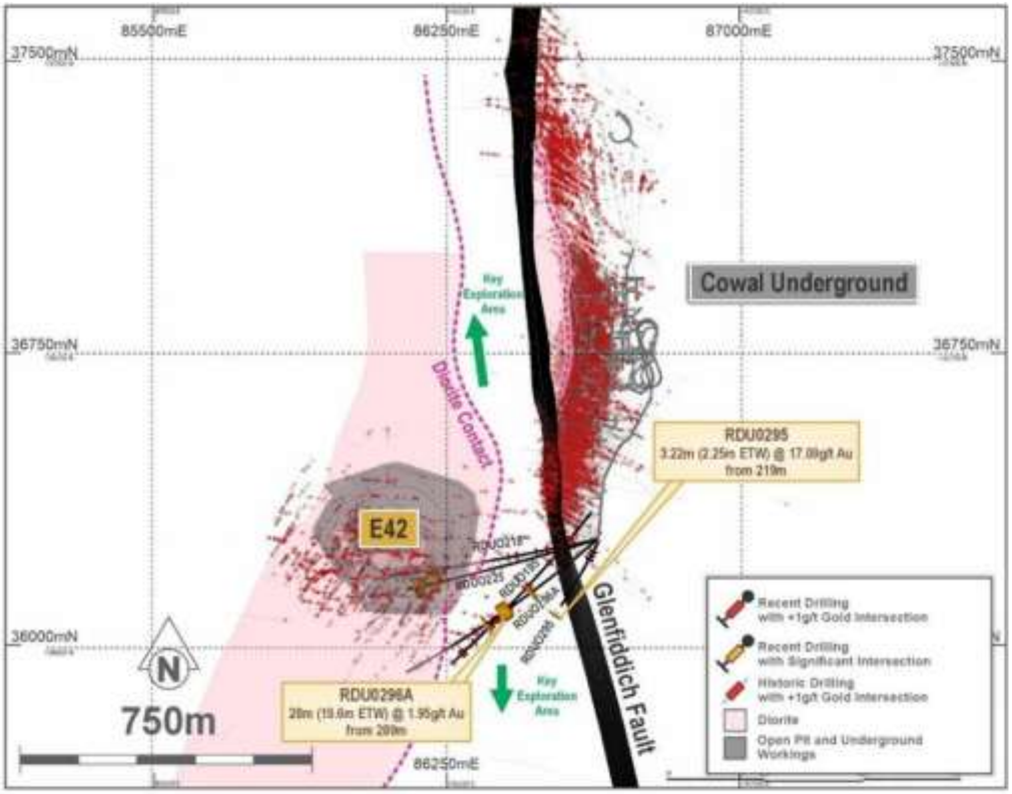

Figure 7: Plan view showing historic drilling along the Gold Corridor with recent Oban results on the western side of the Glenfiddich fault. The map is a 200m slice centred on 650mRL[1]

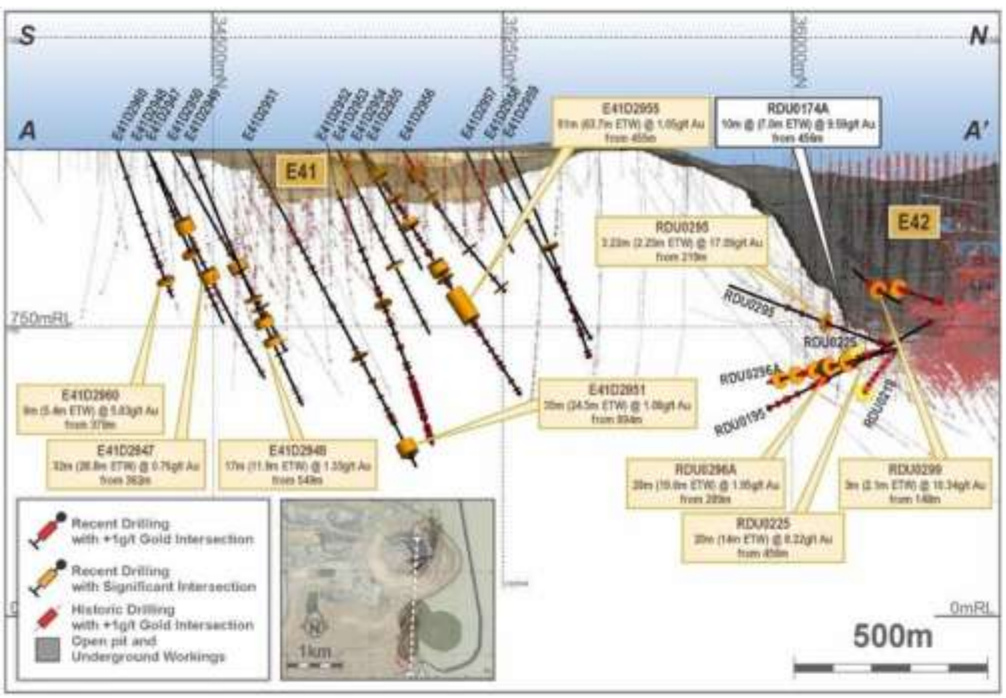

Figure 8: Long section between E41 and E42 showing recent exploration drilling results from drilling around E41 and from the Cowal[1]

1 Refer to ASX Announcement titled ‘Exploration Update’ dated 15 April 2026 and available to view at www.evolutionmining.com.

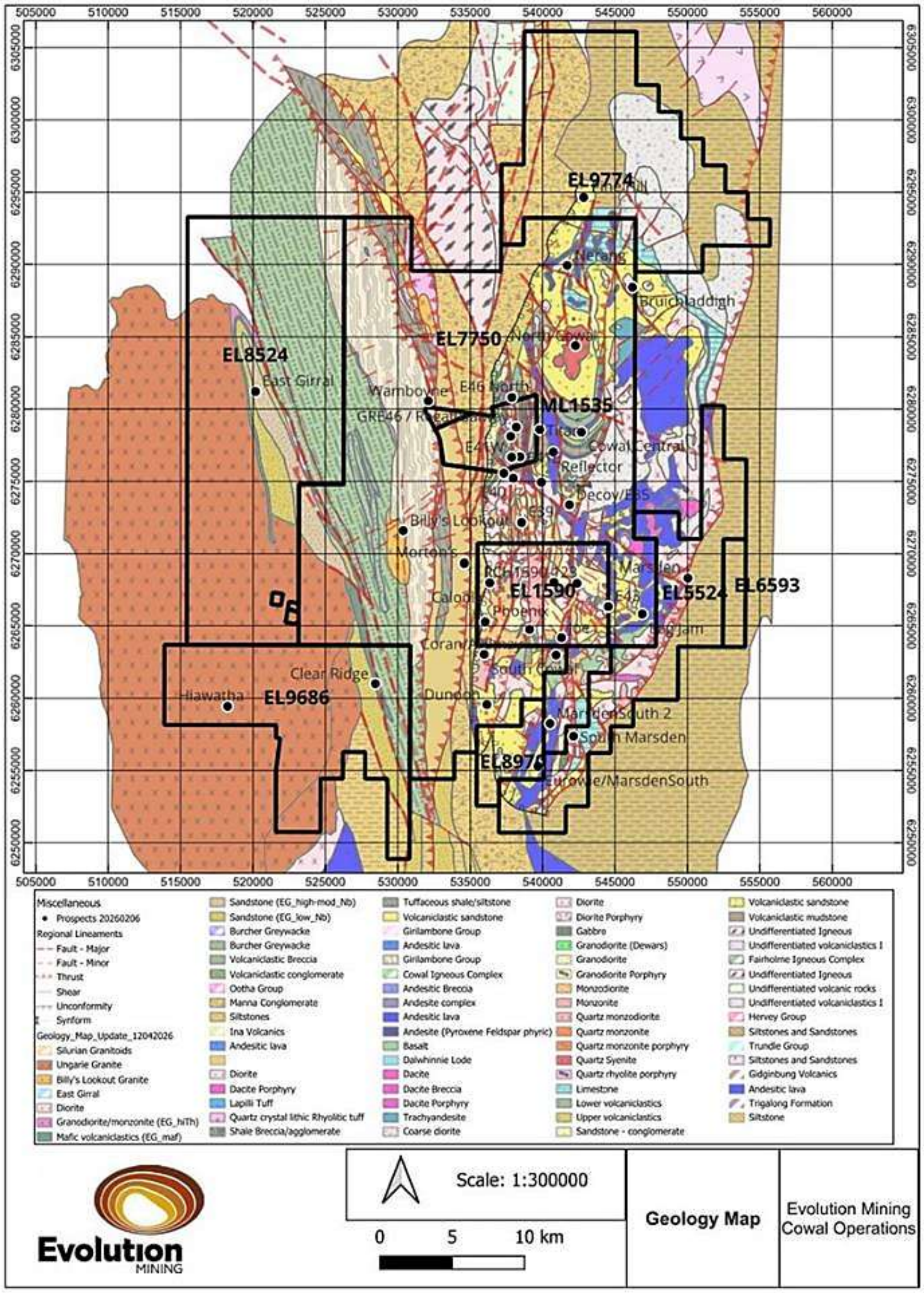

Figure 9: Geology map of Evolution Mining Cowal Operations exploration tenure.

ACKNOWLEDGEMENTS

The authors wish to thank Evolution Mining for their ongoing support of exploration at Cowal. In particular, Glen Masterman, Dan Macklin, Ned Howard, Kevin Gleeson, Ben Reid, Zach Murphy and Tilen Milojkovic have been key in driving the continued exploration and believing there is still more to be found in the Gold Corridor. The authors wish to thank all geologists who have spent time at Cowal, whether as employees, contractors, consultants, academics, or researchers. The understanding of Cowal has been built on the knowledge base of past workers. The authors also acknowledge the incredible work of the field services team led by Braiden Gage, who processes tens of thousands of metres of core each year.

REFERENCES

BURNS-NICHOLS J. 2020. Reconstruction of the volcanic architecture of the host rocks at E41, Lake Cowal Volcanic Complex, Central NSW, Australia. University of Tasmania. Honours Thesis.

EVOLUTION MINING LTD. 2015. Resource & Reserves Increased at Cowal. [online] https://yourir.info/resources/851ef7ffa345f09f/announcements/evn.asx/2A874826/Resources_and_Reserves_increased_at_Cowal.pdf.

EVOLUTION MINING LTD. 2020. Cowal Maiden Underground Ore Reserve Supports Mine Development. [online] https://yourir.info/resources/851ef7ffa345f09f/announcements/evn.asx/2A1238133/Cowal_Maiden_Underground_Ore_Reserve.pdf.

EVOLUTION MINING LTD. 2026. Annual Mineral Resources & Ore Reserves Statement (Dec 2025). [online] https://yourir.info/resources/851ef7ffa345f09f/announcements/evn.asx/2A1669373/Annual_Mineral_Resources_and_Ore_Reserves_Statement.pdf.

HENRY A. D., MCINNES P., & TOSDAL R. M. 2014. Structural Evolution of Auriferous Veins at the Endeavour 42 Gold Deposit, Cowal Mining District, NSW. Australia: Economic Geology, v. 109, p. 1051-1077.

HOWARD N. 2022. Ned Howard - Evolution Mining - Geology of the Cowal Gold Deposit & discovery of the Dalwhinnie - YouTube, Geohug. Available at: https://www.youtube.com/watch?v=5nRHojMcXCg (Accessed: 09 July 2026).

ILA'AVA M., JUTZELER M., CAS R. & CAREY R. 2024. 3D modelling of subsurface ancient volcanic successions: a workflow developed during regional reconstructions of the Cowal Igneous Complex in the Ordovician Macquarie Arc of NSW, Australia. Australian Journal of Earth Science, 71(5), 699-720.

LESLIE CD. 2021. Metallogeny of the Cowal district, New South Wales, Australia. University of Tasmania. PhD Thesis

MCINNES P. & FREER L. 2007. The Cowal Gold Corridor – Opening Other Doors. Mineral Exploration in the Tasmanides. Mines and Wines 2007.

NORTH LTD. 1997. 6th Annual Report on Exploration Licence 2865 for the twelve months ending 1 June 1997.

PEKO-WALLSEND OPERATIONS LTD. 1993. Second Annual Report on EL 2865.

STAUBMANN M., COOKE DR., HALLEY S., MILOJKOVIC T., REID B., GREEN M., HOWARD N., CLIFFORD M. 2025. The GRE46 Epithermal Gold Deposit, Cowal, New South Wales: Geology, Mineralization, Alteration, & Ore Genesis. Economic Geology, 120(4), 847-876.

TUCKER D. 2003. Cowal Gold – Discovery, Disappointment, Recovery. New Gen Gold Conference, Perth.

ZUKOWSKI W., COOKE D. R., DEYELL C. L., MCINNES P., & SIMPSON K. 2014. Genesis & Exploration Implications of Epithermal Gold Mineralization & Porphyry-Style Alteration at the Endeavour 41 Prospect, Cowal District, New South Wales, Australia. Economic Geology, v. 109, p. 1079-1115

CLEVELAND, TASMANIA: GEOLOGY, HISTORICAL TIN/COPPER PRODUCTION AND UNLOCKING FUTURE POTENTIAL

Chris Creagh
Elementos Ltd

Key Words: Cleveland, Luina Group, tin, calcareous sediment replacement, tungsten, greisenisation, porphyry

INTRODUCTION

The tin-copper and tungsten mineralisation at the historical Cleveland Mine site is located approximately 80km to the southwest of Burnie, within the Cambrian Luina Group in northwest Tasmania (Figure 1). Outcrops of gossan were first discovered by prospectors at Cleveland in about 1898. Tin was first identified at Cleveland in 1900 by Harcourt Smith, Government Geologist. Mining by the Cleveland Tin Mining Co NL commenced in 1908 but the mine closed in 1917 after production of about 275 tonnes of tin in the form of cassiterite concentrate (McKeown, 2013).

Figure 1. Location of the Cleveland Mine

From 1935 to 1939, the Mt Bischoff Tin Mining Co undertook exploration by small scale underground mining but no tin production occurred during this period (McKeown, 2013).

Mining was re-commenced at Cleveland by Aberfoyle Ltd in 1968 using trackless methods for mining and ore haulage to the surface. The Cleveland Mine was among the first in the world to use trackless mining, and the mine extended to a depth of over 500 metres below surface (see Figure 4). Production from the mine during the Aberfoyle operation from 1968 to 1986 was 5,645,000 tonnes at a grade of 0.68% Sn as cassiterite and 0.28% Cu (Dronseika, 1986). The current geological tin-copper resource at Cleveland stands at 7.47mt containing 0.75% Sn and 0.3% Cu (Measured Group, 2018).

The tin-copper resource at Cleveland comprises several stratabound lenses of pyrrhotite-cassiterite-stannite-chalcopyrite mineralisation that replaced calcareous beds within a Cambrian marine sequence (Williams, et. al, 1989).

Located beneath the Cleveland tin-copper resource is the Foley Zone tungsten resource. The tungsten resource consists of a quartz vein stockwork system centred around a narrow steeply dipping quartz-feldspar porphyry dyke which intruded the fine-grained Crescent Spur Sandstone. The tungsten mineralisation occurs as wolframite and minor scheelite accompanied by fluorite and very minor molybdenite, bismuthinite, chalcopyrite and cassiterite. The Foley Zone tungsten mineralisation is a separate mineralising event and overprints the overlying tin-copper mineralisation but are both interpreted to have formed during the Devonian, contemporaneous to the intrusion of the nearby Meredith Granite. An increase in exploration activity in recent times has resulted in a significant increase in the geological tungsten resource. The tungsten resource at Cleveland currently stands at 8.49mt containing 0.24% WO_3 (Elementos, 2026). There has been no historical production of tungsten from the Cleveland Mine.

LOCATION

The Cleveland Project is located at Luina approximately 80 km southwest of Burnie in north-western Tasmania. Access to the project area is by way of a sealed all-weather road, which runs from Burnie through Waratah and Luina to Savage River.

The topography around the project area is relatively steep and rugged with elevations ranging from about 300m to over 500m above sea level. The historical Cleveland Mine was developed beneath Crescent Hill which rises to an elevation of 520m while the former township of Luina, the former mine infrastructure and the tailings dams lie in the valleys of the Whyte River and Deep Creek.

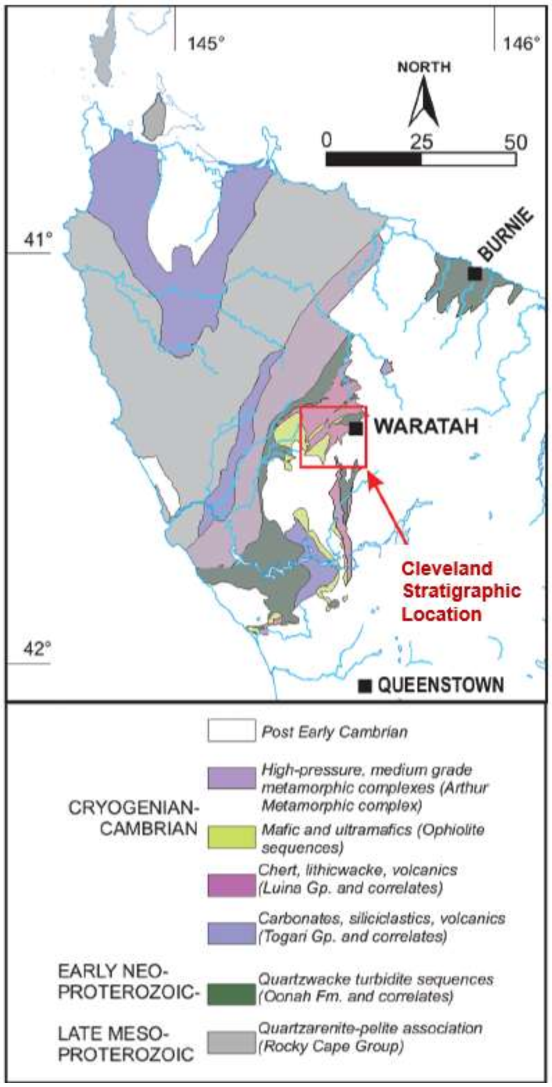

Figure 2. Regional Geology (Cumming et. al. 2016)

GEOLOGY

In north-western Tasmania, the principal metal mines are associated with the Cambrian Mt Read Volcanic rocks, Devonian-Carboniferous granites, or the Precambrian metamorphic rocks of the Arthur Metamorphic Complex. Lead-zinc, copper and gold deposits are associated with the Mt Read Volcanics; tin and tungsten deposits and some silver-lead-zinc deposits are associated with Devonian-Carboniferous granites; large iron deposits are associated with the Arthur Metamorphic Complex. The Cleveland Mine is located within the Cambrian-Silurian Luina Group of north-western Tasmania.

The Cleveland tin-copper mineralisation is hosted in stratabound semi-massive sulphide lenses within a series of sedimentary rocks belonging to the Hall's Formation of Cambrian age. (Figure 3). The Hall's Formation consists of a 100-200m thick sequence of shales, interbedded sandstone-greywacke, calcareous sediments, minor chert, mafic pyroclastics and volcanics.

The Hall's Formation occurs between a basaltic lava sequence (Deep Creek Volcanics) to the southeast, and a turbiditic greywacke sequence (Crescent Spur Sandstone) to the northwest. The Hall's Formation has undergone intense deformation which has resulted in the sequence being slightly overturned and steeply dipping to the southeast, with possible syntectonic thrust faults displacing the sequence in places.

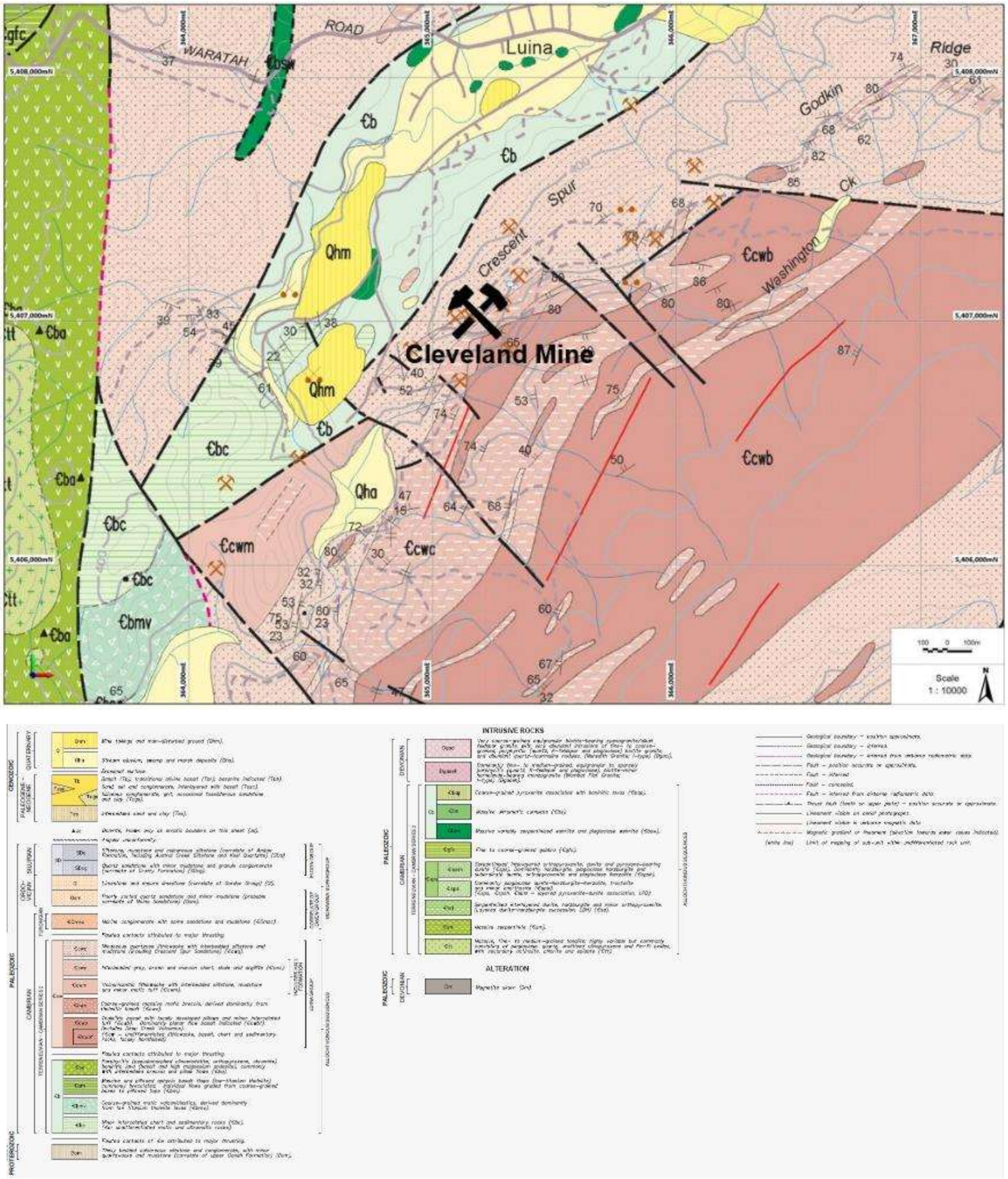

Figure 3. Local Geology (Mineral Resources Tasmania 1:25,000).

The Crescent Spur Sandstone, and to a lesser extent the Hall's Formation, are locally intruded by a narrow, steeply north dipping quartz-feldspar porphyry dyke. The medium grained quartz-feldspar porphyry intrusive occurs deep within the central portion of the mine sequence. Current information limits the top of the porphyry dyke to be at approximately sea level (~300m below the surface), with the deepest drill intersection to-date being at 600m below sea level. Drilling to-date indicates a very steeply dipping dyke (80°) to the north, with a maximum strike length of approximately 80m and up to 33m in horizontal width. The dyke is interpreted to have a strike of approximately 280° with a steep (80°) plunge towards the east. It appears to bifurcate at its extreme upper and western end.

MINERALISATION

The mineralisation at Cleveland consists of two separate but closely related events, both in space and time (Figures 4 & 7).

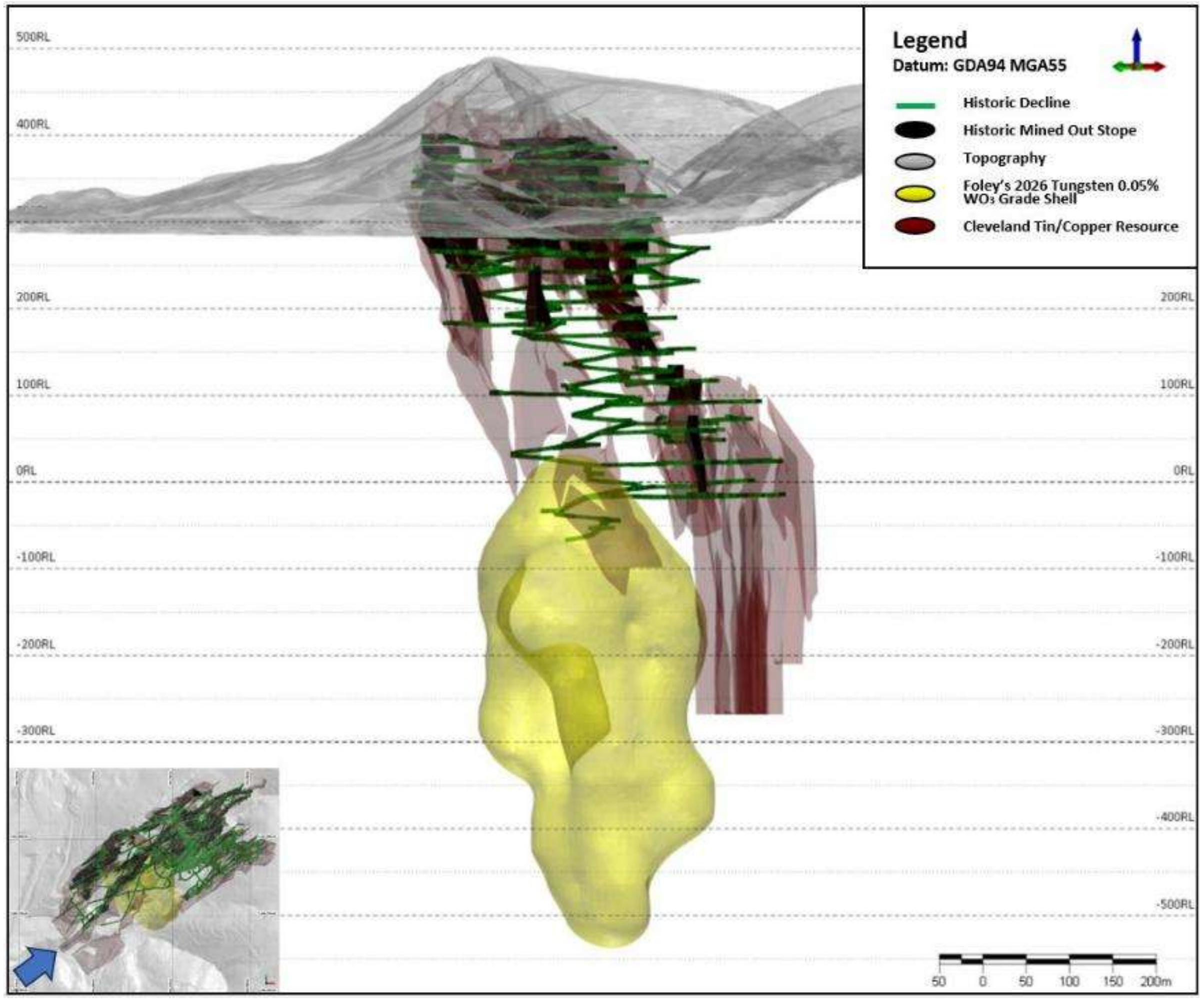

Figure 4. Location of the Foley Zone tungsten resource wireframe boundary (0.05% WO3 cut-off), pre-mining Cleveland tin-copper resource wireframes (geological boundary) and the historical underground mine decline.

Mineralisation – Cleveland Tin-Copper

The Cleveland tin-copper mineralisation (pyrrhotite-cassiterite-stannite-chalcopyrite) is hosted in semi-massive sulphide lenses. The semi-massive sulphide mineralisation is considered to have been formed by the hydrothermal replacement of calcareous sedimentary beds by mineralising solutions contemporaneous with the emplacement of the Devonian-Carboniferous Meredith Granite. The tin-copper lenses that form the Cleveland mineral resource are restricted to the Hall's Formation, however recent drilling to the northwest of the resource has intersected tin-copper mineralisation within the Crescent Spur Sandstone. At least ten discreet lenses of tin mineralisation have been recognised within the Halls Formation, displaying replacement textures after a calcareous unit. The lenses have been observed in close approximation with the contact between calcareous units and chert lenses.

The tin and copper lenses have strike lengths of up to 500 metres, across strike thicknesses of up to 30 metres and down-dip extents of up to 800 metres.

The Cleveland tin-copper deposit is geologically similar to the tin bearing semi-massive and massive sulphide mineralisation at the Renison Mine, near Zeehan.

Figure 5. Drill core from drill hole C2115 (completed in 2117): 1.5m @ 0.83% Sn, 0.76% Cu & 10.4% Zn from 61.3m (Henry's Lode)

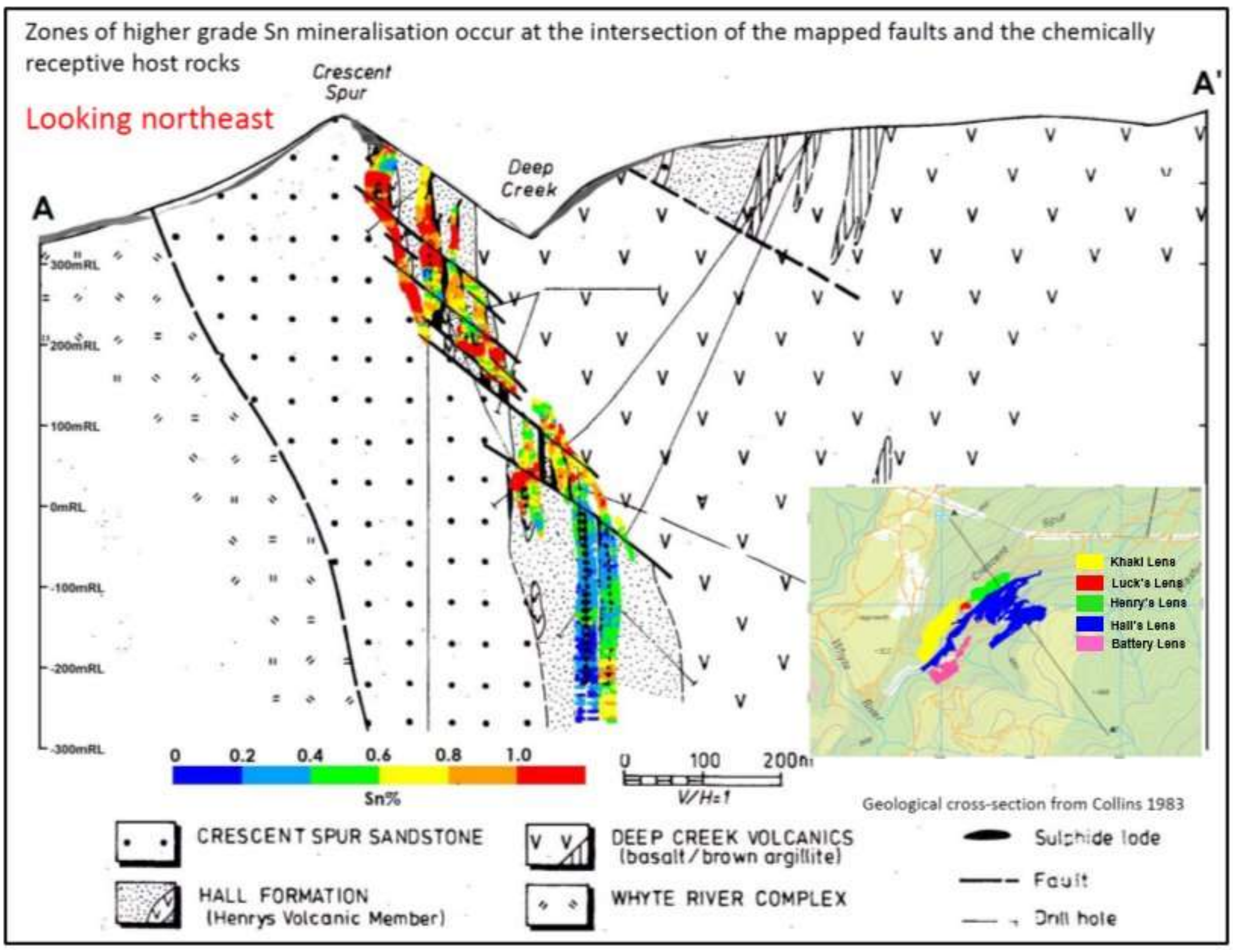

Figure 6. Cleveland tin mineralisation block model (pre-mining) depicting a close spatial association with moderately dipping mapped faults (higher concentrations near the faults), suggesting the faults may have been the feeders for the mineralising fluids. (geology from Collins 1983)

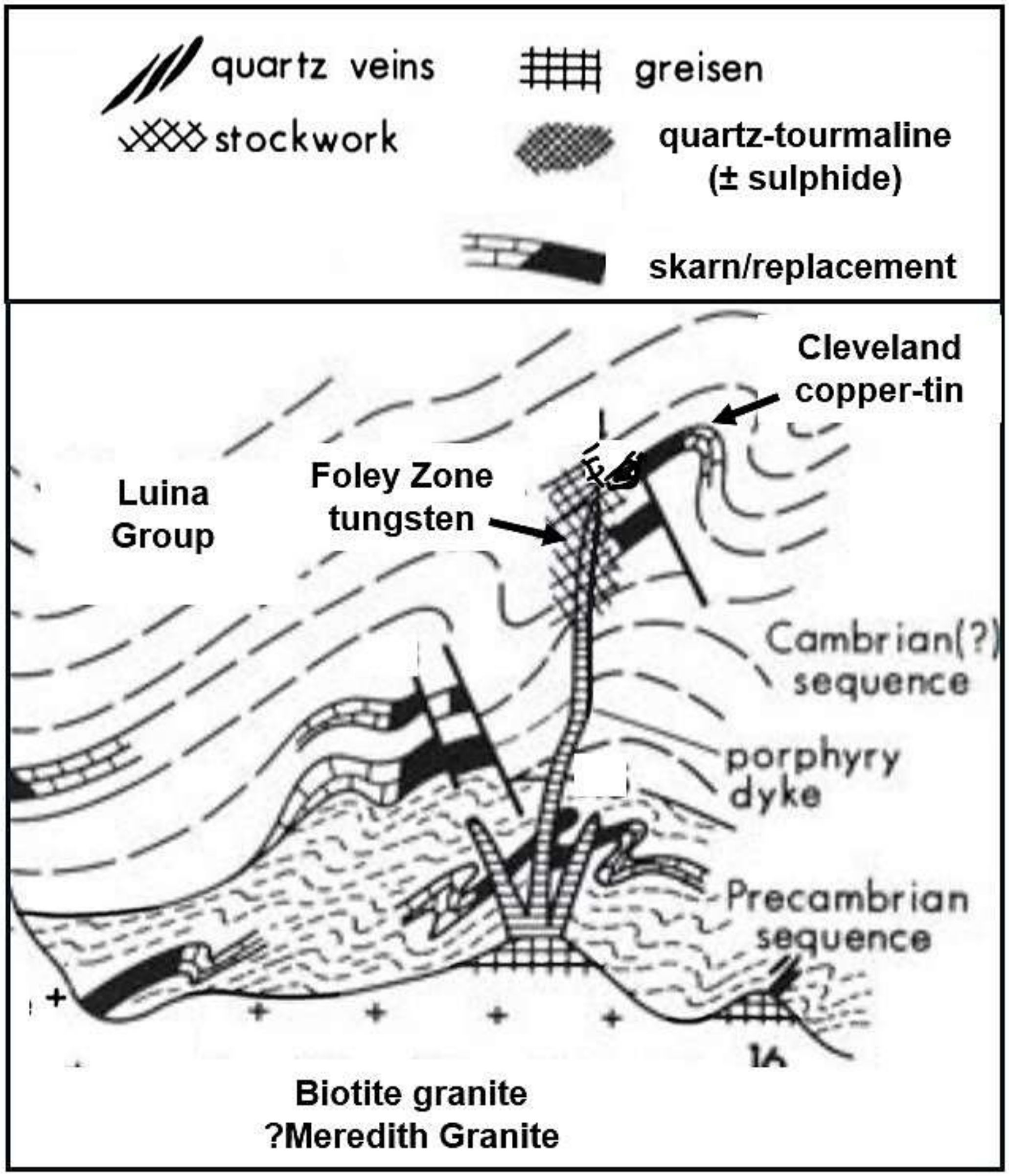

Figure 7. Schematic representation for genetic ore body types at Cleveland (Williams, et. al. 1989)

Mineralisation – Foley Zone Tungsten

The Foley Zone tungsten mineralisation is located beneath the historical tin-copper mine workings at Cleveland and is a separate and later mineralising event to the tin-copper mineralisation. The Foley Zone tungsten mineralisation consists of greisenisation of a near-vertical quartz-feldspar porphyry dyke and development of a quartz fissure stockwork vein system which crosscuts the Crescent Spur Sandstone (and to a much lesser extent the Hall's Formation). Tungsten mineralisation is predominantly wolframite with lesser scheelite, accompanied by minor tin (cassiterite), molybdenum (molybdenite), bismuth (bismuthinite), copper (chalcopyrite) and fluorite mineralisation. Alteration associated with the quartz vein stockwork system extends for several tens of metres into the enclosing Crescent Spur Sandstone which can be recognised by a significant increase in biotite, sericite and silicification. The increase in mica in the alteration zone is accompanied by a significant increase in rubidium.

The Foley Zone tungsten mineralising event is also considered to be associated with the intrusion of the nearby Devonian Meredith Granite with the nearest known occurrence being approximately 4km to the south of Cleveland. The top of the tungsten mineralised zone is approximately 150m above sea level and is known to extend beyond 600m below sea level.

Figure 8. Foley Zone mineralised (wolframite) quartz vein within the Crescent Spur Sandstone in drill hole C2124A (completed in 2024), 2.47m @ 0.57% WO_3 from 887.0m

HISTORICAL EXPLORATION AND MINE PRODUCTION

The Cleveland Mine has been operated sporadically as an open cut or underground operation from 1908 to 1986. Prospectors first discovered outcrops of gossanous material at Cleveland in about 1898. Tin was first identified at Cleveland in 1900 by Harcourt Smith, a Government Geologist. Mining by the Cleveland tin Mining Co. NL commenced in 1908 as a small open cut and underground operation but closed again in 1917 after production of approximately 275 tonnes of tin (cassiterite) in concentrate.

Exploration by the Tasmania Mines Department and the Australian Bureau of Mineral Resources in the 1950s identified the potential for relatively large cassiterite bearing sulphide ore bodies. Consequently, in 1961, the Aberfoyle Tin Development Partnership acquired the leases at Cleveland and commenced systematic exploration based on geological mapping and using diamond drilling. Since then, over 2100 diamond drill holes have been drilled into both the tin-copper and tungsten resources.

Mining of the tin-copper ore at Cleveland re-commenced in 1968 using trackless methods for mining and ore haulage to the surface. The Cleveland Mine was among the first in the world to use trackless mining, and the mine extended to a depth of over 500 metres below surface (Figure 4). Production from the mine during the Aberfoyle operation from 1968 to 1986 was 5,645,000 tonnes at a grade of 0.68% Sn as cassiterite and 0.28% Cu (Dronseika, E.V., 1986). There has been no historical production of tungsten from the Cleveland Mine.

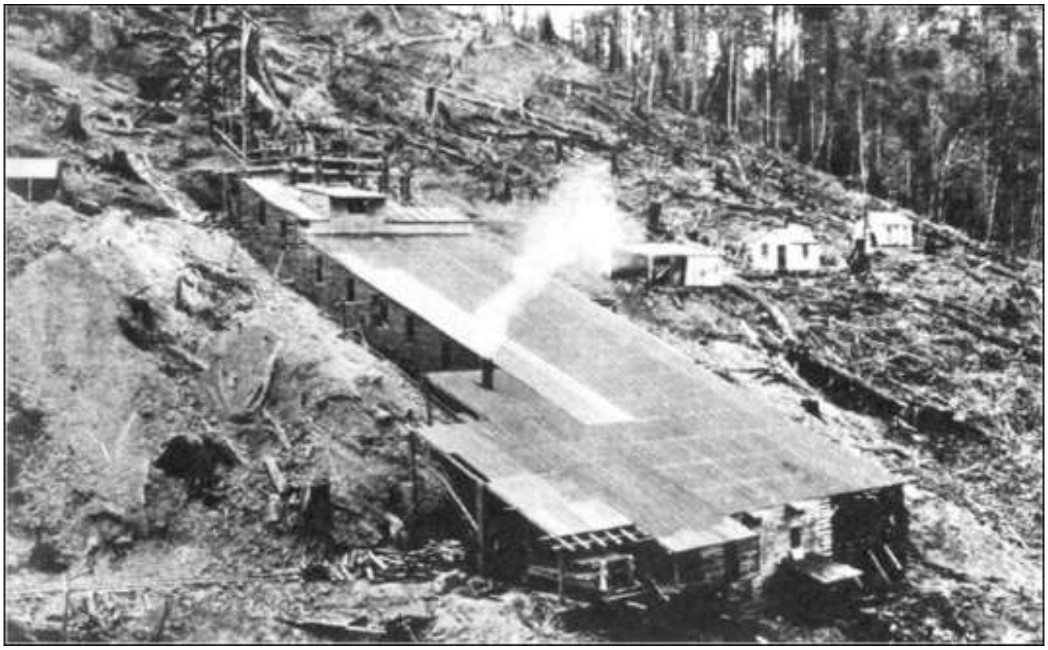

Figure 9. Cleveland historic operations 1908-1917.

Figure 10. Cleveland historic operations 1968-86.

REFERENCES

COLLINS P.I.F.,1983. Geology & mineralisation at the Cleveland mine, western Tasmania. Doctoral thesis, University of Tasmania, Australia.

CUMMING G., EVERARD J.L., MEFFRE S., 2016. Age constraints & provenance of the Mount Bischoff inlier & the Luina Group: evidence from LA-ICPMS U-Pb dating of detrital zircon. Tasmanian Geological Survey Record UR2016/04

DRONSEIKA E.V., 1983. Geological assessment of the Foley zone mineralisation at Cleveland mine Tasmania, May 1983. Unpublished report for Cleveland Tin Ltd.

DRONSEIKA E.V., 1986. Geological Resource Assessment, Cleveland Tin Mine, as at End of Milling-Mining Operations, 12th June 1986. Unpublished report for Aberfoyle Resources Limited.

Elementos Ltd., 2026. ASX Release. Tungsten Mineral Resource Estimate Increase at Cleveland Tin Project

GREEN G. R., 1990. Palaeozoic Geology & Mineral Deposits of Tasmania in Geology of the Mineral Deposits of Australia & Papua New Guinea (Ed. F. E. Hughes). 1207-1223 (The Australasian Institute of Mining and Metallurgy; Melbourne)

MCKEOWN M. V., 2013. Cleveland Mine, Luina, Tasmania Mineral Resource Report. https://www.mrt.tas.gov.au/mrtdoc/tasxplor/download/13_6753/EL72005_201306_01_Appendix.pdf

Measured Group., 2018. Geology & Resource Estimate Report. Cleveland Project. Elementos Ltd. (unpub)

WILLIAMS E., MCCLENAGHAN M.P & COLLINS P.I.F., 1989. Mid-Palaeozoic deformation, granitoids & ore deposits, in Geology & Mineral Resources Tasmania (Eds C.F. Burrett & E.L. Martin), Geol. Soc. Aust. Spec. Publ., 15: 238-292.

KEYS TO DISCOVERY IN THE GOLD-ANTIMONY FIELD OF COSTERFIELD, VICTORIA

Chris Davis & Ryan Eagle

Alkane Resources

Key Words: Gold, Antimony, Discovery, Costerfield

INTRODUCTION

Located central Victoria, alongside the crustal-scale Heathcote Fault, lies a relatively small Gold-Antimony mine with global significance (Figure 1). Costerfield was first discovered in the later stages of the gold rush era of (1861) with mines quickly coming into production and supplying Britan with antimony, most notably through WW1.

In recent decades, Costerfield has been a consistent producer of gold and antimony, operating continuously since the commencement of mining at the Augusta deposit in 2006. Over this modern period approximately 663,000 oz of gold and 71,700t of antimony has been mined between 4 production centres spanning a 4 Km corridor of veining. In 2006 mining began with Reserve of 204,000t at 10.9 g/t Au and 5.7% Sb (71,000Au oz and 11,580t Sb) indicating a mine life of approximately 2 years (McArthur 2005). From this point the mine self-funded its exploration, and with continued success managed to replace mining depletion and build on its mine life through the following 20 years making it one of the most consistent producers in the state.

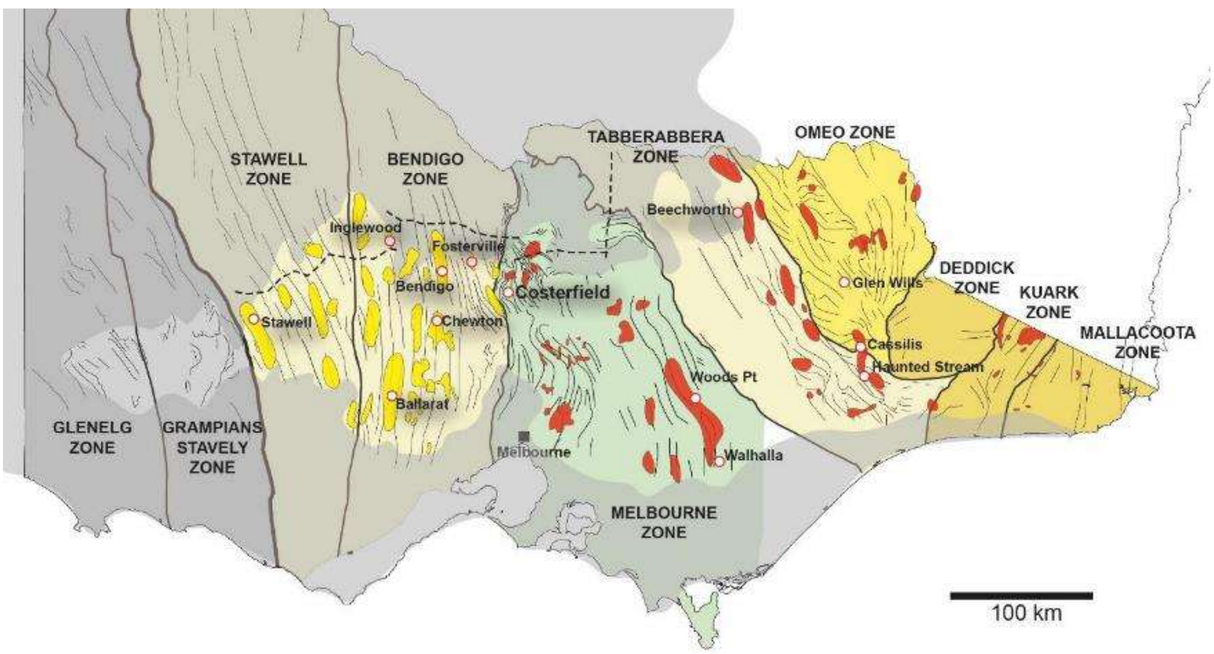

Figure 1. Map of Victoria showing Geological domains, structural features and major mines. Also shown are recognised instances of gold mineralization (yellow), Gold + Antimony (red) and areas of alluvial cover (greyed). From Mandalay Resources internal report prepared by Clive Willman, figure derived from Figure 2 in Willman (2010).

GEOLOGICAL SETTING

Costerfield is located in the Siluro-Devonian Melbourne Zone of Victoria, just 15 kilometres from the footwall of the crustal-scale Heathcote Fault Zone, which represents the boundary with the deep water Ordovician turbidites of the Bendigo Zone. Mineralisation at the property is largely hosted within the Costerfield Dome, an antiformal thrust stack developed within the Lower Silurian Costerfield Formation, comprising siltstone, turbiditic sequences and mudstones up to 550 m thick (figure 2). The dome shows extensive shortening and duplexing, with folding strongly influencing the structural architecture. Folds are typically asymmetric with shallow west limbs and steeply dipping east limbs, the largest such as the Costerfield Anticline form the dominant structural elements of the dome.

Major west-dipping thrusts, including the King Cobra and Adder faults, display apparent offsets of up to 400 m and are marked by fault gouge zones 1–2 m thick, flanked by heavily fractured and sheared rock. These structures truncate or offset stratigraphy and form key structural boundaries within the dome. Postdating dome formation are a series of locally significant brittle faults and thrusts. Bedding-parallel laminated quartz faults are widespread and are the earliest structures. Many have acted as detachment surfaces and ramps during shortening, they exhibit evidence of significant horizontal displacement and stratigraphy is frequently repeated across them.

A series of NW and NE-striking steep faults intersect the dome at angles of 15–30° and are thought to be associated with changes in regional compressional regimes from E–W to NE–SW. Evidence of reactivation is common along these structures.

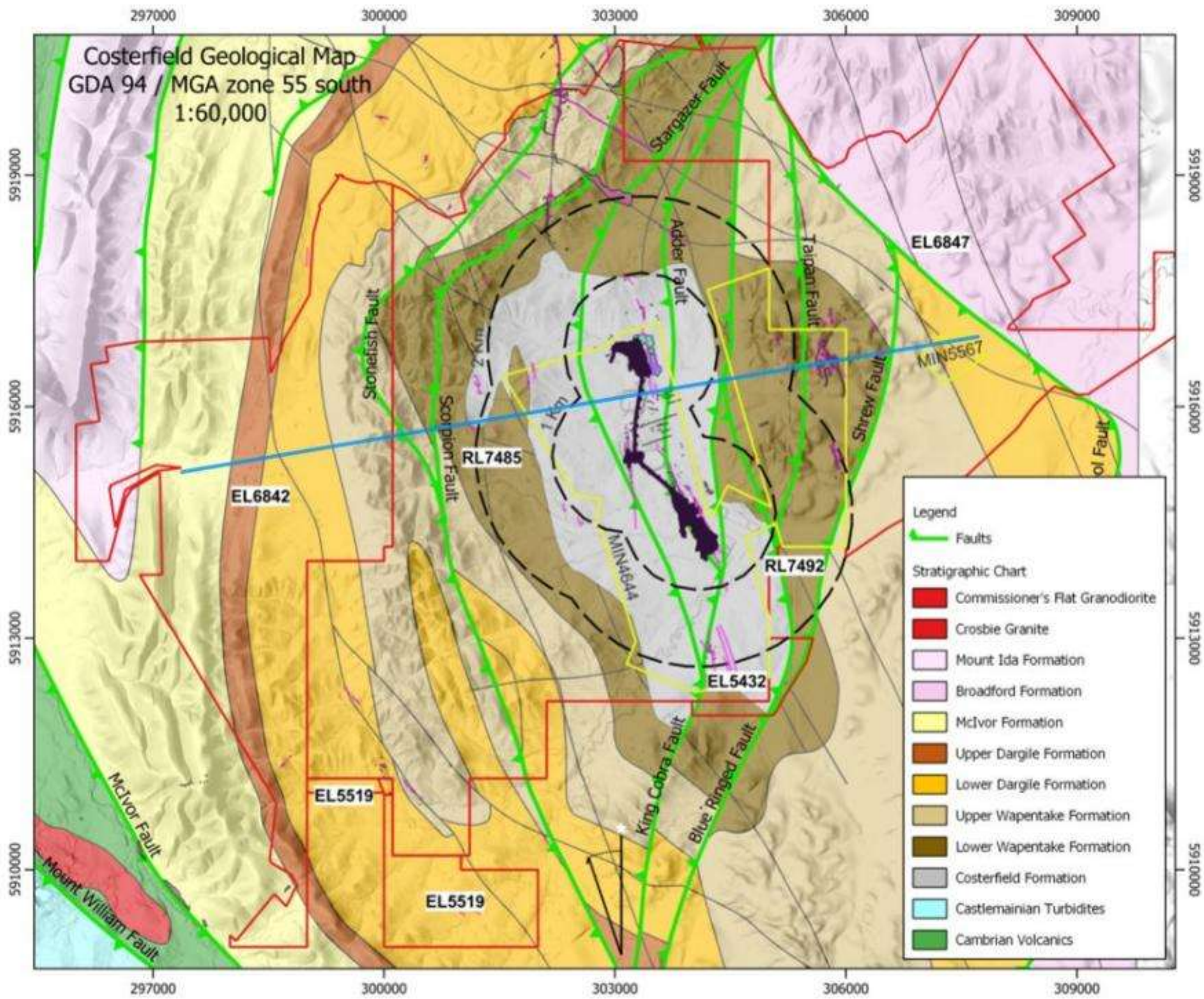

Figure 2. Geological map focused on the Costerfield Dome showing the extent of mine development, mining/exploration tenements (yellow/red) and location of mineralised structures (pink). The blue line indicates the position of the Figure 2 cross section.

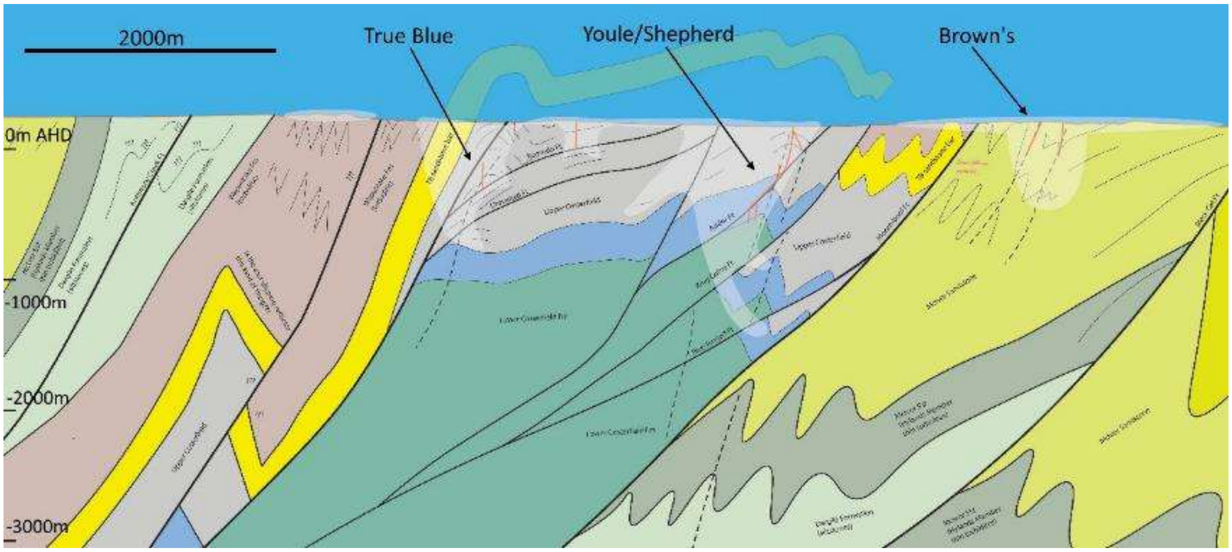

Figure 3. Cross section through the Costerfield Dome, integrating seismic, diamond drilling and outcrop data. White shaded areas show outcrop and drilling-informed interpretation, with red lines schematically representing mineralised veins. A stratigraphic package of sandstones at the top of the prospective Costerfield Siltstone is projected above ground to illustrate approximately how much of the Costerfield Dome has been lost to erosion.

MINERALISATION

The Costerfield Dome hosts narrow, anastomosing and *en echelon* mineralised vein systems developed along a north–south corridor encompassing the Costerfield, Brunswick, and Augusta zones, extending over at least 4km of strike (Figure 3). True Blue sits within a second parallel line of mineralisation 2km to the west.

Individual lodes may persist for up to 800 m along strike and 300 m down dip, with multiple lodes typically occurring in proximity within each deposit. Vein orientations are typically sub-vertical (70–90°) either east or west dipping, or moderately west dipping (30–60 °). Two principal styles of lodes are recognised: stibnitedominant and gold-only. The distribution of stibnite versus gold-only lodes appears to be controlled by depth of emplacement, with gold-only veins occurring more commonly beneath or at the base of stibnite-rich systems, such as in the Shepherd and Sub-King Cobra veins (figure 4 and 7).

The mineralised shoots are structurally controlled, typically forming at the intersection of lodes with major crosscutting, gouge-filled faults and shears. West- to northwest-dipping thrusts commonly bound mineralisation, while shallow, bedding-parallel thrusts with laminated quartz fill link between them, displacing vertical lodes laterally by up to 50 m. The lateral displacement is predominantly pre- to syn-mineralisation, as healed stibnite infill is commonly observed along the shallow thrusts linking between vertical veins. Cross faults and structural intersections create conditions for north–south trending extensional veining, characteristic of the Augusta, Brunswick, Kendall, and Shepherd deposits, while thrust fault reactivation has accommodated the moderately west-dipping Youle Deposit. This litho-structural framework underpins ongoing exploration efforts, which target additional extensional zones.

Figure 4. Underground face photographs of Youle Lode (left) and Shepherd Lode (right). Here, Youle consists of almost equal proportions of laminated quartz and massive stibnite (bluish-gray). Note the hangingwall (and footwall to a lesser extent in this area) bedding discordant to the Youle thrust.

Stibnite lodes range from massive stibnite with microscopic gold to quartz–stibnite veins with visible gold, pyrite, and arsenopyrite, while gold-only lodes are characterised by quartz–carbonate veining containing free gold, typically as sub-millimetre grains with minor pyrite and arsenopyrite. Accessory minerals include sphalerite, galena, pyrrhotite, aurostibite, and sulfosalts such as tetrahedrite and bournonite. Aurostibite is rarely observed due to its similarity to the other sulphides, however the free, “rusty” gold left *in situ* after aurostibite patches have destabilised in the hypogene environment is very common across the field. Patches and veins of native antimony are sometimes observed, usually associated with other reduced assemblage minerals such as pyrrhotite. The mineralogical proportions of each major vein differ; however, their textures and apparent paragenesis is observed to be consistent. The wallrock alteration halo associated with mineralised veins typically consists of very proximal fine-grained arsenopyrite and pyrite, with a cryptic muscovite alteration extending up to 10-20m from mineralisation (House *et al*, 2014). Ferroan carbonate spotting and bleaching of sandy beds is pervasive and extends up to hundreds of meters from the system.

Figure 5. Drill core photos from BC418 (590 Vein) showing the nature of veining with individual assay grades of the samples. Composited interval graded 13.6g/t gold and 16.4% antimony over 2.22m (ETW 1.37m).

HISTORIC DISCOVERY

The Costerfield gold-antimony deposit was discovered in 1861, antimony having been already identified in the district as early as 1853 (Whitelaw, 1926) as prospectors attracted to the McIvor (Heathcote) alluvial gold rush began to explore the surrounding hills for the primary deposits. All of the significant Costerfield deposits were located by trenching across the line of lode, as the structures and host siltstone outcrop very poorly yet are only covered by a thin soil blanket. Several lodes along a 3km corridor were rapidly opened up with the bulk of historical production coming from leases at the northern end of the field; the Costerfield (Main), Bombay and Minerva mines. Production from these mines primarily took place in two phases, between 1861-1883 and 1903-1924 (Figure 6). A short-lived attempt at reopening the mine occurred between 1933-1939. This phase notably included the first use of underground diamond drilling as an exploration tool at Costerfield.

Figure 6. Costerfield *ca*. 1914, photograph taken from the Costerfield Main headframe looking south-east.

MODERN DISCOVERY

Between 1969 and 1971 Mid-East Minerals conducted a large soil and bedrock geochemical survey that highlighted the prospective ground around the historically mined Brunswick, South Costerfield and Margaret deposits. Au, Sb and As were used as the key pathfinder signature of the orebodies. With falling Sb prices the project was shelved, until the next major exploration push which was undertaken between 1975 and 1981 by the Victorian Mines Department, who drilled a series of diamond holes targeting the anomalies and intercepted stibnite veins south of the historic South Costerfield mine. This area had not received much exploration attention previously due to being covered by the wide alluvial plains of Wapentake and Mountain Creeks. This discovery was later named Augusta when AGD Operations followed up on the area, defining two parallel lodes via diamond drilling.

Limited geophysical methods including IP/resistivity and ground gravity were trialled over the new Augusta deposit and the Margaret prospect to the south in 2005. Results were inconclusive, with no firm identification of mineralisation able to be derived from the data. Later processing integrated with the large drilling dataset on hand, has shown that some features in the geophysical data, particularly chargeability do correlate well with the large west-dipping thrusts such as the King Cobra Fault.

After 2 years of production by AGD, Mandalay Resources acquired the property, continuing production and exploration with a keen interest in structural geological modelling and a short-term reserve replacement mindset. This approach saw the company build a robust stratigraphic and structural model, resulting in the growth of resources and reserve through further near mine discoveries (Figure 7). In 2014, a campaign of top of bedrock auger geochemistry was completed over the most prospective ground on the mining licence and exploration tenements, which has continued to serve as a foundation for both near-mine and regional exploration through to the present. Around this time, the Cuffley lode was discovered, offset below the historic Alison mine which terminated on a shallow thrust fault. Accounting for thrust offsets was rapidly included in the exploration playbook for Costerfield, and has been a key characteristic in almost all deposits found since. In 2016 the Youle orebody was discovered, approximately 2km north of development at the time. Youle was unique in that it was the first orebody at Costerfield found to be hosted within a west-dipping thrust fault, a model not systematically tested for as extensive drilling through similar structures elsewhere had usually found them to be barren, or containing trace incidental mineralisation. Therefore they had been previously associated with bounding and offsetting mineralisation, not a target in themselves. Initial feasibility checks were positive thus infill and extension drilling ramped up quickly, integrating the lower-grade Brunswick deposit as a northward stepping stone.

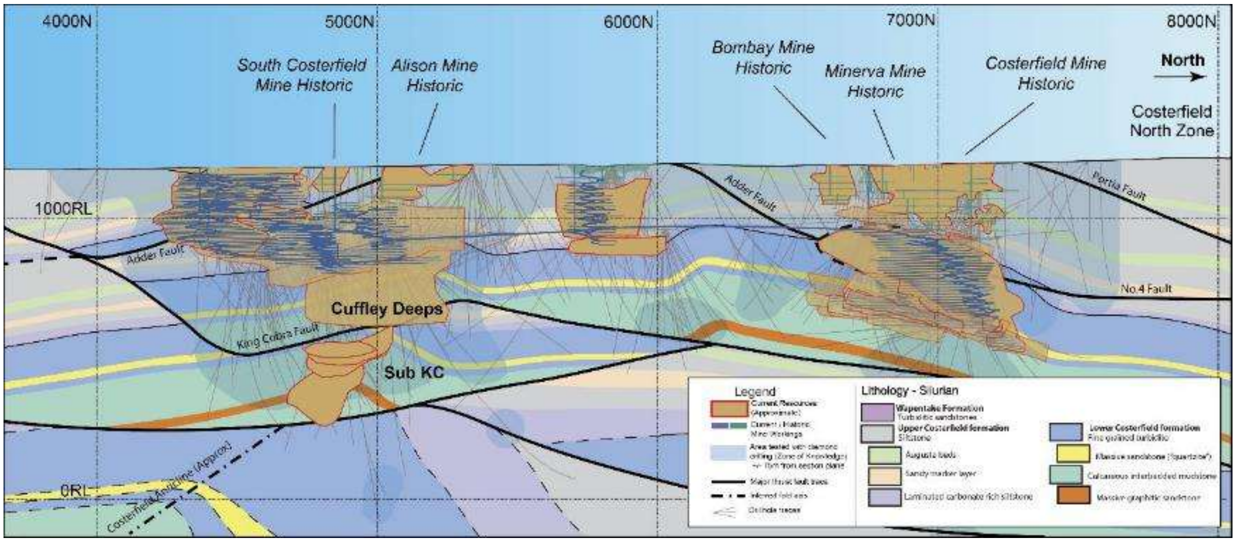

Figure 7. Longitudinal section of the central corridor showing interpreted geology with discovery years and total modelled endowment (estimated total resources including depleted areas) of institute deposits.

With the discovery and infill of Youle completed in 2019 and medium-term production secured, Exploration took a back seat while the lion's share of available funding was allocated to developing the required 2 km-long access drive. During this time of quiet, a keen Mandalay graduate geologist was given access to a mineral systems expert, mapping tablet and a Leapfrog licence to model the field and identify further regional targets. This model, when integrated with the geochemical and geophysical data, delivered key targets that were then assessed, prioritised and tested in a program of 4 short diamond drilling campaigns (figure 8). 3 of these campaigns saw the discovery of significant mineralisation in corridors both to the east and west of the central mining corridor.

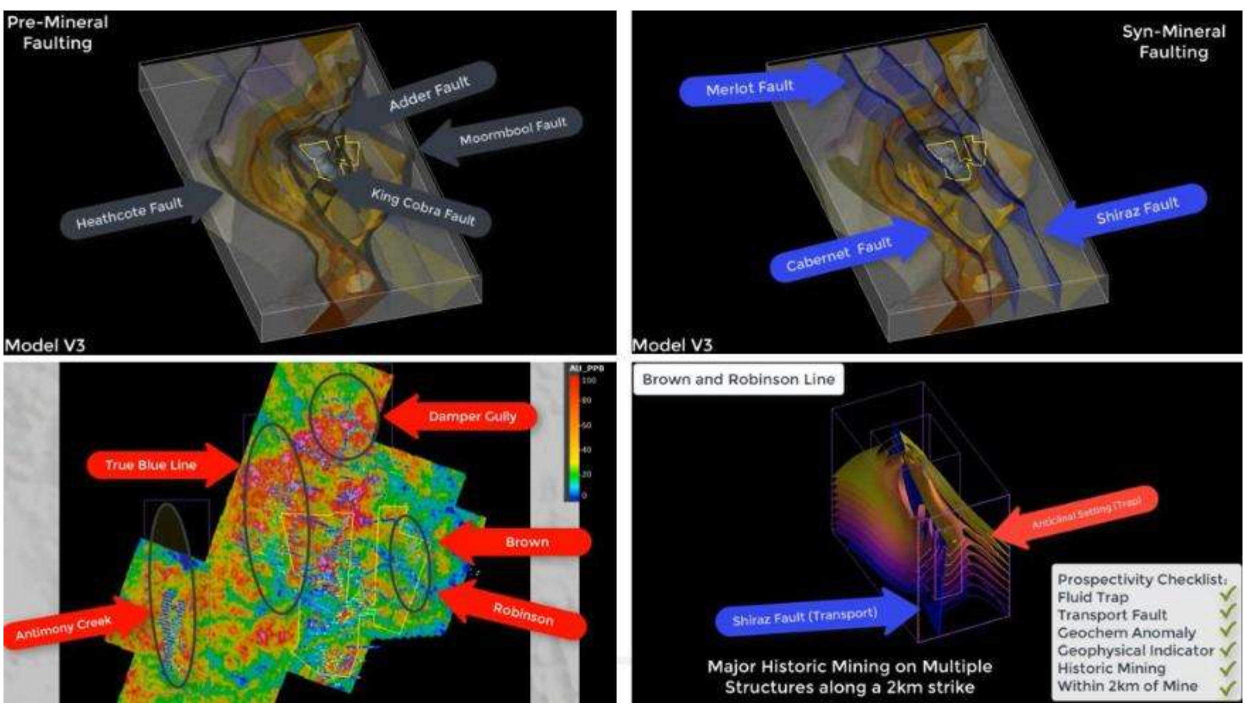

Figure 8: Images from the Costerfield Regional Geological model developed in the post-Youle exploration lull.

Once the high grade of Youle was finally in production the focus returned to Exploration. Follow-up drilling on the best targets along the eastern line ramped up, however after finding ore grade intercepts it was eventually understood that the host lithology was not conducive to the formation of continuous and easily minable veins. This led to a reassessment of the initial targeting program and armed with the understanding that the host formation was key control on mineralisation. Taking cues from successes in the Central corridor, the stratigraphic sequence built up by the site geologists was to be applied to these new areas. The “favourable” mine-sequence lithology was modelled within both the eastern and western corridors and found to be approximately 300m below the initial intercepts within the western corridor. This target was then drilled, resulting in high grade intercepts in the first drillholes, although still not quite enough to continue rapid testing.

From this point the focus changed to the True Blue prospect, which stood out as an exceptionally prospective area from the bedrock geochemistry and supporting regional model. The historically mined surface expression of True Blue was found to be relatively small, but as testing progressed deeper high-grade intercepts came to light. These intercepts were the first of the Freeman deposit, which is hosted in the west limb of an anticlinal duplex stack and effectively capped at 250m below surface by its bedding-parallel roof thrust, the Wombat Fault. Exploration on this prospect continues today utilising seismic traverses (Figure 9), mapping and drilling to extend the targeting model at depth and along strike (Alkane, 2006b).

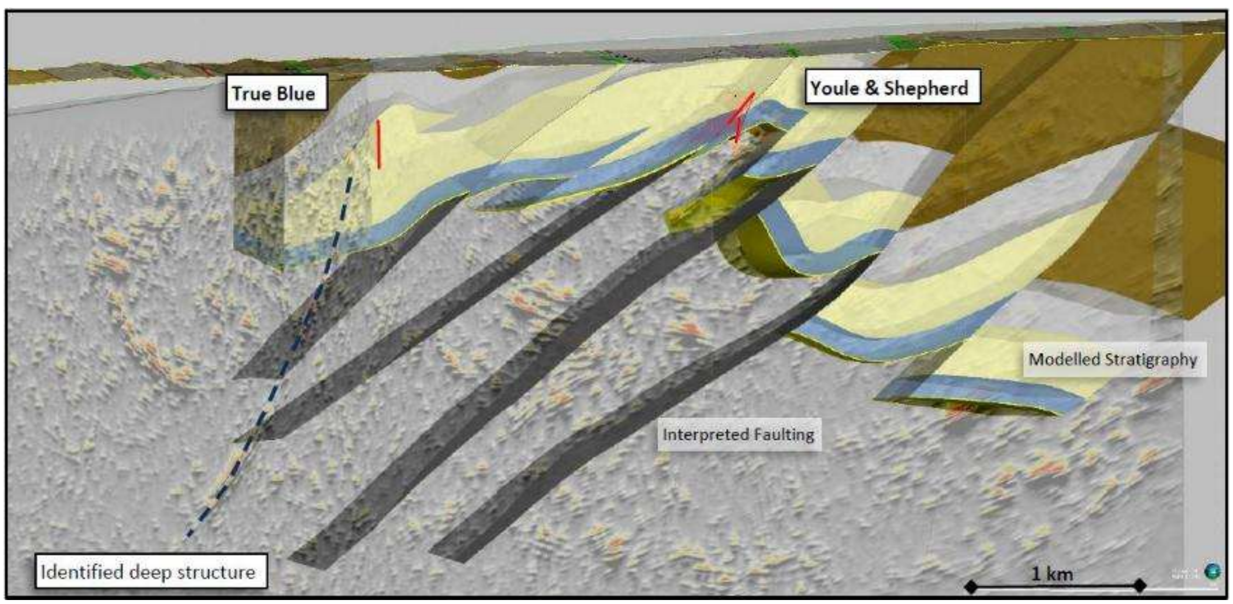

Figure 9: East-west section though Costerfield showing interpreted geology recent seismic traverse.

DISCOVERY THROUGH MINING

In a structurally complex deposit such as Costerfield, geological understanding is typically sufficient to support confident mining decisions; however, additional mineralisation is often revealed as development progresses. Rather than relying solely on extensive and costly drilling programs, the operation utilises an agile mine geology team equipped with the time, skills, and drilling capability required to identify small-scale splay veining and optimise extraction from existing orebodies. Mine and exploration geologists work closely together, allowing discoveries made during production to be rapidly assessed and advanced through targeted exploration. It is estimated that approximately 20% additional ore was identified during the mining of the Cuffley deposit. The success of this approach is also dependent on a responsive engineering team capable of adapting quickly to an evolving geological model.

CONCLUSION

The discovery success at Costerfield has been underpinned by a combination of high-quality geology, persistent exploration, and a willingness to challenge established interpretations. Over more than two decades of continuous operation, the mine has repeatedly replaced depletion through a series of discoveries made by integrating detailed structural analysis, stratigraphic understanding, geochemistry, and observations from active mining. Key advances have come from recognising the importance of fault offsets, favourable host stratigraphy, and the evolving structural framework of the Costerfield Dome. Equally important has been the close collaboration between exploration and mining teams, allowing new geological concepts to be rapidly tested and incorporated into targeting strategies. The continued success of Costerfield demonstrates that mature mining districts can still yield significant discoveries when geological models are continually refined and exploration remains driven by observation, curiosity, and disciplined interpretation.

REFERENCES

Alkane Resources (2025). Costerfield Resource & Reserve statements FY25. ASX Announcement, 15 October 2025

Alkane Resources (2026a). Alkane Advances Near-Mine Kendal Deposit with High Grade Antimony-Gold Intercepts at Costerfield. ASX Announcement, 25 February 2026

Alkane Resources (2026b). Costerfield - True Blue Exploration Update. ASX Announcement, 6 July 2026

McArthur Ore Deposit Assessments Pty Ltd. (2005) “Augusta Project, Mineral Resource & Reserve Assessment” (Report prepared for AGD Operations Pty Ltd) AGD Operations Pty Ltd.

Mandalay Resources (2025). Mandalay Intersects New High-Grade Gold-Antimony Veining & Expands True Blue with 27 g/t AuEq over 4.9 Meters”. TSX media release, 21 July 2025

HOUSE E.R., ARNE D.C. & PONTUAL S., (2014). The Hyperspectral Interpretation of Selected Drill Cores from Orogenic Gold Deposits in Victoria. Geological Survey of Victoria Technical Record 2014/1. Department of State Development, Business & Innovation.

WHITELAW H.S., (1926). The Costerfield Auriferous Antimony Veins. Geological Survey of Victoria Bulletin 50. Department of Mines, Victoria, 29 pp.

WILLMAN C.E., (2010). Gold Undercover - summary of geological findings: Exploring for buried gold in northern Victoria. GeoScience Victoria Gold Undercover Report 24. Department of Primary Industries.

UNRAVELLING COMPLEX POLYMETALLIC MAGMATIC-HYDROTHERMAL MINERAL SYSTEMS AT THE BYGOO TIN PROJECT

Ben Kimpton[1], Garry Dick[1], Greg Miles[1], Jon Hronsky[1]

[1] Caspin Resources Ltd, West Perth, WA, 6005.

Key Words: Tin, Wagga-Omeo Zone, Central Lachlan Orogen, Magmatic, Hydrothermal

INTRODUCTION

Primary Sn(-W) mineralisation occurs globally within highly reduced intrusion-related magmatic-hydrothermal mineral systems. Sn is increasingly recognised as a critical metal and has experienced a historic and sustained price increase as forecast demand is predicted to outstrip supply. Despite clear strategic importance, understanding of these systems remains arguably limited, specifically as it relates to exploration targeting (including undercover) and the synthesis of a unifying mineral systems model.

The Bygoo Tin Project (Caspin Resources Ltd) represents a globally significant laboratory for increasing understanding into these important mineral systems. Situated within the Wagga-Omeo Zone of the Central Lachlan Orogen, mineralisation is associated with increasingly fractionated pulses within the encompassing 414.7 ± 2.3 Ma (Bodorkos et al., 2013) reduced, ilmenite-series Ardlethan Granite. Deposits include greisen-hosted Sn (Kelpie Deposit; 3.94Mt @ 0.5% Sn for 19,300t of contained Sn) and breccia pipe-hosted Sn (Ardlethan Mine), while local occurrences also include sediment-hosted Sn and greisen-hosted W. The collective scale of magmatic-hydrothermal activity and associated mineralisation across the wider area is substantial. The Bygoo Project is situated at the intersection of several major trans-lithospheric structures which have allowed for voluminous, long-lived and readily evolving melt flux. Mineralised intrusions are likely derived from hybridisation of lower crustal partial melts and metasomatised upper mantle derived alkalic-mafic melts which have ascended through a large sedimentary reservoir (Ordovician Abercrombie Formation).

Ongoing exploration by Caspin has included geological mapping, surface geochemistry, Reverse Circulation (RC) drilling and extensive geophysical survey programs. Work has helped build rapidly evolving models for mineralisation and exploration targeting across the broader region. Critical learnings, driven in large part by geophysics, include recognition of highly fractionated granitic, variably textured intrusive pulses or sub-intrusions and associated alteration centres within the broader Ardlethan granite batholith. A series of major intersecting structures are observed to define sub-intrusion geometry and control the transport and concentration of mineralised hydrothermal fluids at both the deposit and regional scales. Importantly, these critical controls on Sn mineralisation have distinct signatures that are readily identifiable in magnetic, gravity and Induced-Polarisation (IP) datasets. In addition to learnings taken from sporadic outcrop and historical workings, the newly developed model allows for increasingly confident targeting of blind mineralisation across the Bygoo Project and prioritisation of land access negotiations. In addition to resource expansion drilling, targeting has defined a range of greisen targets directly surrounding the Kelpie Deposit, as well as a variable combination of greisen, breccia, sediment hosted and gold targets at Ardlethan, Bald Hill, Dullah and Gibsonvale.

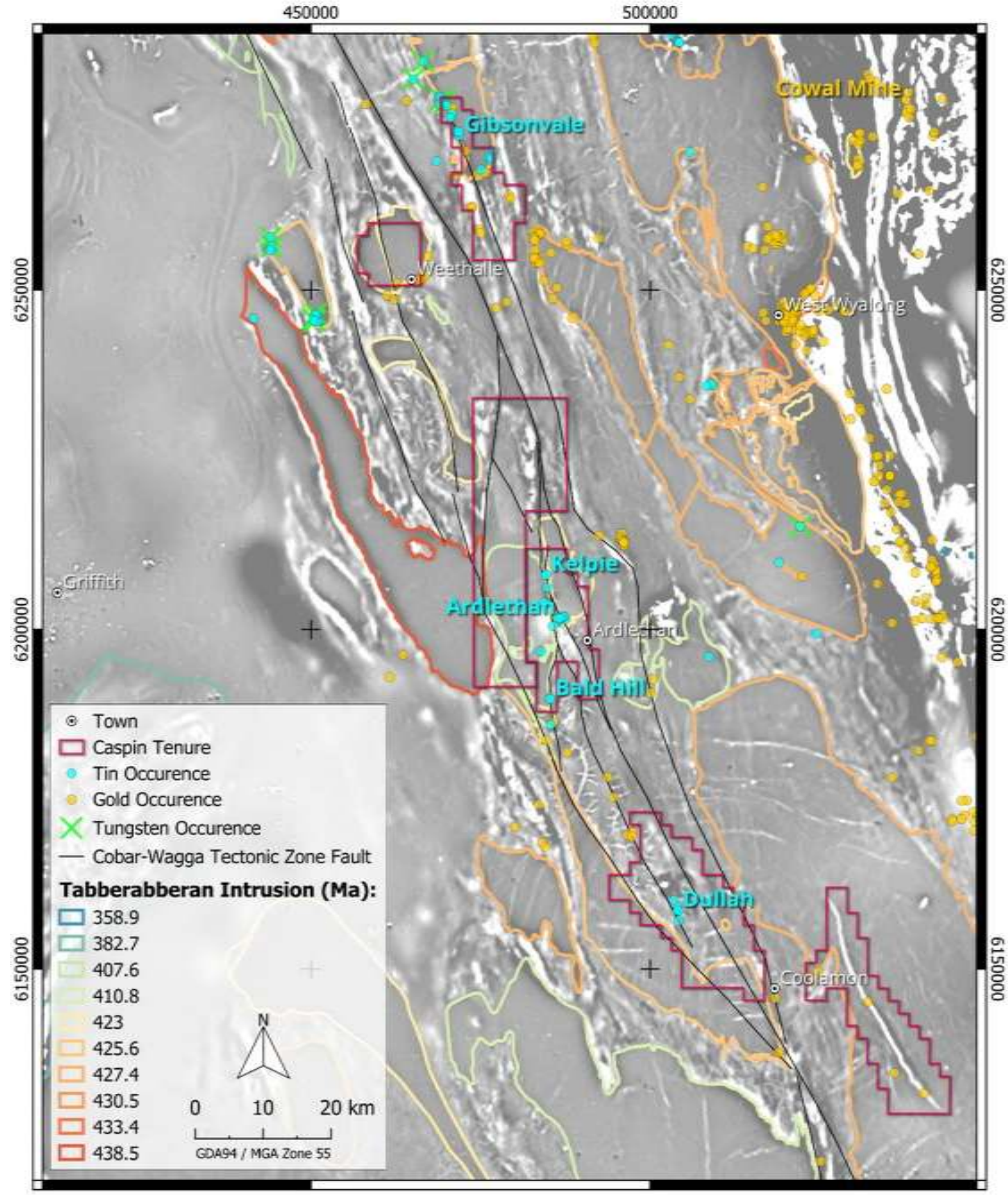

Figure 1. Location of the Bygoo Tin Project (Caspin Resources Ltd) in relation to prospective Siluro-Devonian Tabberabberan Intrusions of the Central Lachlan Orogen. Over NSW First Vertical Derivative of TMI RTP (1VD TMI RTP) Upward Continued to 250m.

KELPIE DEPOSIT AND SURROUNDS

Greisen-hosted cassiterite Sn mineralisation at Kelpie (Bygoo North, Little Bygoo) has seen a long history of artisanal mining and exploration dating back to the early 20th century (Godfrey, 1915). Caspin Resources defined a maiden inferred resource at Kelpie in 2025 of 3.94Mt @ 0.5% Sn for 19,300t of contained Sn. Mineralisation is hosted about the cupola of a late-stage highly fractionated and reduced pulse or sub-intrusion within the encompassing Ardlethan granite. Sn-bearing magmatic-hydrothermal fluids are readily transported along major NE trending fault structures. High-grade mineralisation is concentrated down a plunge defined by the intersection lineation of the intrusive hanging wall contact and cross-cutting faults. Ongoing resource and exploration drilling is focused on following existing lodes down-plunge where they remain open, and delineation of new lodes (e.g. Errol's) driven in large part by interpretation of repeated fault structures in Gradient Array Induced Polarisation (GAIP) imagery.

The Kelpie sub-intrusive suite and associated hydrothermal alteration halo are interpreted from overlapping gravity-high and magnetic-low zones, spanning an area of ~0.3km^2. The interpretation is supported by surface geochemistry signatures and geological mapping. A second variably textured sub-intrusive centre is defined from the same parameters entirely within the Ardlethan granite. Here, stockscheiders which may mark early stages of the magmatic-hydrothermal transition (Zhang et al., 2026) are observed locally on the edge of the sub-intrusion some 600-700m in-board of the main Ardlethan granite contact and the Kelpie resource. The second sub-intrusion appears to have a distinct metal deportment, with both Sn and minor W occurrences noted along intersecting structural planes. Despite the presence of significant historical workings here including shafts, no historical exploration drilling has been completed.

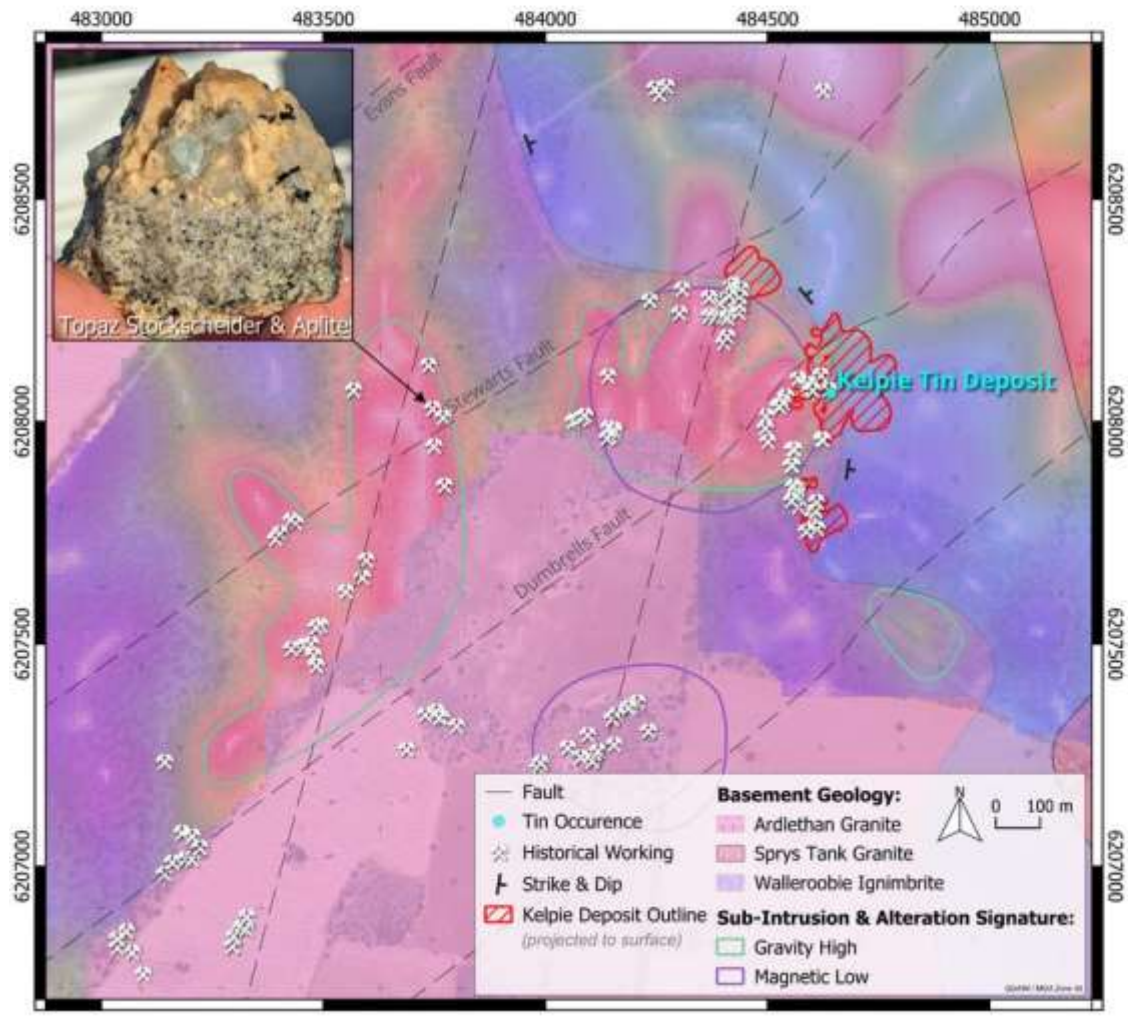

Figure 2. Kelpie Deposit and Surrounds highlighting sub-intrusion and alteration centres visible in magnetic and gravity imagery, crosscut by prominent faults in GAIP imagery which serve as dominant pathways for hydrothermal fluids. Over ground gravity (KelpieA_OTB2p39_Bp_Hwet) and satellite imagery.

REGIONAL TARGETS AND MINERAL SYSTEMS FRAMEWORK

Sn mineralisation and historical occurrences are observed over large portions of the outcropping Ardlethan granite, although the majority remains buried under both thin shallow and residual cover. Ongoing exploration by Caspin has focused primarily on discovering blind breccia pipe and sediment-hosted tin within the Ardlethan near-mine area 'Ardlethan East'. Expansive hydrothermal alteration halos in Ordovician Sediments are now recognised at Ardlethan East, with geochemistry and geophysics allowing for prioritisation of a range of targets primarily at major structural intersections. Aeromagnetic and ground gravity data has allowed for precise mapping of the main Ardlethan granite contact undercover which has highlighted Kelpie-style exploration opportunities at Ardlethan South, Taylors Hill and Bald Hill. Numerous Sn and W occurrences are noted throughout these areas; however, historical exploration and drilling remain limited.

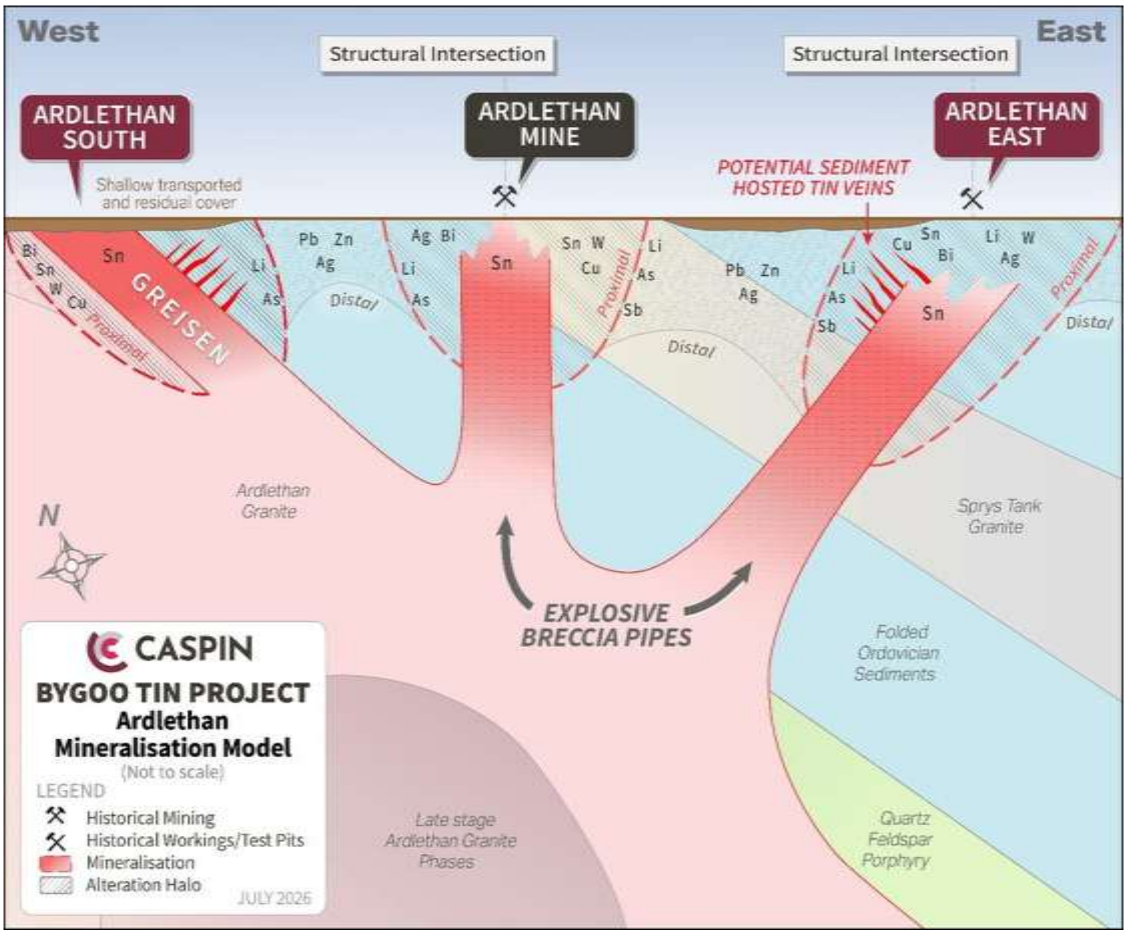

Figure 3. Model for various prospective mineralisation styles in the Ardlethan area, especially highlighting the importance of large hydrothermal alteration halos for vectoring to blind occurrences.

Historical mining of sediment hosted Sn occurred at the Dullah prospect, while Gibsonvale is unique for hosting closely overlapping (<1km lateral distance) historical occurrences of hardrock Sn, W and Au mineralisation associated with the Tabberabberan Kikoira Granite. Study and exploration of these prospective polymetallic zones in the Gibsonvale area are considered especially important for growing understanding of magmatic-hydrothermal Sn, W and Au systems.

Sn mineralisation in the Central Lachlan Orogen and globally is associated with highly reduced, ilmenite-series granitic intrusions. Unlike similar magmatic-hydrothermal mineral systems, a unifying mineral systems framework is not commonly recognised. Like other Sn-W belts globally, Reduced Intrusion Related Gold (RIRG) deposits are spatiotemporally associated at the belt scale (Thompson et al., 1999). Although the RIRG model is underexplored in the district, it is recognised as a style of mineralisation associated with contemporaneous Tabberabberan intrusions. A large and enigmatic magnetic and moderately dense intrusion is noted at the Bygoo Project and is thought to immediately precede the late Sn mineralised stages of the Ardlethan Granite. The deep geophysical anomaly dubbed 'Kraken' sits well in-board of the main Ardlethan granite contact and therefore postdates magnetic extrusive suites. It is hypothesised that in areas of significant hybridised melt flux with adequate sedimentary reservoirs; highly Reduced Intrusion Related Tin (RIRT) systems may represent Au depleted endmembers of a melt evolution that can include an immediately preceding generation of intermediate moderately reduced IRG systems. Where varying degrees of potentially rapid crustal assimilation as a function of depth or lateral emplacement may define a predictable melt continuum. The Kraken target represents a globally unique opportunity to test this theory with deep diamond drilling.

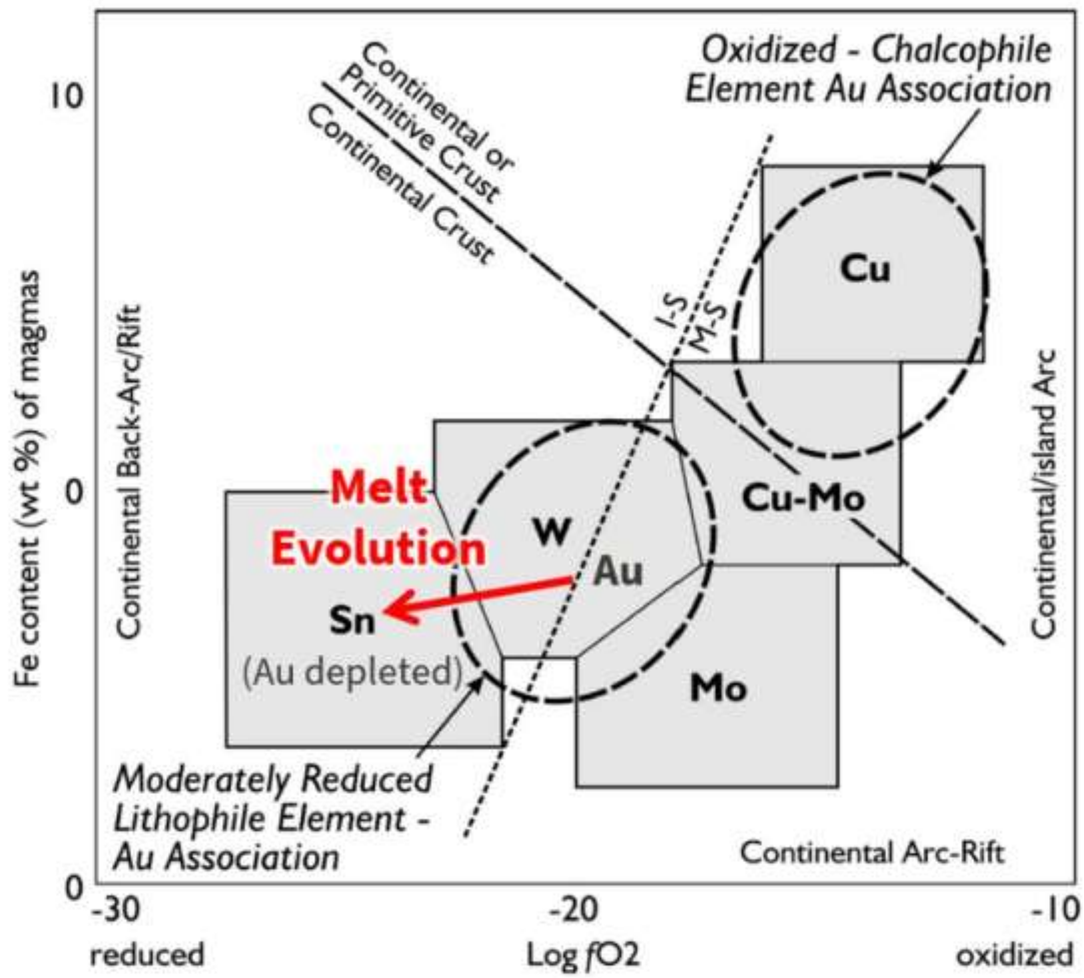

Figure 4. Hypothesised evolution of Moderately Reduced Intrusion Related Au-W-Cu (RIRG) to Au depleted, Highly Reduced Intrusion Related Tin (RIRT). After Thompson et al. (1999).

ACKNOWLEDGEMENTS

- Fiona Letchford, Evan Brittlebank, Dave McInnes (Montana GIS), Dr Roger G. Taylor, Kelvin Blundell
- NSW Resources (Critical Minerals and High-Tech Metals Exploration Program)
- The London Hotel Ardlethan, Resolution Drilling, AMWD Drilling, Daishsat Geodetic Surveyors, Merlin Geophysical Solutions and Planetary Geophysics

REFERENCES

BODORKOS, S., BLEVIN, P. L., SIMPSON, C. J., GILMORE, P. J., GLEN, R. A., GREENFIELD, J. E., & QUINN, C. D. (2013). New SHRIMP U-Pb zircon ages from the Lachlan, Thomson and Delamerian orogens, New South Wales. Tech. Rep. GS2013/0427, Geological Survey of New South Wales, Maitland.

CASPIN RESOURCES LIMITED. (2025, September 1). Maiden resource estimate with significant growth potential at the Bygoo Tin Project [ASX announcement]. Australian Securities Exchange.

GODFREY, J. R. (1915). Report Upon the Ardlethan Tinfield (No. 20). WA Gullick, government printer.

MATTHEWS S.J. (2026). New South Wales Statewide magnetic merge, version 4.0 [Digital Dataset]. Geological Survey of New South Wales, Department of Primary Industries and Regional Development, Maitland.

THOMPSON, J. F. H., SILLITOE, R. H., BAKER, T., LANG, J. R., & MORTENSEN, J. K. (1999). Intrusion-related gold deposits associated with tungsten-tin provinces. Mineralium Deposita, 34(4), 323-334.

ZHANG, X., ZHAO, J., GUO, C., WEBB, S., QIN, K., WU, F., & ZHOU, Q. (2026). Fluids in stockscheiders record the magmatic-hydrothermal transition in rare-metal granites. Lithos, 108562, 536-537.

A TALE OF TWO BASINS: UNDERSTANDING THE SILURODEVONIAN BACK-ARC BASINS OF THE LACHLAN OROGEN

Fitzherbert J.A., Simpson B.P., Mahoney L. and Downes P.M.

Geological Survey of NSW

Key Words: eastern/central Lachlan Orogen, Cobar Basin, Hill End Trough, basement terrane, successor basin, isotopes, metamorphism, deformation.

INTRODUCTION

The Siluro-Devonian successor basins of the Lachlan Orogen developed following the Benambran Orogeny, which amalgamated the Ordovician Macquarie Arc and flanking turbidite packages of the Wagga, Hermidale and Bega terranes to the east Gondwanan margin (Glen et al 2007). Subsequent eastward migration of subduction established a broad back-arc setting where the successor extensional basins developed over the deformed and heterogeneous substrate (Oversby 1971; Scheibner & Basden 1998; Collins 2002; Glen 2005). We consider the contrasting evolution of two spatially separated Siluro-Devonian basins, the Cobar Superbasin in the central Lachlan Orogen (CLO) and the Hill End Trough–Goulburn Basin in the eastern Lachlan Orogen (ELO) (Figure 1). Although both basins formed within the same regional tectonic setting, they display fundamentally different magmatic, metallogenic and thermal histories, with differences primarily reflecting the nature of the underlying basement terranes and subsequent modification during orogenesis. This discussion presents new data and ideas but necessarily relies on a vast published database and many ideas/models from past workers that unfortunately cannot all be cited.

BASEMENT ARCHITECTURE, MAGMATIC PROVINCES AND CONTRASTING BASIN EVOLUTION

Fundamental differences in the Cambro-Ordovician basement substrate between the central and eastern Lachlan Orogen are expressed as zones of unique Siluro-Devonian magmatic character (e.g. S/I line of Chappell et al 1988); a crustal-scale seismic interpretation of the present-day basement configuration is presented in Figure 1 (Mahoney et al. 2024, 2026) and the changing character of magmatism over time and space is illustrated in Figure 2. The major basement elements relevant to the Siluro-Devonian basins discussed here are the Wagga, Hermidale, Macquarie Arc, Bega and Kosciuszko terranes, that have been defined and discussed in the extensive body of prior work (e.g. Chappell et al 1988; Direen et al 2001; Glen et al 2002; Finlayson et al 2002; Vassallo & Glen 2003; Glen et al 2007; Doublier & Korsch 2024; Connors 2024; Mahoney et al 2024, 2026).

The Wagga Terrane comprises structurally thickened continental-derived turbidite underlain by attenuated continental crust (Delamerian/Neoproterozoic?) and is characterised by predominantly S-type and A-type magmatism in basement and successor basin. In contrast, the Hermidale and Bega terranes are interpreted as comprising continental-derived turbidite thrust imbricated with or underlain by oceanic crust and are characterised by predominantly I-type magmatism in basement and successor basin. The Macquarie Arc terrane is the most compositionally juvenile and characterised by I-type magmatism in basement and successor basin. The Kosciuszko Terrane displays characteristics consistent with continental basement, reflected in a mixed S-type and subordinate I-type magmatic signature along its length.

These basement terranes influenced the spatial and temporal evolution, as well as the volcanic character of the back-arc basin development that followed (Summarised here from Colquhoun et al (2026) and GSNSW explanatory notes referenced therein). The key magmatic features of the CLO and ELO are depicted in Figure 2 and involve:

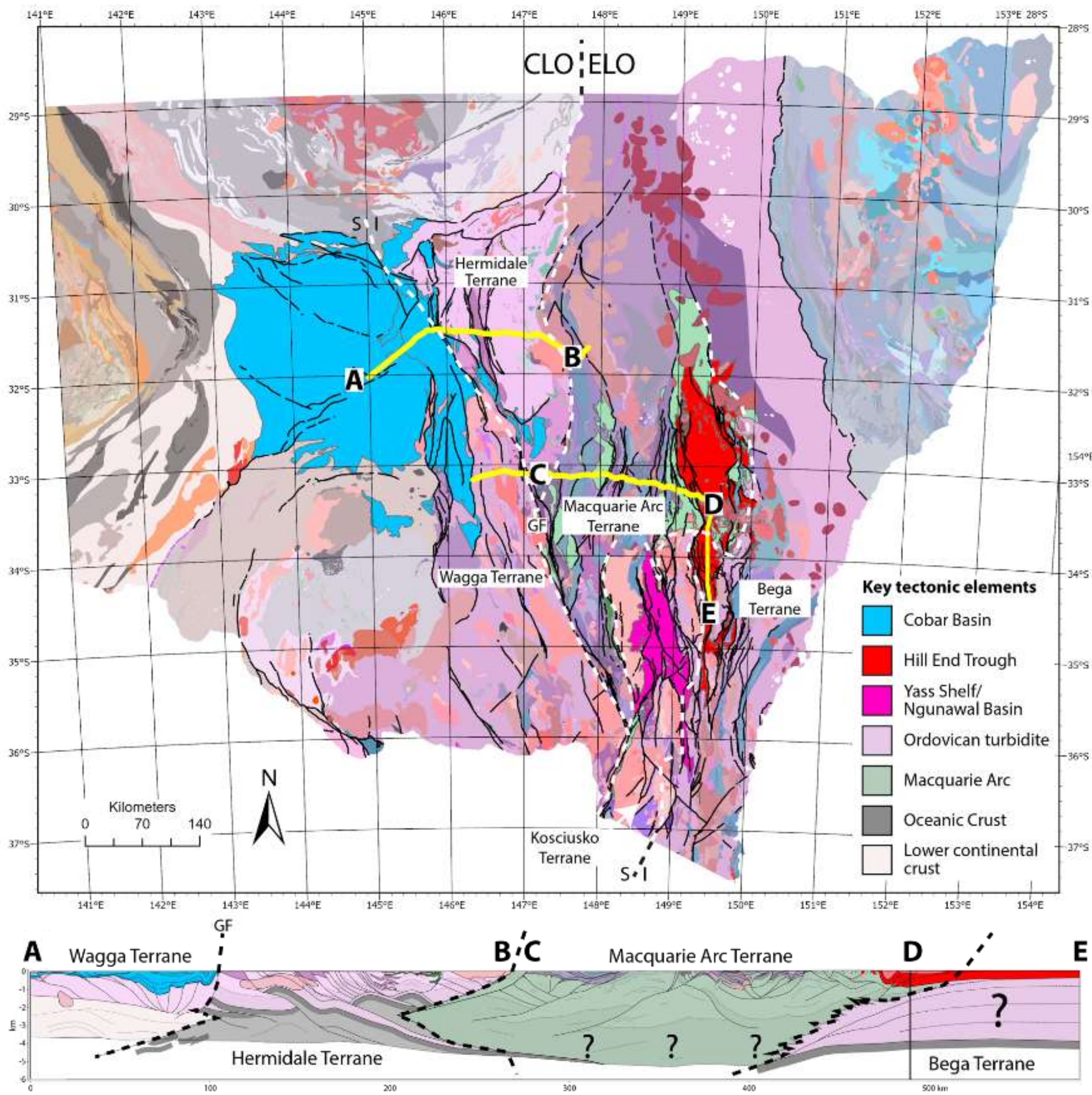

Figure 1. Simplified geological map and schematic based on composite seismic section representing the main tectonic elements discussed. Northern seismic transect (A-B) is a composite line comprising 23NSW-CY1 and 25NSW-CL2, while the southern transect (C-D) is line 25NSW-CL1 (mod. from Mahoney et al. 2024, 2026). The schematic is jump tied along the Gilmore Fault (GF) zone (i.e. B-C). Transect D-E is purely interpretive.

435-423 Ma early extension to peak-rift in the ELO

Widespread subaerial and shallow-marine volcanism in the eastern Lachlan Orogen between 435 and 423 Ma, particularly within the Canberra–Yass Shelf (S-type over Kosciusko Terrane) and Ngunawal Basin (I-type over Bega Terrane). This period culminated in extensive peak rift submarine volcanism within the southern Hill End Trough and Goulburn Basin (Bega Terrane) but is also recorded in basal sequences of the Mumbil Shelf, Cowra Trough, northern Hill End Trough and Capertee High. These volcanic successions are closely associated with the main period of VMS (volcanogenic massive sulfide) mineralisation in the ELO (e.g. Captains Flat, Woodlawn, Wet Lagoon and Lewis Ponds). In contrast, the central Lachlan Orogen records exclusively S-type intrusive magmatism during over this time interval.

423-415 Ma peak rift in the CLO and sag transition in ELO

The Cobar Superbasin records peak rift phase submarine volcanism between 423–415 Ma focused in volcanic troughs and early rift shallow marine environments over the Wagga and Hermidale terranes. The main phase of submarine volcanism has been linked with possible VMS mineralisation (e.g. Mallee Bull; Edgecombe & Soininen 2019). In the southern Wagga Terrane, the Siluro-Devonian volcanism is exclusively subaerial (predominantly S-type in the Riverina High) occurring between 419–418 Ma. By comparison, in the eastern Lachlan Orogen there is a continuous I-type intrusive magmatic record over this period, but much of the Hill End Trough–Goulburn Basin had already commenced thermal subsidence. Volcanic activity diminished (still recorded on the Mumbil Shelf, Capertee High and subaerial volcanism in the Ngunawal Basin) and thick siliciclastic and volcaniclastic sequences began accumulating throughout the basin system.

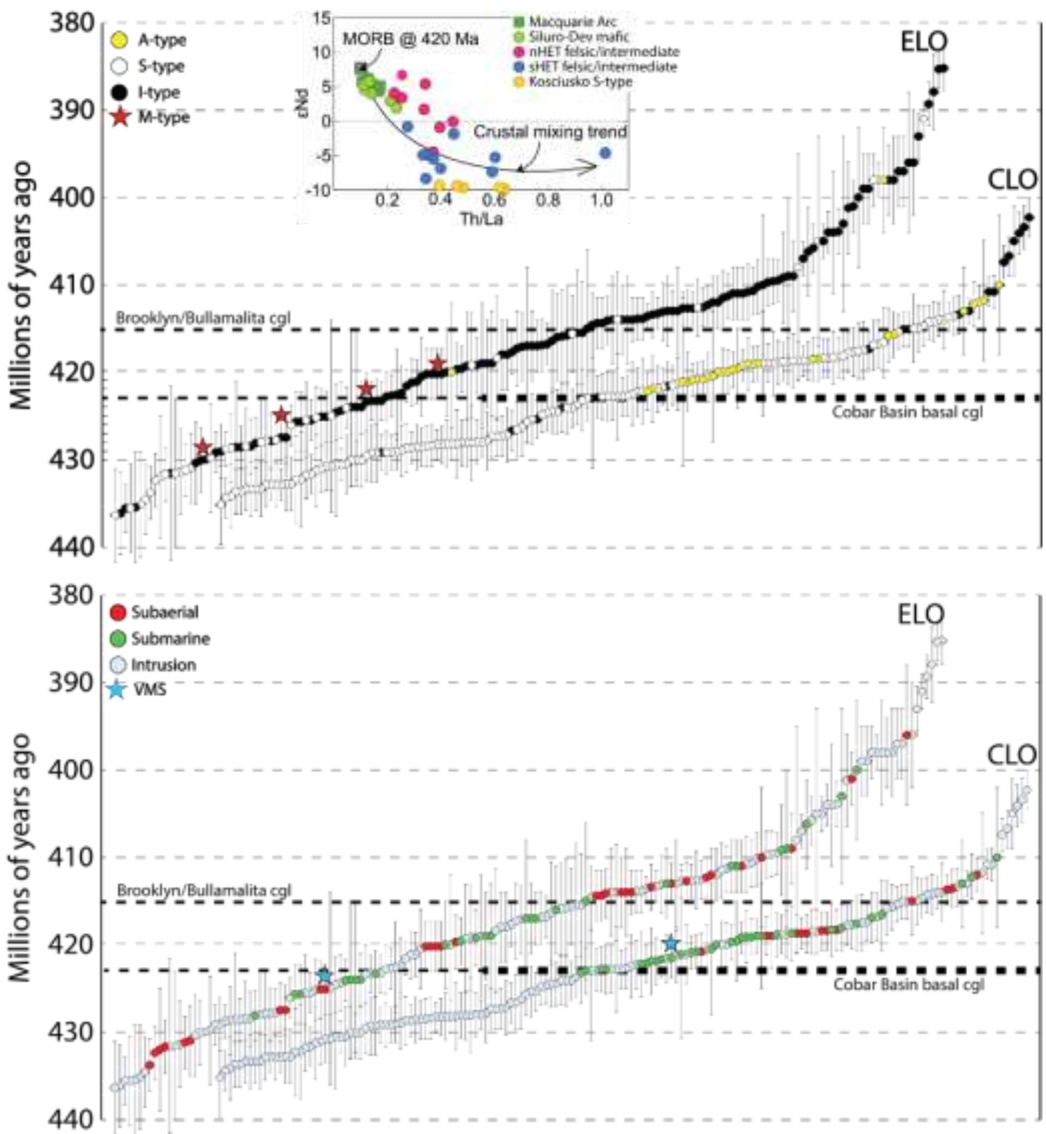

Figure 2. Plot of all (within reason) available U-Pb zircon geochronology for igneous rocks of the CLO and ELO symbolised according to, a) igneous rock S-I-A-M classification (Chappell et al 1988) and b) three different geological settings, intrusion, submarine volcanic and subaerial volcanic (from Colquhoun et al 2026). εNd V Th/La inset data from this study, Maas et al (1987) and Carr et al (2003). nHET = northern Hill End Trough; sHET = southern Hill End Trough–Goulburn Basin.

415-408 Ma ELO renewed volcanism and CLO sag transition

The eastern Lachlan Orogen experienced renewed subaerial volcanism across the Bungonia and Yass shelves, while the CLO records a smaller volcanic pulse in the Cobar Superbasin represented by the Shepherds Hill and Tarran volcanics. Towards the end of this period the Cobar Superbasin had commenced thermal subsidence, and thick siliciclastic sequences were accumulating within the deep-water parts of the basin.

BASEMENT ARCHITECTURE, SILURO-DEVONIAN MAGMATISM AND VMS POTENTIAL

Based on current understanding, key controls on the development of a VMS mineralisation relevant to this discussion include, an extensional setting, crustal-scale fault systems, deepwater setting, seafloor or near seafloor interface, character of intrabasin magmatism, size and abundance of subvolcanic intrusions, and direct mantle involvement (e.g. Galley et al 2007; Shanks et al 2012; Tornos et al 2015; Hart et al 2004; Yang & Scott 1996), along with evidence such as seafloor exhalation and metal ratios consistent with direct leaching of footwall stratigraphy.

Both the Cobar Superbasin and Hill End Trough–Goulburn Basin developed in a tectonic setting favourable for VMS mineralisation involving rifting over or adjacent to crustal-scale boundaries and rapid subsidence during the early stages of back-arc extension combined with discrete intervals of magmatism at or near paleo-seafloor (e.g. Edgecombe & Soininen 2019; Fitzherbert & Downes 2020; Deyssing & Fitzherbert 2017; Thomas & Pogson 2012).

The Cobar Superbasin occupies the transition between the continental Wagga Terrane and the more juvenile crust of Hermidale Terrane. Despite being developed largely over buoyant continental crust, the basin evolved to accommodate deep marine deposition around the terrane boundary. Mineralisation is often associated predominantly with continental crust derived felsic S/A-type magmatism and resembles a continental–margin felsic association VMS system with some characteristics like the Iberian Pyrite Belt and Bathurst mining camp (Yang & Scott 2003). Metal associations are dominated by Zn–Pb–Ag in the western-central Cobar Basin (e.g. Mallee Bull), consistent with the leaching of the footwall stratigraphy. Conversely, the turbidite-hosted Cu(Zn)–Au(Ag)-rich orebodies of the eastern Cobar Basin (e.g. CSA mine) are a mismatch for their footwall. There is limited evidence for seafloor exhalation, exposed subvolcanic intrusions are rare, and there is little evidence for a direct mantle input.

In contrast, the southern Hill End Trough–Goulburn Basin (and Ngunawal Basin) developed over the more juvenile mixed turbidite/oceanic crust of the Bega Terrane. Mineralisation is associated predominantly with intermediate to felsic I-type and mafic M-type volcanism resembling a continental-margin intermediate/felsic-bimodal association VMS system akin to Kuroko-style (Shanks et al 2012). Metal associations are consistent with leaching of the footwall stratigraphy, varying from Pb–Zn-rich to Cu-rich between felsic and mafic footwall volcanics. There is abundant evidence for seafloor exhalation (the region hosts most barite occurrences in the Lachlan Orogen), extensive bimodal subvolcanic intrusions are commonly exposed, and direct mantle input is common throughout the stratigraphy.

The northern Hill End Trough represents its own unique metallogenic environment, having developed over the juvenile Macquarie Arc Terrane. Mineralisation here is associated with intermediate to felsic I-type and rare M-type volcanism broadly resembling the intermediate/felsic-bimodal association VMS system of the southern Hill End Trough. However, a key difference when compared with the volcanics of the southern Hill End Trough is that volcanics here display distinctly less evidence for crustal contamination (Figure 2 inset), consistent with Macquarie Arc basement. There is some evidence for seafloor exhalation, exposed subvolcanic intrusions are small or unknown, and there is limited direct mantle input into the basin.

ISOTOPIC CONSTRAINTS ON METAL SOURCE AND AGE OF MINERALISATION

Lead isotopes in the Lachlan Orogen are typically discussed in terms of the plumbotectonic model of Carr et al (1995) which affords a visual representation of both age and the mantle versus crustal signatures of mineralisation (See also Huston et al 2016; Liebmann et al 2024). There are two simple isotope ratio maps relevant to this study, μ = calculated U^{238}/Pb^{204} (Figure 3a; Stacey & Kramers 1975); illustrates mantle versus crustal Pb sources) and $Pb^{206}/^{204}$ (Figure 3b; illustrates ~Pb extraction age). Lead isotopes for successor basin mineralisation display first order variation that correlates with different basement terranes, and second order, intrabasin variation associated with inferred/observed magmatism.

Where successor basins are developed over siliciclastic turbidite (Cobar Superbasin and southern Hill End Trough) the first order Pb isotope signature is high μ and crustal (Figure 3a). Second order variation for the Cobar Superbasin involves a shift to lower μ in areas hosting skarn mineralisation and/or limited mafic magmatism (Hera/Nymagee/Federation and Norma Vale; e.g. Fitzherbert et al 2021) as well as Yellow Mountain/Blind Calf/Mineral Hill in the Kopyje Shelf. Second order variation for the southern Hill End Trough involves a shift to lower μ centred around the mafic-volcanic associated Currawang deposit. In contrast, the northern Hill End Trough has developed over the low-μ Macquarie Arc Terrane and displays a basin-wide first order lower μ (mantle contaminated) when compared to basins developed over siliciclastic turbidite.

Lead extraction ages can be calculated where continental crust Pb is dominant and there is noteworthy contrast between the Cobar Superbasin v southern Hill End Trough–Goulburn Basin (Figure 3b). The Cobar Superbasin is dominated by ratios consistent with Pb extraction between 400–380 Ma, reflecting known ages for mineralisation during the Tabberabberan Orogeny (Fitzherbert & Downes 2020). Older Pb extraction ages (ca. 420 Ma) occur in the central Cobar Basin (e.g. Mallee Bull) and parts of the Kopyje Shelf, where syn-volcanic VMS and epithermal mineralisation have been proposed (Edgecombe & Soininen 2019; Fitzherbert & Downes 2020). In contrast, the southern Hill End Trough/Goulburn Basin displays Pb extraction ages exclusively between 425–415 Ma consistent with the proposed syn-volcanic genesis (e.g. Deyssing & Fitzherbert 2017). Lead isotope data from the northern Hill End Trough displays variable mantle Pb input and is not easily correlated with crustal growth curve ages and thus not considered further in this context.

Sulfur isotope systematics in the Lachlan Orogen are typically considered in terms of simple reservoirs, such as isotopically heavy (more +ive $\delta^{34}S$) values for seawater/formational derived, versus isotopically lighter (less +ive to -ive $\delta^{34}S$) values for magmatic influences (e.g. Fitzherbert & Downes 2020). Much like the variation for μ above, sulfur in successor basin mineralisation displays first order variation that correlates with different basement terranes (Figure 3c). A first order isotopic shift is evident from heavy isotopic values characteristic of basins that overly the turbidite-dominant Wagga and Bega terranes (Cobar Basin & southern Hill End Trough/Goulburn Basin) to lighter isotopic ratios characteristic of the northern Hill End Trough/Mumbil Shelf that overly the Macquarie Arc Terrain. Second order variation in the Cobar Basin involves a shift from heavier isotopic values in the central-western Cobar Basin to lighter isotopic values preserved in the Hera–Nymagee–Federation and Mount Solar/Solitary areas where skarns and deep-seated intrusions are recorded/inferred; intermediate ‘mixed’ isotopic ratios are preserved in the Cobar Mineral Field where distal igneous influence has been inferred. This transition from heavy to light $\delta^{34}S$ generally coincides with a switch from Pb-Zn-Ag dominant to Cu-Au dominant mineralisation. Second order variation in the southern Hill End

Trough involves a shift from dominantly heavier sulfur isotope ratios throughout the basin to lighter ratios centred around mafic magmatism at the Currawang copper mine. Changing isotopic ratios display coincidence with changes in metal commodity.

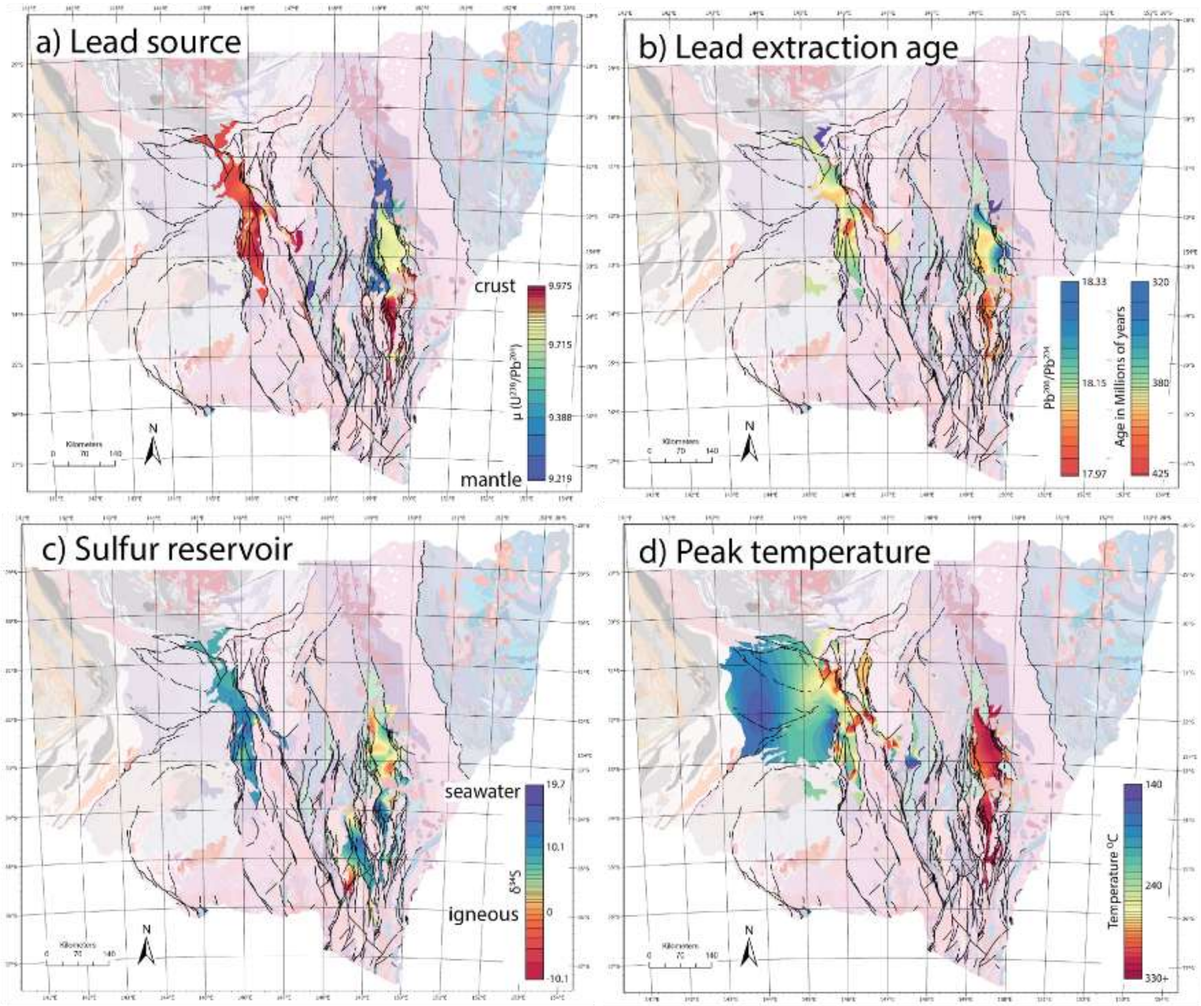

Figure 3. Heat style interpolation maps for key isotopic and thermal characteristics of the Cobar Basin and Hill End Trough discussed here. Map constructed from a/b) >1,600 Pb isotope analyses, c) >4,700 S isotope analyses, and d) >300 Kubler index analyses. Pb^{206}/Pb^{204} values have been approximately calibrated against know ages for mineralisation in the Cobar Basin.

POST DEPOSITIONAL MINERALISATION AND METAMORPHISM IN THE SILURO-DEVONIAN SYSTEM

The Cobar Superbasin and Hill End Trough–Goulburn Basin record markedly different post-depositional histories, with the discriminatory characteristics relevant to this discussion being, distribution of peak metamorphic grade and age of mineralisation/deformation (Figure 3d, 4).

First order variation in peak metamorphic temperature is characterised by an eastward temperature increase from sub-greenschist in the Cobar Basin to middle-greenschist in the Hill End Trough–Goulburn Basin (Figure 3d), synonymous with increased intensity of deformation (Fergusson & Colquhoun 2021). Second order variation within the Cobar Basin is characterised by a transition from sub-greenschist temperatures in the western-central to lower-greenschist in the eastern parts of the basin. This eastward temperature increase coincides with change from Pb–Zn–Ag-dominant to Cu(Zn)–Au(Ag) dominant mineralisation, with highest temperatures coinciding with distal skarn and zones of inferred distal intrusion influence; high temperatures also coincide with deeply exhumed parts of the stratigraphy. By contrast the exposed levels of the Hill End Trough–Goulburn Basin record uniform, higher temperature middle-greenschist facies peak metamorphism.

The age of mineralisation and deformation is complicated, but fundamentally different between these basin systems (Figure 4). For the Cobar Superbasin (CLO) direct dates from mineralisation mostly fall between 410-380 Ma consistent with Tabberabberan inversion related orogenic base-metal systems, with rare syn-depositional ages (ca 420–415 Ma) encountered at Mallee Bull, Mineral Hill and Norma Vale (Fitzherbert & Downes 2020). Foliation formation has been dated between 400–380 Ma, consistent with deformation during peak Tabberabberan metamorphism (Fitzherbert & Downes 2020 and references therein). Recent Ar–Ar dating of granites in the region has resolved a lower temperature (<200°C) Kanimblan (360–320 Ma) thermal event that is almost exclusively recorded by K-feldspar (Simpson et al 2026). For the Hill End Trough (ELO), many of the base-metal systems are considered to be syn-volcanic at ca. 423 Ma (Downes 2009), and there are few direct dates on mineralisation other than those for the orogenic gold systems overlying the Macquarie Arc terrane at 360–340 Ma, consistent with Kanimblan deformation (Lu et al 1996; Downes 2019). The age for foliation development in the Hill End Trough is mostly Carboniferous, with locally preserved Middle Devonian (Tabberabberan) ages more commonly preserved in basement rocks and intrusions (Forster et al. 1999; Glen et al. 1999; Lu et al 1996; Lennox et al 2014). There is little recorded Tabberabberan Orogeny aged mineralisation in the Hill End Trough, although Hill et al (2026) described a base-metal vein system in the Capertee High (Dead Horse–Havilah prospect) with a crustal Tabberabberan age Pb isotope signature akin to the mineralisation in the Cobar Superbasin. Work is ongoing to determine how common Tabberabberan age base-metal systems are in the Hill End Trough–Goulburn Basin system.

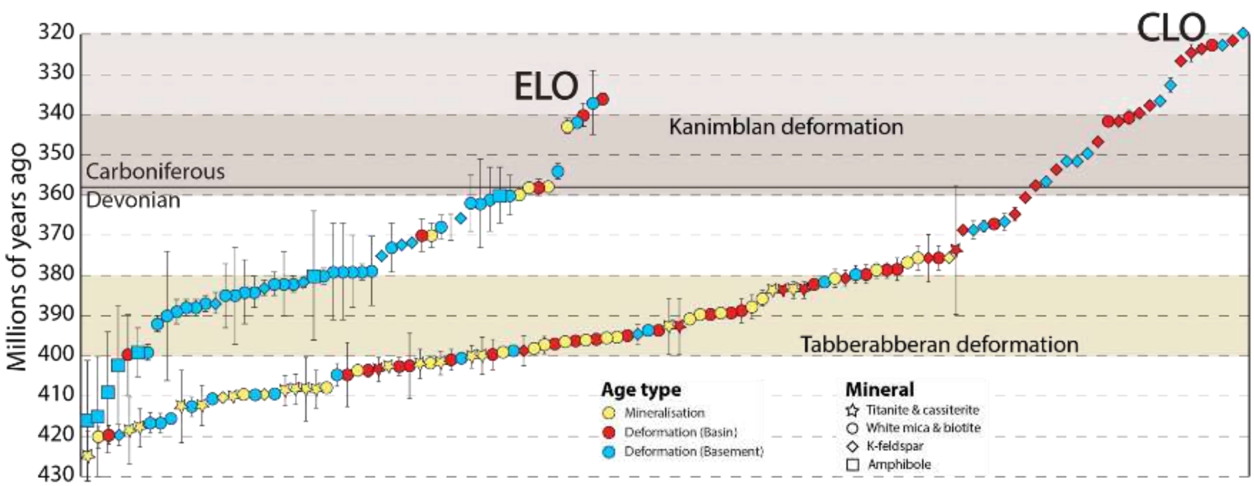

Figure 4. Plot of all (within reason) available geochronology for deformation and mineralisation in the CLO and ELO symbolised according to age type (mineralisation, in basin deformation, in basement deformation/granite) and mineral dated. Data sources are covered in the text, see also GSNSW MinView portal (https://minview.geoscience.nsw.gov.au/#/?lon=148.5&lat=-32.5&z=7&l=).

SUMMARY

Basement architecture imposes first order control on Siluro-Devonian successor basin evolution in the Lachlan Orogen, including character (composition/environment of deposition) of volcanism, metal/fluid source, and in combination with proximity to accretionary boundaries affects the style of overprinting deformation and orogenic mineralisation.

The Cobar Superbasin developed over the Wagga/Hermidale terrane boundary. Its evolution was dominated by S-type and A-type felsic magmatism derived largely from continental crust. Peak volcanic activity, with potential for felsic-association VMS-style mineralisation occurred between 423–415 Ma; this localised supracrustal felsic association is not ideal for VMS-type systems, and the system lacks a strong heat engine. In contrast, the Hill End Trough–Goulburn Basin developed largely over the more juvenile Bega and Macquarie Arc terranes characterised by I-type and mafic magmatism, stronger mantle input, abundant submarine volcanism and extensive seafloor hydrothermal activity. This setting produced VMS systems such as Captains Flat, Woodlawn and Lewis Ponds during peak rifting ca. 435–423 Ma. Overall, volcanism and mineralisation commenced in the Hill End Trough–Goulburn Basin and progressed westward over ~5 million years period into the Cobar Superbasin, with VMS mineralisation restricted to the early rift phase of each basin.

Lead and sulfur isotope data demonstrate strong links between basement architecture and metal sources. The Cobar Basin and southern Hill End Trough/Goulburn Basin display predominantly crustal Pb isotopic signatures and seawater/formation sulfur over the Wagga and Bega terranes; deviation to greater mantle input is associated with restricted Siluro-Devonian mafic magmatism. Conversely, the northern Hill End Trough–Goulburn Basin records a greater mantle metal/sulfur contribution over the Macquarie Arc.

The two basins experienced markedly different post-depositional histories. Most economic mineralisation and deformation in the Cobar Superbasin is linked to Tabberabberan inversion between about 410–380 Ma (with rare VMS recorded), whereas the Hill End Trough–Goulburn Basin largely preserves syn-volcanic VMS mineralisation formed during basin development and was more strongly affected by later Carboniferous Kanimblan deformation with orogenic gold systems developed in the basin, particularly over the Macquarie Arc. Regional metamorphic grade increases eastward from relatively low-grade conditions in Cobar Superbasin to middle-greenschist facies in the Hill End Trough–Goulburn Basin. This increased deformation/metamorphism reflects proximity to the Carboniferous accretionary boundary between the New England and Lachlan Orogens and may mask Tabberabberan age inversion-related mineralisation in the Hill End Trough.

REFERENCES

CARR G.R., DEAN J.A., SUPPEL D.W. & HEITHERSAY P.S., 1995. Precise lead isotope fingerprinting of hydrothermal activity associated with Ordovician to Carboniferous metallogenic events in the Lachlan fold belt of New South Wales. Economic Geology 90,1467–1505.

CARR P. F., FERGUSSON C. L., PEMBERTON J. W., COLQUHOUN G. P., MURRAY S. I. & WATKINS J. 2003. Late Ordovician island-arc volcanic rocks, northern Capertee Zone, Lachlan Fold Belt, New South Wales. Australian Journal of Earth Sciences 50(3), 319–330.

CHAPPELL B.W., WHITE A.J.R. & HINE R. 1988. Granite provinces & basement terranes in the Lachlan Fold Belt, southeastern Australia. Australian Journal of Earth Sciences 35, 505–521.

COLLINS W.J. 2002. Nature of extensional accretionary orogens. Tectonics 21(4), 1258–1272.

COLQUHOUN G.P., BALLARD J.C., HUGHES K.S., DEYSSING L., FOLKES C.B, PHILLIPS G., TROEDSON A.L. & FITZHERBERT J.A. 2026. New South Wales Seamless Geology dataset, version 2.6 [Digital Dataset]. Geological Survey of New South Wales, Department of Primary Industries & Regional Development, Maitland.

CONNORS K. 2024. Importance of crustal type & architecture to exploration: a new look at the eastern Lachlan Orogen. In Greenfield, J.E. (compiler), 2024. Bulletin 76: Discoveries in Tasmanides 2024. Australian Institute of Geoscientists, PO Box 576 Crows Nest NSW 1585.

DEYSSING L. & FITZHERBERT J.A. (compilers). 2017. Braidwood 1:100 000 Geological Sheet 8827, 2nd edition, Explanatory notes. Geological Survey of New South Wales, Maitland.

DIREEN N. G., LYONS P., KORSCH R. J. & GLEN R. A. 2001. Integrated geophysical appraisal of crustal architecture in the eastern Lachlan Orogen. Exploration Geophysics 32, 252–262.

DOUBLIER M. & KORSCH R.J. 2024. Major Crustal Boundaries of Australia (2D) - 2024 Edition. Commonwealth of Australia (Geoscience Australia) dataset.

Downes P.M. 2009. Sulfur- & lead-isotope signatures of selected middle Silurian to Carboniferous mineral systems of the Lachlan Orogen, eastern New South Wales — implications for metallogenesis. PhD thesis, University of Newcastle (unpublished).

DOWNES P.M. 2019. A mineral system model for orogenic gold mineralisation in the eastern Lachlan Orogen, New South Wales. Unpublished Geological Survey of New South Wales report 2019/0173.

EDGECOMBE D. & SOININEN L. 2019. Wagga Tank/Southern Nights & Mallee Bull, evolving stories. Bulletin 69: Discoveries in Tasmanides 2019. Australian Institute of Geoscientists, PO Box 576 Crows Nest NSW 1585.

FERGUSSON C.L. & COLQUHOUN. 2021. Devonian–Carboniferous regional deformation in the northeastern Lachlan Orogen, southeastern Australia. Australian Journal of Earth Sciences 68(8), 1092-1110.

FINLAYSON D. M., KORSCH R. J., GLEN R. A., LEVEN J. H. & JOHNSTONE D. W. 2002. Seismic imaging & crustal architecture across the Lachlan Transverse Zone, a cross-cutting feature of eastern Australia. Australian Journal of Earth Sciences 49, 311–321.

FITZHERBERT J.A. & DOWNES P.M. 2020. A mineral system model for Cu-Au-Pb-Zn-Ag systems of the Cobar Basin, central Lachlan Orogen, New South Wales. Unpublished Geological Survey of New South Wales report GS2021/0042.

FITZHERBERT J.A., MCKINNON A.R., BLEVIN P.L., WALTENBERG K., DOWNES P.M., WALL C., MATCHAN E. & HUANG H. 2021. The Hera orebody: A complex distal (Au–Zn–Pb–Ag–Cu) skarn in the Cobar Basin of central New South Wales, Australia. Resource Geology 71(4), 296-319.

FOSTER D. A., D. R. GRAY & M. BUCHER. 1999. Chronology of deformation within the turbidite-dominated, Lachlan orogen: Implications for the tectonic evolution of eastern Australia & Gondwana. Tectonics 18(3), 452–485.

GALLEY A.G., HANNINGTON M.D., & JONASSON I.R. 2007. Volcanogenic massive sulphide deposits, in Goodfellow, W.D., ed., Mineral Deposits of Canada: A Synthesis of Major Deposit-Types, District Metallogeny, the Evolution of Geological Provinces, & Exploration Methods: Geological Association of Canada, Mineral Deposits Division, Special Publication No. 5, p. 141-161.

GLEN R.A. 2005. The Tasmanides of eastern Australia. In: A.P.M. Vaughan, P.T. Leat & R.J. Pankhurst, eds, Terrane processes at the margins of Gondwana, pp. 23–96. Special Publications 246, Geological Society, London.

GLEN R.A., LENNOX P.G. & FOSTER D.A. 1999. 40Ar–39Ar dating of deformations west of the Hill end Trough, Lachlan Orogen, New South Wales. Quarterly Notes of the Geological Survey of New South Wales 110, 13–22.

GLEN R. A., KORSCH R. J., DIREEN N., G., JONES L. E. A. & JOHNSTONE D. W. 2002. Crustal structure of the Ordovician Macquarie Arc, Eastern Lachlan Orogen, based on seismic-reflection profiling. Australian Journal of Earth Sciences 49, 323–348.

GLEN R.A., MEFFRE S., & SCOTT R.J. 2007. Benambran Orogeny in the Eastern Lachlan Orogen, Australia. Australian Journal of Earth Sciences 54, 385–415.

HART T.R., GIBSON H.L. & LESHER C.M. 2004. Trace element geochemistry & petrogenesis of felsic volcanic rocks associated with volcanogenic massive Cu-Zn-Pb sulfide deposits. Economic Geology 99 (5) 1003–1013.

HILL S., FITZHERBERT J. & SIMPSON B. 2026. Petrographic & isotopic study of the Dead Horse-Havilah Zn-Pb-Ag prospect, Hill End Trough, NSW. Unpublished Geological Survey of New South Wales report GS2026/0008.

HUSTON D.L., CHAMPION D.C., MERNAGH T.P., DOWNES PM., JONES P., CARR G.D., FORSTER D. & DAVID V. 2016. Metallogenesis & geodynamics of the Lachlan Orogen: New (and old) insights from spatial & temporal variations in lead isotopes. Volume 76, July 2016, Pages 257-267.

LIEBMANN J., WARE B., MOLE D.R., KIRKLAND C.L., FRASER G., WALTENBERG K., BODORKOS S., HUSTON D.L, EVANS N.J., MCDONALD B.J., RANKENBURG K., DATTA P. & TESSALINA S. 2024. A crustal Pb isotope map of southeastern Australia. Scientific Data volume 11, Article number: 1222.

LENNOX P.G., FORSTER M. A. & WILLIAMS I. S. 2014. Emplacement & deformation ages of the Wyangala Granite, Cowra, NSW. Australian Journal of Earth Sciences 61:4, 607-618.

LU J., SECCOMBE P.K., FOSTER D., ANDREW A.S. 1996. Timing of mineralization & source of fluids in a slate-belt auriferous vein system, Hill End goldfield, NSW, Australia: Evidence from 40Ar39Ar dating & O- & H-isotopes. Lithos 38(3-4), 147-165.

MAAS R., NICHOLLS I.A. & LEGG C. 1997. Igneous & metamorphic enclaves in the S-type Deddick Granodiorite, Lachlan Fold Belt, SE Australia: petrographic, geochemical and Nd–Sr isotopic evidence for crustal melting & magma mixing. Journal of Petrology 38, 815-841.

MAHONEY L., FITZHERBERT J. & MILZ M. 2024. New constraints on the subsurface structure & geological evolution of the Cobar Basin & Hermidale Terrane. Exploration in the house seminar. Geological Survey of NSW.

MAHONEY L., MILZ M. & FITZHERBERT J. 2026. The Central Lachlan seismic project – revealing the Macquarie Arc. Exploration in the house seminar. Geological Survey of NSW.

OVERSBY B. 1971. Palaeozoic plate tectonics in the southern Tasman Geosyncline. Nature, 234(15), 45–48.

SCHEIBNER E. & BASDEN H. (eds) 1998. Geology of New South Wales — Synthesis. Volume 2, Geological Evolution. Memoir Geology 13(2). Geological Survey of New South Wales, Sydney.

SHANKS W.C. PAT, III, & THURSTON R. (eds) 2012. Volcanogenic massive sulfide occurrence model: U.S. Geological Survey Scientific Investigations Report 2010–5070.

SIMPSON B.P. & FITZHERBERT J.A. 2026. National Argon Map (NAM) - Insights from Ar-Ar geochronology in the Cobar Basin. Unpublished Geological Survey of New South Wales report GS2026/0002.

STACEY J. S. & KRAMERS J. D. 1975. Approximation of terrestrial lead isotope evolution by a two-stage model. Earth & Planetary Science Letters, 26(2), 207–221.

THOMAS O.D. & POGSON D.J. (COMPILERS), 2012. Goulburn 1:250 000 Geological Sheet SI/55-12, 2nd edition, Explanatory Notes. Geological Survey of New South Wales, Maitland, NSW.

TORNOS F., PETER J.M., ALLEN R. & CONDE C. 2015. Controls on the setting & style of volcanogenic massive sulphide deposits. Ore Geology Reviews 68, 142-163.

VASSALLO J.J. & GLEN R.A. (EDS) 2003. Evolution of the Hill End Trough: Hill End Trough Geoscience Database. Geological Survey Report GS2003/291. Geological Survey of New South Wales, Sydney, Australia.

YANG Y. & SCOTT S.D. 1996. Possible contribution of a metal-rich magmatic fluid to a sea-floor hydrothermal system. Nature 383, 420–423.

YANG Y. & SCOTT S.D. 2003. Geochemical Relationships of Felsic Magmas to Ore Metals in Massive Sulfide Deposits of the Bathurst Mining Camp, Iberian Pyrite Belt, Hokuroku District, & the Abitibi Belt", published in Massive Sulfide Deposits of the Bathurst Mining Camp, New Brunswick, & Northern Maine (Economic Geology Special Publication 10, edited by W. D. GOODFELLOW S. R. McCutcheon, & J. M. Peter), pages 517–539.

TORPY'S: A NEW INTRUSIVE-RELATED AG-PB-ZN SYSTEM

Edward S. K. Fry

Ballymore Resources Limited, Suite 606, Level 6, 10 Market Street, Brisbane, QLD, 4000

Key Words: Torpy's, Intrusive-Related Mineral System (IRMS), silver, lead, zinc, gold, copper, Hodgkinson Formation, Kennedy Igneous Association, Mossman Orogen, Tasman Orogenic Zone, Devonian, Permian-Carboniferous

INTRODUCTION

North Queensland is one of Australia's most prolific mineral provinces, hosting over 40Moz of identified gold resources, with nearly half the deposits being recognised as Intrusive-Related Gold Systems ("IRGS") (Morrison, 2017). Most recognised intrusion-related systems in North Queensland are gold-dominant and are commonly characterised by Bi ± Te geochemical associations, potassic to calc-silicate alteration assemblages and emplacement at shallow crustal levels. IRGS deposits form a significant class of ore deposits and are closely associated with Permo-Carboniferous intrusives.

The Chillagoe Mineral Field hosts a diverse suite of intrusion-related mineral systems (IRMS) associated with long-lived magmatic-hydrothermal activity from Late Devonian to Permo-Carboniferous magmatism of the Kennedy Igneous Association. Mineralisation occurs as a spectrum of genetically related deposit styles including porphyry Cu-Au systems (e.g., Ruddygore), endogreisens (Scardons Top and Bottom Camps), skarns (e.g., Maniopota), breccias/breccia pipes (e.g., Red Dome/Mungana) and unclassified structurally controlled polymetallic veins.

These systems are characterised by variable associations of Au, Ag, Cu, Pb, Zn, Bi, Mo, W, As and Sb, reflecting differing levels within evolving magmatic-hydrothermal systems along with influences from local host-rock lithologies. Many of the district's polymetallic Ag-Pb-Zn deposits may represent distal or base-metal-rich expressions of broader intrusion-related mineral systems rather than isolated mineralising events, highlighting the importance of intrusive centres as long-lived drivers of fluid flow and metal transport throughout the Chillagoe district.

The Torpy's Prospect is part of Ballymore's Ruddygore Project Group and is located 29 km southeast of Chillagoe and 5 km east of Almaden (Figure 1). The Torpy's high-grade Ag-Pb-Zn historical mine along with other historical silver-lead-zinc deposits within the Chillagoe Mineral Field differ from other sediment-hosted base-metal deposits such as SEDEX, MVT and carbonate replacement deposits and may represent overlooked components of larger magmatic-hydrothermal systems rather than discrete sedimentary-hosted or structurally controlled base-metal occurrences.

Collectively, these observations suggest a probable magmatic-hydrothermal fluid source and structurally controlled mineralisation consistent with other North Queensland intrusion-related mineral systems, although the geochemical signature is dominated by silver, lead and zinc rather than gold. This paper presents the geological, petrographic and geochemical characteristics of the Torpy's Prospect and proposes that it represents a previously unrecognised intrusion-related Ag-Pb-Zn hydrothermal system. Identification of this mineralisation style expands the spectrum of intrusion-related mineral systems within the Chillagoe Mineral Field and has broader implications for regional exploration.

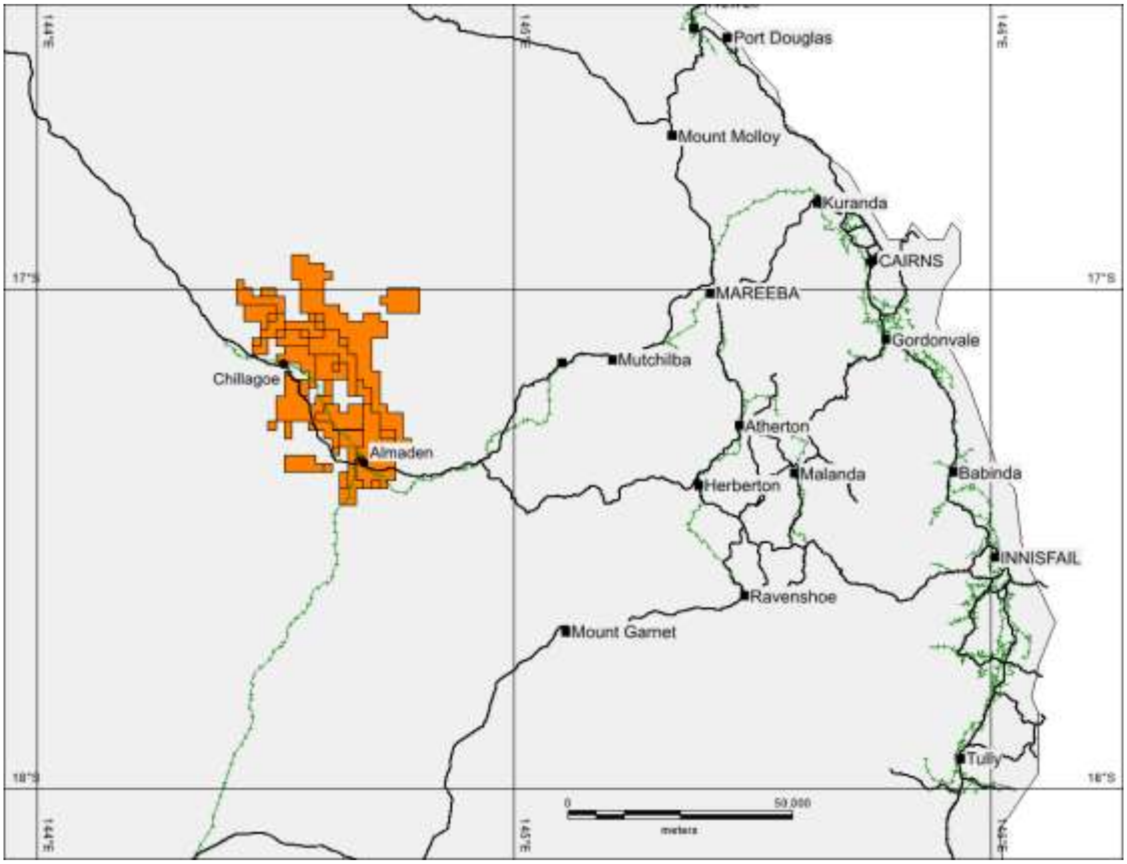

Figure 1: Ruddygore Project Group location.

HISTORY

Torpy's Crooked Creek Mine was one of the most significant Ag-Pb producers of the district during the early twentieth century. Lead carbonate veins were initially discovered at surface, with subsequent underground development intersecting a high-grade lens of silver-bearing galena approximately 20 m below surface. Mining commenced in 1903, and the property was acquired by E.B. Torpy in 1904, who installed a concentrating plant to process ore for shipment to the Chillagoe Smelters. Early production reportedly averaged around 30% Pb and 25 oz/t Ag, with selected ore containing up to 60–70% lead.

Between 1905 and 1908 the mine underwent substantial development, including sinking of multiple shafts to depths exceeding 90 m and construction of water supply, milling and transport infrastructure. Government geological reports described the mineralisation as a series of irregular, lenticular masses of silver-bearing galena hosted within altered sedimentary rocks. Individual ore lenses reached up to approximately 15 m in width, with mineralisation remaining open at depth. Zincblende became increasingly abundant in the deeper workings, suggesting metal zonation within the hydrothermal system.

Mining declined after 1908 owing to the irregular geometry of the ore bodies and difficulties securing smelting capacity. Operations recommenced in 1912 following rehabilitation of the mine and processing plant, with production peaking during 1913 at approximately 500–550 tons of ore per month. Ore shipped to the Chillagoe Smelters averaged 24–28 % Pb and 16–22 oz/t Ag, although mining ceased again in 1914 after the principal orebody pinched out. Limited attempts to reopen the mine during the 1920s focused on dewatering the workings and recovering additional Ag-Pb and Zn mineralisation, but only small quantities of ore were produced before operations finally ceased.

REGIONAL GEOLOGY

The Torpy's Crooked Creek Prospect is situated within the Hodgkinson Province of north Queensland (Figure 2). The region forms part of the Mossman Orogen and is underlain by a thick succession of deformed Palaeozoic sedimentary rocks that have been intruded by numerous granitoid bodies and locally overlain by younger volcanic sequences (Henderson, Donchak & Withnall 2013).

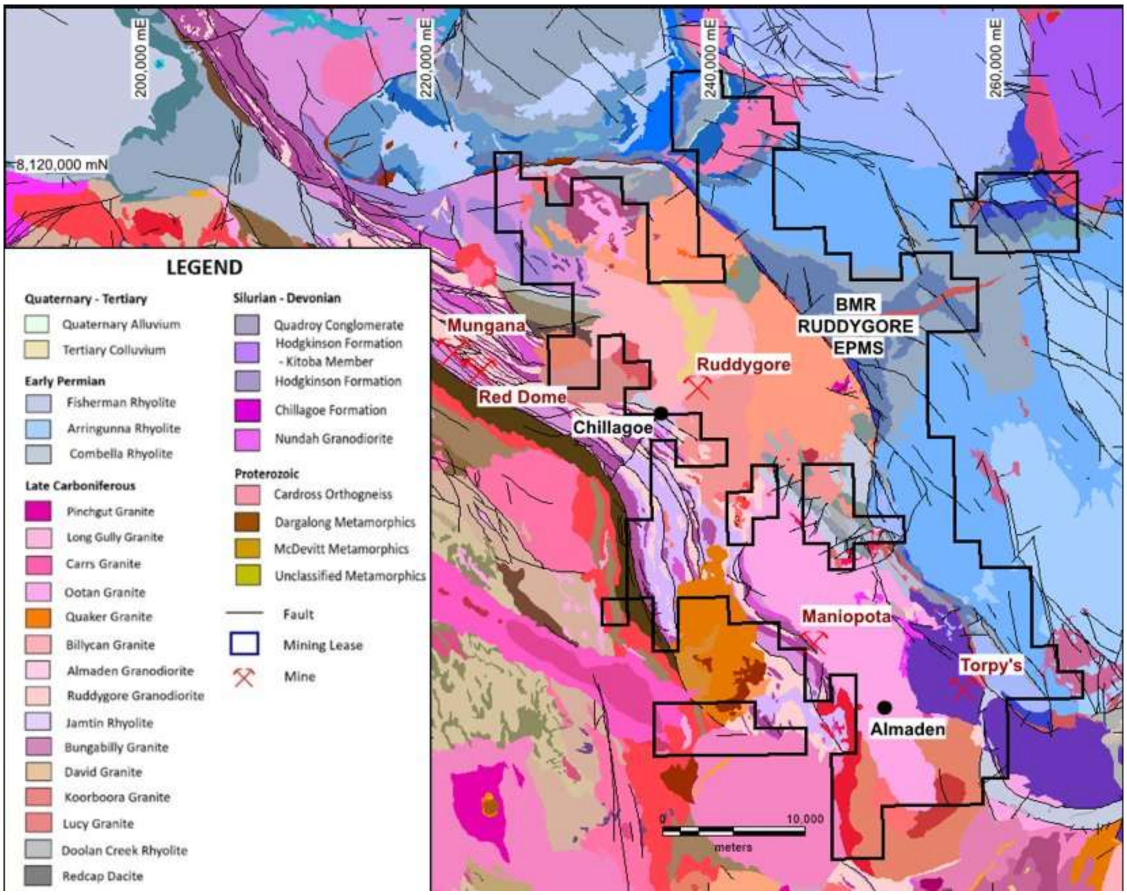

Figure 2: Regional geology at the Ruddygore project group.

The sedimentary succession is dominated by the Devonian Hodgkinson Formation, a thick turbiditic sequence of greywacke, siltstone and mudstone that has undergone multiple episodes of folding, faulting and low-grade regional metamorphism.

The district was extensively intruded by granitoid bodies of the Kennedy Igneous Association, including the Herbert River, Almaden and Elizabeth Creek granites, which are interpreted to have driven widespread magmatic-hydrothermal activity. To the east, the sedimentary succession is unconformably overlain by felsic volcanic rocks of the Featherbed Volcanics, representing a later phase of Permian magmatism.

The Almaden–Chillagoe district is also characterised by a complex structural framework comprising north–south, northeast–southwest and northwest–southeast faults and shear zones that exert an important control on fluid flow and mineralisation.

The Chillagoe Mineral Field contains numerous intrusion-related mineral systems, including porphyry Cu-Au deposits, skarns, greisens, breccia-hosted systems and structurally controlled polymetallic veins, together with several historical Ag-Pb-Zn deposits. The close spatial relationship between mineralisation and Late Palaeozoic intrusive rocks suggests that prolonged magmatic activity was a fundamental control on hydrothermal fluid circulation and ore formation throughout the district, providing the regional context for evaluating the origin of the Torpy's Prospect.

PROJECT GEOLOGY

The Torpy's Ag-Pb-Zn historical mine is hosted within metamorphosed sedimentary rocks of the Devonian Hodgkinson Formation, comprising predominantly greywacke, siltstone and conglomerate with narrow rhyolite dykes cutting the sedimentary succession (Figure 3). The timing of these dykes are unknown but they appear to predate the Ag-Pb-Zn mineralisation.

The greywackes commonly contain interbedded siltstone horizons, while the conglomeratic units locally incorporate slump breccia textures. Within the broader prospect area, carbonaceous black shales are structurally juxtaposed against a package of greywacke and siltstone-dominated sediments. Resistant conglomeratic units form prominent topographic ridges through the central part of the prospect area.

To the north, the sedimentary sequence is intruded by the Torpy's Granite, while the Cottel Rhyolite occurs to the southeast. Further to the northeast, volcanic and intrusive rocks associated with the Featherbed Volcanics, including the Lags Microgranite and Fisherman Rhyolite, are present. The district has undergone multiple episodes of deformation, resulting in complex faulting and locally developed tight to isoclinal folding. These structures are interpreted to have exerted a significant control on the distribution of lithological units and mineralisation throughout the prospect area.

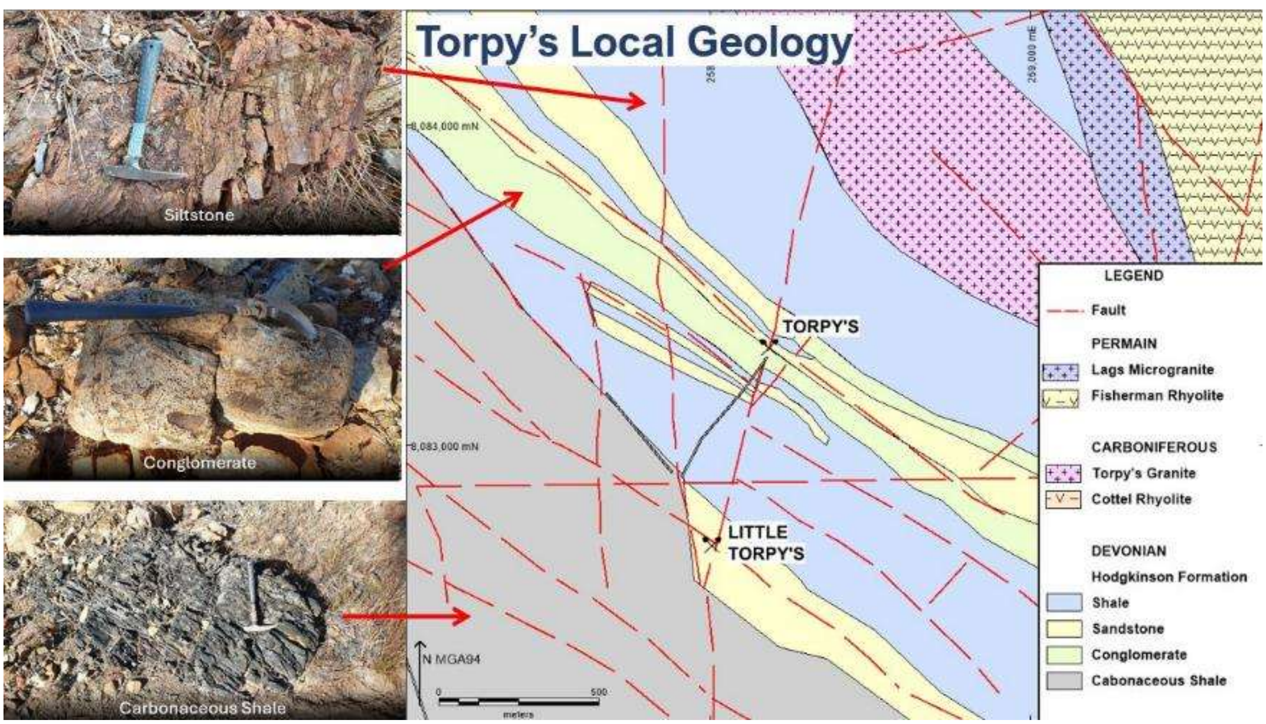

Figure 3: Local geology at the Torpy's Prospect.

MINERALISATION

Mineralisation at Torpy's is associated with a complex, multi-stage hydrothermal system developed within clastic metasedimentary host rocks. Geological observations from surface mapping, drill core logging and petrographic studies (Brown 2026) have enabled the development of a preliminary paragenetic sequence as outlined in Table 1.

Table 1: Torpy's Mineralisation Paragenesis.

Stage	Hydrothermal Event	Representative Minerals	Interpretation
I	Early fracturing and quartz veining	Quartz	Initial fluid ingress
II	High-temperature prograde alteration	Amphibole ± Biotite ± Magnetite ± early Sphalerite	Magmatic fluid influx
III	Potassic–calc-silicate alteration	Biotite + Garnet ± Magnetite	Peak thermal conditions
IV	Main Ag-Pb-Zn mineralisation	Massive Sphalerite + Galena ± Magnetite	Principal ore stage
V	Retrograde alteration	Chlorite ± Magnetite ± Sphalerite	Cooling and fluid evolution
VI	Cu-bearing hydrothermal veins	Chalcopyrite ± Carbonate ± Sphalerite	Late magmatic-hydrothermal pulse
VII	Late carbonate veining	Carbonate	Waning hydrothermal activity

GEOCHEMISTRY

Geochemical data indicate that Torpy's is a polymetallic Ag-Pb-Zn system with elevated Bi, Sb, Te, As, Se and locally Cu, In and W. Drill intersections returned exceptionally high silver grades (up to 987 g/t Ag) with associated lead (38.6% Pb), zinc (20.8% Zn), indium (82.9 g/t In) and copper (0.95% Cu), while elevated bismuth, tellurium, selenium and tungsten provide evidence for a metal association which is characteristic of an intrusion-related mineral system as opposed to a sediment-hosted base-metal system.

Element association analysis demonstrates a strong Ag-Pb-Bi-Se ± Te-Au-S-Cu-As association together with a Zn-Cd-S ± Co assemblage, suggesting the coexistence of both precious metal and base-metal signatures. Relative to average shale, Pb, Ag, Bi, Zn, Sb and Te display enrichment factors ranging from approximately 65× to over 2,700×, highlighting an unusually metal-rich hydrothermal system (Figure 4).

The elevated Bi-Te-In association, together with anomalous Cu and W, is considered significant as these elements are commonly associated with intrusion-related hydrothermal systems. Combined with the observed alteration assemblage of quartz-amphibole-biotite-garnet-magnetite evolving to chlorite and late Cu-rich sulphides, the geochemical signature supports interpretation of Torpy's as a magmatically influenced, intrusion-related Ag-Pb-Zn system.

CLASSIFICATION & ZONING PATTERNS FOR PORPHYRY-RELATED HYDROTHERMAL SYSTEMS

METAL ASSOCIATION CLASSIFICATION	Au	Cu-Au	Cu-Mo	Mo-W-Bi	Sn-W	Sn-B
EXAMPLE Eastern Australia	Fifield	Goonumbla	Mount Leyshon	Kidston	Herberton	Cooktown
EXAMPLE World	Maricunga Chile	British Columbia	Bingham	Climax	Erzgebirge	NE Tasmania
IGNEOUS CHARACTERISTICS						
CHEMICAL TYPE; FRACTIONATION; REDOX	M, U-F, O	M, U-F, SO-O	I, U-F, O	I, F, O-R	I, F, R	S, F, R
IGNEOUS ROCK TYPE ON QAP	DI-QD-TN	DI-MZD-MZ-QMZ	DI-GD-MZG	QMZ-MZG-SYG	MZG-SYG-AFG	SYG-QSY-ASY
METAL ZONING						
MARGINAL	Hg, S	Ca	Ca	F, U	F, Ba, Se, Hg, U	F
DISTAL (As)	As (Au)	Au As Sb	(As, Sb, Au)	(As Ag Sb Au)	As (Au)	As
DISTAL (BM)	Pb, Zn, Ag, Sb, (Au)	Pb Zn Ag Au (Cu Mo Te)	Pb Zn Ag (Au, Bi)	Zn Cu Pb Bi Au	Pb Ag Zn	Zn Pb Ag
PROXIMAL (BM)	Au Cu Mo (Ag, As)	Cu (Zn)	Cu Au Ag (Bi Te)	Cu (Au Bi Te)	Cu Mo Bi	Cu Bi Mo (W)
CORE	Au, Te, (Pt)	Cu Au (Te)	Cu Mo	W Mo Bi	Sn W	Sn B (W)

Figure 4: Classification of element enrichment zonation pattern for generalised porphyry-related hydrothermal systems. The yellow box is positioned according to the enrichment of Bi vs Te, the red box indicates where Torpy's may sit within the system according to the generalised enrichment pattern of As, Sb, Au, Pb, Zn, Ag, Bi, and Te.

INTRUSIVE-RELATED MINERAL SYSTEM GEOLOGICAL MODEL

Northeast Queensland is a prolific mineral province with over 40Moz of identified gold endowment, and nearly half of the deposits are recognised as IRGS deposits. Our understanding of IRGS mineralisation has made great advances in the past 30 years with improved understanding of the magmatic sources, mineralisation styles, tectonic setting and geochemical zonation (Baker, 2002; Hart, 2007; Sillitoe & Thompson, 1998; Morrison, 2017).

The eastern coast of Queensland has a history of discovery and mining IRGS mineralisation. Morrison (2017) presented a mineralisation model for IRGS showing North Queensland examples (Figure 5). He reported that 130 IRGS prospects had been identified to date in North Queensland, with only 30 of these systems being well explored.

Many well-known gold deposits in Northeast Queensland have been assigned to the IRGS model, including Kidston (5 Moz Au), Ravenswood / Mount Wright (5.8 Moz Au), Mount Leyshon (3.5 Moz Au), Pajingo (3.5 Moz), Red Dome / Mungana (3.2 Moz Au), Mount Carlton (1.4 Moz Au) and Mount Morgan (17 Moz Au and 239 Kt Cu). A collation of data by Morrison (2017) suggests that the dominant causative intrusions for North Queensland IRG systems are Permo-Carboniferous age, slightly oxidised to slightly reduced and moderately fractionated. Mineralisation is commonly associated with rhyodacitic intrusive stocks belonging to the Kennedy Igneous Association and are interpreted to have formed in cauldron subsidence complexes. These deposits typically exhibit Au-Sn-W-Mo metallogeny.

The Chillagoe Mineral Field hosts a diverse suite of IRGS/IRMS systems associated with Late Devonian to Permo-Carboniferous magmatism of the Kennedy Igneous Association. IRMS deposits form a significant class of ore deposits and are closely associated with Permo-Carboniferous intrusives and occur at porphyry level (i.e. 2-5 km depth), with most deposits displaying a Bi +/- Te chemical association.

Although Torpy's shares many characteristics with North Queensland Intrusion-Related Gold Systems (IRGS), several aspects of the deposit differ from the established Au-dominated systems at Kidston, Mount Leyshon, Ravenswood and Red Dome. Mineralisation at Torpy's is dominated by Ag-Pb-Zn, with only minor gold, and is characterised by a strong Bi-Te-In association and abundant sphalerite-chalcopyrite mineralisation. These characteristics suggest that Torpy's represents a more distal, base-metal-rich expression of an intrusion-related mineral system.

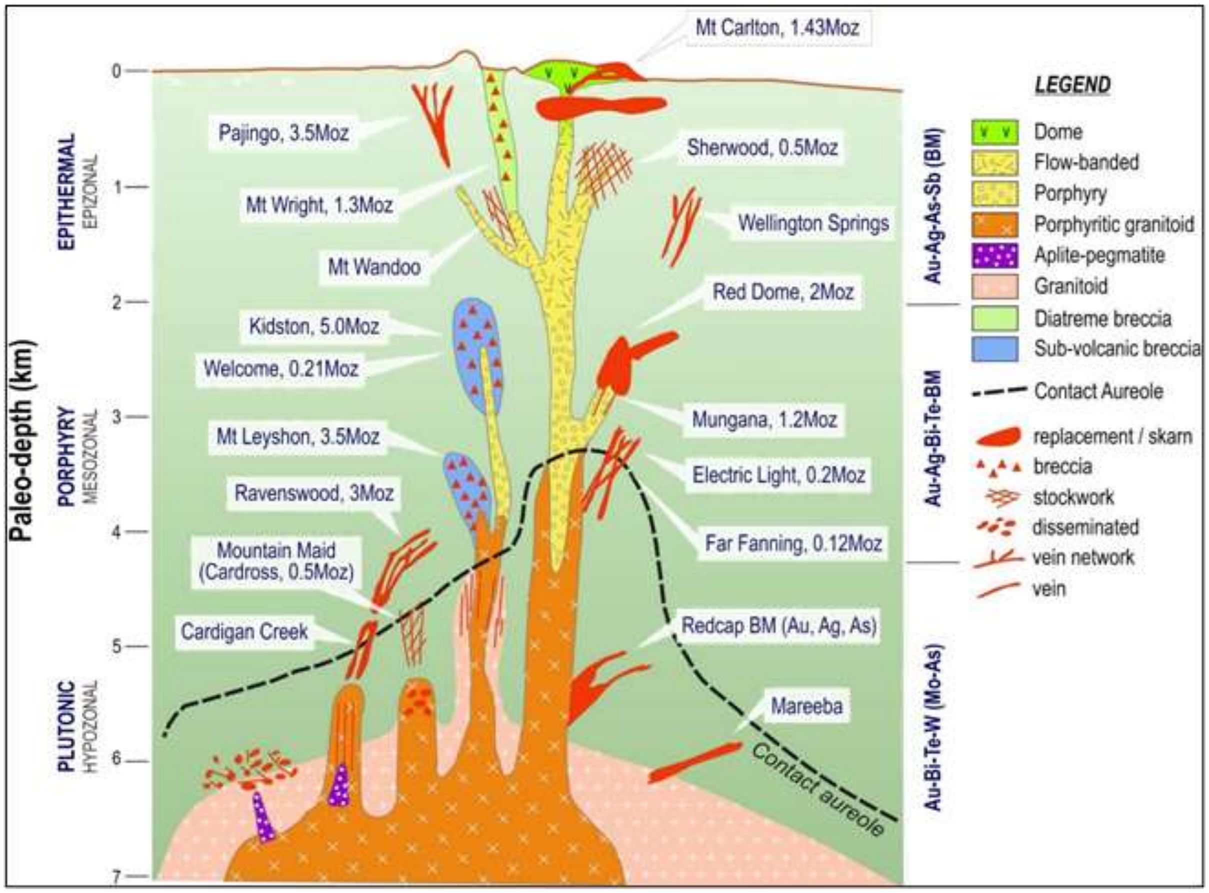

Figure 5: IRGS Mineral System Model with North Queensland Examples (Morrison, 2017)

Petrographic evidence indicates a prolonged, multi-stage hydrothermal evolution involving biotite-garnet-magnetite alteration, retrograde chloritisation and late Cu-rich sulphide assemblages, suggesting repeated magmatic-hydrothermal fluid influxes.

Rather than representing a contradiction to the IRGS model, these characteristics recognised at Torpy's are interpreted to reflect a more distal, base-metal-dominant expression of an IRMS deposit, where metal zonation, host-rock composition and evolving fluid chemistry have produced a polymetallic Ag-Pb-Zn system in place of the more typical gold-dominated deposits recognised elsewhere in North Queensland.

CONCLUSIONS

Exploration completed by Ballymore Resources indicates that the Torpy's Prospect is unlikely to represent an isolated silver-lead-zinc sediment-hosted mineral occurrence. Instead, geological, petrographic and geochemical evidence collectively supports interpretation of the deposit as a long-lived intrusion-related hydrothermal system developed within the Devonian Hodgkinson Formation. The observed alteration evolution from quartz-amphibole through biotite-garnet-magnetite to retrograde chlorite, together with multiple generations of sulphide mineralisation and late Cu-rich hydrothermal veins, records repeated pulses of mineralising fluids rather than a single mineralisation event.

The geochemical signature further reinforces this interpretation, with exceptional Ag-Pb-Zn grades accompanied by enrichment in Bi, Te, In, Sb, As, Se, Cu and W—an elemental association consistent with distal intrusion-related hydrothermal systems recognised elsewhere in North Queensland. These results suggest that Torpy's may represent the base-metal-rich expression of a larger magmatic-hydrothermal system and demonstrate that intrusion-related mineralisation within the Chillagoe Mineral Field extends beyond the traditional gold-dominated IRGS model. Recognition of this broader IRMS framework has important implications for exploration across the district, where many historical Ag-Pb-Zn occurrences may represent distal expressions of concealed intrusive centres capable of hosting larger mineral systems.

ACKNOWLEDGEMENTS

Many people have contributed to the development of the understanding of the Torpy’s deposit and models described, and special acknowledgement goes to David Webb, Deanna Houston, William Bladen & David A-Izzeddin.

REFERENCES

BAKER, T 2002, 'Emplacement depth and CO_2-rich fluid inclusions in intrusion-related gold deposits', Economic Geology, vol. 97, pp. 1109–1115.

BROWN, A 2026, Petrographic observations on 12 samples from Torpy's Prospect, Ballymore Resources, report no. TECHREP-26-011, Lithinsight Pty Ltd, Mount Isa, Qld.

HART, CJR 2007, 'Reduced intrusion-related gold systems', in WD Goodfellow (ed.), Mineral Deposits of Canada: A Synthesis of Major Deposit-Types, District Metallogeny, the Evolution of Geological Provinces, & Exploration Methods, Special Publication 5, Geological Association of Canada, Mineral Deposits Division, St John's, Newfoundland, pp. 95–112.

HENDERSON, RA, DONCHAK, PJT & WITHNALL, IW 2013, 'Mossman Orogen', in PA Jell (ed.), Geology of Queensland, Geological Survey of Queensland, Brisbane, pp. 225–304.

MORRISON, G 2017, Intrusion-Related Gold Deposits in North Queensland, presentation to the Geological Survey of Queensland Project Final Meeting, 7 December 2017.

QUEENSLAND DEPARTMENT OF MINES 1903–1924, Queensland Government Mining Journal, Queensland Government, Brisbane. Consulted reports: CR47932, CR47945, CR47947, CR47952, CR47953, CR47955, CR47956, CR47960, CR47962, CR47963, CR47967, CR47969, CR47977, CR47979, CR47980, CR47992, CR48015, CR48030, CR48031, CR48034, CR48037, CR48039, CR48041, CR48042, CR48043, CR48051, CR48123, CR48124, CR48166, CR48172, CR48177, CR48178, CR48179 & CR48277.

SILLITOE, RH & THOMPSON, FH 1998, 'Intrusion-related vein gold deposits: types, tectono-magmatic settings & difficulties of distinction from orogenic gold deposits', Resource Geology, vol. 48, no. 2, pp. 237–250.

RIDGEWAY: A FRESH LOOK IN A MATURE DISTRICT

Kerrison, A., West, J., Hart, E., Finn, D., Willcox, A., Brabham, G.
Newmont Australia

ABSTRACT

Newmont's Cadia Valley Operation hosts world-class porphyry-style mineralisation across three main deposits (Figure 1): the active Cadia East underground, the historic Cadia Hill open pit and Ridgeway underground, which is currently on care-and-maintenance. Collectively, these deposits and associated stockpiles have a combined mineral reserve of 1Bt @ 0.42g/t Au for 13.5Moz and 0.29% Cu for 2.9kt Cu, estimated December 2025. Ridgeway production ended in 2017, with a total production of 87Mt @ 1.67g/t Au and 0.62% Cu for 3.9Moz of gold and 487kt of copper. Mineralisation remains open at depth, with evidence for local high-grade, including 16m @ 10.8g/t Au and 3.4% Cu in UR333 (Figure 2). Despite the exploration upside, Ridgeway had not been drilled for 15 years, and fundamental questions remained regarding the geological controls on high-grade mineralisation at depth.

The Ridgeway deposit is a subvertical body of quartz–sulphide vein stockwork mineralisation with an elliptical, pipe-like geometry, elongated along a northwest-striking axis. Stockwork dimensions are approximately 400 m east–west, 250 m north–south and the deposit extends to a depth in excess of 1,000 m. High-grade mineralisation at Ridgeway occurs within dense quartz vein stockworks and sheeted arrays developed in and around small (50–100 m diameter), early-, inter- and late-mineral monzonite to quartz-monzonite intrusions. These monzonite dykes exploit early pyroxene- and plagioclase-porphyritic dykes that themselves intrude along broader structural discontinuities. The deposit is located at the intersection of multiple regional fault systems and is localised at the contact between the reactive Forest Reef Volcanics and underlying, less-reactive Weemalla Formation. The Weemalla Formation consists of thinly bedded siltstone with less common sandy marl interbeds and mafic lavas.

Newmont's acquisition of Newcrest in 2023 and the formation of a new site exploration team in 2024 created an opportunity to revisit Ridgeway and evaluate its remaining exploration potential. Building on previous exploration, the team designed and executed a 10,000 m drill program testing the remaining potential at Ridgeway. The work program included relogging 6,000 m of historic Ridgeway drill core. Newly drilled core was also scanned using Veracio's Truscan 2 unit to generate a real-time multi-element geochemical dataset. The relogging and drilling program was undertaken to better understand the controls on mineralisation at depth and to refine the characterisation of early-, inter- and late-mineral porphyry and country rock.

Integrated drilling, relogging and lithogeochemical datasets indicate that the early-, inter- and late-mineral porphyries at Ridgeway are distinguishable geochemically by degree of hornblende fractionation (V/Sc) and evolved from a common parental magma. Mineralisation at depth remains strongly focussed along the margins of the Ridgeway intrusive complex within the less-reactive Weemalla Formation, with lithogeochemistry assisting to identify two preferentially mineralised units: 1) sandy and silty marl interbeds within the Weemalla Formation that locally host skarnoid (Mt-Kfs-Act-Chl-Cp-Bn) mineralisation, and 2) pyroxene-porphyry dykes and sills that act as a rheological contrast between high-K igneous units and the low permeability, comparatively unreactive thinly-bedded Weemalla siltstones. Veracio's Truscan predictive logging was utilised to rapidly identify marl stratigraphic horizons and mafic sills and dykes amongst otherwise uniform and less-reactive bedded siltstones. Our interpretation is that these stratigraphic horizons and dykes were instrumental in the development of high-grade, localised mineralisation during prolonged injection of porphyry magmas through the Weemalla Formation

along structural discontinuities, until reaching complete devolatilisation in the overlying Forest Reef Volcanics.

The integration of multi-element geochemistry with relogging and recent drilling has refined the understanding of the geological controls on mineralisation at Ridgeway and identified new vectors for targeting extensions to the existing resource within country rock historically viewed as less prospective. This work highlights the value of revisiting mature deposits using new technologies, integrated datasets and modern workflows to generate new geological insights and uncover previously unrecognised exploration opportunities.

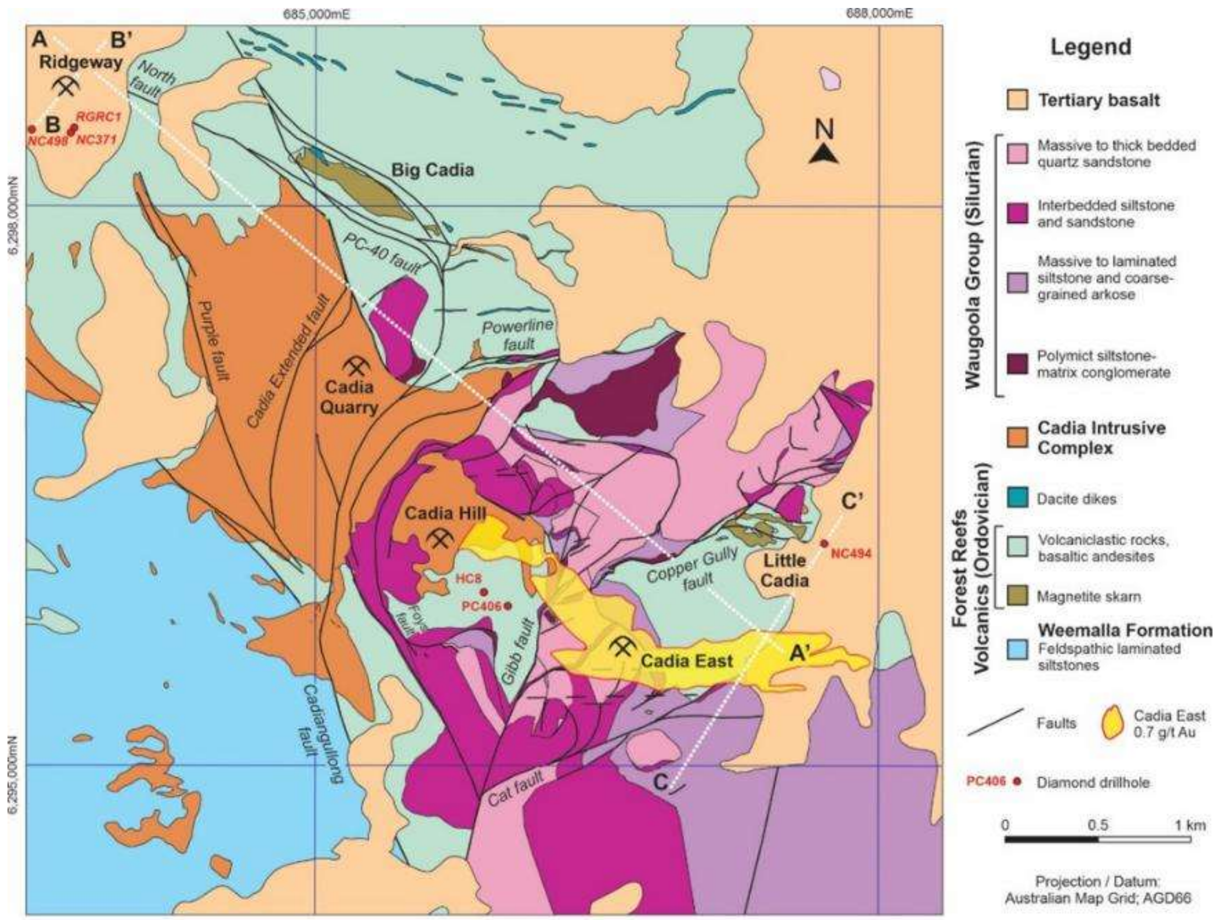

Figure 1 – Geology and deposits of the Cadia District (Harris et al., 2020).

Figure 2 – Example of vein-hosted and disseminated sulphide mineralisation within a locally brecciated pyroxene porphyry dyke. Image of UR333 showing subsection of 16m @ 10.8g/t Au and 3.4% Cu.

REFERENCES

HARRIS, A., COOKE, D., CUISON, A. L., GROOME, M., WILSON, A., FOX, N., HOLLIDAY, J., & TOSDAL, R. (2020). Geologic Evolution of Late Ordovician to Early Silurian Alkalic Porphyry Au-Cu Deposits at Cadia, New South Wales, Australia (Version 1). University of Tasmania.

SEISMIC CLUES FOR DISCOVERY: REFLECTIONS ON OVER 1000 KM OF NEW DEEP-CRUSTAL SEISMIC ACROSS THE LACHLAN OROGEN

Luke Mahoney, Joel Fitzherbert, Max Milz

Geological Survey of NSW

Key Words: seismic reflection, mineral systems, Lachlan Orogen, crustal architecture, covered terranes, Macquarie Arc.

INTRODUCTION

The Lachlan Orogen hosts several economically significant mining provinces, including major deposits of copper, zinc, and silver that are critical to clean-energy technologies (DPIRD, 2024). It is also the leading region for mineral exploration investment in New South Wales, attracting AUD $147 million and accounting for 36% of the state's total exploration expenditure in FY24-25 (Cathers, 2026).

Despite strong exploration expenditure and periodic discovery success in the Lachlan Orogen, the region faces a global challenge: the search for new mineral deposits is becoming increasingly difficult as readily identifiable geophysical anomaly-based targets are progressively exhausted (e.g., Schodde, 2025). Consequently, exploration is increasingly focused on subtle and difficult-to-detect prospects, including deposits concealed beneath younger cover sequences. In response, the minerals industry is adopting holistic mineral systems approaches that seek to understand the spatial and temporal relationships between mineralisation and the broader geodynamic, tectonic, structural, and stratigraphic processes that govern its formation and preservation (e.g., McCuaig and Hronsky, 2014). Such approaches rely on multidisciplinary investigations and the integration of datasets that have not traditionally formed part of exploration workflows.

Among these datasets, seismic reflection has emerged as a particularly valuable tool. Traditionally associated with hydrocarbon exploration and tectonic-scale studies, seismic reflection is now being applied throughout mineralised terranes across a range of scales from individual structures to the entire crust. Since 2023, the Geological Survey of NSW (GSNSW) has conducted three deep-crustal seismic reflection surveys across the central and eastern Lachlan Orogen to improve understanding of crustal architecture and to place mineral deposits within their broader tectonic framework. Collectively, these surveys have acquired more than 1,000 km of modern 2D seismic data. As processing and interpretation remain ongoing, the datasets and associated geological models are at varying stages of maturity.

This paper provides an update on the status of the seismic program and presents three case studies illustrating how the data and interpretations are improving understanding of mineralisation, constraining mineral system components, and supporting exploration targeting in brownfield and greenfield settings.

SEISMIC PROGRAM OVERVIEW AND STATUS

Three seismic surveys were acquired between 2023 and 2026: the Cobar–Yathong Seismic Survey (2023), the Central Lachlan Seismic Survey (2025), and the Macquarie Arc Seismic Survey (2026). Survey line layouts were designed to balance logistical considerations, such as vehicle access, with key technical objectives. In particular, the program sought to acquire multiple overlapping seismic lines across geologically and metallogenically significant regions, thereby reducing the interpretational uncertainty associated with individual seismic transects. The survey locations are shown in Figure 1, together with a summary of the status of data acquisition, processing, and interpretation.

Acquisition parameters were developed in collaboration with Geoscience Australia to optimise imaging of both shallow and deep crustal structures. All three surveys utilised modern 2D seismic acquisition systems comprising vibroseis source trucks and wireless nodal receivers. A listening time of 20 seconds was used for all surveys except Cobar–Yathong, which employed a 16-second record length. High-fold seismic data were acquired using a 20 m source interval, with reflections recorded across a 12 km receiver spread at 10 m geophone spacing. At the time of submission, data acquisition had been completed for all three surveys.

Processing seismic data in structurally complex hard-rock terranes such as the Lachlan Orogen presents significant challenges and requires specialised expertise. To address these challenges, the GSNSW is collaborating with Thrust Belt Imaging to apply prestack time migration workflows that are well suited to areas where subsurface velocity structures are poorly constrained. Processing has focused on attenuating traffic and other cultural noise associated with acquisition along road corridors, particularly near population centres where signal-to-noise ratios are lowest (Figure 2(I)). Equally critical is the seismic migration stage, which relies on geologically constrained velocity models to accurately position reflections within the subsurface. This work requires close collaboration between seismic processors and geological interpreters (e.g., Figure 2(II)). Detailed descriptions of the processing methodology are provided by Vestrum and Cameron (2022) and in the processing reports accompanying the survey data packages available through MinView. At the time of writing, processing of the Cobar–Yathong and Central Lachlan surveys is complete, and the processed datasets have been publicly released, while processing of the Macquarie Arc survey is underway.

The resulting seismic profiles are being integrated with legacy geological and geophysical datasets within a three-dimensional interpretation framework. This approach allows interpretations to be informed by correlations between adjacent seismic lines and along-strike geological constraints. The resulting interpretations are evaluated through 2.5D potential-field modelling and incorporated into 3D geological models. Readers are referred to Mahoney et al. (2024; 2026) and Milz and Mahoney (2025) for examples of the processed seismic sections and preliminary interpretations. Given the overlapping nature of the survey network, these interpretations should be regarded as evolving and may be revised following completion of processing and interpretation of the Macquarie Arc Seismic Survey.

MINERAL SYSTEMS CASE STUDIES

Given the ongoing nature of this project, we do not attempt to present a complete interpretation of the seismic datasets. Instead, we highlight three case studies that demonstrate how seismic data are improving understanding of the distribution and geological context of known mineralisation within the Lachlan Orogen. The seismic data and interpretations are presented alongside geological constraints and mineral occurrences within three-dimensional visualisations (Figures 3 to 5), providing context that closely reflects the framework used to develop the subsurface interpretations. Collectively, the case studies demonstrate the value of seismic reflection data for constraining mineral system architecture and reducing geological uncertainty in mineral exploration.

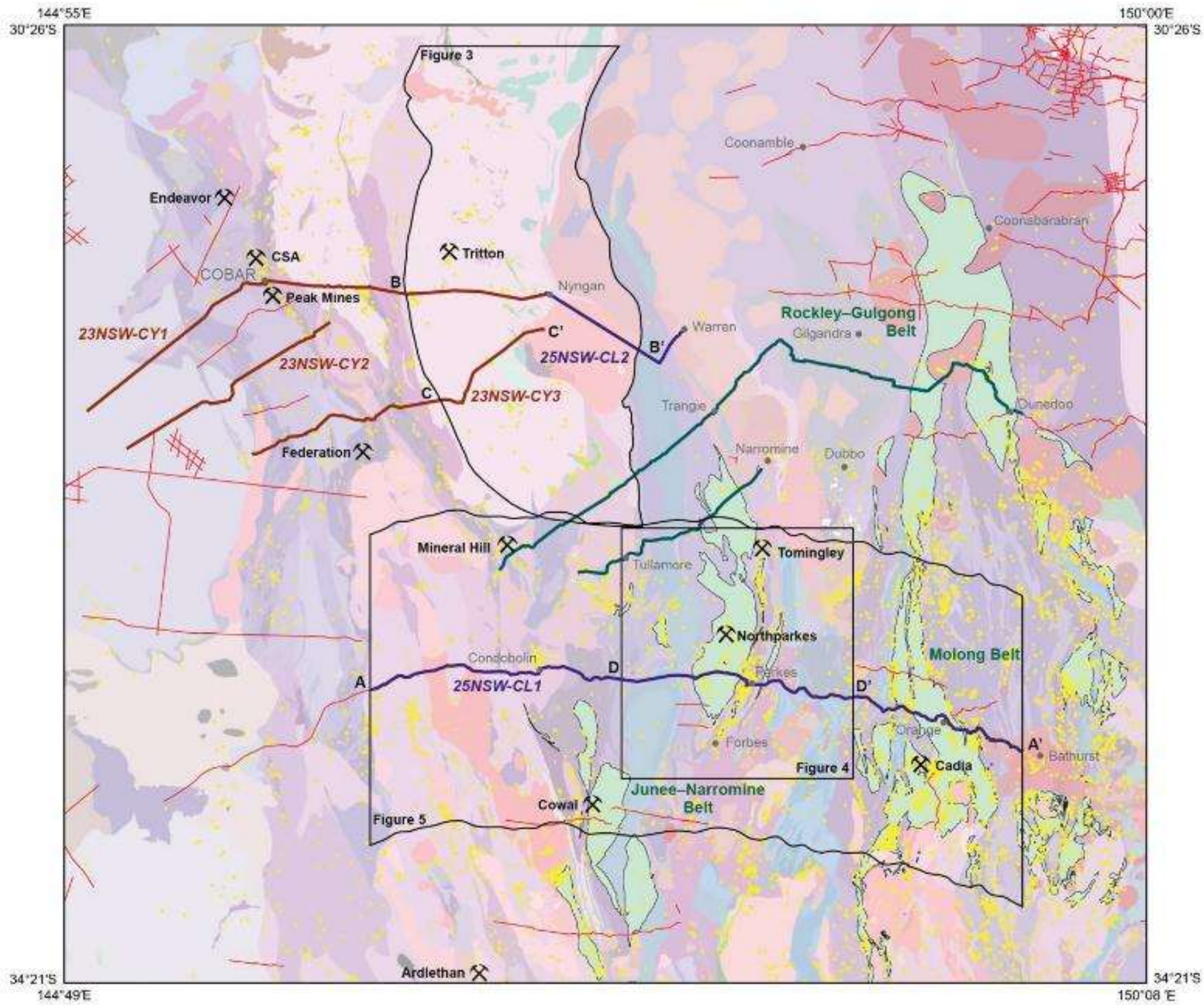

YEAR	SURVEY	LINE KILOMETRES	AQUISITION	PROCESSING	INTERPRETATION
2023	Cobar–Yathong Sesimic Survey	506	Complete	Complete	Complete - subject to review
2025	Central Lachlan Sesimic Survey	420	Complete	Complete	Underway
2026	Macquarie Arc Sesimic Survey	395	Complete	Underway	Awaiting processed data

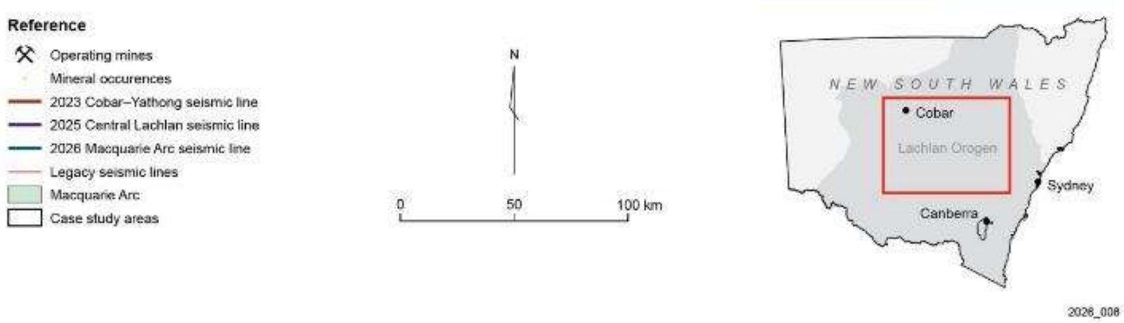

Figure 1. Overview of the GSNSW seismic program. Map shows locations of seismic surveys conducted since 2023, shown relative to legacy seismic lines, Lachlan Orogen layer from Seamless Geology (Colquhoun et al., 2026), and NSW mineral occurrences from MinView. Table summarises the status of acquisition, processing, and interpretation for each survey.

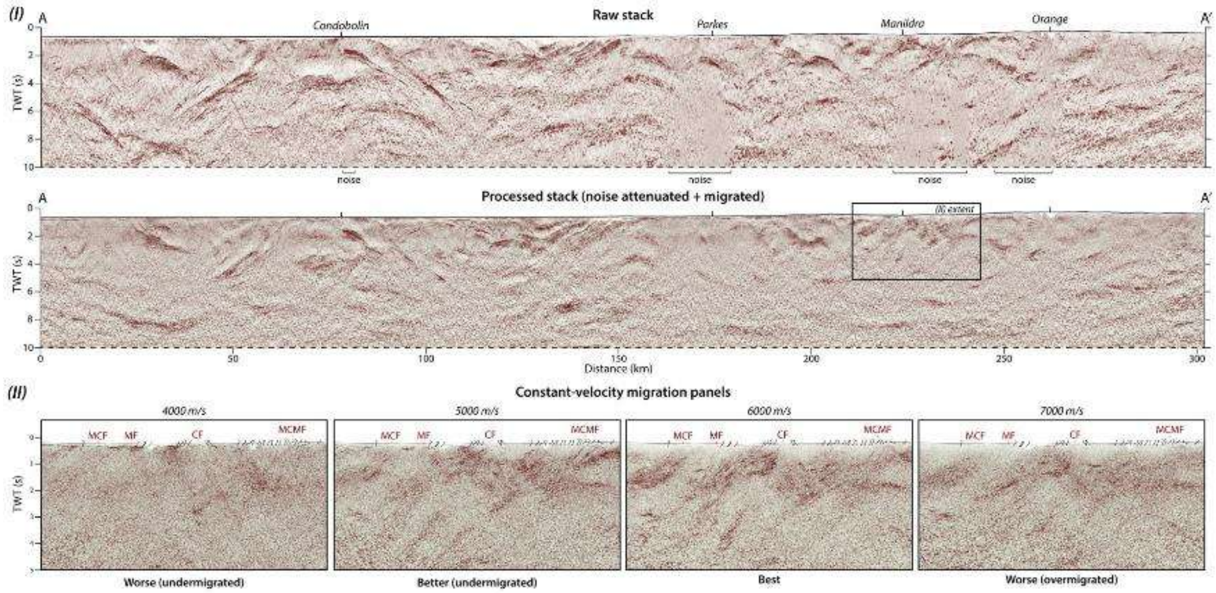

Figure 2. (I) Comparison of the raw and processed seismic stacks from Central Lachlan Seismic Survey Line 1 (25NSW-CL1), cropped at 10 s two-way time, illustrating the substantial improvement in subsurface imaging achieved through noise attenuation and migration. Prominent noise cones associated with the Parkes and Orange areas, together with numerous cross-cutting reflectors visible in the raw stack, are largely removed in the processed section, resulting in a clearer and more geologically meaningful image. (II) Seismic panels showing the seismic data migrated at constant velocities between 4000 and 7000 m/s, illustrating the sensitivity of seismic imaging to migration velocity selection. Geological observations, including bedding dip and mapped surface fault locations (red), provide important constraints on selecting appropriate migration velocities, particularly in areas where subsurface velocity information is sparse. The panels demonstrate the importance of close collaboration between seismic processors and geological interpreters in structurally complex terranes such as the Lachlan Orogen. Fault abbreviations: MCF = Mandagery Creek Fault; MF = Manildra Fault; CF = Cudal Fault; MCMF = Molong–Columbine Mountain Fault.

Hermidale Terrane / Girilambone Zone

The Hermidale Terrane is one of several terranes within the Lachlan Orogen composed predominantly of Ordovician siliciclastic turbiditic sedimentary rocks deposited along the eastern margin of Gondwana (Glen et al., 2009). The eastern part of the terrane, corresponding to the Girilambone Zone of Scheibner and Basden (1998), hosts numerous copper-rich mineral deposits, many of which contain elevated gold, zinc, lead and silver. These deposits form a mineralised belt extending from the Girilambone–Hermidale district in the north to the Tottenham–Albert district in the south (Figure 3). The region has a long history of mining and remains an active producer, with Aeris Resources currently operating the Tritton, Avoca Tank, Budgerygar and Murrawombie mines (Figure 3).

The genesis of these deposits has been the subject of considerable debate. They have variously been interpreted as syngenetic and stratabound (e.g., volcanic-associated massive sulphide (VAMS) deposits) or as epigenetic and structurally controlled. More recent studies seeking to reconcile evidence supporting these end-member models propose that mineralisation was originally emplaced within a VAMS system and subsequently remobilised during later deformation, producing the complex orebody geometries observed today (e.g., Murphy and Cox, 2019). A detailed discussion of the mineral system and the relevant literature is provided by Gilmore et al. (2018).

Much of the Hermidale Terrane comprises variably metamorphosed sandstone, siltstone and claystone of the late Cambrian to early Ordovician Narrama Formation, which is largely concealed beneath extensive Quaternary alluvial cover (Figure 3 inset). Consequently, bedrock exposure is sparse, discontinuous and commonly affected by deep weathering. Exploration drilling and most documented mineral occurrences are concentrated within the Girilambone–Hermidale and Tottenham–Albert districts, where outcrop is comparatively abundant.

The Girilambone–Hermidale district is the most intensively studied area, reflecting ongoing exploration and mining activity (e.g., Aeris Resources, 2023). Significant mineral occurrences occur stratigraphically beneath the regionally extensive, quartz-rich Budgery Sandstone Member, a 75–125 m thick metasandstone unit. Mineralisation is also spatially associated with mafic rocks of MORB affinity (Gilmore et al., 2015; Gilmore et al., 2018 and references therein). Together, these competent lithologies contrast strongly with the surrounding Narrama Formation and form an erosion resistant corridor that, despite folding and deformation, maintains an overall north–south trend. This corridor defines the primary prospective trend and exploration fairway within the district.

The continuation of this prospective trend beneath younger cover to the south remains poorly constrained. Increasing thickness and extent of alluvial cover obscure its trajectory, making geological mapping difficult. Nevertheless, the apparent genetic relationship between deposits in the Girilambone–Hermidale district, the Collerina area, and the Tottenham–Albert district suggests that the primary mineralised corridor may be continuous beneath cover (e.g., Gilmore et al., 2015).

This setting is well suited to seismic investigation. The competent lithologies associated with the primary mineralised corridor contrast strongly with the surrounding, less competent pelitic rocks that comprise much of the Narrama Formation. This marked difference in acoustic properties generates a pronounced acoustic impedance contrast that is clearly expressed on the two seismic lines acquired as part of the Cobar–Yathong Seismic Survey, which transect the region (Figure 3).

On seismic line 23NSW-CY1 (B–B'; Figure 3), a series of east-dipping listric thrust sheets can be traced directly to the primary mineralised corridor at the surface. These reflectors are interpreted as thrusted sheets of the competent lithologies associated with mineralisation and appear to merge downward into a regional detachment at approximately 10 km depth. The inferred structural configuration is consistent with regional metamorphic constraints (Fitzherbert et al., 2017), and the reflector near-surface dip of ~ 45° is broadly consistent with fault geometries mapped at the surface (Shields, 1996; Trigg, 2017), and the geometry of known ore systems (Fogarty, 1998; Erceg and Hooper, 2006; Murphy and Cox, 2019).

Seismic line 23NSW-CY3 (C–C'; Figure 3) traverses an area where prospective basement is almost entirely concealed beneath younger cover (Figure 3 inset). Nevertheless, the line images a remarkably similar set of east-dipping listric thrust sheets. These structures align closely with known copper occurrences, including those in the Collerina area approximately 20 km to the southeast (Figure 3), and are therefore interpreted to define the likely continuation of the primary mineralised corridor beneath cover. This demonstrates the potential value of seismic reflection data for mapping prospective trends in regions where conventional geological mapping is challenged by extensive cover. For future brownfields exploration within this region, higher-resolution infill seismic surveys could further delineate the geometry and continuity of the primary mineralised corridor. Elsewhere, recognising similar seismic signatures in the existing dataset and other legacy data, particularly in covered areas, may assist in defining new exploration targets.

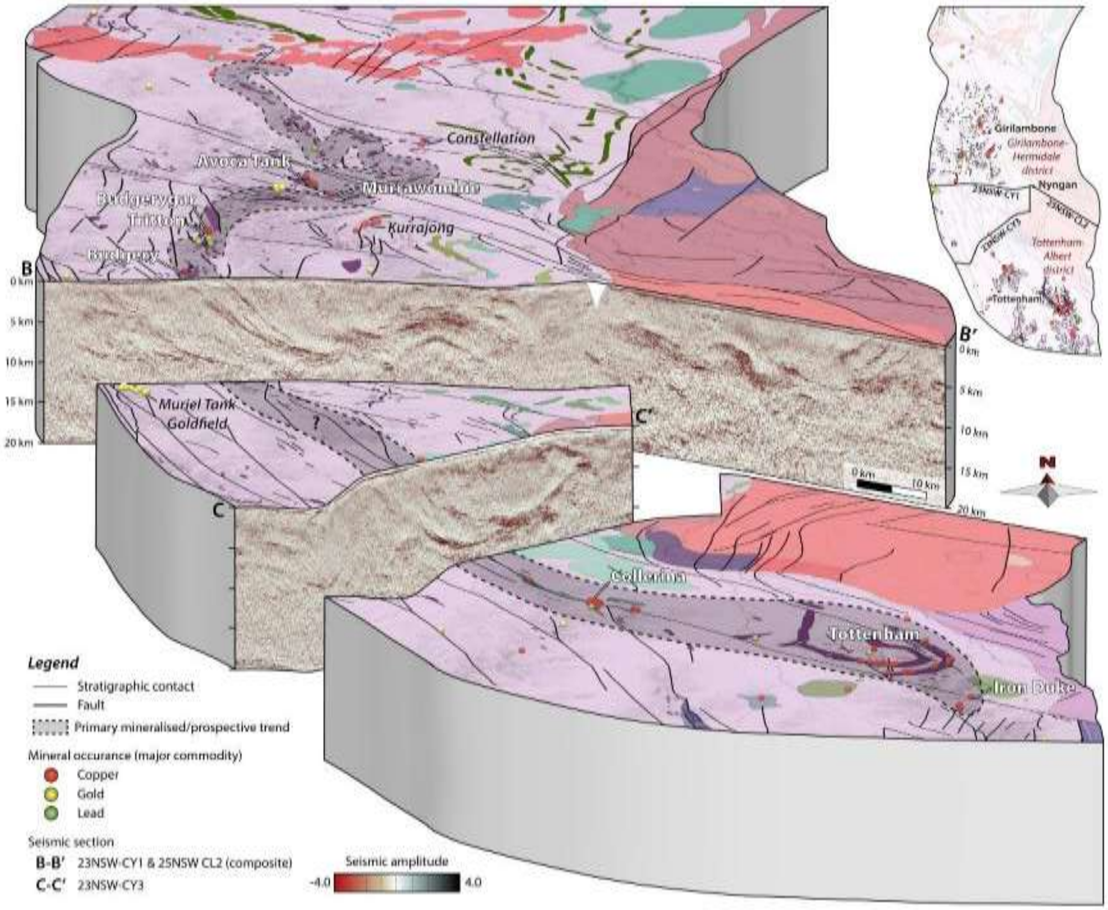

Figure 3. 3D block model of the Girilambone Zone within the Hermidale Terrane, showing the locations of the Cobar–Yathong seismic lines 23NSW-CY1 and 23NSW-CY3 in the context of Lachlan Orogen basement geology and NSW mineral occurrences from MinView. The western boundary of the model approximates the Muriel Fault Zone and its lateral equivalents. The Lachlan Orogen basement geology is shown using an updated version of the map of Colquhoun et al. (2026), scheduled for release in a future Seamless Geology update. The primary mineralised trend is modified from Aeris Resources (2023) for the Girilambone–Hermidale district and Gilmore et al. (2015) southward where it is increasingly interpretive and uncertain. The inset map illustrates the distribution of basement outcrop (opaque) and cover sequences (transparent) across the region. Approximately 95% of the area is concealed beneath Quaternary alluvial cover. Stratigraphic legend and mineral occurrence data are available through MinView.

Forbes-Parkes-Tomingley Gold Belt

The Forbes-Parkes-Tomingley gold belt is a narrow (< 10 km wide), elongate (> 100 km long) curvilinear structural corridor trending north–south to northeast–southwest. It lies immediately east of the regionally significant Parkes Thrust and Forbes Anticline within the Junee-Narromine Belt of the Macquarie Arc. The belt comprises a complex assemblage of interlayered volcanic and volcanoclastic/sedimentary units that host numerous vein- and lode-style orogenic gold fields (e.g., Tomingley, London-Victoria, Lachlan). Mineralisation is strongly controlled by rheology, with gold concentrated in the most intensely deformed zones, including highly sheared and faulted contacts between volcanic and volcaniclastic–sedimentary units, as well as within brittle volcanic rocks (Clarke, 1990; Chalmers et al., 2007). Although the source of gold-bearing fluids remains poorly constrained, the abundant mafic rocks of the Macquarie Arc provide a plausible reservoir, and the Parkes Thrust is widely considered the primary fluid conduit (Downes, 2019). The Peak Hill epithermal system also occurs within the belt but is genetically distinct from the orogenic deposits (Downes et al., 2025) and is therefore excluded from this study.

Following the nomenclature of the Forbes 1:250,000 and Parkes 1:100,000 geological map sheets (Lyons et al., 2000; Raymond et al., 2000), the faults within this high-strain corridor are collectively referred to as the "Parkes Fault Zone". This zone comprises the Parkes Thrust along its western margin, together with a set of structures to the east that may be linked at depth. The first-order geometry of the Parkes Fault Zone is generally interpreted as west-dipping, consistent with the exhumation of Macquarie Arc rocks and formation of the Forbes Anticline in its hanging wall (e.g., Lyons et al., 2000; Raymond et al., 2000; Glen et al., 2007; Meffre et al., 2007), although alternative east-dipping geometries have been proposed (e.g., Krynen et al., 1990; Owens et al., 2017). The magnitude of uplift and the broad wavelength of the Forbes Anticline support a west-dipping configuration and imply development above a deep-rooted fault system. Until recently, however, this deep-rooted geometry could not be demonstrated conclusively, owing to the absence of subsurface constraints on the geometry and crustal-scale characteristics of the Parkes Thrust.

Figure 4 presents a 115 km segment of the Central Lachlan Seismic Survey Line 1 (25NSW-CL1; D–D'), which traverses the Jemalong Trough/Tullamore Syncline, the Forbes Anticline, the Parkes Fault Zone, and continues eastward into the Cowra Trough. Because seismic imaging performs best in areas with gently dipping strata, the broad, long-wavelength folding of the Tullamore Syncline and Forbes Anticline is well resolved in the section. In contrast, the steep dips and structural complexity of the Parkes Fault Zone produce significant scattering and redirect seismic energy beyond the recorder spread, resulting in poor reflector continuity. These imaging characteristics are consistent with surface bedding measurements extracted from Colquhoun et al. (2026), which show average dips of 30° (n = 75) in the Tullamore Syncline and Forbes Anticline, compared with 60° (n = 72) in the Parkes Fault Zone (Figure 4(I)).

Although the Parkes Fault Zone is poorly imaged in the shallow portion of the seismic section, several deeper features provide important new constraints on its geometry. A set of reflectors at approximately 10 km depth displays folding that parallels the surface trace of the Forbes Anticline, while offsets in high-amplitude packages within the mid- to lower crust (20–40 km) demonstrate that the structure extends through most of the crust. When integrated with existing geological constraints, the new seismic observations can be reproduced using a fault-bend fold model (Suppe, 1983), providing a plausible geometric and kinematic framework for a transcrustal fault system accommodating more than 25 km of displacement (Figure 4(II)). Much of this displacement could be accommodated within the uppermost crust across the Parkes Fault Zone.

Recognising such deep-rooted structures is important for understanding how orogenic gold systems develop. The association of major gold districts with crustal-scale faults is well demonstrated elsewhere in the Tasmanides (e.g., Kreuzer et al., 2007; Willman, 2007; Downes, 2019) and indeed globally (e.g., Kerrich et al., 2000; Groves et al., 2018); however, the deeper crustal-scale architecture of these faults is rarely well constrained. With new deep-crustal seismic data, the Parkes Fault Zone now provides a robust example of a crustal-scale system that has been capable of focusing fluid flow and localising significant orogenic gold mineralisation. This provides explorers with a tangible structural template to incorporate into mineral system analyses and, ultimately, exploration models.

Macquarie Arc (and related deposits)

Macquarie Arc rocks are a critical component of mineral exploration within the Lachlan Orogen. In addition to hosting significant porphyry and epithermal deposits, they are interpreted as important sources of metals and mineralising fluids for mineral deposits within the overlying and adjacent mid-Silurian to mid-Devonian rocks (e.g., Carr et al., 1995; Downes et al., 2008; Downes, 2009; Fitzherbert et al., 2026; Greenfield, 2026). Consequently, both direct proximity to

Macquarie Arc rocks and the structural pathways that link them to overlying rocks, are regarded as key indicators of prospectivity. Exploration activity, and much of the associated discovery success, has therefore been concentrated in areas where these relationships are readily apparent, such as at Tomingley and McPhillamys, which occur adjacent to the Junee–Narromine and Molong belts, respectively.

However, more than 60% of the area shown in Figure 5(I) is concealed beneath Cenozoic cover, while Macquarie Arc rocks comprise less than 5% of the exposed basement geology. Consequently, the structure, continuity and true extent of the Macquarie Arc beneath much of the region remain poorly constrained. As a result, an important exploration frontier may lie in identifying previously overlooked structures that have more subtle but significant connections to Macquarie Arc rocks concealed beneath younger cover.

Central Lachlan Seismic Survey Line 1 (25NSW-CL1) provides an unprecedented dataset for examining the surface and subsurface distribution of Macquarie Arc rocks at regional and crustal scales along a profile exceeding 330 km (A–A'; Figure 5). The transect provides continuous sampling under cover from the westernmost interpreted occurrence of Macquarie Arc rocks in the footwall of the Gilmore Fault Zone (Glen et al., 2002), across the Junee–Narromine and Molong belts, and into the northern Hill End Trough, where Macquarie Arc rocks clearly form the basement (e.g., Fitzherbert et al., 2026).

In addition, smaller exposures located along strike of the transect, including those at Fairholme, Cowal and Cargo (Figure 5(III)), provide important controls on the seismic interpretation. Many of these exposures occur within exhumed thrust sheets bounded by major faults that can be traced into the seismic section. The Cargo area provides a particularly well-constrained example, where Macquarie Arc rocks are exposed within thrust sheets associated with the Cudal and Manildra faults (e.g., Krynen et al., 1997; Colquhoun et al., 2026).

North of Cargo, these structures pass beneath the Silurian–Devonian Cowra Trough, where direct exposure of Macquarie Arc rocks is absent. However, the thrust sheets and their bounding faults are well imaged in the seismic data (i.e., Figure 2(II)) and can therefore be traced beneath cover. Correlation with exposed Macquarie Arc rocks at Cargo and within the Molong Belt indicates that Macquarie Arc rocks are likely preserved within the shallow subsurface beneath the eastern Cowra Trough (Figure 5).

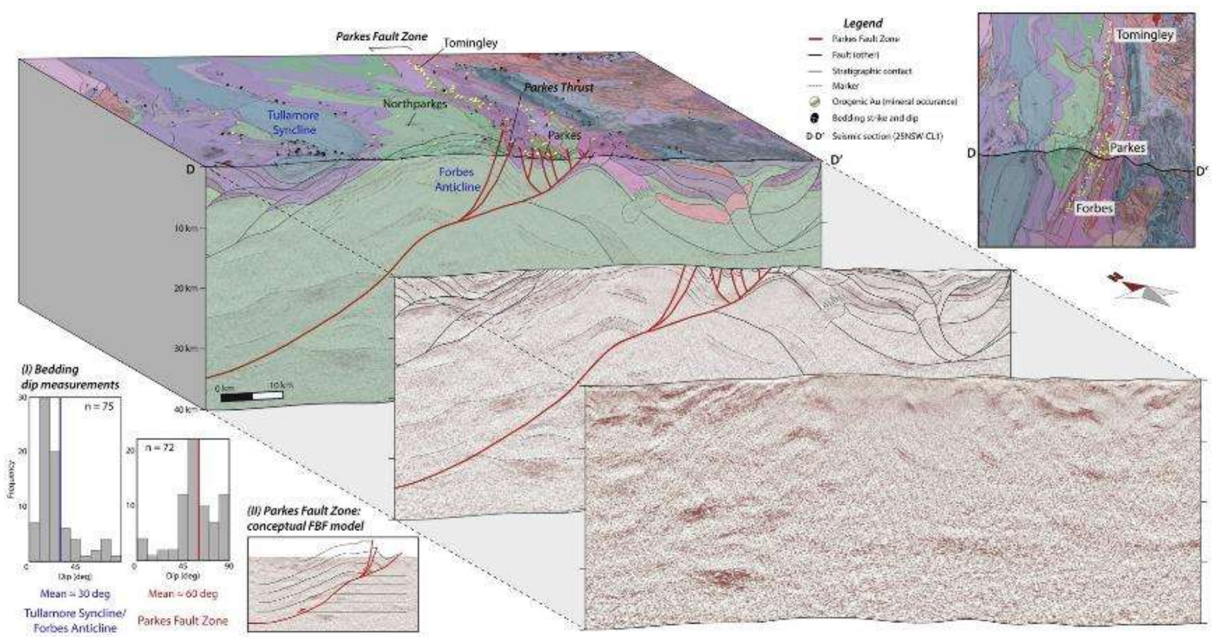

Figure 4. 3D block model showing the relationship between the Forbes-Parkes-Tomingley gold belt and seismic line 25NSW-CL1. Both uninterpreted and interpreted seismic sections are displayed. Geology is based on the Lachlan Orogen interpretation from Seamless Geology (Colquhoun et al., 2026) presented without Cenozoic sedimentary cover. Orogenic gold occurrences are sourced from the NSW Mineral Occurrences database. Geological mapping, stratigraphic legend, and mineral occurrence data are available through MinView. (I) Comparison of surface bedding measurements in the Tullamore Syncline and Forbes Anticline versus the Parkes Fault Zone. (II) Conceptual fault-bend fold model testing the geometric and kinematic plausibility of the fault interpretation.

This interpretation has important exploration implications. The faults bounding these thrust sheets provide direct structural connections between shallow basin rocks and Macquarie Arc basement, creating potential pathways for the migration of arc-derived magmas, metals and mineralising fluids. Together, the interpreted proximity of Macquarie Arc rocks in the subsurface and the direct structural connectivity make this series of faults within the eastern Cowra Trough an attractive, historically underexplored target.

A similar case can be made for the proximity of Macquarie Arc rocks in thrust sheets imaged beneath the western Jemalong Trough and easternmost Hermidale Terrane, based on along strike constraints from exposures and drilling within the Cowal, Fairholme and Trundle areas (Figure 5(III)). However, faults are mapped much less confidently in this area and are therefore harder to target, largely due to the more extensive Cenozoic cover (e.g., Figure 5(I)).

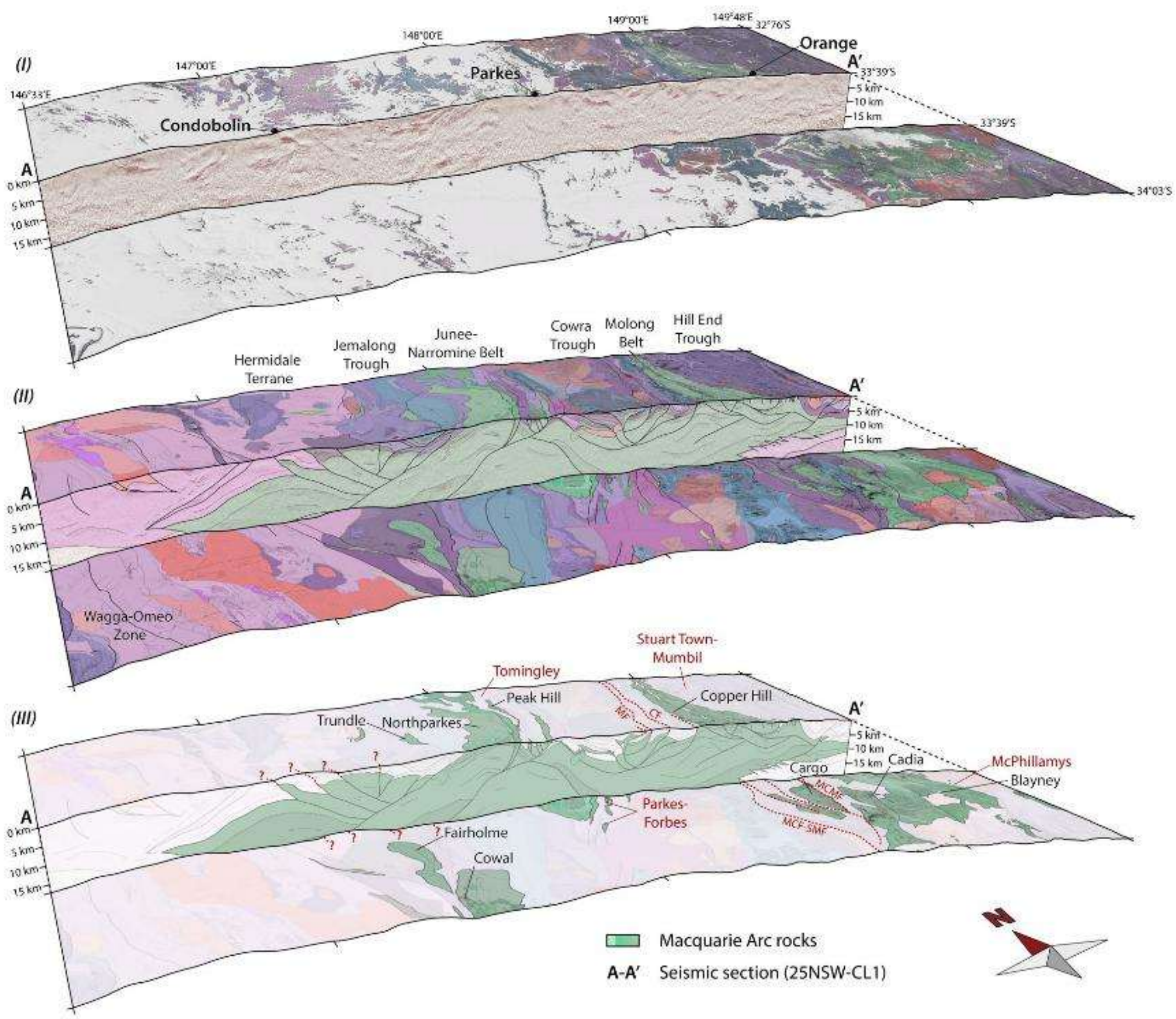

Figure 5. 3D perspectives of seismic line 25NSW-CL1 shown in both uninterpreted and interpreted form within the broader context of the Lachlan Orogen. (I) Illustrates the distribution of Lachlan Orogen basement outcrop (opaque) and cover sequences (grey) across the region, highlighting the value of seismic data for providing continuous lateral sampling across areas of limited exposure. (II) Displays the seismic interpretation alongside the interpreted Lachlan Orogen layer from Seamless Geology (Colquhoun et al., 2026). (III) Highlights the interpreted surface and subsurface distribution of Macquarie Arc rocks, together with associated mineral deposits. Black labels denote mapped areas of Macquarie Arc rocks many of which host porphyry and epithermal deposits, whereas red labels identify deposits interpreted to be sourced from Macquarie Arc rocks but are hosted within mid-Silurian to mid-Devonian strata. Red dashed lines indicate faults bounding Macquarie Arc–involved thrust sheets, revealing concealed but direct structural links between shallow basin successions and Macquarie Arc basement. Fault abbreviations: MCF-SMF = Mandagery Creek Fault-Soldiers Mountain Fault; MF = Manildra Fault; CF = Cudal Fault; MCMF = Molong–Columbine Mountain Fault.

CONCLUSIONS AND FUTURE DIRECTION

The GSNSW seismic program is demonstrating the value of deep-crustal seismic reflection data for understanding mineral systems and supporting exploration across the Lachlan Orogen. By acquiring overlapping regional-scale seismic lines, applying specialised processing methodologies, and interpreting the results within an integrated 3D geological environment, the program is building a new framework for understanding the region's crustal architecture, geological evolution, and metallogeny. The case studies presented here show how seismic reflection data can map concealed prospective corridors, image the mineralising structures that feed entire mineral districts, and constrain the distribution of fertile geological units beneath cover. Together, these results demonstrate the growing value of seismic reflection as a practical mineral systems tool that links insights across tectonic, crustal and deposit scales. Ongoing interpretation of the Macquarie Arc Seismic Survey, together with the reprocessing and integration of legacy seismic datasets, will continue to refine this framework and deepen understanding of the geology and metallogeny of the Lachlan Orogen.

ACKNOWLEDGEMENTS

Geoscience Australia is gratefully acknowledged for its assistance with the planning and acquisition of the seismic surveys. The authors also acknowledge the many staff of the GSNSW and external collaborators whose contributions to the acquisition, processing, and interpretation of the seismic surveys made this study possible. Kate Holdsworth is thanked for drafting Figure 1.

REFERENCES

AERIS RESOURCES 2023. Annual Report.

CARR G.R., DEAN J.A., SUPPEL D.W., & HEITHERSAY P.S. 1995. Precise lead isotope fingerprinting of hydrothermal activity associated with Ordovician to Carboniferous metallogenic events in the Lachlan fold belt of New South Wales. Economic Geology 90, 1467–1505.

CATHERS G. 2026. NSW Exploration & Discovery Highlights (NSW Parliament House, Sydney).

CHALMERS D.I., RANSTED T.W., KAIRAITIS R.A., & MEATES D.G. 2007. The Wyoming gold deposits: volcanic-hosted lode-type gold mineralisation in the eastern Lachlan Orogen, Australia. Mineralium Deposita 42, 505–513.

CLARKE I. 1990. Primary deposits in the Forbes-Parkes-Peak Hill-Tomingley gold belt. In Geological Setting of Gold and Copper Deposits in the Parkes Area, New South Wales, I. Clarke, and L. Sherwin, eds (New South Wales Department of Minerals and Energy), pp. 139–190.

COLQUHOUN G.P., HUGHES K.S., DEYSSING L., BALLARD J.C., FOLKES C.B., PHILLIPS G., TROEDSON A.L., & FITZHERBERT J.A. 2026. New South Wales Seamless Geology dataset, version 2.6 [Digital Dataset] (https://minview.geoscience.nsw.gov.au: Geological Survey of New South Wales, NSW Resources, Department of Primary Industries & Regional Development).

DOWNES P.M. 2009. Sulfur- & lead-isotope signatures of selected middle Silurian to Carboniferous mineral systems of the Lachlan Orogen, eastern New South Wales - implications for metallogenesis. Doctor of Philosophy. University of Newcastle.

DOWNES P.M. 2019. A mineral system model for orogenic gold mineralisation in the eastern Lachlan Orogen, New South Wales (Geological Survey of New South Wales).

DOWNES P.M., COLQUHOUN G.P., FITZHERBERT J.A., & BLEVIN P.L. 2025. Metallogenic map of New South Wales 1:1 500 000 (Geological Survey of New South Wales).

DOWNES P.M., SECCOMBE P.K., & CARR G.R. 2008. Sulfur- & lead-isotope signatures of orogenic gold mineralisation associated with the Hill End Trough, Lachlan Orogen, New South Wales, Australia. Mineralogy and Petrology 94, 151–173.

DPIRD 2024. NSW critical minerals & high-tech metals strategy 2024–35 (Department of Primary Industries & Regional Development).

ERCEG M., & HOOPER B. 2006. The Tritton copper mine, New South Wales: New understandings of the deposit & its potential from mining of this blind discovery. In Mineral Exploration Geoscience in New South WALES P.C. Lewis, ed. (Cessnock, New South Wales: Sydney Mineral Exploration Discussion Group (SMEDG)), p. 4.

FITZHERBERT J., SIMPSON B., HILL S., HUGHES K., EASTLAKE M., & LOGAN D. 2026. Thermal & Isotopic Mapping of NSW Orogens – Mapping the Footprints of Mineralisation (NSW Parliament House, Sydney).

FITZHERBERT J.A., MAWSON R., MATHIESON D., SIMPSON A.J., SIMPSON C.J., & NELSON M.D. 2017. Metamorphism in the Cobar Basin: current state of understanding & implications for mineralisation (Geological Survey of New South Wales).

FOGARTY J.M. 1998. Girilambone district copper deposits. In Geology of Australian and Papua New Guinean Mineral Deposits, D.A. Berkman, and D.H. Mackenzie, eds (The Australasian Institute of Mining & Metallurgy, Melbourne), pp. 593–600.

GILMORE P., DAVIDSON G., TRIGG S., & CAMPBELL L. 2015. Mapping, magnetics and microscopes: Understanding the setting of VAMS mineralisation in the Ordovician Girilambone Group, western NSW. In Mineral Exploration in the Tasmanides, p. 11.

GILMORE P.J., TRIGG S.J., & CAMPBELL L.M. 2018. Coolabah 1:100 000 geological sheet 8235 (Geological Survey of New South Wales).

GLEN R.A., KORSCH R.J., DIREEN N.G., JONES L.E.A., JOHNSTONE D.W., LAWRIE K.C., FINLAYSON D.M., & SHAW R.D. 2002. Crustal structure of the Ordovician Macquarie Arc, Eastern Lachlan Orogen, based on seismic-reflection profiling. Australian Journal of Earth Sciences 49, 323–348.

GLEN R.A., PERCIVAL I.G., & QUINN C.D. 2009. Ordovician continental margin terranes in the Lachlan Orogen, Australia: Implications for tectonics in an accretionary orogen along the east Gondwana margin. Tectonics 28, 2009TC002446.

GLEN R.A., SPENCER R., WILLMORE A., DAVID V., & SCOTT R.J. 2007. Junee–Narromine Volcanic Belt, Macquarie Arc, Lachlan Orogen, New South Wales: components & structure. Australian Journal of Earth Sciences 54, 215–241.

GREENFIELD J. 2026. East Lachlan Post-Ordovician Metallogeny: The Siluro-Devonian After Party (Club York Sydney).

GROVES D.I., SANTOSH M., GOLDFARB R.J., & ZHANG L. 2018. Structural geometry of orogenic gold deposits: Implications for exploration of world-class & giant deposits. Geoscience Frontiers 9, 1163–1177.

KERRICH R., GOLDFARB R., GROVES D., GARWIN S., & JIA Y. 2000. The characteristics, origins, & geodynamic settings of supergiant gold metallogenic provinces. Science in China Series D: Earth Sciences 43, 1–68.

KREUZER O.P., BLENKINSOP T.G., MORRISON R.J., & PETERS S.G. 2007. Ore controls in the Charters Towers goldfield, NE Australia: Constraints from geological, geophysical & numerical analyses. Ore Geology Reviews 32, 37–80.

KRYNEN J.P., MORGAN E.J., RAYMOND O.L., SCOTT M.M., & WARREN A.Y.E. 1997. Molong First Edition (1:100 000 geological map 8631) (Geological Survey of New South Wales).

KRYNEN J.P., SHERWIN L., & CLARKE I. 1990. Stratigraphy & structure. In Geological Setting of Gold and Copper Deposits in the Parkes Area, New South Wales, I. Clarke, and L. Sherwin, eds (New South Wales Department of Minerals and Energy), pp. 1–76.

LYONS P., RAYMOND O.L., & DUGGAN M.B. 2000. Forbes 1:250 000 Geological Sheet 2nd Edition SI55-7 (Geological Survey of New South Wales).

MAHONEY L., FITZHERBERT J., & MILZ M. 2024. New constraints on the subsurface structure & geological evolution of the Cobar Basin & Hermidale Terrane (NSW Parliament House, Sydney).

MAHONEY L., MILZ M., FITZHERBERT J., FOLKES C., & EASTLAKE M. 2026. The Central Lachlan Seismic Project – Revealing the Macquarie Arc (NSW Parliament House, Sydney).

MCCUAIG T.C., & HRONSKY J.M.A. 2014. The mineral system concept: the key to exploration targeting. In Building Exploration Capability for the 21st Century, K.D. Kelley, and H.C. Golden, eds (Society of Economic Geologists, Special Publication 18), pp. 153–175.

MEFFRE S., SCOTT R.J., GLEN R.A., & SQUIRE R.J. 2007. Re-evaluation of contact relationships between Ordovician volcanic belts & the quartz-rich turbidites of the Lachlan Orogen. Australian Journal of Earth Sciences 54, 363–383.

MILZ M., & MAHONEY L. 2025. Insights into the Cobar-Hermidale-Yathong region from seismically constrained potential field modelling (NSW Parliament House, Sydney).

MURPHY T., & COX B. 2019. Development in understanding of the Tritton-Girilambone Cu District, Lachlan Fold Belt, Australia; Resolving hydrothermal mineralisation in multiply-deformed Rocks. (The Australasian Institute of Mining & Metallurgy, Melbourne), p. 34.

OWENS J., PRIEST D., JAGO C., & PACEY A. 2017. Northparkes copper-gold deposits. In Australian Ore Deposits, G.N. Phillips, ed. (The Australasian Institute of Mining & Metallurgy, Melbourne), pp. 763–770.

RAYMOND O.L., SHERWIN L., WALLACE D.A., WYBORN D., YOUNG G.C., PERCIVAL I.G., & GLEN R.A. 2000. Parkes 1:100 000 geological map 8531 (Geological Survey of NSW).

SCHEIBNER E., & BASDEN H. 1998. Geology of New South Wales - Synthesis (Geological Survey of New South Wales).

SCHODDE R. 2025. Deposit exploration—discovery trends: 1900–2023. SEG Discovery 142, 19–35.

SHIELDS P. 1996. Geology of the Girilambone Copper Deposit. In The Cobar Mineral Field - A 1996 Perspective, W.G. Cook, A.J.H. Ford, J.J. McDermott, P.N. Standish, C.L. Stegman, and T.M. Stegman, eds (The Australasian Institute of Mining & Metallurgy, Melbourne), pp. 293–304.

SUPPE J. 1983. Geometry & kinematics of fault-bend folding. American Journal of Science 283, 684–721.

TRIGG S.J. 2017. Structural geology of the Coolabah & Mount Oxley 1:100 000 map sheets (Geological Survey of New South Wales).

VESTRUM R., & CAMERON G. 2022. Seismic imaging in fold-and-thrust belts. In Andean Structural Styles, G. Zamora, and A. Mora, eds (Elsevier), pp. 29–41.

WILLMAN C.E. 2007. Regional structural controls of gold mineralisation, Bendigo & Castlemaine goldfields, Central Victoria, Australia. Mineralium Deposita 42, 449–463.

FROM ROCK TO RESOURCE: SCANDIUM AND OTHER CRITICAL METALS IN THE TOUT IGNEOUS COMPLEX, NSW

Ria Mukherjee[1], Paul Ashley[2], Marco Fiorentini[3], Alexandra Bonner[4], Mike Wood[5], Geoffrey Newcombe[5]

[1] Department of Earth Sciences, University of New England, NSW
[2] Paul Ashley Petrographic and Geological Services
[3] Centre for Exploration and Targeting, University of Western Australia
[4] Orthosa Mineral Exploration Services
[5] Sunrise Energy Metals Limited

Key Words: Scandium, Tout Complex, Alaskan-type ultramafic-mafic, laterite, critical metals

INTRODUCTION

The Tout Complex forms part of the Fifield Alaskan-type ultramafic-mafic intrusive belt and hosts economic reserves of scandium (Sc) in its laterite profile. Scandium is a critical metal (Critical Minerals Strategy 2023-2030) of growing importance in the aerospace, automotive and defence industries because of its use in producing lightweight, high strength aluminium superalloys (Chassé et al. 2017). In addition to Sc, the laterite profile hosts significant nickel (Ni) and cobalt (Co), together with minor platinum (Pt) mineralization. The Sunrise Project (Sunrise energy Metals Ltd, ASX: SRL) is classified as an oxide-type nickel laterite deposit with enriched Co and Sc mineralization rather than the more common silicate-type laterite deposit (Syerston Scandium Project, Mineral Resource Estimate, October 2025). This study investigates the distribution of Sc, Ni, Co and Pt in the primary ultramafic mafic rocks of the Tout Complex and examines the processes responsible for their subsequent enrichment within the laterite profile. We show that the Tout Complex represents an exceptional critical metal system in which both primary igneous and secondary processes contributed to ore formation. Magmatic processes established the initial distribution of these metals within the intrusion, whereas serpentinization redistributed Ni and Co into secondary alloy and sulfide phases. Subsequent prolonged supergene weathering produced a thick (~ 40–45 m) laterite profile that further concentrated Sc, Ni, Co and Pt into economically significant resources. The interplay between these magmatic, alteration and weathering processes is therefore fundamental for the critical metal potential in the Tout Complex.

GEOLOGY OF THE TOUT COMPLEX

The Tout Complex is one of ~61 Ural-Alaskan-type ultramafic-mafic intrusions within the Fifield Belt, a ~500 km long and ~80 km wide N–S to NW–SE trending province (Figure 1a). These circular to elliptical, locally lens-shaped intrusions are characterised by strong concentric aeromagnetic anomalies coincident with local gravity highs (Barron et al. 2004). They intrude Cambrian-Ordovician meta-greywackes, quartz-mica schists and slates of the Girilambone Group, within the Lachlan Fold Belt (Glen et al. 2012; Keays et al. 2021).

The Tout Complex is an elliptical intrusion (~16 × 6.5 km) elongated WNW and comprises a concentrically zoned ultramafic-mafic succession with a central dunite core surrounded by pyroxenite and a monzonite-rich western zone (Figure 1b). These rocks are interpreted as the plutonic equivalents of shoshonitic (high-K) volcanic rocks of the Lachlan Fold Belt (Barron et al. 2004; Crawford et al. 2007). U-Pb SHRIMP zircon dating of hornblende gabbro yielded an age of 439.6 ± 8.5 Ma (Webb 2014), temporally overlapping with Phase 4 (440–437 Ma) of Macquarie Arc magmatism (Crawford et al. 2007; Glen et al. 2012).

Phase 4 of the Macquarie Arc coincidentally hosts the highly mineralised Cu-Au porphyry systems at Northparkes and Cadia (Glen et al. 2012). The linear distribution, regular spacing and shoshonitic affinity of the Fifield Alaskan-type complexes have been interpreted as evidence for a feeder system (Barron et al. 2004). This temporal and tectono-magmatic association perhaps suggest a possible genetic link between mineralisation in the Alaskan-type complexes and the Macquarie Arc Cu-Au porphyries, which warrants further investigation in the future.

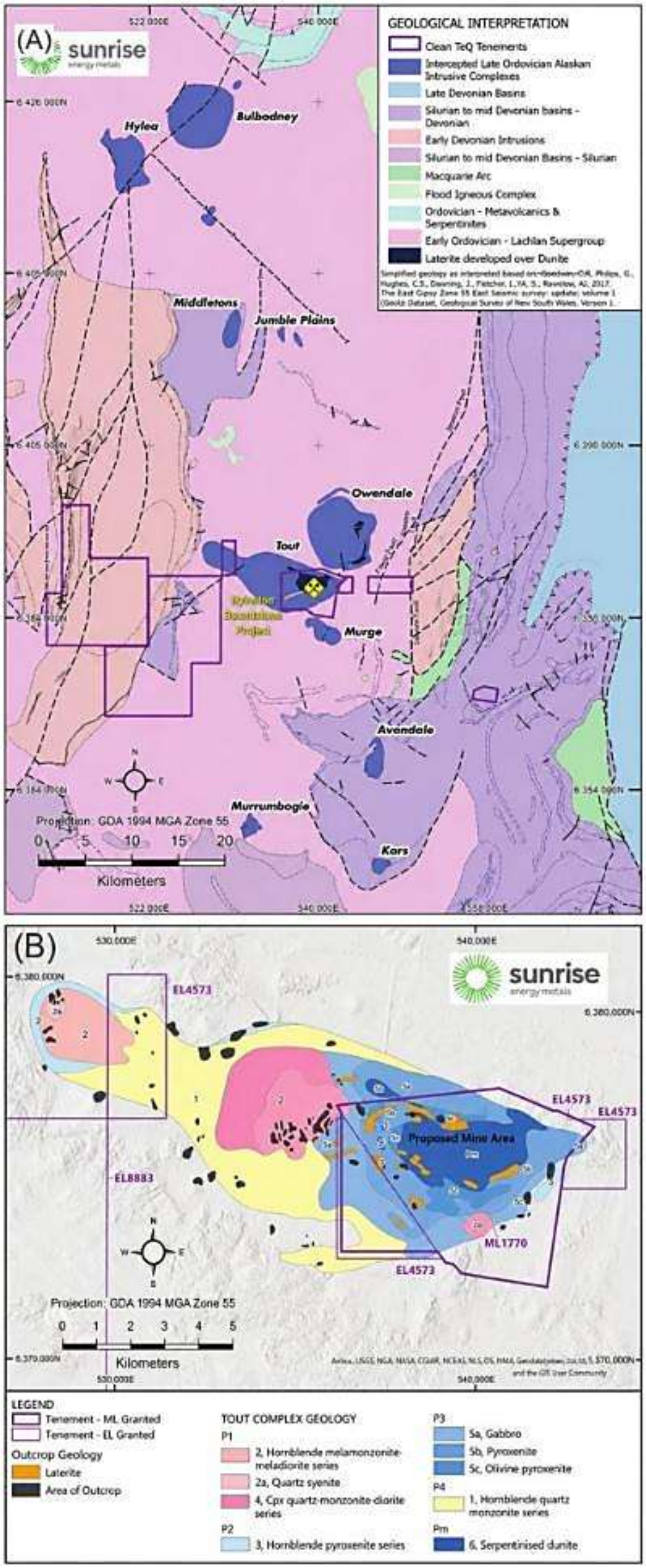

Figure 1. (A) Geology of the Fifield Alaskan-type ultramafic-mafic complex showing individual outcrops as circular to elongated bodies (in blue) that intrude metasedimentary rocks of the Girilambone Group (in pink) (B) Geology of the Tout Complex. Maps are taken from Syerston Scandium Project, Mineral Resource Estimate (October 2025).

LATERITE PROFILE

The laterite profile developed over the Tout Complex reaches ~35–40 m thickness over the dunite core and thins laterally across the flanking pyroxenites over which they form low rises of ~ 20 m relief (Figure 2A) (Syerston Scandium Project, Mineral Resource Estimate, October 2025). High-grade Sc mineralisation in laterite is largely associated with the pyroxenite rim, whereas Ni, Co and platinum enrichment is concentrated over the central dunite core (Figure 2B).

The lateritic profile comprises five distinct zones from top to base: an upper overburden/alluvium zone (Figs. 2C-D), transition zone (Figure 2E), goethite zone (Figure 2F), silicified goethite zone (Figure 2G) and a saprolite zone overlying the ultramafic bedrock (Figure 2H) (Syerston Scandium Project, Mineral Resource Estimate, October 2025).

High-grade Sc mineralisation (~600 ppm) in the laterites is concentrated within the goethite and silicified goethite zones (Figure 2I) (Chassé et al. 2017). Higher Ni and Co values (0.56%Ni and 0.09% Co) are also strongly concentrated in the goethite zone (ASX Announcement, Sunrise Energy Metals Ltd. Sept 2025; Syerston Scandium Project, Mineral Resource Estimate, October 2025).

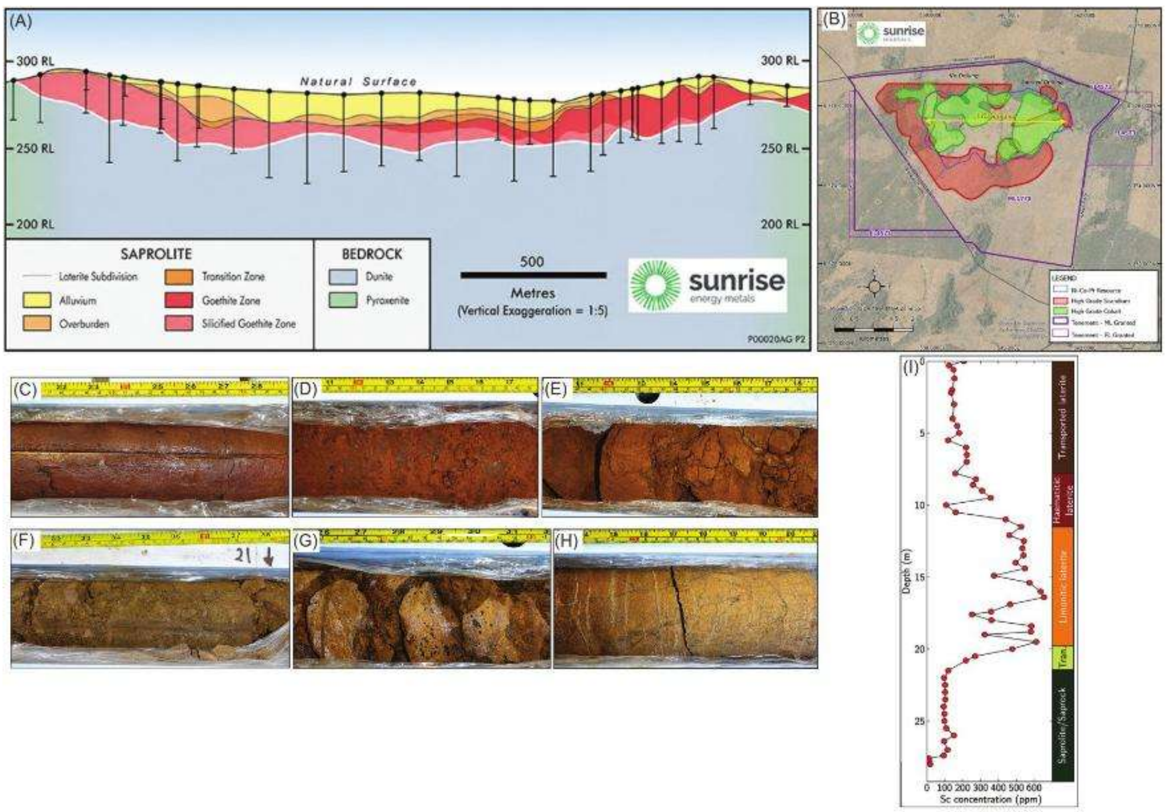

Figure 2. (A) Cross-section of the laterite profile in the Tout Complex (B) Sunrise deposit (Tout Complex) in GDA 1994 MGA Zone 55 coordinates. Ni-Co-Pt resources depicted in blue outline coinciding with dunite outcrop; high grade Co-resource is depicted in green shading and high-grade Sc shown in red (C-H) photographs of samples in sequence representing alluvial zone, overburden zone, transition zone, goethite zone, silicified goethite zone and the saprolite zone of the laterite profile. Figures (A-H) taken from Syerston Scandium Project, Mineral Resource Estimate (October 2025) (I) Sc distribution in Tout Complex across the laterite profile; limonite zone is equivalent to the goethite and silicified goethite zone (from Chassé et al. 2017).

HISTORICAL ASSOCIATION OF PGE OCCURRENCE IN THE TOUT COMPLEX REGION

The Fifield Alaskan-type complexes are renowned for platinum (Pt) mineralization, historically producing ~650 kg of placer Pt from Tertiary paleochannel deposits near Fifield, which was the only significant major Pt production in Australia (Slansky et al. 1991; Hoatson 2014). The nearby Owendale Complex (10 km north of Tout Complex; Figure 1A) hosts high-grade Pt mineralization (as Pt-Cu & Pt-Cu alloys and sulfides such as cooperite, or within disseminated Cu-sulfides) in wehrlites, dunites, and pegmatoidal clinopyroxenite, together with a lateritic Pt resource of 12.7 Mt at 0.28 g/t Pt (Suppel and Barron 1986; Johan et al. 1989; Keays et al. 2021). In contrast, Pt at the Tout Complex is largely confined to the lateritic profile as Pt–Fe alloys at relatively low grades (0.2–2 g/t), with only minor placer occurrences in alluvial channels (Ivanplats Syerston Technical Review Report, 2005) and sparse primary PGE alloys mainly associated with chromite veins or schlierens within dunites.

PRIMARY IGNEOUS ROCKS AND RELATIONSHIPS WITHIN THE COMPLEX

We identified four principal lithologies in ~450 m deep diamond drill cores from the Tout Complex: (1) dunite, the dominant rock type (Figure 3A); (2) wehrlite (Figure 3B); (3) dunite containing clinopyroxenite veins (Figure 3C); and (4) dunite containing mica-rich veins (Figure 3D). Contacts between dunite and wehrlite are gradational, whereas clinopyroxenite and mica veins are sharp, transgressive, and highly variable in thickness. Clinopyroxenite veins range from 2–3 cm and commonly branch into subsidiary veinlets (~1 mm), while mica veins vary from 1 mm to ~2 cm. Clinopyroxenite veins are dominated by coarse clinopyroxene, whereas the mica veins consist mainly of biotite with minor interstitial clinopyroxene and accessory magnetite. Dunite, in contrast, is strongly serpentinized but has small relict grains of olivine and chromite and uncommon accessory clinopyroxenes. Micron-sized disseminated sulfides (millerite and Co-pentlandite) occur in serpentinites and are mostly replaced by anhedral magnetite along with scattered sub-micron to micron-sized Ni-Co alloys (awaruite).

Figure 3. Hand specimen images of the primary ultramafic-mafic rocks sampled from diamond drill core SDD026 from the Tout Complex (A) Dunite (B) Dunite showing a gradational transition to Wehrlite (C) Dunite showing a distinct clinopyroxenite vein (1 cm wide) (D) Wehrlite showing mica vein (0.5 cm wide)

The bulk-rock geochemical data presented from one of the representative diamond drill cores show little variation in Ni and Co concentrations with depth, whereas Sc reaches its highest concentrations (40-50 ppm) at shallow levels (Figure 4A-C). Platinum exhibits a heterogeneous distribution, with only isolated depth intervals showing elevated concentrations (Figure 4D).

TIMA analyses that we conducted indicates that Ni and Co are primarily hosted by awaruite (Ni_3Fe), Co-bearing pentlandite [$(Co,Fe,Ni)_9S_8$], and millerite (NiS) (Figure 4E H). These minerals formed during serpentinization, when hydration of olivine generated serpentine, magnetite and H_2, creating reducing conditions that promoted the conversion of primary magmatic Ni-Cu sulfides to awaruite (Sciortino et al. 2015; Evans et al. 2023), and millerite.

Co-bearing pentlandite is also observed to be most abundant in wehrlite and within clinopyroxenite and mica-bearing veins, whereas awaruite predominates in dunite (Figure 4E-H). Millerite is the next most abundant Ni-bearing phase and is also most common in dunite. Awaruite and Co-bearing pentlandite are principally associated with serpentine, with occasional preservation in relict olivine (Figure 4I, K), while millerite occurs mainly with serpentine and magnetite (Figure 4J). Platinum is closely associated with chromite, consistent with previous investigation by Sunrise Energy Metals that found PGE minerals to preferentially occur within or adjacent to chromite veins and schlieren in the dunite. We followed up our TIMA investigation with Laser ablation ICP-MS analyses of the major silicate minerals and the disseminated oxides (magnetite and chromite) and observed that Sc is hosted predominantly by clinopyroxene, followed by biotite and, to a lesser extent, chromite (Figure 4L-N).

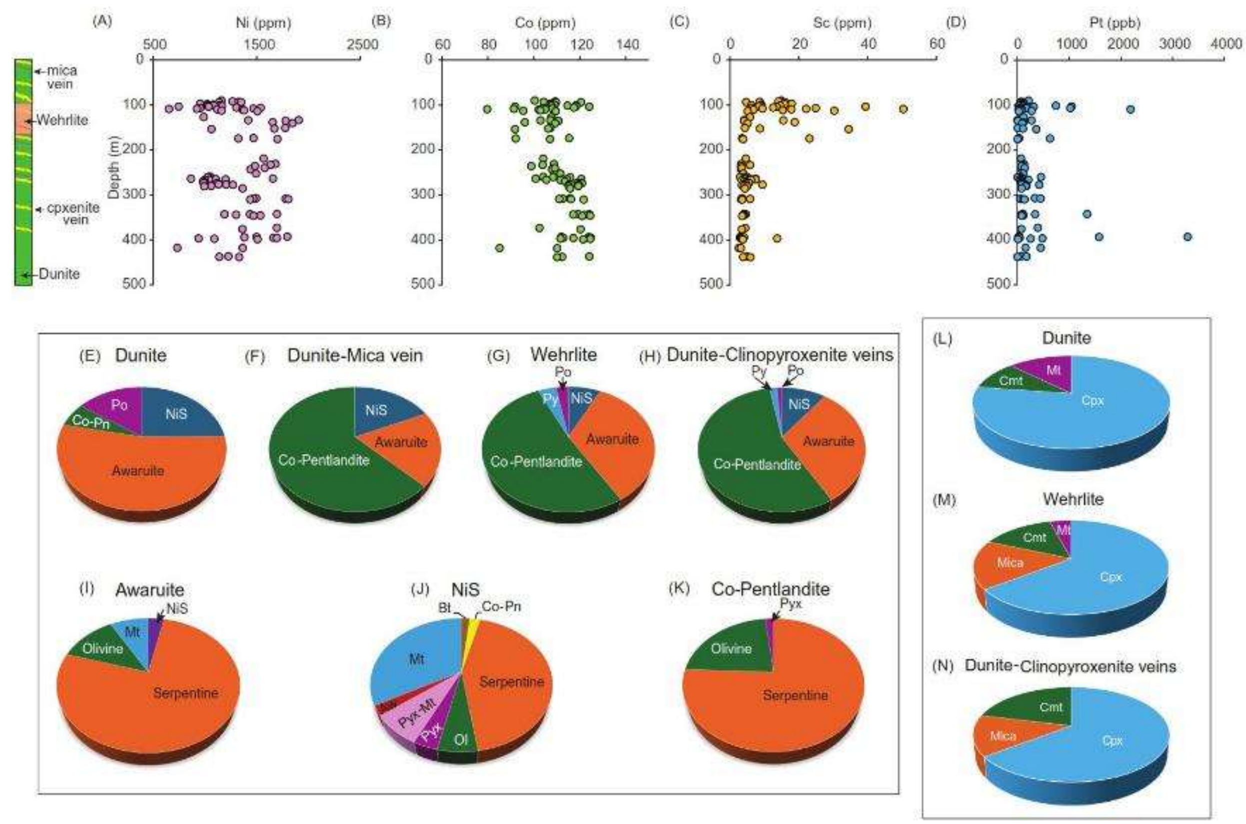

Figure 4. Bulk-rock assay of rocks from drill core SDD026 (core log presented on the left) showing distribution of (A) Ni (B) Co (C) Sc and (D) Pt (E-H) Pie-charts showing distribution of major Ni-Co bearing phases across the four distinct lithologies recognised from the drill core. Ni is dominantly in Awaruite (Ni_3Fe) and Millerite (NiS), Co is in Co-Pentlandite $(Co,Fe,Ni)_9S_8$. Data obtained from automated mineralogy (TIMA) (I-K) Pie chart showing association of

the Ni-Co bearing phases with other silicate and oxide minerals in the rocks. Data obtained from automated mineralogy (TIMA) (L-N) Pie chart showing Sc distribution in the rocks. Data obtained from LA-ICPMS.

REGOLITH PROFILE: MINERALOGICAL, AND GEOCHEMICAL CHARACTERISTICS

The Tout Complex hosts one of the world's highest-grade scandium (Sc) laterite deposits, with Sc concentrations typically ranging from 400 to 1200 ppm (Syerston Scandium Project, Mineral Resource Estimate, October 2025). This enrichment has been attributed to Sc-rich clinopyroxene-bearing ultramafic–mafic rocks in the basement, affected by prolonged weathering, perhaps since the late Cretaceous (Chan 2009), and long-term tectonic stability, which together promoted the development of thick Sc-rich lateritic profiles (Chassé et al. 2017).

Sc rarely forms discrete minerals but substitutes into clinopyroxene and other silicates (amphibole, garnet and mica; Samson and Chassé 2016), with lateritic weathering concentrating Sc in the profile. During weathering, Sc is initially retained in smectite and subsequently adsorbed onto goethite, which hosts 80% of the Sc budget. Consequently, the highest Sc grades have been reported from goethite zones, and its concentrations drops upwards due to progressive replacement of goethite by hematite towards the surface (Chassé et al. 2019).

Our investigation of recently drilled Sunrise Energy Metals laterite samples reveals some important information. We recorded markedly higher Sc concentrations (~1200 ppm) at shallow depths (5–10 m; Figure 5A–B), compared with the maximum values of ~500 ppm reported previously. Whereas Chassé et al. (2017, 2019) examined an in-situ laterite developed over pyroxenite, our samples are strongly magnetic throughout the 30–40 m drill interval and preserve remnant mesh textures and chromite pseudomorphs indicative of a dunite substrate (Figure 5C-H). This interpretation is further supported by increasing Ni, Co and Mg concentrations and decreasing Al contents towards the base of the profile (Figure 5A-B). Unlike previous studies that interpreted Sc enrichment as predominantly an in-situ process controlled by clinopyroxenite basement (Chassé et al. 2019), our data indicate that exceptionally high Sc concentrations (up to ~1200 ppm) also occur within transported laterite developed above serpentinized dunite. This suggests that secondary transport and redistribution played a much larger role in Sc concentration than previously recognised. Our finding is also consistent with Figure 2A, which indicates that the inferred substrate beneath much of the laterite is dunite.

SUMMARY

The Tout Complex represents a distinctive critical-metal system in which primary igneous processes concentrated Sc, Ni, Co and Pt into specific minerals, serpentinization redistributed Ni and Co into awaruite, millerite and Co-bearing pentlandite, and prolonged weathering further upgraded these metals into economically significant laterite ores. Our findings also demonstrate that Sc enrichment is more complex than previously recognised, with transported laterite capable of hosting exceptionally high Sc concentrations.

The unusually high Sc concentrations in the deposit may reflect an unusual mantle source, such as a fluid-metasomatized fertile mantle (Wang et al. 2021) that are also capable of producing the high-K (shoshonitic) magmas characteristic of Phase 4 volcanism of the Macquarie Arc Glen et al. 2012), which may have genetic links to the Alaskan-type ultramafic–mafic intrusions.

The Tout and Owendale complexes also exhibit contrasting critical-mineral potential. Unlike Owendale, the Tout Complex shows little evidence for primary Ni-Cu sulfide or significant primary PGE mineralisation. Instead, its economic potential is dominated by Sc and lateritic Ni–Co mineralisation, with Ni and Co-hosted mainly in serpentinization related awaruite, millerite and Co-bearing pentlandite, whereas Sc remains principally controlled by primary clinopyroxene and biotite before secondary enrichment during lateritization.

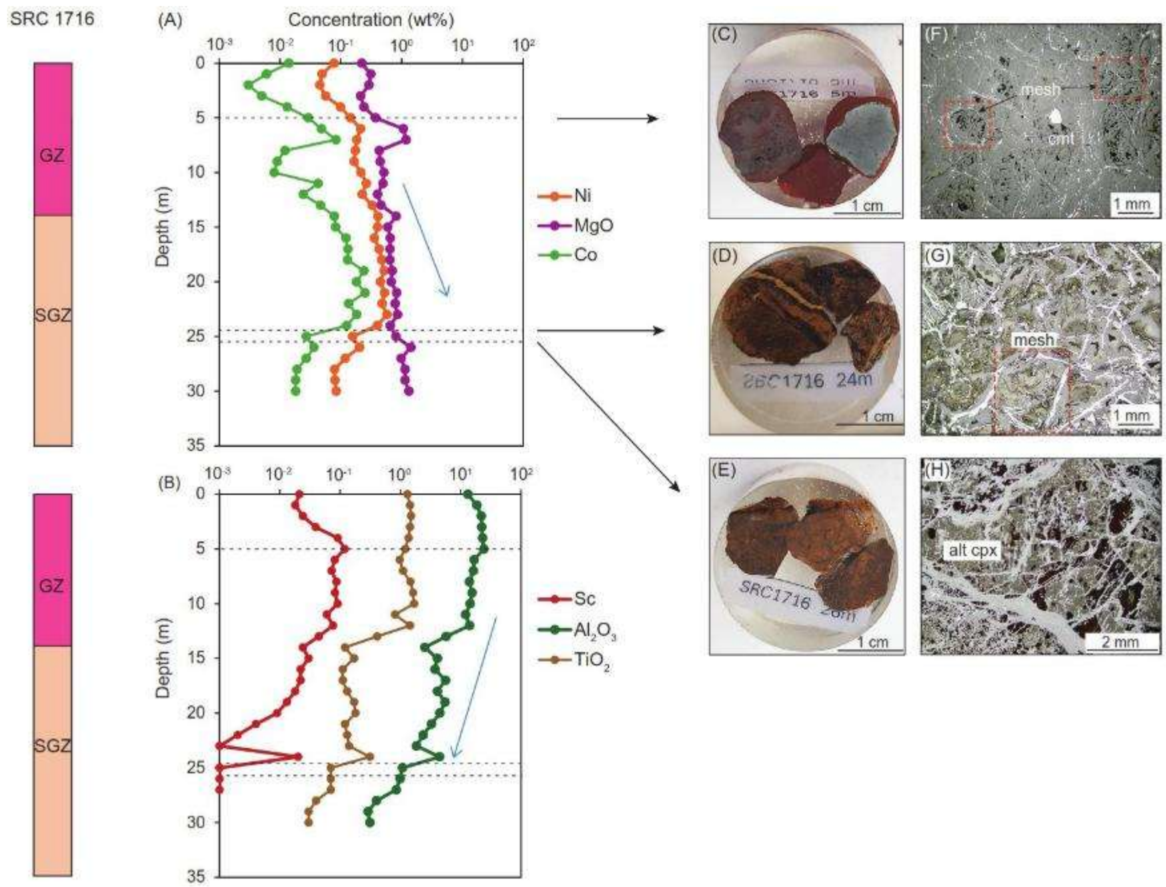

Figure 5. Assay showing variation of elements across a laterite profile. An overall log of the drilled RC chips is illustrated on the left, which shows the Goethite Zone (GZ) and Silicified Goethite Zone (SGZ). (A) Illustrates Ni, MgO and Co increasing with depth across the laterite and (B) shows progressive decrease in Sc, Al2O3 and TiO2 with depth. Blue arrow highlights the trend of changing concentration, while dashed line corresponds to the depth intervals of rock chips studied petrographically. (C) RC chip with highest Sc concentration at shallower depth (D-E) RC chip at depth with low Sc concentration but showing remnant layered texture (defined by magnetite) and mesh texture, respectively (F-G) corresponds to petrographic images of the RC displaying remnant mesh texture (highlighted by red-dashed box), defined by hematite; Fig. F shows chromite grain (cmt) altered to hematite (H) some remnant altered clinopyroxene (cpx) also observed.

FUTURE WORK

We propose that future investigations should focus on detailed geological mapping of both the ultramafic-mafic basement and the laterite profile to better constrain the controls on Sc mineralisation. Particular emphasis should be placed on mapping paleochannels to evaluate the extent of Sc redistribution within transported laterites, as suggested by this study. Detailed mineralogical and geochemical characterisation of the laterite profile is also required to determine the deportment of Sc, Ni, Co and Pt across the different weathering zones. Such work will improve understanding of ore-forming processes, resource potential and metallurgical behaviour during processing (Downes 2021).

UPDATE ON SRL’S PLANNED SCANDIUM MINING AND PROCESSING OPERATION

The Syerston Feasibility Study, completed March 2026, demonstrates excellent economics for a long-life, low-lost and scalable operation. Site works are due to start in the second half of 2026 with a 24-month construction and commissioning period followed by a 32-year mine life (21 years mining, 11 years processing stockpiled ore). At this stage no further exploration drilling is planned, however infill drilling to further define the Mineral Resource for mine planning and extraction purposes is planned over the lifetime of the operation.

The operation will mine the scandium bearing ore using conventional open-pit mining methods to feed a High Pressure Acid Leach circuit (ASX Announcement, Sunrise Energy Metals Ltd. Sept 2025), with the leachate fed to a Resin in Pulp extraction circuit followed finally by a refinery to produce a 99.9% pure scandium oxide product for use in the defence, aerospace, semi-conductor, communications and fuel cell markets.

ACKNOWLEDGEMENTS

The University of New England (UNE) is acknowledged for supporting the fieldwork. Grant Harris (UNE) is thanked for preparing the petrographic sections. The ARC Centre of Excellence for Critical Resources for the Future (ARC CCRF) is acknowledged for supporting the TIMA and LA-ICP-MS analyses. Louise Schoneveld (CSIRO, Perth) is thanked for assistance with the LA-ICP-MS data analysis, and Michael Verrall (CSIRO, Perth) for assistance with the TIMA analysis.

REFERENCES

ASX ANNOUNCEMENT 2025. Sunrise Energy Metals Ltd. 9th September 2025. BARRON L.M., OHNENSTETTER M., BARRON B.J., SUPPEL D.W. & FALLOON T. 2004. Geology of the Fifield Alaskan-Type Complexes, New South Wales, Australia. Geological Survey Report GS2004/323, 1-36.

CHAN R.A. 2009. Evolution of the Girilambone Regolith Landscape, Central-Western New South Wales. Australian Journal of Earth Sciences 56, 106–123.

CHASSÉ M., GRIFFIN W. L., O'REILLY S. Y. & CALAS G. 2017. Scandium speciation in a world-class lateritic deposit. Geochemical Perspective Letters 3, 105–114. doi:10.7185/geochemlet.1711

CHASSÉ M., GRIFFIN W.L., O'REILLY S.Y., ALARD O. & CALAS G. 2018. Insights into the mantle geochemistry of scandium from a meta-analysis of garnet data. Lithos 310-311 (2018) 409–42. https://doi.org/10.1016/j.lithos.2018.03.026

CRAWFORD A.J., MEFFRE S., SQUIRE R.J., BARRON L.M. & FALLOON T.J., 2007. Middle & Late Ordovician magmatic evolution of the Macquarie Arc, Lachlan Orogen, New South Wales. Australian Journal of Earth Sciences 54 (2-3), 181–214. https://doi.org/10.1080/08120090701227471.

CRITICAL MINERALS STRATEGY 2023-2030. Department of Industry, Science and Resources, Australian Government. June 2023, 1-58.

DOWNES P.M. 2021. A mineral system model for scandium-enriched regolith-hosted deposits in NSW. Geological Survey Report 2021/0343, 1-19.

EVANS K.A., FROST B.R., REDDY S.M. & BROWN T.C. 2023. Causes, effects, and implications of the relationships amongst fluids, serpentinisation, & alloys. Lithos 446 447 (2023) 107132. https://doi.org/10.1016/j.lithos.2023.107132

GLEN R.A., QUINN C.D. & COOKE D.R. 2012. The Macquarie Arc, Lachlan Orogen, New South Wales: its evolution, tectonic setting & mineral deposits. Episodes, 35 (1), 177 186.

HOATSON D.M. 2014. Evolution of Australia's platinum-group-element industry. In: Hoatson D.M., Lewis B. (eds) Platinum-group elements in Australia: geological setting, mineral systems, & potential. Record 2014/51. Geoscience Australia, Canberra.

IVANPLATS SYERSTON PVT LTD. 2005. Syerston Project – Technical Review of Resources prepared by McDonald Speijers (unpublished).

JOHAN Z., OHNENSTETTER M., SLANSKY E., BARRON L.M. & SUPPEL D. 1989. Platinum mineralisation in the Alaskan-type intrusive complexes near Fifield, New South Wales, Australia: Part 1, Platinum-group minerals in clinopyroxenites of the Kelvin Grove prospect, Owendale intrusion. Mineralogy and Petrology 40, 289–309.

KEAYS R.R., HOLWELL D.A. & PRICHARD H.M. 2021. Platinum mineralisation in the Owendale Uralian-Alaskan-type complex, New South Wales, Australia: The effects of serpentinization on Cu-PGE-Ni sulphides. Ore Geology Reviews 130 (2021) 103928. https://doi.org/10.1016/j.oregeorev.2020.103928

SAMSON I.M. & CHASSÉ M. 2016. Scandium. In: White W.M. (Ed.) Encyclopedia of Geochemistry. Springer International Publishing, Cham, Switzerland, 1–5.

SCIORTINO M., MUNGALL J.E. & MUINONEN J. 2015. Generation of high-Ni sulfide and alloy phases during serpentinization of Dunite in the Dumont Sill, Quebec. Economic Geology 110(3), 733–761. https://doi.org/10.2113/econgeo.110.3.733.

SLANSKY E., JOHAN Z., OHNENSTETTER M., BARRON L.M. & SUPPEL D.W. 1991. Platinum mineralization in the Alaskan-type intrusive complexes near Fifield, New South Wales, Australia. Part 2. Platinum-group minerals in Placer Deposits at Fifield. Mineralogy and Petrology 43, 161- 180.

SUPPEL D.W. & BARRON L.M. 1986. New data on the occurrence of platinum at Fifield. In: Geological setting of precious metals in New South Wales. Geological Society of Australia Abstract 18, 1-5.

SYERSTON SCANDIUM PROJECT, MINERAL RESOURCE ESTIMATE, October 2025. JORC Mineral resource estimation of the Syerston Scandium project for Sunrise Energy Metals Limited. Document 338_M_8937_v1 [Unpublished]

WANG Z., LI M.Y.H., LIU Z-R.R. & ZHOU M-F. 2021. Scandium: Ore deposits, the pivotal role of magmatic enrichment & future exploration. Ore Geology Reviews 128 (2021) 103906. https://doi.org/10.1016/j.oregeorev.2020.103906

WEBB K. 2014. The age & tectonometallogenic setting of the Fifield "Alaskan-type" intrusive suite, Lachlan Orogen, NSW. B. Sc. thesis, University of Wollongong.

STRUCTURAL CONTROLS ON GOLD MINERALISATION AT THE LONDON-VICTORIA DEPOSIT, PARKES DISTRICT, NSW: PROGRESSIVE DEFORMATION AND TARGETING IN THE EASTERN LACHLAN FOLD BELT

Ian E Neilson[1], Andrew Moulder[2], Alistair Hack[3]

[1] Structural Geology Consultant / GeoAugment
[2] Adavale Resources Limited
[3] ACH Geoscience Pty Ltd

Key Words: orogenic gold, Lachlan Fold Belt, London-Victoria, Tabberabberan, Kanimblan, structural targeting, Parkes, progressive deformation

INTRODUCTION

The London-Victoria gold deposit lies within the Parkes district of central New South Wales, hosted in Ordovician volcaniclastic rocks of the Macquarie Arc within the eastern Lachlan Fold Belt (Lachlan Orogen). The deposit forms part of a broader gold-copper mineral system shaped by Palaeozoic orogenic events of the Tasmanides. Understanding how progressive deformation partitioned strain, created fluid pathways, localised gold is essential for effective exploration beneath and along strike from the existing open pit.

This extended abstract presents a structural model for London-Victoria based on integrated analysis of pit mapping and diamond drillhole ALD001, calibrated against field-verified kinematic observations. All structures are explained by progressive strain accumulation under a single progressive E-W to ENE-WSW maximum principal stress, consistent with the published Kanimblan and Tabberabberan orogenic framework of the eastern Lachlan Fold Belt (Glen, 2005; Foster and Gray, 2000). Gold mineralisation is hosted in a NNE dextral shear zone that reactivated earlier thrust and axial planar fabrics. The model has direct implications for structural targeting of high-grade shoots in boudin necks, dilational jogs and shear intersections.

DATA SOURCES AND QUALITY HIERARCHY

Interpretations presented here rest on a strict data-quality hierarchy. Highest confidence is assigned to diamond drill core (ALD001), which provides continuous lithology, oriented structural measurements, reliable overprinting relationships. Pit mapping spanning 2025 and May 2026 supplies the second tier: direct outcrop observation of shear sense, fold geometry, lithology. Historic reverse-circulation (RC) drilling is used only cautiously for structural orientation where available; RC lithological assignments are treated as low confidence.

The VIO over-representation problem

Historic RC chip logging systematically over-assigns the rock code VIO (intermediate andesite / volcanic intermediate Ordovician) across much of the drilled stratigraphy. This is contradicted by two independent high-quality datasets. Diamond hole ALD001 identifies the host sequence below the oxide zone as dominantly lapilli tuff, tuffaceous ash siltstone, volcaniclastic sediment; intermediate andesite is restricted to the uppermost weathered interval (approximately 0-32 m). Pit mapping records fine-grained volcaniclastic sediments and chlorite-altered tuffaceous units, with no andesite mapped in the pit walls or floor.

The RC misidentification of fine-grained, altered volcaniclastic sediment as andesite is a common chip-logging error where alteration textures obscure primary grain size and composition. Consequently, any cross-sections, lithological wireframes, or resource models that rely on RC lithology to define andesite distribution should be regarded as low confidence. Structural interpretations in this abstract are built exclusively from measured orientations and direct observations in diamond core and pit outcrop, are independent of RC lithological assignments.

REGIONAL TECTONIC FRAMEWORK

The eastern Lachlan Fold Belt records a protracted history of accretionary orogenesis along the eastern margin of Gondwana (Glen, 2005; Foster and Gray, 2000). In the Parkes-Macquarie Arc region, two Palaeozoic events are particularly relevant to gold systems. The Tabberabberan Orogeny (approximately 390-380 Ma) involved broadly E-W shortening, producing ~N-S to NNW-trending folds and thrust systems. The subsequent Kanimblan Orogeny (approximately 340-320 Ma), the terminal orogenic event of the Lachlan Orogen, also involved E-W shortening, with widespread reactivation of pre-existing ~N-S fabrics and the development of strike-slip fault systems.

Both orogenies share approximately E-W σ_1. At London-Victoria, the full structural inventory, folds, thrusts, conjugate shears, the gold-hosting ~NNE-SSW dextral shear is explained by progressive strain accumulation under this common regional stress orientation. The transition from folding and thrusting to strike-slip faulting and fault reactivation records the order of strain accommodation as the fold-thrust system strain-hardened. This progressive model is consistent with published Kanimblan stress orientations and with analogous architecture at Hill End, where it is suggested that gold is likewise hosted on reactivated ~N-S faults under E-W compression.

PROGRESSIVE DEFORMATION MODEL

London-Victoria structures can be explained by progressive strain accumulation under a common ~E-W to ENE-WSW σ_1. The deformation sequence comprises progressive stages that record a continuous evolution from compressional folding and thrusting through conjugate strike-slip nucleation to fault reactivation and gold mineralisation.

Stage 1 — Early folding and thrusting

Early deformation under E-W σ_1 produced ~N-S regional folds with an axial-planar S1 cleavage, ~N-S to NNE-striking thrust faults with moderate east dips. S0 bedding is steeply East-dipping to locally overturned and vergence to both East and West. S1 occurs low-angle to sub-parallel to S0 and is interpreted as axial-planar cleavage to F1 folds. Reverse shear zones and reverse faults with moderate east dips record reverse geometry under ~E-W compression. Strain was accommodated by ductile folding and thrust imbrication, establishing a strong ~N-S mechanical anisotropy that controlled all subsequent deformation.

Stage 2 — Strain hardening and conjugate shear nucleation

As the fold-thrust system strain-hardened and could no longer accommodate further E-W shortening by pure compression, σ_2 and σ_3 swapped and the regime transitioned to transcurrent (σ_3 now horizontal ~N-S). Conjugate strike-slip faults nucleated at angles resultant from E-W σ_1: a NE-SW dextral set and a NW-SE sinistral set, rupturing the early ~East-dipping reverse faults. The bisector of these conjugates reflects the published Kanimblan E-W shortening within a few degrees of due east.

Stage 3 — Fault reactivation and the gold event

The principal gold-controlling structure is a steeply east-dipping ~N-S to NNE dextral shear zone that reactivated the earlier ~N-S thrust and S1 fabrics. Field observation suggests this as the dominant pit structure and the primary gold host, with sulphide and ankerite alteration also associated with lower-angle reverse structures that acted as link structures during reactivation. Kinematic evidence from pit mapping and ALD001 is consistent with dextral shear sense.

Mapped boudin axes (BAX) on the steep host form a steep SE-plunging cluster (typically 65–70° toward 130–150°), with a minor gentle NNW set.

On the steep N–S to NNE fabric this implies ~NE–SW extension during wrench-dominated dextral reactivation.

Earlier thrust faults are cross-cut with S2 crenulation cleavage overprinting S1 at an acute angle to the main shear. Quartz-carbonate shear veins were emplaced sub-parallel to the dextral shear (predominantly ~N-S, steep dips) in overstepping dilation sites. Further evidence of early fault reactivation occurs at the south end of the pit, where a ~ESE moderately dipping reverse fault is intensely altered and associated with low-angle tension veins.

Progressive dextral shearing boudinaged early veins. In ALD001 an early quartz vein is attenuated and transposed by D2 fabrics, showing that at least some quartz veins pre-date S2 and the steep shear and were deformed during progressive shearing. Late brittle normal-sense faults associated with pit-wall collapse are interpreted as post-orogenic modification, not part of the primary gold event.

ALD001 DRILLHOLE FINDINGS

Diamond hole ALD001 provides the only available qualified modern oriented-core window through the deposit. Drilled from the eastern pit wall toward the west, it intersects east-dipping ~NNE-SSW structures at a high angle and records a coherent structural architecture that supports the progressive deformation model.

Key observations include: S2 fabric crenulating S1; shear-parallel and tension vein populations; Z-fold dominance associated dextral shear sense; systematic west vergence at depth indicating a reverse component on the main shear and boudinaged early quartz veins attenuated by the D2 fabrics. A vergence transition and fabric overturning in the mid-hole interval are consistent with the hole crossing a shear-zone margin or inverted limbs, rather than a simple single-limb anticline.

At depth, stockwork veining in the lower interval demonstrates that structural preparation and fluid pathways persist well below the current pit floor. Combined with the steep easterly dip of the main shear, this supports significant down-dip exploration potential east of the pit.

EXPLORATION IMPLICATIONS

The progressive deformation reframes targeting at London-Victoria around the architecture of the reactivated ~N-S to NNE dextral shearzone and its intersections with conjugates. Priority vectors are:

- Along strike (~N-S to NNE): the gold-hosting dextral shear should continue beyond the current pit along strike with minor offsets associated with step overs and accommodation across sinistral conjugate features and associated reactivated D1 reverse fault systems. Systematic mapping and drilling along this corridor are the first-order exploration priority.
- Down dip (east): the main shear dips East. Deeper drilling stepped to the East should intersect the shear at depth, including the vein dominated domain indicated in ALD001
- Boudin necks and dilational jogs: high-grade shoots are predicted where progressive dextral shear created dilational sites.

- Shear intersections: where NE-SW dextral shears intersect the ~N-S gold-bearing shear, structural complexity enhances fluid focusing and creates high-priority drill targets.
- Data quality: future resource and targeting work to prioritise diamond drilling and pit mapping over historic RC lithology. pXRF-assisted logging is recommended to mitigate VIO over-representation in the existing database.

CONCLUSIONS

Structural analysis of the London-Victoria deposit demonstrates that progressive deformation under a single ~E-W to ENE-WSW σ_1 accounts for the full structural inventory: early ~N-S folds and thrusts, the onset of ~NNE-SSW dextral and NW-SE sinistral conjugates, a gold-hosting ~N-S to NNE dextral shear that reactivated the earlier thrust fabric. Gold mineralisation is controlled mechanically by the shear, with precipitation focused in boudin necks, dilational jogs, shear intersections. Diamond drilling (ALD001) and pit mapping provide the high-confidence data foundation; historic RC lithology is lower confidence for structural data acquisition. Exploration should target the ~N-S to NNE dextral shear along strike and down dip, with particular emphasis on boudin-neck geometry and intersections with NE-SW conjugates.

ACKNOWLEDGEMENTS

The authors thank Adavale Resources Limited for permission to present these results, the geology team who supported the collection of the oriented structural data from the London-Victoria pit and drillhole ALD001.

REFERENCES

FOSTER D. A. & GRAY D. R. 2000. Evolution and structure of the Lachlan Fold Belt (Orogen) of eastern Australia. Annual Review of Earth and Planetary Sciences 28, 47-80.

GLEN R. A. 2005. The Tasmanides of eastern Australia. In: Vaughan A. P. M., Leat P. T. & Pankhurst R. J. eds. Terrane Processes at the Margins of Gondwana. Geological Society, London, Special Publications 246, 23-96.

THE MS2 STRUCTURAL CORRIDOR: TESTING A SOUTHERN ANALOGUE OF THE PEAK GOLD FIELDS IN THE MOUNT HOPE TROUGH, COBAR BASIN, NSW

Mick Oates[1]

[1] 7PsXploration Pty Ltd, Candelo, NSW, 2550

Key Words: Mount Solitary, Mount Solar, MS2, New Occidental, Peak Goldfields, gold, bismuth, Cobar Basin, Mount Hope Trough

INTRODUCTION

The MS2 structural corridor is the name designated by Mount Hope Mining (MHM) to represent an 8km long north-south trending line of gold prospects defined by four topographic highs: Mt Solitary, Little Mount Solitary, Powerline Hill and Mt Solar. The entire MS2 structural corridor is currently held by Mount Hope Mining under EL6837 and forms part of a 606 km^2 tenement holding in the southern Cobar Basin (Figure 1).

MHM hypothesise that the MS2 corridor represents a southern analogue to the structurally controlled Peak Goldfields. This paper tests this hypothesis by comparing the structural evolution and compositional and physical characteristics of the hydrothermal fluids associated with mineralisation in the MS2 corridor, primarily the Mount Solitary prospect, with those documented from the Peak Goldfields, including the New Occidental mine. Establishing these similarities may provide a refined framework for exploring the MS2 corridor and gauge its potential to host significant Cobar-style gold mineralisation, both down plunge at the four prospects and along strike under cover.

Recent base metal discoveries by Aeris Resources (ASX:AIS), Australian Gold & Copper (ASX:AGC), Aurelia Metals (ASX:AMI) and Peel Mining (ASX:PEX) outside of the main Cobar mining district have driven a resurgence for base metal exploration throughout the Cobar basin. MHM considers that this resurgence in base metal exploration has overlooked the importance of stand-alone gold mines in the historic production of the Cobar basin and that an opportunity exists to explore for gold in the southern basin.

BACKGROUND

Tectonic Setting

Glen (1990, 1994, 1995) established that the Cobar Trough evolved through Early Devonian transtensional basin development followed by Tabberabberan inversion, during which NW-trending listric growth faults and associated NE transfer faults were reactivated to form the high-strain structural corridors that localised mineralisation throughout the Peak Goldfields. David (2005) extended this tectonic framework across the entire Cobar Basin by demonstrating that the Mount Hope and Rast troughs share the same basin architecture, structural inheritance and inversion history. His basin-scale synthesis showed that mineralisation throughout the Mount Hope Trough is consistently associated with reactivated syn-rift faults, eastward reverse tectonic transport and discrete high-strain corridors developed during inversion. Within this framework, the MS2 Structural Corridor is interpreted as a structurally equivalent inversion-related hydrothermal corridor to that hosting the Peak Goldfields, rather than as an isolated gold occurrence.

MS2 - Mt Solitary

According to Mines Department records, gold was first discovered at Mount Solitary in 1904 by Dowd and David where samples returned assays of up to 233 g/t Au and 8% Bi. Sporadic mining up until the1940s led to the development of underground workings, a glory hole style open pit and a cyanide treatment plant with total recorded production of approximately 1331 (Oz t) of gold at a bulk grade of 2.62 g/t Au (Mc Clatchie 2001)

The Mount Solitary prospect is hosted by siliciclastic facies sandstone, siltstone and intraformational pebbly conglomerates of the Early Devonian Broken Range Group within the Mount Hope Trough, a southern depocenter of the Cobar Basin (Schiebner 1987, Suppel and Gilligan 1993). Approximately 5km west of Mount Solitary, the coeval Mount Hope Group volcanics comprise a bimodal volcanic succession, where recent petrographic studies by Simpson 2014, suggest potential for the existence of a volcanic eruptive centre she termed the Nombinnie-Regina Eruptive Centre, an interpretation further supported by a recent deep crustal seismic interpretation by Milz and Mahoney 2025.

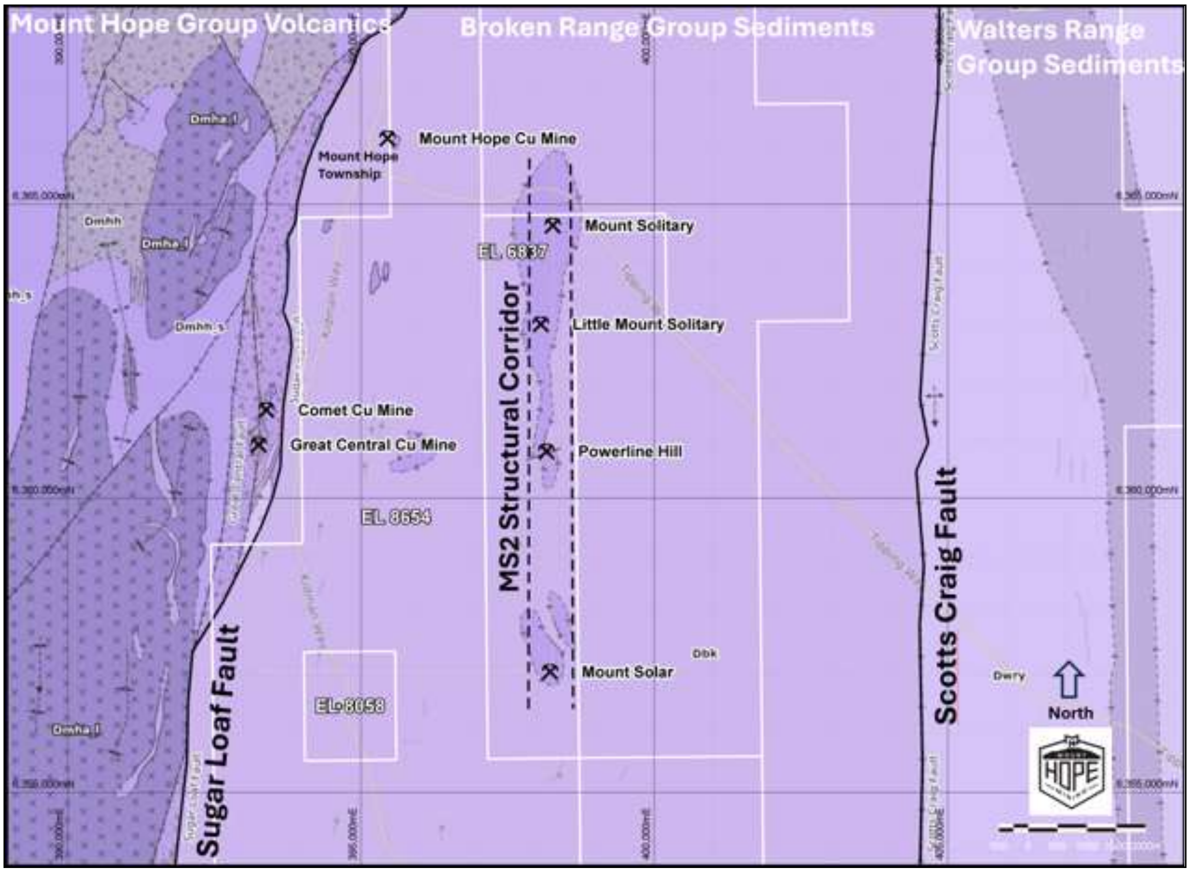

Figure 1. Location of Mount Hope Mining's 8km long North South trending MS2 Structural Corridor hosting the four prospects Mount Solitary, Little Mount Solitary, Powerline Hill and Mount Solar, proposed in this paper to represent a single hydrothermal system developed along a major structure. The MS2 is hosted by Broken Range Group sediments and is centrally located between the Scotts Craig Fault which separates the Walters Range Group sediments to the East and the Sugar Loaf Fault which sperates the Mount Hope Group volcanics to the West.

The MS2 structural corridor is centrally located between and parallel to the regionally significant Sugar Loaf and Scotts Craig faults (Figure 1). The Sugar Loaf fault is proximal to the copper and gold dominated mineralisation at the Great Central and Comet Mines. The Scotts Craig fault separates the Broken Range Group sediments to the west, that host the MS2 structure from the shallow water Walters Range Group to the east and according to Downes et al 2016 is more extensive than previously mapped, extending north to link up with the Rookery Fault in the vicinity of the Queen Bee mine near Cobar. Both faults have been interpreted as normal listric faults created during basin extension and reactivated as thrust faults during basin inversion.

During the 1980's, The Electrolytic Zinc (EZ) company modelled regional airborne magnetic and gravity datasets. The magnetic modelling identified two circular magnetic anomalies, measuring approximately 5km in diameter each and modelled at depth beneath the MS2, and NE and NW trending paleo drainage patterns that cross through the MS2 (Figure 2). From gravity data the MS2 structural corridor was interpreted to be located along the contact between a granite to the east and the Mt Hope volcanics to the west. The two deep magnetic anomalies were interpreted to have been intruded into this contact. (Slade 1985). A recent interpretation of a seismic line that passes just south of Mount Solar by Milz and Mahoney 2025 supports the EZ modelling and suggests that the Sugarloaf fault and the Scotts Craig fault's may be connected at depth where they host the roots of Simpson's Nombinnie-Regina eruptive center. Schiebner s' tectonic map of the Cobar basin in 1976 interpreted basin oblique lineaments. One of them, the Mount Hope Lineament, crosses only a couple kilometers to the north of Mount Solitary on the same orientation as the linear magnetic features.

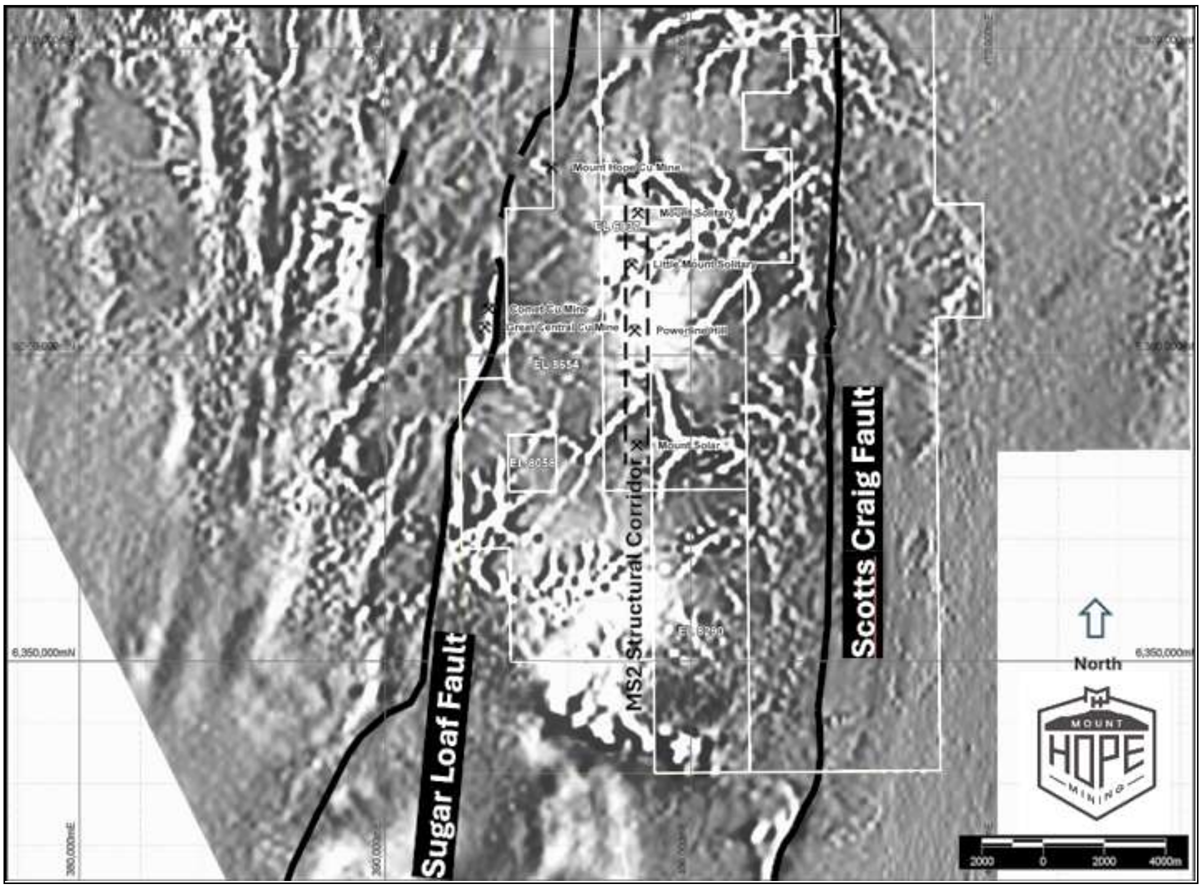

Figure 2. Reduced to pole first vertical derivative image highlights the deep magnetic anomalous sources described as two 5km diameter circular features as well as the shallow NE and NW palaeo drainage patterns that cross the MS2 structural corridor and are interpreted as cross faults linking the Scott's Craig and the Sugar Loaf faults.

The structural and geological source of all widespread mineralisation has not yet been defined; however one possible cause may be related to the concealed intrusive bodies, basement highs and cross faults, which are all prominent features in the Mount Hope Trough, which further highlight the structural prospectivity of the MS2 corridor at depth.

Peak Goldfield – New Occidental

The Peak Goldfields are located approximately 10km south of Cobar within the eastern margin of the Cobar trough and comprise a cluster of structurally controlled gold and polymetallic deposits associated with the Great Chesney Fault and the Peak Shear.

Mineralisation is hosted by siliciclastic facies sandstone, siltstone, mudstone and basal conglomerates of the early Devonian Nurri Group within the Cobar Trough, a northern depo-center of the Cobar Basin. These volcano-sedimentary successions were deposited during Early Devonian extension before undergoing basin inversion during the Tabberabberan Orogeny (ca. 400–395 Ma).

The New Occidental gold deposit is one of the principal deposits within the Peak Goldfields and is hosted within a steeply dipping structural corridor characterised by intense silica–chlorite–carbonate alteration, sheeted and stockwork quartz veins, sulphide-rich breccias and brittle-ductile deformation developed within competent fine-grained sediments. Detailed structural studies demonstrate that gold mineralisation was emplaced during progressive deformation associated with Early Devonian basin inversion, with repeated fault movement creating transient permeability for hydrothermal fluid flow and high-grade gold deposition (Stegman, 2007). The Occidental mine was initially discovered in the 1880s and later reopened as the New Occidental mine in 1935 where it has since produced roughly 1.5 million ounces of gold. It is also worth noting that The Peak and Perseverance deposits, also part of the Peak Goldfields are spatially associated with an intrusive rhyolite where mineralisation is localised along fault contacts between sediment and rhyolite blocks and shears within the rhyolite. Perseverance was identified in the 1980s from a coincident gravity and magnetic anomaly centered on historical workings. The relationship between anomalous magnetic and gravity features further highlights the similarities between the Peak Goldfields and the MS2.

HYPOTHESIS: A SOUTHERN ANALOGUE

MHM's exploration model is based on the premise that if the MS2 corridor evolved through the same geological processes as the Peak Goldfield, then both systems should display comparable:

- Structural architecture and deformation history; and
- Compositional and physical characteristics of the hydrothermal fluids associated with mineralisation

Each of these criteria provides an independent line of evidence that can either support or reject the proposed analogue.

Evidence 1: Structural architecture and deformation history.

Three independent lines of structural evidence support the interpretation that the MS2 corridor represents a single long-lived hydrothermal system rather than a series of isolated mineral occurrences.

Historical Mining Evidence

The earliest evidence comes from historical mining records between 1904 and 1935, which document mineralisation hosted within a near-vertical, approximately 30 cm wide, NW–SE striking rubbly quartz vein emplaced along a fault that cross-cut steeply dipping north–south sedimentary beds. The vein was traceable from the base to the crest of Mount Solitary and contained a west-plunging bismuthinite-rich shoot aligned subparallel to bedding despite the vein itself being discordant to stratigraphy. Underground development subsequently identified several parallel mineralised veins. Collectively, these observations indicate that mineralisation was controlled by repeated structural reactivation and localised fluid flow rather than a single quartz vein event (Mine Record 2391; Mc Clatchie 2001).

Evolution of structural models

A second line of evidence is provided by the progressive evolution of structural interpretations developed during modern exploration. Although successive explorers proposed different geological models, each recognised increasingly larger scales of structural organisation. Initial exploration by Electrolytic Zinc interpreted mineralisation as a silicified shear zone, followed by models involving north-plunging pipe-like ore bodies, steep west-dipping lodes, polyphase fold interference, and regional north–south fault corridors containing en-echelon dilational zones. More recent workers have incorporated concealed intrusive bodies and linked northeast-trending splays into a broader Cobar-style structural framework. Despite differences in interpretation, these models collectively document an expanding recognition that mineralisation is controlled by a long-lived north–south structural corridor rather than isolated veins or individual prospects. Outside this corridor, deformation intensity and hydrothermal alteration diminish rapidly, further indicating that the line of hills defines a discrete zone of enhanced strain developed within the Mount Hope Trough.

Corridor-scale geological continuity

The third line of evidence is provided by observations made during recent field investigations by Mount Hope Mining. Micro-XRF analysis of high-grade vein samples collected from historical workings identified abundant visible gold intimately associated with native bismuth and bismuth minerals hosted within crustiform banded quartz veins. The crustiform textures indicate repeated episodes of hydrothermal fluid influx during progressive vein growth rather than a single mineralising event. At the scale of the entire MS2 corridor, Mount Solitary, Little Mount Solitary, Powerline Hill and Mount Solar all display the same fundamental geological characteristics, including:

- Intense cleavage development;
- Pervasive silicification;
- Abundant quartz veining and hydrothermal brecciation;
- Steeply dipping mineralisation; and
- Evidence for repeated hydrothermal alteration and fluid flow.

The persistence of these features over approximately 8 km strongly suggests that the four prospects developed within a single structurally controlled hydrothermal corridor.

Comparison with the New Occidental deposit

Collectively, these three independent lines of evidence define a structural architecture that closely resembles that documented by Stegman (2007) for the New Occidental deposit. At New Occidental, gold mineralisation is localised within a major reverse-fault system where repeated deformation generated transient permeability and focused hydrothermal fluids into short strike-length dilational segments. Cyclic fault movement produced repeated episodes of brecciation, crustiform quartz veining and gold deposition through fault-valve behaviour. The remarkable similarities in structural geometry, vein textures, hydrothermal brecciation and evidence for episodic fluid flow provide the first independent line of evidence supporting the interpretation that the MS2 corridor represents a southern analogue of the Peak Goldfields.

Evidence 2 – Hydrothermal Fluid Evolution

Four independent lines of hydrothermal evidence support the interpretation that the MS2 corridor formed within a long-lived mineralising system comparable to that responsible for the New Occidental deposit.

Historical geochemical evidence

The earliest indication of a distinctive hydrothermal system comes from historical mining records, which describe exceptionally high-grade gold intimately associated with abundant bismuthinite hosted within quartz veins at Mount Solitary. This unusual Au–Bi association was later recognised throughout the MS2 corridor by successive exploration programs that undertook extensive multi-element geochemistry, XRD, petrography and metallurgical investigations of rock, soil, lag, stream sediment and drill samples.

Electrolytic Zinc (1981–1982) first recognised a district-scale quartz–chlorite alteration system associated with Au–Bi–As mineralisation and a separate Cu–Pb–Zn association. They also documented a systematic west-to-east transition from Pb through Cu towards a Bi-rich core, providing the first evidence that mineralisation was accompanied by large-scale metal zonation across the corridor. Aberfoyle (1983–1984) subsequently demonstrated that mineralisation occupied fracture-controlled zones of silicification and chloritisation in which chlorite alteration formed halos around mineralised fractures while intense silicification generated jasperoidal rock. They also recognised that the widespread sub-horizontal bucky quartz veins post-dated the principal gold event.

Normandy Resources (1985–1986) and Placer (1991–1995) expanded this work through detailed whole-rock geochemistry, XRD and alteration studies. Their investigations demonstrated consistent depletion of K_2O, Na_2O, Al_2O_3, TiO_2, Ba, Rb and muscovite accompanied by enrichment in Au–Bi, pyrite, quartz, chlorite and a distal Cu–Pb–Zn association together with anomalous As, Sb, Sn and W.

Collectively these studies established that the MS2 corridor is characterised by a coherent hydrothermal alteration and metal zonation rather than isolated mineralised veins (Table 1).

Table 1: Summary of geochemical studies conducted by Normandy and Placer Mt Solitary and Mt Solar

Depleted	Enriched
K_2O	Ore Zone Au-Bi-Fe+/-Cu
Na_2O	Adjacent Ore - Bi
Al_2O_3	Hanging Wall Zonation Cu-Pb-Zn
TiO_2	Quartz
Minor MgO/CaO/P2O5	Anomalous As-Sn-Sb-W
Muscovite	Chlorite
Ba and Rb	Pyrite

Alteration mineralogy and hyperspectral evidence

A second independent line of evidence is provided by alteration mineralogy and hyperspectral analysis.

As part of the Geological Survey of New South Wales Nymagee Mineral Systems Project, drill core from Mount Solar was analysed using the HyLogger™ hyperspectral scanner together with sulphur and lead isotope investigations (Downes et al. 2016). The HyLogger™ data demonstrate that mineralised intervals are characterised by increasing silica abundance, increasing chlorite wavelength, decreasing white mica abundance and a measurable change in the white mica wavelength.

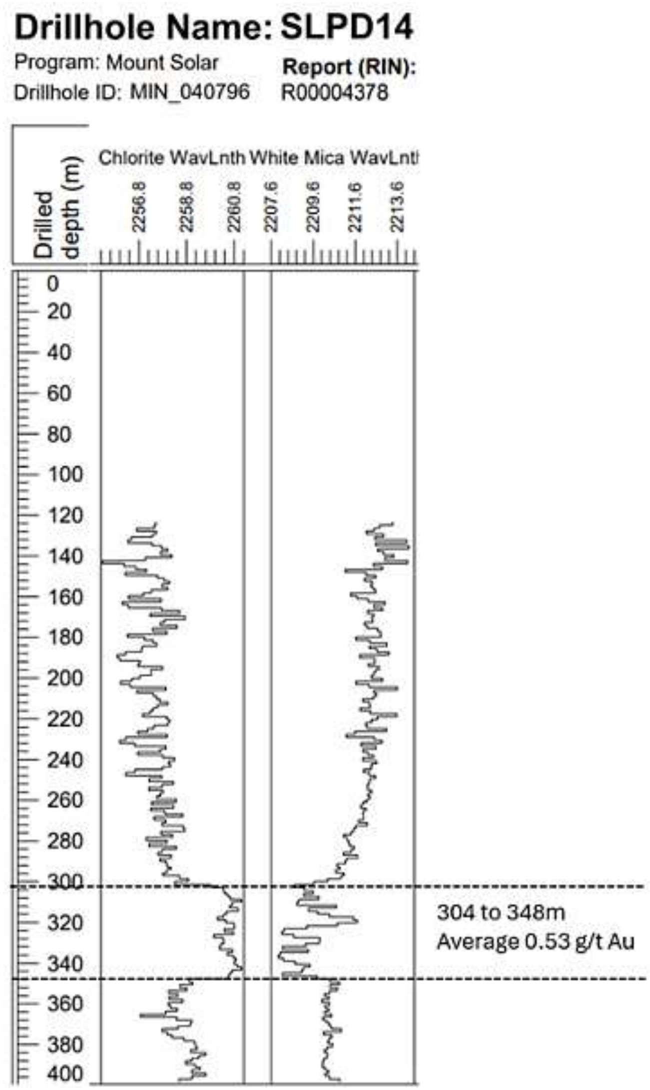

Figure 3. Downhole plot of spectral changes associated with mineralised zone at Mount Solar in SLDOP014 where an interval from 304m to 348m averages 44m @ 0.53 g/t Au incl 4m @3.39 g/t Au from 312 to 316m in SLDP014 correlates with an increase in the chlorite wavelength and a change in the white mica wavelength.

These spectral responses indicate progressive enrichment in Fe-rich chlorite, together with replacement and destruction of regional metamorphic muscovite during fluid-rock interaction. Importantly, the alteration vector directly coincides with gold mineralisation within drill hole SLDP014, where an interval grading 44 m @ 0.53 g/t Au, including 4 m @ 3.39 g/t Au, corresponds to systematic increases in chlorite wavelength and a change in white mica wavelength (Figure 3.)

Stegman (2007) demonstrated that gold mineralisation at the New Occidental deposit was accompanied by a systematic evolution of the alteration assemblage, characterised by increasing Fe-rich chlorite, progressive destruction of regional metamorphic white mica and the development of increasingly more phengitic white mica with increasing proximity to the New Occidental orebody. The measurable hyperspectral response recognised within the MS2 corridor—expressed as silica alteration, increasing chlorite wavelength and abundance together with a change in white mica wavelength and abundance—indicates that hydrothermal alteration and fluid–rock interaction are measurable with hyperspectral tools.

It should be stressed that the above observations are based on a very limited number of samples which would benefit from further test work to test these observations. That said identifying a measurable trend in the available data offers potential for hyperspectral data to be used as a tool to vector towards and map alteration along the MS2 in outcrop and under cover.

Sulphur isotope evidence

The third line of evidence is provided by sulphur isotope geochemistry.

Pyrite collected from quartz–chlorite veins at Mount Solar yielded $\delta^{34}S$ values ranging from +5.43 to +5.67‰. These values overlap the lower portion of the ore-sulphide field reported by Stegman (2007) for the New Occidental deposit (+4.2 to +11.4‰) Figure 4

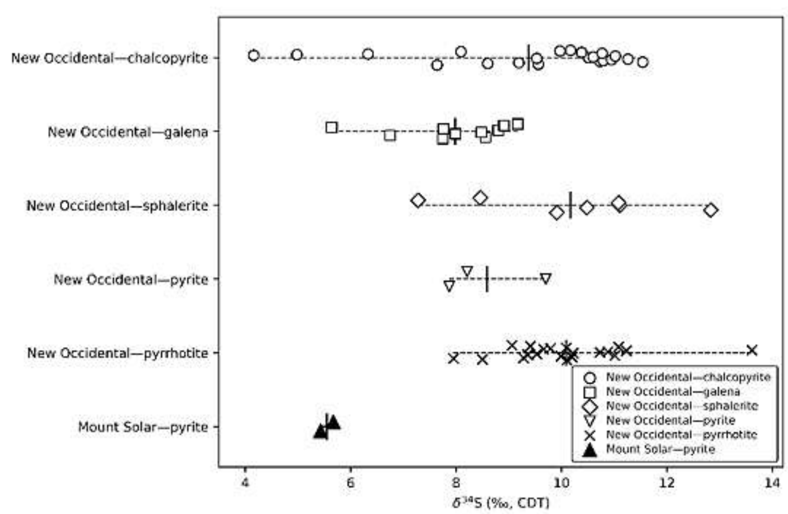

Figure 4. Comparison of $\delta^{34}S$ values for ore sulphides from the New Occidental deposit (Stegman, 2007) and pyrite from Mount Solar. Individual analyses are grouped by sulphide mineral, with dashed horizontal lines indicating the observed isotopic range and vertical bars denoting the mean for each mineral. The Mount Solar pyrite values (+5.43 to +5.67‰) overlap the lower end of the New Occidental ore sulphide field, supporting derivation from a broadly similar hydrothermal sulphur reservoir involving reduced seawater sulphate with a possible magmatic contribution

Stegman interpreted the New Occidental sulphur isotope compositions as reflecting sulphur ultimately derived from Devonian seawater sulphate that underwent high-temperature inorganic reduction during deep crustal fluid circulation. Downes et al. (2016) independently concluded that the Mount Solar values similarly indicate Sulphur derived from a mixed magmatic and reduced seawater sulphate reservoir.

Although the Mount Solar dataset remains limited, the close agreement between both deposits indicates that the MS2 corridor and the Peak Goldfields were mineralised by hydrothermal fluids derived from comparable crustal-scale Sulphur reservoirs. The inferred magmatic contribution at Mount Solar also raises the possibility that concealed intrusive bodies associated with the deep magnetic anomalies beneath the MS2 corridor contributed heat and Sulphur to the hydrothermal system.

Lead isotope evidence

The fourth line of evidence is provided by lead isotope compositions.

Three galena-bearing samples collected from Mount Solitary and Mount Solar during Geological Survey investigations by Supple in 1997 and 1998 display remarkably similar Pb isotope compositions to ore sulphides from the New Occidental deposit (Table 2 , Figure 5). Despite representing different sample types (surface gossan and drill chips) and separate prospects, the Mount Solitary sample together with the repeat Mount Solar analysis fall directly within the isotopic field defined by New Occidental. The higher-quality Mount Solar analysis is slightly more radiogenic but plots along the projected trend of the New Occidental array.

Table 2. Comparison of Pb isotope compositions for the Mount Solar and Mount Solitary prospects (Supple, 1997 and 1998) with ore sulphides from the New Occidental deposit (Stegman, 2007). The Mount Solitary gossan and the repeat Mount Solar analysis (QF = 9) fall within the New Occidental isotopic field, whereas the higher-quality Mount Solar analysis (QF = 2) is slightly more radiogenic. Overall, the MS2 corridor displays Pb isotope compositions comparable to those of the Peak Goldfield’s, consistent with derivation from a similar regional crustal lead reservoir and an Early Devonian mineralising event.

Deposit	Sample	$^{206}Pb/^{204}Pb$	$^{207}Pb/^{204}Pb$	$^{208}Pb/^{204}Pb$	Pb (ppm)
New Occidental (Stegman, 2007)	Ore sulphides (n = 13)	18.06–18.12	15.59–15.64	38.13–38.27	—
Mount Solar	Drill chip (QF = 2)	18.171	15.726	38.536	3000
Mount Solar	Repeat (QF = 9)	18.096	15.637	38.242	1764
Mount Solitary	Gossan (QF = 3)	18.048	15.623	38.204	236

Overall, the MS2 analyses indicate derivation of lead from the same regional crustal reservoir recognised at New Occidental and are consistent with mineralisation during the Early Devonian hydrothermal event responsible for many Cobar-style deposits. Although the limited number of samples warrants cautious interpretation, the remarkable isotopic similarity between two independent districts strongly suggests that both systems accessed comparable crustal metal reservoirs through long-lived basin-tapping structures.

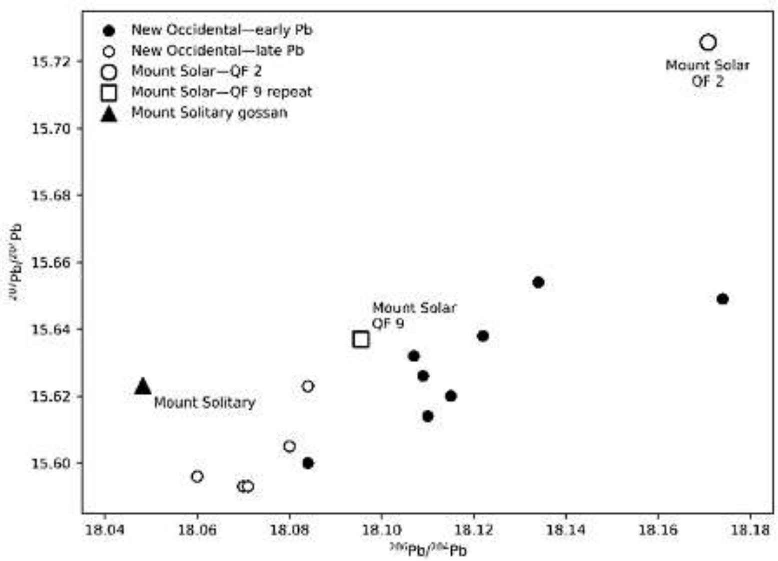

Figure 5. Comparison of Pb-isotope compositions from the MS2 corridor with early- and late-stage lead mineralisation from the New Occidental deposit. New Occidental data are from Stegman (2007, Table 44). The Mount Solitary gossan and the lower-quality Mount Solar repeat analysis plot close to the New Occidental isotopic array. The higher-quality Mount Solar analysis is more radiogenic in both $^{206}Pb/^{204}Pb$ and $^{207}Pb/^{204}Pb$ and plots beyond the main New Occidental cluster, although broadly along its projected trend. The similarity of most MS2 values to the restricted New Occidental isotope field is consistent with derivation of lead from a comparable regional crustal reservoir, but the Mount Solar dispersion and limited number of MS2 samples require cautious interpretation.

Comparison with the New Occidental deposit

Collectively, these four independent datasets define a hydrothermal evolution remarkably like that documented by Stegman (2007) for the New Occidental deposit. Both systems exhibit early Au–Bi-dominated mineralisation followed by progressive development of Cu–Pb–Zn assemblages as hydrothermal fluids evolved through time. Both display pervasive silica–chlorite alteration, destruction of regional white mica, enrichment in Fe-rich chlorite and quantitative hyperspectral vectors towards mineralisation. Sulphur isotope compositions indicate comparable contributions from reduced seawater sulphate, while lead isotope signatures demonstrate derivation from similar regional crustal reservoirs.

Rather than representing isolated observations, these independent datasets consistently indicate that the MS2 corridor and the New Occidental deposit formed within analogous long-lived hydrothermal systems controlled by repeated structural reactivation during Devonian basin inversion. Together they provide the second major line of evidence supporting the interpretation that the MS2 corridor is a southern analogue of the Peak Goldfields.

EXPLORATION IMPLICATIONS

The comparison with the Peak Goldfields fundamentally changes the exploration strategy for the MS2 corridor. Rather than viewing Mount Solitary, Little Mount Solitary, Powerline Hill and Mount Solar as isolated gold occurrences, they can instead be interpreted as expressions of a single kilometre-scale hydrothermal system developed along a long-lived structural corridor. The coincidence of Au–Bi mineralisation, systematic Cu–Pb–Zn metal zonation, extensive silica–chlorite alteration, crustiform banded quartz veins and intense cleavage development indicates that mineralisation was controlled by repeated structural reactivation and sustained hydrothermal fluid flow rather than isolated episodes of quartz veining.

This interpretation shifts the exploration focus from tracing individual quartz veins to identifying the structural sites that repeatedly generated permeability and focused hydrothermal fluids. If the MS2 corridor represents a true southern analogue of the Peak Goldfields, then high-grade mineralisation should be concentrated within structurally favourable sites such as fault intersections, dilational jogs and linked shear segments, both beneath the historic workings and within concealed portions of the corridor.

Accordingly, exploration should adopt a corridor-scale exploration model that integrates structural geology, alteration mineralogy, geochemistry and geophysics to identify and drill test these fluid pathways and depositional sites. The following methodology has been developed to systematically test this exploration model

EXPLORATION METHODOLOGY

The proposed hypothesis will be tested using an integrated exploration workflow designed to determine whether the MS2 corridor exhibits the same structural architecture and hydrothermal alteration characteristics as the Peak Goldfields.

The workflow begins with the compilation, validation and integration of historical geological mapping, drilling, structural and geochemical datasets to establish a consistent corridor-scale geological database. These data will be combined with a regolith model to distinguish areas of outcrop, sub-crop and transported cover, enabling bedrock sampling to be targeted appropriately.

Detailed geological and structural mapping will then be undertaken to validate historical interpretations and produce both factual and interpretive geological maps of the corridor. Existing drill-hole geochemistry from Mount Solitary will be used to characterise the geochemical signatures of unaltered host rocks, hydrothermal alteration and mineralised zones, providing a baseline for interpreting new datasets.

Systematic bedrock sampling across the corridor will then be completed for four-acid digest geochemistry to map alteration halos and develop geochemical vectors towards mineralisation. These results will be integrated with quantitative mineralogical modelling, hyperspectral data and targeted geophysical surveys based on ore-related physical properties to define alteration zonation, structural architecture and potential hydrothermal fluid pathways beneath cover.

The integrated datasets will be used to rank exploration targets and design diamond drill holes to intersect the most prospective structural and alteration zones. Oriented drill core will provide the structural, mineralogical and alteration data required to constrain the controls on mineralisation at Mount Solitary and test whether these are representative of the broader MS2 corridor.

The workflow incorporates an iterative feedback loop in which observations from mapping, geochemistry, mineralogy, geophysics and drilling are continually integrated to refine the geological model, improve drill targeting and progressively test the proposed analogue with the Peak Goldfields.

CONCLUSIONS

This study demonstrates that the MS2 structural corridor shares many of the defining characteristics of the Peak Goldfields. Comparable structural architecture, hydrothermal alteration, Au–Bi association, regional metal zonation, hyperspectral alteration signatures and sulphur and lead isotope compositions indicate that both regions evolved from long lived hydrothermal systems within regional structures.

Although further work is required to quantify the structural evolution and hydrothermal fluid history of the MS2 corridor, the convergence of these independent geological, geochemical, mineralogical and isotopic datasets provides strong support for the hypothesis that the corridor represents a southern analogue of the Peak Goldfields and has significant potential to host additional Cobar-style gold mineralisation.

The principal outcome of this study is therefore not simply a reinterpretation of the Mount Solitary prospect, but the development of a new corridor-scale exploration model for the southern Cobar Basin in which the entire MS2 structural corridor is recognised as a highly prospective hydrothermal system worthy of systematic exploration.

If validated through ongoing exploration, the MS2 structural corridor has the potential to establish a new search space for Peak-style gold mineralisation within the southern Cobar Basin and demonstrate that the geological processes responsible for the Peak Goldfields extend significantly farther south than previously recognised.

ACKNOWLEDGEMENTS

The author wishes to thank the board of Mount Hope Mining Ltd for approving this paper and in particular Fergus Kiley for his unwavering support, encouragement and constructive criticism. A special thanks also goes to Emma Oerlemans and Seb Hind for reviewing the document.

REFERENCES

DAVID V. 2005. Structural setting of mineral deposits in the Cobar Basin. Unpublished PhD thesis, University of New England, Armidale.

DOWNES P. M., BLEVIN P. L., ARMSTRONG R., SIMPSON C. J., SHERWIN L., TILLEY D. B. & BURTON G. R. 2016. Outcomes of the Nymagee mineral system study—an improved understanding of the timing of events & prospectivity of the central Lachlan Orogen. Geological Survey of New South Wales Quarterly Notes 147.

FITZHERBERT J. A. & DOWNES P. M. 2021. Mineral systems of the Cobar Superbasin: an updated geological framework for mineral exploration. Geological Survey of New South Wales.

FITZHERBERT J. A., DOWNES P. M. & BLEVIN P. L. 2022. District-scale characteristics of mineralisation in the Cobar Superbasin: attempting to understand timing & genesis. In: Discoveries in the Tasmanides Conference Proceedings. Australian Institute of Geoscientists.

GLEN, R. A., 1990. Formation of inversion of trans-tensional basins in the western part of the Lachlan Fold Belt, Australia, with emphasis on the Cobar basin. In A.E. Grady, P.R. James, A.J. Parker and J.P. Platt (Editors), Australian Tectonics. J. Structural Geol., 12: 601-620.

GLEN R. A. 1995. Thrusts & Thrust-Associated Mineralisation in the Lachlan Orogen. Economic Geology, Vol 90, (1995) 1402-1429.

GLEN R. A., DRUMMOND B.J., GOLBEY B.R., PALMER D., & WAKE-DYSTER K.D, 1994. Structure of the Cobar Basin, New South Wales, bawed on seismic reflection profiling., Australian Journal of Earth Sciences (1994) 41, 341-352

Mc CLATCHIE L., 1996. Mount Solitary Gold Prospect, Mount Hope NSW (EL1466) report on drill holes DD43, DD44. GSNSW Report GS1996/450

Mc CLATCHIE L., 1997. Exploration licence EL1466, Mount Hope district Report for period ending 16th October 1997. GSNSW Report GS1998/053

Mc CLATCHIE L., 2001. Exploration licence EL1466, Mount Hope district Report for period 16.10.1999 to 15.10.2000. GSNSW Report GS2002/261

Mc CLATCHIE L., 2007. Report for period 19.02.2006 to 18.02.2007, EL6055 Mount Hope. GSNSW Report GS2007/278

McQUEEN K. G. 2021. Beneath the copper 'tablecloth': history of the Mount Hope mines, northwest New South Wales. Journal of Australasian Mining History 19, 85–107.

MILZ M. & MAHONEY L. 2025. Insights into the Cobar–Hermidale–Yathong region from seismically constrained potential field modelling.

SIMPSON, C. 2014. Nymagee project: petrographic reassessment of the Mount Halfway Volcanics & other formations in the Mount Hope Group. Geological Survey of New South Wales, Report GS2015/0221.

SCHEIBNER E. 1987. The Mount Hope & Rast troughs: Early Devonian volcano-tectonic rifts of the Lachlan Fold Belt. Geological Survey of New South Wales.

SCHEIBNER E. 1989. The tectonic of the New South Wales in the second decade of application of the plate tectonic paradigm. Journal of Proceedings of the Royal Society of New South Wales, 122, 35-74.

SCHWEBEL P.J., 1986. EL1466, Mt Solitary, NSW, six monthly report for period ending October 1986. GSNSW Report GS1986/213

SLADE J. 1985. Review of magnetic & gravity data over the Mount Hope & Mount Solitary areas, New South Wales. Appendix 7 in EL 1466 Mount Solitary, NSW: Six Monthly Report for the Period Ending October 1985. NSW Geological Survey open-file report R00009740.

STEGMAN C. L. 2007. Structural evolution & controls on gold mineralisation at the New Occidental Deposit, Peak Gold Mines, Cobar Basin, New South Wales. Unpublished PhD thesis, University of Tasmania.

SUPPLE D.W. & GILLIGAN L.B. 1993. Nymagee 1:250000 Metallogenic Map S1/55-2: Metallogenic Study & Mineral Deposit Data Sheets. 171 pp. Geological Survey of New South Wales, Sydney.

TAYLOR G., 1989. Eighteenth report on exploration activities for the six months ending 16 October, 1989. GSNSW Report GS1989/393

TAYLOR G., 1988. Exploration licence 1466 (Mt Solitary Project) Report for the six month ended 16th April, 1988. Mt Hope NSW GSNSW Report GS1986/213

TAYLOR G., 1990. Nineteenth report on exploration activities for the six months ending 16 April, 1990. GSNSW Report GS1989/392

TRIGG S. J. 1987. Stratigraphy & tectonic evolution of the Mount Hope region, central western New South Wales. Geological Survey of New South Wales.

YANG B., OFFLER R., FITZHERBERT J. A., FOLKES C., DWYER R. & CLARK C. 2024. Basin provenance & its control on mineralisation within the Early Devonian Cobar Basin, western Lachlan Orogen, eastern Australia. Australian Journal of Earth Sciences 71, 211–230.

UNCORKING THE BOTTLE OF GEOCHEMICAL VALUE: OPTIMIZING SAMPLE SUBMISSION AND ANALYSIS FOR THE IMPATIENT GEOLOGIST

Mark Pirlo

Australian Laboratory Services Pty. Ltd.

Key Words: geochemical analyses, pathfinder element, lithogeochemistry, alteration, mineralogy, machine learning, turn-around-time, sample submission

INTRODUCTION

Compositional analysis of geological materials, usually in the form of elemental analysis of samples, has long been a fundamental, objective measurement used by many geoscientists. These measurements can provide a powerful tool to address a range of important questions connected to the mineral resource lifecycle. As the exploration and mining industry continues to evolve and mature, recent interest in and uptake of machine learning tools for addressing these questions typically requires high-quality geochemical composition data for input. Without it, models tend to hallucinate and fail. The adage that garbage in = garbage out holds true no matter how advanced models become. Good decisions are made easier with good data.

Thoughtfully framing questions can be a key driver of success in applied geochemistry, and questions usually differ depending on the stage of the process a project occupies. Generative exploration may seek to map out how elements are dispersed in the near-surface environment. Or it might require knowing if the rocks in the project are the right part of a minerals system. Can the target be enlarged and/or the search space reduced in size? What kind of rock might this be, has it been altered and if so, in what way? Can I use geochemical composition data to link to mineralogy, and can I get indications on a likely mineral processing route? Will the mine tailings and mine waste leave an environmental legacy and an economic liability? These are examples of some questions that may be tackled with good quality geochemistry data.

TIMING OF DATA DELIVERY

Commercial geochemical analysis laboratories have existed for many years; however, they continue to evolve. The methods offered even 20 years ago have been refined and improved on, providing more options and more tools that can be deployed to address questions – a suitable tool for almost every purpose. Consequently, commercial geochemical analysis laboratories remain an indispensable part of the resource life cycle.

As the resources industry experiences periodic cyclicity – the “boom and bust”, demands on commercial laboratories tend to track exploration expenditure (Figure 1), albeit often with a slight lag. Drilling, performed to obtain samples at depth, is often a major cost in mineral exploration. However, the relationship between meters drilled (Figure 2) and total expenditure is not always straightforward. Alternate sample sources (e.g. the surface), alternate exploration technologies (e.g. geophysics, computerised legacy data review), changing costs, and even doing more with fewer samples (e.g. wider and more comprehensive geochemical analysis suites) can confound the relationship. Over time, overall sample throughput through commercial laboratories has increased (Figure 3), though some laboratories do experience occasional year-on-year reductions. This increase comes despite an uptake of technologies that operate outside of the central commercial laboratory environment. Portable instrumentation that can be operated with minimal technical training or limited skill, and single-element analysis systems provide two examples.

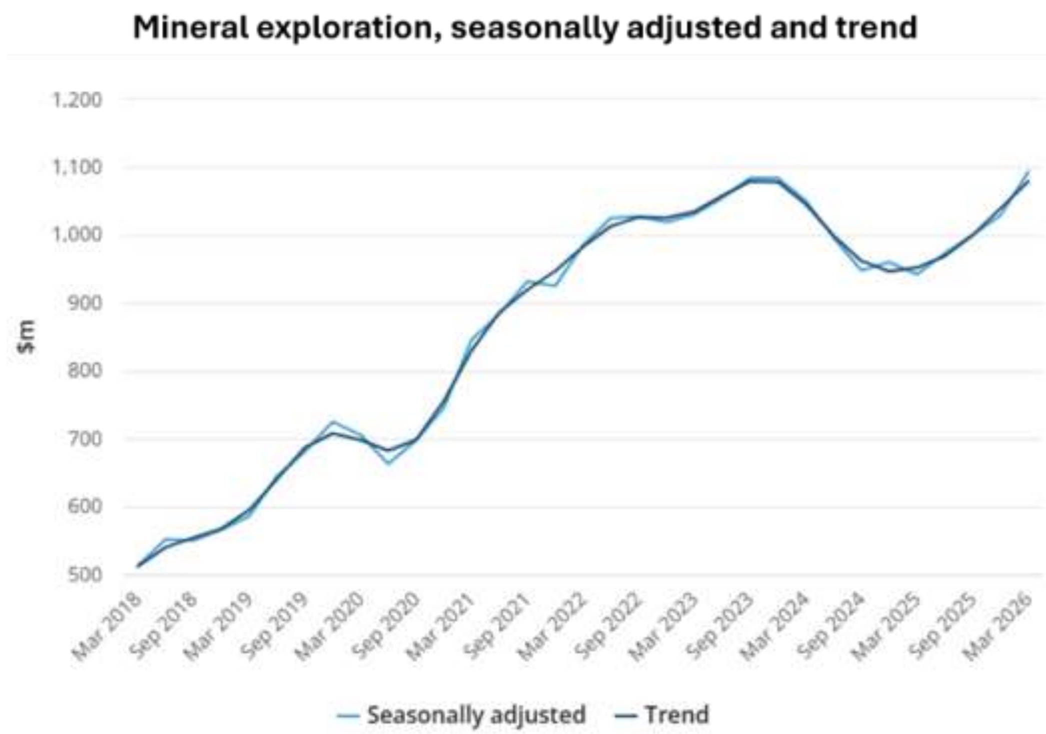

Figure 1. Total mineral exploration expenditure for Australia from March 2018 to March 2026. Source: Australian Bureau of Statistics.

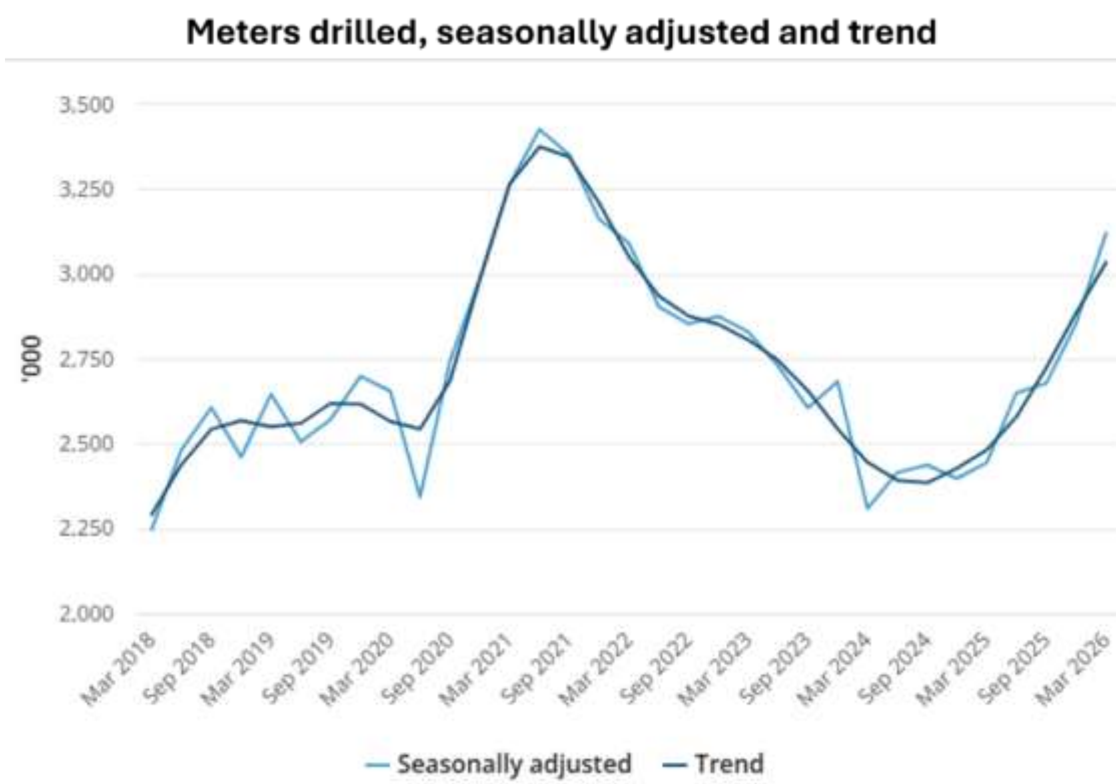

Figure 2. Meters drilled for mineral exploration purposes in Australia from March 2018 to March 2026. Source: Australian Bureau of Statistics.

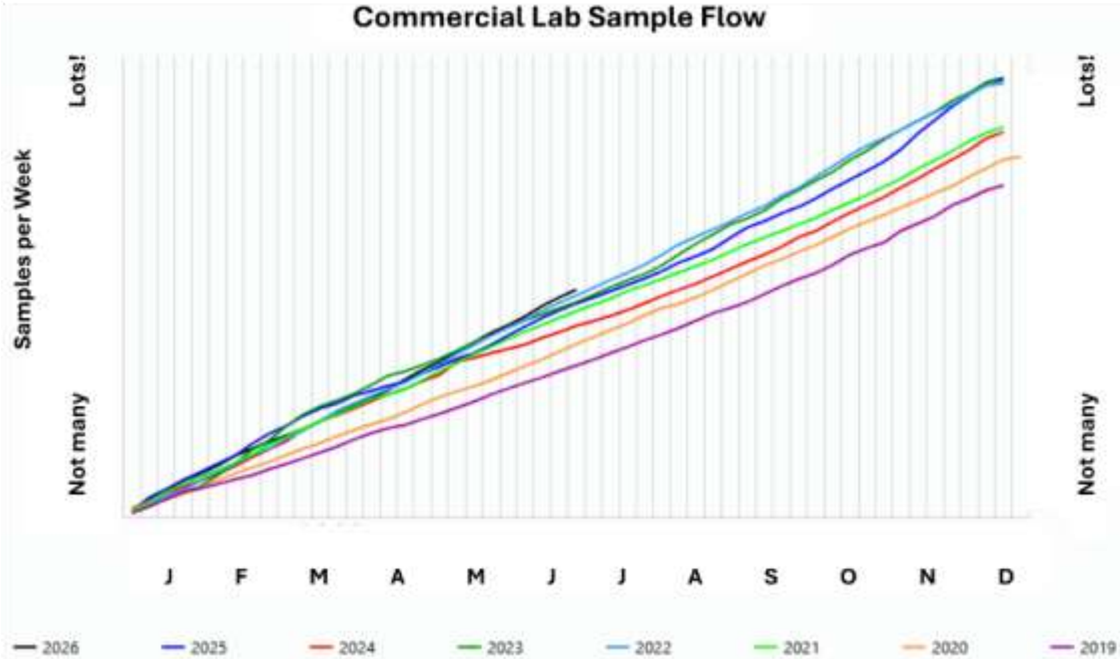

Figure 3. Example of changes in the cumulative samples received per week at an Australian commercial laboratory over 7.5 years. A significant general year-on-year increase exists for most years, demonstrating the increasing recent demands on commercial geochemical analysis laboratories.

Of course, the sample flow into laboratories is not consistent, and large swings in response to seasonality provide a regular challenge for commercial laboratories to schedule staff, equipment, maintenance and often disruptive capacity expansions (Figure 4).

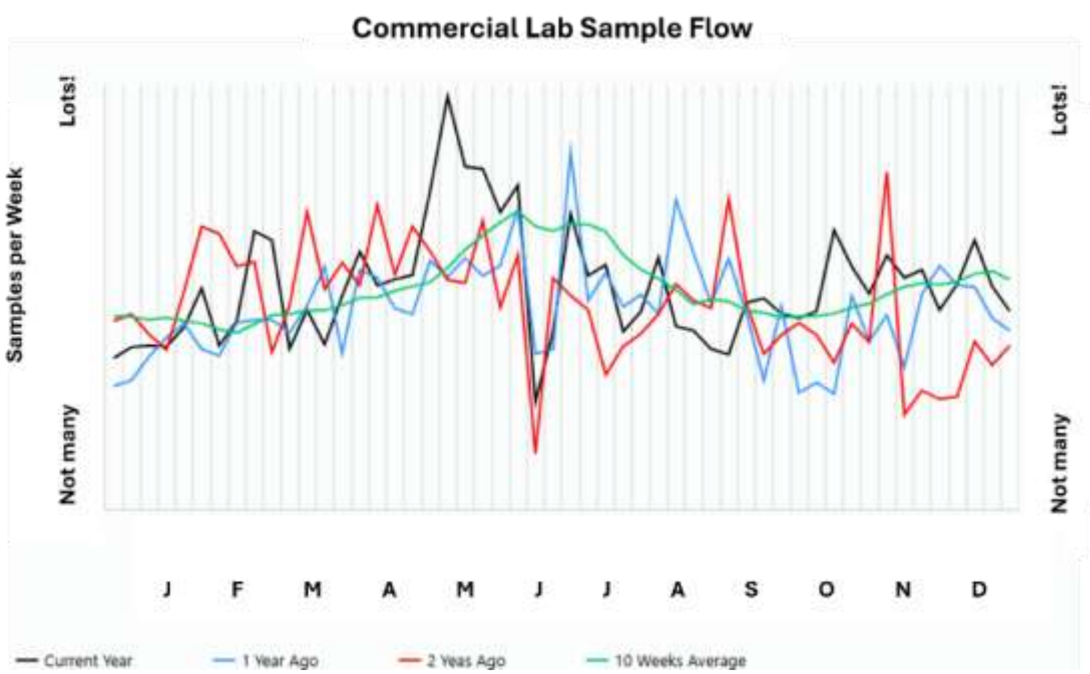

Figure 4. Sample flow into an Australian commercial geochemical analysis laboratory on a fortnightly basis. Trends can be observed; however, the data can be somewhat noisy, representing a “snapshot” of what may be happening in the mineral exploration industry at a given time.

However, unlike a fine wine, aging geochemical data delivery in the form of slow turn-around-times (TATs) is rarely appreciated by clients!

THE VALUE IN GEOCHEMICAL DATA

Realising value in geochemical data ultimately comes from how it is used. Opportunities to use data are controlled by the range of analytes (elements, species, isotope and compounds including minerals), and the concentration range across which they are effectively determined. However, these are in turn controlled by the available separation and analysis techniques. Laboratories that can offer a range of relevant methods provide flexibility and optimisation potential to clients that engage their services. As an example, a large commercial geochemical analysis group may offer upwards of 200 different active methods that can each report a Cu concentration. These methods can report Cu concentrations from partial leaches as benign as water, selective leaches designed to target specific mineral groups, through to total analyses that consider all the Cu in the sample. The concentration range can cover 1ppb through to 100%. Importantly, methods can be developed and optimised for applications linking to typical sample matrices.

The ability of a commercial laboratory to convert samples into fit-for-purpose data is the key driver of success. Appropriate accuracy and precision of data is a fundamental requirement, however a spatial network of laboratories in the places that matter, capacity to process the sample volumes generated by industry, the technical ability to identify, diagnose and rectify issues, and an ability to track samples and their progress all help to deliver value to clients.

Commercial geochemical analysis laboratories offer more analytes now than they did 20 years ago. They do this because they can, but also because they are requested by industry. Moving from a single element or a very limited group of elements to “full” suites of elements has been enabled by advances in instrumentation and data management. This has made significantly more data available – more analytes, across wider (and specifically lower) concentration ranges, at a fit-for-purpose quality and delivered at an acceptable price.

More data is only of use if it is put to work. Geochemistry is not simply plotting single-element thematic maps in 2D or 3D, or downhole strip logs of element concentration. Understanding how to use different elements to answer different questions has enabled many geoscientists to do more.

R&D-driven improvements in our understanding of the mobility of elements in primary and secondary dispersion settings have been another key driver in the uptake of geochemical analysis data. Enabling this further has been the widespread of tools in the hands of end-users. These tools have been in the form of software e.g. ioGAS and GIS plug-ins, but also in the “how to” from workshops, webinars and online teach-yourself guides. In turn, this has increased confidence amongst some users. Though occasionally this confidence has been unsupported by understanding and skill.

WHAT ADVERSELY AFFECTS LABORATORY TURN-AROUND-TIME (TAT)?

Sample preparation is often a bottleneck in the commercial laboratory process and has perhaps the biggest influence on laboratory turn-around time. The physical demands and logistics of taking larger samples, drying, crushing, splitting and pulverising, to produce a homogeneous and representative sample requires space, workers and specialised equipment. Thinking of sample preparation as part of a “rock factory” often sounds simple – until it isn’t. Input variability, where subsequent, consecutive samples can have vastly different geology, mineralogy, hardness, grindability and carry-over potential takes skill and time to effectively manage. Automated sample preparation can sometimes be thought of as a panacea to sourcing workers that are willing, able and productive in the often-undesirable workplace of sample preparation. However, the economic challenges associated with designing, manufacturing and configuring automated options and then operating these efficiently and cost effectively due to very high Capex in the highly variable industry that is exploration and mining often proves to be an unappreciated barrier.

Quality and optionality also take time. Preparing a sample for a single element analysis, such as gold by PhotonAssay, does take less time than preparing a sample for gold by fire assay. However, the pulverised sample for fire assay can be immediately used for other analytes that require the same sample preparation. Saving time on one analysis is an unrealistically simplistic view, unless that single analysis is all that really matters. For most applications though, the industry has moved on and embraced geochemistry. This requires having access to and using key geochemical data prior to making decisions.

Higher-technology methods have evolved to help drive detection limits of some elements down to levels necessary to be useful in generative exploration settings. However, higher-technology methods require highly specialised procedures and instruments, and optimising for analytical performance often comes at the expense of speed. The uptake in low-level methods, underpinned by 4-acid digests and ICP-MS instruments has been significant, particularly over the past 20 years. Clients are asking more of commercial laboratories, and the laboratories are fulfilling the task. However, scaling to match the inherent variability in the industry whilst maintaining a profitable business is an ongoing challenge.

WHAT CAN GEOSCIENTISTS DO TO GET BETTER DATA, FASTER?

Nobody disputes that rapid delivery of geochemical data is important, since it allows the data to be interpreted and decisions to be made. Some geochemical analysis options have attempted to address TAT issues by using advances in analytical instrumentation, changes to decomposition/digestion process, or by considering samples that have less preparation. However, these options typically do so with several important compromises. They may be in the form of detection limits, where faster options simply cannot match the performance of "conventional" laboratory options. This can become a real issue in mineral exploration when detection limits are not reporting key pathfinder elements to at least average crustal abundance, making anomaly definition difficult or impossible in many cases. Another example is in single element reporting. Using a technology to expedite reporting time for a single element will simply not advance a project where actual geochemical data interpretation is required. "Fixing" for one analyte and ignoring the rest can add risk. Are you comfortable with faster decisions at a higher risk of being incorrect? Fast data may be of only very limited use if you still can't adequately answer a question, or you are left with doubts. Often, a fast fix for TAT is more benefit to the proponent of the option than to the overall client requirements.

The primary levers that influence and indeed control TAT reside with the laboratory. Nevertheless, there are several things that clients can do to assist in the process of getting better data, faster.

Carefully frame your questions

Understand what stage of the resource life cycle your project currently occupies, and where you expect to take it. Archiving prepared sample material often allows for subsequent analyses, as project requirements dictate. However, knowing what data you need to have to answer immediate questions can save time on large, fully comprehensive analysis packages.

Changing analysis requirements after a workorder has been written up and analysis started is not impossible. However, it typically tends to contribute to delays. Understanding your questions, the options to address them, and the process involved is a good way to help avoid unnecessary delays.

Understand your options

Quality sample preparation takes time. How samples arrive at the laboratory – their masses, moisture content, packaging, labelling, declarations etc can all influence TAT and what options may be available for subsequent analysis. Sample digest or decomposition, ranging from partial, through selective, near total and finally to total recovery can have a huge influence on data interpretation options. Instrumental analysis options will determine whether you can “see” background at very low levels, or if most of your data is incapable of showing the signals that you seek amongst geochemical noise.

Many modern instrumental analysis methods are multi-element, producing fit-for-purpose data from a single instrumental analysis. However, some elements can benefit from specialised digest/decomposition/analysis options, that are optimised for recovering the element, keeping it available for analysis and minimising interferences. Sometimes these specialist options are required to advance a project with confidence. Knowing what to do and when can save confusion and ultimately time. Key laboratory staff can be of assistance in this regard.

Understand the process

A solid understanding of the process that samples go through from departing their source at your project site, through receipt at the laboratory, sample preparation, digest/decomposition, analysis and reporting is important. A visit to your nearest laboratory, even if it is a regional laboratory that offers sample preparation and a restricted range of methods can help clients understand the steps involved. It can raise awareness of sources of error and opportunities for improvement. Laboratory visits are usually available with a polite request and a small amount of notice.

Developing a working relationship with the local or hub laboratory manager, client services officers, business development officers and technical specialists (such as the geochemist) can often help to ensure that you are getting the methods you need to answer your key questions and to quickly resolve any issues as they arise.

Understanding the difference between laboratory QAQC and your own QAQC responsibilities, including criteria for assessing a result as a failure against data quality objectives is another important task that can prevent unnecessary rework.

Taking advantage of electronic sample submission documentation can help to reduce the time required for workorder writeup, checking and getting your samples started in the laboratory. E-submissions help to remove ambiguity and may reduce a large potential source of errors, and subsequent delays from re-work.

Communicate with your lab

In the laboratory environment at least, surprises are rarely good! Communicating clearly and early with your laboratory is a proven way to reduce surprises. This can really help with planning and scheduling of staff, equipment, maintenance etc, since the laboratory has a better idea of what to expect and when to expect it. Consistent input helps to produce a more consistent output, and this is particularly so in laboratory TAT.

Sample volumes also help to drive discounts, so communicating these early to business development teams can ensure you are getting the best available pricing, and that the laboratory is sufficiently resourced to perform the work.

As can be seen in Figure 4, there is cyclicity in sample receipt in commercial laboratories through a regular year. An influx of samples prior to Christmas, samples that peak and then fall with dry/wet seasons' fieldwork opportunities, drilling delays (or capacity expansions) are examples that can be communicated to the laboratory.

As the primary source of samples, clients tend to know or suspect at least something about them before they arrive at the laboratory. Communicating to the laboratory about expected concentrations can help ensure that the samples go through the most appropriate process, and do not contaminate equipment – requiring long clean times to restore backgrounds or prevent unacceptable carry-over. Advising on sample hazards, including the likelihood of naturally occurring radioactive materials (NORM), fibrous minerals, or reactive sulphides can ensure that the samples proceed directly to a preparation facility that can process hazardous samples without placing people at an elevated risk.

Think about the future

On the pathway to discovery (in the Tasmanides or elsewhere), your immediate questions often have a generative or even a targeted exploration focus. But what comes next? Ensuring that you prepare, preserve and archive material so that it might be used for subsequent analysis improves optionality. This might include mineralogy to inform geometallurgical models, or acid-base accounting to inform closure requirements. Samples often cost a lot of money to obtain, so consideration of what might come next can reduce the need to spend more money again later.

ACKNOWLEDGEMENTS

The author would like to thank several colleagues at Australian Laboratory Services. Ben Cooke and Shaun Crabb provided thoughtful input and review of this abstract.

PAST, PRESENT AND FUTURE OF THE LIONTOWN VMS DEPOSIT

Matt Price[1], Tav Bates[1]

[1] Sunshine Metals Ltd, Townsville, QLD, 4810.

Key Words: Mount Windsor Volcanics, VMS, copper, gold, lead, zinc, mineralisation, North Queensland

INTRODUCTION

The Liontown VMS deposit is located in northeast Queensland, approximately 150km southwest of Townsville and 42km southwest of the historic mining town of Charters Towers. The deposit was originally mined for gold and copper from 1905 to 1911 producing approximately 28,000oz Au at an average grade of 22g/t Au. Sunshine Metals have been highly active at the deposit since acquisition in 2023, with plans to again bring Liontown back into production in 2027.

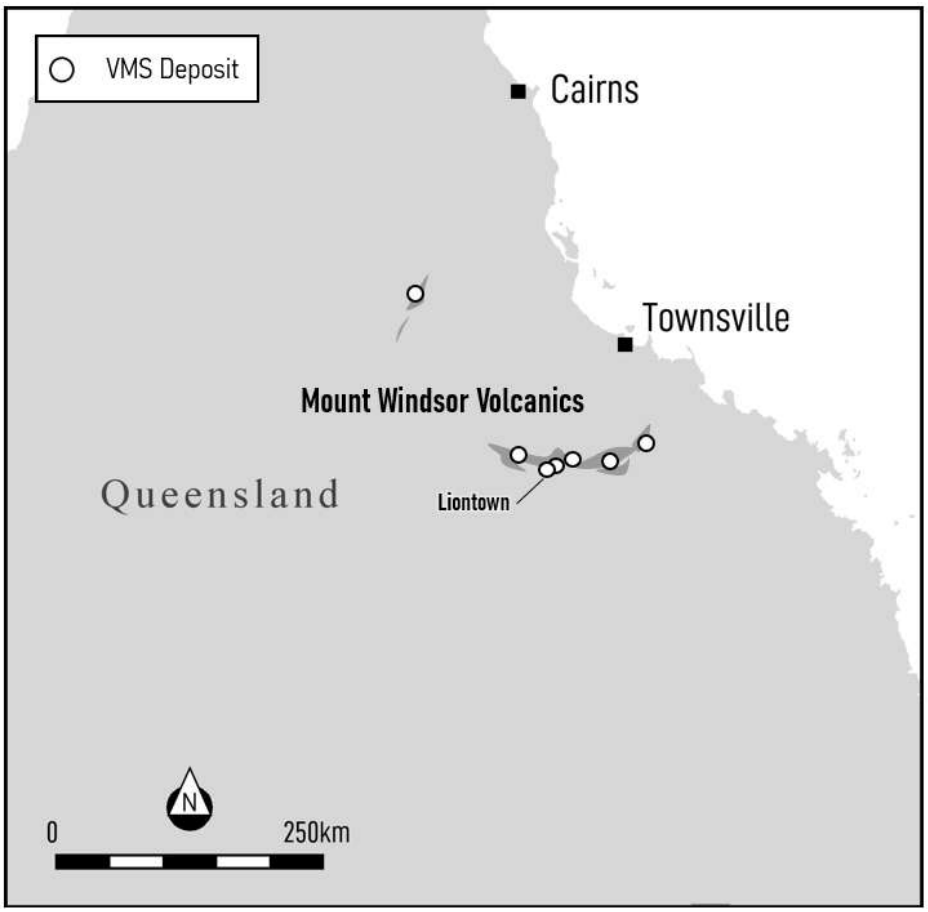

Figure 1. Location of the Mount Windsor Volcanics & major VMS Deposits

REGIONAL GEOLOGY

The Liontown deposit is located within the Charters Towers Province which extends inland from the coast at Townsville to 150km west of Charters Towers. The rocks are typically Neoproterozoic to Palaeozoic age. It is bound in the southeast by the New England Orogen and to the north by the Broken River Province of the Mossman Orogen.

The known VMS deposits, including Liontown and Highway-Reward, are hosted within the stratigraphy of the Mt Windsor Sub-province, which encompasses the dismembered remnants of a thick volcanic and sedimentary succession predominantly of Late Cambrian and Early

Ordovician age located within the northern part of the Tasman Orogenic Zone (Henderson, 1986). The succession comprises four identified formations collectively known as the Seventy Mile Range Group, which outcrop discontinuously in an east-west belt south of the Ravenswood Batholith.

The Seventy Mile Range Group (499 – 479 Ma) ranges from Late Cambrian to Early Ordovician and is represented by the Puddler Creek Formation at the base, followed by the Mt Windsor Volcanics, the Trooper Creek Formation and the Rollston Range Formation at the top (Figure 2).

The Puddler Creek Formation comprises continentally derived siltstone, sandstone and greywacke and mafic dykes. The Mt Windsor Volcanics overlie the Puddler Creek Formation and are a thick succession of rhyolitic to dacitic lavas, autoclastic and reworked breccia facies, and minor andesite and sedimentary rocks (Henderson, 1986). The transition from Mt Windsor Volcanics to the overlying Trooper Creek Formation appears to represent a change from felsic to intermediate-mafic volcanism. The Trooper Creek Formation consists of intermediate lavas, volcaniclastics (including mass flow deposits), minor felsics and marine sediments (Henderson, 1986). The facies assemblage has been interpreted as being deposited proximal to submarine volcanic centres and is known to host VMS deposits, such as Thalanga, Liontown and Highway-Reward. The Rollston Range Formation consists of laminated volcaniclastic siltstones and sandstones, with rare intercalations of vitric tuff (Henderson, 1986).

In the Project area, the Seventy Mile Range Group is variably overlain by Tertiary and Quaternary cover sequences, including the Campaspe Formation which comprises immature and pebbly sandstone and minor siltstone interbeds and is interpreted to represent erosive channel fill and fluvial sheet deposition.

Structurally, the Seventy Mile Range Group experienced early compactional foliation followed by three main deformation events owing to the emplacement of the Ravenswood Batholith. The first produced north-south folds; the second resulted in a major east-west fold with a spaced cleavage; and the third formed northeast-trending slaty cleavage and steep faults (Simpson, 2001).

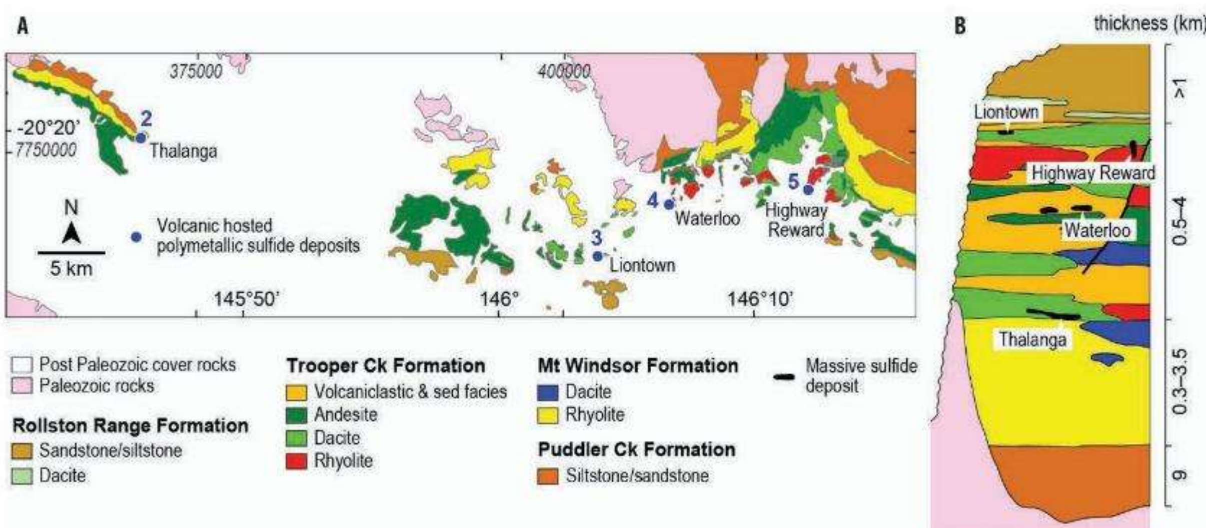

Figure 2. Regional Geology and Stratigraphy of the Mount Windsor Volcanics (from Beams et al, 2017).

LOCAL GEOLOGY

The Liontown deposit is located within the Trooper Creek Formation sediments and volcaniclastics of the Seventy Mile Range Group. The deposit stratigraphy comprises (in a general order from footwall to hangingwall) of a hangingwall of dacite, siltstone, black shale and tuffs, and a footwall of volcaniclastic, known locally as the dacite pumice breccia. The dacite pumice breccia is interpreted as a volcaniclastic flow breccia of dacitic composition, where pumaceous clasts have been altered to chlorite during low-grade metamorphism.

The dacite pumice breccia and immediately overlying siltstones are the main host of mineralisation at Liontown. Mineralisation and alteration do not persist above the lower black shale, suggesting this unit is either post-mineralisation or may have been deposited pre/syn-mineralisation and acted as an aquiclude.

The Seventy Mile Group units in the area have undergone tilting and deformation, leading to a general steep southerly dip to the package at about 70 degrees, likely during the D2 event of east-west folding and regional cleavage emplacement. Locally, the sequences are variably deformed with localised shearing and parasitic-style folding seen within both the sediments and volcanic units.

The sequences are overlain to the north, south and east of the deposit by the Tertiary Campaspe Formation sediments, which comprise of poorly consolidated sandstone, claystone, conglomerate.

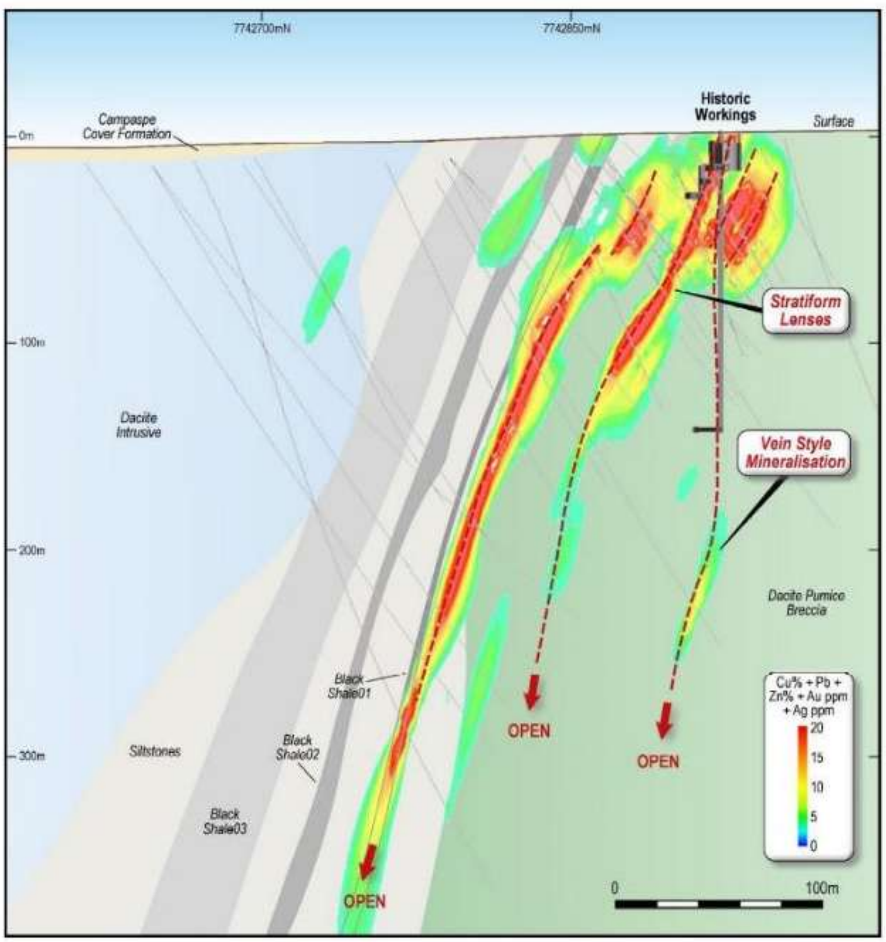

Figure 3. Schematic cross section of the Liontown deposit with geology & mineralisation

MINERALISATION

The Liontown deposit is considered a volcanic hosted massive sulphide deposit (VMS). The mineralisation at Liontown comprises of both stratiform sulphide lenses and cross-cutting vein style sulphide (Figure 4). The primary mineralisation comprises varying proportions of sphalerite, galena, with associated silver, pyrite and chalcopyrite. Gold is present as free gold and spatially associated with the sulphides.

Alteration associated with mineralisation is not particularly well-defined and comprises of chloritic to sericitic alteration assemblages. The entire package of Trooper Creek Formation has undergone weak, broad-scale metamorphism to lower greenschist facies, resulting in widespread weak chlorite development. Furthermore, localised shearing has produced strong, Fe-rich chlorite shear zones. Silica flooding is also present locally and is more commonly seen closer to the hanging-wall contact between the pumice breccia (PBX) and the overlying sediments and volcanics.

Mineralisation is believed to have been deposited syn-genetically at or near the seafloor. The standard genetic model for VMS deposits is that hydrothermal fluids are driven by convection around a deeper magmatic body. The mineralisation can be zoned as ascending hydrothermal fluids deposit the Cu-Au at higher temperatures (~300°C) compared to the zinc, lead and silver (~250°C) which can lead to a vertical zonation of the ore body. Laterally, the model suggests that still cooler temperatures deposit other gangue such as barite and silica.

Metal zonation studies by Sunshine suggest that stratiform Pb-Zn-Ag dominant sulphide lenses were likely fed by the Cu-Au enriched vein style mineralisation.

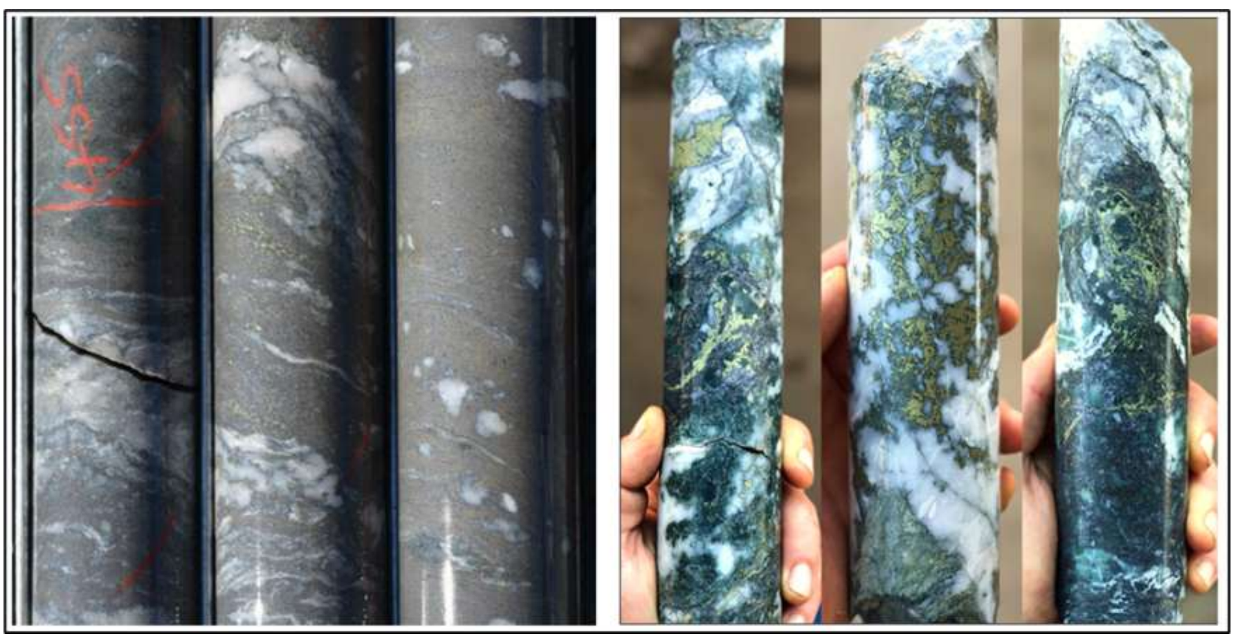

Figure 4. Stratiform Zn-Pb mineralisation (left) & Vein hosted Cu-Au mineralisation (right)

DISCOVERY & EXPLORATION HISTORY

The Liontown deposit was discovered in 1905 by William Fredrick Carrington, whilst searching for his horses “Lion and Noble”. The Cu-Au enriched zone was mined from 1905 to 1911, producing 28,000 ounces of gold at an average grade of 22g/t Au (Levingston, 1972). A second phase of mining occurred from 1951 to 1954 after Parsons and Jansen discovered the Pb-Zn-

Ag enriched stratiform sulphide lenses, producing 54,000 ounces of silver and 9 tonnes of lead (Levingston, 1972).

Recognition that the Seventy Mile Range Group shared similarities to the Mt Read Volcanics in Tasmania (and elsewhere) spurred exploration for volcanogenic massive sulphide deposits in the 1970s onwards, which resulted in the first regional discoveries of the Warrawee deposit in 1974 and shortly after the Thalanga deposit. Considerable exploration in the area between the 1970s to early 2000s by Jododex, Esso Australia and Liontown Resources amongst others put Liontown back on the map as a polymetallic deposit, with considerable resource definition work undertaken by Red River Resources ("Red River") between 2014 – 2022 to establish a Mineral Resource at the project.

In 2016, polymetallic mineralisation was discovered approximately 500m east of the modelled Liontown deposit in an area termed "Liontown East". The discovery was the culmination of drill testing a chargeability anomaly located below significant Campaspe Formation cover, where shallow historical drilling had previously noted weakly elevated base metals. Red River drill hole LTED01 intersected two zones of massive and semi-massive mineralisation, reporting 4.3m @ 1.6g/t Au, 56g/t Ag, 15.1% Zn, 0.6% Cu and 6.6% Pb, from 452.7m (ASX:RVR, 2016).

RECENT EXPLORATION

In 2023, Sunshine Metals acquired the Liontown deposit and has since completed a total of 252 drill holes for 19,744 metres, increasing resource confidence and extending the modelling to incorporate the Liontown East area into the broader Liontown deposit. The current Liontown Mineral Resource Estimate (ASX:SHN, 2025) is:

- 6.31Mt @ 1.49g/t Au, 27g/t Ag, 0.79% Cu, 1.57% Pb and 4.28% Zn

Sunshine's early drilling highlighted the Liontown deposit as locally gold-rich, with significant intercepts including 17m @ 22.05g/t Au from 67m (23LTRC002). A Scoping Study was completed in February 2026 in preparation for potential future mining of select gold-dominant zones.

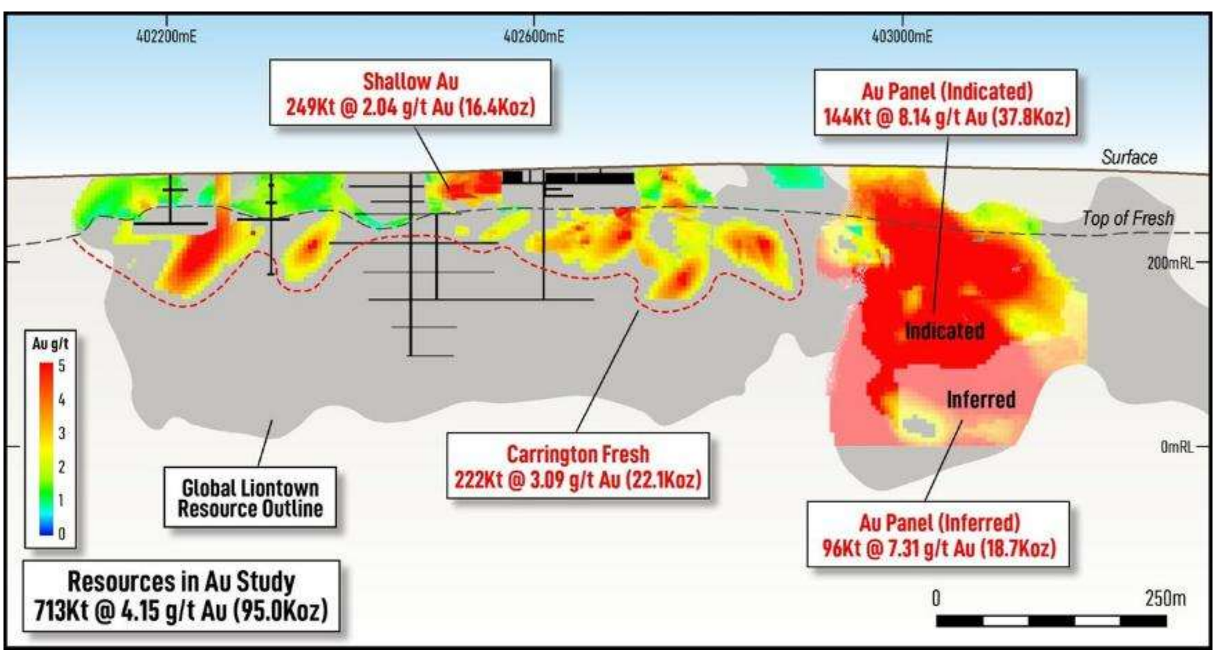

Figure 5. Long section of Au resource in February 2026 Mining Study.

ANTICLINE CONCEPT

The spatial relationship between the Au-Cu mineralisation and the adjacent Zn-Pb mineralisation has long been a point of contention for previous workers. A recent review of geophysical and geochemical data sets supports the concept of an anticlinal hinge being situated approximately 500m north of the Liontown deposit (Figure 6).

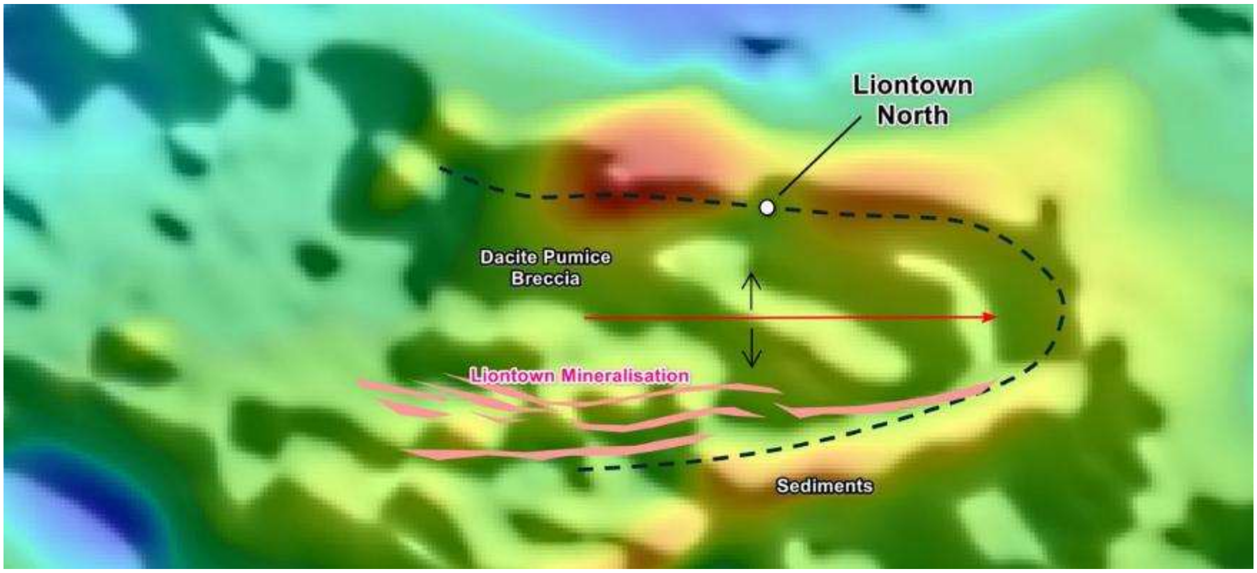

Figure 6. Ground Magnetics Image with interpreted anticlinal hinge

The unusual geometry of the known mineralisation at Liontown could potentially be explained by isoclinal folding. The low angle of the “feeder” vein style mineralisation to the stratiform mineralisation is possibly due to north-south shortening inducing east-west folding during D2; effectively maintaining the general geometry of the vein style mineralisation (fold axial planar) whilst rotating the stratiform mineralisation to sub vertical.

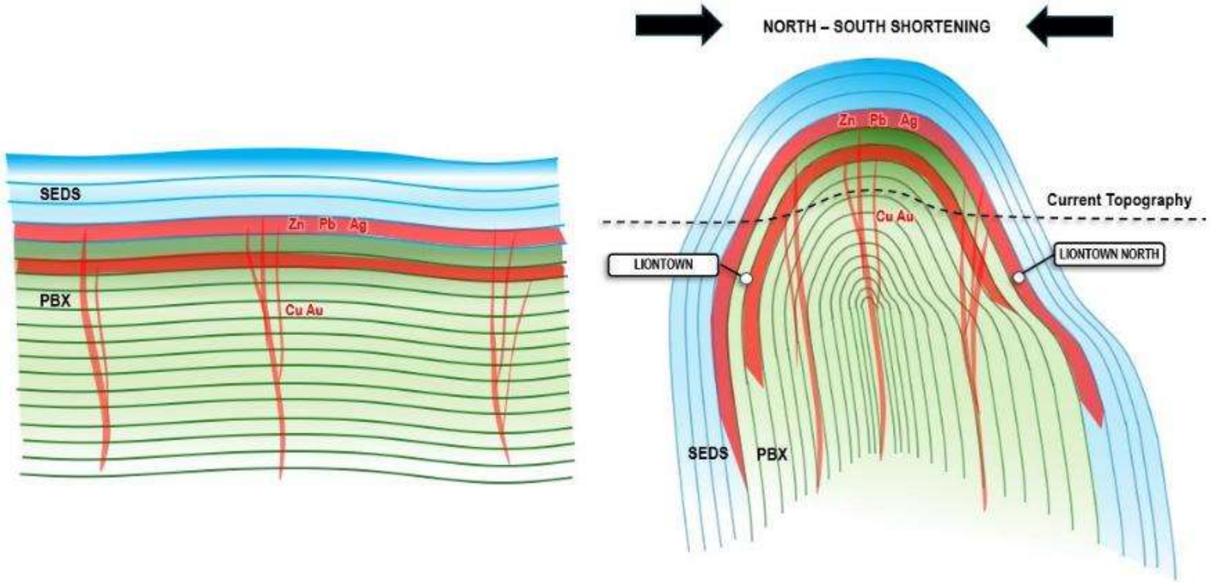

Figure 7. Schematic of proposed north-south folding of the Liontown deposit host stratigraphy

METAL ZONATION

Assuming the anticlinal deformation of the system as discussed above, Sunshine Metals translated the block model to orient the stratiform mineralisation Zn-Pb mineralisation to a horizontal (seafloor) position in order to investigate the metal zonation of the "unfolded" system.

As Figure 8 illustrates, a strong thermal zonation can be seen from the footwall Au-Cu "feeder" style mineralisation out to Zn-Pb dominant mineralisation at the seafloor position, further supporting the anticlinal folding concept.

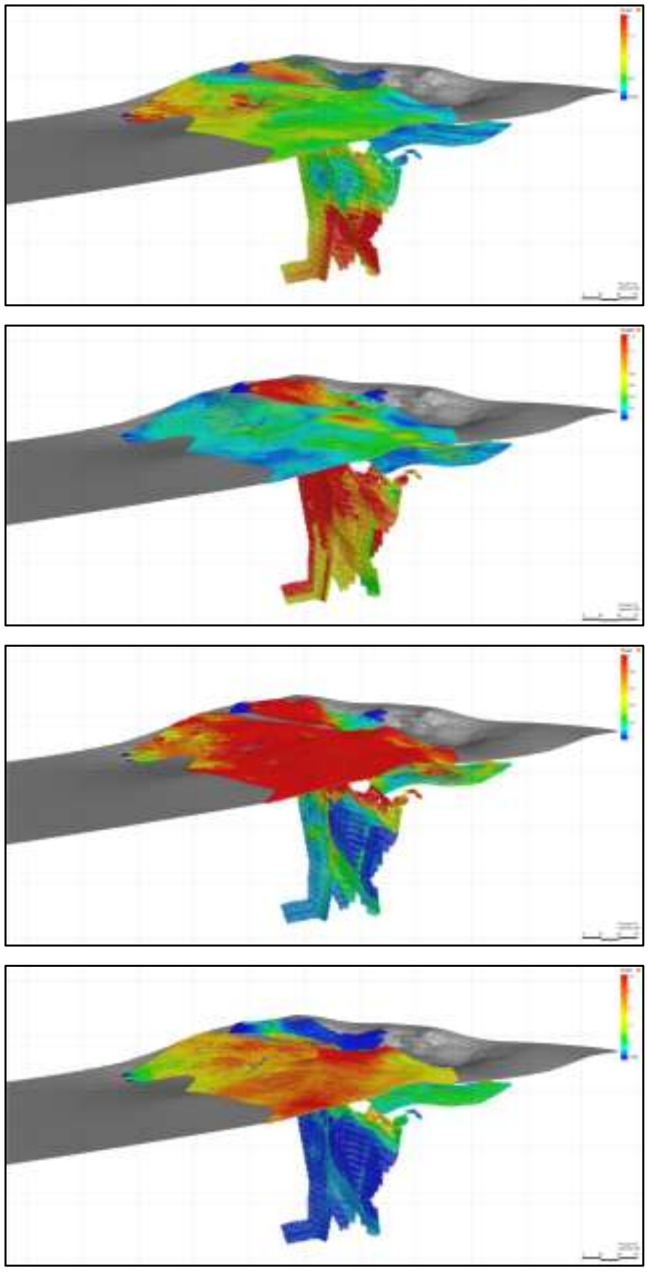

Figure 8. Oblique cross sections (looking NNW) of translated block model coloured (from top to bottom image): copper (max. 2% in 4 increments), gold (max. 1.5ppm in 7 increments), lead (max. 1% in 5 increments) & zinc (max. 10% in 5 increments). Scale bar (bottom right) is 75 metres across.

Sunshine Metals continues to develop the Mineral Resource at Liontown and, with the recent acquisition of its Mt Moss processing facility, is undertaking preparations to potentially mine the select gold-dominant zones at Liontown (ASX: SHN, 2026)

REFERENCES

BEAMS S.D., BATES T., HUSTON D.L. & MORRISON I.J. 2017 Polymetallic massive sulfide deposits of the Mount Windsor Subprovince. In Philips (ed), Australian Ore Deposits. AusIMM. Monograph 23

BERRY, RF, HUSTON, DL, STOLZ AJ, HILL, AP, BEAMS, SD, KURONEN, U & TAUBE, A, 1992. Stratigraphy,structure, & volcanic-hosted mineralisation of the Mt Windsor Subprovince, North Queensland. Economic. Geology, 87:739-763.

DOYLE M. G., & MCPHIE J., 2000: Facies architecture of a silicic intrusion-dominated volcanic centre at Highway-Reward, Queensland, Australia. Journal of Volcanology & Geothermal Research, 99(1-4), 79-96

DOYLE, MG, 1997. A Cambro-Ordovician submarine volcanic succession hosting massive sulphide mineralisation: Mt Windsor Subprovince, Queensland. PhD Thesis (unpublished), CODES, University of Tasmania.

DUHIG N. C., STOLZ J. S., DAVISON G., & LARGE R., 1992: Cambrian microbial & silica gel textures in silica iron exhalates from the Mount Windsor volcanic belt, Australia; their petrography, chemistry & origin. Economic Geology, 87(3), 764-784

HENDERSON, RA, 1986. Geology of the Mt Windsor Subprovince – a Lower Palaeozoic volcano- sedimentary terrane in the northern Tasman orogenic zone. Australian Journal of Earth Sciences,33:343-364.

LEVINGSTON K.R. 1972. Ore deposits & mines of the Charters Towers Sheet area, north Queensland. Rep. geol. Surv. QLD. .57

RED RIVER RESOURCES (ASX:RVR), 2016, Exceptional High Grade Zinc Discovery at Liontown East, ASX Release – 4th August 2016

SIMPSON K.A., 2001. Volcanic facies architecture of the Cambro-Ordovician Seventy Mile Range Group, northern Queensland, Australia, PhD thesis (unpublished), CODES, University of Tasmania.

SUNSHINE METALS (ASX:SHN), 2025, Significant Upgrade in Liontown Shallow Gold Resource, ASX Release – 26th November 2025

SUNSHINE METALS (ASX:SHN), 2026, Robust Mining Study for Liontown Gold Operation, ASX Release – 16th February 2026

SUNSHINE METALS (ASX:SHN), 2026, Mt Moss Acquisition Completed & Production Pathway Advanced, ASX Release – 2nd July 2026

VICTORIA'S SECRET: GOLD MINERALISATION IN THE STAWELL ZONE, VICTORIA.

Bill Reid

North Stawell Minerals Ltd

Key Words: Tasmanides, Victoria, Stawell Zone, Narrow Vein Gold, Exploration, Cover

INTRODUCTION

North Stawell Mineral Ltd ("North Stawell", "NSM") is a gold explorer focused on 445 km2 of contiguous tenements over 60km strike-length immediately north of Stawell Gold Mines' ("SGM") multi-million-ounce namesake deposit at Stawell, Victoria, Australia (ASX:NSM 22-Sep-2020). The NSM ground is bound by the two major regional structures – the eastern Coongee Fault and the western Moyston Fault which define the 10km wide, gold-prospective (Moornambool Metamorphic Complex ("Stawell Gold Corridor")(Cayley and Taylor 2006)(Figure 1.h.) comprising the highly disrupted, arc-proximal section of the accretionary prism immediately east of the west-subducting Stavely Arc – and the far western margin of the Tasmanides (Cayley & Taylor 2006).

Gold mineralisation is emplaced by the same structural events that control all mineralisation as far east as the Western Bendigo Zone (Benambran (440 Ma) and Bindian (420-400 Ma) orogenic gold (Bucher, 1998, Glen, 1995)). However, the Stawell Corridor includes Delamerian structural emplacement of large slabs of Cambrian basalts into the sedimentary pile - derived from the subducting sea floor sequence (Schofield, 2018). The basalts are an important pre-cursor to later mineralisation acting as structural buttresses focus mineralisation adjacent to the basalt margins and in the roof zones above them.

Exploration potential, despite 40 years of modern mining at Stawell, is significant and has been preserved by a necessary focus on the mining operation, and by a thin blanket of Murray Basin cover (Johns and Lawrence, 1964) that is ubiquitous from 5km north of the mine, masking 85% of NSM's tenement footprint in the Stawell Gold Corridor (Figure 1.a.).

The geological history at Stawell, the vast amount of mine data and the important role that the geophysics-responsive basalts play in focusing mineralisation make the Stawell Corridor an ideal location to explore for narrow-vein gold mineralisation, particularly through cover.

REGIONAL GEOLOGY

The Victorian Goldfields account for approximately 15% of Australia's gold production, with 90+ Moz production recorded since 1853 (GSV, Mudd, 2007). Geology is dominated by monotonous Cambrian and Ordovician turbidites deposited in an early Palaeozoic ocean basin. Ocean floor basalts do not typically outcrop, but several are exhumed in major regional structures, and basalt slabs are common in the Stawell Gold Corridor. The sedimentary pile was limited to the west by the Cambrian, west-subducting Stavely Magmatic Arc (the same age/arc as the Mt Read Volcanics in Tasmania and the Mt Arrowsmith Volcanics in NSW) (Schofield, 2006).

Silurian-Devonian (Benambran) orogenesis closes the ocean basin, developing a thick-skinned (30-40km) orogenic belt comprising thrust slices of the oceanic basin sequence (Cayley et al, 2006). Associated metamorphism and structural development are the engine that drives gold mineralisation throughout western Victoria (Glen, 1995, Ramsay et al, 1998)). These regional structures divide Victoria into several discrete geological zones with interpreted deep-tapping regional faults defining their boundaries (Moore et al, 1998)(Figure 1.h).

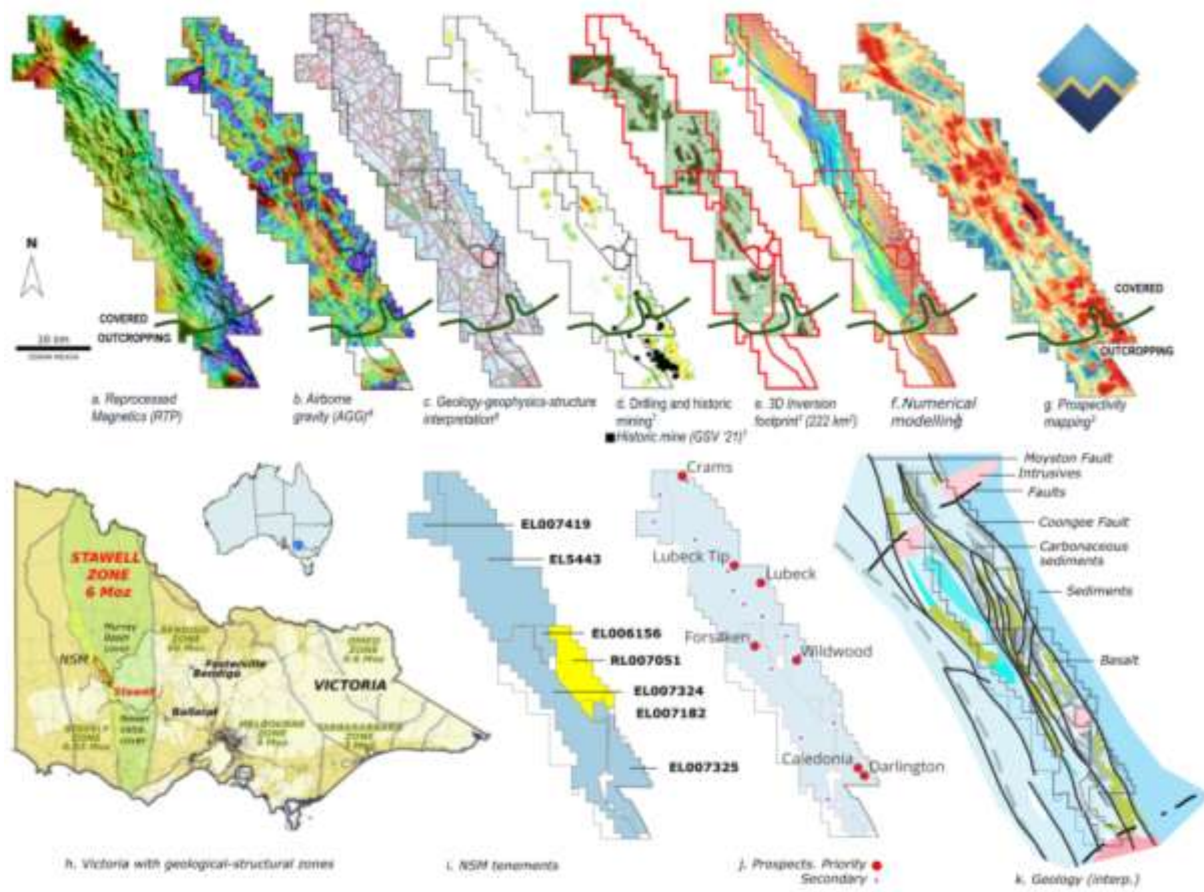

Figure 1: Locations, data sets, tenements, prospects and simplified geology, North Stawell Minerals.

The Stawell Zone is the westernmost structural zone impacted by Benambran orogenic events, emplacing typical narrow vein orogenic gold systems (Cayley and Taylor 2006, Hronsky 2021, Miller and Wilson 2004).

The metasedimentary sequence is intruded by several post-tectonic suites of Silurian and Devonian intrusives (Cayley and Taylor 2006). An additional gold event is associated with the intrusives (Bindian Orogeny). The Bindian is best developed east of the Stawell Zone.

During the Paleogene - Miocene, the Murray Basin was deposited over the northern continuation of the gold-prospective geology (Bush et al, 1995)(Figure 1.a). To the south, the Newer Volcanics mask basement geology (Geurin, 1995).

Stawell Zone

During the Cambrian, the Stawell Zone's western margin was the then-active Stavely Arc (Schofield, 2006). An accretionary prism with seaward-facing thrusts and back-thrusts was developed along the margin. The Stawell Gold Corridor is preserved on the far-western margin of the Stawell Zone and comprise greenschist through amphibolite grade, strongly disrupted and faulted, underthrust and exhumed slices of the down-going basalt-turbidite oceanic sequence.

The Stawell Gold Corridor can be traced in drilling and geophysics over 170km strike and is approximately 10km wide. The regional Coongee Fault (Figure 1.k) is the eastern margin of the Stawell Gold Corridor and is locally west-dipping – an orientation interpreted to reflect its origins as a back-thrust(s) (Cayley and Taylor, 2006). The Moyston Fault is a moderately east-dipping basal thrust and the western margin of the Stawell Corridor, Stawell Zone and the Tasmanides. The fault trace approximates the contact with the Stavely Arc (Cayley and Taylor, 2006).

Underplated and thrust-exhumed ocean tholeiites are incorporated into the accretionary prism – and are particularly common in the in the Stawell Corridor (Cayley and Taylor 2006)(Figure 1.k). The structurally emplaced (fault-bounded) basalts are a critical preparatory step in the gold-geology model at Stawell - they serve as structurally resistive buttresses during the gold-event. The geology focuses dilation on the margins of, and proximal to, the basalts (Winterbottom and Holland, 2016). Multiple belt-parallel thrusts occur within the Stawell Gold Corridor, repeating the basalts. Sub-parallel faults crosscut the geology and mineralisation and are penecontemporaneous with the late intrusive event (Hronsky, 2021).

Gold mineralisation is emplaced during the Benambran and Bindian Orogenies – the same events that emplace the early orogenic gold occurrences throughout the western Victorian goldfields (Cayley and Taylor, 2006, Hronsky, 2021). Unique to the Stawell Corridor (in Victoria) structures (and mineralisation) find and follow the margins of the resistive basalt (Winterbottom and Holland, 2016). Irregularities in structural orientation and the basalt margins promotes dilation, and interactions with reduced sediments and sulphide facies volcanogenic rocks peripheral to the basalt focus ore development. Locally, in the pressure shadows above the buttressed basalts, additional splays and veins of orogenic gold mineralisation occur (Fredericksen and Gane, 1998, Winterbottom and Holland, 2016).

Other mineral systems described in the Stawell Corridor include potential IRGS (Bierlien and McKnight 2005) and Besshi-type VHMS (Murphy, 2017). Of note, strandline HM-REE and WIM-type REE occur in the cover sequence (Murray Basin, see below), comprising billions of tonnes of declared resources (see ASX:ATM, ASX:WIM).

Late (post-tectonic) S-type and I-type intrusives occur throughout the Stawell Zone (Cayley and Taylor 2006). The Silurian-Devonian intrusives are frequently preferentially oriented northeast, parallel to a late a generation of faulting (Figure 1.k.)(Hronsky 2021. Locally, the intrusives interact with, and potentially re-mobilise or upgrade, pre-existing orogenic gold mineralisation. Possible intrusive-related gold is discussed (Bierlien and McKnight 2005).

Cover sequences mask approximately 85% of the gold-prospective geology in the Stawell Zone (c.f. 40% in the Bendigo Zone). Only 30km of the Stawell Gold Corridor is exposed (Figure 1.h.). To the north, the Murray Basin covers the Paleozoic basement from 5km north of the Stawell Mine. The basin sediments thicken at approximately 1m/km near the margin, but steepen rapidly beyond this, with depths to 300m recorded (Bush et al 1995) (Figure 1.a, 1.b.). The Cenozoic Newer Volcanics occur, masking basement geology from 25 km south of Stawell. 100km south of Stawell, normal faulting on the margin of the Otway Basin down-drops the gold-prospective basement geology to approximately 1 km depth.

Regional geophysics effectively maps basement geology – particularly the gold-prospective basalts. Unlike the Newer Volcanic cover, Murray Basin cover does not have a significant geophysical signature in regional surveys (magnetics or gravity) (Figure 1.a, 1.b.).

DEPOSIT MODELS

Magdala (Stawell Mine)

The type-example of a fault-emplaced basalt in the Stawell Zone is the Magdala Basalt that cores the mineral deposit at Stawell (Winterbottom and Holland 2016)(Figures 2.b., 3). The operating mine at Stawell is owned and operated by Stawell Gold Mines Pty Ltd. The Magdala Basalt is 300-400m wide, 5.5 - 8 km in length and at least 1,600m deep. The basalt core is largely non-tectonised by regional structural fabrics, although late thrusts cut it. The basalt is chlorite +/- epidote altered, weakly deformed on its margins, with minor quartz +/- carbonate veins.

Mariners-type mineralisation

The Magdala Basalt does not outcrop and was found by a progressive mining from alluvial systems (0.8 Moz Au produced (Stawell Gold Mines, 2024)) and identified outcropping/sub-cropping metasediment-hosted orogenic gold mineralisation to depth. The Mariners Lodes occur in the 300m faulted sedimentary roof above the basalt – and returned historic production of 0.74-0.95 Moz Au at 28-30 g/t Au) (NSM:ASX 15 Apr 25)(Figure 2.b.). The Mariner Lodes are faulted, plunging narrow vein, high grade gold system, with broad similarities to many other Victorian resources (e.g. Ballarat). The historic Mariners Lodes are brecciated quartz-carbonate veins with abundant visible gold (Fredericksen and Gane, 1998). They are an attractive exploration target-type – high-grade gold in Victoria. At depth, the Mariners Lodes led mining to the basalt-margin-hosted mineralisation ("Stawell-type").

Stawell-type mineralisation

The western basalt-margin Central Lodes and the deeper, fault-offset Golden Gift, the eastern-basalt margin Hampshire Lodes) (Winterbottom and Holland 2016, Stawell Gold Mines 2024)(Figure 2.b.) are grouped as "Stawell-type" mineralisation for their common characteristic – proximity to the Magdala Basalt margin.

Geology differs on each flank of the basalt and the basalt roof. The basalt margins on the western Magdala Basalt includes reduced, carbonaceous sediments and sulphide-facies volcanogenic sediments. Sulphides (pyrrhotite, pyrite and arsenopyrite), silica, chlorite and magnetite occur and are variably developed (Winterbottom and Holland 2016). The western Magdala Lodes extend to approximately one mile depth (1,600 m). The ores and the basalt are open at depth – a vertically persistent mineral system (Figure 2.b.).

On the roof of the basalt locally on the basalt flanks, the volcaniclastics are also mineralised, particularly where they occur as embayments in basalt margin (termed "waterloos"), focussing dilation and mineralisation (Winterbottom and Holland 2016, Stawell Gold Mines 2024). The waterloos are interpreted as primary features that have been exploited and reactivated by structures. Mineralisation is highly variable, including pyrrhotite-pyrite-arsenopyrite-chlorite-stilpnomelane-magnetite-quartz in the alteration-mineralisation system and quartz-carbonate veining haloes with more distal carbonate spotting (Winterbottom and Holland 2016).

Following ownership change in 2017, mining focused on the eastern, less-reduced flank of the basalt for the first time (Robinson, 2018). Mineralisation is more silicic and sulphidic with lesser chloritic with very minor white mica. Gold mineralisation is demonstrated to be well-developed and economic, with ore plunging sub-parallel to mineralisation on the western Magdala Basalt (Stawell Gold Mines 2024). The sedimentary host rocks are also less reduced on the east flank compared to the west flank.

Metasedimentary host rocks are highly deformed by multiple events, and primary sedimentary structures are often disrupted and obscured (the fold-fault reconstructions typical of Victorian turbidites are challenging).

Late felsic porphyry dykes occur, frequently exploiting existing structures and are unmineralised at Stawell, but has a spatial relationship to mineralisation at Wonga, a satellite deposit 900m south of Stawell within the contact aureole of the Stawell Granite (Beirlien and McKnight 2006).

EXPLORATION AND DISCOVERY

NSM was spun out of Stawell Gold Mines in 2020 to focus on the regional gold prospectivity in the northern Stawell Gold Corridor. The regional exploration thesis north of Stawell is that Stawell-type mineral systems associated with basalts are primary targets as the basalts are a regional vector to mineralisation and provide a clear "marker horizon/footwall" at the drilling/deposit scale. The basalts respond variably to magnetics and are well-defined by gravity (Figure 1.a, 1.b). The geophysics response is particularly advantageous in covered terrane – 85% of the NSM tenement package and 100% covered from 6 km north of the Stawell Mine) (ASX:NSM 16 Sep 25, 15 Nov 23). Potential for Mariners-type mineralisation is tested when targeting the deeper (causative) basalt(s).

Wildwood

The Wildwood Prospect, 25km north of Stawell Figure 1.j.), is cored by the 4.5 km Wildwood Basalt on the far eastern margin of the Stawell Gold Corridor. The basalt is doubly-plunging, and the central area is unroofed and eroded. The basement rocks are masked by 10-30 m Murray Basin cover. At depth, the basalt and (minor) mineralisation is demonstrated to extend to 500m depth and remains open (ASX:NSM 15 Apr 25) (Figure 3). Wildwood is effectively tested to approximately 150 m vertical. The southern 1.6 km of the Wildwood Basalt and a 1.3 km basalt 600 m to the east (Wildwood East) are poorly explored.

Wildwood was identified in 1993, through shallow cover, with high resolution, regional, government-flown magnetics (Figure 1.a). The basalt was confirmed with drilling in 2001, and Stawell-type mineralisation confirmed with the 78th hole into the target in 2003.

Table 1: Mineral Resource Estimate – Wildwood (ASX:NSM 29 Jun 2023).

	Indicated	**Inferred**				
	Tonnes	Grade	Ounces (oz Au)	Tonnes	Grade	Ounces (oz Au)
	(t)	(g/t Au)		(t)	(g/t Au)	
Maslin	328,100	2.3	24,600	361,900	2.2	25,500
Clontarf	140,400	2.3	10,500	90,100	1.9	5,400
Trinity	121,800	2.4	9,500	112,600	3.3	11,800
TOTAL	590,300	2.4	44,600	564,600	2.4	42,700

Note: All resource figures are reported in accordance with the JORC Code 2012 Edition. •All figures are rounded to reflect the appropriate levels of confidence, with apparent differences potentially occurring due to rounding. •Mineral Resources are reported at a 1.0 g/t Au cutoff grade.

Wildwood includes a modest global resource of 87.3 Koz Au at 2.4 g/t Au (ASX:NSM 29 Jun 23, Table 1, Figure 2, 3) occurring as three discrete resources that occur on both margins of the basalt. The mineralisation, alteration, structures and controls are very similar to the system at Magdala (Stawell) – pyrrhotite-arsenopyrite-pyrite-quartz-chlorite-stilpnomelane-magnetite.

In contrast to Magdala, however, identified mineralisation at Wildwood occurs principally on the top/crest of the basalt and in "waterloo" embayments – lacking the large-tonnage, basalt-flank resources (ASX:NSM 14 Apr 25)(Figure 3). Basalt-flank drilling intercepts occur, are encouraging, and open at depth. Locally, the gold-prospective volcanogenic unit on both the basalt flanks is faulted out.

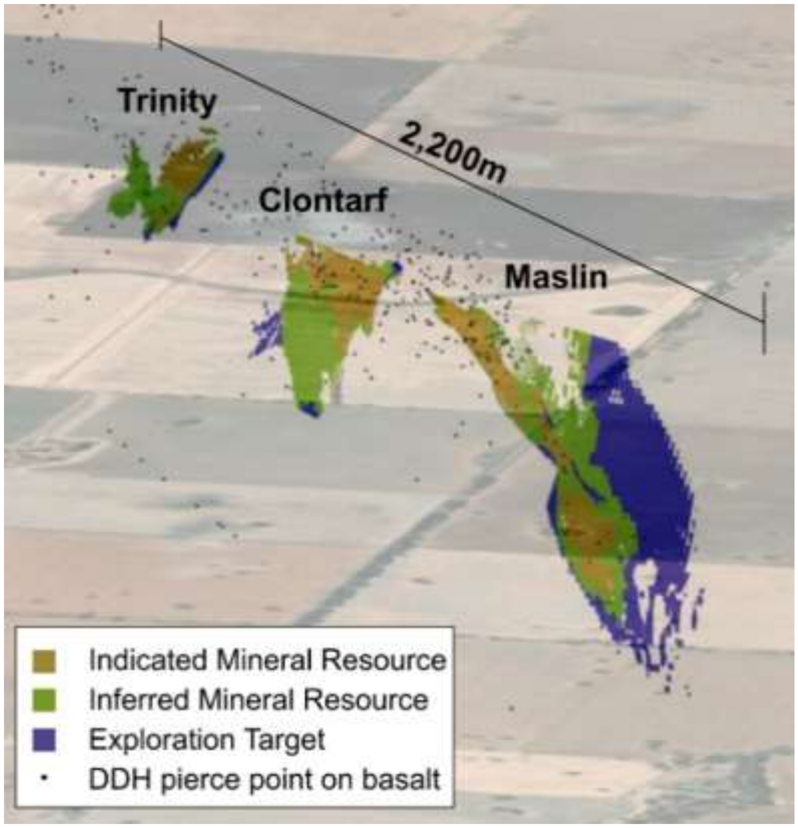

Figure 2: a. Oblique image Wildwood Mineral Resource (view down and toward the south).

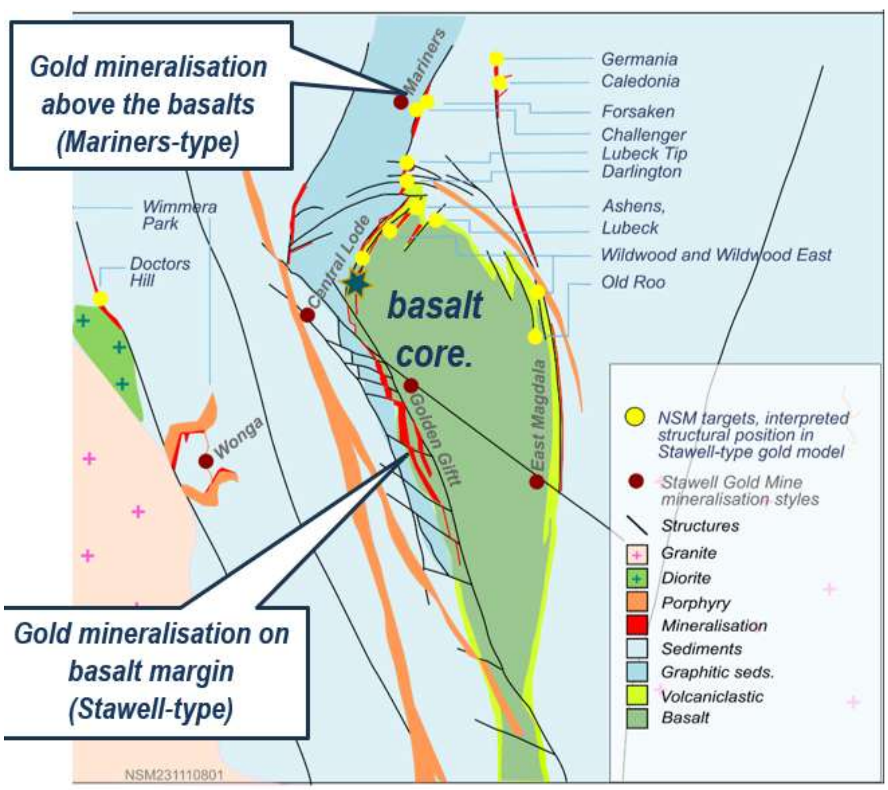

Figure 2: b. Stylised model of Stawell showing the mineralisation architecture and NSM Prospects superimposed in their relative position against the model.

Regional Exploration

On listing, NSM's focus on regional gold-prospectivity was accelerated, augmented by a large, historic drill database (200+km of shallow drilling (heavily skewed towards the Wildwood Prospect) (ASX:NSM 31 Jan 21)(Figure 1.d.) and disappointing results from programs targeting basalt flank mineralisation to extend mineralisation at the Wildwood.

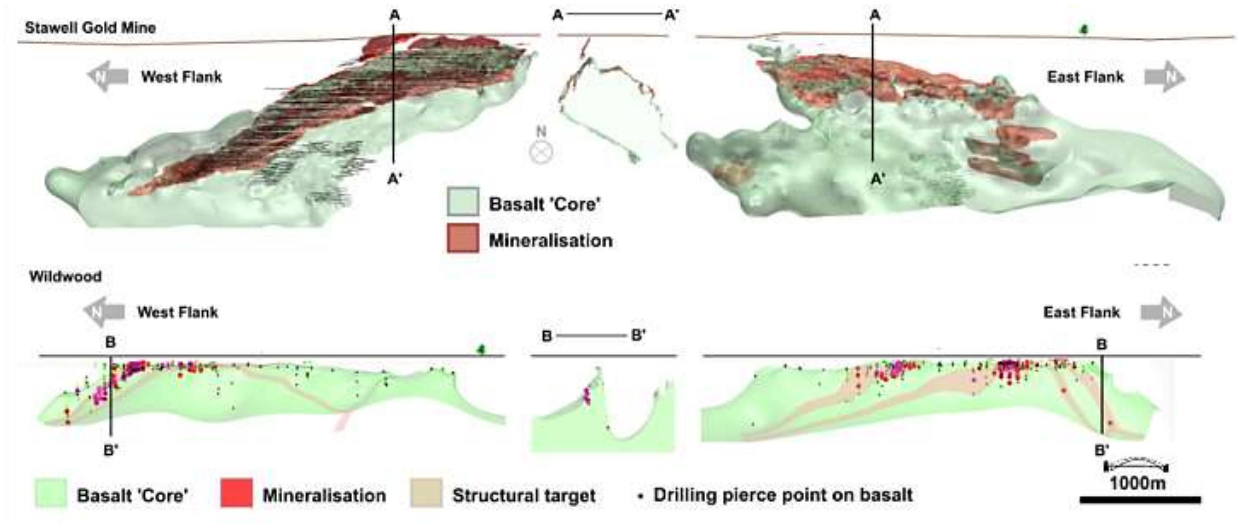

Figure 3: Comparison of Stawell and Wildwood - west flank long-section, section, and east flank long-section at the same scale.

Acquisition of Falcon AGG data (Figure 1.b.) improved gravity resolution by two orders of magnitude and highlighted additional blind basalt targets, significantly improving target vectoring (ASX:NSM 8 Jun 21). Over 60km of basalt strike was interpreted – with potential for mineralisation on each flank and the crest (if not unroofed)(Figure 1.k.). Complicated by a poor surface geochemistry response, targets were ranked and prioritised against the Stawell models and drilled with campaign air core drilling, with targets that responded to the model-driven targeting being prioritised from 12 tested targets. (Wildwood, Darlington, Caledonia, Forsaken and Lubeck Tip) (ASX:NSM 23 Mar 23)(Figure 1.j.). The result is a substantially more robust project pipeline from resources through generative targets.

To further refine the exploration fairways, 222 km^2 of 3D inversion modelling (ASX:NSM 29 Oct 21, 31 Jan 22)(Figure 1.e.) of basalts was completed using the AGG gravity data and numerical modelling (Figure 1.f.) of potential fluid flow along basalt margins completed to predict prospective sites on the basalt margins. Darlington West, discussed below, is a critical test of targeting directly against the inversion-numerical modelled vectors.

Darlington-Caledonia trend

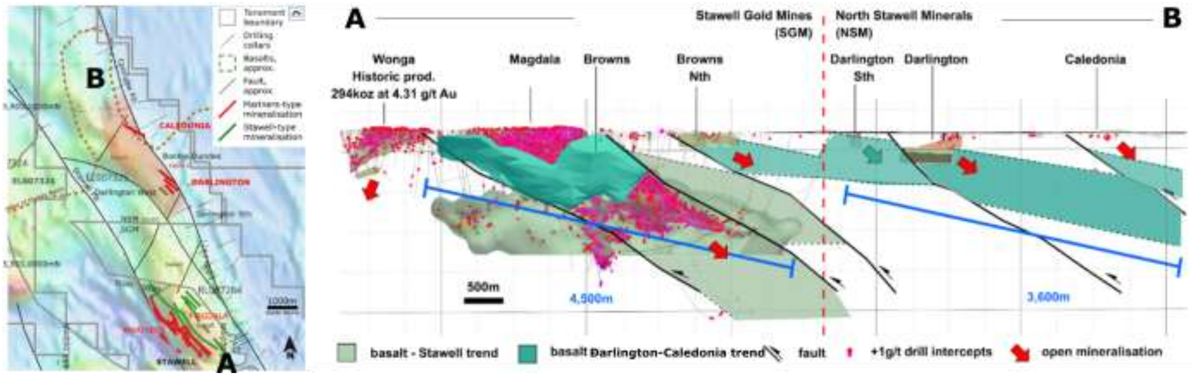

Figure 4: Darlington – Caledonia trend and the Stawell Mine. Plan and long-section.

The Darlington-Caledonia trend is a 3.6km structural-geophysics target that follows the northern continuation of the Magdal Basalt into NSM's tenements (Figure 4.). The basalt has been intersected with only a small number of holes, with depths varying from 20-300 m vertical.

The trend includes four historic small-scale mines, notable for their historic production grades (10-30 g/t Au). Darlington and Caledonia are NSM's current exploration focus – each returning near-surface, high-grade gold intercepts in drilling and multiple low-grade hits defining a larger mineralised target. Mineralisation occurs above the basalts is interpreted as lodes sub-parallel (NNW) to the trend of the basalt (Figure 2.a., b.).

At Darlington, drilling has intersected a deeper, weakly carbonate altered basalt in two locations – in both intersects the gold-prospective margin is faulted out (ASX:NSM 26 Jul 23, 23 Apr 25). However, the high-grade gold intercepts occur 100m above the basalt – a similar structural position as the Mariners Lode (at Stawell). The mineralisation includes brecciated and quartz-flooded veining with coarse visible gold (NSD053) (ASX:NSM 19 Mar 25, 23 Apr 25). High grade intercepts occur in parallel narrow, vertical vein. Determining continuity and plunge of a possible higher-grade shoot is the current focus for exploration. The Darlington system includes 1+ g/t Au gold intercepts over 800m of strike and is open along strike and at depth (ASX:NSM 29 May 26).

Caledonia, a vein system two km north of Darlington includes 600 m of gold-mineralised strike – identified through shallow cover (ASX:NSM 30 Jun 26) (Figure 4). Deeper basalts have been intersected but are interpreted at depth from geophysics. The target is open.

Darlington West

Darlington West tested one of several priority geophysics-only targets generated from high-resolution AGG 3D inversions (Figure 1.e.) coupled to numerical modelling of fluid flow (Figure 1.f.) against a Stawell Mine exploration model (Figure 2.b.). The modelling highlighted northern and eastern flanks of the interpreted basalt as matching the mineralisation conditions that control Stawell. Recognising that the inversion shapes are approximate, drill planning included a broad error window. Drilling (NSD054) (ASX:NSM 13 May 25) has confirmed basalt margin-hosted (Stawell-type) mineralisation on both margins of a weakly tectonised basalts. Follow up holes have intersected additional basalt-flank mineralisation, also mineralised. Refining targeting to identify broader or high-grade intercepts are the next steps at Darlington West. Two other priority inversion-3D modelling targets – the Crams and Lubeck Prospects (ASX:NSM 13 May 25)(Figure 1.j.) – have similar 3D Inversion-numerical modelling targets.

CONCLUSION

NSM is exploring a 445 km^2 highly gold-prospective, cover dominated 10km wide structural corridor on the far western margin of the Stawell Zone, Victoria, Australia. The Stawell Gold Corridor geology includes large slabs tholeiitic basalt incorporated into the sedimentary pile prior to the gold mineralisation events, a point of difference c.f. other Victorian gold systems.

The basalts are structurally resistive (buttressed) against the gold mineralisation events and focus mineralisation onto the basalt margins (Stawell-type mineralisation). The type-deposit is the 5.3Moz Stawell Gold Mine, 5km south and along strike of the NSM tenement package.

In addition, high-grade, narrow-vein gold is also identified as splays off the basalt into the sedimentary rocks above the basalt (termed Mariners-type gold). The type-deposit is the historic Mariners (historic production of 0.74-0.95 Moz Au at 28-30 g/t Au). The difference to more typical Victorian narrow vein gold systems is the association with the deeper, pre-structural basalt buttresses.

The basalts provide a strategic geological control on the mineralisation systems – find the basalt to find mineralisation. The basalts respond to geophysics, in particular high-resolution gravity, hugely assisting exploration targeting. This is doubly important north of Stawell, where the Murray Basin forms a thin blanket of unmineralised cover above the gold-prospective basement geology. The cover sequence also preserves the potential for large, shallow repeats of Stawell.

NSM has identified multiple basalts totalling 60 km strike length. Twelve are drill-tested. Five are prioritised (with the remainder contributing to a robust project pipeline). The Wildwood Prospect includes a modest Mineral Resource (87.3 Koz Au at 2.4 g/t Au) and is open along strike and at depth. The 3.6km Darlington-Caledonia trend includes multiple high grade gold intercepts above the far northern continuation of the basalt that controls the Stawell Mine, 5km to the south of NSM's tenement boundary). The Darlington and Caledonia Prospects have both returned high grade gold intercepts. The Darlington Prospect includes geology, structure and mineralisation that may be a repeat of the Mariners-type gold system above a drill-confirmed basalt.

Modelling the geophysics (3D inversion) and most likely fluid flow pathways (numerical modelling) further refines drill targeting ahead of drilling, predicting the most likely mineralisation pathways. The Darlington West Prospect is a geophysics-numerical modelling only target that returned thin (but highly encouraging) basalt-flank mineralisation in the first drill hole targeting the previously undrilled target. Additional modelled targets are identified in data.

NSM was spun out of Stawell Gold Mines in 2021 to focus on the regional search for a repeat of the multi-million-ounce deposit at Stawell. Building on a large inherited database, NSM has added campaign drilling, revised and refined exploration models, improved geophysical data (and derived products and targets) and an upgraded Mineral Resource Estimate at Wildwood. The cornerstone strategic advantages are the association between gold mineralisation and basalt slabs in the pre-gold mineralisation geology (unique to the Stawell Corridor in Victoria) and the mask of thin cover to preserve shallow gold potential. Currently focused on three key projects – Darlington, Caledonia and Wildwood – multiple additional targets are identified for further exploration with significant potential to discover a repeat of the mineralisation at Stawell.

REFERENCES

BIERLEIN F. & McKNIGHT S. 2005. Possible intrusion-related gold systems in the western Lachlan orogen, southeast Australia. Economic Geology, 100(2): 385.

BUCHER M. 1998. Timing & deformation, plutonism & cooling in the western Lachlan Fold Belt, Southeastern Australia. Ph. D thesis, Latrobe University, Melbourne (unpublished).

BUSH M. D., CAYLEY R. A., ROONEY S., SLATER K. R. & WHITEHEAD M., 1995. Geology & prospectivity of the southern margin of the Murray Basin. Victorian Initiative for Minerals & Petroleum Report 4. Department of Agriculture, Energy & Minerals, Victoria.

CAYLEY R. A. & TAYLOR D. H. 2001. Ararat 1:100,000 map area geological report. Geological Survey of Victoria Report 115.

CAYLEY R. A., KORSCH R. J., MOORE D. H., COSTELLOE R. D., NAKAMURA A., WILLMAN C. E., RAWLING T. J., MORAND V. J., SKLADZIEN P. B. & O'SHEA P. J. 2011. Crustal architecture of central Victoria. results from the 2006 deep crustal reflection seismic survey. Australian Journal of Earth Sciences 58, 123–156.

FREDERICKSEN D. C. & GANE M. 1998 - Stawell gold deposits: in Berkman D A, Mackenzie D H (Ed.s), 1998 Geology of Australian & Papua New Guinean Mineral Deposits. The AusIMM, Melbourne Mono 22 pp 535-542

GUERIN B., 1992. Scoria & tuff quarrying in Victoria. Geological Survey of Victoria Report 96

GLEN R. A. 1995. Thrusts & thrust associated mineralisation in the Lachlan Orogen. Economic Geology 90 pp. 1402-1429.

HRONSKY J. 2021. North Stawell Mines Metallogenic Analysis & Targeting Study. Internal report, Western Mining Services61 pages.

JOHNS M. W & LAWRENCE C.R. 1964. Aspects of the geological structure of the Murray Basin in north-western Victoria. Department of Mines.

MILLER J. McL & WILSON C. J. L. 2004. Structural analysis of faults related to a heterogeneous stress history: reconstruction of a dismembered gold deposit, Stawell, western Lachlan Fold Belt. Journal of Structural Geology, Volume 26, 6-7, pp 1231-1256

MUDD G. M. 2007. Gold Mining in Australia: linking historical trends & environmental & resource sustainability. Environmental Science & Policy. Vol 10 7-8 pp 629-644.

MURPHY J. 2017. EL4758 TARGET Mineralisation exploration initiative Milestone 1 report for downhole electromagnetic survey at the Carrols Prospect. Stavely Minerals Ltd report.

MOORE D. H., VANDENBERG A. H. M., WILLMAN C. E & MAGART A. P. M. 1998. Paleozoic geology & resources of Victoria. AGOS Journal of Australian Geology & Geophysics, 17(3) 107-122.

RAMSAY W. H. R. & WILLMAN C. E. 1998. Gold. In J. G. Douglas & J. A. Ferguson (eds.) Geology of Victoria, pp 454-481. Victorian Division, Geological Society of Australia Incorporated.

ROBINSON B. 2018. Stawell Gold Mines: Finding new life in an old mine. GPIC presentation. (https://ballaratgeology.wordpress.com/wp-content/uploads/2018/04/20180419-ballarat-geology-stawell-gold-mines-b_robinson.pdf) Ballarat. pp 27.

SCHOFIELD A. (ed.) 2018. Regional geology & mineral systems of the Stavely Arc, western Victoria. Record 2018/02. Geoscience Australia, Canberra.

STAWELL GOLD MINES. 2024. Stawell Gold Mines. Stawell Gold Corridor Conference 2024. Online resource (https://minedocs.com/27/Stawell-Gold-CP-11272024.pdf) (pdf). pp 15.

WINTERBOTTOM J. & HOLLAND I. 2017. Report on the Mineral Resources & Reserves of the Stawell Gold Mine in the state of Victoria, Australia. Technical Report. Kirkland Lake Gold.

THE E37 TREND PORPHYRY SYSTEMS: DIFFERENTIATING AN ENDMEMBER OF THE NORTHPARKES PORPHYRY SPECTRUM

Henry Schaumburg[1], Cameron Buchanan[1], Nathan Fox[2], Jonathon Hoye[1]

[1]Evolution Mining (Northparkes) Pty Ltd

[2]Sustainable Minerals Institute - University of Queensland

Key Words: Northparkes, E37W, Porphyry, Copper

INTRODUCTION

Evolution Mining's Northparkes Operations (NPO) has been in production since 1993. The Northparkes porphyry district has been actively explored for Cu-Au porphyry deposits since the discovery of porphyry mineralisation at E22 in 1976 (Jones 1985; Lye et al. 2006). Since then, nine economic porphyry deposits have been defined, four of which have each undergone periods of either open pit and/or block cave mining (E22, E26, E27, and E48) with underground development currently underway for a new block cave beneath the open pit at E22. Although these deposits are broadly similar to one another, they differ in areas such as host lithologies, stock position, vein assemblages, and characteristics of porphyry magma. While the porphyry systems on the mining leases are the best described multiple porphyry systems exist on the NPO exploration leases (Lye et al. 2006) that have undergone multiple phases of exploration and are still comparatively poorly understood.

Further work is warranted to characterise the Northparkes porphyry systems to assist with regional exploration targeting and to better understand the evolution of the Northparkes porphyry district and Macquire Arc as a whole.

The E37 Trend is located approximately 6km's directly west of the current NPO mining lease. This area has been periodically explored since 1978 (Lye et al. 2006). Over this time three porphyry systems, E37, E37W and Veedas, have been identified within the E37 Trend, with which each corresponding to a distinct magnetic high geophysical anomaly (Fig. 1), with only E37 having a corresponding geochemical anomaly in aircore/RAB (Lye et al. 2006). Geochemical classification of these systems has identified four phases of porphyry intrusion within host lithologies that are dominated by the andesitic latites and volcaniclastic sandstones of the Goonumbla Volcanics with lesser amounts of fiamme and trachyte clast bearing volcaniclastic breccias of the Wombin Volcanics.

In this paper we aim to characterise the E37W porphyry system, using data from drillhole E37D136, as a representative of the porphyry system along the E37 Trend, and then compare the magma fertility, alteration zonation, and mineralisation styles to porphyry deposits on the NPO mining leases.

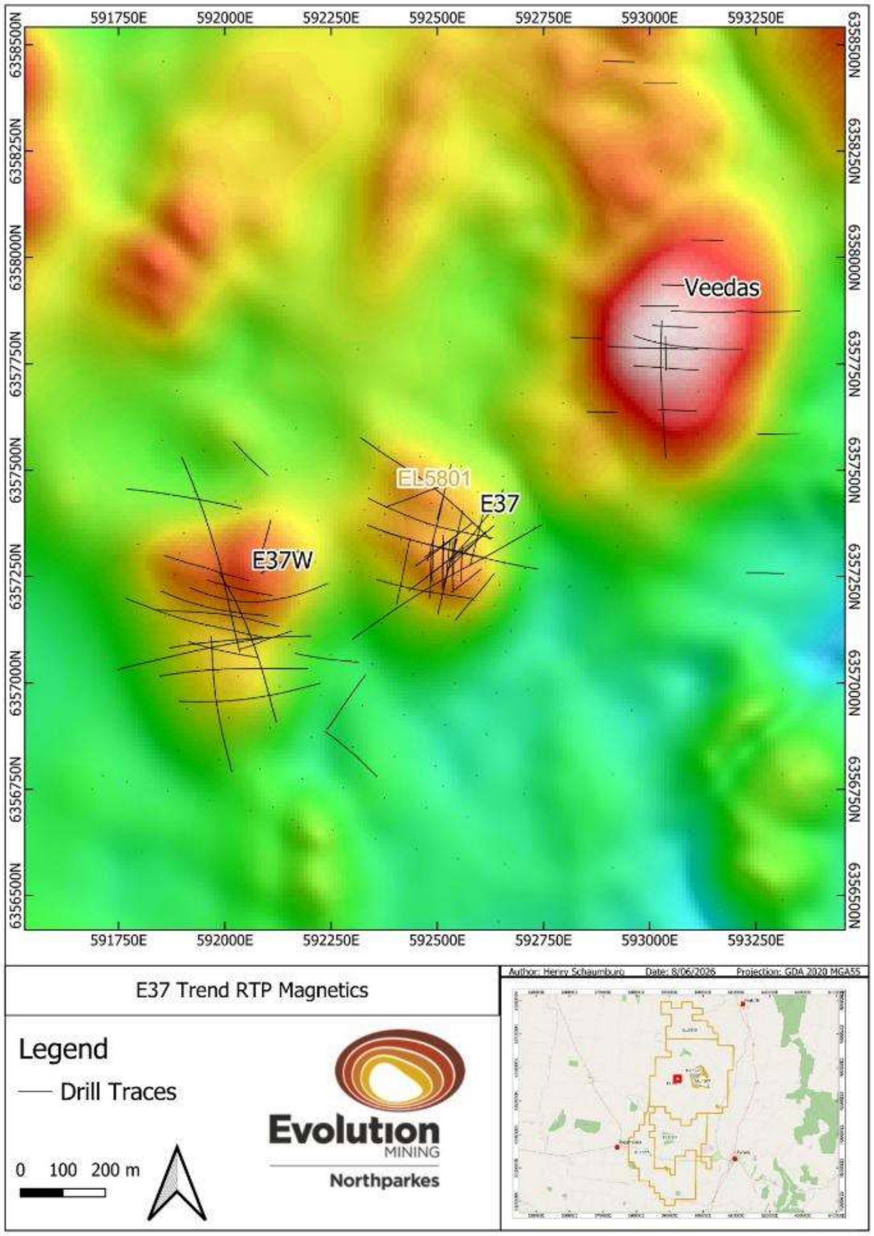

Figure 1: RTP magnetics map over the E37 Trend highlighting the location of the E37, E37W and Veedas porphyry systems. Coordinates in MGA2020 Zone 55. Red dotted circles are Cu haloes (>0.1%) represent drilling geochemistry projected to surface.

REGIONAL GEOLOGY

The Northparkes porphyry district is hosted within Late Ordovician to Early Silurian Wombin and Goonumbla Volcanics of the north-south trending Junee-Narromine volcanic belt of the Macquarie Arc in Central NSW, Australia. The Wombin Volcanics are characterised by an andesitic to trachyandesitic composition, while the Goonumbla Volcanics are more andesitic to basaltic andesite in composition (Simpson et al. 2005). The volcanic belt is broadly folded with these features striking roughly NE-SW. These folds have subsequently been intruded by a large volume monzonite stock complex with a U-Pb (SHRIMP) zircon age date of 445.2±3.9Ma (Lickfold, 2002).

The Northparkes porphyry systems are composed of a series of narrow, vertically continuous, alkalic monzonite porphyry intrusions, with these intrusions hosted with the volcanic host sequences and monzonite stock (Jones 1985; Lickfold 2002). Four phases of porphyry intrusion have been identified to date, with each phases becoming progressively less mineralised. The final unmineralized porphyry intrusions are believed to be emplaced at a similar time to basaltic dykes.

Cu-Au mineralisation at Northparkes is zoned with bornite ± chalcocite cores of the systems trending laterally to chalcopyrite dominated and then pyrite dominated. These sulfides are both disseminated and hosted in quartz ± anhydrite or quartz ± carbonate vein sets. Host lithologies are seen to impact the dispersion of the alteration halos and mineralising fluids with volcanic sequences constraining mineralisation close to the causative porphyry intrusion while the monzonite stock leads to large, low-grade halos. Localised white mica overprinting of economic systems are magnetite destructive forming broken magnetic donuts in regional magnetic imagery.

DEPOSIT GEOLOGY

The E37 Trend is characterised by three distinct magnetic highs related to monzonite porphyry intrusions that run roughly parallel to the Milpose Syncline. The area is composed of the Late Ordovician Goonumbla Volcanic sequence, with a conformable overlying unit of Wombin Volcanics (Fig. 2). The Goonumbla volcanic sequences consist of shoshonitic basaltic trachyandesite lavas and sills, volcaniclastic breccias, and volcaniclastic sandstone, while the Wombin Volcanics consist of trachyte clast bearing volcaniclastic breccia and lesser amounts of ignimbrite. These units dip shallowly to the south-east (Fig. 3). An erosional unconformity occurs between these units and the west-dipping sedimentary cover, consisting of fine-grained, massive to locally bioturbated/fossiliferous siltstone, quartz-mica sandstones and basal conglomerates. The basal conglomerates are composed of the Ordovician Goonumbla Volcanics. The Department of Primary Industries and Regional Development have provided faunal ages on these fossiliferous rocks of late Silurian to Early Devonian.

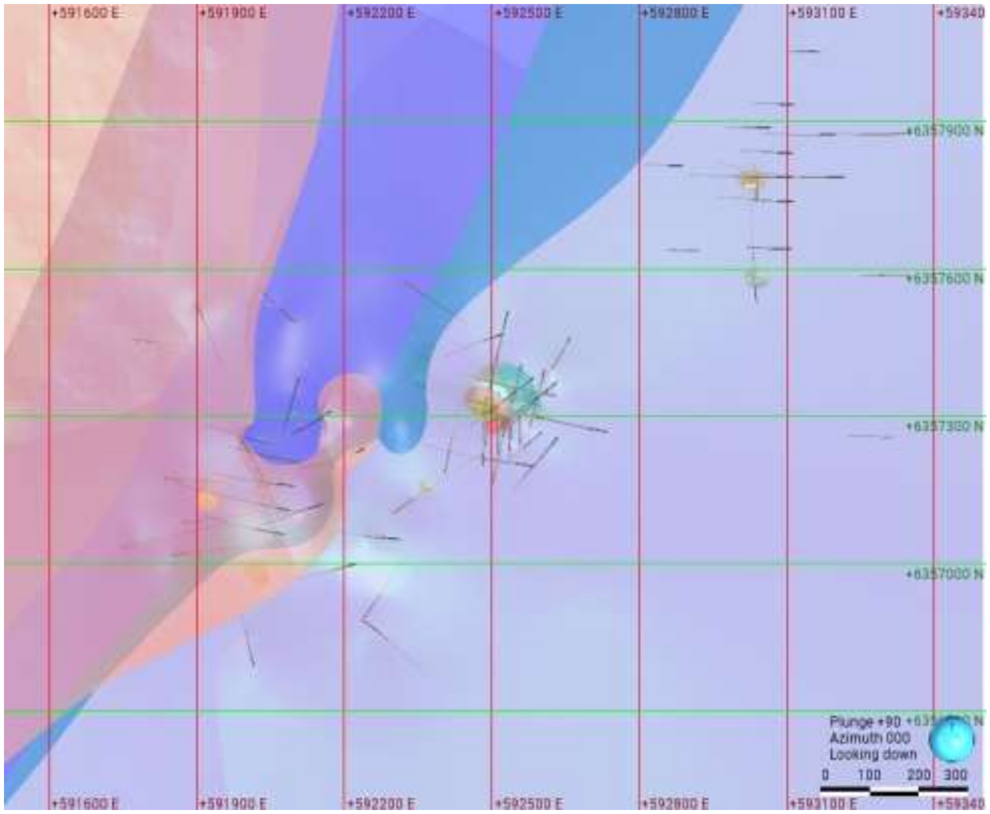

Figure 2: Interpreted basement geology map of the E37 Trend with Devonian cover in the west, Wombin Volcanics in the southeast, and the Goonumbla Volcanic seen between the two. Drill traces shown in grey. Coordinates in MGA2020 Zone 55.

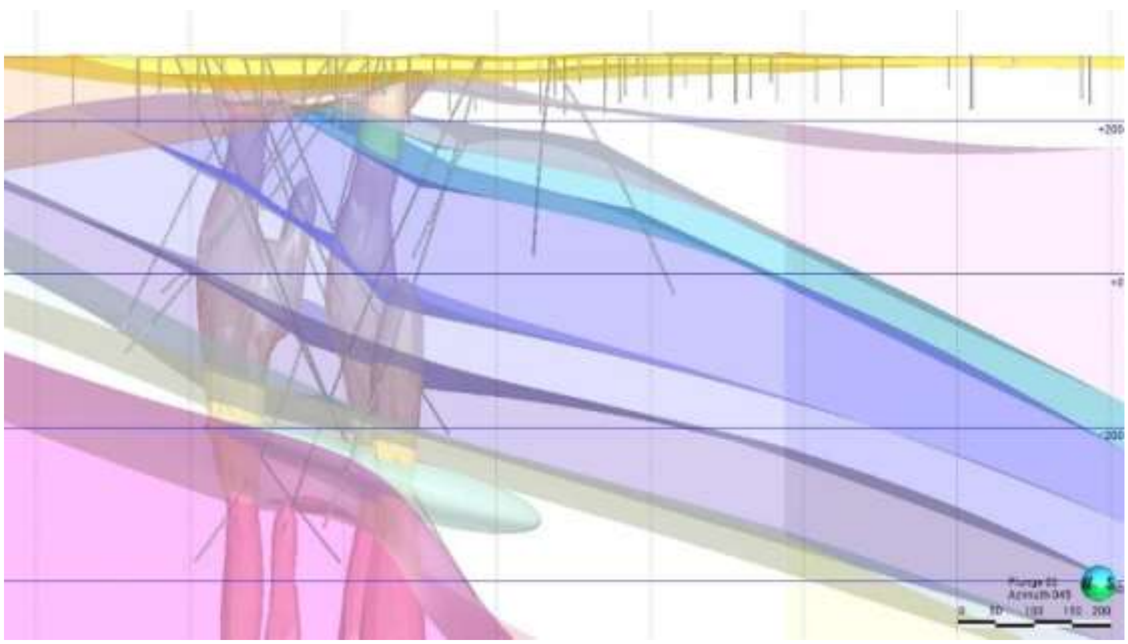

Figure 3: Geological model of E37W highlighting the south-easterly dipping host sequences and the erosional unconformity between the Devonian cover and Ordovician host sequences. Slice taken following A-A' in Figure 2. Coordinates in MGA2020 Zone 55.

Host Sequences

The host sequences of the E37 Trend are dominated by the Goonumbla Volcanics and the first units of the Wombin Volcanics. These units were lithogeochemically classified using Halley's (2026) geochemical classification method on 2m HQ core intervals that underwent ALS's 4-Acid Near Total Digest (HCl, HNO3, HF, H2SO4) with combination Inductively Coupled Mass Spectrometry (ICP-MS) and Atomic Emission Spectroscopy (AES) finishes to allow determination of both pathfinder suite metals and rock forming major elements, excluding Si. Scandium works well to differentiate units and allowing them to be correlated between drillholes across the whole of the E37 Trend.

The Goonumbla volcanics are characterised as andesitic latites with 10-20ppm Sc alongside minor interbeds of andesitic volcaniclastic >20ppm. The andesitic latites can be further separated through elements like P, Cr, and Nb (Fig. 4).

The Wombin Volcanics consist of ignimbrites and fiamme bearing volcaniclastic breccia that includes clasts of trachyte and contain <10ppm scandium. Several felsic intrusive trachyandesites are present at the base of current drilling and these can be differentiated from volcaniclastic breccias in Zr, Nb, V, and Th concentrations (Fig. 4).

Bedding measurements from volcaniclastic units shows a shallow south-easterly dip which is supported in the alignment of these classified units in 3D space during modelling. This shows that the host sequences are largely continuous flows and beds over ~1500m between the three porphyry systems.

Porphyry Phases

Across the E37 Trend four phases of monzonite porphyry intrusion have been identified through lithogeochemical classification (Fig.5). The first phase of monzonite porphyry occurs only at E37 and is characterised by low Ti, Sc, Th, V, Nb, P and Zr. The second phase of porphyry intrusion (Fig. 6) is slightly more elevated in Ti, Sc, Th, V, Nb, P and Zr. A vein hosted molybdenite sample that crosscuts a second phase mineralised porphyry at E37W has a Re-Os molybdenite age of 447.3 ± 2.7 Ma. The geochemical classification of this unit is more varied than other porphyries on the E37 Trend which is attributed to these intrusions containing varying amounts of volcanic xenoliths. Interestingly this doesn't explain why the northern porphyries at E37W while geochemically similar to the mineralised porphyry to the south of the prospect contain considerably lower grades. The mineralising porphyry at Veedas appears to be more closely associated with the Cu poor porphyries present in the northern proportion of E37W. Both the first and second phases of mineralised porphyry intrusion are steeply dipping towards the NNE. The mineralised intrusion intersected in E37D136 showing a steeply (76.5 degrees) NE (53.2 degrees) dipping body which is supported by the orientation of sulfide bearing quartz veining. The final two phases of monzonite porphyry along the E37 Trend are unmineralized. The first of these phases occurs at E37 and Veedas. The unmineralised porphyry at E37 crosscuts the two phases of mineralising monzonite porphyries which is visible in the magnetic response over the system. This un mineralised porphyry has a U-Pb (SHRIMP) zircon age of 436.7 ± 3.3 Ma (Lickfold 2002). These intrusions are characterised by coarse, square K-feldspar crystals amongst tabular euhedral-subhedral plagioclase with a fine-grained groundmass. Geochemically this unit is elevated in Sc, Th, and Nb, while depleted in V and Cr. This unmineralized porphyry has been modelled striking roughly E-W based off drill intercepts. The second phase of the unmineralized monzonite porphyries is interpreted to be only narrow intrusions that have been contaminated by the host rocks it has intruded and is best seen distally at E37. A monzodiorite intrusion is also present at E37 within the centre of the system but has only been intersected in a single hole. It is elevated in Sc, Ti, V, P, Zr and Nb while being depleted in Cr.

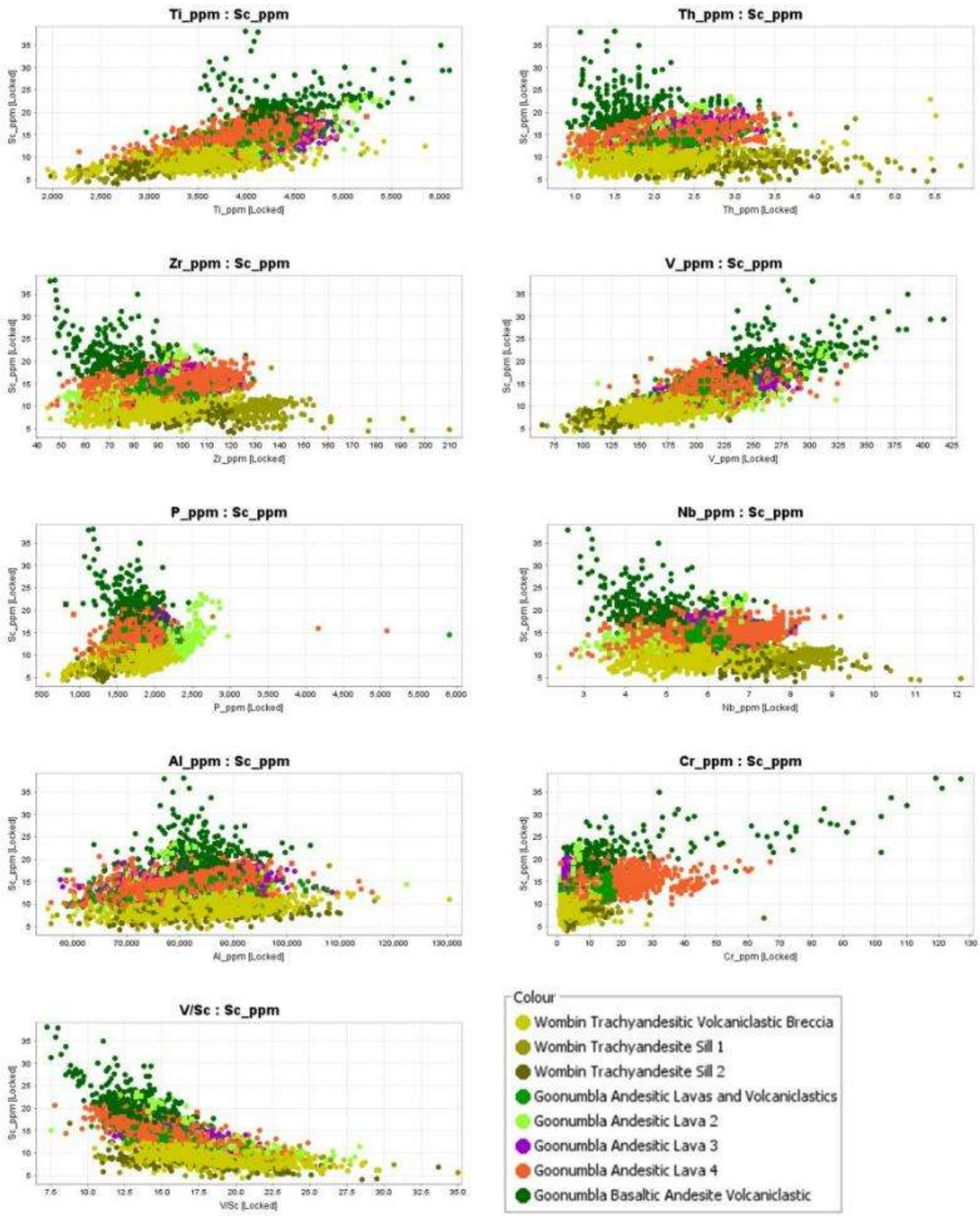

Figure 4: Lithogeochemical classification of the E37 Trend volcanic and volcaniclastic host sequences.

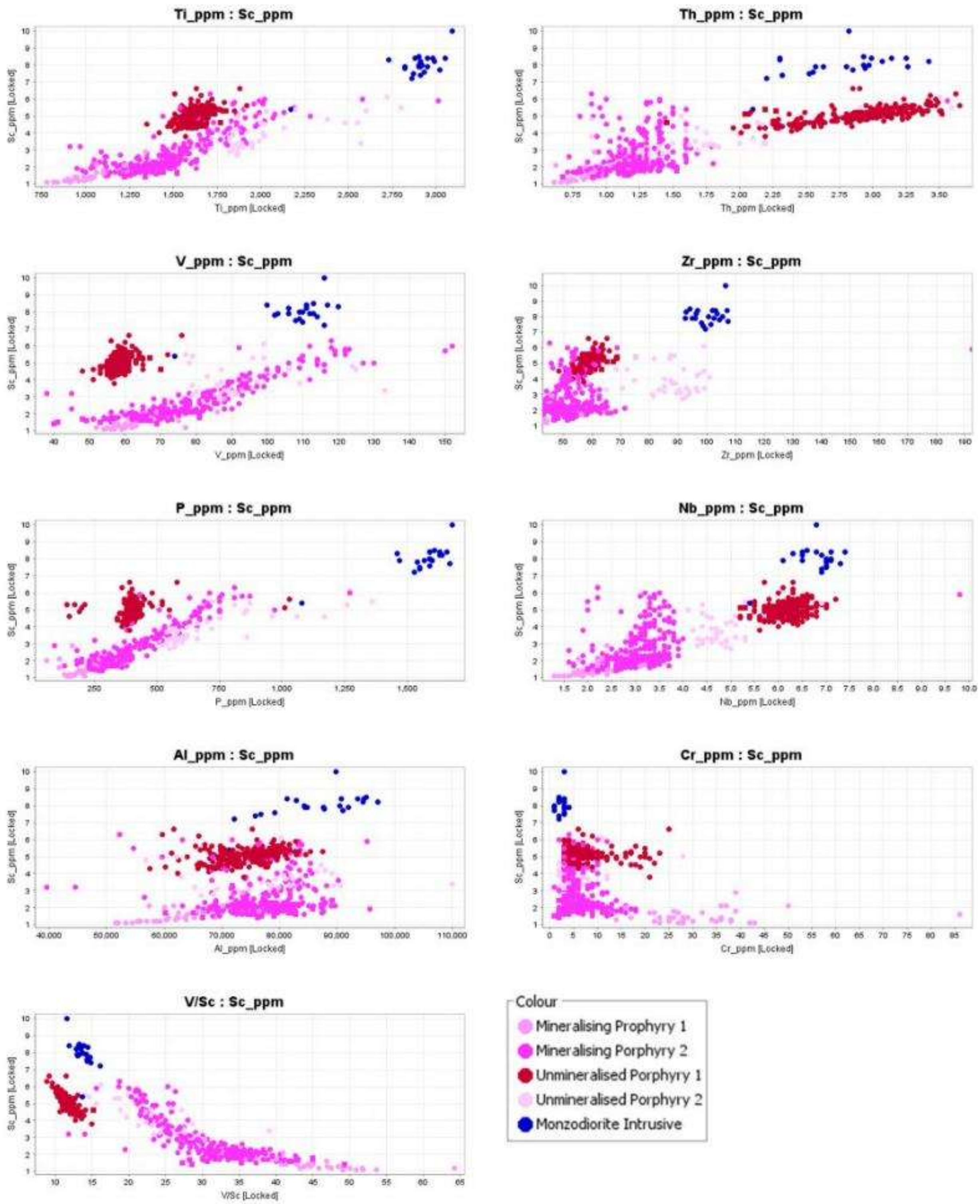

Figure 5: Lithogeochemical classification of intrusive units along the E37 Trend.

Figure 6: Mineralising monzonite porphyry intrusion from E37D136 from 360.4-366.75m

ALTERATION ZONATION THROUGH SPECTRAL RESPONSE

The spectral response of E37W is best seen in drillhole E37D136 which intersects a mineralising porphyry at depth (Fig. 7). Each sample that underwent assay analysis was sent for AiSIRIS analysis as part of the dispatch. E37D136's spectral response is dominated by white mica and chlorite in SWIR spectral contributions. White mica classification shows phengite and muscophengite is dominate, with muscovite seen directly adjacent to the intercepted porphyry intrusions (Fig. 7).

Chlorites spectral contribution is dominated Mg chlorite alongside phengite transitioning to Mg-Fe chlorite and epidote indicating the start of the propylitic halo (Fig. 8). A drop in magnetic susceptibility corresponds with this transition into the propylitic halo. Using magnetic susceptibility, epidote alteration and the transition to Mg-Fe chlorite it is estimated that propylitic alteration begins at 90-100m from the modelled location of the causative porphyry intrusion.

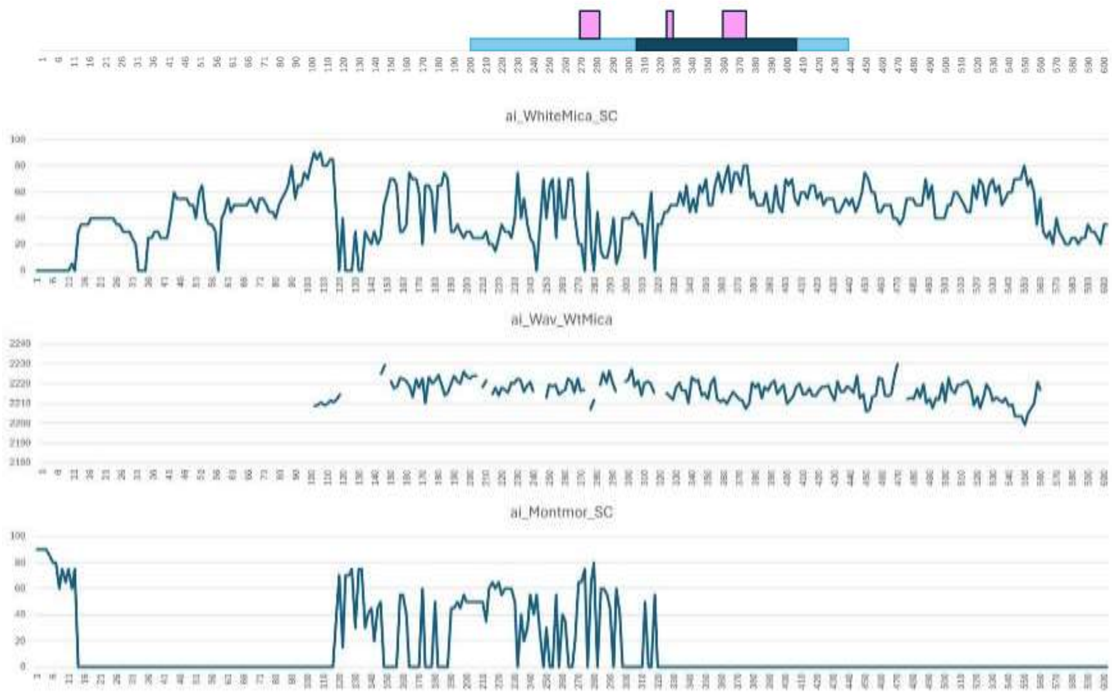

Figure 7: Downhole spectral response from drillhole E37D136 alongside A) white mica spectral contribution. B) white mica wavelength. C) montmorillonite spectral contribution. D) Porphyry intrusions (pink box), Cu grades >0.1% (blue box), and Cu grades >0.5% (navy box).

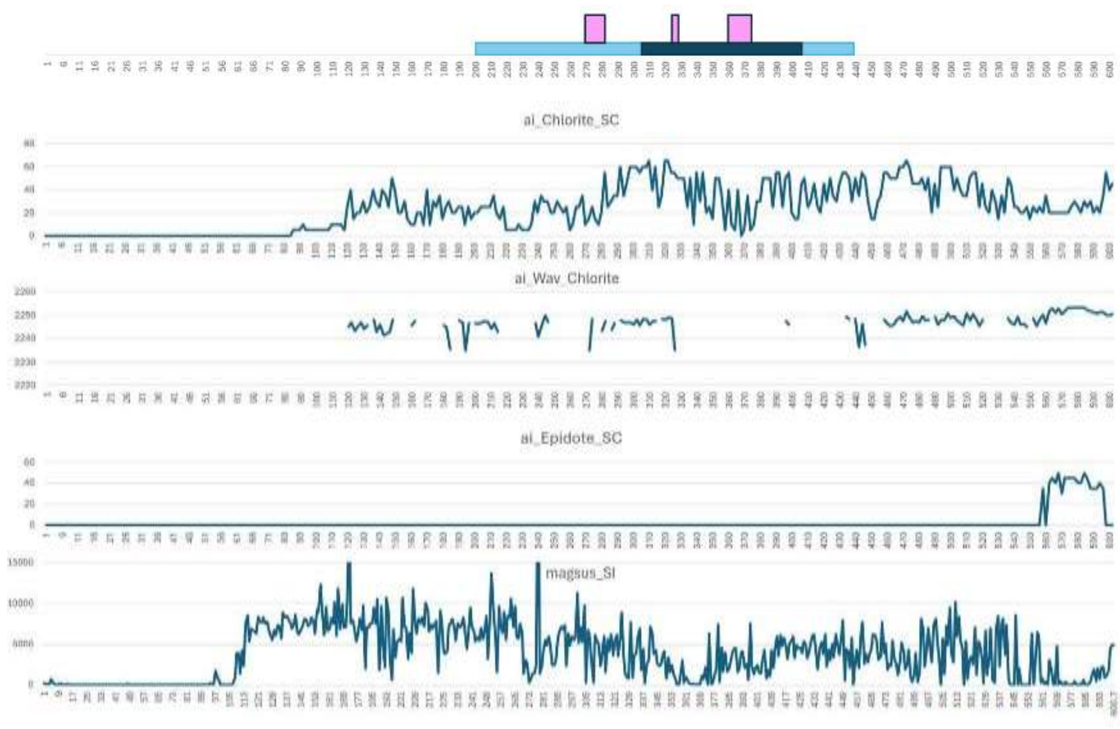

Figure 8: Downhole spectral response from drillhole E37D136. A) chlorite spectral contribution. B) chlorite wavelength. C) epidote spectral contribution. D) magnetic susceptibility. E) Porphyry intrusions (pink box), Cu grades >0.1% (blue box), and Cu grades >0.5% (black box).

The dominance of phengite/muscophengite and narrow zone of muscovite alteration alongside the rapid onset of propylitic alteration suggest that the porphyry at E37W was relatively cool (<350ºC) with a small hydrothermal cell. At E37W montmorillonite is present towards the top of the systems as a low temperature overprint that is distal from the mineralising porphyry intrusion. This overprinting montomorillonite is seen to correspond with an erratic magnetic susceptibility response away from the mineralising intrusion. A similar relationship is seen with chlorite spectral contributions which drop around the mineralising porphyry and are elevated but erratic around areas attributed to montmorillonite overprint. Feldspar stable alteration associated around the mineralising porphyry produces a subdued magnetite response with a higher response adjacent to the system which is associated with a muscovite response.

Figure 9: Epidote-chlorite-haematite propylitic altered peperitic andesite of the Goonumbla Volcanics intersected in E37D136 from 575.12-581.8m

MINERALISATION

E37D136 intercepted the mineralising porphyry in the southern proportion of E37W which includes an interval of >0.1% Cu exceeding 200m which has an average Cu:Au of 18.9:1, in contrast to E22 which has a Cu:Au ratio of 1.34:1. Mineralisation is zoned with a bornite>chalcopyrite potassic core becoming chalcopyrite>pyrite and pyrite>>chalcopyrite present in the propylitic halo.

Vein Stages

A clear zonation is present at E37W with porphyry intrusions with K-feldspar – quartz -bornite +/- chalcopyrite veins (Fig. 8) trending to quartz-chalcopyrite-bornite veining with an outer halo of carbonate+/-zeolite and epidote veins. Epidote veining is only present in areas dominated by propylitic alteration. D-veins composed of pyrite-chalcopyrite with sericite vein halos are seen sporadically throughout the hole. Trace carbonate-fluorite veining is present as you approach the propylitic halo. The orientation of veining and porphyry intrusions are closely aligned indicating that the intercepted porphyries are the causative intrusions of observed veining.

Figure 10: Intense quartz-bornite-chalcopyrite veining hosted in the Goonumbla Volcanics adjacent to the mineralising monzonite porphyry intrusion intersected in E37D136 from 353.8-360.4m.

Comparing the E37 Trend Alteration Assemblages to Northparkes Porphyry Deposits

While located within the same volcanic belt and rock package the porphyries of the E37 Trend differ from those seen on the mining leases. A clear example of this is their associated magnetic anomalies with the E37 Trend porphyry systems all associated with large magnetic highs, while the deposits on the mining lease are all associated with magnetic high donuts (Hoschke et al. 2022). This is attributed to the strength of phyllic overprint present at each of the mining lease deposits which isn't reflected on the E37 Trend as shown above with the prevalence of low temperature white mica alteration and montmorillonite overprint.

Comparing magma fertility between the E37W and E22 porphyry system shows similar zircon and apatite fertility indicators with both systems hosted predominately in the Goonumbla Volcanics (Buchanan 2025). The volume of porphyry magma and the depth of emplacement are two variables that may impact the scale alteration and mineralisation at the systems.

A final potential contributor could be the ages of the systems. The Re-Os molybdenite date at E37W that crosscuts the porphyry system shows this intrusion is older than the porphyry systems and emplacement of the monzonite stock on the mining leases (Lickfold 2002). This may highlight the importance of the monzonite stock as a heat source and provider of porosity that allows for the concentration of porphyry magmas at Northparkes. Allowing for the rise and concertation of porphyry magmas in a single location.

CONCLUSIONS

The Northparkes district has been actively explored since the late 1970's identifying multiple porphyry deposits with numerous regional porphyry systems. Each of these porphyry systems while broadly similar is unique in its host rock environment and magma characteristics, which leads to changes in vein assemblage, alteration strength and mineralisation. This characterisation of the E37 Trend highlights that these systems have a less intense white mica overprint compared to the porphyry systems on the NPO mining leases. Further work is needed to better understand how this relates to the evolution of the Northparkes district and to the economics of Northparkes porphyry deposits.

REFERENCES

BUCHANAN, C. M. (2025). Evaluating magma fertility and controls on metal tenor: The E37W prospect - Northparkes District. Bachelor of Science (Honours). Brisbance, QLD: The University of Queensland.

HALLEY, S. (2026, July 9). Geochemistry at a Regional Scale. Retrieved from Mineral Mapping: https://www.scotthalley.com.au/geochemistry-information

HOSCHKE, T., HARRIS, A., & HOYE, J. (2022). Geophysical response of alteration and mineralisation at the Cadia and Northparkes porphyry districts, NSW, Australia. Discoveries in the Tasmanides 2022 (pp. 195-202). Orange: Australian Insitute of Geoscientists.

JONES, G. J. (1985). The Goonumbla porphyry copper deposits, New South Wales. Economic Geology, 591-613.

LICKFOLD, V. (2002). Intrusive history and volatile evolution of the Endeavor porphyry Cu-Au deposits, Goonumbla district, NSW, Australia. Doctoral Dissertation. University of Tasmania.

LYE, A., CROOK, G., & KOLFF VAN OOSTERWIJK, L. (2006). The discovery history of the Northparkes deposits. Mines & Wines 2006 (pp. 1-5). Cessnock: Mines and Wines Conference.

SIMPSON, C. J., CAS, R. A., & ARUNDELL, M. C. (2005). Volcanic evolution of a long-lived Ordovician island-arc province in the Parkes region of the Lachlan Fold Belt, southeastern Australia. Australian Journal of Earth Sciences, 863-886.

THE ACHILLES AG-AU-ZN-PB DISCOVERY IN THE SOUTHERN COBAR BASIN

Martin Scott

Australian Gold and Copper (AGC), 14 Edward St Orange, 2800

Key Words: Cobar Basin, Cobar-type orogenic mineral system, Achilles Ag Au Zn Pb deposit, mineral systems approach

INTRODUCTION

The discovery of the Achilles Ag Au Zn Pb deposit in early 2024 is an example of exploration persistence in an area explored sporadically during the last 50 years. AGC drilled the Achilles deposit for most of the previous two and a half years and announced a maiden mineral resource in December 2025. The deposit stratigraphy, mineralisation, structure, alteration are briefly described, as well as discussion of exploration using a mineral systems approach.

ACHILLES GEOLOGY AND MINERALISATION

The Achilles deposit is located 25km NW of the town of Lake Cargelligo in the southern Cobar Basin (Figure 1). The Achilles deposit is hosted by Early Devonian Ural Volcanics and mafic dolerite along the eastern margin of the Kilparney Shear Zone and is mostly concealed beneath Quaternary soil and transported regolith (Figure 1, Colquhoun et al 2005).

The Ural Volcanics form a moderately east-dipping and younging volcanic sequence of pumice breccia, thin bedded shard and pumice facies, siltstone, volcaniclastic sandstone and siltstone, and dacite sills (Figures 2 and 3, Simpson 2026). These volcanic units are intruded by fine-moderate grained dolerite sills and dykes, with multiple intrusive pulses recognised from changes in grainsize and overprinting chilled margins. The dolerite intrusives are also deformed (foliated, folded, sheared) and mineralised, helping constrain the timing of mineralisation.

Higher-grade mineralisation is focussed in the thinly bedded shard and pumice facies and the Achilles Fault Zone, with lower grade mineralisation plus pathfinder elements continuing into the immediately adjacent enveloping units. Sulphides are disseminated, massive, banded, and form blebs, patches, veins, and are within veins and along the foliation (Figure 4). There is also early laminated framboidal pyrite with associated coarse sphalerite (Fitzherbert and Downes 2026). Mineralisation is interpreted to be pre-, syn- and post deformation with sulphides cut by the foliation, smeared by the foliation, cutting across the foliation and redistributed after deformation (Fitzherbert and Downes 2026).

Ag-Au-Pb-Zn mineralisation is as freibergite, tennantite-tetrahedrite, dycrasite?, gold, sphalerite, secondary smithsonite? and galena. Additionally, there is chalcopyrite, secondary bornite, chalcocite, covellite and digenite?, plus stibnite, pyrite, arsenian pyrite, arsenopyrite and pyrrhotite (petrography by Simpson 2026, Fitzherbert and Downes 2026, plus Hylogger, MicroXRF and QEMSCAN data).

Early syn-eruptive or early diagenetic silica-albite alteration indurates most of the felsic volcanic sequence and is followed by sericite-silica-pyrite-chlorite alteration with mineralisation and deformation that is most intense in the thinly bedded shard and pumice facies, plus late carbonate, secondary mineralisation, and hematite/limonite alteration along fractures (Simpson 2026, Fitzherbert and Downes 2026). Dolerite is altered by albite-chlorite-actinolite ± carbonate-titanite-epidote (Simpson 2026).

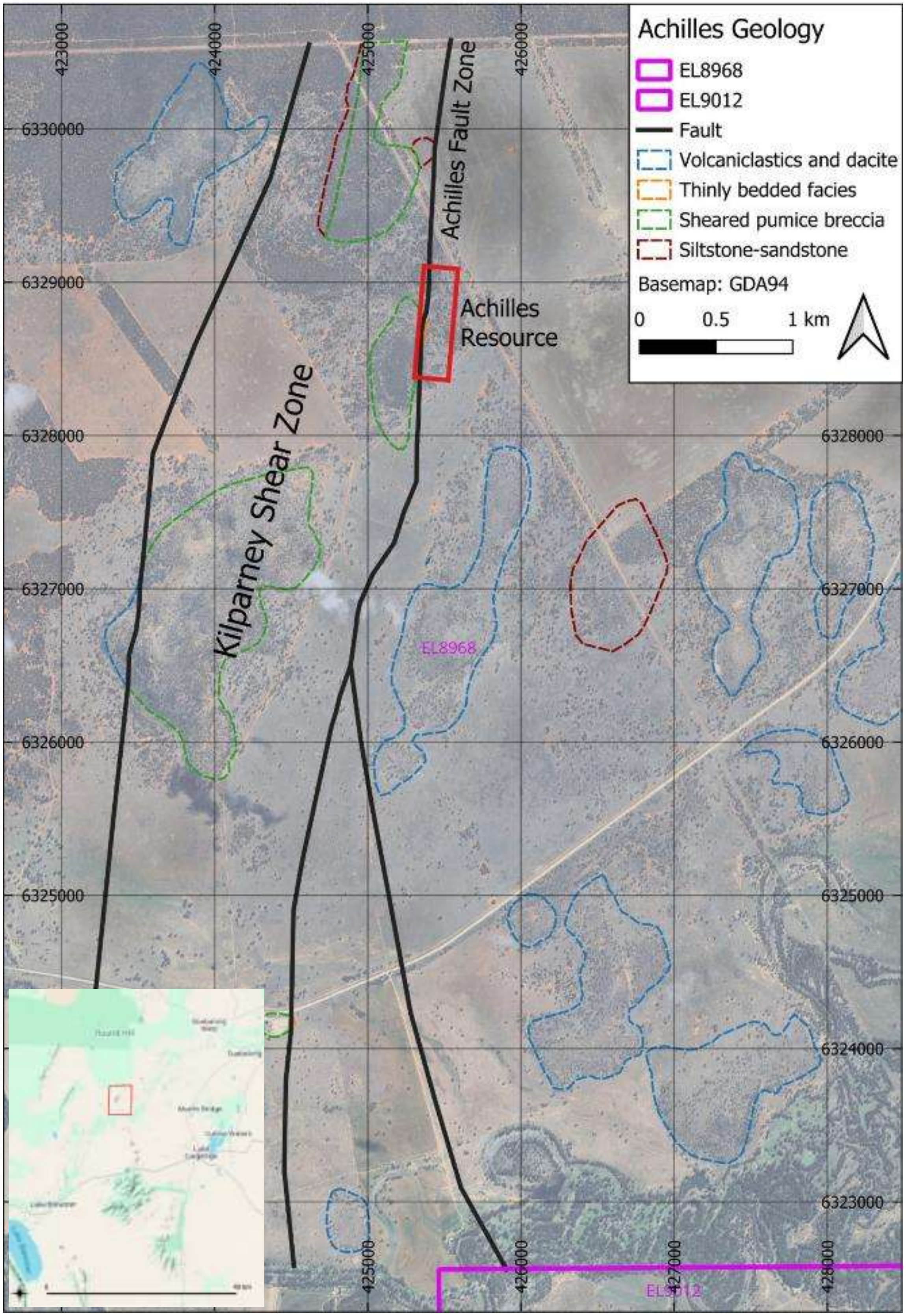

Figure 1 Outcrop geology of Achilles area showing polygons of outcrop and residual regolith. Surrounding areas are covered by Quaternary transported regolith.

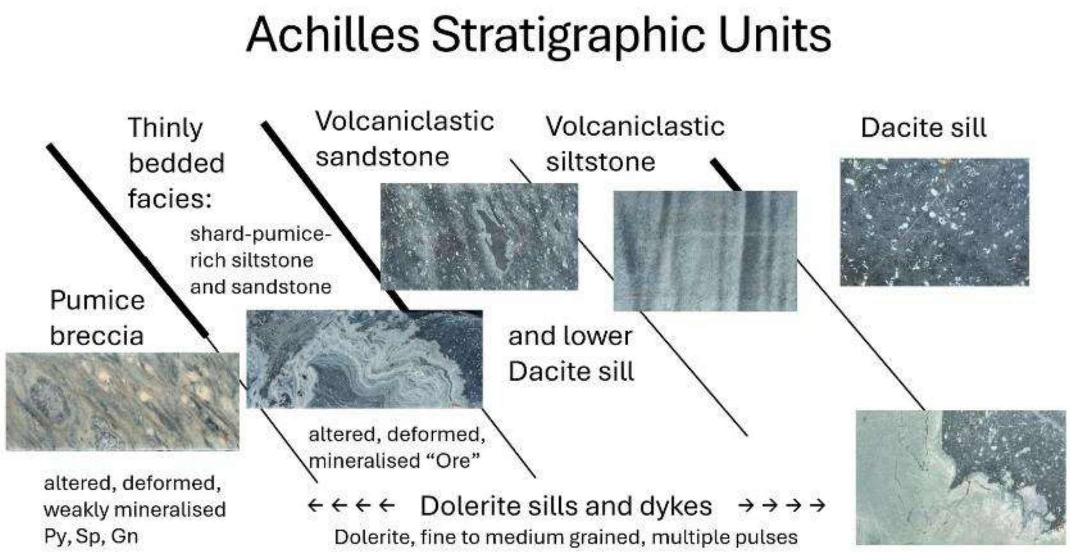

Figure 2 Schematic cross section of the Achilles deposit with stratigraphy, faults (bold black lines) and photographs of units (Simpson 2025)

The Achilles deposit has consistent structure, with moderate to steep ESE-dipping bedding and flow banding, foliation, veins with sulphides, dolerite sills and faults (Figure 5). The lower units of pumice breccia and thinly bedded facies are strongly deformed by the Kilparney Shear Zone and the Achilles Fault Zone, with S-C fabrics, crenulation cleavage, mantled pumice clasts, mineral lineations, tight-isoclinal mesofolding, and faulting. Slickenlines and steps on foliation, veins and dolerite contacts indicate multiple fault movements, and late east over west reverse displacement.

Based on the structural analysis, mineralisation and alteration at the Achilles, the deposit is interpreted as being controlled by east over west reverse movement on the Achilles Fault Zone at the margin of the major kilometre-wide Kilparney Shear Zone. Geological mapping reveals that the Achilles Fault Zone is the localised eastern dilatant margin of a significant 1-2km wide silica-sericite-pyrite-chlorite altered Kilparney Shear Zone. The timing of deformation and mineralisation is consistent with during the Mid-Devonian Tabberabberan Orogeny (Fitzherbert and Downes 2026). The structurally controlled Achilles polymetallic deposit is consistent with it being a Cobar-type orogenic mineral system (Skirrow et al 2013).

In December 2025 AGC announced an initial Indicated (58%) and Inferred (42%) Mineral Resource of 10.3Mt at 116g/t AgEq (51g/t Ag, 0.37g/t Au, 0.7% Zn, 0.5% Pb) from 68 drillholes (Figure 6). The resource is approximately 900m long and extends 300m down dip. Drilling in 2026 extended the mineralisation, stratigraphic units and the Achilles Fault Zone 550m down dip to a depth of ~400m from the surface (Figures 6 and 7).

DISCUSSION

The discovery of the Achilles deposit is another example of exploration persistence and is reviewed herein using a mineral system approach. Previous explorers of the Achilles area (Figure 1) found anomalous geochemistry in surface sampling and shallow drilling (to 106m depth) in the Kilparney Shear Zone (in the footwall pumice breccia): Shell (EL0921) 1977-78, Santa Fe (EL5082) 1998, Western Plains Gold (EL6367) 2006-2007, and Thomson Resources / Platsearch (EL7746) 2012. They found the major fault conduit with lower grade mineralisation, but didn't find a significant trap.

AGC started exploring at Achilles in 2020, following up on the anomalous geochemistry of previous explorers. Over 4 years prior to the discovery to early 2024, AGC explored the Achilles area by geological mapping, soil and rockchip sampling, drilling auger, aircore, reverse circulation (RC) and 1 diamond hole, airborne magnetic and radiometric survey, induced polarisation (IP) survey, petrology, geophysical processing and modelling. Their persistence paid off, and by exploring along strike and east of previous sampling, they tested a subtle IP anomaly and anomalous surface geochemistry with success in early 2024.

AGC drilled into the Achilles deposit and found an excellent conduit and trap along the eastern margin of the Kilparney Shear Zone. The combination of the Achilles Fault Zone along the easily deformed thinly bedded facies, the moderate dip of the fault zone, and the indurated, previously silica-albite altered hangingwall and footwall volcanic units provided geochemical and geotechnical traps to mineralising fluids. The low erosion rates and a depositional regime in the western Lachlan Orogen beside the Murray Basin have led to the mineralisation to be preserved below a shallow veneer of transported regolith cover.

The discovery of Achilles also highlights the challenge of exploring in areas of extensive transported regolith cover, and in using geophysics to locate narrow Ag-Au-Zn-Pb mineralisation in basinal sedimentary-felsic volcanic stratigraphy. The basinal stratigraophy and the mineralisation have similar low magnetic response, similar densities, and the sulphides lack an EM response. IP was useful for the exploration of Achilles, as there is disseminated pyrite within and around the mineralised zone and in the weakly mineralised pumice breccia footwall within the Kilparney Shear Zone. However, magnetics and gravity are useful for locating the Early Devonian dolerites that have higher magnetic susceptibilities and densities than the mineralised zones and the felsic volcanics.

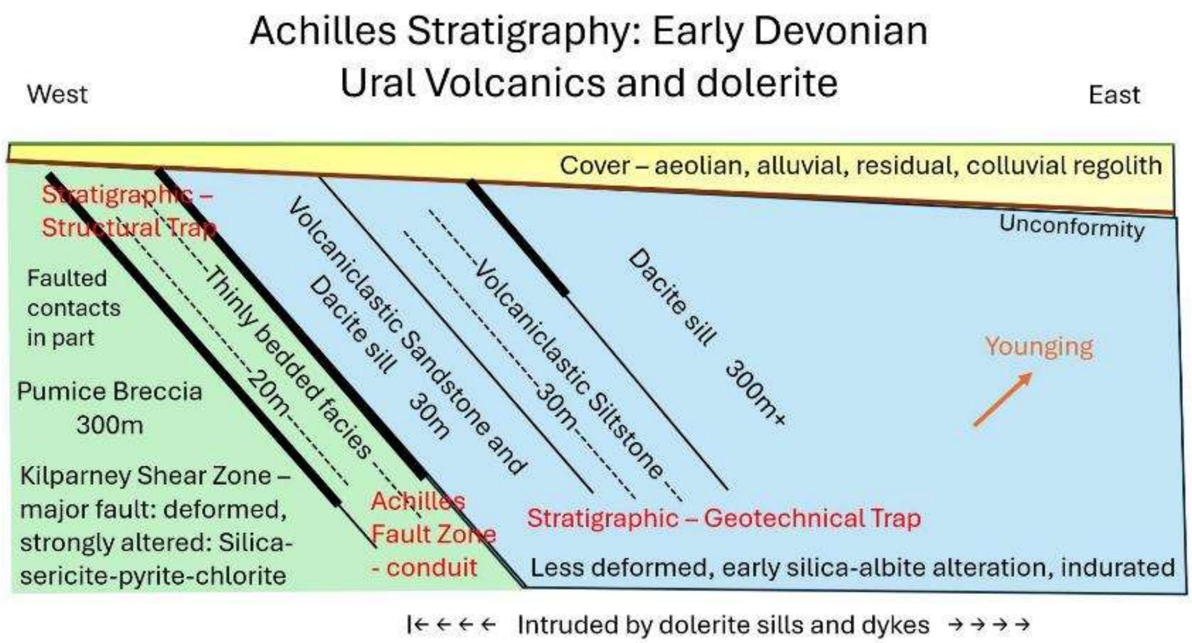

Figure 3 Schematic cross section of the Achilles deposit with unit average thicknesses, alteration, fault and shear zones and the interpreted mineralising conduit and traps.

Figure 4 A3DD004 core with the Achilles Fault Zone, massive sulphides and intercept of 9.1m from 126.5m at 3.0g/t Au, 698g/t Ag, 19.4% Pb+Zn and 1.2% Cu, and altered pumice breccia in the footwall. AGC ASX announcement 13/11/2024

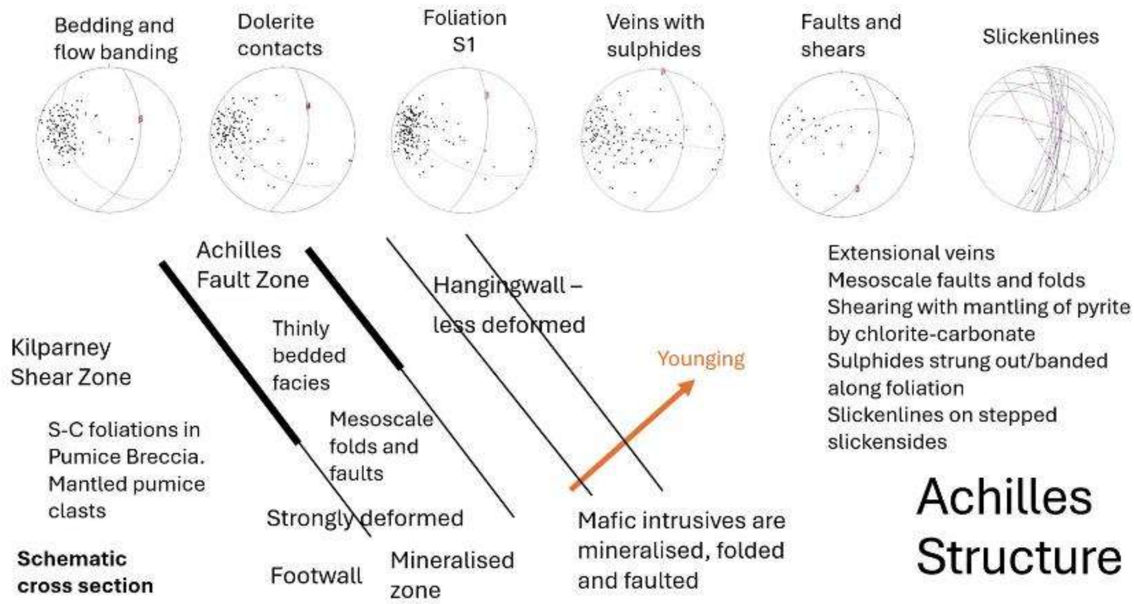

Figure 5 Structure of Achilles with moderate to steep ESE-dipping bedding and flow banding, foliation, veins with sulphides, dolerite sills and faults. Slickenlines on steps indicate a late east over west reverse fault displacement. Equal area strereographic projections using Georient (Holcombe 2023).

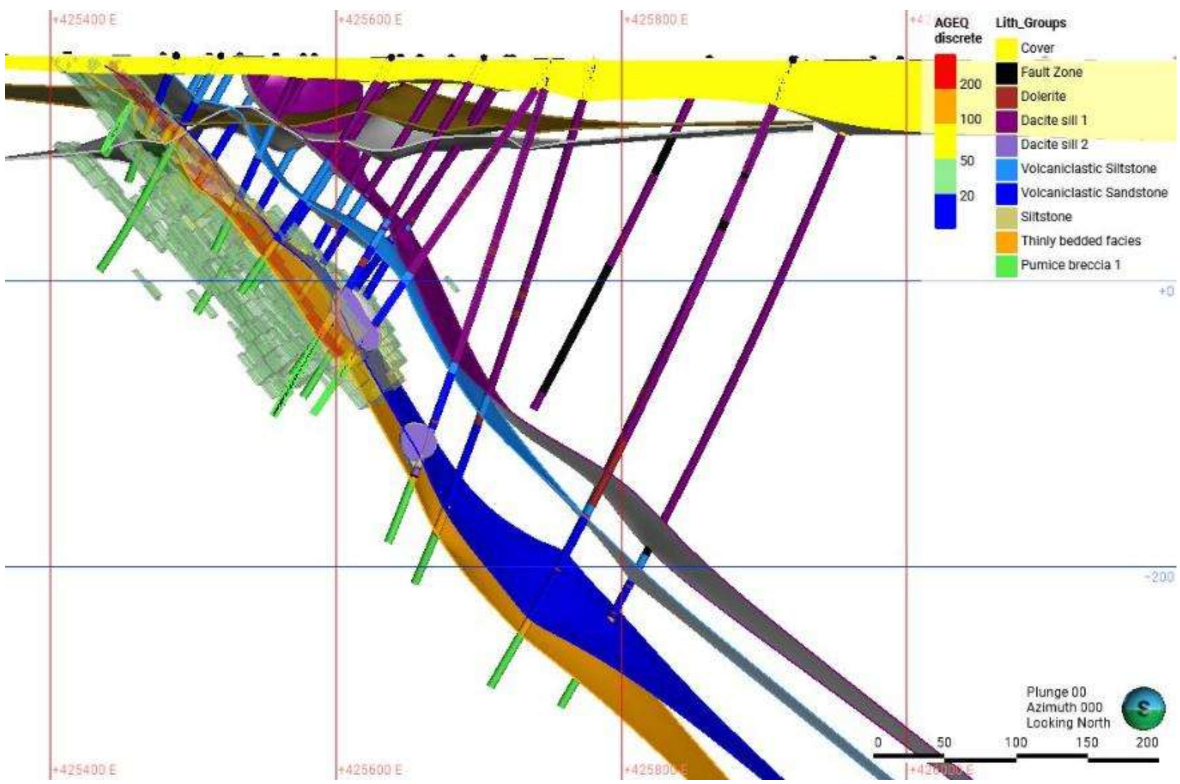

Figure 6 Cross section of Achilles deposit geological units at MGA94N 6329100 with current drilling, the 2025 resource blocks in Ag equivalent g/t, the base of complete oxidation (BOCO) and the base of weathering (BOW).

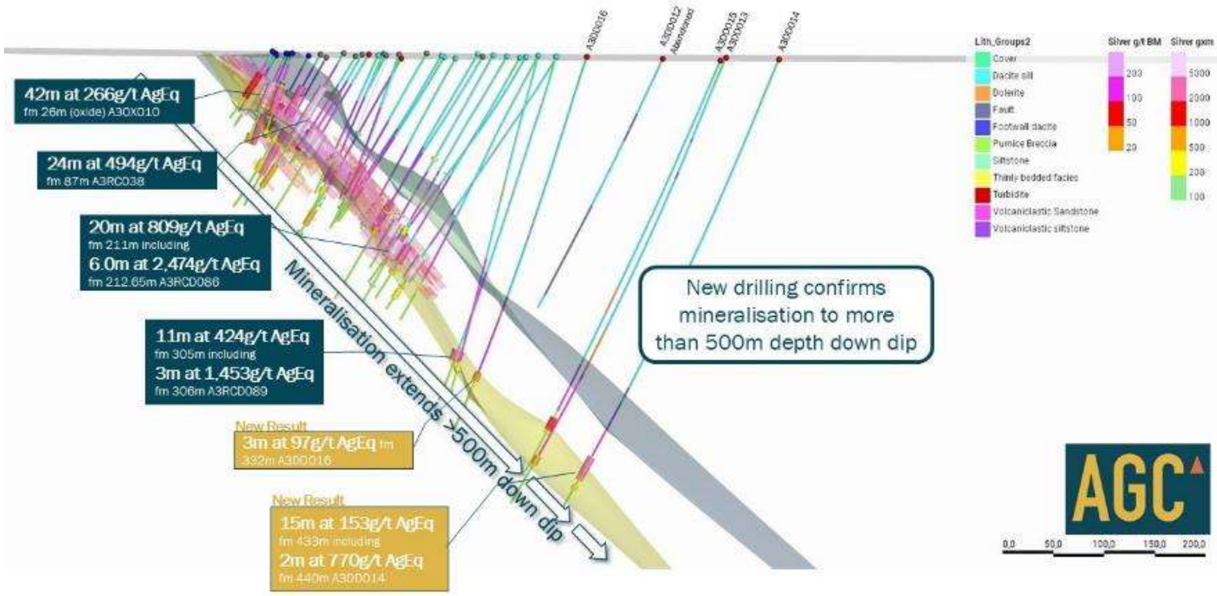

Figure 7 Achilles cross section looking north at 6329070N showing mineralisation continuing from surface down dip, including recent intercepts from A3DD014 and A3DD016. AGC ASX announcement 15/07/2026

ACKNOWLEDGEMENTS

With thanks to the team at AGC, and Carol Simpson (petrography and volcanics), Mark Arundell (IMEx, geochemistry) and Joel Fitzherbert (GSNSW, isotopes, petrography, mica crystallinity) for their observations.

REFERENCES

COLQUHOUN G.P., MEAKIN N.S. & CAMERON R.G. (compilers) 2005. Cargelligo 1:250 000 Geological Sheet SI/556, 3rd edition, Explanatory Notes. Geological Survey of New South Wales, Maitland, NSW, 291 pp.

FITZHERBERT J. A. & DOWNES P. M. 2026. Petrographic, isotopic character & thermal indexing of mineralisation from Achilles prospect, Rast Trough, Cobar Superbasin, NSW. Draft, Department of Primary Industries & Regional Development, 65pp.

HOLCOMBE R. 2023. GEOrient v10. www.holcombe.net.au/software/

SKIRROW R.G., HUSTON D.L., MERNAGH T.P., THORNE J.P., DULFER H., & SENIOR A.B. 2013. Critical commodities for a high-tech world: Australia's potential to supply global demand. Geoscience Australia, Canberra, 118pp.

SIMPSON C. 2025. Key features & photo atlas of Achilles 3 facies. Report for Australian Gold & Copper, 31pp.

SIMPSON C. 2026. Achilles 3 geological framework, alteration, structure & mineralisation report 2026. Report for Australian Gold & Copper, 41pp.

PORPHYRY COPPER IN THE TASMANIDES: A FAILED MARGIN OR A MARGIN OF OPPORTUNITY?

Stuart Smith[1] and Gideon Rosenbaum[2]

[1]Inflection Resources Ltd

[2]School of the Environment, The University of Queensland

Key Words: porphyry copper, exploration strategy, Tasmanides.

INTRODUCTION

Subduction-related convergent continental margins are the loci of many of the world's major porphyry copper provinces, including the Andean Cordillera, the world's premier porphyry copper province. In eastern Australia, a series of subduction-related orogens, collectively referred to as the Tasmanides, developed on the Gondwanan convergent margin over a period of more than 300 million years from the Cambrian to the Triassic (Glen, 2005; Glen, 2013; Rosenbaum, 2018).

Exploration for copper deposits in the Tasmanides and elsewhere in Australia has been active since the mid 1800's. Since these early efforts Australia-wide copper prospecting and exploration has been highly successful with Australia ranking 2nd in the world for contained copper resources (11% of global resources) and 8th for production (4% of global production). Despite this, porphyry deposits in the Tasmanides account for only 14% of Australian copper production and 4% of Australian copper resources.

In this contribution we seek to determine if this apparent lack of porphyry copper endowment is fundamental to the geology of the Tasmanides or can be attributed to other factors.

PORPHYRY COPPER SYSTEMS vs DEPOSITS

It is well documented that only a small proportion of exploration programs generate real value, with the vast majority of wealth generated by few large-scale deposits (e.g., Schodde and Hronsky, 2005; Schodde, 2023). In this context, we use the general term "*porphyry system*" for any occurrence, regardless of size or significance, that displays the recognised characteristics of porphyry mineral systems (e.g., stockwork or sheeted quartz-sulphide veins, association with porphyritic igneous rocks, zoned alteration typically with potassic, phyllic, and/or advanced argillic facies present). In contrast, we use the terms "*major porphyry deposit*" for those systems that are economic (or potentially economic); these deposits typically correspond to the "very large" category of Clark (1993) with >1 Mt contained copper.

PORPHYRY COPPER DEPOSITS - FAVOURABLE TECTONIC SETTINGS

Porphyry copper deposits typically develop at convergent plate margins where subduction of oceanic lithosphere generates oxidised, hydrous I-type magmas (e.g., John et al., 2010). However, these magmatic characteristics are typical of arc-magmas generally (e.g., Maury and Pallares, 2024), most of which are not responsible for formation of significant porphyry copper systems. The distinct spatial and temporal clustering of *major porphyry deposits* within broadly favourable magmatic arcs of enormous extent (1000's kilometres of strike length) and extended time frames (10's to 100's million years) indicates that *major porphyry deposits* are the product of exceptional geological processes in particular localised regions at specific periods during the evolution of much larger arcs (e.g., Farrar et al., 2023; Ward et al., 2024).

In continental convergent margins, major porphyry deposits are associated with, or immediately subsequent to, periods of contractional deformation accompanied by significant crustal thickening (e.g., Mpodozis and Cornejo, 2012; Farrar et al., 2023; Favorito and Seedorff, 2024). Such periods of crustal thickening have been documented to be associated with periods of accelerated plate convergence, flat-slab subduction, and/or the subduction of anomalously thick oceanic crust (e.g., Mpodozis and Cornejo, 2012; Rosenbaum et al., 2005). In island arc tectonic settings, the formation of porphyry deposits does not seem be associated with crustal thickening. Critical factors in such settings are linked to plate reorganisations, subduction of buoyant oceanic elements, and slab segmentation due to slab tearing (Garwin et al., 2005; Ward et al., 2024).

We consider that *porphyry systems* are developed as a natural consequence of the typical oxidised I-type magmas of magmatic arcs. However, the generation of *major porphyry deposits* requires particular circumstances that are only developed within certain arcs, and furthermore, only within certain restricted times and regions of such arcs.

TASMANIDES - TECTONIC EVOLUTION

The Tasmanides has commonly been referred to as an accretionary orogen (eg Coney, 1992; Cawood and Buchanan, 2007). However, there is relatively little evidence of accreted terranes in the Tasmanides (e.g., Glen et al., 2016). Tectonic models for the evolution of the Tasmanides typically consider switches from trench advance to trench retreat, which resulted in repeated episodes of reactivation and recycling of the continental margin (Collins, 2002a, b). Such models are consistent with the spatial and temporal distribution of tectonic elements (e.g., fold-thrust belts, magmatic belts, and sedimentary basins), which indicate short periods of contraction within longer periods of crustal extension (Collins, 2002a, b; Rosenbaum, 2018). Due to the repeated phases of crustal extension, the crust in the Tasmanides has remained relatively thin, with limited opportunities for the development of thicker (>40 km) crust that can be sustained over extended time periods.

Within the overall continental margin setting of the Tasmanides, the Macquarie Arc represents an unusual setting. This arc is considered to represent an intraoceanic arc that developed outboard of the continental margin (Crawford et al. 2007, Glen et al. 2007).

ANDEAN CORDILLERA – PORPHYRY and TECTONIC EVOLUTION

Subduction processes and related tectono-magmatic activity have affected the western margin of South America since the late Neoproterozoic. The earlier history of subduction, from ~570 Ma to ~240 Ma, involved accretion of exotic terranes and several periods of subduction-related magmatism (Mpodozis and Cornejo, 2012), but porphyry systems associated with these early arcs all are minor (Sillitoe and Perello, 2024).

Following the breakup of Pangea, from the Middle Triassic to Early Jurassic, subduction processes along the Andean margin recommenced. This subduction has continued uninterrupted until the present day (Mpodozis and Cornejo, 2012). Early Andean (Jurassic to Late Cretaceous) subduction occurred under extensional or transtensional conditions and resulted in accumulation of thick volcano-sedimentary basins. Isolated and generally minor porphyry deposits are associated with the Triassic and Cretaceous arcs (Sillitoe and Perello, 2005). Acceleration of westward plate motion, associated with the final stages of Atlantic opening, produced strongly contractional conditions during the Late Cretaceous and early Cenozoic; this broadly compressional settings have dominated until the present day (Mpodozis and Cornejo, 2012). Importantly, the broadly compressional conditions were punctuated by periods of extreme compression and crustal thickening linked to subduction of buoyant oceanic elements and/or flattening of the slab dip angle (e.g., Kay and Coira, 2009; Mpodozis and Cornejo, 2012; Carlotto et al., 2023). Major porphyry deposits were generated during three major periods, which were synchronous with or postdated the major compressional events (e.g., Sillitoe and Perello, 2005): (1) early Palaeocene; (2) mid Eocene to early Oligocene; and (3) Miocene to early Pliocene. The USGS database compilation of porphyry occurrences in the

Andes (USGS, 2022) documents 194 occurrences within an approximate 2 million km^2 area, equating to approximately 0.1 occurrences per 1000 km^2.

PORPHYRY SYSTEMS OF THE TASMANIDES

Porphyry systems are widely distributed in time and space throughout the magmatic provinces of the Tasmanides. A comprehensive compilation of Tasmanide-wide porphyry occurrences was presented by Bookstrom et al. (2014), who recognised nine porphyry-permissive tracts and sub-tracts, which could be considered metallogenic belts within the broader tectonic province of the Tasmanides. We have used the database of Bookstrom et al. (2014) as a base and have edited it with more recent knowledge, additional references, and our own experience (where applicable). The original database of Bookstrom et al. (2014) contains 232 deposits, out of which 198 are porphyry Cu or Mo occurrences, and 34 are "porphyry related" occurrences. Our edited database contains 152 *porphyry systems* (Cu, Mo, Au or combinations thereof) and an additional 18 "porphyry related" occurrences (skarns, high sulphidation epithermal). To compare occurrence density (see previous section for the Andes), we used the 232 deposits from Bookstrom et al. (2014). These porphyry and porphyry-related systems occur within permissive magmatic tracts with an area of approximately 500,000 km^2, thus corresponding to an average occurrence density of 0.45 per 1000 km^2.

The oldest known Tasmanide *porphyry systems* are associated with the Cambrian and Early Ordovician (~500–480 Ma) Delamerian Orogen; they occur in South Australia, Victoria and New South Wales (Bookstrom et al., 2014; Schofield, 2018; Hong et al., 2023). A total of 10 *porphyry systems* are recognised, with the most significant of these to-date being the Thursdays Gossan system of western Victoria with a mineral resource of 59 Mt at 0.43% Cu, 0.08 g/t Au, and 2.7 g/t Ag (Angus et al., 2026). Mineralisation includes supergene chalcocite developed above low-grade porphyry-style veins hosted by a multi-phase intrusive complex and nearby magma-style veins and massive sulphide replacement systems (Angus et al., 2026). Several low-grade Cu-Mo *porphyry systems* are recorded in the Delamerian Orogen in South Australia and New South Wales, with the best drill result reported from the Netley Hill prospect (350 m @ 0.1% Cu, 0.015% Mo, and 1g/t Ag; Clifford, 2008 *in* Hong et al., 2023). Mineralisation is associated with diorite, granodiorite and monzonitic intrusions cut by multi-phase porphyry-style veining and associated potassic and phyllic alteration (Hong et al., 2023). Host intrusion ages range from 485 to 465 Ma and Re-Os molybdenite records mineralisation events at 480 and 470–460 Ma (Hong et al., 2023). Mineralisation is interpreted to have formed following a phase of subduction-related magmatism, at 514–490 Ma, in an inverted back-arc setting (Hong et al., 2023).

The Macquarie Arc porphyry and porphyry-related systems — the most significant porphyry belt in the Tasmanides — have been widely documented. Our dataset includes a total of 49 *porphyry systems* and porphyry-related systems in the Macquarie Arc. These include Cadia and Northparkes, which are Australia's only currently economic porphyry deposits, hosting combined total resources and past production in excess of 55 Moz Au and 14 Mt Cu (Kincora Copper https://kincoracopper.com/; NSW Geological Survey https://www.resources.nsw.gov.au/sites/default/files/2022-11/copper.pdf). The Boda and Kaiser porphyry deposits contain an additional 8.3 Moz Au and 1.5 Mt Cu (Alkane Resources https://alkres.com/projects/northern-molong-porphyry-project/). Other significant districts that host currently sub-economic *porphyry systems* include Copper Hill, Temora, Narromine, and Bushranger, as well as recently drilled systems in the extreme north, deeply covered, section of the belt, up to 200 km north of Northparkes (e.g., Inflection Resources https://inflectionresources.com/inflection-resources-intercepts-porphyry-style-alteration-at-the-duck-creek-target/; https://inflectionresources.com/inflection-resources-intercepts-porphyry-gold-copper-mineralisation-in-new-south-wales/).

Other districts hosting *porphyry systems* and potentially related vein or skarn systems include Cowal and Cargo; both districts contain low-grade porphyry-style Cu-Au and significant epithermal Au style vein systems (Waratah Minerals https://waratahminerals.com/spur-project/). Skarn-style systems also occur in the Cadia, Northparkes and Trundle districts (Kincora Copper https://kincoracopper.com/the-trundle-project/). In addition to the porphyry and skarn-style systems, significant high-sulphidation epithermal deposits (e.g., Gidginbung, Temora district and Peak Hill, Parkes district) occur within the Macquarie Arc and are considered broadly porphyry related. Porphyry Cu and Au endowment in the Macquarie Arc is dominated by alkalic porphyry-style mineralisation, which was emplaced during a brief period at ~440–435 Ma (within the overall ~40 m.y. arc evolution). This phase of porphyry-style mineralisation was accompanied by small volume post-collisional intrusions. This short fertile period was coincident with a major plate reorganisation event associated with the collision of the postulated VanDieland microcontinent (Cayley, 2011).

Younger rocks in the Lachlan Orogen (post-early Silurian) contain *porphyry systems* within late-Silurian to early-Devonian I-type suites. This belt, termed “Yeoval tract” by Bookstrom et al. (2014), essentially coincides with the oxidised early Devonian I-type Boggy Plains Supersuite (Wyborn et al., 1987). The belt contains 9 Cu-Mo *porphyry systems* (Bookstrom et al., 2014; this study), including the Yeoval complex of Central West NSW. Principal occurrences, such as Goodrich and Cyclops, contain a published resource of 12.8 Mt at 0.38% Cu, 0.14 g/t Au, 2.2 g/t Ag, and 120 ppm Mo; more recent drill intersections of 18 m include 0.52% Cu and 18m@ 0.41% Cu (Godolphin Resources https://godolphinresources.com.au/yeoval; Bookstrom et al., 2014). Other porphyry-style occurrences have been reported in Victoria, where some systems are associated with felsic intrusions and are Mo-dominated; significant intersections include 29 m @ 0.11% Mo, 89 m @ 0.13% Cu; 46 m @ 0.09% Mo and 86 m @ 0.2% Cu (e.g., Mt Unicorn; Hochwimmer, 2012). The late Silurian to early Devonian Lachlan Orogen magmatic suites and associated porphyry systems are interpreted to have developed in extensional back-arc settings (Bookstrom et al., 2014; Hochwimmer, 2012), potentially from remelting of underplated Macquarie Arc (Wyborn et al., 1987). It is notable that despite voluminous potentially permissive I-type magmatism, no porphyry Cu occurrences are noted in the Lachlan Orogen outside the Macquarie Arc or the “Yeoval tract”.

The dataset of Bookstrom et al. (2014) also includes an “East Tasmanide” tract comprising igneous rocks of the New England, Thompson and Mossman Orogens. This has been sub-divided into northern, central and southern sub-tracts. The northern sub-tract (wholly within the Mossman Orogen) does not contain known porphyry systems. The southern sub-tract (occupying the region of the southern New England Orogen) contains only two occurrences (Bookstrom et al., 2014). The central sub-tract (northern New England Orogen and northern Thompson Orogen) contains 75 *porphyry systems* and an additional 15 potential porphyry-related systems (e.g., skarns, high-sulphidation epithermal, Au-Ag veins, and breccia) (Bookstrom et al., 2014, and this study). The oldest porphyry occurrences, Early Ordovician in age, are within the Greenvale Province; they include the rare, possible *porphyry systems,* of Bottletree and Cockie Creek. These prospects are possibly associated with 486–477 Ma intrusions related to the nearby Lynwater Complex (Fergusson et al., 2007; Corbett, 2023; Superior Resources https://www.superiorresources.com.au/projects/). Mineralisation is reported to be associated with deformed quartz-chalcopyrite porphyry-style A and D veins within potassic (biotite), phyllic, and propylitic altered meta-andesites and pelitic sedimentary rocks, intruded by polyphase diorite to dacite dykes (Corbett, 2023). Reported drill intercepts include 632m @ 0.21% Cu, 0.03 g/t Au, 18.0 ppm Mo; 292m @ 0.22% Cu; 463m @ 0.15% Cu, 0.02g/t Au, 9ppm Mo; 320m @ 0.21% Cu, 0.05g/t Au, 31ppm Mo (Superior Resources https://www.superiorresources.com.au/). An historical resource of 13 Mt @ 0.42% Cu has been estimated for the Cockie Creek prospect (Superior Resources https://www.superiorresources.com.au/projects/greenvale/cockie-creek/). The Lynwater Complex and equivalent volcanic rocks are considered to have developed in a back-arc extensional rift setting (Fergusson et al., 2007).

Potential *porphyry systems* of Late Silurian to Devonian age (e.g., The Bank, Barrabas Creek, and Titov) have been reported southwest of Townsville. They consist of Cu-Mo systems with weak fracturing, phyllic and propylitic alteration, and uncommon potassic alteration (Bookstrom et al., 2014).

The Late Carboniferous to Middle Permian continental magmatic arc contains *porphyry systems,* related skarns, and vein systems. The most significant deposits are those of the Chilligoe district, with the previously mined Red Dome (pre-mining resource 15 Mt @ 2.6 g/t Au; Porter Geoscience https://portergeo.com.au/database/mineinfo.php?mineid=mn791), the Mungana Au-skarns (Ewers et al.1990; Bookstrom et al., 2014). Other, more classic, porphyry-style prospects include Ruddygore and Dimbulah, where Bookstrom et al. (2014) reported resources of 10 Mt @ 0.4 % Cu and 20 Mt @ 0.25 % Cu, respectively (see also Ballymore Resources https://www.ballymoreresources.com/site/projects/ruddygore-project and Tartana Minerals https://www.tartanaminerals.com.au/projects/other-exploration-projects/dimbulah-porphyry-copper-project). Mineralisation is described as moderate stockwork and fracturing, associated with common phyllic and propylitic alteration, but rare potassic alteration (Bookstrom et al., 2014).

In the New England Orogen, the most richly endowed porphyry deposits are associated with Late Permian to Late Triassic magmatism. The contained Cu reported by Bookstrom et al. (2014) is 1.8 Mt, divided into eight separate systems with tonnages of 71.5–200 Mt @ 0.01 – 0.65% Cu. Reported Au in two systems, Mount Cannindah and Chinaman Creek, are 0.16 g/t Au and 0.33 g/t Au, respectively. Three of the systems have Mo (0.01 to 0.04 % Mo). These resource numbers are historic and likely based on limited data; they are therefore considered indicative only.

Among the most significant of these Triassic systems is the Mt Cannindah with a JORC compliant resource of 14.5 Mt @ 0.72% Cu, and 0.42 g/t Au (Cannindah Resources, https://app.sharelinktechnologies.com/announcement-preview/asx/3e408112499e9d8d2e87b74d32d9230e). Despite this modest resource, recent exploration has delivered significant drill results, such as 282m @ 0.94% Cu, 0.3g/t Au, 19g/t Ag; 58m @ 0.47% Cu, 0.16g/t Au; 54m @ 0.69% Cu, 0.95g/t Au; 128m @ 0.39% Cu, 0.21g/t Au (Cannindah Resources https://cannindah.com.au/project/mt-cannindah-project/). Mineralisation is hosted by Carboniferous sedimentary rocks, Triassic volcanic rocks, and associated multi-phase diorite to granodiorite intrusions (Cook et al., 2021). The system contains a major hydrothermal breccia component, as well as classic porphyry stockwork and skarn (Cannindah Resources; Cook et al., 2021). Alteration is zoned from potassic (biotite and K-feldspar) to sericitic and outer sericite-silica-pyrite. Mineralisation is considered to have developed coevally with the ~230 Ma Glassford Igneous Complex and Bobby Volcanics (Cook et al., 2021 and references therein). Other significant Triassic *porphyry systems* include Limonite Hill, Coalston, and Yeppoon; all of which contain potassic alteration, porphyry-style veining, and significant breccia components (Bookstrom et al., 2014).

Within the Late Permian to Triassic belt, two temporally distinct groups of porphyry deposits are recognised: an earlier (253–244 Ma) belt of copper-molybdenum deposits and a younger (235–230 Ma) belt of copper-gold porphyry deposits (Rosenbaum, 2026). The younger group of porphyry deposits includes Coalstoun and Coalstoun Lake copper deposits (Ashley et al., 1978), as well as the Late Triassic (~230 Ma) coppergold porphyry deposits of Chinamans

Creek, Mount Cannindah, and Mount Cannindah East. Farther north, the slightly younger (~225 Ma) copper-molybdenum Yeppoon deposit is associated with a small granodiorite stock (Ford et al., 1976). The older porphyry deposits (Late Permian to Middle Triassic) were developed mainly during the second stage of contractional deformation associated with the Hunter-Bowen orogeny, at ~250 Ma. It has been suggested that this porphyry belt formed in an arc segment that coincided with a shallower slab dip angle (Rosenbaum, 2026). The third and last phase of Hunter-Bowen contractional deformation coincided with the development of the younger porphyry group.

Early Cretaceous *porphyry systems* are relatively poorly defined. However, the presence of six Early Cretaceous *porphyry* systems have been reported by Horton (1978) and Bookstrom et al. (2014). These systems are generally considered weakly developed, dominated by Cu with minor Mo. Estimated resources are 434.6 kt of contained Cu in four systems (Bookstrom et al., 2014), with the major one being Mount Abbott (300 kt of contained Cu at 0.15 % Cu). Two of the systems are dated at 132–123 Ma (hydrothermal biotite and magmatic hornblende in Juvilon Creek) and 119 Ma (U-Pb zircon on associated quartz syenite in Mt Abbott). The older age is consistent with subduction related magmatism and the younger age with extension-related magmatism associated with slab rollback (Allen et al., 1997).

In addition to the occurrences discussed above, several major Au deposits have been considered porphyry-related, including the significant Kidston and Mt Leyshon breccia-hosted deposits, which have a combined estimated contained Au of 7 Moz (Porter Geoscience https://portergeo.com.au/database/index.php; Blevin and Morrison, 1997). Importantly, in addition to these substantial Au deposits, the Tasmanides host other multi-million-ounce intrusion-related or epithermal Au deposits and districts such as Ravenswood and the Drummond Basin deposits. The high Au endowment of the Tasmanides is in stark contrast to the modest Cu endowment.

PRESENT ENDOWMENT – A TRUE REFLECTION OR AN OPPORTUNITY?

Our analysis demonstrates that although numerous *porphyry systems* developed within the various magmatic provinces of the Tasmanides, none of these systems, except for the Macquarie Arc, reached the threshold of a *major porphyry deposit*. This lack of significant Cu endowment in the Tasmanides, outside of the Macquarie Arc, could have two possible explanations: (1) a relative lack of exploration maturity or (2) a fundamental lack of Cu endowment. Each explanation carries critical implications for exploration strategies.

Since the 1800's, eastern Australia has been considered as a favourable exploration and mining destination. As a consequence, extensive exploration has been conducted in eastern Australia, benefitting from favourable government policies, land access, and access to funding. The overall exploration success is reflected in discoveries forthcoming for a range of deposit types during the 20th and 21st Centuries, including Mt Read Volcanics in Tasmania (Zn-Pb-Ag-Au), Cobar Basin in NSW (Zn-Pb-Ag-Au-Cu), Macquarie Arc (Au-Cu), and Drummond Basin in northern Qld (Au). The Macquarie Arc is the only porphyry Cu-Au belt that has yielded economic deposits and created value in the sense of Schodde and Hronsky (2005) and Schodde (2023). Exploration over decades has unearthed many *porphyry systems* outside the Macquarie Arc, but no *major porphyry deposits*, providing further support that exploration maturity is not a valid reason for the lack of known endowment.

During the same time period, exploration efforts in other global porphyry provinces, with far more challenging exploration circumstances (e.g., Andean Cordillera, British Columbia, SW Pacific margin), have led to discoveries of multiple *major porphyry deposits*. Compared with many global porphyry provinces, it appears that exploration in the Tasmanides was relatively mature (with the exception of the deeply buried sections of the Lachlan and Thompson Orogens). A lack of exploration efforts, therefore, cannot explain the scarcity of Cu endowment.

It appears, therefore, that the current lack of Cu endowment (outside of the Macquarie Arc) is fundamental to the geology of the Tasmanides. Most of the porphyry systems in the Tasmanides occur in extension-related (e.g., back-arc) magmatic provinces, which were driven by repeated periods of trench retreat. This tectonic setting, in contrast with highly endowed continental margin porphyry Cu provinces, generated extensional deformation at the overriding plate and prevented development of extensive and long-lived thick crust critical for the development of highly fertile porphyry Cu provinces and *major porphyry deposits*. Based on the USGS databases for the Andes and the Tasmanides, the density of porphyry occurrences is 4.5 times greater in the Tasmanides (using only the favourable tracts of Bookstrom et al., 2014) than the Andes; nonetheless, the Cu endowment is orders of magnitude less. This supports the suggestion that the development of *porphyry systems* is a natural consequence of I-type arc magmas, but that *major porphyry deposits* require particular circumstances. We consider that, in contrast to the Andes, the Tasmanides generally lacks those particular circumstances. The exception to this is the Macquarie Arc, which was likely developed as an intra-oceanic arc, subjected to a major plate tectonic reorganisation event, and ultimately established the appropriate circumstances for development of *major porphyry deposits.*

Our conclusions are similar to those of Sillitoe (2018) for the Japan-South Korea convergent margin. Both the Tasmanides and the Japan-South Korea margin are host to substantial Au systems of various types.

EXPLORATION IMPLICATIONS

Future exploration strategies recognising the commodity balance and the predominantly extensional tectonic setting of major deposits in the Tasmanides will optimise probabilities of success. In the future, under future economic conditions, some non-Macquarie Arc Tasmanide porphyry systems may become economic. However, we believe that exploration probabilities are maximised by appropriate strategies.

We specifically suggest that maximum value creation is likely through exploration strategies focussing on opportunities such as:

- Macquarie Arc-age systems in less mature areas or in novel structural settings outside the main “recognised” arc;
- low sulphidation epithermal Au-Ag deposits in back-arc positions of major thermal phases;
- intermediate sulphidation Au-Ag-Pb-Zn-(Cu) epithermal deposits in Permian and younger extensional settings;
- distal Au-rich deposits in intrusion-related districts that may or may not have porphyry characteristics; and
- siderophile metal associations and intrusion-related Au deposits associated with reduced to mildly oxidised magmatic suites.

Recent diverse exploration success in Australia indicates that future exploration activities can be successful. However, strategies should reflect the realities of the underlying geology.

REFERENCES

ALLEN C.M., WOODEN J.L. & CHAPPELL, .B.W., 1997. Late Paleozoic crustal history of central coastal Queensland interpreted from geochemistry of Mesozoic plutons—The effects of continental rifting: Lithos, 42, 67–88.

ANGUS M., CAIRNS C., KONOPA S. & MEAKIN A., 2026. Mineral Resource Estimate for the Thursday's Gossan Deposit Technical Report for Staveley Minerals Ltd.

ASHLEY P.M., BILLINGTON W.G., GRAHAM R.L. & NEALE R.C., 1978. Geology of the Coalstoun porphyry copper prospect, Southeast Queensland, Australia. Economic Geology, 73, 945–965.

BOOKSTROM A.A., GLEN R.A., HAMMARSTON J.M., ROBINSON G.R., Jr., ZIENTEK M.L., DRENTH B.J., JAIRETH S., COSSETTE P.M., & WALLIS J.C., 2014, Porphyry copper assessment of eastern Australia: U.S. Geological Survey Scientific Investigations Report 2010–5090–L, 160 p. & GIS data, http://dx.doi.org/10.3133/sir20105090L.

BLEVIN P.L. & MORRISON G.W., 1997, Kidston breccia pipe-magmatic & hydrothermal evolution. Unpublished report, AMIRA Project P425: Magmatic & Hydrothermal Evolution of Major Intrusive-related Gold Deposits in Eastern Australia

COOK N., ALLAN S. & SAVINOVA K., 2021. Mt Cannindah, East Queensland Mineral Deposit Atlas, Ch. 23, Geological Survey of Queensland, 577 – 597.

CAWOOD, PA, BUCHAN C. 2007. Linking accretionary orogenesis with supercontinent assembly. Earth-Sci. Rev., 82, 217–56.

CAYLEY R.A. 2011. Exotic crustal block accretion to the eastern Gondwanaland margin in the Late Cambrian–Tasmania, the Selwyn Block, & implications for the Cambrian–Silurian evolution of the Ross, Delamerian, & Lachlan orogens. Gondwana Res. 19, 628–649.

CONEY P.J. 1992. The Lachlan belt of eastern Australia & Circum-Pacific tectonic evolution. Tectonophysics, 214, 1–25.

CORBETT G., 2023. Comments on the exploration potential of the Bottletree Project, North Queensland. Unpubl. Report to Superior Resources Ltd., 37 pp. https://www.superiorresources.com.au/wp-content/uploads/2023/04/Corbett_Bottletree_Report_20March2023.pdf. Accessed 15 June 2026.

CARLOTTO V., CARLIER G., VAN HEININGEN P.V., HODGIN E.B., CARDENAS J., LIGARDA R., CERPA L. & MAQQUERA V., 2023. Andean evolution, orogenic deformation & uplift of the Western Cordillera & Altiplano of southern Peru, northern Bolivia and Chile: Eocene-Oligocene lithospheric delamination, Journal of South American Earth Sciences. v. 128.

CLARK A.H., 1993.Are outsize porphyry copper deposits either anatomically or environmentally distinctive? Society of Economic Geologists Special Publication 2, 213–282.

COLLINS W.J., 2002a. Hot orogens, tectonic switching, & creation of continental crust. Geology, 30, 535–538.

COLLINS W.J., 2002b. Nature of extensional accretionary orogens. Tectonics, 21, 6.1–6.12.

CRAWFORD A.J., MEFRE S., SQUIRE R.J., BARRON L.M., & FALLOON J., 2007. Middle & Late Ordovician magmatic evolution of the Macquarie Arc, Lachlan Orogen, New South Wales. Aust. J. Earth Sci. 54,181–214.

ENEVER J., 2008. 'Not for Want of Trying' The history of the Coopers Creek Copper Mine, Victoria Journal of Australasian Mining History, 6, 150-175.

EWERS G.R., TORREY C.E., & ERCEG M.M., 1990. Red Dome Gold deposit: in Hughes F E (Ed.),1990 Geology of the Mineral Deposits of Australia & Papua New GuineaThe AusIMM, Melbourne Mono 14, 2, 1455-1460.

FARRAR A.D., COOKE D.R., HRONSKY J.M.A., WOOD D.G., BENAVIDES S. B., CRACKNELL M.J., BANYARD J.F., GIGOLA S., IRELAND T., JONES S. M. & Jose PIQUER J., A Model for the Lithospheric Architecture of the Central Andes & the Localization of Giant Porphyry Copper Deposit Clusters. Economic Geology, 118, 1235-1259.

FAVORITO D.A., & SEEDORF E., 2024. Temporal & Spatial Relations Between Porphyry Copper Deposits & Crustal Shortening: Insights from the Laramide Arc of Arizona & New Mexico. Economic Geology, 119, 1261-1288.

FERGUSSON C.L., HENDERSON R.A., WITHNALL I.W., & FANNING C.M., 2007. Structural history of the Greenvale Province, north Queensland: Early Palaeozoic extension & convergence on the Pacific margin of Gondwana. Australian Journal of Earth Sciences, 54, 573-595.

FORD J.H., WOOD D.G., GREEN D.C., 1976. Geochronology of porphyry copper-type mineralization near Rockhampton, eastern Queensland, Australia. Econ. Geol., 71, 526–534.

GARWIN S., HALL R., WATANABE Y., 2005. Tectonic Setting, Geology, & Gold & Copper Mineralization in Cenozoic Magmatic Arcs of Southeast Asia & the West Pacific. Economic Geology 100th Anniversary Volume, 891–930.

GLEN R.A., 2005. The Tasmanides of eastern Australia. In Terrane Processes at the Margins of Gondwana, ed. APM Vaughan, PT Leat, RJ Pankhurst, pp. 23–96. London: Geol. Soc. Lond.

GLEN R.A., CRAWFORD A.J., PERCIVAL I.G. & BARRON L.M. 2007a. Early Ordovician development of the Macquarie Arc, Lachlan Orogen, New South Wales. Australian Journal of Earth Sciences. 54,167–179.

GLEN R.A., 2013. Refining accretionary orogen models for the Tasmanides of eastern Australia. Australian Journal of Earth Sciences, 60, 315–370.

GLEN, RA, BELOUSOVA, E, & GRIFFIN W.L., 2016. Different styles of modern & ancient non-collisional orogens & implications for crustal growth: a Gondwanaland perspective. Canadian Journal of Earth Sciences., 53, 1372–415.

HONG W., FABRIS A., WISE T., COLLINS A.S., GILBERT S., SELBY D., CURTIS S., & REID A.J., 2023, Metallogenic Setting & Temporal Evolution of Porphyry Cu-Mo Mineralization & Alteration in the Delamerian Orogen, South Australia: Insights From Zircon U-Pb, Molybdenite Re-Os, & In Situ White Mica Rb-Sr Geochronology, Economic Geology, 118, 1291–1318.

HOCHWIMMER B., 2012. The Unicorn Climax-type Mo Porphyry - a Urad-Henderson Analogy. Australian Institute of Geoscientists Quarterly Newsletter 107.

HORTON D.J., 1978, Porphyry-type copper-molybdenum mineralization belts in eastern Queensland, Australia. Economic Geology, 73, 904–921.

JOHN D.A., AYUSO R.A., BARTO M.D., BLAKELY R.J., BODNAR R.J., DILLES J.H., GRAY, F, GRAYBEAL F.T., MARS J.C., MCPHEE D.K., SEAL R.R., TAYLOR R.D., & VIKRE P.G., 2010, Porphyry copper deposit model, chap. B of Mineral deposit models for resource assessment: U.S. Geological Survey Scientific Investigations Report 2010–5070–B, 169 pp.

LEVIELLE R.A. & STEGEN R.J.,2012. The southwestern North America porphyry copper province, Society of Economic Geologists Special Publication 16, 361–401.

MAURY R.C. & PALLARES C., 2024. Spatial & temporal evolution of magmatic arcs: Geochemical diversity & tectonic controls. Journal of South American Earth Sciences, 144, 1-5.

MPODOZIS C., & CORNEJO P., 2012. Cenozoic Tectonics & Porphyry Copper Systems of the Chilean Andes. Society of Economic Geologists, Inc. Special Publication 16, 329–360.

PEARSON M., 2003. The Early Copper Mining Industry in Central Queensland, 1863-1879 - History & Place, Journal of Australasian Mining History, Vol. 1, No.1, September 2003, 121-143.

ROSENBAUM G., 2018. The Tasmanides: Phanerozoic Tectonic Evolution of Eastern Australia, Annual Review of Earth & Planetary Sciences, 46, 291-325.

ROSENBAUM G., GILES D., SAXON M., BETTS P.G., WEINBERG R.F., DUBOZ C., 2005. Subduction of the Nazca Ridge & the Inca Plateau: Insights into the formation of ore deposits in Peru. Earth & Planetary Science Letters, 239, 8– 32.

SCHODDE R.C., 2023. Outlook for the Australian Junior Sector. Keynote Presentation for Mines & Money Conference, Melbourne, 14th June 2023, Melbourne, Australia

SCHODDE R.C. & HRONSKY J.M.A., 2005. The Role of World-Class Mines in Wealth Creation. Society of Economic Geologists Special Publication v. 12.

SCHOFIELD A. (ed.), 2018. Regional geology & mineral systems of the Stavely Arc, western Victoria. (No. 2018/02). Geoscience Australia, Canberra.

SILLITOE R.H., Why No Porphyry Copper Deposits in Japan & South Korea? Resource Geology, 68, 107-125.

SILLITOE R.H., PERELLO J.,2005. Andean copper province: Tectonomagmatic settings, deposit types, metallogeny, exploration, & discovery. Economic Geology 100th Anniversary Volume, 845–890.

SILLITOE R.H., PERELLO J., 2024. Porphyry copper recurrence in the Andes of Chile & Argentina. Economic Geology, 119, 995-1003.

USGS, 2022. Porphyry copper deposits & prospects in the Andes Mountains of South America. https://www.sciencebase.gov/catalog/item/625dae34d34e85fa62b7a712

WARD J.F., ROSENBAUM G., UBIDE, T, SANDIFORD M., 2024., Slab segmentation, anomalous arc volcanism, & giant porphyry copper deposits in Indonesia. Earth & Planetary Science Letters, 626.

WYBORN D., TURNER B.S., & CHAPPELL B.W., 1987, The Boggy Plain Supersuite—A distinctive belt of I-type igneous rocks of potential economic significance in the Lachlan Fold Belt: Australian Journal of Earth Sciences, 34, 21–43.

THE GEOLOGY AND GEOLOGICAL SETTING OF THE BRIGGS PORPHYRY COPPER-MOLYDENUM DEPOSIT, CENTRAL QUEENSLAND

Frazer Tabeart

Alma Metals Limited

Key Words: Northern New England Orogen, convergent margin, porphyry copper deposit

INTRODUCTION AND SUMMARY

The Briggs deposit is located 60km west of Gladstone in central Queensland. Briggs is currently the largest known porphyry copper deposit in the Northern New England Orogen and contains a total mineral resource estimate of 932Mt @ 0.21% Cu, 36ppm Mo and 0.6ppm Ag at a 0.15% Cu cut-off grade. Mineralisation is related to quartz-sulphide stockwork veining associated with early Triassic tonalitic to granitic intrusions emplaced into volcanic sediments of the older Devonian Calliope island-arc. The mineralisation and associated alteration are typical of porphyry deposits, with a sodic-potassic core surrounded by propylitic alteration. Phyllic alteration gradational into greisen/silica flooding and subsequent argillic alteration is locally present. Post mineral weathering has produced a thin oxide cap with local supergene enrichment at the base of weathering.

TECTONIC SETTING AND AGE DATING

Briggs is in the Yarrol Province of the New England Orogen (Figure 1). Basement rocks comprise tholeiitic to moderately calk-alkaline island arc basalts and andesites of Devonian age which formed part of the Calliope Arc. The Calliope Arc was thrust onto the leading edge of the Lachlan Orogen during the formation of the Connors-Auburn Arc during the Lower Carboniferous and subsequently intruded by widespread Permo-Triassic magmas during the Bowen Orogeny between 260 Ma and 250 Ma (Jessop *et al* 2019).

SHRIMP U-Pb dating of zircons in the syn-mineral tonalitic intrusions at Briggs give an average age of 247.2 +/- 1.2 Ma with some older components reflecting ages of 258-262 Ma (Pollard 2021). Re-Os dating of molybdenite associated with chalcopyrite at Briggs gives ages of 248.35 +/- 0.90 Ma (Pollard 2022).

DISTRICT SCALE SETTING

The Briggs porphyry copper-molybdenum prospect is centred on porphyritic tonalites that intrude the Capella Creek Beds sequence, a mid-late Devonian package of volcanoclastic and sedimentary sequences ranging in composition from basaltic to andesitic volcanoclastic sediments to thinly interbedded fine-grained sandstone and siltstone with andesitic to dacitic clasts. To the south of the Briggs porphyry the Capella Creek Beds are truncated by the Permo-Triassic aged Galloway Plains granodiorite batholith (Figure 2).

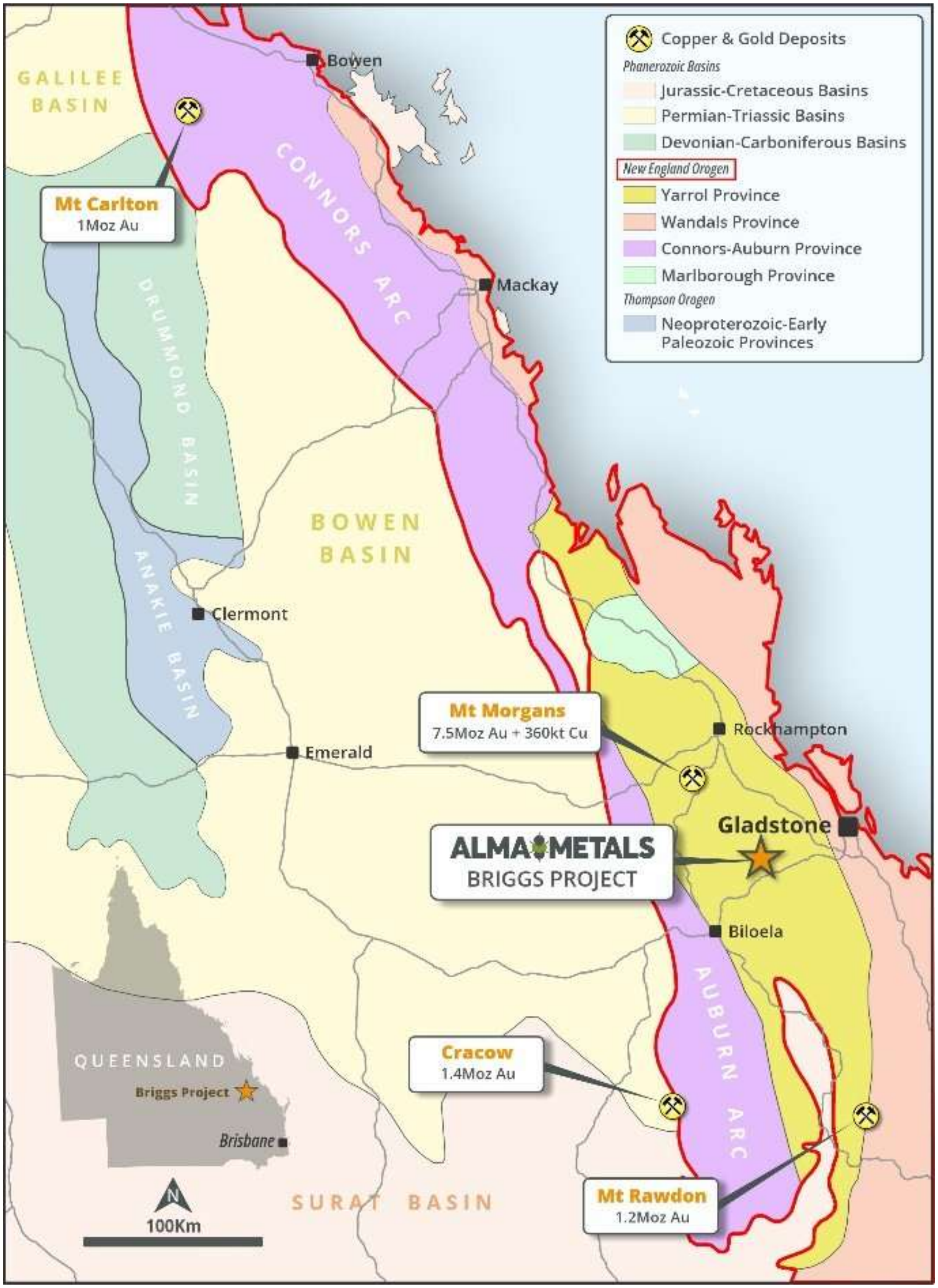

Figure 1. Regional Setting of the Briggs Porphyry Cu Deposit.

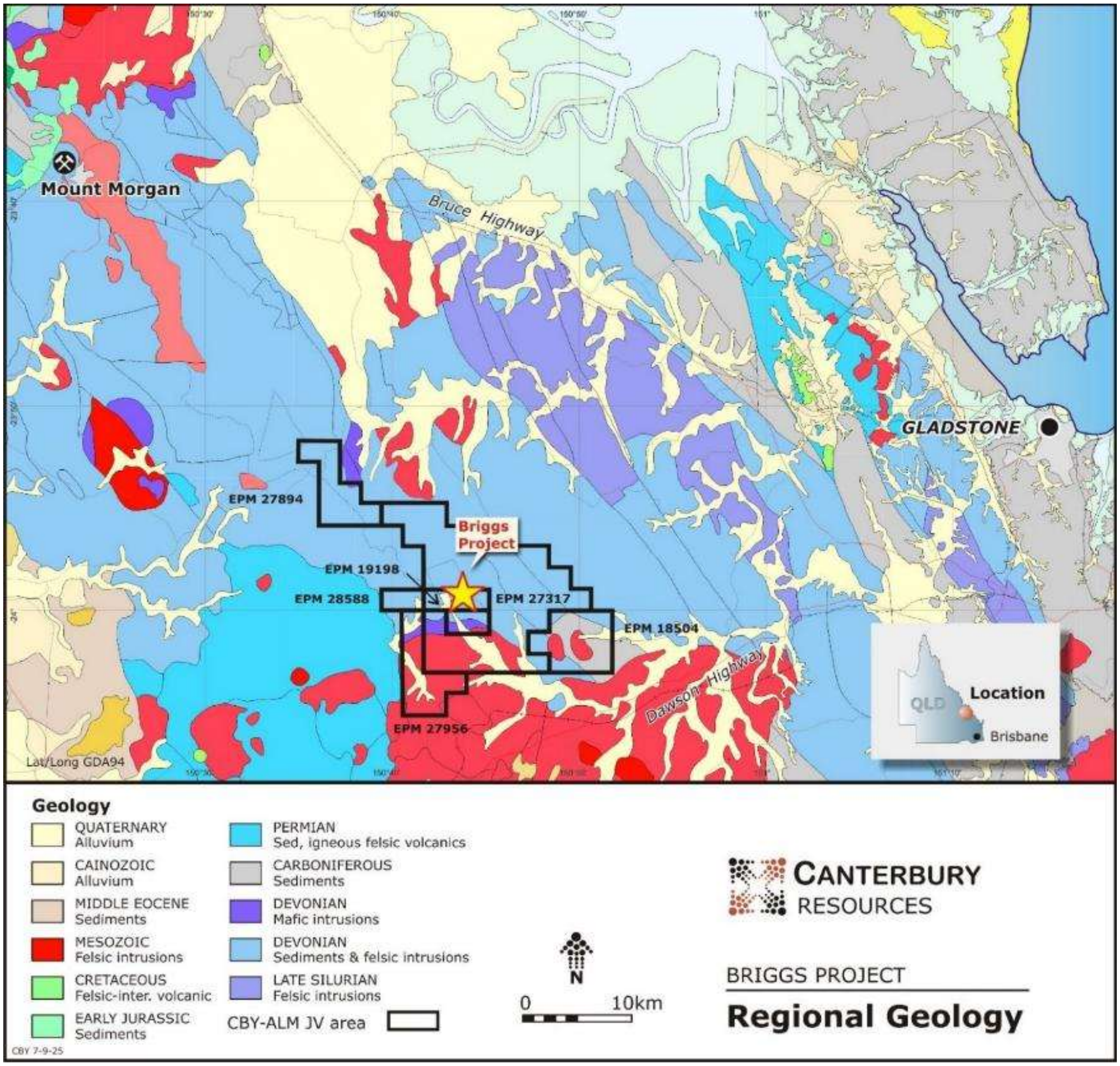

Figure 2. District Scale geological setting of the Briggs Porphyry Copper Deposit.

DEPOSIT SCALE GEOLOGY

Detailed surface geological mapping and characterisation of the litho-geochemistry of core drilling in the top ~400m of the Briggs deposit highlights that mineralisation is spatially related to three porphyritic tonalitic stocks (Figure 3). Mineralisation occurred during two major phases, with an early syn-mineral phase comprising predominantly crowded porphyry textured tonalites with lesser volumes of weakly porphyritic to glomeroporphyritic tonalites and diorites. Late mineral phases include quartz-feldspar porphyry, hornblende porphyry and granite and aplite dykes. Three chemically/texturally distinct phases of post-mineral dyke are also recognised.

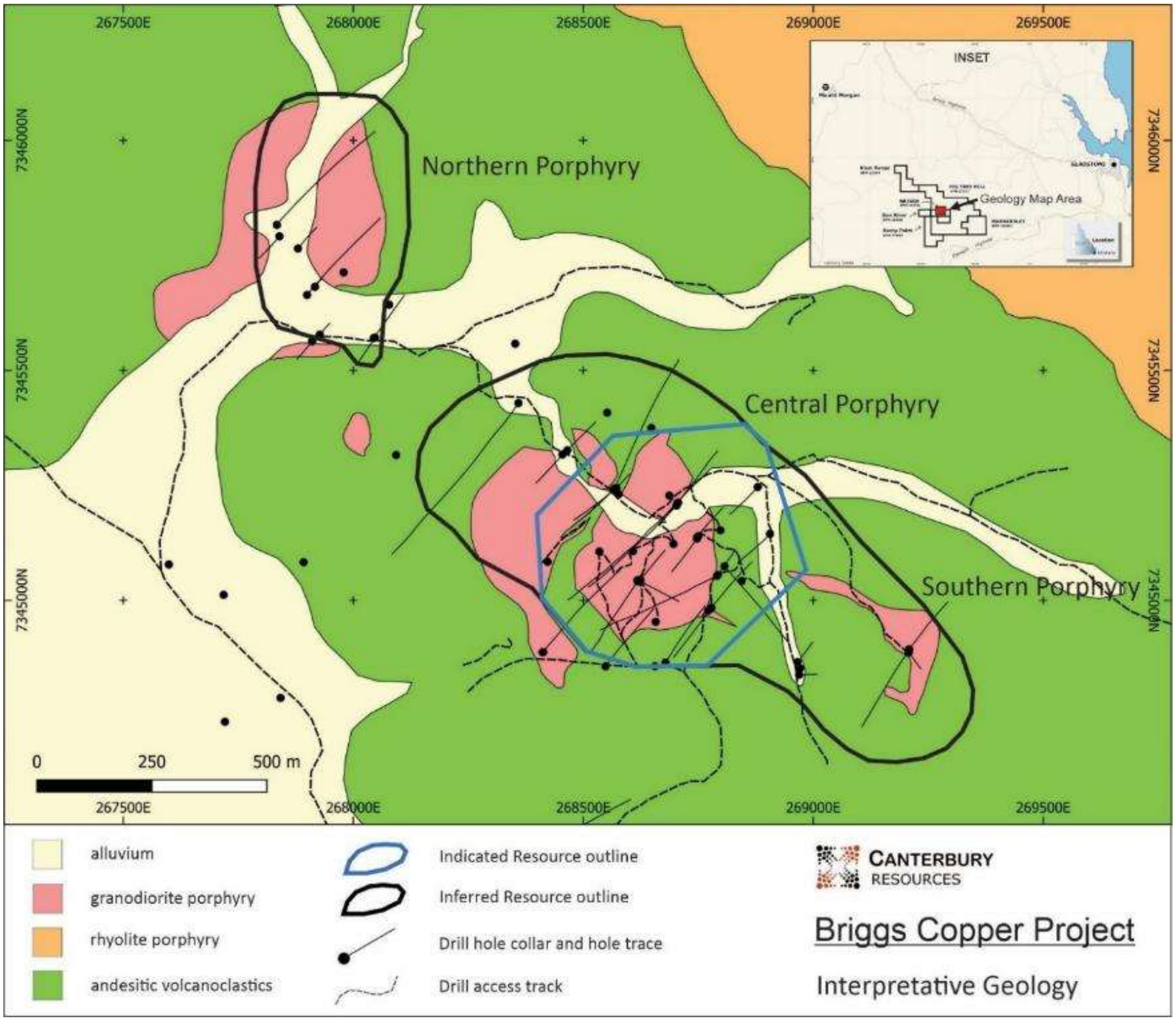

Figure 3 Deposit Scale Geology of the Briggs Porphyry Copper Deposit.

PORPHYRY MINERALISATION AND ALTERATION STYLES

Mineralisation at Briggs consists of chalcopyrite and pyrite with minor molybdenite and very minor amounts of bornite. The chalcopyrite is observed both disseminated in the rock mass, and within quartz and k-feldspar porphyry style veins and is present in both the intrusions and the enclosing volcanic sediments (see Figure 4).

The earliest syn-mineral intrusions (porphyritic tonalites) typically contain A- and B-type porphyry veins with varying ratios of quartz, albite, orthoclase and anhydrite (sodic-potassic alteration, e.g. Figure 5). These veins extend into the enclosing volcanic sediments, along with local C-veins characterised by earthy green chlorite and chalcopyrite (e.g. Figure 6). Later stockwork veining events associated with the more granitic phase of mineralisation show the presence of red/pink k-feldspar, quartz and anhydrite, and also extend into the volcanics. These veins may contain more molybdenite than the earlier veins. Local development of UST's in the intrusive phases are observed in outcrop and drill core, often with high copper tenors approaching 1% Cu. Local D-type porphyry veins containing quartz, pyrite and muscovite/sericite overprint the earlier A/B vein assemblages (Figure 7), and form part of late phyllic overprint which is locally present. Minor argillic alteration in the form of kaolinization (+/- sericite/illite) of feldspars is observed in the top 200-300m of the deposit.

Secondary copper is also present as malachite, azurite, covellite and tenorite, generally in the top 10-30m above the base of oxidation. A thin, discontinuous zone of supergene enrichment at the base of the oxide profile contains chalcocite and locally native copper on fracture surfaces (e.g. Figure 8).

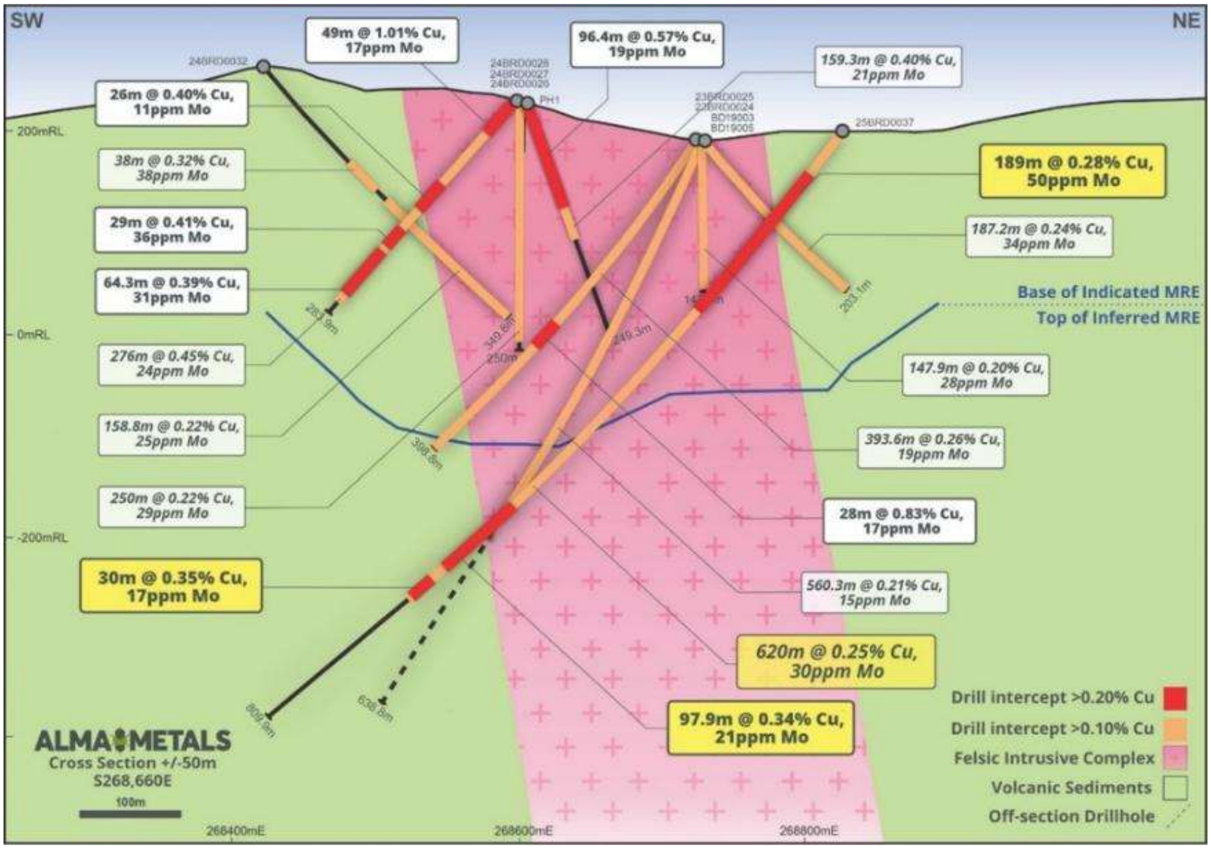

Figure 4 Cross Section across the central part of the Briggs deposit showing the mineralisation extends up to 100m away from the contact between the porphyritic tonalite into the enclosing volcanic sediments. Note that the deposit remains open at depth.

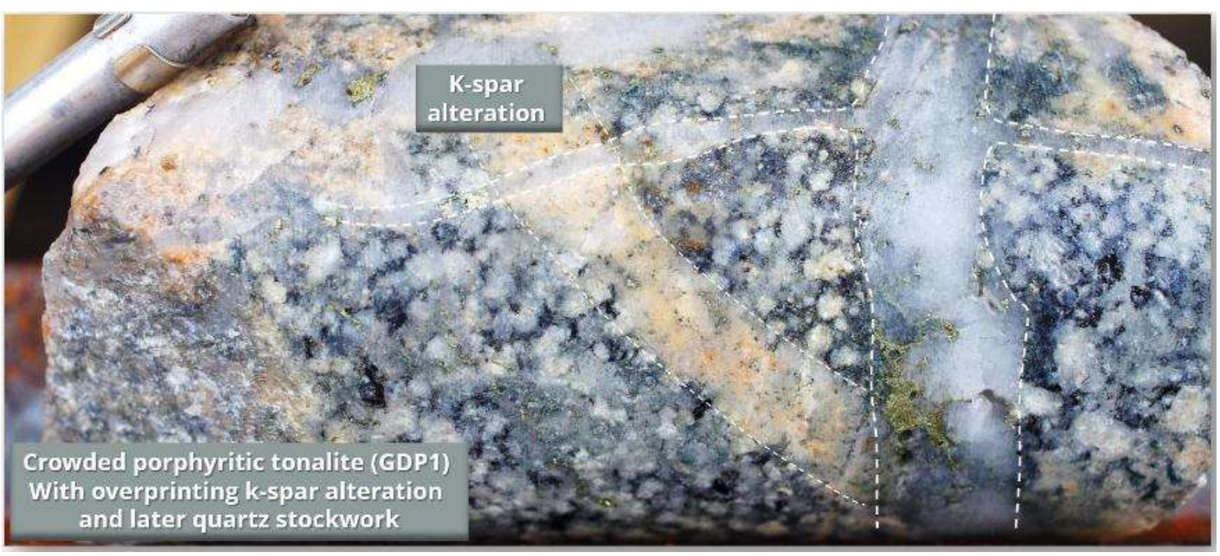

Figure 5. Porphyritic tonalite with multiple veining and alteration events

Figure 6. Mineralised Devonian volcaniclastic rocks with overprinting A, B and C-veins.

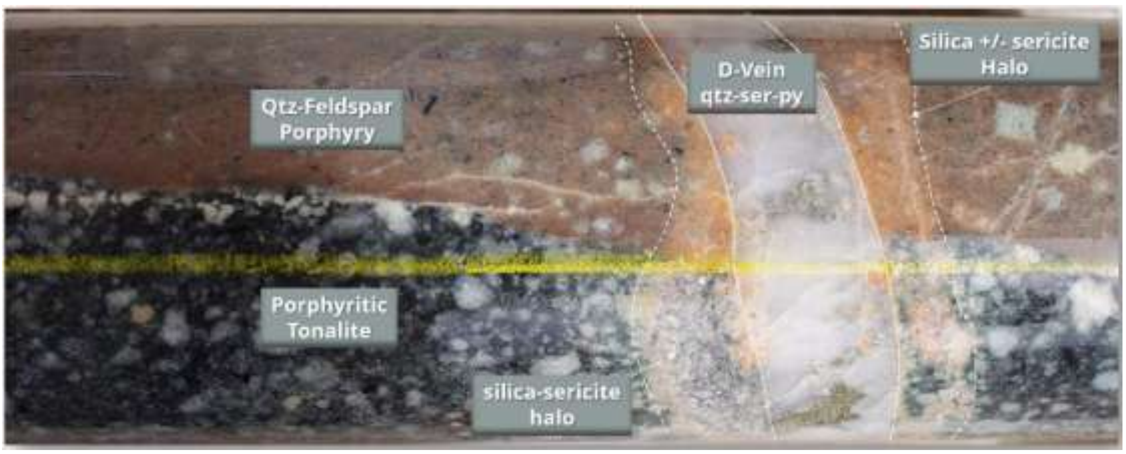

Figure 7. Porphyritic tonalite cut by a later quartz--feldspar porphyry and subsequently overprinted by a D-Vein.

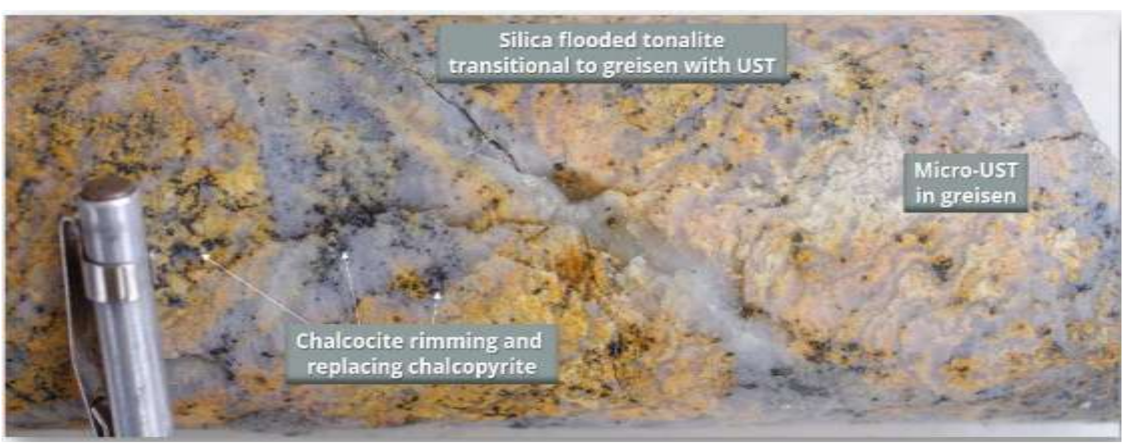

Figure 8. Supergene enriched mineralisation hosted in silica flooded tonalite transitional to greisen with micro-UST.

CONCLUSIONS

Briggs shows many broad characteristics of a typical porphyry system with a central core of intense sodic-potassic alteration dominated by secondary albite overprinting igneous plagioclase with lesser k-feldspar and some biotite (particularly in the volcanics). This zone is locally overprinted by a phyllic assemblage of sericite after biotite and muscovite, locally gradational into greisen assemblages. The sodic-potassic alteration event grades into a propylitic assemblage in the volcanics and sediments dominated by chlorite and epidote before a gradational change to metamorphic epidote. A later argillic overprint is locally present.

Mineralisation is related to porphyritic tonalite stocks which were emplaced into Devonian arc-related mafic to intermediate volcanics during intense shortening associated with the Bowen Orogeny.

REFERENCES

JESSOP K., DACZKO N.R. & PIAZOLO S. 2019 Tectonic cycles of the New England Orogen, eastern Australia: A Review. Australian Journal of Earth Sciences v66 459-496

POLLARD P.J. 2021. U-Pb & Re-Os dating of intrusive rocks & mineralization at the Briggs porphyry copper deposit, central Queensland. Internal Company Report prepared for Canterbury Resources.

POLLARD P.J. 2022. Re-Os dating of mineralisation from the Southern Porphyry target (BRIG0001) at the Briggs porphyry copper deposit, central Queensland. Internal Company Report prepared for Alma Metals & Canterbury Resources.

CONSTELLATION: STRUCTURALLY CONTROLLED COPPER MINERALISATION IN THE GIRILAMBONE GROUP, NSW

Vassallo J[1], Cox N[2], & Raymond C[1]

[1] Aeris Resources Ltd, Tritton Operations, Yarrandale Rd, Hermidale, NSW 2831

[2] TrueDip Geoscience, 6/1 Wylie Place, Leederville, WA 6007

Key Words: Girilambone Group, Copper Mineralisation, Structurally Controlled.

INTRODUCTION

The Constellation deposit is a cornerstone project for Aeris Resources' Tritton Operations in central NSW with a Mineral Resource Estimate of 7.6Mt @ 2.01% Cu, 0.66 g/t Au & 2.5g/t Ag (Aeris Resources 2025). The deposit has a strike length of 250 m, a down-plunge extent of 1,100 m to the ESE and remains open at depth (Figure 1). The upper part of the deposit resides near the surface (~5m) and has oxide-supergene copper components to 100m depth. Open-cut mining is due to start in July 2026 and will later be followed by conventional Long Hole Open Stope (LHOS) underground mining.

Constellation is a large and important example of the suite of similar deposits hosted in the highly deformed turbidite-rich Cambrian-Ordovician Girilambone Group. The discovery of Constellation in November 2020, was previously presented at Mines and Wines by Brad Cox (2022). Since its discovery, 110 reverse circulation holes totalling 11318.7 m and 171 diamond holes totalling 43,121.1 m have been completed. Through collaboration, the Aeris team, with the assistance of consultants and the Geological Survey of NSW, has developed a stronger understanding of the deposit.

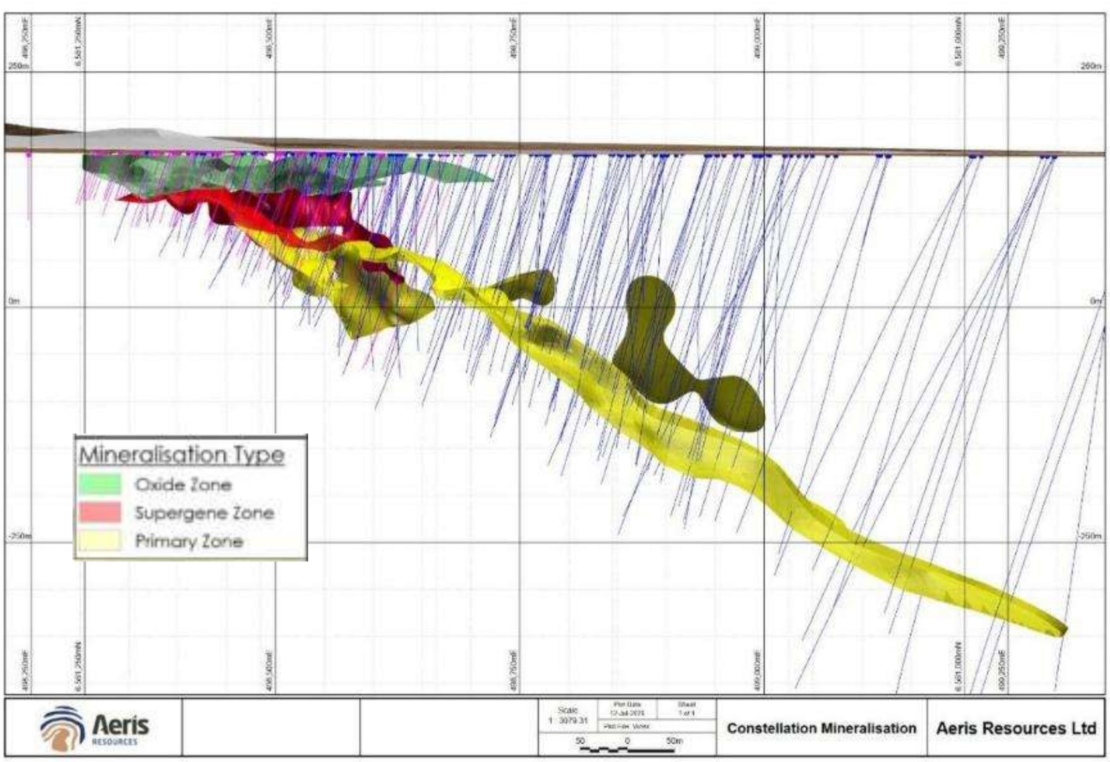

Figure 1 Constellation long section looking NNE, showing the oxide, supergene and primary copper-bearing mineralogical domains. Purple strings are RC, and blue strings are diamond holes.

KEY QUESTIONS

During the initial project drill-out, lithological and structural logging, down-hole EM (DHEM), four acid digest low-level detection geochemical analysis of drill core, geochemical modelling, and petrography were undertaken. During the 2023-2025 Resource upgrade program, structural analysis using graphic logs and paper sections was incorporated, including downhole petrophysics (i.e. Optical Televiewer-Acoustic Televiewer), and Short Wave Infrared and Thermal Infrared (SWIR-TIR) spectral analysis of selected core using Hylogger 4, and RC chips using Hylogger 3.

During the process, the key questions the team tried to answer included:

- What is the stratigraphy, and are there any mafic rocks or marker units in the package?
- What controls the large-scale, gently SE-plunging ribbon-style geometry of the deposit?
- Why is the northern margin markedly different and steeply dipping to the south?
- What fault systems offset the deposit?

LITHOLOGY, STRUCTURE AND MINERALISATION

The extensive lithological logging by the Aeris team and Hylogger data indicate that the deposit is hosted by a highly deformed turbidite package (psammite-pelite) underlain by graphitic schist. No significant volume of mafic rock types has been identified to date. Chlorite-dominant domains <1m wide are present, though no petrographic or geochemical data suggest evidence for a mafic protolith. This differs from other deposits in the region (i.e. Budgery, Avoca Tank, Kurrajong) where mineralisation occurs near mafic rocks (volcanics and intrusions).

As the rock package has been strongly deformed, a structural history became important to document. Based on careful review of the crosscutting/overprinting relationships in drill core (Figure 2), a deformation sequence has been constructed. Evidence of at least four deformation events (D1-D4) was identified.

- D1-D2 penetrative foliations with quartz-dominant veins. S1-2 are relatively coplanar with compositional contacts.
- D3 is represented by a well-formed, moderately N-NE dipping spaced cleavage, shear bands and close-to-tight fold hinges. Shear offsets and vergence suggest the dominant transport direction was to the SW. D3 transitions to brittle-ductile behaviour with late quartz-chlorite ± carbonate and sulphide vein emplacement.
- D4 is dominated by brittle-ductile structures along with open folds with NW-striking steep axial planes and weakly-formed fracture cleavage and micro-crenulation. The vein type is dominated by tension and en-échelon arrays with carbonate ± sulphide infill.

Tight cm-scale parasitic folds and localised shear offsets have rendered the use of sedimentary structures or marker horizons redundant, based upon the observed drill cores from a resource drill pattern on a 40-80 m-spaced grid. Therefore, the challenge was to track the broad changes of the S1-2 and S3 form surfaces to better link key features and/or patterns across drill strings. Using 1:1,000 scale interpretations on graphic logs was a significant challenge for the team. While interpretations varied between team members, D3 features were interpreted similarly to the detailed structural features present in the drill core: tight asymmetrical folds with crosscutting reverse shears (thrusts).

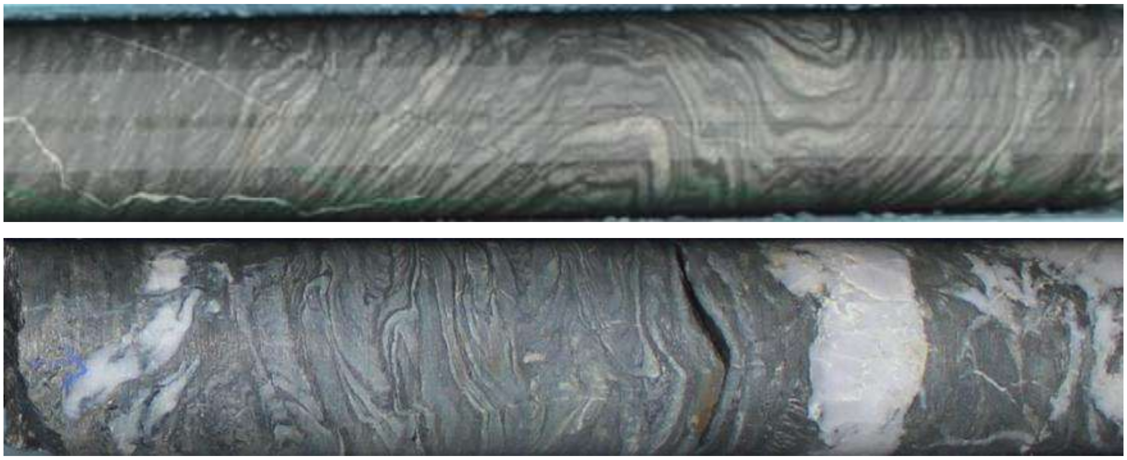

Figure 2 Moderate (top) to high strain (bottom) D3 folding of S1-S2 in HQ core at Constellation.

At the deposit scale, the mineralisation at Constellation resolves into a relatively continuous planar ribbon-style feature which plunges 28º to 106º and transgresses the compositional layering (Figure 1). This is not unlike the geometry of other deposits in the terrane (i.e. Tritton, Budgery). Considering the very high amount of strain recorded in the host rocks, the simpler geometry of the Constellation deposit does not accord with the intense early structures that are present in the host rocks.

There are some possible pre to syn-D2 pyrite, which are elongate in the early fabrics, with ragged grain boundaries. These have been identified in the graphitic schist and are a very minor part (<1%) of the sulphide system.

Two styles of economic mineralisation were identified:

- Phase 1: Pyrite-chalcopyrite ± minor sphalerite lenses in banded-massive form, and
- Phase 2: Fracture-controlled chalcopyrite-pyrite±pyrrhotite that overprint Phase 1.

The relationship of mineralisation to the structures was of key importance in deposit modelling and for regional targeting efforts by the Tritton Exploration team. Detailed observations showed that both Phase 1 & 2 mineralisation had infiltrated the host rock package, utilising both the pre-existing S1-2 and S3 structures as pathways.

The Phase 1 banded-to-massive sulphides are a replacement style mineralisation, most evident on the margins of the deposit, where Phase 1 alteration minerals such as albite-sericite have grown along the tectonic fabrics to infiltrate the surrounding host rock. In places where the alteration is much stronger, the original rock textures are increasingly overprinted, mineralisation becomes massive and crosscuts the tectonic fabrics.

Phase 2 mineralisation is hosted by discrete fractures, forms veins and breccias that incorporate foliated host-rock fragments.

Petrography (Fitzherbert 2024) showed that the Phase 1 mineralisation has overgrown early stilpnomelane, while syn-D3 albite porphyroblasts only have sulphides in their rims, suggesting Phase 1 pyrite formed late during D3. Therefore, the Phase 1 mineralisation is interpreted to be syn to post-D3 (Figure 3). The lack of pyrite pressure shadows, or sulphide grain refinement, further supports Phase 1 mineralisation as being late in the tectonic history of the Girilambone Group. Phase 2 mineralisation, hosted by highly brittle structures with wall rock fragments, is evidently post-D3 (Figure 3).

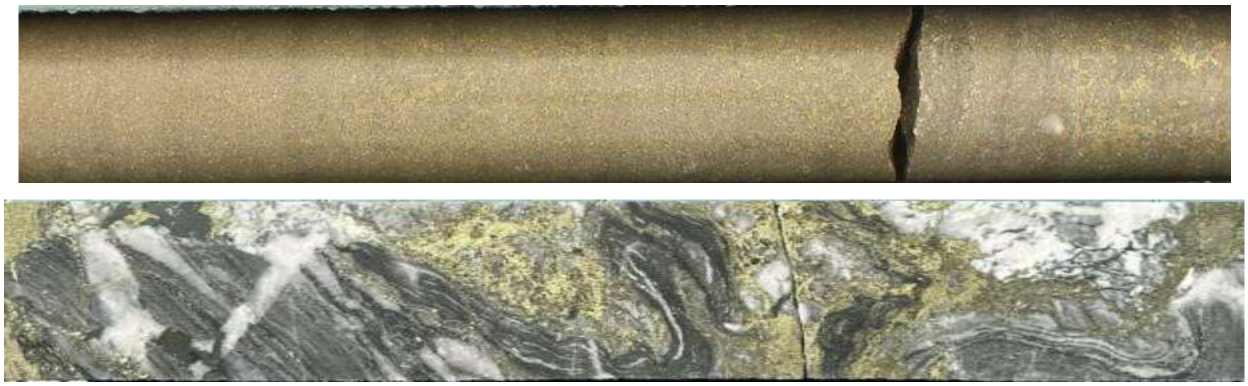

Figure 3 Phase 1 (top) and Phase 2 (bottom) mineralisation in HQ core at Constellation.

LATE FAULTS

Late to post-mineral brittle faults are prevalent across the deposit with offsets of up to 50m. The key challenge for the team was identifying how to ink fault intervals due to poor preservation of core orientation through the fracture zones. One method used to overcome this issue was downhole geophysical logging using ATV and OTV, which measured the faults in situ. While these methods were only trialled in a few holes, the results did assist the team in connecting fractures across section lines and even identified that the east-dipping faults crosscut and offset the west-dipping faults. One further unexpected benefit was also achieved. Slowing down the rate of tool retrieval allowed the capture and subsequent in-situ measurement of the tectonic fabrics. This provided a valuable independent data check.

GEOPHYSICS

With the assistance of the NSW government through the Critical Minerals and High-Tech Metals Exploration Program, two geophysical surveys were completed over Constellation in May 2026, which included:

- 50-100m station Dipole-Dipole Induced Polarisation (IP) surveying, achieving 35.1-line km of ground coverage, and
- 75m gridded ground gravity surveying with data collected at 2509 stations.

The reasoning for completing the surveys was threefold:

- To fingerprint the deposit via IP and gravity geophysical responses,
- Explore for deposit extensions,
- Characterise the broader geological package hosting the mineralisation.

While results are awaited, in combination, they have the potential to generate drill targets and screen false-positive geophysical anomalies caused by the graphitic schist. We are aiming to generate further discoveries in the Tasmanides.

CONCLUSIONS

Whilst not all our initial questions about Constellation have been answered to date, we have come a long way since discovery. Our work suggests that the deposit is late in the complex history of the highly deformed Girilambone Group. The economic mineralisation both follows and crosscuts tectonic fabrics and clearly is not as deformed as the host rock sequence. The deposit is structurally controlled, and the evidence we have collected suggests it is epigenetic. It is crosscut by several late faults, most of which are not mineralised.

Results from the recent geophysical programs are pending, with the aim of generating further targets for future drill testing.

We look forward to the increased geological exposure that will occur during mining. This will certainly raise more questions for the team during our future investigations and hopefully, find some more answers that assist towards the discovery of further copper resources.

ACKNOWLEDGEMENTS

The authors would like to thank Aeris Resources Ltd for permission to publish this work & the ongoing input from the past & present geologists within the Exploration, Mining & Corporate teams for their assistance in improving our understanding of this complex & important company asset. We would especially like to thank: Phil Jones, Joel Fitzherbert, Groundsearch Australia, Harvey Rock Physics, Mitre Geophysics, Fender Geophysics & Paul Ashley, amongst others. Thanks to Dan Logan, Kyle Hughes & all the staff from the Geological Survey of New South Wales for their ongoing interest in our work, important data collection & interactions during this exciting geological journey.

REFERENCES

AERIS RESOURCES. 2025. Aeris Delivers Material Increase in Copper & Gold at Constellation. Australian Stock Exchange Announcement, 31 March 2025.

COX B. 2022. Evolution of Aeris Resources Exploration Strategy within the Tritton Exploration Package. Aeris Resources Ltd. Abstract 2022 Mines & Wines Conference, Orange, NSW.

FITZHERBERT J. 2024. Summary & recommendations for future work on 6 sulfide etched petrographic samples from Constellation. Unpublished Report for Tritton Resources by Joel Fitzherbert Consulting.

EXPLORATION AND DISTRICT POTENTIAL OF THE SLASHERS FLAT PROJECT, GULGONG, NEW SOUTH WALES

Charlie Voorn

Xpedra Resources Ltd, 215 Hay Street, Subiaco, Perth WA 6005

OVERVIEW

The Slashers Flat Project is located within the Rockley-Gulgong Volcanic Belt in the Eastern Sub-province of the Lachlan Orogen, 10km south of Gulgong in New South Wales. The project hosts the Springfield gold deposit, as well as the Divide 4, Orchard, Belinfante, Whales, and Tower Hills South primary gold occurrences, which are all hosted within Late-Ordovician intermediate to mafic volcanics, intrusions and volcaniclastic sedimentary rocks of the Macquarie Arc.

The Gulgong alluvial fields are in the north of the project area which according to mine records produced upwards of 500,000 oz of gold between 1870 to 1927 (Jones, 1940), and for which a bedrock source of feasible size has never been identified. The presence of widespread alluvial gold sitting adjacent to - and in places lying unconformably above - late-age Macquarie Arc volcanics of the Burranah Formation provides an attractive exploration opportunity in a region that has seen no exploration activity over the past 25 years.

The Springfield deposit was first drilled in 1981 by Endeavour Resources. Two diamond holes were drilled to test beneath historic shafts and pits that are located along two parallel, NNW-trending elongate quartz veins, situated up-stream from the Springfield Lead alluvial workings. Drilling completed by subsequent explorers between 1981 and 1991 outlined a shallow (<60m depth) resource estimate of 60 koz @ 1.4 g/t Au, hosted within stockwork quartz veins and sulphide disseminations.

In 2025, Xpedra Resources acquired the project with the view that potential exists to expand the known extents of primary mineralisation at Springfield, as well as to deploy modern exploration techniques to discover additional mineralisation along strike within the reverse-dextral Mudgee-Home Rule Fault system, which bounds a belt of deformed Macquarie Arc volcanics. Xpedra completed an initial confirmatory drilling program in April 2026 which included initial testing of the Springfield deposit at depth. This program returned the best intercept yet reported from the deposit, comprising 94m @ 2.00 g/t Au from 80m including 13m @ 10.21 g/t Au from 81m, in mineralisation situated down-dip from previous drilling.

AREA GEOLOGY

The Slashers Flat project covers Late-Ordovician Burranah Formation rocks of the Cabonne Group within the northern portion of the Rockley-Gulgong volcanic belt. The Burranah Formation rocks consist generally of deep-water, mafic to intermediate volcanics, volcaniclastics and syn-volcanic intermediate intrusions, which are fault-bound to the east and west by Mid-Silurian quartz and felsic volcanic-rich sandstone of the Tannabutta Group, and to the east by siliciclastic sedimentary rocks of the Early Devonian Queens Pinch and Kandos Groups. The Carboniferous Home Rule, Gulgong and Ulan granites intrude to the north and east.

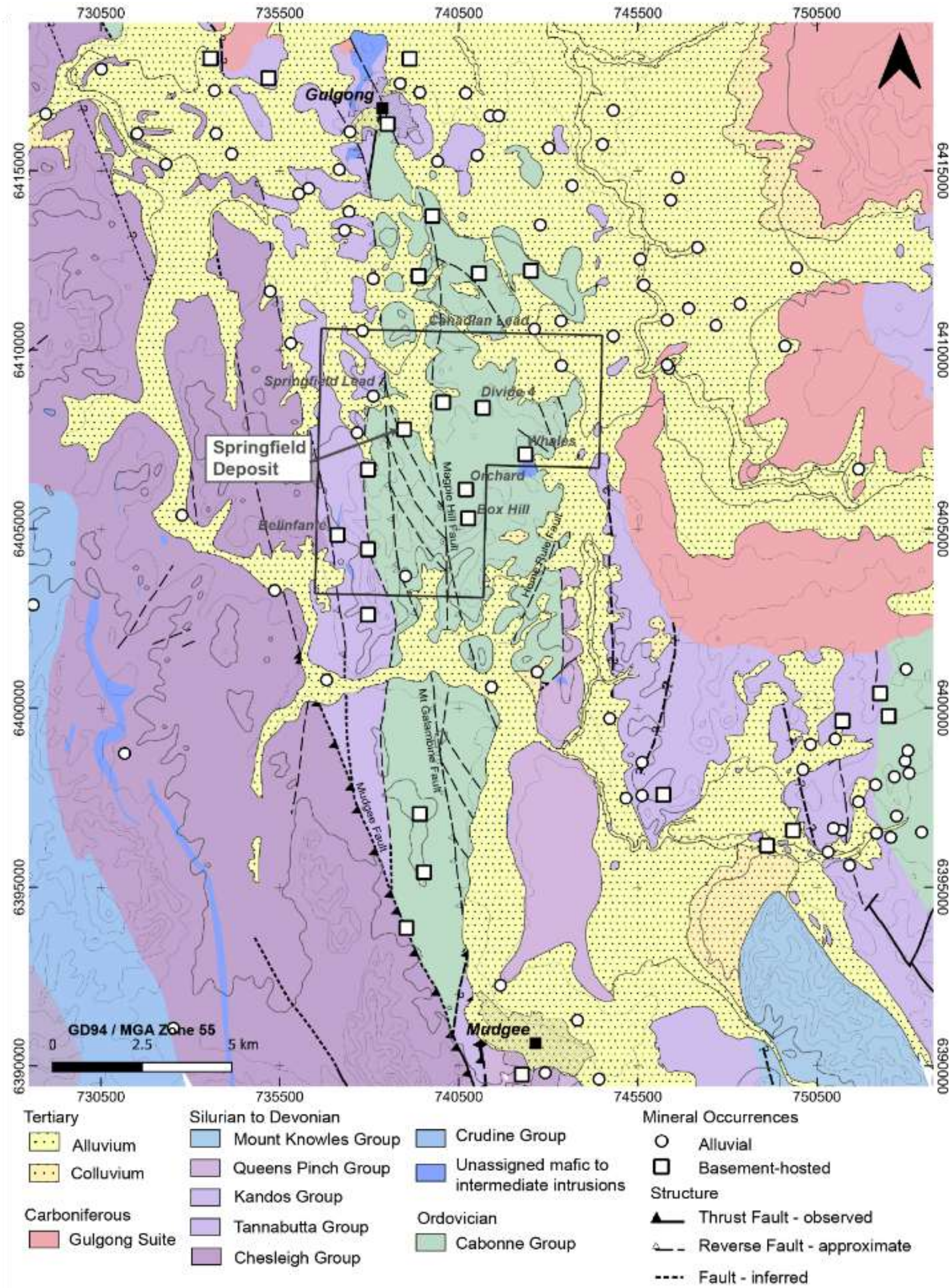

Figure 1: Slasher's Flat project area geology (GSNSW Seamless Geology).

The area is dissected by broadly north-south oriented faulting of Early-Carboniferous age, with north to northwest-trending folding generally tight and gently plunging to the south. Structures are generally west-dipping and, between the Mudgee and Home Rule faults, define a zone of considerable shortening within which most of the primary gold mineralisation in the area is located (Watkins, 1996). The Magpie Hill Fault and the Mount Galambine Fault together define the margins of a 1km-wide deformational zone which hosts the Springfield deposit.

PREVIOUS WORK AND EXPLORATION THESIS

The Early Tertiary ‘Gulgong deep leads’ alluvial deposits are principally located to the south and southeast of the township of Gulgong, with recorded historical production totalling 555,000 oz between 1870 and 1927. Although deep lead deposits supplied most of the production in the area, some primary deposits also made contributions to the total gold production. A total of fourteen primary gold deposits are known in the Mudgee-Gulgong district, however production details are generally unknown (Watkins, 1996; Kirkpatrick, 2003).

The Gulgong granite was historically thought to be the hard-rock source for deep lead gold in the area, however work by Rayner (1940) showed that the deep leads drained north in a radial nature, partially from an area south of Gulgong (Watkins, 1996). Elevation data from the project area shows modern drainage radiating north from a topographic high approximately 12km SSE of Gulgong, consisting mainly of Late-Ordovician Cabonne Group intermediate to mafic intrusive and volcanic rocks and volcaniclastics.

The Springfield deposit, situated on the margin of these erosional and depositional domains (Figure 1), was first drilled by Endeavour Resources in 1981 and subsequently drilled by Sabminco and IMC/Newcrest in the early 1990s. IMC used drill results down to a vertical depth of 60m to estimate a shallow resource of 1.4 Mt @ 1.4 g/t Au for 63,000 oz at a 0.5 g/t cut-off (Hawley, 1990). The deposit was considered by Newcrest to be an encouraging example of porphyry-related mineralisation in an area that historically produced large quantities of alluvial gold, however gold grades were considered sub-economic at the time. Subsequent work by M. Phillips and Jaguar Minerals included one drillhole into the Springfield deposit in 1999 and the evaluation of regional targets, however the strike and depth potential of the Springfield deposit was largely untested.

The shallow nature of the historical resource, paired with mineralisation being intercepted over 400m of strike, down to 170m vertical depth, and open along strike and at depth, provides clear exploration potential in an area that has historically produced significant quantities of alluvial gold.

DRILLING RESULTS

The initial phase of drilling completed by Xpedra during mid-2026 comprised 27 reverse circulation holes for 2,579m. Holes were designed to confirm historic drilling results and begin testing for depth extensions of the deposit. Both objectives were achieved, with continuous mineralisation confirmed to be present along 400m of strike and, in places, widening at depth. Selected assay results from Xpedra’s initial drilling are listed in Table 1.

Figure 2: SFRC025 gold grades by metre (g/t Au)

Table 1. Selected assays from Xpedra's initial drilling

Hole ID	Intercept
SFRC025	90m @ 2.00 g/t Au from 80m
including	13m @ 10.21 g/t Au from 81m
SFRC018	44m @ 2.03 g/t Au from 1m
including	7m @ 4.04 g/t Au from 1m
and	12m @ 3.46 g/t Au from 25m
SFRC017	24m @ 2.97 g/t Au from 0m
including	15m @ 4.27 g/t Au from 0m
including	8m @ 6.71 g/t Au from 0m
SFRC011	55m @ 1.32 g/t Au from 0m
including	15m @ 2.79 g/t Au from 7m
SFRC004	52m @ 1.35 g/t Au from 20m
including	11m @ 3.03 g/t Au from 39m

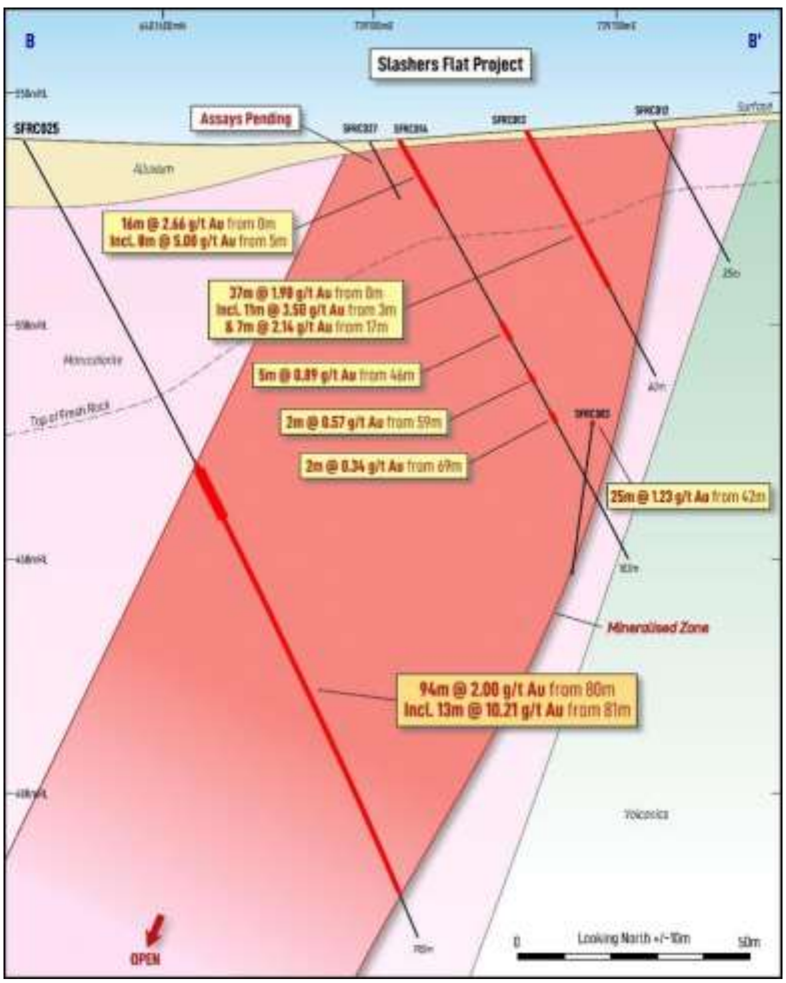

Figure 3: Cross-section and select drill results.

DEPOSIT GEOLOGY, ALTERATION AND MINERALISATION

The Springfield deposit itself is hosted within an elongate, west-dipping, NNW-trending monzodioritic to syenitic intrusion hosted within Burranah Formation basalts, crystal lithic tuffs and volcaniclastic siltstone. Hydrothermal alteration is focussed along a west-dipping fault which obliquely dissects the monzodiorite.

Alteration within the intrusion is zoned, grading from an outer epidote-chlorite +/- carbonate ‘propylitic’ assemblage, grading to inner muscovite-ankerite/siderite-quartz-albite-sulphide ‘sericitic’ alteration (Figure 4). Irregular zones of sericite-poor, silica-dominant alteration are also present, with gold mineralisation confined to the sericitic and silicic alteration zones. Arsenopyrite and pyrite are the dominant sulphides with minor chalcopyrite, occurring within sheeted to stockwork quartz +/- albite-carbonate veins and as disseminations within the altered monzodiorite.

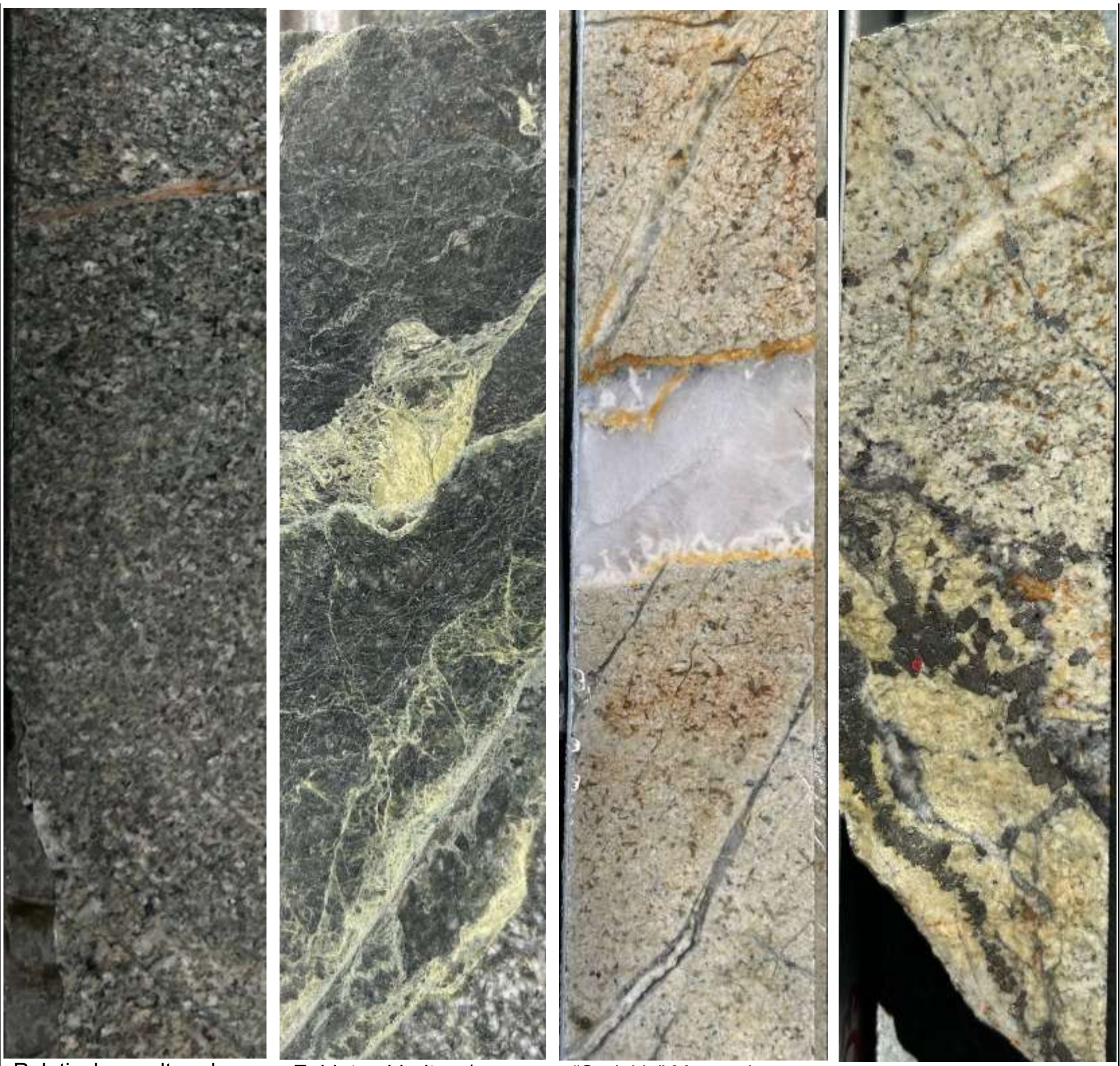

Relatively un-altered monzodiorite	Epidote-chlorite +/- carbonate alteration	“Sericitic” Muscovite - carbonate-quartz-albite-sulphide alteration	“Sericitic” Muscovite - carbonate-quartz-albite-sulphide alteration

Figure 4: Summary of alteration and mineralisation types of the Springfield Gold Deposit

STRUCTURE AND CONTROLS ON MINERALISATION

Historical mapping of old workings delineated two parallel, west-dipping quartz veins 50m apart, with widths of roughly 30cm at surface. Subsequent drilling outlined a broad, steeply west-dipping zone of gold-bearing hydrothermal alteration. The following observations on gold grade distributions are based on Xpedra's recent RC drilling:

- Gold grade is variable within the broader alteration envelope;
- The true width of the west-dipping alteration envelope varies considerably, from 30m to 90m;
- Coherent, higher-grade zones exist within the alteration envelope As yet, their continuity has not been established;
- The southern-most high-grade zone is west-dipping, and plunges shallowly to the south.

Mineralisation appears primarily controlled by steeply west-dipping reverse faults which cross-cut the Springfield monzodiorite, with possible lower-order splays and/or linking structures forming relatively flat-lying high-grade zones. A possible intersection in the central-southern portion of the deposit between the dominant west-dipping fault and an east to north-east trending off-set is visible in magnetics and correlates with higher gold grades.

GENETIC MODEL

Low-sulphide structurally-controlled orogenic gold mineralisation is widespread in the eastern part of the Lachlan Orogen, where major districts include Adelong, Gulgong, Hill End, Lucknow and the Parkes area (Downes, 2019).

The Springfield deposit's alteration and sulphide assemblage, geometry, and structural association are all consistent with a structurally-controlled orogenic gold model of deposition. Isotope studies by Downes et al (2008) and detailed field mapping of the region by Watkins (1996) support this, assigning a probable Early-Carboniferous age with mineralisation likely associated with regional deformation in a back-arc setting coeval with the development of subduction in the New England Fold Belt (Murray et al. 1987). Sulphur isotope data suggests sulphur was sourced directly from the host sequence or from sediments of the Hill-End Trough (Downes, 2008).

FUTURE WORK

Follow-up drilling programs are planned for later in the year to (i) begin testing deeper beneath current drilling; (ii) continue following shallow mineralisation along strike, and (iii) to begin investigating extensive arsenic anomalism in historical shallow aircore drilling at Springfield North (Figure 5).

The Company also plans to utilise low-detection multi-element analysis of soil samples across the entire project area. This, paired with targeted geological mapping, has the potential to lead to discovery of further economic mineralisation in addition to that defined at Springfield.

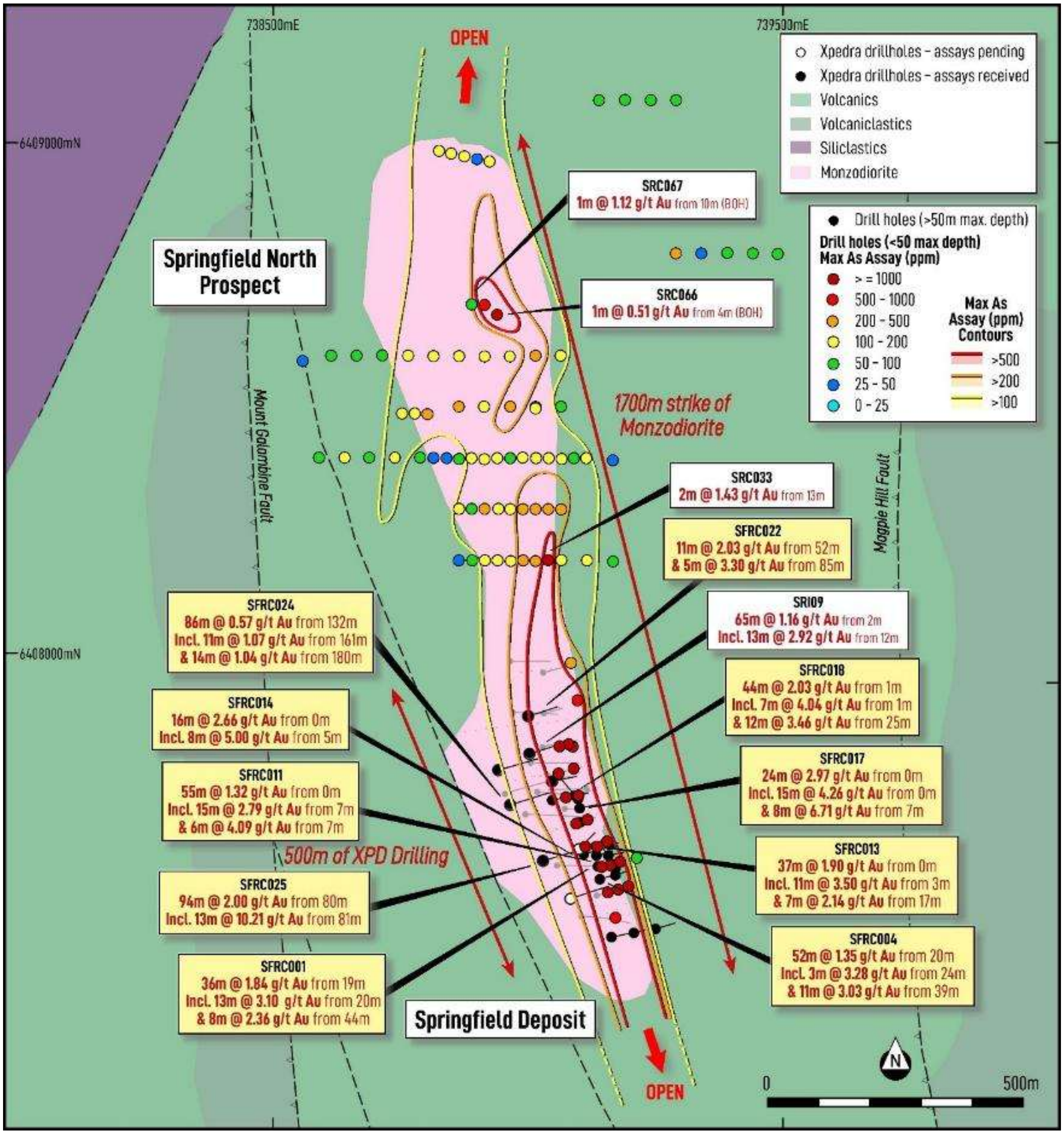

Figure 5: Recent company drilling results (yellow boxes) with select historical results (white boxes), shown with maximum-in-hole arsenic values for shallow aircore drilling across the Springfield monzodiorite.

REFERENCES

DOWNES, P.M., SECCOMBE, P.K., CARR, G.R., 2008, Sulfur- and lead-isotope signatures of orogenic gold mineralisation associated with the Hill End Trough, Lachlan Orogen, New South Wales, Australia, Miner Petrol,, 94: 151-173

DOWNES, P.M., 2019, A mineral system model for orogenic gold mineralisation in the eastern Lachlan Orogen, New South Wales, Geological Survey of NSW, (GS 2019/0173)

HAWLEY, D.L., 1990, Springfield Prospect, EL 2893 Annual Report for the period 1989-1990.

JONES, L.J., 1940, The Gulgong gold field: Department of Mines, New South Wales, Mineral Resources No.38, part 1.

KIRKPATRICK, B.L., 2003, Springfield Project, EL 5991 Annual Report for the period 2002-2003.

MURRAY. C.G., FERGUSSON, C.L., ROOD, P.G., WHITAKER, W.G., AND KORSCH, RJ., 1987, Plate Tectonic model for the Carboniferous evolution of the New England Fold Belt: Australian Journal of Earth Sciences, v. 34. p. 213-236.

RAYNER, J.M. 1940. Magnetic prospecting of the Gulgong deep leads: Department of Mines, New South Wales, Mineral Resource No. 38, part 2.

WATKINS, J. J. 1996, Regional setting of structurally hosted gold mineralisation in the Mudgee-Gulgong district, N.S.W., Master's Thesis, CODES University of Tasmania.

MT CARRINGTON GOLD-SILVER AND BASE METAL PROJECT: NEW EXPLORATION INSIGHTS AND GROWTH POTENTIAL

Thomas Wall, Chris Byrne, John Greenfield

Legacy Minerals Holdings Limited, 12/217 Howick St, Bathurst NSW 2795

Key Words: Mt Carrington, Drake, New England Orogen, Permian, low-sulphidation epithermal, intermediate-sulphidation epithermal, silver, gold, copper, caldera, scoping study

INTRODUCTION

The Mt Carrington Project is one of New South Wales's most endowed polymetallic epithermal systems, carrying a global Mineral Resource Estimate (MRE) of 47.9 Mt at 1.02 g/t AuEq for 1.57 Moz AuEq, comprising 715 Koz gold, 35.0 Moz silver, 40 Kt copper, 37 Kt lead and 164 Kt zinc (JORC 2012; LGM 2026b). The project is 5 km north of Drake in the Tenterfield Shire of northern NSW (Figure 1), within tenements EL6273, EL9616, EL9727 and assessment lease ALA75, collectively covering around 350 km² of the Permian Drake Volcanics and associated units (Figure 2).

Legacy Minerals Holdings Limited (ASX: LGM) acquired the project in March 2024 (LGM 2024a), from previous explorer White Rock Minerals Ltd (WRM). Since acquisition, Legacy Minerals has carried out systematic re-evaluation of the district's potential via generative exploration and research, leading to the May 2026 Ausenco-led Scoping Study that confirmed a compelling development case: a pre-tax net present value (NPV_7) of A$716 million, a 19-year mine life and first-quartile AISC of A$1,061/oz Au (including silver credits) at spot-case metal prices (LGM 2026a).

This paper summarises the geological setting, mineralisation controls, exploration history and key datasets that underpin Legacy Minerals exploration at Mt Carrington and outlines the development path that the company is now pursuing. The district is viewed not simply as a near-term mine, but as a large, under-explored mineral system with genuine potential for further discoveries.

Figure 1. Mt Carrington Project Location, NSW.

DECISION TO EXPLORE AT DRAKE / MT CARRINGTON

Legacy Minerals' decision to acquire the Mt Carrington tenements was largely informed by the company's experience having worked in JV with world class explorers and major miners and was driven by the observation of indicators at the early exploration stage that were suggestive of a world class deposit setting:

- Recognition of a large mineralising system footprint:
- Abundance of 100 gram x metre Au drill intercepts (greater than 100) across multiple deposits and prospects.
- Extensive km^2 scale anomalous surface geochemistry (soils and rock samples).
- Wide distribution of historic workings and multiple prospects with resources.
- Extensive km^2 scale alteration footprint across multiple prospects.
- Polymetallic intercepts showed known deposits were open in all directions (especially at depth) and this upside had been excluded from previous studies and exploration focuses,
- Historical shallow depth of drilling meant potential high-grade feeder structures had received very limited testing at depth (average depth of drilling <50m), and
- Opportunity to apply modern exploration approaches to a district that had received limited modern systematic exploration and regional prospect testing.

Previous operators had defined resources using pit-shell constraints optimised for a gold-only carbon-in-leach (CIL) operation. Thus, significant silver-dominant, zinc-lead and copper mineralisation lying outside those shells was excluded from the reported inventory. Legacy Minerals recognised that the combined JORC 2004 and JORC 2012 MRE at acquisition (356 Koz Au and 23.3 Moz Ag) did not represent the full mining potential. The broader polymetallic system remained largely untested against modern resource estimation standards and commodity prices.

Prior to the acquisition, Legacy Minerals had gained experience exploring calc-alkaline, low- to intermediate-sulphidation mineral systems. The 15-20 km diameter Drake Quiet Zone (DQZ) caldera system shares characteristics with world-class Western Pacific epithermal districts. Multi-episode calc-alkaline volcanism, abundance of D-vein style copper-gold lodes acting as vectors towards porphyry Cu-Au source rocks (Corbett and Menzies 2013), and the presence of structurally controlled silver-dominant deposits at the caldera margin (Figure 2) all point to a magmatic-hydrothermal system of considerable scale. Isotopic data now confirm a major heat and metal source below the centre of the DQZ (Quan et al., 2025), consistent with an unexposed intrusive centre driving district-scale mineralisation.

The brownfield nature of the project offered significant capital cost advantages. Existing infrastructure included near ready office and core yard set up, accommodation, helipad, sealed access roads, power to site, a cleared plant pad, near empty tailings storage facility and pre-stripped open pits. Thus, the initial capital expenditure is materially lower than for a comparable greenfield operation.

GEOLOGICAL SETTING

The Mt Carrington Project lies near the northeastern margins of the southern New England Orogen (NEO), the easternmost tectonic element of the Palaeozoic Tasmanides. The NEO extends from eastern Queensland through northern New South Wales and hosts numerous major gold, silver and base metal deposits, including Cracow (2.5 Moz Au; Worden & Shepherd 2016), Mt Carlton (1.2 Moz Au, 12 Moz Ag; Sahlström 2018), Mt Rawdon (2.5 Moz Au; Howard 2015) and Mt Morgan (8 Moz Au; Taube 1986).

Mineralisation during the mid to late Permian along the NEO formed during back-arc extensional volcanism along the eastern margin of Gondwana (Jessop et al. 2019). Extension produced rift-related volcanic basins in which subaqueous to subaerial bimodal magmatism deposited thick sequences of andesite flows, dacitic to rhyolitic volcaniclastics and associated sub-volcanic intrusions, which are the principal hosts to epithermal Au-Ag-Cu-Pb-Zn mineralisation (Rosenbaum 2026).

The Drake Volcanics form a NW-trending corridor approximately 60 km long and 10 km wide within the Wandsworth Volcanic Group. U-Pb zircon geochronology constrains the eruption of the Drake Volcanics to ~264-265 Ma (Waltenberg et al. 2016) and $^{40}Ar/^{39}Ar$ plateau ages have a range of ~269-251 Ma (Quan 2022). The sequence is defined as a complexly interbedded assemblage of rhyodacitic to andesitic flows, tuffs, breccias and volcaniclastics, deposited into a shallow marine environment (Barnes et al. 1991). It unconformably overlies the Early Permian Emu Creek Formation and Razorback Creek Mudstone to the east and is conformably overlain by the Gilgurry Mudstone (Brown et al. 2001). The western boundary is marked by the Demon Fault and the Early Triassic Stanthorpe Monzogranite. Permian and Triassic granitoid plutons, including the Dumbudgery Creek Granodiorite, Bruxner Granodiorite, Morgans Creek Leucomonzogranite, Yellow Gully Syenogranite, and Bungulla Monzogranite intrude the sequence (Brown et al. 2001). The eastern side of the Drake Volcanics are unconformably overlain by Jurassic sedimentary rocks of the Clarence-Moreton Basin.

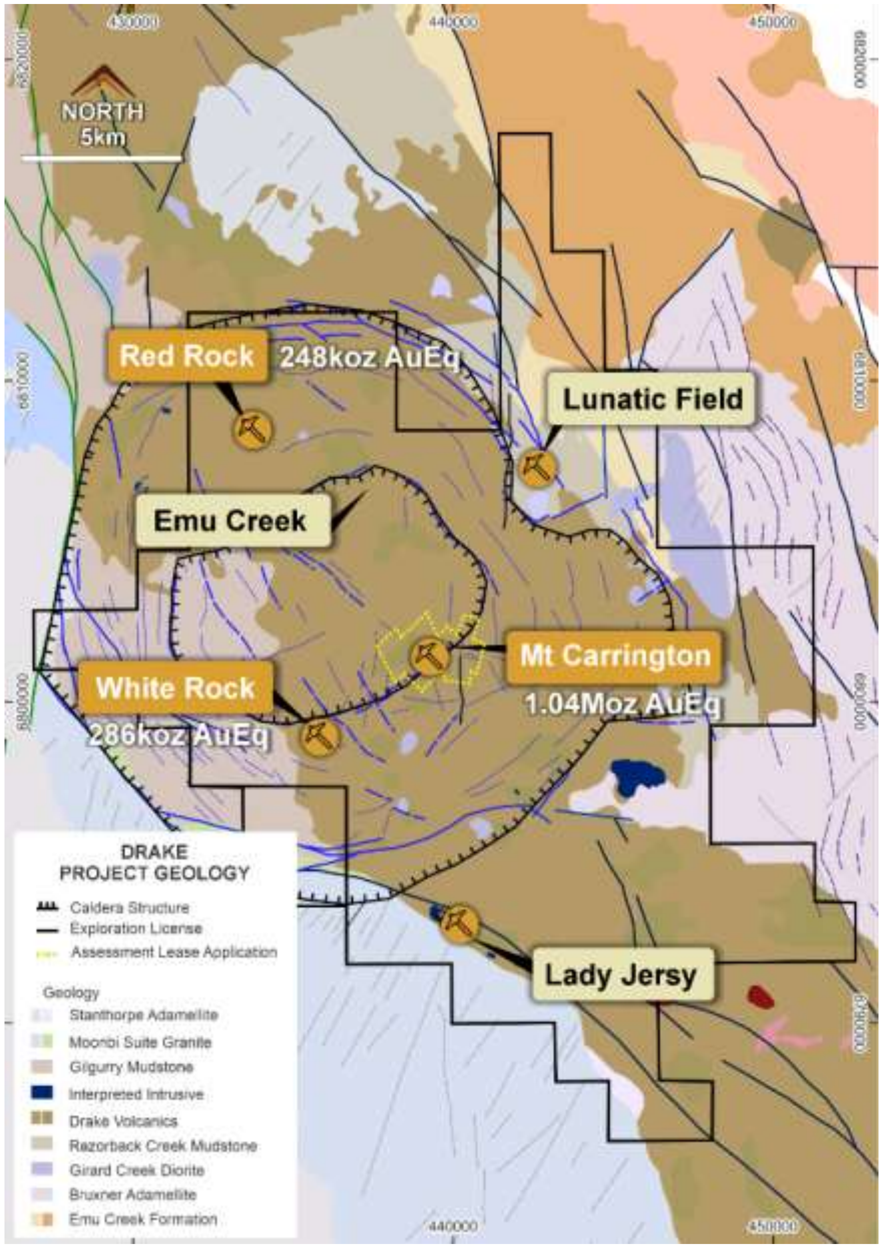

Figure 2. Drake Project area showing deposits and major prospects.

LOCAL GEOLOGY

The volcanic architecture of the Drake Volcanics records at least three distinctive eruptive events (Cumming 2011). The first was dominated by coherent basaltic to andesitic lavas, dykes and sills with associated volcaniclastics, followed by slope collapse and debris flow/avalanche deposits. Rhyolite and dacite domes were then emplaced in the west of the Drake caldera. The third and most volumetrically significant event comprised widespread rhyolitic and dacitic volcanism, primarily as extensive tuff-breccias interpreted as caldera-forming eruption products (predominantly dacitic with minor rhyolitic units). Emplacement of rhyolitic-dacitic lavas and synvolcanic intrusions related to caldera resurgence followed, culminating in quiescent shallow-water sedimentation. Regional low-grade greenschist metamorphism and very weak regional deformation have gently tilted the entire succession (Cumming, 2011).

Cumming (2011) subdivided the Drake Volcanics into five stratigraphic facies associations (DV1 to DV5, oldest to youngest). There is a broad progression from mafic to felsic volcanism followed by epiclastic deposition, summarised in Figure 3.

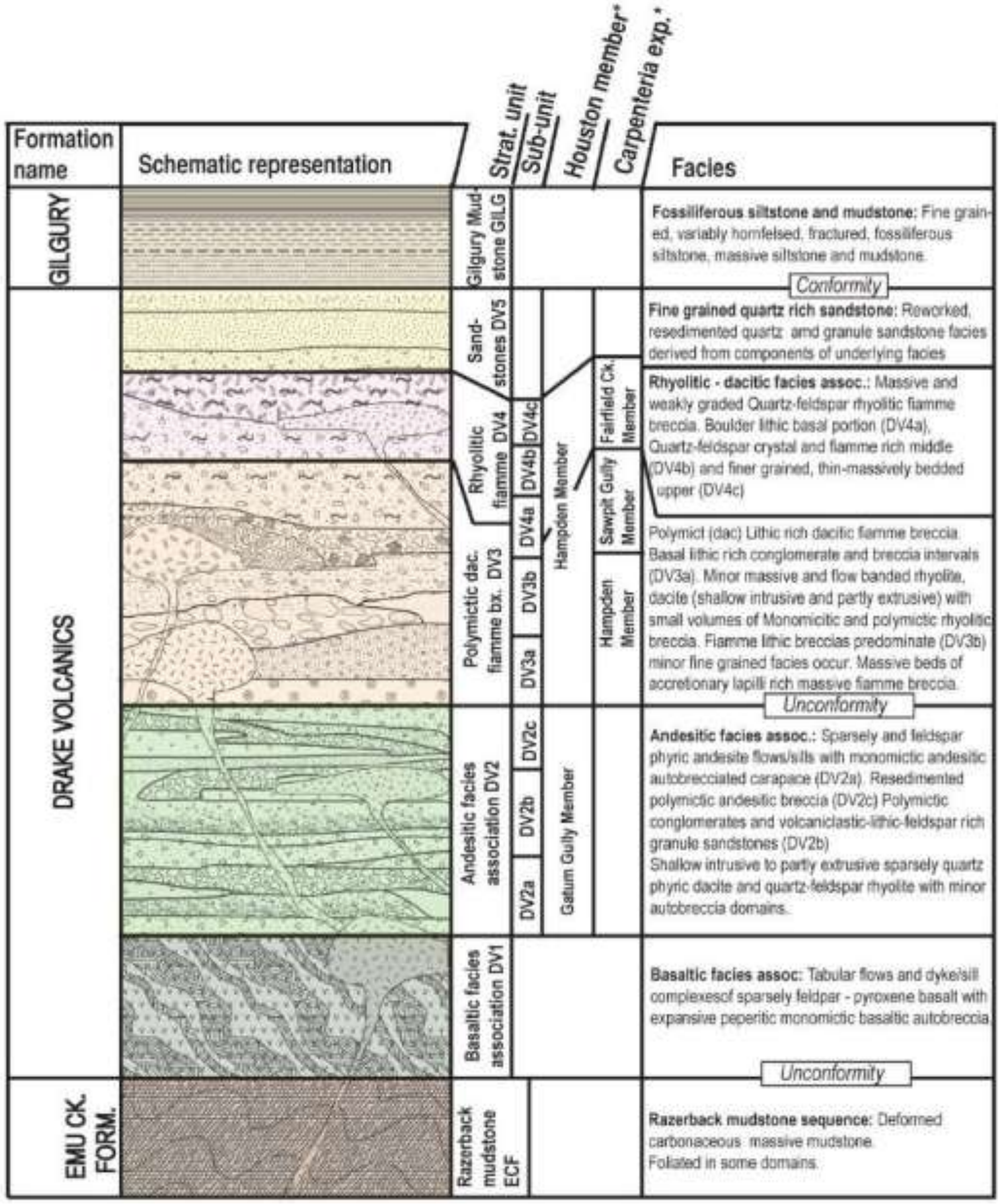

Figure 3. Stratigraphic framework for the Drake Caldera (Cumming 2011) showing schematic lithofacies and major facies associations for each unit. Previous subdivisions from Offenberg and Cochrane (1975) and Houston (1983) are included on separate columns.

The sequence is intruded by subvolcanic flow-laminated rhyolites and coarse to fine-grained diorite intrusions, with conjugate NE-NW basalt to diorite dykes cross-cutting the succession (Figure 4; Cumming 2011). Lithologies include porphyritic lavas, rhyolitic to andesitic crystal-lithic tuffs, breccias and agglomerates, with epiclastic rocks including breccias, conglomerates, sandstones and mudstones with marine fossils (Barnes et al. 1991).

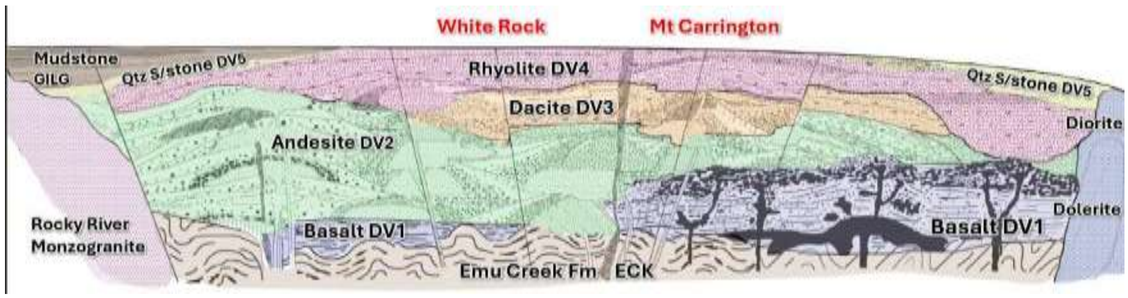

Figure 4. Schematic cross-section across the Drake Caldera showing lithofacies distribution (Cumming 2011).

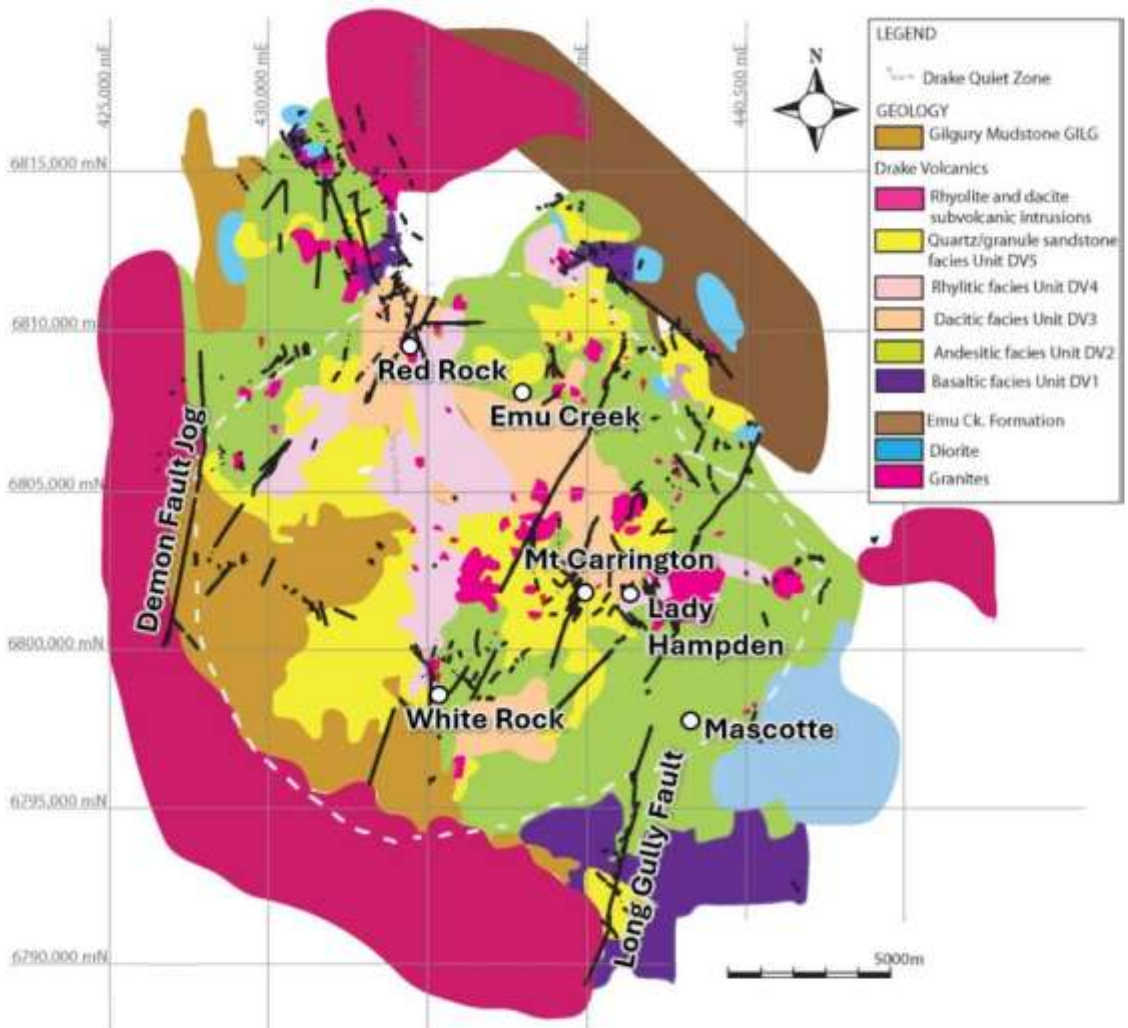

Figure 5. Lithofacies map across the Drake Caldera (Cumming 2011). Significant faults shown in black.

Structure

The Drake Volcanics have not undergone significant deformation, with bedding upright and generally dipping 20-30° to the east. The main structural feature, which hosts most of the mineralisation, is the Drake Quiet Zone (DQZ), first documented by Houston (1993) as a 15-20 km diameter circular aeromagnetic low (Figure 5). Considered to represent a volcanic caldera, the DQZ was studied by Davies (2010) who reprocessed geophysical data and identified concentric faults and radial fractures marking the caldera perimeter, and an inner structural domain representing a coherent anomaly with clear boundaries (inner caldera margin shown in Figure 2). An interpreted switching of fault polarity between outer margin faults and those bounding the inner domain suggests the presence of an uplifted central zone (Davies 2010). This was later corroborated by Cumming (2011) who recognised rhyolitic fiamme breccias (unit DV4) that were produced from large volume explosive eruptions, which either predated or accompanied incremental caldera collapse. Explosivity was followed by rhyolite/dacite dome and andesite sill/dome growth and caldera resurgence focussed in the central zone accompanied by low angle extensional faults (e.g., the Red Rock area and Mascotte area).

Extensional (normal) faults, dominate the structural framework and provided the principal pathways for mineralising hydrothermal fluids. Strike-slip (wrench) faults, particularly the dextral Demon Fault system, controlled NNE-trending mineralised trap sites, e.g. the Long Gully Fault at Mt Carrington (Davies 2010). The NNE-trending Long Gully Fault (Figure 5) is parallel to a jog segment of the Demon fault that bounds the western side of the caldera. MT data shows the Long Gully Fault to be a coherent conductive lineament to at least 1.5 km depth (Figure 9).

At the prospect scale, Hammond (2005) proposed that sub-volcanic dome emplacement drove local uplift of fault-bounded blocks, with structures adjacent to emplacement pathways activated by local extension (Figure 6). Corbett and Menzies (2013) noted mineralisation physically trapped by bedding planes, sigmoidal tension veins and brecciated brittle silicified rocks.

MINING AND EXPLORATION HISTORY

Gold was first discovered in the Drake district in 1853, and silver first found at Boorook in 1878, but the productive era began in earnest in March 1886 with the discovery of the gold-bearing Adeline Reef, shortly followed by discoveries at Mt Carrington, White Rock, Lady Jersey, Mascotte and Red Rock (Andrews 1908). Most deposits were discovered and developed between 1886 and 1888, with production dominated by near-surface secondary mineralisation. Polymetallic ore containing copper, gold, silver, lead and zinc was characteristic from the outset. Historical production from the nineteenth and early twentieth centuries is estimated at approximately 62,000 oz Au and 0.5 Moz Ag, though water ingress and metallurgical problems with complex sulphide ores limited the depth and longevity of many operations (McQueen 2017).

Modern exploration and mining resumed in the late twentieth century. Between 1969 and 1972, approximately 10,000 t of mixed sulphide ore were mined at Emu Creek and Red Rock by Mt Carrington Mines Ltd. Between 1988 and 1990, approximately 233,000 t of ore grading 2.38 g/t Au and 7.44 g/t Ag were mined by open cut. Total twentieth-century production is recorded at approximately 28,000 oz Au and 1 Moz Ag (McQueen 2017).

Significant exploration was conducted by Aberfoyle, MCM, CRAE, Drake and Rex Minerals Ltd (ASX: RXM), with RXM announcing JORC 2004 gold-silver MREs in 2008 for the Strauss, Kylo, Guy Bell, Lady Hampden, Silver King and White Rock deposits. White Rock Minerals Ltd (ASX: WRM), spun out of Rex in 2012, upgraded and expanded the MREs through diamond drilling campaigns. This culminated in JORC 2012 MREs for Kylo and Strauss and Prefeasibility Studies (2017 and 2020) centred on a modest CIL gold-only operation. Thomson Resources Ltd (ASX: TMZ) announced a JORC 2012 polymetallic MRE for Strauss and Kylo in 2022, though this remained conservative as it was constrained by WRM's gold-only pit shells.

WRM entered administration in 2023, and Legacy Minerals acquired 100% of the project tenements in March 2024 (LGM 2024a). The August 2026 MRE update delivered the current global resource of 1.57Moz AuEq, constituting the most comprehensive estimate of the district's endowment to date (LGM 2026b).

MINERALISATION

Base metal and precious metal (Au-Cu-Pb-Zn-Ag) mineralisation is abundant in the Drake Volcanics and encompasses a wide range of occurrence types, with over 3000 mine workings identified, including 11 deposits with reported production (Brown et al. 2001). The mineralisation is multi-stage, with an early pyritic stage overprinted by later base and precious metal stages (Bottomer 1986), occurring as steep-dipping fissure veins, stockworks, breccia matrix and disseminations within intrusions and permeable volcaniclastics (Offenberg and Cochrane 1975; Quan 2022). Mineralisation is commonly located in and around the margins of felsic sub-volcanic domes, intruded during late caldera resurgence (Houston 2010, Cumming 2011).

Based on available U-Pb zircon dating (Waltenberg et al. 2016) and Ar-Ar plateau ages (Quan 2022) mineralisation at Drake was directly associated with the main stage of volcanism at around 265 Ma, followed by minor silver mineralisation in the White Rock area associated with a distinctive later hydrothermal event around ~251 Ma (Quan 2022).

Economic mineral deposits can be divided into Au(-Cu) rich (Mt Carrington gold group- Strauss, Kylo, Guy Bell, Carrington, Gladstone; Red Rock; Adeline; Lady Jersey; Border Chief; Nobles Creek), and Ag(-Au) rich (Mt Carrington silver group- Lady Hampden, Silver King, Mozart, Lead Block; White Rock, White Rock North; Mascotte). Outside of this dichotomy is Emu Creek Mine, which is Cu-rich with Zn(-Mo) credits (Brown et al. 2001).

Typical mineralisation mineralogy comprises, in approximate paragenetic order: pyrite, galena, sphalerite, chalcopyrite, electrum, and tennantite-tetrahedrite (Herbert 1983; Smith 1989; Quan 2022). Smith (1989) defined four stages of mineralisation: (1) quartz-hematite brecciation and veining; (2) sphalerite ± pyrite-galena veining; (3) quartz-chalcopyrite-tennantite-pyrite ± bornite-hematite-electrum; and (4) quartz-chalcopyrite-pyrite ± carbonate.

Mineralisation shares affinity with intermediate- (Au-rich deposits) to low-sulphidation (Ag-rich deposits) epithermal deposits. Fluid cooling or mixing rather than boiling interpreted as the dominant metal deposition mechanism, particularly in Au-rich-deposits. Stable isotopic data from Quan et al. (2025) suggest a district-scale spatial zonation: Au-Cu intermediate-sulphidation deposits are concentrated within the centre of the DQZ, reflecting a dominantly magmatic fluid source with limited meteoric mixing (Gulson and Bottomer 1984); while Ag low-sulphidation epithermal deposits occur at the periphery, where greater meteoric water mixing resulted in larger $\delta^{34}S$ and $\delta^{18}O$ variations. This concentric Au-Ag zonation, centred on the DQZ, is consistent with a major heat and metal source below the centre of the caldera, with the Red Rock area potentially hosting a second, localised heat source (Quan et al. 2025).

Madayag (2020) classified the Au-rich Strauss deposit as an intermediate-sulphidation epithermal deposit based on the dominant sulphide assemblage of pyrite, chalcopyrite, sphalerite and galena with minor tennantite-tetrahedrite, Fe-poor sphalerite composition, and stable isotope evidence for a magmatic sulphur source (Figure 7).

At the deposit scale, the silver-rich White Rock and White Rock North deposits carry Ag sulphosalts including members of the Ag-Cu-As-Sb polybasite-pearceite group, while tennantite dominates at Lady Hampden and Silver King (Figure 8). Low-temperature (<177°C) jalpaite (Ag-Cu) was identified for the first time in the White Rock and White Rock North deposits by Lay (2019). White (2017) suggested the distribution of silver in the White Rock field is largely controlled by lithology, defined by low Zr units (reflecting less fractionated magmas) and distinct permeability contrasts in stratigraphic units.

For the silver-rich deposits, Lay (2019) constrained the ore-forming fluid temperature evolution from approximately 300°C for gold deposition, declining to 200–250°C for sphalerite and galena, and 117–197°C for silver mineralisation. Mineralisation within the deposits occurred in separate discrete hydrothermal convective cells for the White Rock field and the Silver King–Lady Hampden field.

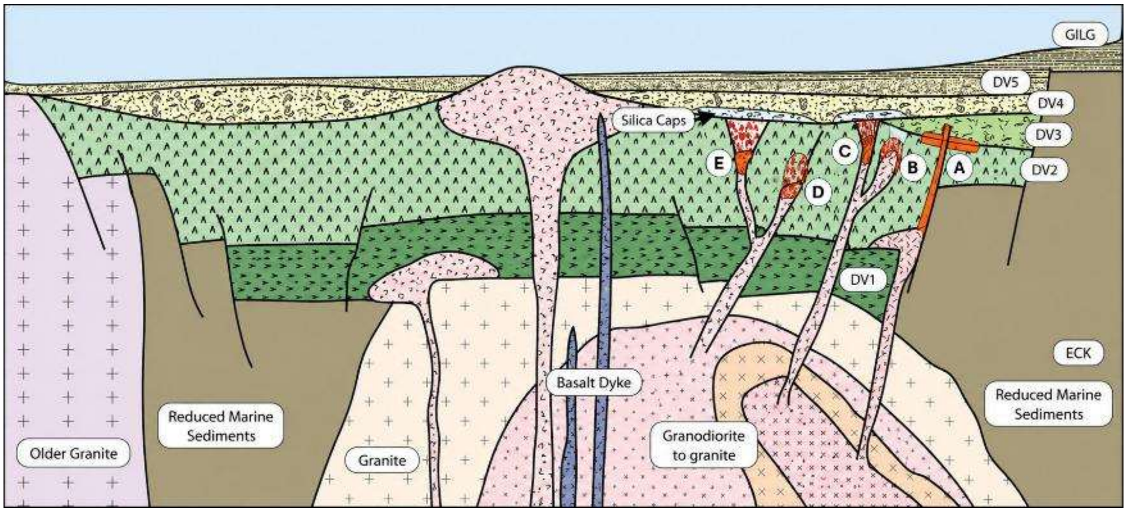

Figure 6. Schematic lithofacies setting of major deposits in the project area (based on Cumming 2011; Corbett & Menzies 2013). A - Silver King, B – Strauss, C – White Rock, D – Gladstone, E – Red Rock. See Figure 3 for lithofacies descriptions and Figure 5 for deposit locations.

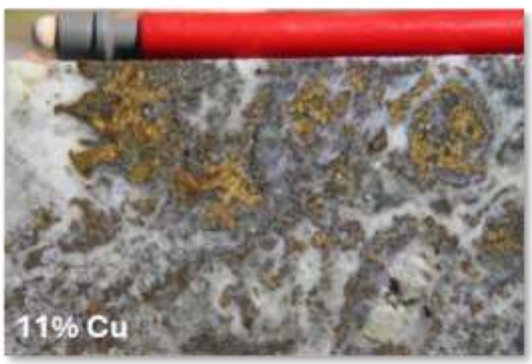

Quartz vein comprising quartz-pyrite-chalcopyrite – KYDD001 62.5m, **11.9% Cu**, 2% Zn.

Quartz-sulphide vein in andesite porphyry - KYDD011, 140.5m, **99.7g/t Au**, 3.17% Cu & 231g/t Ag.

Vein comprising banded quartz-pyrite-pale sphalerite and local galena-Ag sulphosalts – SRDD006, 89m, **18.6g/t Au** & 9.6% Zn

Quartz-polymetallic Au-Ag lode from the Strauss pit area. SRDD001, 30.1m, **21.9 g/t Au**.

Figure 7. Core photographs showing textural examples of the major gold dominant deposits (Corbett 2008, 2011, Corbett & Menzies 2013). Strauss and Kylo are part of the cluster of deposits collectively called Mount Carrington.

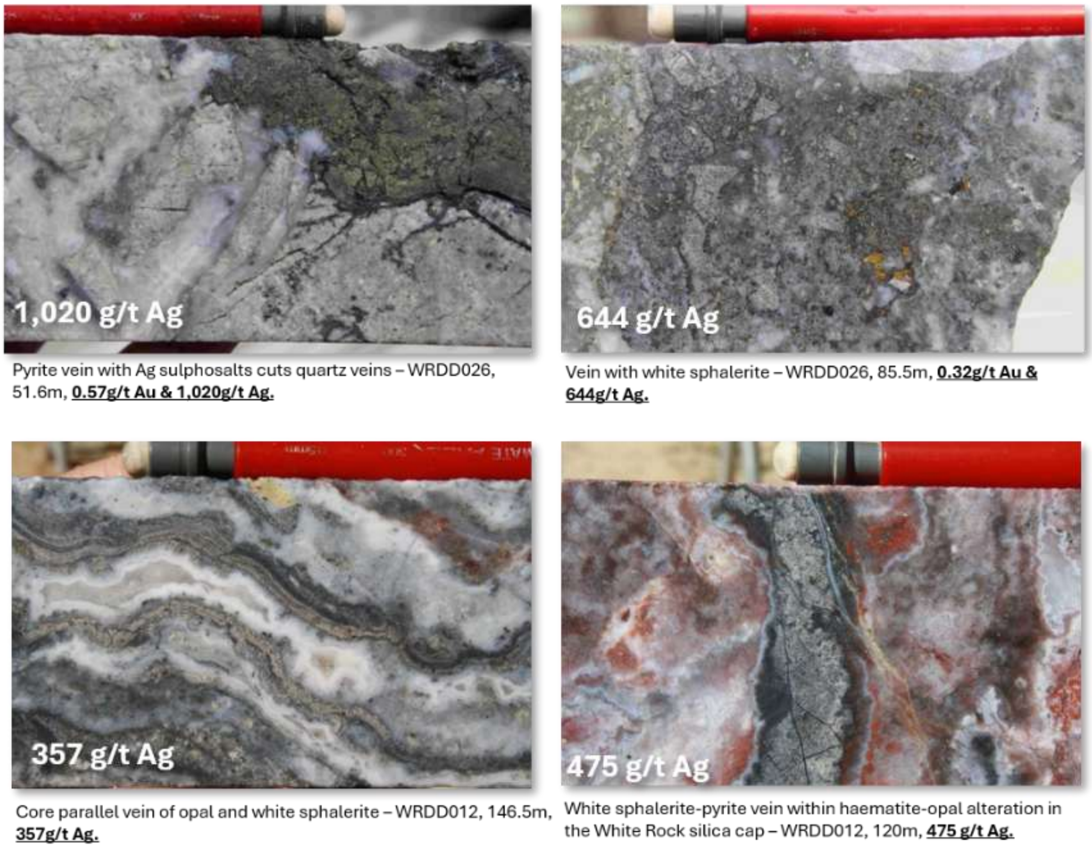

Figure 8. Core photographs showing textural examples of the silver dominant deposits at White Rock (Corbett, 2011, Corbett & Menzies 2013).

ALTERATION

The principal alteration facies in the Drake Goldfield are widespread argillic, locally pervasive phyllic (with associated silicification), and propylitic (Herbert, 1983; Bottomer, 1986; Perkins, 1987; Chomiszak, 2016; Zhang, 2016; White, 2017; Madayag, 2020; Quan, 2022).

Argillic alteration is widespread across the DQZ and is dominant in the Cu prospects. Illite-quartz argillic alteration is ubiquitous, with quartz-illite-clinochlore and quartz-illite-kaolinite/dickite assemblages identified at Gladstone, Kylo and Strauss, the latter indicating more acid pH conditions (Corbett and Leach, 1998). Rare advanced argillic minerals (kaolinite, dickite) occur in Cu- and Au-dominant deposits. The alteration facies can be separated into clay-dominant (illite/muscovite, kaolinite) facies reflecting fluid-buffered conditions, and adularia-dominant facies reflecting rock-buffered conditions. Mapping the K gradient between these facies is important for mineralisation vectoring (Quan, 2022).

Phyllic alteration (sericite-pyrite-quartz-chlorite-carbonate) is also locally pervasive, forming at temperatures of 200–250°C and pH 4–5. The transition from illite to muscovite marks the argillic-to-phyllic boundary at approximately 200–300°C (Lay 2019). Propylitic alteration (quartz-chlorite-epidote-zeolite-calcite-dolomite-adularia-albite-pyrite) occurs in localised zones at Mozart, White Rock, Silver King, the upper part of Lady Hampden, and the basal parts of Strauss and Kylo, indicating peak fluid temperatures above 240°C in near-neutral pH waters. Propylitic alteration is commonly overprinted by both phyllic and argillic alteration.

Deposit-scale alteration sequences differ between the Au-Cu dominant and Ag-dominant groups. At Strauss, at least three mineralisation events and multiple alteration events have been identified, with argillic alteration and mineralisation intimately connected (Madayag, 2020). At White Rock and White Rock North, intense and pervasive silicification and illitisation are prominent, with at least two phases of argillic alteration: chlorite ± carbonate ± illite near surface, and adularia ± carbonate ± illite at depth, while advanced argillic alteration is limited to zones with intense silicification (Chomiszak, 2016). At Lady Hampden, three alteration stages are defined: early propylitic (epidote ± clinochlore ± albite), pervasive illitisation (illite ± alunite ± carbonate), and late phyllic alteration (quartz ± pyrite ± muscovite), with mineralisation largely associated with the late phyllic stage (Zhang, 2016).

Despite the detailed alteration characterisation available, at the scale of the Drake Goldfield there is presently no definitive relationship between lithology or alteration assemblage and mineralisation that can serve as a simple vector (Quan 2022). The extremely widespread argillic alteration assemblage across the entire DQZ limits its utility as a proximity indicator. LGM is currently working with CSIRO to investigate future vectoring work. Based on current research, K-gradient (clay-to-adularia ratio), isotopic signatures and structural position provide the best promise as reliable mineralisation vectors (Quan 2022).

GEOCHEMISTRY

The bulk chemistry of the Drake Volcanics varies from rhyolitic to andesitic, mostly dacitic to andesitic, showing typical calc-alkaline trends (Barnes et al. 1991; Cumming 2011). Herbert (1983) identified a Na-rich series in the dacitic, rhyodacitic and rhyolitic tuffs. The calc-alkaline Drake Volcanics formed in a continental arc environment during the late Permian (~265 Ma), with Dy/Dy* vs. Dy/Yb relationships indicating that clinopyroxene/amphibole fractionation had a major effect on source magmas rather than garnet fractionation (Quan 2022). The dacitic and andesitic tuffs in the Ag-rich deposits (Lady Hampden, Mozart, Silver King, White Rock North) show two distinguishable fractionation trends, suggesting derivation from different magmatic sources (Quan 2022).

Multi-element geochemical surveys cover most of the project area, with stream sediment, soil and rock chip datasets providing first-pass anomaly definition. At White Rock North, elevation of As, Hg in soil data define the distal geochemical footprint, with elevated Sb and Mo in drill samples defining the proximal signal (Houston 2010).

Drillcore geochemistry of Drake mineralisation displays systematic spatial zonation consistent with a caldera-hosted dome-related low-sulphidation epithermal system (Corbett and Menzies 2013). Core-to-margin zonation broadly follows: Cu ± Bi ± Te (proximal, near domes and D veins) → Zn-Pb-Ag → As-Sb → Ca ± Hg (distal). D vein lodes at Gladstone carry strongly elevated Bi, consistent with proximal quartz-sulphide Au ± Cu mineralisation formed at depth close to intrusion source rocks.

Carbon and oxygen isotope studies of vein carbonates confirm a mantle-derived carbon source with limited meteoric mixing (Quan et al. 2025). Au-Cu dominant deposits (except Red Rock) show an initial magmatic origin for late-stage fluids, which then mixed with fluids associated with low-temperature alteration. $\delta^{34}S$ values for sulphides in Au-Cu deposits cluster close to 0‰, confirming a predominantly magmatic sulphur source. In contrast, Ag-dominant deposits and the Red Rock deposit show greater meteoric water mixing, reflected in larger $\delta^{34}S$ and $\delta^{18}O$ variations. This isotopic distinction confirms the district-scale Au-Ag zonation described above and provides a geochemical vectoring framework: deposits with magmatic-dominant isotopic signatures indicate proximity to the central heat source, while mixed-fluid signatures characterise the peripheral Ag-enriched zone.

Late-stage carbonates (ankerite, calcite, dolomite, magnesite, siderite) across the goldfield are characterised by wide $\delta^{18}O$ variation but a relatively narrow $\delta^{13}C$ range, reflecting fluctuating Mg/Ca ratios and disequilibrium assemblages from multiple fluid sources. These carbonates post-date the main mineralisation events and are not directly related to ore deposition (Quan et al. 2025).

GEOPHYSICS

Close-spaced airborne magnetic data provide the primary framework for geological interpretation at district scale. The dominant aeromagnetic expression in the centre of the sequence is the Drake Quiet Zone (DQZ), a 15-20 km diameter circular feature of low magnetic signature, interpreted as a semi-resurgent collapse caldera filled with less magnetic volcanics than the surrounding terrain (Houston 1993).

Within the DQZ, discrete magnetic highs define intrusive dome complexes and dyke swarms, while circular and arcuate features map caldera ring fractures and structural corridors that focused hydrothermal fluids (Davies 2010). Airborne radiometrics showed K and K/Th highs, and U/K lows in radiometric data. Strong K-rich responses occur at Mt Carrington and Emu Creek, possibly reflecting surface argillic alteration. Also, K-rich highs define the prominent NNW structures, and K-poor zones are related to Th-rich Gilgurry Mudstone and early andesite units.

Airborne gravity data define significant NNE-trending structural corridors, including a major gravity break at the southern caldera margin (Corbett and Menzies 2013). The data also highlight a low-density substrate below a line that divides the DQZ into low northeastern and high southwestern halves. This asymmetry in the gravity signature was interpreted by Davies (2010) to infer that greater subsidence (collapse?) occurred in the northeastern parts of the DQZ.

Expert Geophysics Pty Ltd. conducted a helicopter-borne MobileMT electromagnetic and magnetic survey over the Drake project over a 298 km^2 area (Figure 7). The survey consisted of 1642 line-km flown with a 200m East-West line spacing between February and April 2025 (LGM 2025). The results from the Airborne MT survey have revealed an excellent correlation between known mineral deposits and more conductive bodies and linear trends, particularly imaging the Long Gully Fault as a >1km deep conductive structure.

Airborne EM (DIGIHEM) was also flown across the DQZ, defining conductive anomalies along the outer caldera margin plus Mount Carrington. Electrical (IP, MIMDAS) surveys over the main prospects defined high chargeability, low resistivity anomalies associated with disseminated to stockwork pyrite in phyllic-altered zones peripheral to economic mineralisation. Resistivity does sometimes show areas of known mineralisation as resistivity highs due to silicification of the host rock (Houston 2010).

Light detection and ranging (LiDAR) topography survey was conducted over the DQZ and proved very effective at seeing outcrops, bedding and structural trends, as well as drill-pads, costeans and old mine workings (LGM 2024b). The survey detected over 3,367 historical mining features.

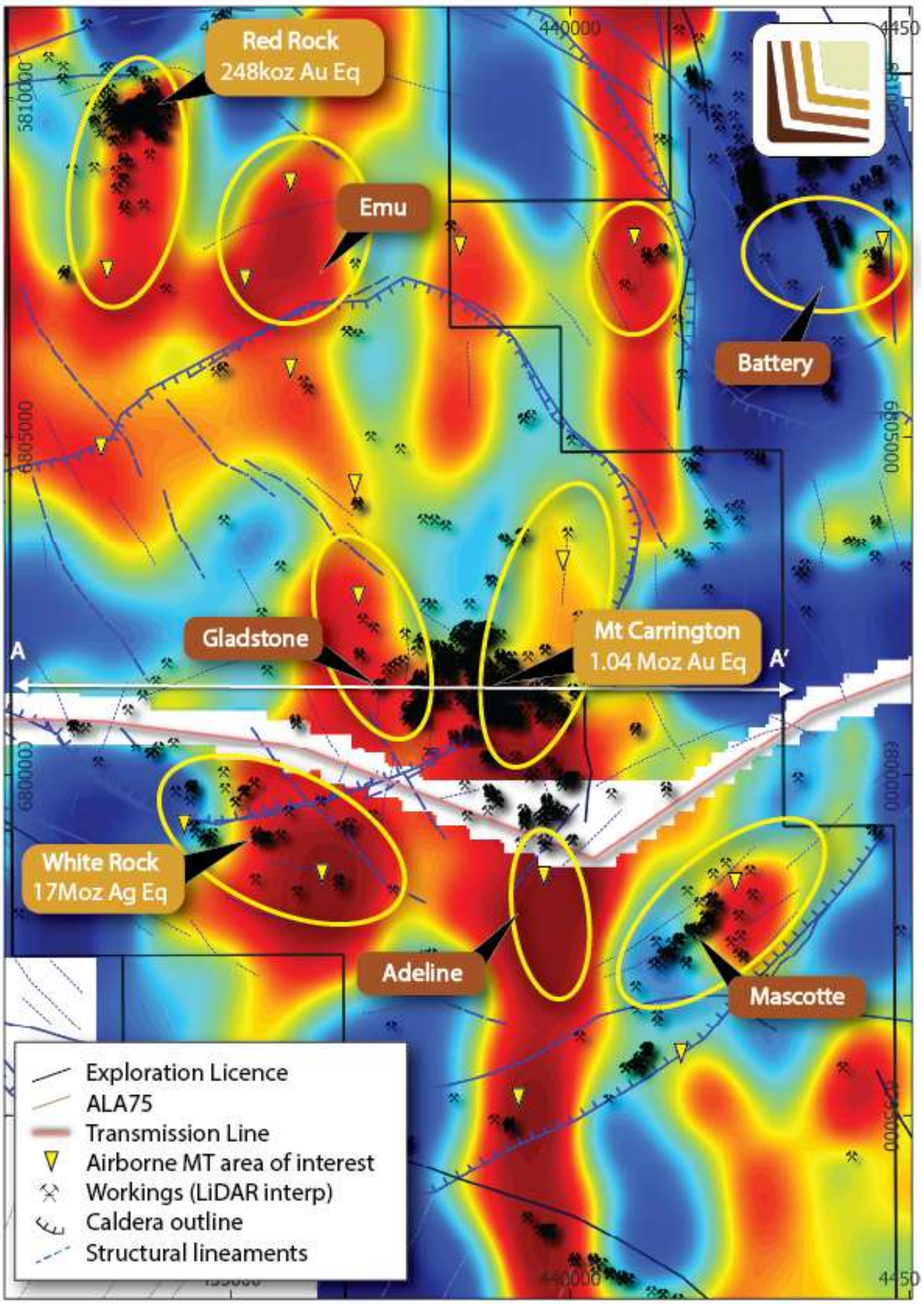

Figure 9. Plan view of fluid flow interpretation over regional Airborne MobileMT (-500mRL) with powerline interference removed through central portion of survey (white area). Priority areas of interest shown (yellow triangles and outlines).

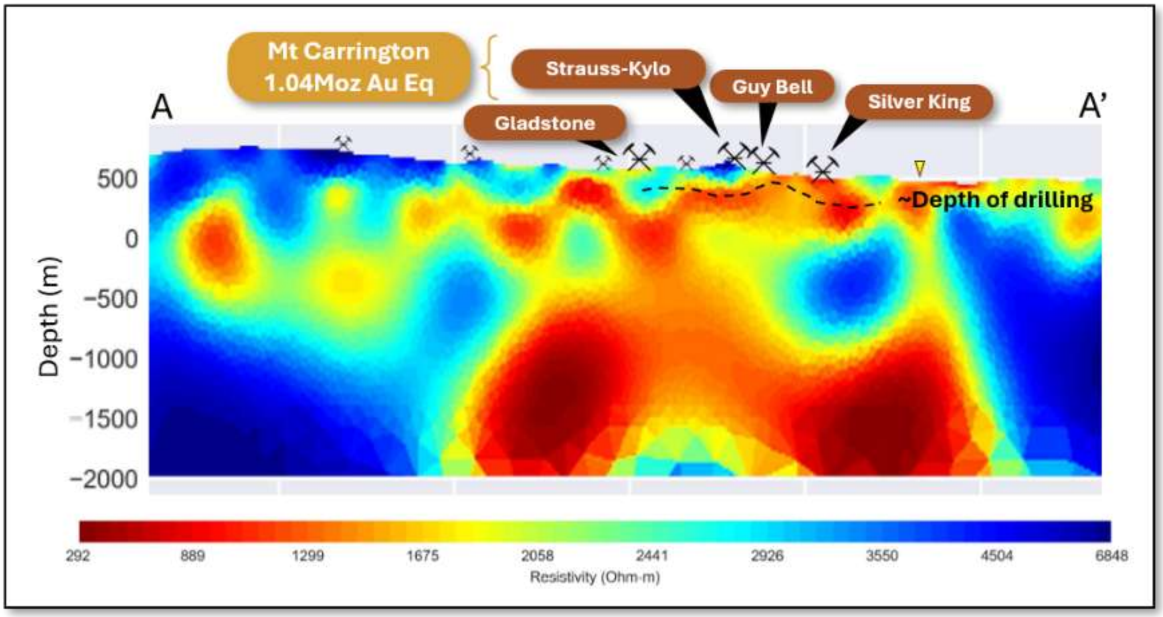

Figure 10. Airborne MT (LGM 2025) conductivity cross-section (A-A' in Figure 9) through the Mt Carrington Group of prospects, historic workings and new areas of interest (yellow ovals).

RECENT EXPLORATION

Since acquisition Legacy Minerals has pursued a systematic program assessing the full caldera-scale and designed to test the district's polymetallic potential beyond the historically focused gold-only pit shells. To date, each new drill campaign has converted a priority target into a new mineralisation discovery. The close-spaced airborne MobileMT and DIGIHEM surveys (LGM 2025), integrated with reprocessed radiometrics and gravity, surface geochemistry and the LiDAR-mapped historical workings (LGM 2024b), generated a ranked pipeline of targets across the DQZ (Figure 7). Prospects were prioritised that combine proximity to a coherent conductive MobileMT lineament, historical workings, surface geochemical anomalism and elevated K/Th radiometric response. At Mascotte, approximately 5 km south of the Mt Carrington deposits along a 1.3 km line of historical workings, a maiden eight-hole diamond program (MSDD001 to MSDD008, 1,841 m) confirmed a new low-sulphidation epithermal gold-silver discovery, with significant intercepts of 40 m at 1.0 g/t Au from 151 m in MSDD001, 3 m at 3.3 g/t Au from 167 m in MSDD007, and a high-grade polymetallic breccia of 2 m at 9.4% Pb, 4.7% Zn and 22.8 g/t Ag from 180 m in MSDD003 (LGM 2026d). The mineralisation remains open along strike and at depth.

The discovery pattern has been repeated at the copper-gold targets. At the Battery prospect, a porphyry-epithermal copper-gold target originally identified by CRA Exploration marked the first regional target tested at Mt Carrington in three decades (LGM 2026c; Figure 9) and intersected wide zones of copper mineralisation associated with sheeted quartz-pyrrhotite-chalcopyrite veining, returning 52 m at 0.15% Cu from 142 m within a broader 95 m at 0.13% Cu (uncut) from 114 m in BCDD002, which the company considers indicative of intrusion-related copper (gold) system mineralisation (LGM 2026c). Drilling has since extended to the Emu copper-gold prospect, the first drilling there in approximately 50 years, testing porphyry-epithermal targets adjacent to the district's largest historical copper mine (LGM 2026e). Within roughly twelve months, systematic modern exploration has therefore delivered a new gold-silver discovery at Mascotte and wide copper mineralisation at Battery from targets that had been untested for decades, demonstrating that the caldera hosts additional mineralised systems and underpinning the importance of the company's dual-track strategy of resource growth within the defined deposits and new discovery focus across the wider caldera.

RESOURCE, DEVELOPMENT AND THE FUTURE

The global MRE (August 2026, JORC 2012) for the Mt Carrington Project totals 47.9 Mt at 1.02 g/t AuEq for 1.57 Moz AuEq, comprising 715 Koz gold, 35.0 Moz silver, 40 Kt copper, 37 Kt lead and 164 Kt zinc (LGM 2026b). The resource is broadly divisible into four groups:

- Gold-rich resources (Strauss, Kylo, Guy Bell, Carrington, Gladstone): 18.6 Mt at 1.02 g/t AuEq for 607 koz AuEq, with Indicated category in Strauss and Kylo. Hosted predominantly in DV2–DV3 andesitic to dacitic tuffs.
- Silver-rich Mt Carrington Group (Lady Hampden, Silver King, Mozart, Lead Block): 11.8 Mt at 70 g/t AgEq for 27 Moz AgEq; dominated by resources at Lady Hampden and Silver King. Hosted in DV2–DV3 andesitic tuffs with bedding-parallel structural control.
- Red Rock Group: 10.2 Mt at 0.76 g/t AuEq for 248 koz AuEq; entirely Inferred, hosted in NS-trending structural corridors at the northern caldera margin, with high conversion potential given the structurally continuous mineralisation style and possible second heat source (Quan et al., 2025).
- White Rock Group (White Rock and White Rock North): 7.3 Mt at 72 g/t AgEq for 17 Moz AgEq. Hosted in DV4 rhyolitic breccias and tuffs.

The May 2026 Ausenco-led Scoping Study confirmed the financial robustness of a conventional 1 Mtpa open-pit, cyanide-free flotation operation targeting gold and silver from 17.04 Mt of plant feed across eight shallow pits (LGM 2026a). Key financial outcomes at the May Spot Case (Au A$6,500/oz, Ag A$105/oz) include a pre-tax NPV_7 of A$716 M, a pre-tax IRR of 38%, a payback period of 32 months from first production and a life-of-mine AISC of A$1,061/oz Au – first quartile globally. Initial capital expenditure is A$220.5 M, leveraging the brownfield site infrastructure and grid power connection. The Scoping Study explicitly excluded zinc, lead and copper credits (approximately 180 kt Zn-Pb-Cu in the 2025 MRE), the White Rock North silver resource, and mill throughput above 1 Mtpa – all representing near-term value-uplift opportunities.

Legacy Minerals is now advancing Mt Carrington toward an updated Scoping Study prior to initiating a Pre-Feasibility Study (PFS). The updated Scoping Study will include the large increase in Indicated Resources and will assess potential increases to the mill throughput and potential improvements to the mining schedule and processing. Key workstreams post-delivery of the updated Scoping Study will include targeted extensional resource drilling, infill drilling to convert further Inferred to Indicated Resources, geotechnical and hydrological studies, metallurgical test work across all principal ore types, and offtake discussions with potential concentrate buyers.

In parallel, Legacy Minerals is pursuing a broader exploration program targeting the under-explored portions of the caldera system. The Emu, Battery and Mascotte prospects represent the most immediate new discovery opportunities. The copper corridors at Gladstone and along the Mt Carrington trend have not been systematically drill-tested and have potential for both open-pit and underground mining targets and potential for a porphyry Cu-Au source (Corbett and Menzies, 2013).

The primary conceptual target at Drake represents high-grade gold-silver epithermal veins formed from fluids from deeper buried intrusion source rocks into shallow structural traps, potentially obscured beneath overlying incompetent host rocks or younger sequences (Corbett and Menzies 2013). This model is analogous to El Peñón (Chile), Palmarejo (Mexico) and Hishikari (Japan) and is supported by the stable isotope evidence for a deep magmatic heat source below the DQZ centre, and by the presence of two NS-trending structural corridors (Red Rock North and offshoots from Long Gully Fault) that have not been adequately tested. The Porgera goldfield and Kainantu System in Papua New Guinea provide further analogies where persistent exploration resulted in the Porgera bonanza-grade Zone VII low- to intermediate sulphidation epithermal quartz Au-Ag mineralisation and extensions to the Kainantu's Kora-Judd-Irumafimpa vein system. Both these systems are interpreted to have been emplaced in relatively shallow crustal levels from fluids derived from a deeper, later felsic magmatic source (Corbett 2005; K92 2020), and a similar scenario remains geologically viable at Drake.

ACKNOWLEDGEMENTS

The authors would like to acknowledge and thank local stakeholders of Drake including landholders, Forestry Corp NSW, and Ngullingah Jugun Aboriginal Corporation for their support during work on the project. Furthermore, acknowledgement is made to all the Legacy Minerals field team, the Directors and contractors who have been a part of the exploration effort to date. The foundations of this work draw substantially on the contributions of Greg Corbett and Doug Menzies, Grace Cumming, and the UNSW research of Hao Quan, Emmanuel Madayag, Winnie Lay, Zach White and Kathrine Zhang, whose work on the Drake Goldfield has greatly advanced understanding of this complex epithermal system. We also acknowledge the fundamental exploration and resource work conducted by Rex Minerals, White Rock Minerals and Thomson Resources.

REFERENCES

ANDREWS E. C. 1908. Report on the Drake gold & copper field. Mineral Res. GSNSW. 12.

BARNES R. G., BROWN R. E., BROWNLOW J. W., CAMERON R. G. & KRYNEN J. P. 1991. Tenterfield 1:250,000 Metallogenic Map, SH/56-5: Metallogenic Study & Mineral Deposit Data Sheets. Geological Survey of New South Wales.

BOTTOMER L. R. 1986. Geology & geochemistry of the Drake Goldfield, New South Wales. Unpublished PhD thesis, University of New South Wales.

BROWN R. E., BROWNLOW J. W. & KRYNEN J. P. 2001. Warwick-Tweed Heads 1:250,000 sheet Geology, Mineral Occurrences, Exploration & Geochemistry. GSNSW, GS2001/087.

CHOMISZAK M. 2016. Alteration & mineralisation at the White Rock & White Rock North deposits, Drake, NSW. Unpublished Honours thesis, University of New South Wales.

CORBETT G. J. 2005. New mineralisation & alteration styles at the Porgera gold deposit, Papua New Guinea. PACRIM 2005 Congress, Australasian Institute of Mining & Metallurgy.

CORBETT G. J. & LEACH T. M. 1998. Southwest Pacific rim gold-copper systems: structure, alteration, & mineralisation. Society of Economic Geologists Special Publication 6, 234 p.

CORBETT G. J. 2008. Comments on the Controls to Au Mineralisation at the Mt Carrington Project, Drake Goldfield, North East New South Wales. Corbett Geological Services Pty Ltd, unpublished report, April 2008.

CORBETT G. J. 2011. Comments on Recent Exploration in the Mt Carrington Region, Eastern Australia. Corbett Geological Services Pty Ltd, unpublished report, September 2011.

CORBETT G. J. & MENZIES D. 2013. Comments on Exploration at the Drake Project, Northeast NSW. Corbett & Menzies Consulting Pty Ltd, unpublished report, August 2013.

CUMMING G. 2011. New geological constraints for the Drake Volcanics, Northern New South Wales. Unpublished report for White Rock Minerals Ltd.

DAVIES B. 2010. Structural framework of the Drake Goldfield, northern NSW. Unpublished report.

GULSON B. L. & BOTTOMER L. R. 1984. Lead isotope studies of mineralisation at Drake, New South Wales. Economic Geology 79, 1640–1648.

HAMMOND R. 2005. Geological interpretation of the Drake district, northern NSW. Unpublished report.

HERBERT H. K. 1983. Geology & geochemistry of the Drake mining district. Unpublished MSc thesis.

HOUSTON M. J. 1993. The geology & mineralisation of the Drake mining area, northern NSW, Australia. In: Flood P. G. & Aitchison J. C. eds., New England Orogen, Eastern Australia, pp. 337–348. University of New England, Armidale.

HOUSTON M.J., 2010. A review of the White Rock prospect & surrounding area. Unpublished report for Rex Minerals.

JESSOP K., DACZKO N. & PIAZOLO S. 2019. Tectonic cycles of the New England Orogen, eastern Australia: A review. Australian Journal of Earth Sciences 66, 459–496.

K92 MINING INC. 2020. Kainantu Project NI 43-101 Technical Report & Preliminary Economic Assessment (Kora Gold Deposit, Papua New Guinea). Effective date 2 April 2020.

LAY W. 2019. Mineralogy & fluid evolution of silver-dominant epithermal deposits, Drake goldfield, NSW. Unpublished Honours thesis, University of New South Wales.

LEGACY MINERALS HOLDINGS LIMITED (LGM) 2024a. Transformational Acquisition of the Mt Carrington (Drake) Project. ASX Announcement, 21 March 2024.

LEGACY MINERALS HOLDINGS LIMITED (LGM) 2024b. Over 100% Increase in Historical Mines & Workings Identified at Drake. ASX Announcement, 16 December 2024.

LEGACY MINERALS HOLDINGS LIMITED (LGM) 2025. Significant Gold-Copper Airborne MT Targets Defined at Drake. ASX Announcement, 3 July 2025.

LEGACY MINERALS HOLDINGS LIMITED (LGM) 2026a. Study Confirms Compelling Potential of Mt Carrington Project. ASX Announcement, 4 May 2026.

LEGACY MINERALS HOLDINGS LIMITED (LGM) 2026b. Mt Carrington Mineral Resource Grows to 1.6Moz Gold-Equivalent. ASX Announcement, 30 July 2026.

LEGACY MINERALS HOLDINGS LIMITED (LGM) 2026c. Silver-Gold-Copper Drilling Update at Mt Carrington. ASX Announcement, 30 January 2026.

LEGACY MINERALS HOLDINGS LIMITED (LGM) 2026d. Maiden Drilling Makes New Greenfields Gold Discovery. ASX Announcement, 19 March 2026.

LEGACY MINERALS HOLDINGS LIMITED (LGM) 2026e. Mt Carrington Gold-Copper-Silver Drilling & Resource Update. ASX Announcement, 28 July 2026.

MADAYAG E. 2020. Characterisation of the Strauss epithermal deposit, Drake goldfield, NSW. Unpublished Honours thesis, University of New South Wales.

MCQUEEN K. G. 2017. Mining history of the New England region. Geological Survey of New South Wales Report GS2017/0650 (R00034616).

MINING PLUS PTY LTD 2025. Mt Carrington JORC 2012 Mineral Resource Estimate. Prepared for Legacy Minerals Holdings Limited, March 2025.

HOWARD N. 2015. Geochemistry & hydrothermal alteration at the Mount Rawdon gold deposit. In: Mineral Exploration in the Tasmanides, Mines and Wines 2015, Sydney Mineral Exploration Discussion Group (SMEDG) Bulletin. smedg.org.au

OFFENBERG A. C. & COCHRANE G. W. 1975. Drake 1:100,000 Geological Map Sheet. Geological Survey of New South Wales.

PERKINS C. 1987. Alteration at the Drake goldfield, New South Wales. Unpublished report.

QUAN H. 2022. Geological & geochemical controls on precious metal epithermal mineralisation, Drake Goldfield, northern NSW. Unpublished PhD thesis, University of New South Wales.

QUAN H., GRAHAM I., WORLAND R., ADLER L., DIETZ C., MADAYAG E., WANG H. & FRENCH D. 2025. Interpreting the Complexity of Sulfur, Carbon, & Oxygen Isotopes from Sulfides & Carbonates in a Precious Metal Epithermal Field: Insights from the Permian Drake Epithermal Au-Ag Field of Northern New South Wales, Australia. Minerals 15, 134. https://doi.org/10.3390/min15020134

ROSENBAUM G. 2026. The plate tectonic setting of mineral deposits in the New England Orogen (Australia). Earth-Science Reviews 276, 105435. https://doi.org/10.1016/j.earscirev.2026.105435

SAHLSTRÖM F. 2018. The Mt Carlton high-sulfidation epithermal deposit, NE Australia: geologic character, genesis & implications for exploration. Unpublished PhD thesis, James Cook University. researchonline.jcu.edu.au/54844

SIMMONS S. F., WHITE N. C. & JOHN D. A. 2005. Geological characteristics of epithermal precious & base metal deposits. Economic Geology 100th Anniversary Volume, 485–522.

SMITH R. J. 1989. Geology & mineralisation of the Drake gold-silver district, northern New South Wales. Unpublished PhD thesis, University of Queensland.

TAUBE A. 1986. The Mount Morgan gold-copper mine & environment, Queensland: a volcanogenic massive sulfide deposit associated with penecontemporaneous faulting. Economic Geology 81(6), 1322-1340. doi.org/10.2113/gsecongeo.81.6.1322

WALTENBERG K., BLEVIN P., BULL K., CRONIN D. & ARMISTEAD S. 2016. New SHRIMP U–Pb zircon ages from the Lachlan Orogen & the New England Orogen, New South Wales: Mineral Systems Projects, July 2015–June 2016. Geoscience Australia Record 2016.028.

WHITE Z. 2017. Volcanic facies & silver distribution at White Rock & White Rock North, Drake goldfield, NSW. Unpublished Honours thesis, University of New South Wales.

WORDEN K. & SHEPHERD R. 2016. Cracow gold field. In: Australian Ore Deposits (ed. Phillips G.N.), pp. 559-562. Australasian Institute of Mining & Metallurgy, Melbourne.

ZHANG K. 2016. Alteration & mineralisation at the Lady Hampden deposit, Drake goldfield, NSW. Unpublished Honours thesis, University of New South Wales.

PRIMARY AND SECONDARY GEOSCIENCE EDUCATION FOR THE NEXT GENERATION OF GEOSCIENTISTS

Phil Gilmore, Malte Ebach

Teacher Earth Science Education Programme Limited (TESEP).

The future of geoscience education in Australia has been of serious concern for over two decades due to a combination of cuts to the university sector, a lack of geoscience-trained secondary science teachers, changes to the Australian curriculum, lack of schools offering senior secondary school Earth and Environmental Science courses, and a disconnect between society and understanding the Earth.

As an example, the rock cycle and plate tectonics – fundamental processes on Earth – are now taught in year 8. If these subjects are not taught by a knowledgeable and passionate teacher, then students will most likely never study geoscience again.

In the school systems, geoscience education organisations like the Teacher Earth Science Education Programme Limited (TESEP) and others provide professional development workshops and field trips to upskill teachers and laboratory technicians and inspire students.

TESEP is an Australia-wide, not-for-profit organisation that started in 2007. Our workshops and content are designed to “teach the teachers” – to upskill and provide confidence to Australian Curriculum K-12 and state / territory syllabi. As one teacher teachers many students a year let alone over a career, the multiplier effect of teaching that teacher is enormous.

TESEP advocate for improved geoliteracy in schools and the community, given we all depend on the Earth for life and our resources. TESEP promotes the overlap of STEM in geoscience – for example the opportunities for students interested in chemistry to contribute to critical mineral exploration and recovery, physics students to understand the structure of the Earth using a variety of techniques, and mathematicians to maximise the geoscience sector’s vast data science repository. We also highlight the career opportunities in geoscience outside tertiary qualifications which are important for our METS sector.

The generous support of partners including the *Discoveries in the Tasmanides* organisers – the Australian Institute of Geoscientist and the Sydney Mineral Exploration Discussion Group, and other organisations present at this conference enable TESEP to operate. And many professional societies offer support for geoscience education initiatives, such as the recent international GeoSciEd X conference for geoscience educators in Adelaide.

Current statements from peak bodies and professional societies like the Australian Academy of Science National Committee for Earth Sciences, and the Australian Geoscience Council Inc highlight the issues and needs for a geoscience education.

However, all geoscience education providers require further ongoing financial support to maintain and expand their programs. And we as a sector require a single and powerful voice to government to bring real change and ensure geoscience is taught well for both our society and for our next generation of geoscientists to flourish.

PORPHYRY CU-AU EXPLORATION IN NORTHERN JUNEE-NARROMINE VOLCANIC BELT, NSW – EXPANDING FRONTIERS

Doug Menzies*, Kristen Marris*, Alistair Waddell and Stuart Smith

Inflection Resources Ltd.

Keywords: Macquarie Arc, Lachlan Orogen, porphyry Au-Cu, Junee-Narromine Volcanic Belt, exploration, geochronology

INTRODUCTION

Recent exploration success in Australia has been dominated by discovery of concealed deposits in poorly explored extensions to known productive belts (eg Paterson Province, Gawler Craton). The Macquarie Arc is Australia's premier porphyry province and has delivered exploration success on a consistent basis, however the far northern deeply buried interpreted extension to the arc has seen very little exploration.

Inflection Resources Ltd is a Canadian Securities Exchange (CSE) listed exploration company formed in 2020 with the strategy of exploring the immature interpreted northern extension of the Macquarie Arc. The availability of high-quality public domain data sets such as airborne magnetics, gravity, geological interpretations and previous exploration data was key to attracting the capital required to undertake such frontier exploration. It was also recognised that success would depend on being able to test numerous targets within large landholdings that could be acquired at relatively low cost and that this could be achieved in NSW.

In this contribution we briefly discuss aspects of the exploration completed, the tactics and techniques applied as well as selected results that have bearing on the understanding of the Macquarie Arc and the Lachlan Orogen more broadly.

PROJECT DEVELOPMENT and EVOLUTION

During 2018 Dr Douglas Haynes undertook an interpretation of the public-domain magnetic and gravity data extending from Parkes to Lightning Ridge and developed 12 specific high-priority Cu-Au targets. This work was presented to the founders of Inflection Resources. Initial seed capital was raised and eight exploration license applications, extending from Trangie to Brewarrina, were lodged which together with two licenses already held by Dr Haynes and associates formed the initial project portfolio. These were supplemented by additional exploration license applications such that by April 2020 the company held seventeen licenses for a total of approximately 3,500 square kilometres. Following further capital raising, extensive landowner liaison and development of a small team the first drill hole commenced on 28th June in Dr Haynes's Myallmundi target approximately 10 km northwest of Trangie township. Inflection Resources began trading on CSE on 16th July 2020.

Inflection Resources self-funded all exploration activities from this initial period until mid-2023 when an exploration agreement was executed with AngloGold Ashanti Ltd (AngloGold) whereby AngloGold fund exploration activities and provide extensive technical and other expertise on selected Exploration Licenses. Exploration is ongoing, with an aircore drill program recently undertaken at the Trangie prospect. The company currently holds 3200 square kilometres of Exploration Licenses in the Macquarie Arc project.

EXPLORATION APPROACH and TACTICS

The strategy employed is to maximise "dollars in the ground" and to prioritise drilling. Historic exploration success since the 1970's in the Junee-Narromine Belt and adjacent areas has been achieved by employing RAB, aircore or RC drilling through cover sequences in order to obtain consistent basement samples. This style of exploration, aided by geophysical interpretations, was critical to economic discoveries at Northparkes, Cowal, Wyoming and encouraging results in the Temora and Narromine complexes. Recognising this but taking into account the deeper cover expected in the Inflection areas, initial drilling employed mud rotary drilling through cover followed by short diamond tails. Encouraging initial results were followed up with deeper diamond tails. At that time aircore was not considered an option due to the cover thickness (>150 m), however more recently aircore has been proven to be a viable basement sampling technique in areas with up to 200 m of cover and has dramatically reduced overall drilling costs. A total of 192 mud rotary-diamond holes have been completed encompassing an area of more than 300 km from south of Trangie to west of Walgett. Aircore drilling is underway at time of writing, with approximately 100 holes completed.

Other exploration techniques have been employed, as an adjunct to drilling, with more detailed airborne magnetic surveys, ground gravity, Ambient Noise Tomography (ANT) and IP-resistivity surveys conducted. Detailed potential field data have assisted in refining targets and interpretations, however conductive material in the cover sequences has rendered the IP-resistivity of little applicability. The ANT surveys have provided useful data for depth-to-basement interpretations and some information regarding regional architecture however the technique is in its infancy in porphyry environments.

All basement samples have been analysed by 4-Acid ICP-MS and spectral data is routinely collected. A total of 402 samples have been described petrographically, 144 samples were analysed for “green-rock” epidote and/or chlorite mineral chemistry. A total of 63 new U-Pb, 7 Re-Os and 9 conodont dates have been collected. Within the units dated by Inflection there had only been one previous geochronological result.

A disciplined approach has been taken to testing of targets and discarding of licenses if first pass testing does not produce evidence of porphyry style mineralisation or Macquarie Arc sequences. As a result 15 licenses have been relinquished during the life of the project.

SELECTED RESULTS

Interpreted Macquarie Arc equivalent rocks, as determined by geochronology, petrography and geochemistry have been encountered approximately 150 km north of the northernmost Macquarie Arc as it is interpreted on the NSW seamless geology coverage. Preliminary age relationships, petrographic descriptions and geochemical associations indicate that the arc may young to the north and involve higher crustal components than in the better-studied southern section of the arc. Data are sparse in this northern area and interpretation is ongoing.

Drilling of high magnetic complexes in the extreme north of the project area, between Walgett and Brewarrina, encountered medium grained, equigranular dioritic intrusions that yielded U-Pb zircon ages from 392.8 to 416.4 Ma, consistent with their interpretation as early Devonian intrusions in the NSW Geological Survey seamless geology interpretation.

Several significant areas of interpreted porphyry-style mineralisation have been encountered and exploration is ongoing. Here we provide summary details of two target areas where exploration is ongoing. The Trangie target occurs north and west of the township of Trangie and occurs beneath 120 to 200 m of post-mineral cover. The target has yielded a best intersection (TRNDH023) to-date of 54.37 m at 0.37 g/t Au and 0.07% Cu from 194.63 m, including 8.00 m at 0.67 g/t Au and 0.11% Cu. Deeper intervals included 35.47 m at 0.40 g/t Au and 0.06% Cu from 259.53 m and 21.45 m at 0.22 g/t Au and 0.04% Cu from 346.00 m (Inflection Resources, 2025a). Gold, Cu and Ag are positively associated, and Au shows low or negative association with Te and Sb. Together with the vein and alteration assemblages, this favours a porphyry rather than shallow epithermal interpretation. The higher Au values are spatially associated with centre-lined quartz–pyrite–chalcopyrite-gypsum veins classified as porphyry-style B veins. These veins occur in epidote-chlorite and epidote-actinolite-biotite-magnetite-pyrite altered monzodiorite to monzonite porphyries and andesitic volcaniclastic host rocks (Crawford, 2025, Wilson, 2025).

Follow-up drilling at Trangie identified porphyry-related alteration, local B-style veining and associated gold mineralisation sporadically developed across a greater than 500 m by 500 m. Drillhole TRNDH028, designed to intersect the mineralised zone encountered in TRNDH023, intersected a volcaniclastic sedimentary sequence affected by epidote-chlorite and biotite–magnetite ± K-feldspar alteration and containing significant quartz–pyrite–chalcopyrite B-style veins. The hole returned 42.67 m at 0.33 g/t Au and 0.05% Cu from 263.33 m. Drillhole TRNDH027, drilled on a section approximately 200 m south of TRNDH023, intersected epidote-chlorite and biotite–albite-altered siltstone and sandstone and a monzodiorite intrusion, returning 4.0 m at 1.24 g/t Au from 225.0 m (Inflection Resources, 2025b).

Preliminary, unpublished Re–Os molybdenite and U–Pb zircon results provide the first direct age constraints on mineralisation and intrusive activity at Trangie. These results place hydrothermal mineralisation and intrusive crystallisation within an approximately 470–460 Ma Early to Middle Ordovician interval (CODES, 2025; Creaser, 2026). At district scale, the preliminary Trangie dates indicate protracted Ordovician magmatic–hydrothermal activity but do not yet define a single continuous event. The Trangie range broadly overlaps published ages for mid-Ordovician intrusive activity in the Cowal district, including the pre-mineralisation Muddy Lake Diorite and related dioritic to monzodioritic phases. At Cowal, these pre-mineralisation intrusions were followed by a younger epithermal gold event at approximately 455 Ma (Zukowski, 2010; Zukowski et al., 2014).

The Duck Creek target (Inflection Resources, 2022, 2024; Crawford, 2024) occurs approximately 35 km northeast of Nyngan and was targeted due to the presence of a subtle gravity low within high a magnetic domain interpreted to be potential Macquarie Arc. Drilling has encountered mixed shoshonitic basaltic to dacitic volcanics and monzonite to quartz monzonite intrusions beneath deep cover (200-400 m). Complex, multiphase alteration is extensive occurring over an area of approximately 2 x 2 km and known to depths up to 300 m below the base of cover. Alteration consists of high temperature biotite-actinolite-magnetite-K-feldspar mixed with and overprinted by lower temperature sericite-bearing phyllic alteration. A notable feature of both the higher and lower temperature alteration at Duck Creek is the presence of significant tourmaline as alteration and in veins. Poorly defined albite alteration has also been encountered. Other vein styles encountered include various combinations of quartz, magnetite, actinolite, tourmaline, gypsum, pyrite, chalcopyrite with A- and B-vein textural characteristics recognised. To-date Cu and Au results have been modest and data interpretation is ongoing to determine any further next steps at Duck Creek.

CONCLUSIONS

Frontier exploration built on a strategy of exploring poorly tested extensions to the Macquarie Arc has been ongoing since 2020. Extensive data sets have been acquired that will contribute significantly to the geological understanding of New South Wales. The known Macquarie Arc has been extended well north of previous interpretations, and the Devonian age of several igneous complexes has been confirmed. Several zones of interpreted porphyry-style alteration and mineralisation have been identified and exploration is ongoing. Although active since 2020, exploration is still in its infancy and large areas of poorly tested, prospective Macquarie Arc remain.

ACKNOWLEDGEMENTS

Numerous people have contributed to the exploration programs, and we particularly acknowledge the important technical contributions of AngloGold Ashanti Greenfields Exploration geoscientific team and consultants Anthony Crawford, Alan Wilson, Josh Phillips and Terry Hoschke. Carl Swensson, Tobias Erskine, Jess Askew contributed significantly to the project in previous campaigns and the critical contribution of Margus Madissoo is acknowledged.

REFERENCES

CODES, 2025. U–Pb zircon geochronology from the Trangie Project, NSW. Unpublished analytical results prepared for Inflection Resources Ltd.

CREASER, R.A., 2026. Re–Os molybdenite geochronology from the Trangie Project, NSW. Unpublished analytical results prepared for Inflection Resources Ltd., University of Alberta.

CRAWFORD, A.J., 2024. Petrographic Report, 29 Rocks from the Duck Creek Prospect, EL8965, Nyngan District, NSW. Unpublished report to Inflection Resources Ltd.

CRAWFORD, A.J., 2025. Petrographic Report, 23 Samples from Trangie Prospect Drillholes TRNDH027 through TRNDH032. Unpublished report to Inflection Resources Ltd.

INFLECTION RESOURCES LTD, 2022. Inflection Resources Intercepts Porphyry Style Alteration at the Duck Creek Target. News release, 13 June 2022.

INFLECTION RESOURCES LTD, 2024. Inflection Resources Provides Drilling Update From Phase II Duck Creek Exploration Program in New South Wales. News release, 3 October 2024.

INFLECTION RESOURCES LTD, 2025a. Inflection Resources Intercepts Porphyry Gold-Copper Mineralisation in New South Wales. News release, 4 February 2025.

INFLECTION RESOURCES LTD, 2025b. Inflection Resources Provides Update on Trangie Project Drilling in New South Wales, Australia. News release, 18 August 2025.

ZUKOWSKI, W., 2010. Geology and mineralisation of the Endeavour 41 gold deposit, Cowal district, NSW, Australia. PhD thesis, University of Tasmania, Hobart, 275 p.

ZUKOWSKI, W., COOKE, D.R., DEYELL-WURST, C., MCINNES, P. and SIMPSON, K.A., 2014. Genesis and exploration implications of epithermal gold mineralization and porphyry-style alteration at the Endeavour 41 prospect, Cowal district, New South Wales, Australia. Economic Geology, 109, 1079–1115.

DEVELOPING 3D GEOLOGICAL FRAMEWORKS THROUGH VOLCANIC FACIES ANALYSIS AND INTEGRATED LITHOGEOCHEMISTRY AT THE SPUR PROJECT, EAST LACHLAN, NSW, AUSTRALIA

Malai Ila'ava[1,2,3], Jessica Askew[1,2], David Willis[1]

[1]Waratah Minerals, [2]CODES - University of Tasmania, [3]Ila'ava Lava

Key Words: Spur-Consols, volcanic facies architecture, geochemistry, 3D modelling, Molong Volcanic Belt, Macquarie Arc, Eastonian uplift, tectonics

INTRODUCTION

Spur and Consols are emerging gold deposits in the Macquarie Arc of central New South Wales, recently discovered by Waratah Minerals. Systematic diamond drilling is currently underway to support a maiden Mineral Resource Estimate. This has generated a dense three-dimensional dataset through the volcanic succession.

Drill core samples have been analysed using modern four-acid digest lithogeochemistry providing a high-density geochemical dataset across a substantial volume of the Cargo Volcanics. This is a great opportunity to build on the work of Simpson et al. (2007) who documented the volcanics of the Cargo Complex through regional-scale mapping and reconnaissance sampling, but only had limited diamond drill core available from the early-stage exploration drilling of that time.

This contribution presents a facies-led workflow for building three-dimensional geological frameworks in ancient volcanic successions. The workflow first reconstructs the preserved volcanic architecture of the host succession, then uses that architecture as a scaffold for integrating lithogeochemistry, alteration, mineralisation, structure and intrusive relationships. This paper focuses on methodology, volcanic facies architecture, lithogeochemistry, 3D modelling, and regional implications for the Cargo Complex and the broader Macquarie Arc. Further details on project history and deposit characteristics are provided by Askew (this volume).

REGIONAL SETTING

The Macquarie Arc of the Lachlan Orogen in central New South Wales comprises three major, structurally bounded, meridional mafic volcanic belts separated by Siluro-Devonian basins. From west to east, these are the Junee-Narromine, Molong, and Rockley-Gulgong Volcanic Belts. The belts are widely regarded as the structurally dismembered remnants of a once contiguous intra-oceanic island arc that remained outboard of Gondwana throughout the Ordovician (Glen et al., 1998; Percival and Glen, 2007; Fergusson and Colquhoun, 2018; Aitchison and Buckman, 2012). The Macquarie Arc docked onto the Gondwanan margin during the 440 Ma (Phase 1) to 430 Ma (Phase 2) Benambran Orogeny (Glen et al., 2007). Post-orogenic extension was accompanied by alkalic-shoshonitic magmatism and the development of alkalic porphyry-epithermal systems (Cooke et al., 2007), including the pencil porphyry deposits of the Cadia (Fox et al., 2015; Harris et al., 2014., Wilson, 2003) and Northparkes districts (Lickfold et al., 2007; Pacey et al., 2019; Wells et al., 2020).

Previous correlations across the volcanic belts, based on geochemistry, geochronology and biostratigraphy, interpreted two volcanic hiatuses at approximately 475-460 Ma and a more temporal and spatially variable volcanic hiatus across the Ordovician-Silurian boundary around ~ 455-440 Ma (Percival and Glen, 2007). More recent geochronology has reduced the inferred temporal and geographic extent of these hiatuses and, in some areas, has called their existence into question (Kemp et al., 2020). Within the Molong Volcanic Belt, the younger hiatus is locally expressed by volcanic and volcaniclastic successions of the Kenilworth Group passing upward into geographically extensive Barrajin Group limestones, interpreted to reflect regional uplift during the Eastonian [Crawford et al., 2007; Simpson et al., 2007]. The Barrajin Group limestones are overlain, unconformably at many localities, by deep-water sedimentary successions of the Cabonne Group (Percival and Glen, 2007).

Simpson et al. (2007) assigned the Cargo Volcanics to the Kenilworth Group and mapped conglomerates containing rounded cobbles resembling the Cargo Volcanics that were in turn, overlain by Barrajin Group limestones. They suggested that resolving the volcanic and geochemical evolution of the Cargo Volcanics may provide key insights into the tectonic evolution of the Macquarie Arc immediately preceding Eastonian uplift and the subsequent volcanic hiatus. The extensive drill core and high-density lithogeochemical dataset at Spur-Consols provides an opportunity to reassess the volcanic evolution at deposit scale and to consider its broader tectonic implications.

METHODS

Rationale

Ancient volcanic basins preserve volcano-sedimentary successions that are commonly overprinted by intrusive, alteration-mineralisation, metamorphic, and deformational events. The methodology applied here seeks first to look through these later overprints and establish the primary volcanic architecture of the host succession. The underlying premise is that volcanic facies architecture forms the primary geological scaffold that may influence the distribution, geometry, and preservation of later features, including intrusion emplacement, fluid flow, alteration zonation, mineralisation, and deformation.

The workflow begins with blind graphic logging of drill core. Crystal cargoes, textures, contacts, grading relationships, clast populations, and sedimentary structures, are used to interpret the setting, and depositional and emplacement processes, without reference to assays, lithogeochemistry, alteration-indices, structural interpretations or modelled domains. The objective is to produce a down-hole vertical succession of lithofacies, interpreted solely from physical evidence in drill core, that can be tested against independent datasets. This approach builds on a methodology developed by the author for 3D volcanic reconstructions at the Cowal Gold deposit (Ila’ava et al., 2024, 2025).

Blind graphic logging and iterative data integration

A total of 6.1 km of detailed graphic logging has been completed across 14 drill holes from the Spur and Consols deposits. Graphic logs were hand drawn digitally on a Remarkable tablet using A4 logging templates at a scale of 50 m per page. Because the logs are digital and can be exported as consistent scalable vector graphic (SVG) files, downstream automated outputs can be produced based on the graphic logs.

For example, an R script was developed to automatically overlay lithogeochemical interpretations and strip logs of Au, As, Cu and magnetic susceptibility onto the graphic logs (Fig. 1). With these automated R script driven outputs, the core premise of the workflow can effectively be contained within a single drill hole: the volcanic succession is first interpreted independently through detailed graphic logging, then complementary datasets are overlaid to stress-test, refine and revise the interpretation. Mismatches between the graphic logs and datasets are productive points of interrogation rather than issues to be overlooked during modelling.

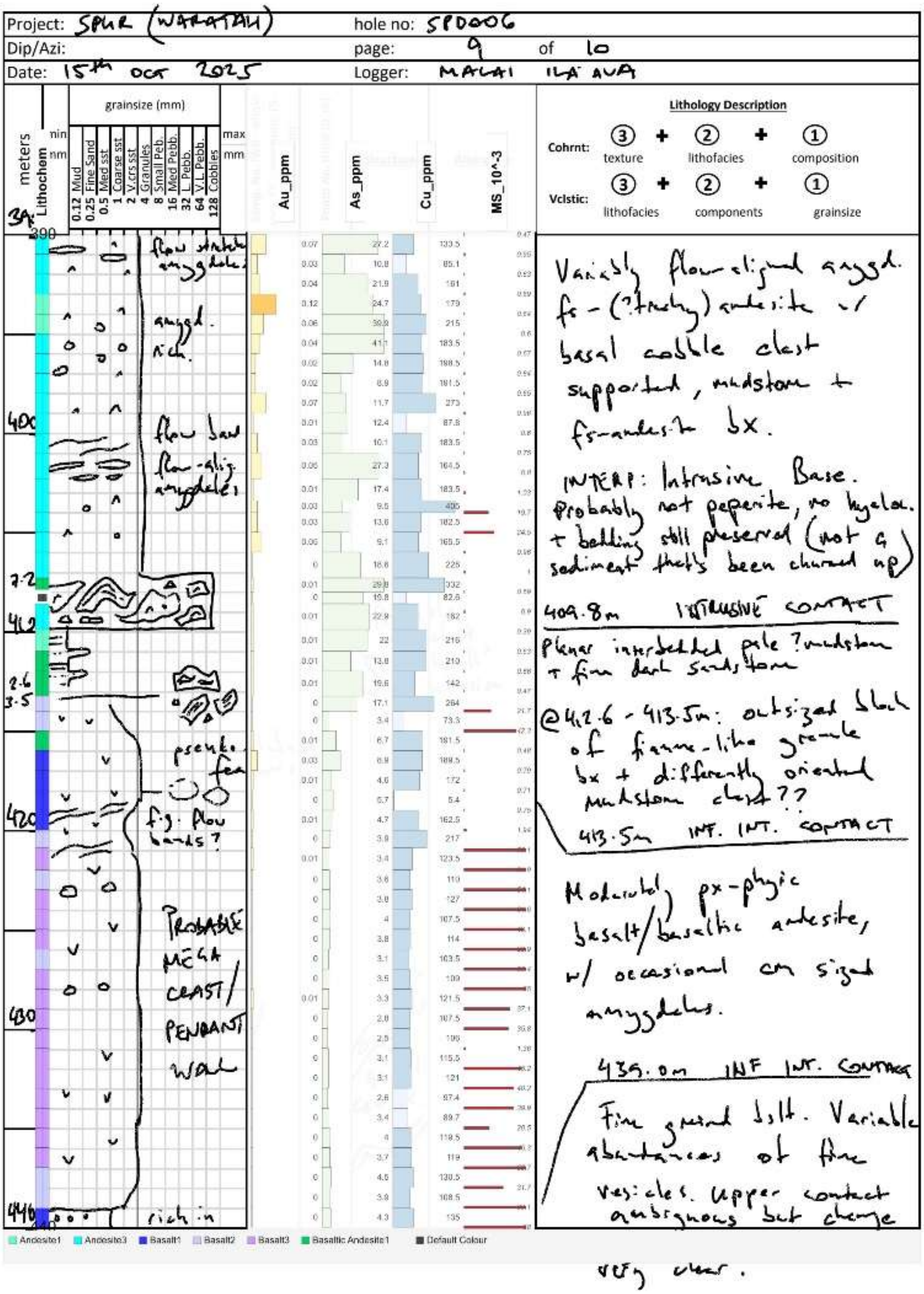

Figure 1: Example of blind graphic logging from SPD006, 390-440m, completed at 50m per A4 page on a Remarkable Tablet. Lithogeochemical populations, Au, As, Cu, and magnetic susceptibility were added later using an R script, allowing core-derived facies interpretations to be interrogated against independent datasets.

Summary lithofacies at Spur-Consols

The Spur-Consols deposits are dominated by thick, massive coherent volcanic units that transition to monomict clast supported breccias with lobate and/or blocky clasts, generally interpreted as massive and pillowed lavas passing to auto-brecciated and hyaloclastite margins. There is some variety in crystal cargoes; increases in relative feldspar abundance generally corresponds to changes in the lithogeochemical compositions defined by Sc, V, Ti abundance, ranging from aphyric basalt, to sparsely-feldspar phyric basaltic andesite, to feldspar-glomerophyric andesites. Sedimentary units such as volcaniclastic turbidites or planar stratified mudstones are volumetrically minor but provide key evidence for interpreting a below wave base, deep marine setting for the volcanics.

In comparing both deposits, Consols has a much thicker preserved succession of massive coherent units that pass up vertically to wavy flow banded units that, from the geochemistry, correspond to evolved compositions like ‘dacite’. Consols is interpreted as a more vent proximal domain, dominated by thick, massive coherent lavas or sub-volcanic intrusions. By contrast, coherent units at Spur that are interpreted as lavas, appear to be thinner (10-20m downhole thickness) with tabular geometries, and pass up to pillows or hyaloclastite more regularly than at Consols. At Spur, a well-preserved ~40 m thick succession comprising sediment-matrix andesite breccia, coherent feldspar-glomerophyric andesite and vesiculated hyaloclastite tops is interpreted as a submarine lava dome. In the context of the broader volcanic architecture, this is interpreted as a satellite or parasitic dome, in the medial to distal aprons of a submarine stratocone.

Complicating that basin architecture are thick (10’s of m’s thick) occurrences of aphyric basalt with varied vesicularity. At drill core scale, it is possible to track the aphyric, vesiculated texture around other clasts. Where these features have been drawn in graphic logs, this is interpreted as an aphyric basalt sill, stoping out pendants of a precursor volcanic succession. At times the aphyric basalt is clearly associated with lobate / pillowed clasts and in-situ hyaloclastite sheets. Because of alteration induced pseudobreccias, it can be very challenging to interpret whether an interval of aphyric basalt is a sill, a shallow sub-volcanic intrusion, or has vented to sea floor as a lava and / or magma fountaining deposit. Distinguishing between sill emplacement, shallow sub-volcanic intrusion and erupted basaltic deposits remains an important interpretive challenge as drilling progresses.

In summary, Consols appears to be a coherent dominated, relatively vent-proximal ‘block’ of a submarine stratovolcano, with Spur representing the medial- to distal- slopes with parasitic lava domes. This architecture has then had the aphyric basalt ‘event’ superimposed on it, that is generally emplaced as a concordant tabular sill, but in places is clearly deposited as a lava / magma fountaining deposit.

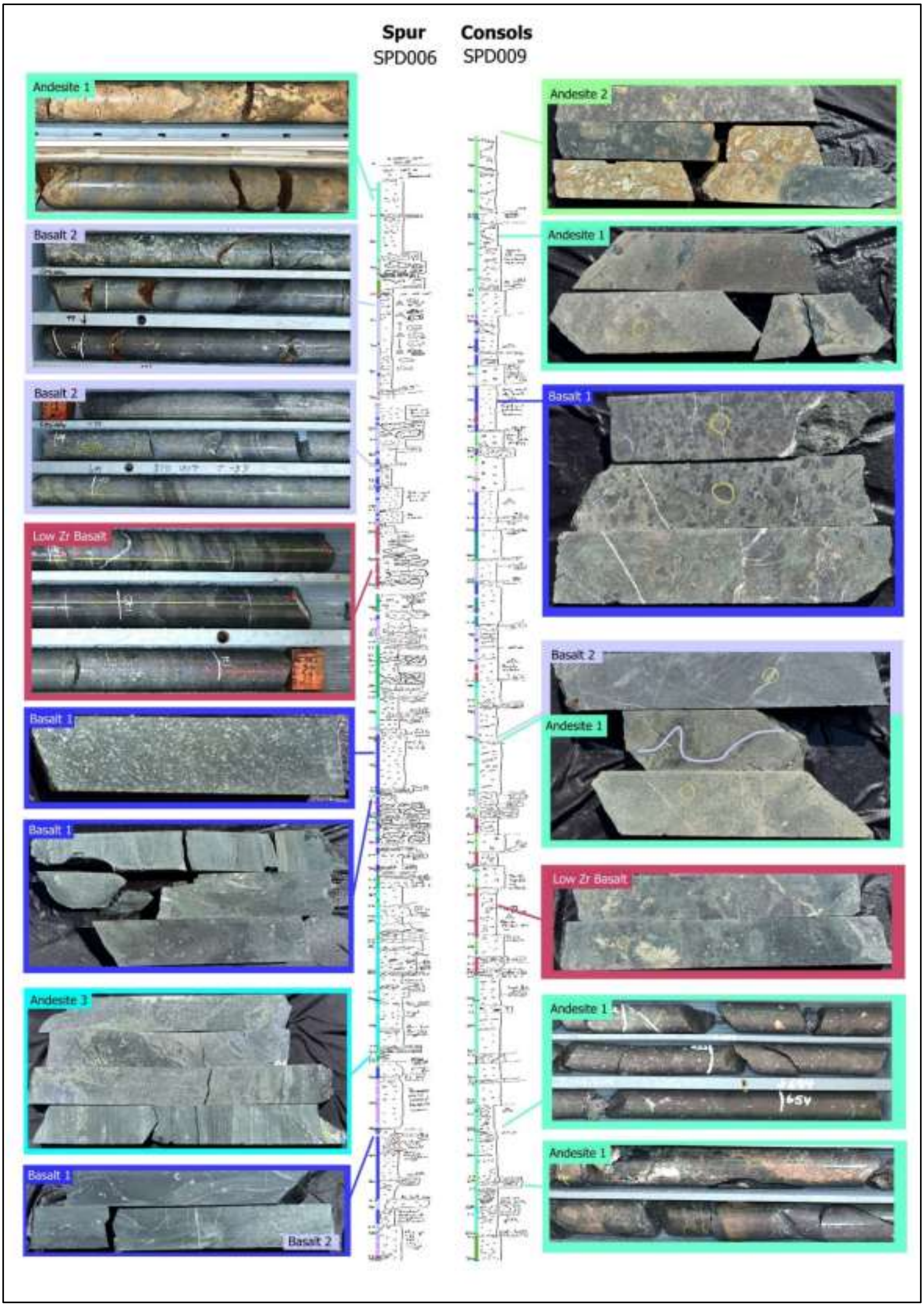

Figure 2: Graphic logs from representative drillholes at Spur (SPD006) and Consols (SPD009), with callout photographs showing volcanic and sedimentary textures. Photographs are colour coded to show how these samples were classified in the lithogeochemistry. Note the variation in textures and crystal cargoes within a given lithogeochemical unit.

Lithogeochemistry analysis

Four-acid digest lithogeochemistry data (n = 34,576) were interpreted using ioGAS. Bivariate plots of immobile high-field-strength elements (HFSE) were used to identify co-magmatic geochemical populations. The ratios Nb/Zr and Y/Zr proved particularly useful for discriminating geochemical populations and for evaluating potential tectono-magmatic affinity (Fig 3).

The interpreted volcanic succession lies largely within a 0.02-0.03 Nb/Zr population, which was subdivided into provisional lithogeochemical units using elements such as Sc, Ti and V as proxies for relative maficity (Halley, 2020). Viewing these units in Leapfrog revealed laterally continuous layers and domains in three-dimensional space. When integrated with graphic logging, these lithogeochemical domains provided a scalable framework for geological modelling.

The blind graphic logging generally correlated with lithogeochemical domains, but several significant mismatches required further interpretation. To reconcile these mismatches, the working hypothesis was that individual lithogeochemical units may represent discrete magmatic, depositional and/or emplacement events. Graphic logging then provided the physical context to assess whether a single lithogeochemical population was expressed through different coherent textures, volcaniclastic facies, intrusive equivalents, or deposit/emplacement processes.

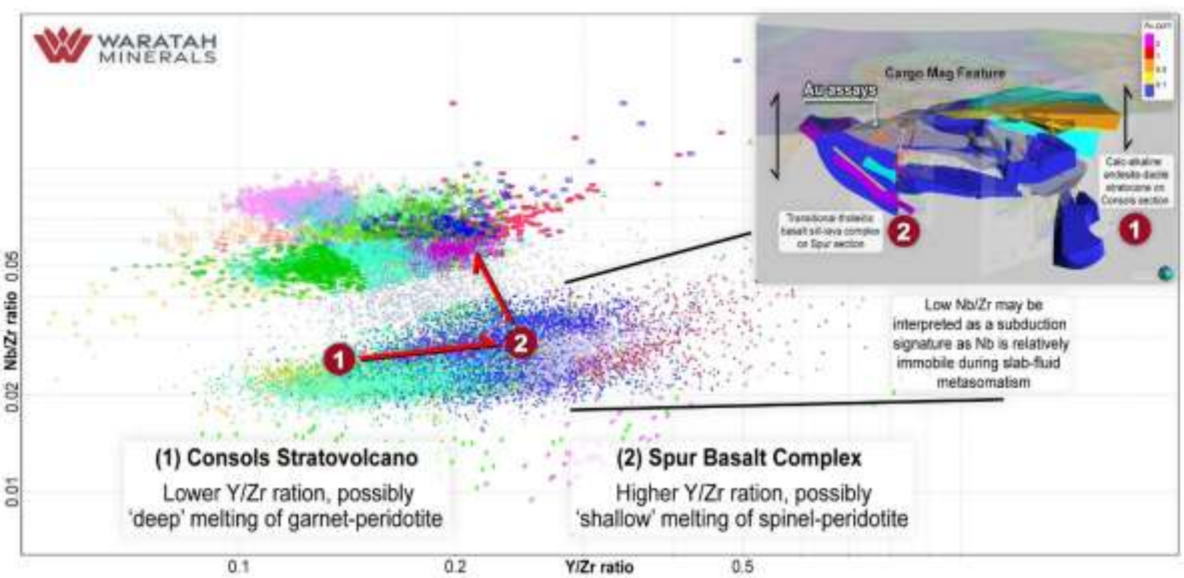

Figure 3: Summary Nb/Zr versus Y/Zr plot for the Spur-Consols lithogeochemical dataset. The plot highlights a low Nb/Zr volcanic population and inferred progression from calc-alkaline andesite-dacite volcanic rocks associated with the preserved remnants of the 'Consols stratocone' (1) towards more mafic transitional-tholeiitic compositions associated with the Spur basalt sill-lava complex (2). Inset – 3D model of volcanic architecture (see Figure 4).

Cross Sections and 3D Modelling

Detailed cross sections were constructed for both Spur and Consols by integrating graphic logging, lithogeochemical interpretations, and geological observations from drill core. Bedding measurements (n = 402) were used to generate isosurfaces in Leapfrog that provided a visual reference for the average S0 orientation which assisted cross-section interpretations of the stratigraphic architecture.

Graphic logging, lithogeochemical interpretations and bedding isosurfaces collectively underpinned multiple iterations of a three-dimensional geological model. With its extensive spatial distribution and sample density, the lithogeochemical dataset proved particularly effective for scaling lithofacies observations from individual drill holes into a deposit-scale framework. The current interpretation is best described as a working geological model that is iteratively constrained by lithogeochemistry and calibrated by targeted lithofacies observations.

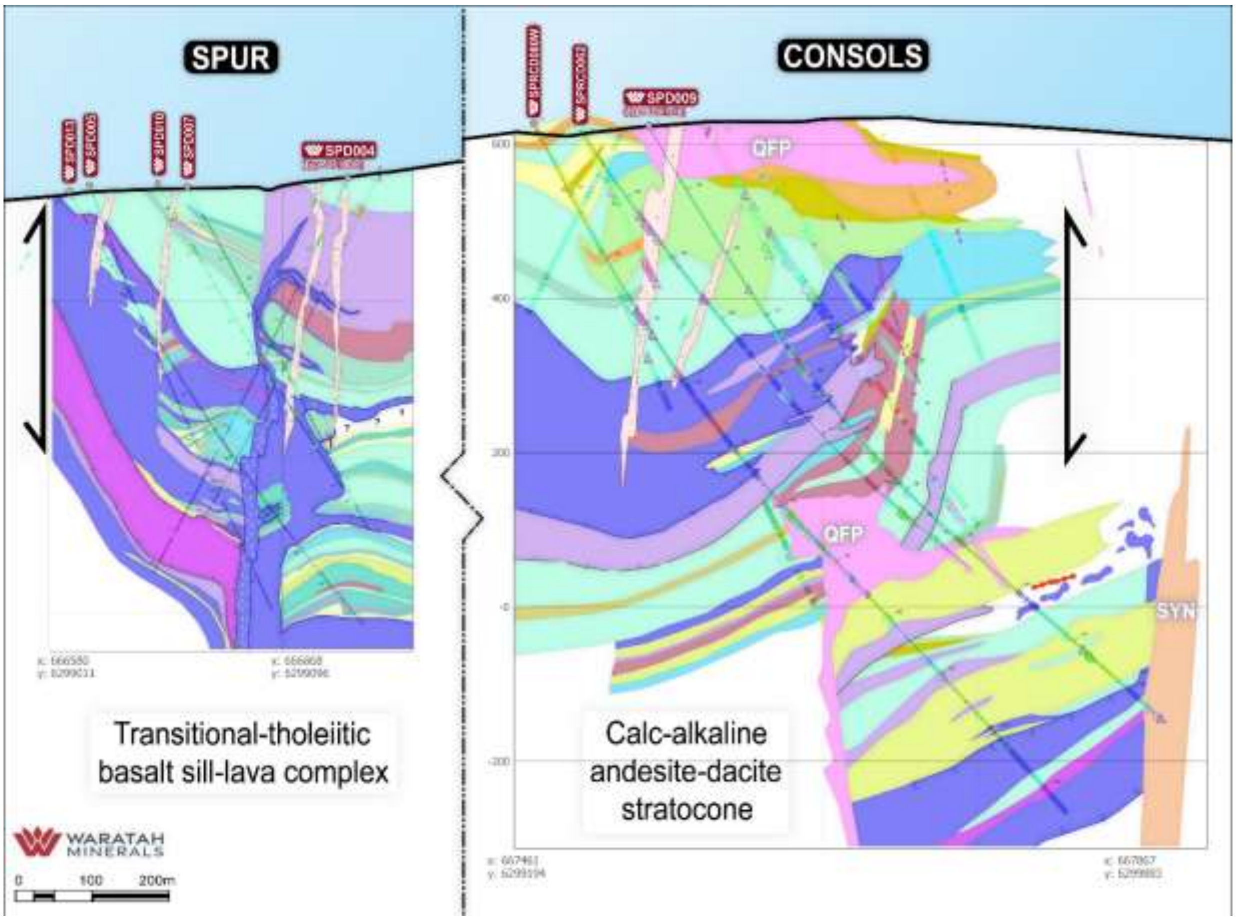

Figure 4: Interpreted representative sections through Spur and Consols. The Consols section is interpreted to preserve a calc-alkaline andesite-dacite stratocone, whereas the Spur section is dominated by a transitional-tholeiitic basalt sill-lava complex that dissects, intrudes and/or overlies the older volcanic architecture.

RESULTS AND SYNTHESIS

The Spur-Consols deposits are interpreted to preserve remnants of a submarine calc-alkaline stratocone (Simpson et al 2007), likely centred on Consols that has subsequently been dissected, intruded and/or overlain by basaltic sills and lavas displaying transitional to tholeiitic affinities, most clearly developed at Spur (Fig. 3 and 4).

At a tectonic scale, the preserved succession may record a transition from calc-alkaline magmatism generated by hydrous flux melting beneath an arc-front, to more mafic transitional-tholeiitic magmatism associated with shallower decompression melting, potentially in a rear-arc or extensional setting. If correct, this transition occurred stratigraphically below the interpreted Eastonian uplift surface and may provide new insight into the tectono-magmatic evolution of the Cargo Complex and broader Molong Volcanic Belt immediately prior to the regional volcanic hiatus.

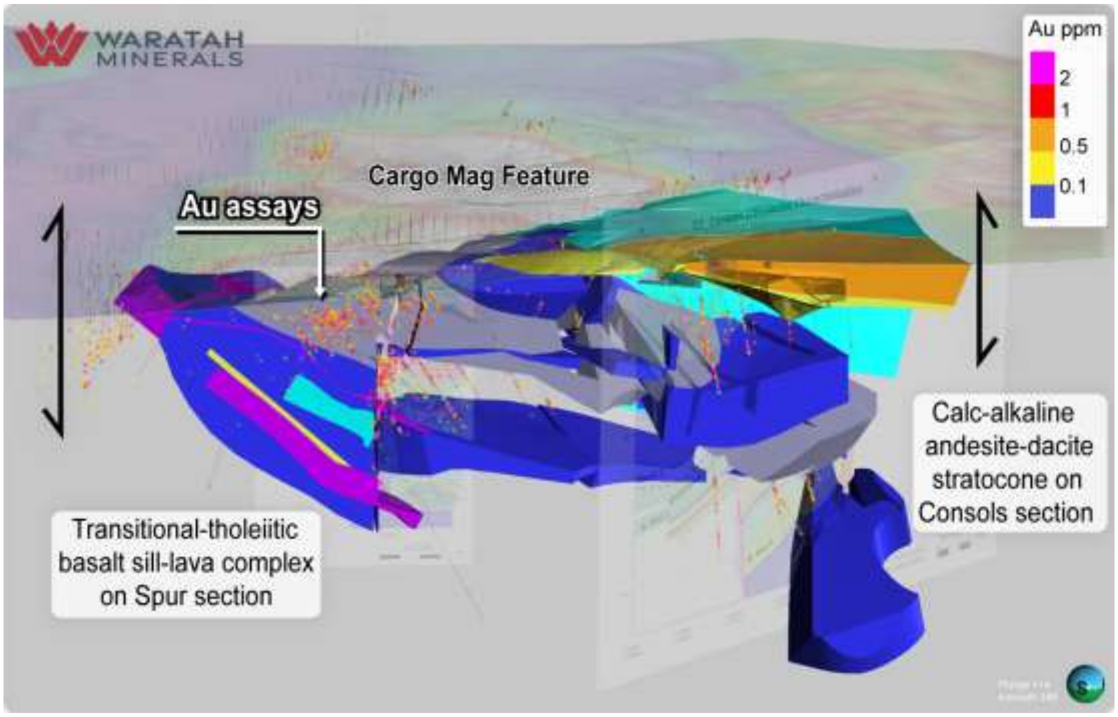

Figure 5: Preliminary three-dimensional geological framework for Spur-Consols, integrating lithogeochemical domains, interpreted cross sections, drill holes, Au assays and geophysical context. The model highlights the interpreted relationship between the Consols calc-alkaline stratocone and the Spur transitional-tholeiitic basalt sill-lava complex.

DISCUSSION

The Spur-Consols workflow demonstrates the value of treating volcanic facies architecture as the primary framework for interpreting complex, overprinted volcanic-hosted mineral systems. In this approach, drill core observations are not used merely to assign lithological codes, but to reconstruct depositional and emplacement processes, establish stratigraphic relationships and provide geological context for lithogeochemical, structural, alteration and mineralisation datasets.

A key outcome of the workflow is that lithogeochemical domains can be interpreted geologically rather than treated only as statistical or compositional populations. Where lithogeochemical units correlate with logged facies, they provide a powerful means of projecting observed volcanic architecture between drill holes and into three-dimensional space. Where mismatches occur, they become useful points of interrogation, prompting reassessment of whether individual geochemical populations represent discrete magmatic events, facies variations within a broader eruptive unit, intrusive equivalents, alteration effects, or structural repetition.

At Spur-Consols, this integrated approach supports interpretation of a submarine calc-alkaline volcanic centre, centred on Consols, that was subsequently dissected and intruded and/or overlain by more mafic transitional-tholeiitic basaltic sills and lavas, most clearly developed at Spur. This interpretation has implications beyond the deposit scale. If the transition from calc-alkaline to transitional-tholeiitic magmatism records a shift from deeper hydrous flux melting beneath a volcanic front to shallower decompression melting in a rear-arc or extensional setting, then the Cargo Volcanics may preserve an important record of tectono-magmatic reorganisation immediately prior to Eastonian uplift in the Molong Volcanic Belt.

More broadly, the study highlights how high-density lithogeochemistry, when calibrated against detailed volcanic facies logging, can be used to construct iterative three-dimensional geological frameworks in ancient volcanic successions. Such frameworks provide a practical basis for testing mineralisation controls, refining exploration models, identifying geological uncertainty and communicating interpretations across project teams.

CONCLUSIONS

- Blind graphic logging provides an independent volcanic facies framework that can be tested against lithogeochemistry, assays, structure, alteration and geophysical datasets.
- High-density lithogeochemistry provides an effective means of scaling core-based facies observations into a deposit-scale three-dimensional model.
- The Spur-Consols succession is interpreted to record a coherent dominated, calc-alkaline andesite-dacite submarine stratocone, likely centred on Consols, later dissected, intruded and/or overlain by a transitional-tholeiitic basalt sill-lava complex most clearly developed at Spur.
- This transition may record tectono-magmatic reorganisation from a volcanic front, to a rear arc or extensional setting in the Cargo Complex immediately prior to Eastonian uplift in the Molong Volcanic Belt and Macquarie Arc.

REFERENCES

Aitchison, J. C., & Buckman, S. (2012). Accordion vs. Quantum tectonics: Insights into continental growth processes from the Paleozoic of eastern Gondwana. Gondwana Research, 22(2), Article 2. https://doi.org/10.1016/j.gr.2012.05.013

Askew, J (2026). Characterising the Spur deposit, NSW, Australia. New insights from an emerging Au-Cu porphyry-epithermal system title and publication details (this volume).

Crawford, A. J., Meffre, S., Squire, R. J., Barron, L. M., & Falloon, T. J. (2007). Middle and Late Ordovician magmatic evolution of the Macquarie Arc, Lachlan Orogen, New South Wales. Australian Journal of Earth Sciences, 54(2–3), Article 2–3. https://doi.org/10.1080/08120090701227471

Cooke, D. R., Wilson, A. J., House, M. J., Wolfe, R. C., Walshe, J. L., Lickfold, V., & Crawford, A. J. (2007). Alkalic porphyry Au – Cu and associated mineral deposits of the Ordovician to Early Silurian Macquarie Arc, New South Wales. Australian Journal of Earth Sciences, 54(2–3), Article 2–3. https://doi.org/10.1080/08120090601146771

Fergusson, C. L., & Colquhoun, G. P. (2018). Ordovician Macquarie Arc and turbidite fan relationships, Lachlan Orogen, southeastern Australia: Stratigraphic and tectonic problems. Australian Journal of Earth Sciences, 65(3), Article 3. https://doi.org/10.1080/08120099.2018.1425909

Fox, N., Cooke, D. R., Harris, A. C., Collett, D., & Eastwood, G. (2015). Porphyry Au-Cu mineralization controlled by reactivation of an arc-transverse volcanosedimentary subbasin. Geology, 43(9), Article 9. https://doi.org/10.1130/G36992.1

Glen, R. A., Walshe, J. L., Barron, L. M., & Watkins, J. J. (1998). Ordovician convergent-margin volcanism and tectonism in the Lachlan sector of east Gondwana. Geology, 4.

Glen, R. A., Crawford, A. J., Percival, I. G., & Barron, L. M. (2007). Early Ordovician development of the Macquarie Arc, Lachlan Orogen, New South Wales. Australian Journal of Earth Sciences, 54(2–3), Article 2–3. https://doi.org/10.1080/08120090601146797

Halley, S. (2020). Mapping Magmatic and Hydrothermal Processes from Routine Exploration Geochemical Analyses. Economic Geology, 115(3), 489–503. https://doi.org/10.5382/econgeo.4722

Harris, A. C., Percival, I. G., Cooke, D. R., Tosdal, R. M., Fox, N., Allen, C. M., Tedder, I., McMillan, C., Dunham, P., & Collett, D. (2014). Marine Volcanosedimentary Basins Hosting Porphyry Au-Cu Deposits, Cadia Valley, New South Wales, Australia. Economic Geology, 109(4), Article 4. https://doi.org/10.2113/econgeo.109.4.1117

Ila'ava, M., Jutzeler, M., Cas, R., & Carey, R. (2024) 3D modelling of subsurface ancient volcanic successions: a workflow developed during regional reconstructions of the Cowal Igneous Complex in the Ordovician Macquarie Arc of NSW, Australia, Australian Journal of Earth Sciences, 71:5, 699-720, DOI: 10.1080/08120099.2024.2356134

Ila'ava, M., Jutzeler, M., Cas, R., Meffre, S., Bruce, M., & Carey, R. (2025). The submarine Cowal Igneous Complex, New South Wales, Australia: embryonic arc volcanism and 20 m.y. of basin evolution at East Gondwana's Cambro-Ordovician margin. Australian Journal of Earth Sciences, 72(7), 872–904. https://doi.org/10.1080/08120099.2025.2564461

Kemp, A. I. S., Blevin, P. L., & Norman, M. D. (2020). A SIMS U-Pb (zircon) and Re-Os (molybdenite) isotope study of the early Paleozoic Macquarie Arc, southeastern Australia: Implications for the tectono-magmatic evolution of the paleo-Pacific Gondwana margin. Gondwana Research, 82, 73–96. https://doi.org/10.1016/j.gr.2019.12.015

Lickfold, V., Cooke, D. R., Crawford, A. J., & Fanning, C. M. (2007). Shoshonitic magmatism and the formation of the Northparkes porphyry Cu – Au deposits, New South Wales. Australian Journal of Earth Sciences, 54(2–3), Article 2–3. https://doi.org/10.1080/08120090601175754

Pacey, A., Wilkinson, J. J., Owens, J., Priest, D., Cooke, D. R., & Millar, I. L. (2019). The Anatomy of an Alkalic Porphyry Cu-Au System: Geology and Alteration at Northparkes Mines, New South Wales, Australia. Economic Geology, 114(3), Article 3. https://doi.org/10.5382/econgeo.4644

Percival, I. G., & Glen, R. A. (2007). Ordovician to earliest Silurian history of the Macquarie Arc, Lachlan Orogen, New South Wales. Australian Journal of Earth Sciences, 54(2–3), 143–165. https://doi.org/10.1080/08120090601146789

Simpson, C. J., Scott, R. J., Crawford, A. J., & Meffre, S. (2007). Volcanology, geochemistry and structure of the Ordovician Cargo Volcanics in the Cargo – Walli region, central New South Wales. Australian Journal of Earth Sciences, 54(2–3), Article 2–3. https://doi.org/10.1080/08120090701221706

Wells, T. J., Meffre, S., Cooke, D. R., Steadman, J. A., & Hoye, J. L. (2020). Porphyry fertility in the Northparkes district: Indicators from whole-rock geochemistry. Australian Journal of Earth Sciences, 67(5), Article 5. https://doi.org/10.1080/08120099.2020.1715477

Wilson, A. J. (2003). The geology, genesis and exploration context of the Cadia gold-copper porphyry deposits, New South Wales, Australia [PhD]. University of Tasmania.